Volume 13 No 1–2 2013

ISSN 1473-6691 (print)
ISSN 1472-3422 (online)

Journal of the ICRU

ICRU REPORT 89

Prescribing, Recording, and Reporting Brachytherapy for Cancer of the Cervix

OXFORD UNIVERSITY PRESS

INTERNATIONAL COMMISSION ON RADIATION UNITS AND MEASUREMENTS

Journal of the ICRU

SUBSCRIPTIONS
A subscription to Journal of the ICRU comprises 2 issues (Reports). All prices include postage, and for subscribers outside the UK delivery is by Standard Air.

Current Subscription Rate
Institutional
Print edition and site-wide online access: £205/$389/€307
Print edition only: £188/$358/€282
Site-wide online access only: £164/$311/€246
Personal
Print only: £98/$186/€147
Please note: £ Sterling or € Euro rates apply in Europe, US$ elsewhere

Reports are available for purchase as single issues. Please see the Journal homepage: http://jicru.oxfordjournals.org/, and go to 'Purchase back reports of the ICRU'.

Full prepayment, in the correct currency, is required for all orders. Orders are regarded as firm and payments are not refundable. Subscriptions are accepted and entered on a complete volume basis. Claims cannot be considered more than FOUR months after publication or date of order, whichever is later. All subscriptions in Canada are subject to GST. Subscriptions in the EU may be subject to European VAT. If registered, please supply details to avoid unnecessary charges. For subscriptions that include online versions, a proportion of the subscription price may be subject to UK VAT. Personal rate subscriptions are only available if payment is made by personal cheque or credit card and delivery is to a private address.

Visit www.jicru.oxfordjournals.org for complete listing of previous reports available from Oxford University Press.

For further information, please contact: Journals Customer Service Department, Oxford University Press, Great Clarendon Street, Oxford OX2 6DP, UK. Email: jnls.cust.serv@oup.com. Tel (and answerphone outside normal working hours): +44 (0)1865 353907. Fax: +44 (0)1865 353485. **In the US, please contact:** Journals Customer Service Department, Oxford University Press, 2001 Evans Road, Cary, NC 27513, USA. Email: jnlorders@oup.com. Tel (and answerphone outside normal working hours): 800 852 7323 (toll-free in USA/Canada). Fax: 919 677 1714. **In Japan, please contact:** Journals Customer Services, Oxford University Press, 1-1-17-5F, Mukogaoka, Bunkyo-ku, Tokyo, 113-0023, Japan. Email: okudaoup@po.iijnet.or.jp. Tel: (03) 3813 1461. Fax: (03) 3818 1522.

Methods of payment. Payment should be made: by cheque (to Oxford University Press, Cashiers Office, Great Clarendon Street, Oxford, OX2 6DP, UK); by bank transfer [to Barclays Bank Plc, Oxford Office, Oxford (bank sort code 20-65-18) (UK); overseas only Swift code BARC GB22 (GB£ Sterling Account no. 70299332, IBAN GB89BARC20651870299332; US$ Dollars Account no. 66014600, IBAN GB27BARC20651866014600; EU€ EURO Account no. 78923655, IBAN GB16BARC20651878923655]; or by credit card (Mastercard, Visa, Switch or American Express).

Journal of the ICRU is published twice a year, June and December, by Oxford University Press, Oxford, UK. Annual subscription price is £205/$389/€307. Journal of the ICRU is distributed by Air Business Ltd, c/o Worldnet Shipping Inc., 156-15, 146th Avenue, 2nd Floor, Jamaica, NY 11434, USA.

US Postmaster: send address changes to Journal of the ICRU, Air Business Ltd, c/o Worldnet Shipping Inc., 156-15, 146th Avenue, 2nd Floor, Jamaica, NY 11434, USA.

Typeset by Nova Techset Private Limited, Bengaluru & Chennai, India
Printed by Bell & Bain, Glasgow, UK

ICRU REPORT No. 89

PRESCRIBING, RECORDING, AND REPORTING BRACHYTHERAPY FOR CANCER OF THE CERVIX

THE INTERNATIONAL COMMISSION ON RADIATION UNITS AND MEASUREMENTS
PREPARED IN COLLABORATION WITH
Groupe Européen de Curiethérapie – European Society for Radiotherapy and Oncology (GEC-ESTRO)
(Published June 2016)

Journal of the ICRU Volume 13 No 1–2 2013
Published by Oxford University Press

PRESCRIBING, RECORDING, AND REPORTING BRACHYTHERAPY FOR CANCER OF THE CERVIX

Report Committee

R. Pötter (Co-Chairman), Medical University of Vienna, Vienna, Austria
C. Kirisits (Co-Chairman), Medical University of Vienna, Vienna, Austria
B. Erickson, Medical College of Wisconsin, Milwaukee, USA
C. Haie-Meder, Gustave Roussy Cancer Campus, Villejuif, France
E. Van Limbergen, University Hospital Gasthuisberg, Leuven, Belgium
J. C. Lindegaard, Aarhus University Hospital, Aarhus, Denmark
J. Rownd, Medical College of Wisconsin, Milwaukee, USA
K. Tanderup, Aarhus University Hospital, Aarhus, Denmark
B. R. Thomadsen, University of Wisconsin School of Medicine and Public Health, Madison, WI, USA

Commission Sponsors

P. M. DeLuca, Jr., University of Wisconsin, Madison, WI, USA
A. Wambersie, Universite Catholique de Louvain, Brussels, Belgium
S. Bentzen, University of Maryland School of Medicine, Baltimore, MD, USA
R. A. Gahbauer, Ohio State University, Columbus, OH, USA
D. T. L. Jones, Cape Scientific Concepts, Cape Town, South Africa
G. F. Whitmore, Ontario Cancer Institute, Toronto, Canada

Consultants to the Report Committee

W. Dörr, Medical University of Vienna, Vienna, Austria
U. Mahantshetty, Tata Memorial Hospital, Mumbai, India
P. Petrič, National Center for Cancer Care and Research, Doha, Qatar
E. Rosenblatt, International Atomic Energy Agency, Vienna, Austria
A. N. Viswanathan, Harvard Medical School, Boston, MA, USA

Journal of the ICRU Vol 13 No 1–2 (2013) Report 89
Oxford University Press

doi:10.1093/jicru/ndw028

International Commission on Radiation Units and Measurements

Introduction

The International Commission on Radiation Units and Measurements (ICRU), since its inception in 1925, has had as its principal objective the development of internationally acceptable recommendations regarding:

(1) quantities and units of ionizing radiation and radioactivity,
(2) procedures suitable for the measurement and application of these quantities in clinical radiology and radiobiology, and
(3) physical data needed in the application of these procedures, the use of which tends to assure uniformity in reporting.

The Commission also considers and makes similar types of recommendations for the radiation protection field. In this connection, its work is performed in cooperation with the International Commission on Radiological Protection (ICRP).

Policy

ICRU endeavors to collect and evaluate the latest data and information pertinent to the problems of radiation measurement and dosimetry and to recommend the most acceptable numerical values for physical reference data and techniques for current use.

The Commission's recommendations are kept under continual review in order to keep abreast of the rapidly expanding uses of radiation.

ICRU feels that it is the responsibility of national organizations to introduce their own detailed technical procedures for the development and maintenance of standards. However, it urges that all countries adhere as closely as possible to the internationally recommended basic concepts of radiation quantities and units.

The Commission maintains and develops a system of quantities and units and concepts (*e.g.*, for radiation therapy) and guidance for measurement procedures and techniques having the widest possible range of applicability. Situations can arise from time to time for which an expedient solution of a current problem is required.

ICRU invites and welcomes constructive comments and suggestions regarding its recommendations and reports. These may be transmitted to the Chairman.

Current Program

The Commission recognizes its obligation to provide guidance and recommendations in the areas of radiation therapy, radiation protection, and the compilation of data important to these fields, and to scientific research and industrial applications of radiation. Increasingly, the Commission is focusing on the problems of protection of the patient and evaluation of image quality in diagnostic radiology and radiation oncology. These activities do not diminish the ICRU's commitment to the provision of a rigorously defined set of quantities and units useful in a very broad range of scientific endeavors.

The Commission is currently engaged in the formulation of ICRU Reports treating the following subjects:

Bioeffect Modeling and Biologically Equivalent Dose Concepts in Radiation Therapy
Key Data for Measurement Standards in the Dosimetry of Ionizing Radiation
Monitoring and Assessment of Radiation Releases to the Environment
Operational Radiation Protection Quantities for External Radiation
Prescribing, Recording, and Reporting Ion-Beam Therapy
Prescribing, Recording, and Reporting Stereotactic Treatments with Small Photo Beams
Retrospective Assessment of Individual Doses for Acture Exposures to Ionizing Radiation
Small-Field Photon Dosimetry and Applications in Radiotherapy

The Commission continually reviews progress in radiation science with the aim of identifying areas

in which the development of guidance and recommendations can make an important contribution.

ICRU's Relationship with Other Organizations

In addition to its close relationship with the ICRP, ICRU has developed relationships with national and international agencies and organizations. In these relationships, ICRU is looked to for primary guidance in matters relating to quantities, units, and measurements for ionizing radiation, and their applications in the radiological sciences. In 1960, through a special liaison agreement, ICRU entered into consultative status with the International Atomic Energy Agency (IAEA). The Commission has a formal relationship with the United Nations Scientific Committee on the Effects of Atomic Radiation (UNSCEAR), whereby ICRU observers are invited to attend annual UNSCEAR meetings. The Commission and the International Organization for Standardization (ISO) informally exchange notifications of meetings, and ICRU is formally designated for liaison with two of the ISO technical committees ICRU is a member of Consultative Committee for Units (CCU) – BIPM and Consultative Committee for Ionizing Radiation (CCRI(I) – BIPM and Observer to CCRI(II) and CCRI (III). ICRU also enjoys a strong relationship with its sister organization, the National Council on Radiation Protection and Measurements (NCRP). In essence, ICRU and NCRP were founded concurrently by the same individuals. Presently, this long-standing relationship is formally acknowledged by a special liaison agreement. ICRU also exchanges reports with the following organizations:

Bureau International des Poids et Mesures
European Commission
International Council for Science
International Electrotechnical Commission
International Labour Office
International Organization for Medical Physics
International Radiation Protection Association
International Union of Pure and Applied Physics
United Nations Educational, Scientific and Cultural Organization

The Commission has found its relationship with all of these organizations fruitful and of substantial benefit to the ICRU program.

Operating Funds

Financial support has been received from the following organizations:

Accuray Incorporated
American Association of Physicists in Medicine
Belgian Nuclear Research Centre
Canadian Nuclear Safety Commission
Federal Office Public Health, Switzerland
Helmholtz Zentrum München Hitachi, Ltd.
International Radiation Protection Association
International Society of Radiology
Ion Beam Applications, S.A.
Japanese Society of Radiological Technology
MDS Nordion
Nederlandse Vereniging voor Radiologie
Philips Medical Systems, Incorporated
Radiological Society of North America
Siemens Medical Solutions
U.S. Environmental Protection Agency
U.S. Nuclear Regulatory Commission
Varian Medical Systems

In addition to the direct monetary support provided by these organizations, many organizations provide indirect support for the Commission's program. This support is provided in many forms, including, among others, subsidies for (1) the time of individuals participating in ICRU activities, (2) travel costs involved in ICRU meetings, and (3) meeting facilities and services.

In recognition of the fact that its work is made possible by the generous support provided by all of the organizations supporting its program, the Commission expresses its deep appreciation.

Hans-Georg Menzel
Chairman, ICRU
Heidelberg, Germany

Journal of the ICRU Vol 13 No 1–2 (2013) Report 89
Oxford University Press
doi:10.1093/jicru/ndw027

Prescribing, Recording, and Reporting Brachytherapy for Cancer of the Cervix

Journal of the ICRU Vol 13 No 1–2 (2013) Report 89
Oxford University Press
doi:10.1093/jicru/ndw004

Preface

The treatment of gynecological malignancies is one of the very earliest applications of radionuclides in medicine, dating from soon after Marie Curie's discovery and isolation of radium (^{226}Ra). The widespread use of radium for the treatment of cervical malignancies rapidly became common practice. Over the many decades since this discovery, incredible advances occurred in the diagnosis and treatment of such tumors. These included the introduction of various radium systems dealing with source application and treatment prescription, mainly in the first half of the last century (*e.g.*, at Manchester and M.D. Anderson Hospital, Houston). Later, intermediate-dose rate, high-dose rate, and pulsed-dose rate radioactive stepping sources were developed. The latter devices employ computer-controlled positioning using afterloading techniques. At present, fully three-dimensional treatment planning derived from CT and MR imaging is considered the paradigm for cervix cancer brachytherapy, replacing the radiographic approach. These techniques are often combined with advanced external-beam therapy and concomitant cytotoxic chemotherapy using three-dimensional image-guided techniques (*e.g.*, image-guided radiotherapy and intensity-modulated radiation therapy using a static or rotating gantry). These and other advances have emerged since the publication of ICRU Report 38 (1985) on intracavitary therapy in gynecology.

Advances in precise, high-resolution, cost-effective volume imaging using MR and spiral CT now allow accurate specification of the relationship between external radiation beams, brachytherapy applicators, and the tumor and normal tissue structures. Brachytherapy treatment of cervix cancer is most frequently used as a boost treatment toward the end of external beam radiation therapy (EBRT) and concomitant chemotherapy. As there is a major tumor response during this combined treatment, tumor volume and shape change significantly and treatment requires an *adaptive* target concept. The resulting high-risk clinical target volume (CTV) is defined using the residual gross tumor volume (GTV) and the pathologically identified tissues at the time of brachytherapy combined with the anatomical topography when the applicator is in place.

In this ICRU report, specific concepts and terminology are developed, comparable to the GEC ESTRO recommendations, for selecting and contouring the various tumor-related (adaptive) volumes, together with the delineation of the adjacent organs at risk (OAR). Detailed contouring of these structures and volumes based on repetitive imaging and gynecologic examination requires a comprehensive understanding of tumor spread and tumor response.

Specific dose-volume and dose-point parameters are introduced and adopted in this ICRU report for the different tumor-related volumes and OARs, based on volumetric imaging as well as on traditional radiographic imaging. This set of parameters fulfill the specific needs for prescribing, recording, and reporting intracavitary and interstitial cervix cancer brachytherapy for the volumes of interest located in the very inhomogeneous dose region characterized by a rapid dose fall off adjacent to the radioactive sources. Essential for dose calculation, treatment planning procedures such as applicator reconstruction are described. This leads directly to three-dimensional treatment planning with optimization procedures based on the evaluation of dose-volume histograms (DVH) and using reference absorbed dose-points. A balanced assessment of the complex set of dose points and dose-volume parameters enables a highly individualized final dose prescription for the volumes of interest. This report, as well as clinical reports based on these parameters, demonstrates that these advances have helped to identify and investigate correlations between dose points and DVH and specific endpoints such as normal tissue damage and local tumor control.

Presently, traditional low-dose rate afterloading techniques with ^{226}Ra or ^{137}Cs sources are being replaced by high-dose rate or pulsed-dose ^{192}Ir or ^{60}Co sources. Computer-controlled, cable-driven afterloading devices place the sources in a variety of positions in the applicator, delivering variable doses at different locations in variable dwell times. A large variety of doses per fraction, dose rates, and total absorbed doses are prescribed and reported for the different volumes of interest, moving away from the traditional implant systems and prescription patterns. These changes and

advances require the use of biophysical modeling to combine the effects of varying dose fractions, total absorbed doses and dose rates (*i.e.*, differing from the conventional 2 Gy per fraction or 0.5 Gy/h) on the corresponding estimates of tumor and normal tissue response. The report discusses such a model and the process to estimate such response variations by means of the equi-effective dose concept, expressed as an EQD2 dose. This report recommends jointly reporting EQD2 results based on modeling as well as traditional absorbed dose in communicating results.

This report provides comprehensive recommendations on prescribing, recording, and reporting brachytherapy focusing on volumetric imaging in cervix cancer brachytherapy. However, it is well recognized that the majority of advanced cervix cancer patients are and will be treated in developing countries with limited resources. Patients in these countries are usually treated with simple radiotherapy methods. This report combines prescribing, recording, and reporting for simple methods of radiotherapy (*e.g.*, point A prescription) with advanced methods using dose-volume parameters (*e.g.*, $D_{90\%}$ prescription in the adaptive target) through an "integrated level" approach. For example, when practicing Level 2 ("advanced standard"), the report recommends also reporting the parameters for Level 1 ("minimum standard"). This facilitates communication between centers with simple and advanced radiotherapy.

The report includes nine appendices providing a spectrum of clinical case examples to guide and suggest various techniques for typical clinical scenarios of radical cervix cancer treatment. These examples include a comprehensive set of treatment-related parameters such as: patient and tumor work up, treatment intention, EBRT and concomitant chemotherapy, brachytherapy, combined reporting of EBRT and brachytherapy, and follow-up. This will facilitate the understanding of prescribing, recording, and reporting across different tumor stages, EBRT and brachytherapy techniques, dose fractions, dose rates, total absorbed doses, in the frame of both a volumetric and a radiographic approach.

Finally, the concepts and terms described in this report follow the tradition of previous ICRU reports on prescribing, recording, and reporting external beam radiotherapy (from ICRU Report 50 to 83). In particular, the concepts for GTV, CTV, and planning target volume are elaborated within the context of cervix cancer brachytherapy, and now introduce a new adaptive target concept. Dose-volume parameters are introduced addressing the specific needs of image-guided brachytherapy. Changes of tumor topography are integrated into these concepts and terms. What still remains to be solved is an integrated assessment of volumes and doses from EBRT and brachytherapy, which reflect the considerable changes during the overall treatment time.

The current report on prescribing, recording, and reporting cervix cancer brachytherapy is a joint report from the ICRU and the GEC ESTRO highlighting the intensive and effective collaboration on cervix cancer brachytherapy during the last two decades.

Paul M. DeLuca Jr
Christian Kirisits
Richard Pötter

Journal of the ICRU Vol 13 No 1–2 (2013) Report 89
Oxford University Press
doi:10.1093/jicru/ndw001

Abstract

This ICRU/GEC-ESTRO report starts with the essential background, including a clinical introduction, historical and current techniques including the concepts of volumetric imaging for cervix cancer. One key element is the four-dimensional adaptive target concept at certain time points during treatment by clinical examination and imaging. For the rectum, bladder, sigmoid, adjacent bowel, and vagina in addition to contours including the entire organ the report emphasizes the presence of different morbidity endpoints and related substructures within the organ. The radiobiology chapter explains the limitations of the linear-quadratic model, but encourages the use of the EQD2 concept as the current best option for treatment planning and overall dose reporting. A detailed concept is recommended to report dose and volume parameters related to contours and reference points. The report includes detailed chapters on treatment planning, especially for three-dimensional volumetric approach, but also the underlying concepts of dosimetry which remains essential for volumetric and radiography-based planning.

Journal of the ICRU Vol 13 No 1–2 (2013) Report 89
Oxford University Press
doi:10.1093/jicru/ndw002

Acknowledgements

The Committee would like to thank the following colleagues for their essential support for some clinical examples and some figures in this report:

Bethany Anderson, University of Wisconsin, Madison Wisconsin, USA,
Daniel Berger, Medical University of Vienna, Vienna, Austria,
Marisol de Brabandere, University Hospital Gasthuisberg, Leuven, Belgium,
Isabelle Dumas, Gustave Roussy Cancer Campus, Villejuif, France,
Martine Franckena, Erasmus Medical Center, Rotterdam, The Netherlands,
Tijana Frank, Medical University of Vienna, Vienna, Austria,
Jesper F. Kallehauge, Aarhus University Hospital, Aarhus, Denmark,
Bruce Libby, University of Virginia, Charlottesville, VA, USA,
Nicole Nesvacil, Medical University of Vienna, Vienna, Austria, and
Maximilian Schmid, Medical University of Vienna, Vienna, Austria.

Journal of the ICRU Vol 13 No 1–2 (2013) Report 89
Oxford University Press
doi:10.1093/jicru/ndw003

1. Introduction

During the past few decades, there have been dramatic changes in the field of radiotherapy (Thwaites and Malicki, 2011). These changes include significant developments in imaging, computer technology, treatment planning, and treatment-delivery technology, and also in understanding the nature of malignant disease and the effects of radiation on both malignant and normal tissue (Leer, 2011; Overgaard, 2011; Rodemann and Wouters, 2011; Thwaites and Malicki, 2011). Due to these developments and the increasing incidence and significance of cancer worldwide (Cavalli, 2006; IAEA, 2013), radiation oncology has become one of the major disciplines in modern medical care and research.

Modern oncology includes a large variety of specialties both in research and in clinical medicine, ranging from prevention to diagnostic and therapeutic procedures. Surgical, radiation, and medical oncology are the major therapeutic strategies, and—because of the necessary sub-specialization of expertise—multidisciplinary approaches have become the standard in research, education, and patient care (Croke and El-Sayed, 2012; Kesson *et al*., 2012; Pötter *et al*., 2012; Reade and Elit, 2012). Major progress in the field is leading to increasingly patient-specific treatment approaches tailored to the individual patient risk, based on tumor stage, histology, prognostic factors, and response to treatment (Reade and Elit, 2012). Cure rates have increased significantly in many oncological fields, initially most notably for pediatric and hematological malignancies (O'Leary *et al*., 2008; Pritchard-Jones *et al*., 2006), but increasingly also for solid tumors (Ferlay *et al*., 2007; Kesson *et al*., 2012). The reasons for such improvements are multifold, including the introduction of more tailored multimodality treatments. The combination of radiotherapy with cytotoxic chemotherapy or hormonal therapy has, for example, become standard particularly for advanced high-risk disease for various malignancies such as breast (Goldhirsch *et al*., 2009), rectum (Valentini *et al*., 2009), prostate (Mottet *et al*., 2011), and cervical cancers (Eifel, 2006; Thomas, 1999), with new approaches in combined targeted therapies and immunotherapies as major future pathways (Specenier and Vermorken, 2013). Long-term treatment-related morbidity and quality of life have consequently become major concerns in the increasing population of cancer survivors (Heirs *et al*., 2012; McCabe and Jacobs, 2012). In parallel, palliative medicine, including radiotherapy, has improved and is playing an increasing role in relief of symptoms, and its role is increasingly emphasized in research and education.

1.1 Developments in Epidemiology and Treatment of Cervical Cancer

Cervical cancer had the highest incidence among female cancers in high-income countries in the first half of the last century [Annual Reports of the International Federation of Gynecology and Obstetrics (FIGO)] (Boyle *et al*., 2003; Denny, 2012; Pecorelli, 2009; Pettersson and Benedet, 1998; Quinn *et al*., 2006). Cervical cancer remains frequent, about 500 000 new cases per year worldwide (Jemal *et al*., 2012, Parkin *et al*., 2005), even increasing in numbers (Forouzanfar *et al*., 2011), particularly in developing countries. Cervical cancer incidence will further increase in countries lacking systematic vaccination and screening programs (Jemal *et al*., 2011; Sherris *et al*., 2001).

In the *developed* world, there has been a dramatic shift in the initial presentation of cervical cancer due to the widespread implementation of cytological screening that began about 50 years ago and is now further expanded to include human-papilloma-virus-based DNA testing (Cuzick, 2010; Cuzick *et al*., 2008). Screening has led to a dramatic decrease in cervical cancer mortality (Cuzick *et al*., 2008). This progress in screening coupled with advances in therapy has divided the "world of cervix cancer" into two groups of countries:

- Countries in South-Central–Eastern Asia, Eastern/Western/South/Middle Africa, South and Central America, and Central/Eastern Europe that have limited resources and a high incidence/mortality of cervical cancer per 100 000 women-years: 15/6 Central and Eastern Europe, 25/15 in South-Central Asia, 24/11 South and Central America, 34/25 Eastern/Western Africa (Jemal *et al*., 2011; Sherris

et al., 2001). Patients are treated mainly with simple methods of radiotherapy (IAEA, 2013);
- Countries such as those in Western/Northern/Southern Europe and in North America and Japan that have extensive resources and a decreasing incidence/mortality of cervix cancer per 100 000 women years: 7/2 Western Europe, 6/1.7 North America (Jemal *et al*., 2011; La Vecchia *et al*., 2010). Patients are treated increasingly with advanced methods of radiotherapy combined with chemotherapy.

This ICRU report deals with the treatment of cervical cancer by radiation therapy with particular emphasis on intracavitary brachytherapy, which has played a major role for more than a century in the treatment of cervical cancer patients (Adler, 1919; Eifel *et al*., 1995; Fletcher, 1971; Gerbaulet *et al*., 1995; Kottmeier, 1954; Logsdon and Eifel, 1999; Paterson, 1954; Quinn *et al*., 2006; Sandler, 1942). FIGO Annual Reports, published annually starting 1937 and then 3-yearly from 1973 onwards (Pettersson and Benedet, 1998) are a major source of information. The need for treatment of invasive cervical cancer will likely increase due to the less-widespread availability of vaccines and screening in developing countries.

This report will address the role of brachytherapy for cancer of the cervix in both advanced countries and those countries where a large number of patients are treated in centers with limited resources.

1.2 Outline of Report

1.2.1 Prevention, Diagnosis, Prognosis, Treatment, and Outcome

To provide an overview of cancer of the cervix, Section 2 begins with an outline of the currently available methods of prevention (vaccination), screening, diagnosis, and staging, followed by a discussion of stage- and risk-adapted treatment strategies, which consist of conservative and radical surgical interventions, radiotherapy, and chemotherapy alone or in various combinations. These will be discussed in the context of therapeutic challenges and treatment outcomes.

Surgery is the main treatment option for early and limited disease, except for patients with lymph-node involvement who are primarily treated with radiochemotherapy, including brachytherapy. Since the publication of five randomized trials in 1999, combined external-beam radiotherapy (EBRT), brachytherapy, and simultaneous chemotherapy has become the standard of care for advanced disease (stage IB2-IV) (Eifel, 2006; Thomas, 1999; Vale *et al*., 2008).

EBRT in gynecology has benefited from major developments that are well reflected in previous reports of the ICRU (ICRU 1993a; 2000; 2004; 2007; 2010). Those reports elaborated the concepts and terms for target delineation and dose–volume reporting. Therefore, there is limited discussion of EBRT in the present report, although EBRT usually represents an important integral part of the overall treatment strategy and has impact both on regional and on local control.

1.2.2 Brachytherapy Techniques and Systems

Intracavitary gynecologic brachytherapy is the most widely used application of brachytherapy. The "rules" of the classical schools with various application and radium-loading systems developed 70 years to 90 years ago, were widely adopted during the first half of the last century. Changes during the last several decades include the decline in the use of radium with the introduction of artificially produced radionuclides. These radionuclides together with the spread of afterloading, stepping-source technology, computer and imaging technology led to the use of novel dose-rate approaches (medium dose rate, MDR, high dose rate, HDR, pulsed dose rate, PDR), computer- and image-assisted treatment planning, modern application and delivery techniques, and most recently the implementation of sectional and volume-image-based applications. These developments largely took place after the publication of ICRU Report 38 on intracavitary therapy in gynecology (ICRU, 1985). Many of these changes and developments are still being incorporated at different rates around the world, often independent of each other, making it difficult and sometimes impossible to describe and compare methods and results in a coherent fashion.

A major aim of this report is to provide definitions of concepts and terms to enable valid and reliable exchange of information about treatment methods and clinical results. Section 3 provides comprehensive information about recent major advances in intracavitary brachytherapy, often referring to the historical roots of current practices. Full understanding of the most advanced, modern image-based brachytherapy techniques is easier with sufficient knowledge of the historical background.

1.2.3 Brachytherapy Imaging for Treatment Planning

Medical imaging has progressed dramatically since the advent of computed tomography (CT) and magnetic resonance imaging (MRI) 30 years to 40 years ago—and is further evolving, particularly in the field of functional imaging such as PET-CT and functional MRI

(fMRI). State-of-the-art imaging such as MRI and CT are being increasingly introduced in the diagnosis and treatment of cervical cancer, particularly in the wealthier countries. Ultrasound imaging has played a limited role, although its potential is significant particularly for applicator placement. Despite the above advances, the majority of patients worldwide still undergo treatments based mainly on FIGO staging determined from clinical examination with or without anatomical drawings and radiographic images.

An overview of the various modalities used for cervical cancer imaging is outlined in Section 4 with particular emphasis on their use in the planning of brachytherapy.

1.2.4 Tumor and Target Volumes and Adaptive Radiotherapy

Brachytherapy in cancer of the uterine cervix can be adaptive and provide better dose conformation if the tumor/target can be precisely assessed and delineated in three dimensions, taking into account the tumor-growth pattern, change during the course of radio-chemotherapy, and the topography of the adjacent OAR. At the time of publication of ICRU Report 38 (ICRU, 1985), treatment planning for cervical cancer was based on gynecologic examination at diagnosis and radiography without the benefit of time-dependent volumetric imaging. The target approach was recommended, referring to the clinical tumor presentation at diagnosis. Reporting the maximum width, thickness, and height of the 60 Gy reference volume covering this target was recommended. It is now well documented that major shrinkage of the initial gross tumor volume (GTV) and variation of topography occurs regularly during treatment, which typically begins with EBRT and simultaneous chemotherapy, leaving various amounts of residual GTV at the time of brachytherapy.

To allow adaptations of the treatment, repetitive gynecologic examinations and imaging are essential to determine tumor width, thickness, and height as a function of time.

The adaptive approach described in Section 5 forms the thrust of the current report. For the boost treatment of the tumor, a special CTV-T terminology is used and specifically defined for the time of brachytherapy after initial radio-chemotherapy. The high-risk CTV-T ($CTV\text{-}T_{HR}$), an adaptive CTV-T,[1] includes the residual tumor, the cervix, and residual adjacent pathologic tissue. A second CTV, the intermediate-risk CTV-T ($CTV\text{-}T_{IR}$), includes the initial tumor extent and the $CTV\text{-}T_{HR}$ with a margin. The area of potential microscopic tumor spread is called the low-risk tumor-related CTV-T ($CTV\text{-}T_{LR}$). The general concepts, terms, and definitions enunciated in the series of recent ICRU reports on prescribing, recording, and reporting different radiotherapy (ICRU, 1993a; 2000; 2004; 2007; 2010) are integrated into the present report, which unlike these previous reports deals with a specific disease site. The GEC ESTRO Recommendations (Haie-Meder *et al*., 2005), generally accepted worldwide, form the basis of this adaptive strategy.

Some attention is paid also to the use of the planning target volume (PTV), which plays a major role in planning and delivering EBRT. However, specific considerations have to be taken into account for brachytherapy due to the inherent absorbed-dose-distribution characteristics, with large absorbed-dose inhomogeneities throughout the target volume and steep absorbed-dose gradients adjacent to the target surface. Therefore, PTV margins have to be utilized with great care in intracavitary brachytherapy. Due to very limited target movement in relation to the position of the applicator, margins for compensation of geometric uncertainties play a minor role. Addition of margins in the orthogonal direction should be avoided as they would lead to a considerable absorbed-dose increase in the whole volume.

1.2.5 OAR- and Morbidity-Related Concepts and Volumes

Section 6 introduces radiotherapy-related morbidity endpoints and (sub-)volumes of OARs based on the typical morbidity profiles as known from clinical experience in cervical cancer radiotherapy. Certain targets in the OAR are selected that correspond to typical pathology and morbidity patterns (*e.g*., telangiectasia/bleeding). Small absolute volumes (2, 0.1 cm^3) are defined corresponding to typical brachytherapy-related morbidities such as telangectasia and ulceration/fistula. These reference volumes might have different locations in the OARs depending on the application technique. The location of such volumes within a given organ can be specified through anatomically defined points in OARs [*e.g*., ICRU bladder point on the bladder floor (bladder balloon), vaginal points (bony reference)]. Larger volumes are of interest for morbidity such as stenosis or organ shrinkage that are due to significant radiation dose to the whole circumference and/or a significant length of a hollow organ (*e.g*., circumference in the upper vagina; length for the mid/lower vagina).

Position variations and uncertainties due to internal motion are observed for OARs (*e.g*., bowel) and should be assessed through repetitive imaging and corrections applied as appropriate. For organs

[1]For simplification, in this Report, CTV refers to CTV-T if not otherwise stated.

with moderate mobility (*e.g.*, rectum, bladder), a static anatomical topography seems to be a suitable approximation for assessing the high-dose region for small volumes in fractionated brachytherapy.

1.2.6 Radiobiological Considerations

Intracavitary brachytherapy always results in a range of highly heterogeneous absorbed-dose rates and absorbed doses per fraction in the different tissues of the patient, with different absorbed-dose distributions characterizing each application. In addition, a large variety of dose and fractionation schedules are in current use. These variations in absorbed dose and absorbed-dose rate have a major impact on tumor and normal-tissue effects. To assess and communicate the effects of such complex dosimetric and clinical situations with such large absorbed-dose inhomogeneities, it is evident that bio-mathematical models would be useful. Such models could serve to describe the assumed biological consequences of the various absorbed doses and absorbed-dose rates encountered. For a long time, efforts have been made to develop and validate biological models, and there still is major controversy about their validity and reliability. A new ICRU Report Committee was recently formed to clarify some of these issues and to propose concepts and methods to make such complex dosimetric, biological, and clinical scenarios meaningful, valid and reliable. In concordance with this ongoing work, the concept of equi-effective dose (EQD2), based on the linear-quadratic model, is discussed, and EQD2 is recommended for gynecologic brachytherapy. These concepts provide a common basis for comparisons of absorbed dose, absorbed-dose rate, and absorbed dose per fraction (rate), and clinical results among different radiotherapy treatment techniques and departments. These are discussed in this report in Section 7, and recommendations are made concerning the choice of alpha/beta values in the linear-quadratic model in the application of the EQD2 concept. Practical ways to implement such concepts into clinical practice are demonstrated in Section 7 (using a spreadsheet). For their application, one must be aware of the limitations of the models, as these concepts still require clinical validation, in particular for their use in brachytherapy.

1.2.7 Dose and Volume Parameters

Based on the volumetric and biological concepts for reporting treatments as outlined in Sections 5–7 of this report, dose–volume parameters are suggested in Section 8 for the residual GTV, the target CTV_{HR}, CTV_{IR}, and OAR, including the application of the EQD2 concept. It is recommended that absorbed-dose coverage and absorbed-dose inhomogeneities of intracavitary brachytherapy be assessed using the dose–volume parameters $D_{98\%}$, $D_{90\%}$, and $D_{50\%}$, which show a wide range of numerical values.

A brachytherapy-specific dose–volume concept for reporting OAR absorbed dose is introduced in the present report, and is essential for evaluating the balance between target coverage and dose–volume constraints in OAR. This concept refers to two small reference volumes, D_{2cm^3} and $D_{0.1cm^3}$, characterizing the maximally exposed region in the adjacent organ walls and the absorbed-dose inhomogeneity over that volume. Concepts for reporting larger intermediate-dose regions irradiated primarily during EBRT are also developed and discussed.

Use and reporting of physical and biological dose–volumes and other relevant parameters is recommended in order to improve future clinical outcomes and to provide the data for new or improved biological models. This will allow future reconstruction of the treatment conditions and correlation with outcome data based on re-evaluation.

In recent ICRU reports, prescription is defined as the final definition of a treatment plan with dose–volume parameters to treat an individual patient, while planning aims are defined within the treatment strategy for patient groups before treatment planning according to their risk profile.

1.2.8 Physics Aspects of Three-Dimensional Volumetric Dose Assessment

The concepts and terms for specifying dose–volumes and absorbed doses at reference points introduced in previous sections (volumes) and in following sections (points) are linked in Section 9 to the brachytherapy applicator and the radioactive-source positions in three-dimensional (3D) space.

The process starts with the applicator reconstruction within the imaging system used for treatment planning, which may be complemented by definition of reference points in these images. Registration and fusion of images with reference systems are important issues that are taken into account in Section 9. These can apply for image fusion in regard to the brachytherapy applicator or for applicator-reconstruction purposes or for fusion of time-dependent target contours within fractionated brachytherapy. Co-registration and fusion as applied to EBRT and brachytherapy still have major unresolved problems. Besides spatial fusion, temporal fusion is also essential, as fractionated treatments are applied to anatomy that changes with time. Various types of uncertainties arising from spatial fusion (3D) and temporal fusion (4D) are systematically addressed and classified as intra-fraction, inter-fraction, and inter-application uncertainties.

1.2.9 Radiographic Localization of Absorbed-Dose Points

The major thrust of this report concerns the concepts of 3D volumetric and 4D assessment and representation of volumes/dimensions and doses, including the application of biological models. However, it is well recognized that due to the expected continuing dichotomy in the global practice of gynecologic oncology, radiography-based methods for assessment of volume/dimensions and of doses will continue to be used in clinical practice. The same biological models as used in 3D volumetric situations can be applied for reference points as defined on radiographs. Therefore, specific attention is given in Section 10 to define these points for 3D radiograph-based practice in limited resource settings for the tumor-related target specification, for OAR, and for lymph nodes. The use of traditional dose points with the volumetric approach enables the various clinical experiences accumulated under different treatment conditions to be evaluated. When a common terminology is established, progress in 3D and 4D gynecologic brachytherapy can influence further developments in institutions with limited resources.

Some of the recommended reference points are taken from the previous ICRU Report 38 (ICRU, 1985) (bladder, rectum, pelvic wall, lymphatic trapezoid) and some additional points are specified (vagina).

Essential to this report is the adoption of Point A as a major reference point with a straightforward definition related to the applicator for absorbed-dose specification: for the planning aim (optional), for prescribing (optional), and for reporting (mandatory) in the volumetric image-based approach as well. Dose at Point A, despite all its limitations, represents the most widely used parameter in gynecologic brachytherapy worldwide. One of the major obstacles to the universal acceptance of ICRU Report 38 (ICRU, 1985) was the fact that Point A was not considered for absorbed-dose reporting because of its inherent limitations. The Point A definition as proposed in the present report is clearly linked to the applicator position. This geometrical definition is recommended in order to provide a clear distinction with the anatomically defined target dose–volume definition that has been introduced here as a new concept.

1.2.10 Sources and Dose Calculation

Section 11 describes the physical background for dose calculation. The source strength is specified in units of reference air-kerma rate (RAKR) at 1 m. It is possible to interpret historical data by converting this unit to milligram Radium equivalent (Raeq), the original unit used to specify dose. The total reference air kerma (TRAK) is defined as the integral of RAKR over the whole treatment duration summed for all sources. Correlations between TRAK and Point A dose/irradiated volumes are indicated in this section. For absorbed-dose calculation, the American Association of Physicists in Medicine (AAPM) Task Group 43 (Nath *et al*., 1995) formalism with recent improvements is recommended.

1.2.11 Treatment Planning

In Section 12, the complete treatment-planning process for image-guided adaptive brachytherapy, incorporating the concepts and methods outlined in this report, is described. Treatment planning includes the decisions related to the use of radiotherapy (EBRT, brachytherapy) and chemotherapy, the planning aims, results of the medical examinations, definition of applicator geometry (pre-planning), imaging information, target-volume determination, OAR contouring, dosimetric-plan optimization, and integration of biological models into the treatment-planning process. The final plan evaluation includes a complete assessment of the various dose-point and dose–volume parameters. The plan selected and prescribed is the most appropriate one that meets the needs of the clinical situation.

1.2.12 Summary of the Recommendations

At the end of the report, a short summary in tabular form gives a quick and complete overview of all the different conditions and parameters that have been described in detail throughout this report, in particular at end of Sections 5 through 8, 10, and 11. For the other sections, “Key Messages” can be found at the end of each section. These stress the major issues outlined in each section that need to be considered in the implementation of brachytherapy for the treatment of cervical cancer.

For the majority of the recommended parameters, reporting is structured following the level approach previously introduced in ICRU reports (ICRU, 1993b; 1999)

Level 1 describes the minimum requirements, which should be followed in all centers, for all patients, and represents the minimum standard of treatment;

Level 2 indicates advanced standards of dose planning and treatment that allow a more complete exchange of information between centers, based on more comprehensive information and which is recommended be followed;

Level 3 describes new forms of planning and treatment largely related to research and development

for which reporting criteria cannot yet be established.

The expected continuing dichotomy in the levels of practice of gynecologic oncology in general and of brachytherapy in particular in different parts of the world (IAEA, 2013) requires a specific solution. To provide a suitable model for both "worlds," a separation within each level is established for a clinical and volumetric approach, on the one hand, and a clinical and radiographic approach, on the other hand. This allows for appropriate selection according to the available resources. Tables of recommendations are therefore provided in two columns (for the two approaches) at the end of Sections 5 and 6, whereas only one column is used for Sections 7, 8, and 10. For a comprehensive exchange of information on brachytherapy for cancer of the cervix among advanced centers with sufficient resources, the Level 2 approach is recommended, whereas for centers with limited resources (developing countries) with large patient numbers, the Level 1 approach should be followed. Through the integration of Level 1 into Level 2 reporting, a broad exchange of information will be possible between centers with limited and sufficient resources.

1.2.13 Clinical Examples

Appendix A consists of nine clinical examples describing in detail the various clinical, imaging, technical, and biological scenarios with respect to the FIGO stage of disease with and without nodes, the various EBRT techniques (3D conformal radiotherapy, IMRT), the different application techniques (tandem-ovoids/tandem-ring/tandem-mold, with and without interstitial needles), different absorbed-dose rates (HDR/PDR/LDR), various physical and biological doses and dose rates, fractionation schedules, treatment planning based on the radiographic (adaptive) approach or the volume-image adaptive approach, and various combinations of these.

The major recommendations as outlined in this ICRU report are applied and specified in these examples. These examples are given in a common format to show how the different steps for treatment planning, for final treatment prescription, and for treatment delivery can be reported.

1.2.14 Electronic Spreadsheet

On the website http://icru.org/content/reports/prescribing-recording-and-reporting-brachytherapy-for-cancer-of-the-cervix-report-no-89, spreadsheets for calculating EQD2 doses for HDR and PDR schedules are provided. This site also contains a printable form for reproducible clinical drawings as used in this report.

1.2.15 Report Organization: Summaries, Recommendations, and Key Messages

To improve clarity and overview for reading, each section ends with a summary of the section contents.

ICRU recommendations are given—partly in tabular form—at the end of Sections 5–8, 10, and 11. These recommendations refer to conditions and parameters as described and defined within the text of these sections. These ICRU recommendations are summarized in tabular form in Section 13. Key messages are given at the end of Sections 2–4, 9, and 12.

Journal of the ICRU Vol 13 No 1–2 (2013) Report 89
Oxford University Press
doi:10.1093/jicru/ndw005

2. Prevention, Diagnosis, Prognosis, Treatment, and Outcome

Cervical cancer is the third most common cause of female cancer mortality. Sexual transmission by human papillomavirus, preventable by vaccination, is responsible for virtually all cases of cervical cancer (Bosch *et al*., 2002). Screening has resulted in a dramatic decrease in mortality from cervical cancer in developed countries (Franco *et al*., 2001). The treatment of cervical cancer is multidisciplinary, based on tumor size and extension as well as nodal involvement.

2.1 Etiology and Screening

About 500 000 new cervical cancer cases occur worldwide each year, responsible for 274 000 deaths (Ferlay *et al.*, 2001). Cervical cancer represents the third most common cause of female cancer mortality (Ferlay *et al.*, 2001). The mortality is 10 times higher in developing countries, where approximately 80 % of the new cases occur (Parkin *et al*., 2005). An early age of first sexual intercourse as well as early pregnancies have been shown as risk factors for cervical cancer (Louie *et al*., 2009). High-risk persistent infection with sexually transmittable human papillomavirus is responsible for virtually all cases of cervical cancer (Bosch *et al*., 2002). HPV-16 and HPV-18 are the most prevalent of the oncogenic types. Human papillomavirus recombinant vaccines are now available and recommended for girls from 12 to 26 years of age and can decrease incidence by as much as 70 % (Cuzick, 2010). During the last half century, the widespread use of screening based on regular pap smears has dramatically changed the presentation of cervical cancer in the developed world, with non-invasive forms of cancer becoming pre-dominant (Franco *et al*., 2001). Therefore, despite the overall potential of vaccination, screening will keep its essential place in invasive-cancer prevention, perhaps combined with virus-based DNA testing (Cuzick, 2010; Cuzick *et al*., 2008).

2.2 Patterns of Spread

In general, more than 50 % of women are infected with the HPV virus, but only from 5 % to 20 % will develop cervical dysplasia (Ho *et al*., 1998). Cervical dysplasia usually represents the starting point of cancer. It generally takes from 10 years to 15 years to progress to invasive carcinoma. The cervical tumor can spread directly to the endo-cervix, the lower uterine segment, the vagina, and laterally to the parametrium (Inoue and Okumura, 1984). Extension to the bladder or the rectum is less frequent and happens at a later stage. The lymphatic involvement usually follows routes of drainage to the parametrial, obturator, internal, external, and common iliac lymph nodes. In some cases, however, rectal, pre-sacral, and para-aortic lymph nodes can also become involved (Benedetti-Panici *et al*., 1996; Henriksen, 1949). The frequency of nodal involvement is related to stage. The overall risk of pelvic lymph-node metastasis ranges from 15 % in Stage IB to about 50 % in Stage III (Touboul *et al.*, 2011). Hematogenous dissemination includes the lung, mediastinum, bone, and liver. The majority of the recurrences occur within 2 years after treatment (Takehara *et al*., 2001).

2.3 FIGO Staging and TNM Classification

Clinical examination, sometimes performed under general anesthesia, represents the basis for the most commonly used FIGO (Fédération Internationale de Gynécologie et d'Obstétrique) staging. It is based on clinically assessed tumor size, vaginal and/or parametrial involvement, and bladder/rectum tumor extension (see Table 2.1). The FIGO staging has recently been updated and now incorporates sub-divisions for IIA tumors, based on clinical tumor size, <4 or ≥ 4 cm (Pecorelli, 2009). The FIGO staging requires basic complementary examinations, including chest x ray and an intravenous pyelogram (IVP).

For TNM classification (Sobin *et al*., 2009), information from any imaging modality including volumetric imaging is used and includes the description of lymph-node involvement. Table 2.1 correlates the TNM classification with FIGO stage.

2.4 Tumor and Lymph-Node Imaging

FIGO staging is based on clinical examination, chest x ray, and IVP. This section describes the additional

Table 2.1. Cervical cancer staging systems (Compton *et al*., 2012).

TNM categories	FIGO stages	
Primary tumor (T)		
TX		Primary tumor cannot be accessed
T0		No evidence of primary tumor
Tis[a]		Carcinoma *in situ* (preinvasive carcinoma)
T1	I	Cervical carcinoma confined to uterus (extension to corpus should be disregarded)
T1a[b]	IA	Invasive carcinoma diagnosed only by microscopy. Stromal invasion with maximum depth of 5.0 mm measured from the base of the epithelium and a horizontal spread of 7.0 mm or less. Vascular space involvement, venous or lymphatic, does not affect classification
T1a1	IA1	Measured stromal invasion 3.0 mm or less in depth and 7.0 mm or less in horizontal spread
T1a2	IA2	Measured stromal invasion more than 3.0 mm and not more than 5.0 mm with a horizontal spread 7.0 mm or less
T1b	1B	Clinically visible lesion confined to the cervix or microscopic lesion greater than T1a/IA2
T1b1	IB1	Clinically visible lesion 4.0 cm or less in greatest dimension
T1b2	IB2	Clinically visible lesion more than 4.0 cm in greatest dimension
T2	II	Cervical carcinoma invades beyond the uterus but not to the pelvic wall or to lower third of the vagina
T2a	IIA	Tumor without parametrial invasion
T2a1	IIA1	Clinically visible lesion 4.0 cm or less in greatest dimension
T2a2	IIA2	Clinically visible lesion more than 4.0 cm in greatest dimension
T2b	IIB	Tumor with parametrial invasion
T3	III	Tumor extends to the pelvic wall and/or involves lower third of the vagina, and/or causes hydronephrosis or non-functioning kidney
T3a	IIIA	Tumor involves lower third of the vagina, no extension to the pelvic wall
T3b	IIIB	Tumor extends to the pelvic wall and/or cause hydronephrosis or non-functioning kidney
T4	IVA	Tumor invades mucosa of the bladder or rectum, and/or extends beyond true pelvis (bullous edema is not sufficient to classify a tumor as T4)
Regional lymph nodes (N)		
NX		Regional lymph nodes cannot be assessed
N0		No regional lymph-node metastasis
N1	IIIB	Regional lymph-node metastasis
Distant metastasis (M)		
MO		No distant metastasis
M1	IVB	Distant metastasis (including peritoneal spread, involvement of supraclavicular, mediastinal, or paraaortic lymph nodes, lung, liver, or bone)

[a]FIGO no longer includes Stage 0 (Tis).
[b]All macroscopically visible lesion, even with superficial invasion, are T1b/1B.

information gained from imaging, which is used in the TNM classification and in the planning of treatment, if available.

2.4.1 Tumor Assessment

Magnetic resonance imaging (MRI) is considered as the reference imaging examination and is regarded as superior to computed tomography (CT) scanning for tumor assessment and is equal or superior to CT scanning for nodal-involvement assessment (Bipat *et al*., 2003; 2011; Hricak *et al*., 2007; Trimble, 2009). Sensitivity for parametrial invasion is particularly high for MRI (75 % *versus* 55 % for CT), as is sensitivity for bladder and rectum invasion.

Post-therapeutic MRI is important as it provides relevant information for follow-up. In this situation, the reliability of MRI studies at 3 months after radiotherapy have been shown to be in the range of 80 % to 100 % with respect to pathological specimens (Hatano *et al.*, 1999; Vincens *et al*., 2008).

2.4.2 Nodal Assessments by Imaging

Nodal status is important as it represents one of the strongest prognostic factors in patients with cervical cancers. In early-stage disease, the 5-year world-average survival is from 90 % to 95 % in node-negative patients, 50 % in pelvic-node-positive patients, and from 20 % to 30 % in patients with positive para-aortic nodes (Fyles *et al*., 1995). The decision to extend radiation fields to include the para-aortic nodes depends on their involvement. For detecting disease in nodes smaller than 1 cm, CT and MRI have low sensitivities, ranging from 38 % to 89 %, and the specificity is within the range from 78 % to 99 % (Scheidler *et al*., 1997). PET-CT appears to be a reliable examination to assess nodal status, especially in advanced disease (Magne *et al*., 2008). In early-stage disease, however, it

is generally agreed that PET-CT is of limited value and cannot replace surgical exploration of pelvic lymph nodes (Bentivegna *et al*., 2010; Chou *et al*., 2006; Reinhardt *et al*., 2001; Roh *et al*., 2005; Sironi *et al*., 2006; Wright *et al*., 2005). In advanced disease, *i.e*., when FIGO stage is greater than or equal to IB2, PET-CT has the potential of showing lymph-node metastases within as well as outside the pelvis, particularly in the para-aortic area. PET-CT can show distant metastasis, not seen by the traditional examinations, *i.e*., chest and abdominal CT and MRI. Comparisons between PET and CT and/or MRI have shown PET sensitivity to be significantly higher than either MRI or CT (Rose *et al*., 1999; Sugawara *et al*., 1999). Positive and negative predictive values of PET/CT have been reported to be 54 % and 88 %, respectively, for microscopic lymph-node-metastases detection (Leblanc *et al*., 2011; Uzan *et al*., 2011). Some authors recommend a para-aortic lymph-node dissection prior to the beginning of concomitant radio-chemotherapy, in order to properly define the target volumes, as PET-CT would miss 8 % of patients with positive para-aortic lymph nodes (Leblanc *et al*., 2011; Uzan *et al*., 2011).

2.5 Invasive Lymph-Node Assessment

2.5.1 Extra-Peritoneal Laparoscopic Para-Aortic Node Staging

The indication for surgical nodal staging for locally advanced cervical cancer remains unclear. Laparoscopic node dissection appears to be safe and effective; an audit of early complications of laparoscopic node dissection in 1000 gynecologic cancer patients showed that 13 open surgeries were required as a result of failure to complete a satisfactory laparoscopic procedure (Querleu *et al*., 2006).

Some authors recommend a pretreatment extra-peritoneal laparoscopic para-aortic node staging and have shown a 24 % incidence of para-aortic nodal involvement and an operative complication rate of 2 % in patients with advanced disease and with positive pelvic and negative para-aortic nodes on PET-CT (Leblanc *et al*., 2007). The management of approximately 20 % of patients might therefore be modified through an extension of the target volumes to the para-aortic area (Leblanc *et al*., 2007). A survival advantage has been suggested in patients after removal of positive nodes (Leblanc *et al*., 2007).

2.5.2 Sentinel Lymph-Node Mapping in Early-Stage Cervical Cancer

Two methods are currently available to detect sentinel lymphatic nodes: one colorimetric with Iso-sulfan blue and a potentially superior one with technetium-99 (Lecuru *et al*., 2011). The laparoscopic approach combined with ^{99m}Tc for the identification and removal of the sentinel lymph nodes identified sentinel lymph node in sites other than expected in 16.7 % of patients with early-stage disease, including 3.8 % in the para-aortic area (Diaz *et al*., 2011; Lecuru *et al*., 2011; Roy *et al*., 2011). Pathologic staging seemed to be an important component in micro-metastasis detection (Diaz *et al*., 2011; Lecuru *et al*., 2011; Roy *et al*., 2011), with some authors concluding that sentinel lymph-node biopsy was a more sensitive procedure in detecting pelvic lymph-node metastases than a complete lymphadenectomy (Gortzak-Uzan *et al*., 2010).

2.5.3 Bulky Lymph Nodes

In patients with bulky lymph nodes in advanced cervical cancer, the role of surgical de-bulking remains unclear. An estimation of the number of patients who might benefit from this procedure showed that, based on published studies, 1 %, 2 %, and 4 % of patients in Stage IB, IIB, and IIIB, respectively, would benefit from a de-bulking procedure if focusing on the potential risk of isolated nodal recurrences (Kupets *et al*., 2002). Other authors estimated 43 patients out of 300 might have an overall benefit from surgical de-bulking (Tammela *et al*., 2004). It has also been shown that the removal of five or more pelvic and/or para-aortic lymph nodes was associated with significant improvement of overall survival (Marnitz *et al*., 2005). With the development of laparoscopic techniques, the resection of bulky lymph nodes ($>$2 cm) becomes possible with a low incidence of complications (9 %) (Tozzi *et al*., 2009).

2.6 Prognostic Factors

Prognostic factors include tumor size, stage, nodal involvement, lympho-vascular space involvement, and histological subtype (Barbera and Thomas, 2009; Delgado *et al*., 1990; Eifel *et al*., 1994a; Fyles *et al*., 1995; Morice *et al*., 2003; Perez *et al*., 1998; Van de Putte *et al*., 2005). Tumor size is a strong prognostic factor. In Stage IB treated with RT, the 10-year actuarial pelvic failure rate is 5 % for tumors smaller than 2 cm, 15 % for tumors from 2 cm to 5 cm, and 35 % for tumors larger than 5 cm (Perez *et al*., 1998). In patients with Stage I disease, a strong correlation has been shown between central- and pelvic-tumor control, disease-specific survival, and tumor size, pelvic-tumor control being from 95 % to 100 % in tumors smaller than 5 cm and from 75 % to 85 % in tumors from 5 cm to 8 cm (Eifel *et al*., 1994a). In patients with Stage IB treated surgically, margin status is significantly associated with an increased recurrence rate. In patients with postoperative positive margins, postoperative

radiotherapy significantly decreases the recurrence rate (Viswanathan *et al.*, 2006a). Even though the FIGO stage does not take into account nodal status, FIGO staging has been identified as a significant prognostic factor (Fyles *et al*., 1995; Stehman *et al*., 1991).

Nodal involvement represents the most significant negative prognostic factor in the majority of studies. In limited-stage disease (Stage I/II), reports indicate 5-year survival rates in excess of 90 % among treated patients with negative pelvic and para-aortic nodes, compared with patients with positive pelvic (from 50 % to 60 %) or para-aortic nodes (from 20 % to 45 %) (Delgado *et al*., 1990). Decreasing 5-year survival rates have been associated with increasing numbers of positive pelvic nodes.

Lympho-vascular space invasion is a significant prognostic factor, especially in early-stage cervical cancer, correlating with pelvic nodal involvement (Delgado *et al*., 1990; Milam *et al*., 2007).

Squamous-cell carcinoma accounts for from 80 % to 90 % of cervical cancers, adenocarcinoma for from 10 % to 20 % (Young and Clement, 2002). Adenocarcinoma has significantly lower survival rates with higher distant failure rates compared stage-by-stage (Baalbergen *et al*., 2004; Gien *et al*., 2010; Kleine *et al*., 1989).

Even though external-beam radiotherapy (EBRT) with concomitant chemotherapy has significantly improved tumor control (Green *et al*., 2001), local failure is still from 10 % to 15 % in early-stage disease (IB2/IIB) increasing to as much as 40 % in more advanced stages [IIB(distal)/IIIB/IVA], especially with topographically unfavorable disease location (such as distal parametrial or utero-sacral ligament involvement) with poor response to initial EBRT and chemotherapy (Barbera and Thomas, 2009). Local tumor control is important, as persistent local disease or local recurrence has a dismal prognosis that does not significantly benefit from salvage treatment (Barbera and Thomas, 2009).

2.7 Stage- and Risk-Adapted Multidisciplinary Treatment

The treatment of patients with cervical cancer is multidisciplinary, based on detailed information about tumor size, extension, and other important prognostic factors such as histology and nodal status. The following treatment outlines are meant to put the report into the perspective of present-day treatment philosophies (Haie-Meder *et al.*, 2010a), and not meant to be treatment recommendations.

2.7.1 FIGO Stage IA1

Standard treatment consists of conisation with free margins or simple hysterectomy (depending upon patient age) (Gadducci *et al*., 2003; Gray, 2008). In the case of lympho-vascular-space involvement, pelvic lymphadenectomy is recommended. In patients with at least two high-risk factors (deep stromal invasion, lympho-vascular-space involvement, large primary tumors), postoperative pelvic radiotherapy with or without concomitant chemotherapy should be considered. In patients with positive margins, parametrial involvement, or pelvic-node involvement, standard treatment consists of postoperative EBRT with concomitant chemotherapy and might be followed by vaginal brachytherapy.

2.7.2 FIGO Stage IA2

Surgery is the standard. Options consist of conisation or trachelectomy in young patients and simple or radical hysterectomy in other patients (Gadducci *et al*., 2003; Gray, 2008). If unexpectedly positive margins or parametrial involvement is seen at surgery, pelvic lymphadenectomy and postoperative EBRT with concomitant chemotherapy is performed and might be followed by vaginal brachytherapy.

2.7.3 FIGO Stage IB1

There is no general standard treatment (Landoni *et al*., 1997). Options consist of surgery, definitive EBRT plus brachytherapy, or combined brachytherapy and surgery plus EBRT in the case of positive nodes (Gerbaulet *et al*., 2002a).

Conservative treatment (radical trachelectomy) combined with pelvic lymphadenectomy can be proposed in young patients presenting with tumors of less than 20 mm in diameter, without lympho-vascular-space involvement or lymph-node involvement. A review of 548 patients treated with radical trachelectomy and lymphadenectomy reported a recurrence rate of about 5 %, in accordance with what has been reported with standard colpo-hysterectomies (Beiner and Covens, 2007). Successful pregnancies outcomes were reported to be within the range of from 41 % to 78 %.

Standard surgery consists of radical hysterectomy, bilateral oophorectomy, and pelvic lymphadenectomy, and is performed if nodes are negative (Gray, 2008). Patients with positive pelvic nodes at surgery, or positive surgical margins, or postoperative findings with disease within parametria or with lympho-vascular space involvement are considered at high risk of recurrence. For high-risk patients, standard treatment consists of complementary EBRT with concomitant chemotherapy followed by vaginal brachytherapy (Keys *et al*., 2003), but the risk of complications (mainly gastro-intestinal) can reach 17 % (Landoni *et al*., 1997). Therefore, EBRT techniques (including brachytherapy) have to be designed with special care, in order to minimize bowel irradiation. As the uterus

has been removed, the bowel might be partly fixed in the pelvis because of adhesions as a consequence of surgery and thus receive high doses.

In the case of nodal involvement detected at diagnosis, mainly on MRI or during laparoscopic lymph-node assessment (prior to tumor resection), definitive EBRT with concomitant chemotherapy followed by brachytherapy are recommended to avoid the more severe morbidity if radical surgery has to be followed by postoperative radiation therapy (Landoni *et al*., 1997).

Preoperative brachytherapy followed 6 weeks to 8 weeks later by hysterectomy, bilateral oophorectomy, and pelvic-node dissection represents another therapeutic option (Gerbaulet *et al*., 1992; Haie-Meder *et al*., 2009).

2.7.4 FIGO Stage IB2–IVA

EBRT with concomitant chemotherapy followed by brachytherapy represents the standard (Green *et al*., 2001; Lukka *et al*., 2002; Vale *et al*., 2008) and is superior to EBRT alone and brachytherapy for local control, freedom from metastasis, and disease-free and overall survival. A meta-analysis based on 18 trials with individual patient data on 3452 patients showed that cisplatin-based chemotherapy was used in 85 % of the patients, although non-platinum-based regimens for radio-chemotherapy appear to be equally effective (Vale *et al*., 2008). The results demonstrated a 6 % improvement in absolute 5-year survival (from 60 % to 66 %) and an 8 % improvement in 5-year disease-free survival (DFS) with EBRT with concomitant chemotherapy compared with EBRT without concomitant chemotherapy. A larger benefit was seen in two trials with additional chemotherapy after EBRT with concomitant chemotherapy and brachytherapy with an absolute improvement of 19 % at 5 years (Duenas-Gonzalez *et al*., 2003). Patients with advanced-stage IB2-IIA/B can benefit more from EBRT with concomitant chemotherapy than those with Stage III and IVA, translating to a 5-year survival benefit of 10 % for women with Stage IB–IIA, 7 % for women with Stage IIB, and 3 % for women with Stage IIIB–IVA. The most common regimen is cisplatin mono-therapy, 40 mg/m^2, on a weekly schedule. EBRT with concomitant chemotherapy increases acute toxicity, particularly for gastrointestinal and hematological side effects. Late effects of this combined treatment have not been extensively reported in the literature.

The role of adjuvant chemotherapy after EBRT with concomitant chemotherapy followed by brachytherapy remains unclear. One randomized study has recently shown the benefit of adjuvant chemotherapy with cisplatin–gemcitabine after EBRT with concomitant chemotherapy followed by brachytherapy, but with a significant increase in complications (Duenas-Gonzalez *et al*., 2011). Adjuvant chemotherapy represents a challenging issue, especially in patients with Stage IB2–IIB for which the main cause of failure is distant metastases. A study comparing standard therapy with EBRT with concomitant cisplatin followed by brachytherapy and the same treatment followed by four courses of adjuvant treatment consisting of carboplatin and paclitaxel (Outback trial) is currently under investigation by the International Gynecologic Cancer Intergroup (NCI, 2015).

The radiation therapy of advanced cervical cancer is based on a combination of EBRT and brachytherapy, and the total treatment duration should remain less than 55 days (Girinsky *et al*., 1993; Perez *et al*., 1995). Complementary extra-fascial hysterectomy after radiotherapy (Keys *et al*., 2003) showed no additional survival benefit, but a potential benefit for patients with persistent disease. This complementary surgery can therefore be considered as an option for patients with persistent disease after EBRT with concomitant chemotherapy and brachytherapy.

Neo-adjuvant chemotherapy remains controversial and is currently under investigation by the EORTC (trial number 55994) and the MRC (Interlace Trial). A systematic meta-analysis has demonstrated the superiority of neo-adjuvant chemotherapy followed by surgery over EBRT and brachytherapy (without concomitant chemotherapy) in terms of overall survival (NCLACCMAC, 2003). In spite of these results, neo-adjuvant chemotherapy has not been considered as a standard for two reasons: one is the inferiority of the control arm (EBRT alone and brachytherapy) compared with the present standard of EBRT with concomitant chemotherapy followed by brachytherapy, and second is the results of the GOG 141 study, showing no advantage of neo-adjuvant chemotherapy with vincristine and cisplatin prior to radical hysterectomy and pelvic/para-aortic lymphadenectomy in bulky Stage IB (Eddy *et al*., 2007).

2.8 Radiation Therapy

In advanced cervical cancer, EBRT and concomitant chemotherapy is applied with brachytherapy in various combinations (total absorbed dose $\geq$85 Gy historically to Point A and more recently to the high-risk CTV (EQD2 dose, see examples in Appendix). Most commonly, the EBRT fields are designed with the use of CT-based planning. The EBRT radiation fields encompass the primary disease, originating from the cervix and the potential areas of tumor

spread into the uterus, the parametria and the vagina, and the internal, external, and common iliac nodes [see, *e.g.*, RTOG recommendations for IMRT (Lim *et al.*, 2011)]. The pelvis is generally treated with from 1.8 Gy/day to 2.0 Gy/day to a total absorbed dose of from 45 Gy to 50 Gy with high-energy photon beams ($\geq$10 MV).

Para-aortic nodes can be included in the target volumes if indicated. In patients with involvement of the lower third of the vagina, EBRT fields are extended to the inguinal lymph nodes because of the risk of metastases linked to the drainage of the lower part of the vagina.

Midline shielding blocks (generally 4 cm wide) have been used during EBRT, especially in early stage disease. Applied after from 20 Gy to 30 Gy of external-beam therapy, the aim is to shield the central part of the fields to maintain bladder and rectal absorbed doses at a low level so as to allow a higher absorbed dose to be delivered with brachytherapy. No real consensus, however, has been reported regarding their use.

In the case of parametrial disease or positive nodes, a boost can be delivered by EBRT to a total absorbed dose ranging from 50 Gy to 65 Gy, including the absorbed dose given by brachytherapy. To achieve this goal, midline blocks have been used for central shielding. Recent data, however, have shown that this technique did not predictably protect organs at risk and did not significantly improve the absorbed-dose coverage of the high-risk clinical target volume (Fenkell *et al.*, 2011).

Intensity-modulated radiation therapy (IMRT) in conjunction with brachytherapy is currently under investigation. The potential benefits of IMRT treatment include a decrease in toxicity, with more conformal absorbed-dose distributions (Ahmed *et al.*, 2004; Brixey *et al.*, 2002; Chen *et al.*, 2011; Heron *et al.*, 2003; Portelance *et al.*, 2001).

Brachytherapy represents a crucial part of the treatment, especially in advanced cervical cancers, as high absorbed doses can be delivered to the tumor while sparing the bladder, the rectum, and the sigmoid because of the rapid absorbed-dose fall-off. The choice of brachytherapy approach, LDR, PDR, or HDR, is usually driven by institutional traditions. Various techniques and applicators are available (see Sections 3.4 and 3.6). Image-based adaptive brachytherapy seems to improve local control, achieving local control rates at 3 years above 90 % even in advanced disease (Castelnau-Marchand *et al.*, 2015; Chargari *et al.*, 2009; Gill *et al.*, 2015; Lindegaard *et al.*, 2013; Nomden *et al.*, 2013b; Pötter *et al.*, 2007; 2011; Rijkmans *et al.*, 2014; Sturdza *et al.*, 2016).

2.9 Treatment Results

2.9.1 Stage IA

In the vast majority of cases, patients are treated with surgery alone, with a 5-year DFS of from 96 % to 100 % (Gadducci *et al.*, 2003). In Stage IA2 with positive lymph nodes, EBRT with concomitant chemotherapy is the standard treatment with a 5-year DFS of from 70 % to 90 % (Gray, 2008; Haie-Meder *et al.*, 2010a).

2.9.2 Stages IB1 and Limited IIA

Treatment options consist of radical surgery or EBRT alone (without concomitant chemotherapy) followed by brachytherapy or combined treatment using brachytherapy and surgery (see Section 2.7.3). Randomized studies have shown comparable outcomes with the two modalities (Landoni *et al.*, 1997; Newton, 1975). Five-year DFS rates are in the range of 73 % to 84 %. If surgery demonstrates positive pelvic nodes or positive margins, EBRT with concomitant chemotherapy followed by vaginal brachytherapy is necessary for these high-risk patients and leads to an 80 % 4-year DFS, but can result in significant toxicity requiring medical or surgical intervention in 22 % of the patients. The toxicity is mainly of hematologic origin, but severe gastrointestinal morbidity is observed in 38 % of the patients (Peters *et al.*, 2000) (see also Section 2.7.3 for IB1). EBRT alone in this patient population leads to a 75 % 5-year DFS, however with less morbidity (Landoni *et al.*, 1997). Another option is preoperative brachytherapy followed by colpo-hysterectomy, with a 4-year DFS of 86 % (Gerbaulet *et al.*, 1992; Haie-Meder *et al.*, 2009). In Stage IB1 and limited IIA, whatever the treatment approach, lymph-node metastasis is the major prognostic factor, with a 5-year DFS of 50 % compared with from 85 % to 90 % in node-negative patients (Gerbaulet *et al.*, 1992; Haie-Meder *et al.*, 2009).

2.9.3 Stage IB2, Extensive IIA, IIB, III, and IVA

EBRT with concomitant chemotherapy followed by brachytherapy is the standard treatment for all these stages (see Section 2.7.4).

In Stage IB2–IIA, studies have shown a dose–effect relationship, with pelvic recurrences reaching 33 % when patients received less than 60 Gy of intracavitary treatment to Point A (Eifel *et al.*, 1994b; Kim *et al.*, 1999; Paley *et al.*, 2000). Tumor diameter is a highly significant prognostic factor; local tumor control generally correlated with regression after EBRT and brachytherapy. In patients with complementary extra-fascial hysterectomy, residual

disease was generally present in 50 % to 60 % of the hysterectomy specimens, and tumor sterilization correlated significantly with the mean absorbed dose to Point A (Paley *et al*., 2000; Perez *et al*., 1998). The DFS was significantly higher in patients with negative specimens, but overall the addition of hysterectomy to EBRT and brachytherapy did not significantly affect survival.

The majority of patients with Stage IIB tumors are now treated with EBRT with concomitant chemotherapy and brachytherapy, with a 5-year survival rate of 60 % to 65 % (Green *et al*., 2001). Concurrent platinum-based chemotherapy reduces the risk of pelvic recurrence by approximately 50 % and extends overall survival by an absolute 5 %–20 % when compared with EBRT alone and brachytherapy (Green *et al*., 2001). The pelvic-failure rate ranges from 18 % to 39 %. A correlation was also reported in Stage IIB for Point A dose and incidence of pelvic failures (Kim *et al*., 1999).

In Stage IIIB carcinoma, the 5-year survival rates range from 25 % to 50 %, and pelvic failure rates from 38 % to 50 % after EBRT alone and brachytherapy (Horiot *et al*., 1988; Montana *et al*., 1986). These patients with very advanced cervical cancers (Stage III and IV) seem to benefit less than patients with Stage IB2–IIB from concomitant chemotherapy (Green *et al*., 2001). A more frequent systematic use of brachytherapy has been shown to correlate with a significant increase in both local control and 5-year survival (Komaki *et al*., 1995).

In patients with Stage IVA disease, the 5-year survival rates range from 20 % to 35 %, and pelvic failures from 60 % to 80 % after EBRT and brachytherapy, even when combined with chemotherapy (Rose *et al*., 2011). In this patient population with large disease, pelvic local control remains the major issue (Rose *et al*., 2011). The development of new interstitial brachytherapy techniques applying image-guided adaptive brachytherapy with a total radiation dose $\geq$85 Gy (EQD2) aims at improving local control in these advanced stages (Dimopoulos *et al*., 2006a; Kirisits *et al*., 2006; Nomden *et al*., 2012; Syed *et al*., 2002).

2.10 Conclusion

Early-stage cervical cancer is a highly curable disease. EBRT with concomitant chemotherapy followed by brachytherapy has significantly improved the prognosis of patients with advanced disease, especially in Stages IB2–IIA and IIB. Local control remains the major issue in Stage IIB, with distal involvement of the parametrium and IIIB–IVA. At present, image-guided adaptive brachytherapy represents the major therapeutic option to improve local control, disease-free and overall survival (Castelnau-Marchand *et al*., 2015; Chargari *et al*., 2009; Gill *et al*., 2015; Lindegaard *et al*., 2013; Nomden *et al*., 2013b; Pötter *et al*., 2007; 2009; 2011; Rijkmans *et al*., 2014; Sturdza *et al*., 2016).

2.11 Summary

"Cervical cancer" is the third most common cause of female cancer mortality. Sexually transmittable human papillomavirus is responsible for the vast majority of cervical cancer cases, which hence may be prevented by vaccination. Screening has resulted in a dramatic decrease in mortality from cervical cancer in developed countries.

"Diagnosis" includes beside gynecologic examination imaging by CT, MRI (reference examination for local tumor extension) and PET-CT (nodal assessment in advanced stages, limited sensitivity). The most accurate lymph node diagnosis is by pathohistological examination after laparoscopic sampling. The "classification" of FIGO (Fédération Internationale de Gynécologie et d'Obstétrique) is most widely used. The frequency of nodal involvement is related to stage.

"Prognostic factors" include tumor size, stage, nodal involvement, lympho-vascular space involvement, and histological subtype.

The "treatment" of cervical cancer is multidisciplinary, based on tumor size and extension. In low stages (FIGO IA), surgery, conisation, trachelectomy, or simple hysterectomy are applied, with 5-year DFS rates of from 96 % to 100 %. In Sage IB1, there is no standard treatment with options for surgery or definitive radiotherapy or combined brachytherapy and surgery. In higher stages (IB2–IVA), concomitant radio-chemotherapy represents the standard, with a 6 % improvement in absolute 5-year survival (60 % to 66 %). Five-year survival and pelvic failure rates decrease with stage. Loco-regional failure remains essential, in particular in advanced Stage II, III, and IVA. The benefit from radio-chemotherapy may be more pronounced for patients with advanced Stage IB2–IIA/B compared with III–IVA. The most common regimen is cisplatin mono-therapy 40 mg/m^2 on a weekly schedule. The role of adjuvant chemotherapy after concomitant radio-chemotherapy remains unclear.

External-beam irradiation is usually combined with brachytherapy, except for very early stages. The overall treatment time should be less than 55 days. The lymph-node target is treated at from 1.8 Gy/day to 2.0 Gy/day to a total absorbed dose of from 45 Gy to 50 Gy with high-energy photon beams (10 MV or higher) and a lymph-node boost in the case of involvement. Brachytherapy is performed with total absorbed doses between 20 Gy and 50 Gy.

The radiation dose correlates with local control and survival.

2.12 Key Messages

- Cervical cancer is the third most common cause of female cancer mortality.
- FIGO staging is the most widely used staging system, which has recently been updated (IIA1 and IIA2). For FIGO staging, clinical examination, chest x ray, and IVP are used. The TNM classification is based on all available clinical and imaging information to be used for actual treatment decisions.
- Lymph-node involvement is related to stage, with from 15 % to 20 % in Stage IB, 30 % in Stage IIB, and more than from 40 % to 50 % in Stage III.
- MRI is regarded as the gold standard for tumor assessment.
- PET-CT is the best available non-invasive examination to assess nodal and distant disease, however with low sensitivity for lymph nodes.
- Prognostic factors include tumor size, stage, nodal involvement, lympho-vascular space involvement, and histological subtype.
- Local failure is about from 10 % to 15 % in Stage IB2/IIB proximal disease and ~40 % in Stage IIB distal disease/IIIB/IVA.
- Lymph-node involvement represents the most significant negative prognostic factor, with 5-year survival rates of 90 % in patients with negative pelvic and para-aortic nodes, compared with from 50 % to 60 % in those with pelvic nodes, and from 20 % to 45 % in para-aortic positive nodes.
- In advanced cervix cancer (IB1-IVA), external beam radiotherapy is combined with brachytherapy aiming at a high total dose, $\geq$75–85 Gy (EQD2) to the CTV_{HR} in the tumor-bearing area, dependent on stage of disease.
- EQD2 doses for EBRT are between 44 Gy and 65 Gy (including lymph-node boost) and for brachytherapy between 20 Gy and 50 Gy (EQD2) for Point A or for the CTV_{HR} (image-guided brachytherapy).
- Radiation dose correlates with local control.
- Overall radiotherapy treatment time should be within 55 days.
- Image-guided adaptive brachytherapy for cervix cancer, applying high radiation doses of $\geq$85 Gy (EQD2), reaches $\geq$90 % local control at 3 years in Stage I/II and about 85 % in Stage III/IV.
- Intensity-modulated radiotherapy in conjunction with brachytherapy for cervical cancer is considered to decrease radiation-associated morbidity and is currently under investigation.

Journal of the ICRU Vol 13 No 1–2 (2013) Report 89
Oxford University Press
doi:10.1093/jicru/ndw008

3. Brachytherapy Techniques and Systems

3.1 The Evolution of Brachytherapy Systems, Techniques, and Absorbed-Dose Rates Applied to Cervical Cancer

When curative treatment is planned, patients with cervical carcinoma treated with radiation should receive brachytherapy. Overall, excellent clinical outcomes have been reported when systematically applying brachytherapy in the definitive management of cervical cancer. Brachytherapy can be used alone in early disease or combined with external-beam irradiation and chemotherapy in more advanced disease. The therapeutic benefit of brachytherapy, if used in addition to external-beam therapy, consists of both a decrease in disease recurrence and treatment-related complications as revealed in the Patterns of Care Studies (PCS) and several major retrospective series (Coia *et al*., 1990; Han *et al*., 2013; Lanciano *et al*., 1991; Logsdon and Eifel, 1999; Perez *et al*., 1983; Tanderup *et al*., 2014). Multivariate analysis indicated that use of an intracavitary implant was the single most important prognostic factor for Stage IIIB cervical cancer with respect to survival and pelvic control in the 1973 and 1978 PCS studies (Lanciano *et al*., 1991). Retrospective series with external beam alone have demonstrated limited benefit (Barraclough *et al*., 2008; Saibishkumar *et al*., 2006), even when applying modern techniques such as IMRT (Han *et al*., 2013; Tanderup *et al*., 2014). The efficacy of brachytherapy is attributable to the inherent physical and biological characteristics that enable the delivery of a well focused and high levels of absorbed dose to the tumor, which contributes to high local control and survival. At the same time, because of rapid absorbed-dose fall-off in all directions from the applicator, surrounding normal tissues, such as the bladder and recto-sigmoid, are relatively spared, making brachytherapy-associated morbidity low. In extensive disease, external-beam irradiation, combined with simultaneous chemotherapy, brings about tumor regression in cervical and vaginal cancers, so that the residual tumor tissue can often be brought within the range of the pear or cylindrical-shaped absorbed-dose distribution around standard utero-vaginal applicators (Erickson and Gillin, 1997).

There are different types of brachytherapy applications used in the treatment of gynecologic cancers. Temporary intracavitary implants are the most common, with interstitial implants less frequently employed. For intracavitary brachytherapy, radioactive sources are placed into the vagina or uterus, using special commercially available applicators, such as a uterine tandem combined with a vaginal cylinder, ovoids, or a ring. With interstitial brachytherapy, the radioactive sources are transiently inserted into tumor-bearing tissues through placement of hollow needles or tubes (Erickson and Gillin, 1997). The most common radioactive sources in use for gynecologic brachytherapy have been ^{226}Ra, ^{137}Cs, and ^{192}Ir.

Absorbed-dose rate also affects the impact of radiation on tumor and normal tissues (see Section 7). Low-dose-rate (LDR) irradiation has been used for decades in gynecologic cancers using ^{226}Ra and, more recently, ^{137}Cs sources for intracavitary insertions, and low-activity ^{192}Ir sources for interstitial insertions. ICRU Report 38 (ICRU, 1985) defined the absorbed-dose rates used in brachytherapy as LDR (0.4 Gy h^{-1} to 2 Gy h^{-1}), medium dose rate (MDR: 2 Gy h^{-1} to 12 Gy h^{-1}), and high dose rate (HDR: $>$12 Gy h^{-1}). However, recent clinical experience indicates that more pronounced differences are observed when moving from standard LDR treatments at absorbed-dose rates of from 0.4 Gy h^{-1} to 0.8 Gy h^{-1} using ^{226}Ra or ^{137}Cs tube-type sources to treatments using ^{137}Cs pellets delivering absorbed-dose rates of 1.0 Gy h^{-1} to 1.4 Gy h^{-1} (Guerrero and Li, 2006; Leborgne *et al*., 1996; 1999; Patel *et al*., 1998; Roberts *et al*., 2004) (see Sections 7.3 and 7.6.2). These clinical findings demonstrate the need for reconsideration of these classifications, in particular low and medium dose rates. New recommendations are provided in this report (see Sections 7.3.1 and 7.3.2). High-dose-rate brachytherapy ($>$12 Gy h^{-1}) has gradually been introduced over the last decades and might become the predominant form of future gynecologic brachytherapy. Pulsed-dose radiotherapy (PDR) (with, for example, hourly intervals between pulses) is becoming more popular, particularly with the scarcity of new ^{137}Cs sources. Pulsed-dose radiotherapy

is capable of applying variable absorbed doses per pulse (*e.g.*, 0.5 Gy to 2 Gy). The effects of PDR are assumed to be comparable to LDR brachytherapy (Swift *et al.*, 1997) (see Section 7).

Essentially, all modern brachytherapy exploits afterloading techniques (Henschke *et al.*, 1963). An appropriate application is established with the unloaded applicator in place in the desired location. The sources are loaded after treatment–planning images have been obtained and the patient has returned to their hospital room or brachytherapy suite. With afterloading, radiation exposure to medical personnel is reduced. Remote afterloading, which eliminates most personnel exposure, entails the use of a computer-driven afterloader to insert and retract a source or sources, from the applicator. Sources are retracted automatically whenever visitors or hospital personnel enter the room. With most modern remote afterloading techniques, a single cable-driven radioactive source is propelled through an array of dwell positions in needles, plastic tubes, or intracavitary applicators. The source stops for a specified duration at a preselected number of locations delivering a specified absorbed dose to a defined volume of tissue. This pattern of absorbed-dose delivery is planned in advance in a computerized dose-planning system, using pretreatment radiographs or volumetric imaging with the applicator in place. Typically, these treatment units are housed in shielded rooms to reduce radiation exposure in the hospital surroundings.

These technical developments have dramatically changed cervical cancer brachytherapy, but were only partially taken into consideration in ICRU Report 38 (ICRU, 1985). In the following review, historical and contemporary techniques will be systematically outlined, providing a foundation for applicator design, loading patterns, and absorbed-dose specification with which to understand the current recommendations in this report. Possibilities for future developments will also be suggested.

3.2 Historical Radium Systems

Intracavitary brachytherapy for cervical carcinoma was profoundly impacted by the development of various "systems" that attempted to combine empirical, systematic, and scientific approaches.

A brachytherapy dosimetric system refers to a comprehensive set of rules involving a specific applicator type and radioactive isotope with a defined distribution of sources in the applicator, resulting in a defined absorbed-dose distribution in a defined target (Stitt *et al.*, 1992). Specification of treatment in terms of absorbed dose at various points and duration is necessary. This systematic approach was necessary and particularly useful at a time when absorbed-dose computation for the individual patient was limited.

The three basic systems developed during the first half of the last century were: the Stockholm system (Kottmeier, 1964), the Paris method (Lamarque and Coliez, 1951), and the Manchester system (Paterson, 1948). A combination of the Paris method and the Manchester system evolved as the MD Anderson system (Fletcher *et al.*, 1953).

3.2.1 The Stockholm System

The Stockholm system began in 1910 and has been modified over the years (Björkholm, 1997; Heyman, 1935; 1947; Walstam, 1954). This system entailed delivery of three "heavy doses," each lasting approximately 20 h to 30 h, separated by 1 to 2 weeks. The use of larger amounts of radium decreased application times from 18 h to 10 h. The uterus contained from 30 mg to 90 mg of radium and the vaginal applicators (cylinders or boxes) from 60 mg to 80 mg (see Figure 3.1). The vaginal and uterine applicators were not joined but held in their appropriate positions by careful gauze packing. There was a large selection of applicators (tandems, plates, cylinders) to meet the need for individualized treatments. There was limited use of external-beam radiotherapy.

3.2.2 The Paris Method

The Paris method (see Figure 3.2) was developed at the Institute of Radium of Paris from 1919 onwards under Regaud, Lacassagne, and associates, and was first described in 1927 (Lenz, 1927; Pohle, 1950). It prescribed a fixed product of source mass and duration (in units of mg h) for a given tumor volume based on the premise that—for any given geometric arrangement of specified sources—absorbed dose at any point is directly proportional to the product of source strength and implant duration. Regaud believed that better results were obtained with small amounts of radium acting over a long time (see Figure 3.2) because more cells would be irradiated during mitosis (Pohle, 1950). The sources were left in place for a minimum of 120 h to deliver from 7200 mg h to 8000 mg h, with the source activity equally divided between the uterus and vagina with 3600 mg h to 4000 mg h each. Brachytherapy was combined in later years with external-beam orthovoltage therapy given before the implant.

3.2.3 The Manchester System

The Manchester system described in 1938 by Tod and Meredith (Meredith, 1950; Sandler, 1942; Tod, 1941; 1947; Tod and Meredith, 1938), and later modified in 1953 (Tod and Meredith, 1953) at the Holt

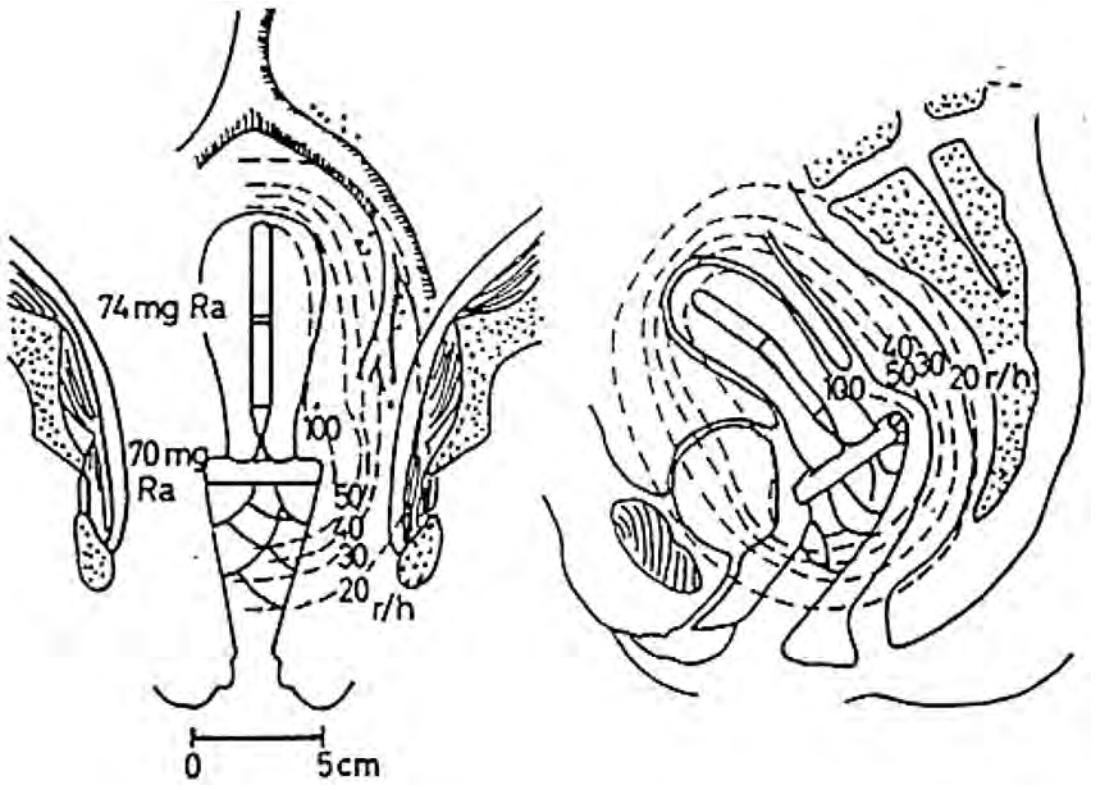

Figure 3.1. The Stockholm system. Typical treatment of a cervix carcinoma with a radium application (uterus normal in size and shape). The total amount of radium is 74 mg + 70 mg = 144 mg of radium. The exposure rates (roentgen per hour) are shown in the frontal and sagittal plane. An amount of 144 mg of radium (1 mm Pt filtration) delivers a total reference air-kerma rate of 964 μGy h^{-1}. After 3 applications of 27 h each, the TRAK would be 78 mGy and a source-mass $\times$ duration of 11.664 mg h (Walstam, 1954) (from ICRU 1985). The relationship between exposure, absorbed dose, and air kerma is described in Section 11.

Radium Institute, had its origin in the Paris method. Initiated in 1932, the Manchester system standardized treatment with predetermined absorbed doses and absorbed-dose rates directed to fixed points in the pelvis in an attempt to reduce the empiricism of the day and the existing high rate of complications. It also developed out of a perceived need to specify intracavitary therapy in terms of the absorbed dose and not in terms of the product of source mass and duration. The paracervical triangle was described as a pyramidal-shaped area with its base resting on the lateral vaginal fornices and its apex curving around with the anteverted uterus. Point A was defined as 2 cm lateral to the central canal of the uterus and 2 cm from the mucous membrane of the lateral fornix in the axis of the uterus. It was thought to correlate anatomically with the point where the ureter and uterine artery cross and was taken as a point from which to assess absorbed dose in the para-cervical region (see also Section 10.1.1). Point B was located 5 cm from midline at the level of Point A and was thought to correspond to the location of the obturator lymph nodes. The fixed Points A and B were selected on the assumption that the absorbed dose in the para-cervical triangle, and not the actual absorbed dose to the bladder, rectum, or vagina, determined normal tissue tolerance (Tod and Meredith, 1938). To achieve consistent absorbed-dose rates at Point A, a set of strict rules dictating the position and activity of radium sources in the uterine and vaginal applicators was devised. The amount of radium varied based on ovoid size and uterine length, such that the same exposure (in roentgens) would be delivered to Point A and the ovoid surface regardless of the size of the patient or the size and shape of the tumor, uterus, and vagina. To provide a uniform absorbed dose at the surface, the amount of radium per ovoid varies by ovoid size. It was recommended to use the largest size ovoid possible and place the ovoids as far laterally as possible in the fornices to carry the radium closer to Point B and increase the depth dose. Vaginal packing was used to limit the absorbed dose to the bladder and rectum to <80 % of the absorbed dose at Point A (see Figure 3.3). Two intracavitary applications of 72 h with a 4–7 day interval between them were given to deliver an exposure of 8000 R[1] at 55.5 R h^{-1} to Point A and 3000 R to Point B. Antero-posterior

[1]Exposure used in the Manchester system corresponds roughly to 9.4 mGy/R.

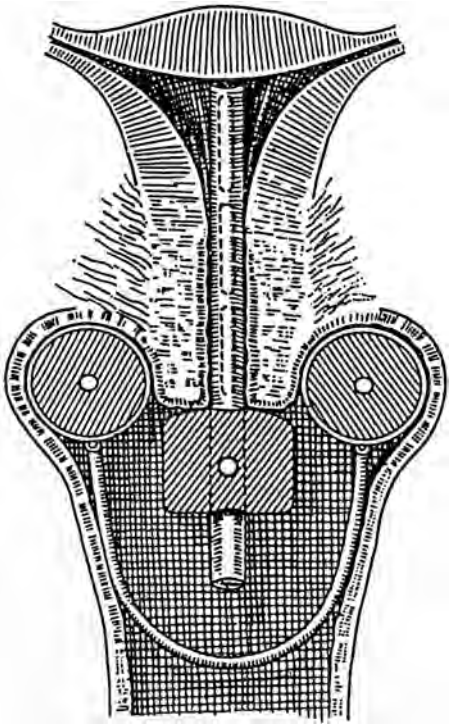

Figure 3.2. Schematic representation of the "historical" Paris method. Assuming three intra-uterine sources of 10 mg radium each and 3 intra-vaginal sources of 10 mg each, the total activity of 60 mg (1 mm Pt filtration) would deliver a TRAK rate of 402 μGy h^{-1}. After an application of 6 days (144 h), the TRAK would be 57.9 mGy and a source-mass × duration of 8.640 mg h (ICRU, 1985; Pierquin 1964).

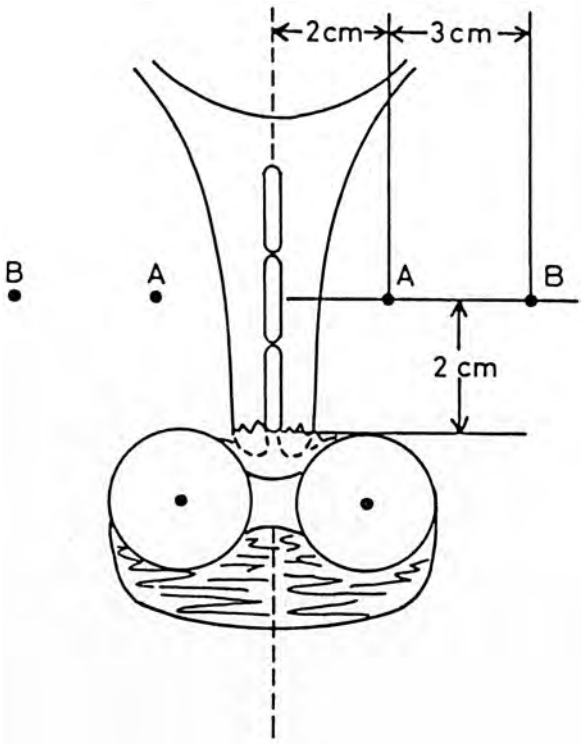

Figure 3.3. The Manchester system. Assuming three intra-uterine sources of 15 mg, 10 mg , 10 mg radium each and 20 mg for each intra-vaginal ovoid, the total activity of 75 mg (1 mm Pt filtration) would deliver a TRAK rate of 469 μGy h^{-1}. After an application of 6 days (144 h), the TRAK would be 67.5 mGy and a source-mass × duration of 10.800 mg h (ICRU, 1985; Meredith, 1967).

and lateral radiographs were taken to verify appropriate applicator position and the applicators were adjusted if needed. However, dosimetry was not based on these radiographs. Ideal geometry was assumed and the absorbed dose at any point in the geometrical framework was calculated by using the Sievert formula based on theoretical arrangements of radium sources and their relationship with pelvic organs (Sievert, 1921). External-beam irradiation with a midline block in place was later used to deliver a total cumulative exposure of 6000 R to Point B. This system was a significant advancement over the source-mass × duration systems as it was realized that variations in applicator dimensions and source configurations could lead to different absorbed doses for the same source-mass × duration. This system underlies many contemporary intracavitary application and dose-specification techniques.

3.2.4 The Fletcher (M.D. Anderson) System

The Fletcher system was established at M.D. Anderson Hospital in the 1940s (Fletcher *et al*., 1952; Lederman and Lamerton, 1948). The Fletcher applicator was subsequently developed in 1953 (Fletcher *et al*., 1953). The initial dosimetric work at M.D. Anderson in the early 1950s was done prior to the development of computerized dosimetry, which became available in the 1960s (Adams and Meurk, 1964; Batten, 1968; Shalek and Stovall, 1968). As in the Paris method, source-mass × duration was used for prescription under the premise that with any geometric arrangement of specified sources, absorbed dose at any point is proportional to the amount of radioactivity and the implant duration. Though previous systems (Paris and Stockholm) had used source-mass × duration and clinical experience to determine the tolerance of tissues, Fletcher believed that better results and less morbidity would ensue if knowledge of the absorbed dose at various points in the pelvis such as the bladder, rectum, and pelvic lymph nodes could be determined. According to Fletcher, a brachytherapy procedure should: (1) ensure that the primary disease in the cervix and fornices and immediate extensions into the para-cervical triangle are adequately treated; (2) ensure that the bladder and rectum are not overdosed (respect mucosal tolerance); (3) determine the absorbed dose received by the various lymph-node groups. External-beam radiotherapy was also used and integrated into the treatment regime.

The decision as to what absorbed dose to give to the primary tumor in the Fletcher system was based initially on tumor volume. Prescription rules were based on maximum time primarily and also maximum source-mass × duration, effectively limiting total absorbed dose and absorbed-dose rate, while taking into account the total external-beam-therapy absorbed dose and the calculated sigmoid absorbed dose. An application was left in place until either of these two maxima was reached while taking into consideration absorbed doses to the rectum, bladder, or vagina, which were considered a tolerance absorbed dose. Large implants were more likely halted by the source-mass × duration prescription while smaller implants were terminated by time (Potish and Gerbi, 1986). A set of tables of maximum source-mass × duration was established for varying tumor volumes and absorbed doses from external beam (Fletcher, 1971). Standardized source arrangements, limits on the vaginal surface absorbed dose, and source-mass × duration were all used to help define treatment (see Figure 3.4).

Despite a more elaborate dosimetry system, the Fletcher system combined many elements of the Paris method and the Manchester system. Some of the same concepts regarding applicator position and loading were re-emphasized by Fletcher. It was recommended to use the largest ovoid diameter that would fit into the vaginal fornices without downward displacement, positioned as far laterally and cranially as possible to give the highest tumor absorbed dose at depth for a given mucosal absorbed dose (as in the Manchester system). By using a larger ovoid, there was a better ratio between the mucosal absorbed dose and the more lateral parametrial/paravaginal absorbed dose (Fletcher *et al*., 1952).

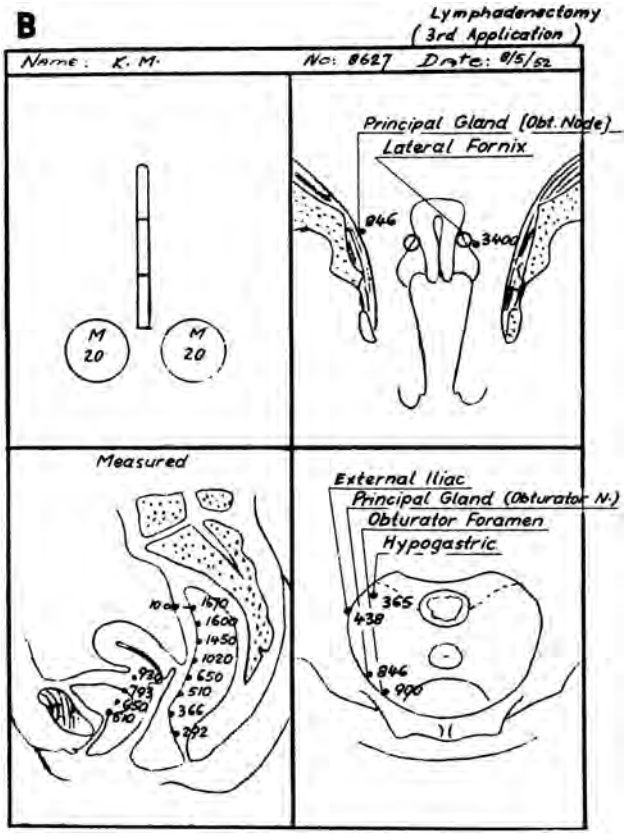

Figure 3.4. The Fletcher (MD Anderson) system (Fletcher, 1980; Fletcher *et al*., 1953).

Unlike prior systems, Fletcher was specific about the position of the tandem and colpostats and their relationship to each other. It was recommended to keep the tandem in mid-plane in the pelvis, equidistant from the sacral promontory and pubis and the lateral pelvic walls to avoid over-dosage to the bladder, sigmoid, or one ureter. The tandem was recommended to bisect the colpostats on the AP films and bisect their height on the lateral films (Fletcher, 1980). The flange of the tandem was to be flush against the cervix and the colpostats surrounding it. This was to be verified by confirming the proximity of the applicators to radio-opaque cervical seeds. Radio-opaque vaginal packing was used to hold the system in place and displace the bladder and rectum. With the use of two or more implants, there was tumor regression from the first implant, which was evident at the second implant, resulting in more optimal absorbed-dose coverage of the remaining tumor volume than achieved at the time of the first implant.

Assuming three intra-uterine sources of 10 mg, 10 mg, 15 mg radium and 20 mg for each intravaginal colpostat, the total activity of 75 mg (1 mm Pt filtration) would deliver a total reference air-kerma rate of 469 μGy h^{-1}. After an application of 6 days (144 h), the total reference air kerma (TRAK) would be 67.5 mGy and a source-mass × duration of 10.800 mg h.

3.3 From Radium to Man-Made Radionuclides

Because of the inherent radiation safety risk, ^{226}Ra has been progressively abandoned and is forbidden in some countries and by several authorities. It has been replaced by artificial radionuclides, such as ^{60}Co, ^{137}Cs, and ^{192}Ir (IAEA, 2006). With ^{226}Ra, the risk of leakage and contamination was high; these risks are considerably reduced with ^{60}Co, ^{137}Cs, and ^{192}Ir sources. The lower energy of the gamma emissions of ^{137}Cs and ^{192}Ir also simplifies the practical problems of room shielding and reduces the exposure to staff.

When radium was the only available radionuclide, the activities of the tube-sources used for intracavitary therapy applications were similar in all institutions.

Typically, the radium tubes were from 1.5 cm to 2.2 cm long with a source mass of from 5 mg to 25 mg of radium and a total platinum filtration of 1 mm for tube sources or 0.5 mm for needles.

The replacement of radium by ^{137}Cs, ^{192}Ir, and ^{60}Co followed one of two options. In the first option, the new sources (^{137}Cs or ^{60}Co) were similar in size and shape and had an output similar to radium sources. The same technique of application could then be used, and the clinical experience gained with radium remained fully relevant. In order to facilitate comparison of substitutes directly with radium itself, sources were specified in "milligram-radium equivalent." The radium-equivalent mass of a source is the mass of radium filtered by 0.5 mm of platinum that gives the same exposure rate at 1 m on the perpendicular bisector of the source. The second option, using ^{192}Ir, takes advantage of improved technology in the preparation of the sources: the increased specific activities possible and the technology to make miniaturized sources.

The large range of source activities available with artificial radionuclides allows greater freedom in the time–dose patterns of the applications, including various forms of fractionated HDR or PDR irradiation. Artificial radionuclides allow new types of sources, wires or seeds, with new shapes and dimensions, better adapted to afterloading techniques and providing more comfort to the patient, as will be discussed in the following section.

These dramatic changes in the brachytherapy-source characteristics and application techniques called for a new method of specification of the radioactive sources. An agreement has now been reached among an increasing number of users and manufacturers (see Section 11.2).

3.4 Contemporary Techniques and the Decline of the Radium Systems

The current practice of gynecologic brachytherapy relies heavily on the influence of historical systems and techniques, but with numerous innovations and adaptations. The Manchester- and Fletcher-based techniques are both related to the original Paris method and have continued to evolve. Evolving techniques have made possible different absorbed-dose rates, including LDR, MDR, HDR, and PDR. With the development of modern manual and remote afterloaders, with computer-controlled stepping source technology and computer- and image-assisted treatment planning systems, dwell-location and dwell-time assignments are open to adaptation and individualization for the patient. Using these modern tools, traditional loading patterns used in the classical systems can be adapted to meet the needs of the individual patient. This freedom to use a variety of absorbed-dose rates, applicators, dose-planning, and treatment-delivery systems has resulted in more frequent combinations of elements from different systems, in order to achieve appropriate and highly customized plans.

3.4.1 Tandem and Ring Techniques (Modified Stockholm Technique)

The ring applicator, an adaptation of the Stockholm tandem-and-box technique, was developed for afterloading techniques using ^{137}Cs and then ^{192}Ir, a much smaller source (Björkholm, 1997; Brooks *et al*., 2005; Walstam, 1965). The vaginal ring is perpendicular and fixed to the rigid tandem and rests against the cervix, secured by gauze packing. Different tandem angles and lengths, and different ring sizes, allow some adaptation to the individual topography. The metal ring is covered by a plastic cap, which places the vaginal mucosa 0.6 cm from the source path. CT- and MRI-compatible variations of the tandem and ring are also available. There are locations all around the ring where the stepping sources stops or dwells to deliver absorbed dose. These dwell locations can be activated as needed. The classical Stockholm loading patterns can be reproduced, and other loading patterns can be used according to the specific needs of the individual clinical situation. The shape of the isodose curves and the volume of tissue irradiated can therefore vary significantly depending on institutional practice and adaptation to an individual patient. The short distance from the ring to the vaginal mucosa can result in very high surface absorbed doses in small areas (Berger *et al*., 2007; Erickson *et al*., 2000; Noyes *et al*., 1995). There have been only very limited number of reports attempting to translate the original Stockholm absorbed-dose prescription into newer modified application techniques and new absorbed-dose rates (Björkholm, 1997; Joelsson and Backstrom, 1970).

3.4.2 Tandem and Ovoid Techniques (Modified Manchester Technique)

The classical Manchester technique was based on the use of an intra-uterine tube of fixed lengths (4 cm and 6 cm) and two vaginal ovoids that were ellipsoid in shape, with diameters from 2.0 cm to 3.0 cm, held apart in the vagina by a washer or spacer. The contemporary Manchester applicators physically mimic the classical models, with the same ovoid diameters, but with more tandem lengths and angles available, and a clamp to hold the ovoids and tandem in a fixed relationship. The whole applicator is stabilized and secured in contact with the cervix and the vaginal fornices by gauze packing. The ovoids are angled at

40° to the vaginal axis and are available to accommodate ^{137}Cs and the smaller size ^{192}Ir sources.

As in the original Manchester system, the absorbed dose and absorbed-dose rate specification at Point A has in principle been maintained in the modified Manchester system, assuming an ideal geometry and a balanced loading between the uterine and vaginal applicators adapted for the new application techniques and the different absorbed-dose rates inherent with ^{137}Cs (MDR) and ^{192}Ir. Absorbed dose at Point A is still the predominant method of absorbed-dose prescription, regardless of the application technique used. This method of Point A prescription includes institutions using the tandem ring as well as the majority of institutions worldwide using the tandem/ovoids. Movement away from a point-dose specification to a volume-based specification is in evolution. However, there is still value in recording and assessing the absorbed dose at Point A, as most of the clinical experience accumulated over the last decades has been based on this absorbed-dose prescription.

3.4.3 Tandem and Ovoid Techniques (Modified Fletcher Technique)

The Fletcher applicator was modified in the 1960s for afterloading (Fletcher-Suit applicator) (Delclos *et al*., 1978; Haas *et al*., 1985; Perez *et al*., 1985; Suit *et al*., 1963) and in the 1970s to accommodate ^{137}Cs sources (Haas *et al*., 1985). In the 1970s, the Delclos mini-ovoid was developed for use in narrow vaginal vaults (Delclos *et al*., 1978; 1980; Haas *et al*., 1983; 1985). The ovoids are 2.0 cm, 2.5 cm, and 3.0 cm in diameter with and without shielding. The mini-ovoids have a diameter of 1.6 cm and a flat medial surface. The mini-ovoids, unlike the standard Fletcher ovoids, do not have shielding, and this—together with their smaller diameter—produces a higher vaginal surface absorbed dose than regular ovoids and the potential for higher absorbed doses to the rectum and bladder. The orientation of the sources in the ovoids affects the absorbed doses to the target and the neighboring normal tissues due to the anisotropy of the sources. Positioning the source axes perpendicular to the tandem in a generally anterior–posterior orientation, as with the Fletcher applicator, produces—for the same absorbed dose to the cervix—relatively lower absorbed doses in the direction of the rectum and bladder than with the sources parallel to the tandem, as in the Henschke applicator (Henschke, 1960). Fletcher tandems are available in four curvatures, with the greatest curvature used in uterine cavities measuring $>$6 cm, and lesser curvatures used for smaller cavities. A flange with keel is added to the tandem once the uterine canal is sounded which approximates the exo-cervix and defines the length of source train needed. The keel prevents rotation of the tandem after packing. The distal end (handle) of the tandem near the cap is marked so that rotation of the tandem after insertion can be assessed and corrected as appropriate. This applicator is referred to as a non-fixed applicator, as the relationship of the ovoids and tandem can be varied.

The current approach to treatment specification reflects the Fletcher system policy of treating advanced cervical carcinoma to normal tissue tolerance (Katz and Eifel, 2000). This includes integrating standard loadings and source-mass $\times$ duration with calculated absorbed doses to the bladder, rectum, sigmoid, and vaginal surface. The activity in the ovoids is limited by the vaginal-surface absorbed dose, which is kept below 140 Gy. Calculated bladder and rectal absorbed doses are noted and sometimes impose limits on the duration of the intracavitary system, with the absorbed doses to the bladder and rectum kept below from 75 Gy to 80 Gy. The treatments are usually limited to 6000–6500 mg (radium-equivalent) h after from 40 Gy to 45 Gy external-beam radiotherapy.

The Fletcher applicator and associated source loading based on tandem length and ovoid diameter led to a predictable absorbed-dose distribution. With current computerized dosimetry, absorbed doses to Point A as well as the adjacent organs at risk also can be accessed easily and have become standard in the Fletcher technique. Adapting the absorbed-dose distribution to the tumor volume, while constraining the absorbed dose to the normal organs for individual patients to best accommodate the tumor volume and the normal-organ absorbed-dose constraints, is also feasible and practical.

Horiot, in Dijon, modified the Fletcher method for treatments based on dimensions (width, thickness, height) and the volume of the 60 Gy reference volume, as outlined in ICRU Report 38 (Barillot *et al*., 2000; ICRU, 1985).

3.4.4 The Tandem and Cylinder Technique

Tandem and cylinder application techniques were designed for various reasons. A major reason for tandem cylinder applications is to accommodate narrow vaginas and to treat varying lengths of the vagina when mandated by vaginal spread of disease. The plastic cylinders vary in diameter from 2.0 cm to 4.0 cm and have varying lengths and curvatures to accommodate varying vaginal sizes (Delclos *et al*., 1980; Haas *et al*., 1983). This approach has also been developed as a general utero-vaginal applicator alone (single line source) without lateralized vaginal sources (Tan *et al*., 1997a; 1997b).

3.4.5 The Tandem and Mold Technique

The tandem and mold technique evolved primarily at the Institut Gustave-Roussy in Paris. This process involves fabrication of applicators made from vaginal molds of each patient as described by Gerbaulet *et al*. (1995). The first step in the preparation of the applicator is the vaginal impression. The second step consists of acrylic molded applicator fabrication. Vaginal catheters are basically located on each side of the cervical limits for cervical cancers. The position of the vaginal catheters, which is determined by the radiation oncologist, is drawn according to the tumor extensions. Their length depends on the tumor size and the vaginal extension. These catheters are fixed in place in the applicator. One hole is made at the level of the cervical os for the uterine-tube insertion and different holes are made in the applicator, allowing daily vaginal irrigation and vaginal-mucosal herniation, which prevent mold displacement. The source position is adapted to the tumor topography. With this technique, no packing is necessary, as the mold itself expands the vaginal walls. In this technique, a customized vaginal applicator is made for each patient from a cervico-vaginal impression, which also enables visualization of the tumor topography at the vaginal surface and guides the positioning of the vaginal and uterine source guides. In the applicator, the vaginal sources are oriented parallel to the anterior-superior surface of the mold, which is parallel to the surface of the cervix (see Appendix examples 1 and 7) (Gerbaulet *et al*., 2002b). This is the most customized of the intracavitary applicators taking into account individual anatomy and pathology.

This technique has been associated with the development of an individualized target concept for prescribing absorbed dose to a clinical target volume (CTV) based on clinical examination and taking into account point absorbed doses for the rectum and bladder. The target concept became the basis for ICRU Report 38 (ICRU, 1985), in which reporting the dimensions of the 60 Gy reference volume and the absorbed doses to the ICRU rectum and bladder points was recommended (Albano *et al*., 2008; Gerbaulet *et al*., 1995; Magne *et al*., 2010).

3.5 Limitations of Historical and Current Brachytherapy Systems, Techniques, and Prescriptions

3.5.1 Applications Based on Amount of Radium

The original systems (Stockholm, Paris) used for prescription in cervical cancer brachytherapy were based mainly on the amount of radium applied and the duration of treatment. These measures gave a reasonable overall estimate of the radiation delivered to both the tumor and lymph nodes and the organs at risk. By empiric means, various treatment schedules were defined, taking into account the loading patterns for the uterine and vaginal sources. Also, different fractionation schedules were used from the beginning, with large fractions with large amounts of radium in the Stockholm System (Heyman, 1935) and a continuous application of smaller amounts of radium in the Paris Method (Lenz, 1927). The amount of radiation prescribed could be adjusted to the tumor volume, with a larger amount of radiation applied for larger tumors (*e.g*., in the later Fletcher system).

The strength of this approach has been its potential for a reproducible generic absorbed-dose estimate dependent only on the amount of radium and the duration of exposure. The weakness was clearly that no precise assessment of absorbed dose for the individual tumor, for the lymph nodes, or for the adjacent organs at risk was possible. This approach produced good clinical results in terms of tumor remission and local control, but with a high rate of complications (Adler, 1919; Kottmeier and Gray, 1961; Paterson, 1954; Sandler, 1942).

3.5.2 Application Based on Dose Points (Point A, Point B, Lymph Nodes, Bony Structures, Organs at Risk)

Dose specification at Point A was a significant step toward more individualized absorbed-dose specification. Point A was modified in 1953 to be "2 cm up from the lower end of the intra-uterine source and 2 cm laterally in the plane of the uterus, as the external os was assumed to be at the level of the vaginal fornices" (Tod and Meredith, 1953). Absorbed dose to Point B was considered to provide an estimate of absorbed dose to the adjacent internal iliac and obturator lymph nodes. In addition, maximum absorbed doses for the bladder and for the rectum were recommended relative to the Point A absorbed dose, keeping the bladder- and rectal-point absorbed doses below 80 % of the Point A absorbed dose (Tod and Meredith, 1938).

In the classical and modified Manchester systems, as well as in more contemporary series, there have been clear rules for absorbed-dose specification at Point A (Katz and Eifel, 2000; Perez *et al*., 1991; 1999; Wilkinson *et al*., 1983). Worldwide, absorbed-dose specification at Point A has been the most frequent form of dose prescription, including the modified tandem and ring techniques (Stockholm) and the tandem cylinder techniques.

With the further development of application techniques, stepping-source technologies, computer-assisted treatment planning systems, and new absorbed-dose

rates used clinically, the degrees of freedom for introducing treatment variations including dwell locations and dwell times have increased dramatically and have led to a large diversification of treatments during the second half of the last century. Dose-point calculations for other than Point A (see Sections 8 and 10), based on orthogonal radiographs, were introduced by various schools and traditions in order to achieve reproducible absorbed-dose prescribing and reporting in the pelvis including the pelvic wall point (Chassagne and Horiot, 1977), lymphatic trapezoid (Fletcher, 1980), and for organs at risk such as the rectum (Chassagne and Horiot, 1977), bladder, and the vagina (Fletcher, 1980). This type of absorbed-dose reporting was also partly merged with absorbed-dose specification and reporting at Point A (Pötter *et al*., 2000; Stitt *et al*., 1992).

There are, however, limitations to the use of Point A for absorbed-dose specification, which are summarized in below.

3.5.2.1 Ovoid Surface Visibility on Radiographs. The failure of localization radiographs to show the surfaces of the ovoids made utilization of the original definition of Point A (Tod and Meredith, 1938) difficult, and hence the definition of Point A was modified in 1953 to be "2 cm up from the lower end of the intra-uterine source and 2 cm laterally in the plane of the uterus, as the external os was assumed to be at the level of the vaginal fornices" (Tod and Meredith, 1953). For the original Manchester applicator, the lower end of the intra-uterine source coincided with the superior vaginal fornices by design. With other applicators, such as the Fletcher, this was not the case. A seed or marker placed near the surface of the cervix and coincident with the tandem flange is used to identify the exocervix on the localization films. The clinical practice using the revised Point A definition, however, becomes problematic if there are deep vaginal fornices and the cervix protrudes between the ovoids, causing a resultant increase in dose rate at point A (Batley and Constable, 1967).

3.5.2.2 Steep Absorbed-Dose Gradient. When Point A is defined with respect to the tandem flange on applicators without fixation between the tandem and colpostats, the location of Point A can occur in a high-gradient region of the absorbed-dose, especially if the vaginal fornices are deep. A consistent location for absorbed-dose specification should fall sufficiently superior to the ovoids where the isodose lines run parallel to the tandem (Nag *et al*., 2000; Potish *et al*., 1995). Reverting to the original definition of Point A rather than the revised version can help to solve this problem (Gerbaulet *et al*., 2002a; Potish *et al*., 1995; Viswanathan *et al*., 2012a).

3.5.2.3 Point A and Tumor Absorbed Dose (According to the Definition Given in this Report). Points A and B are related to the position of the intracavitary sources and the applicator rather than to an anatomical structure. The variation in position and distribution of the sources and the applicator significantly changes the anatomic structures in which Points A and B are located. The Manchester technique was based on the assumption of an ideal cervical and para-cervical anatomy, which is not often encountered in clinical practice. Anatomical and tumor variation can lead to wide variation in the tissues in which Point A is located. Furthermore, and most importantly, the absorbed dose at this point is not a reliable indicator of the minimum tumor absorbed dose. The Point A absorbed dose overestimates the target absorbed dose in large tumors and underestimates the target absorbed dose in small tumors (Batley and Constable, 1967; Lindegaard *et al*., 2008; Potish and Gerbi, 1987; Tanderup *et al*., 2010a).

3.5.2.4 Point B and Lymph-Node Absorbed Dose. The use of Point B has also been criticized, as it does not always represent the absorbed dose to the obturator nodes (Schwarz, 1969). Fletcher concluded that the uterine radium was the main contributor to the pelvic-wall-lymph-node absorbed dose because of its central location. The contribution from the vaginal radium depended on the location of the radium sources, which varies with patient's anatomy and age, and distortion caused by disease (Fletcher, 1971). A strong correlation between absorbed dose to Point B and nodal absorbed doses estimated from CT-assisted analysis does not exist (Gebara *et al*., 2000; Lee *et al*., 2009). Point B is still used in some institutions to help guide decisions about parametrial and nodal boosting.

3.5.3 Further Developments Based on TRAK, Points, and Volumes

As mentioned earlier, dose points were introduced in order to achieve reproducible absorbed-dose reporting based on orthogonal radiographs for the pelvis, for lymph nodes, and for organs at risk such as the rectum, bladder (see Sections 8.4 and 10.3), and vagina (see Sections 8.4 and 10.2).

This dose-point assessment was used together with the overall estimate of radiation delivered by the product of source mass and duration within the Fletcher system. Except for the vagina, most of these absorbed-dose points were also recommended for reporting in the ICRU Report 38 (ICRU, 1985).

The use of Point A was discouraged in ICRU Report 38 for reasons outlined above. The use of

Point A had also not been recommended in the M.D. Anderson approach following the classical Fletcher system, not in the classical Stockholm system, nor in the classical Paris method. Worldwide, however, absorbed-dose specification at Point A has been the most frequent form of absorbed-dose prescription, even though it was intended only for absorbed-dose reporting. Tracking Point A absorbed doses is useful when converting to volumetric absorbed-dose specification to avoid dramatic alterations in practice.

With the development of computer-assisted dose planning based on orthogonal radiographs with the applicator in place, individualized dose planning became possible and is currently utilized both in the volume-image-based and radiographic approaches (see Section 10.1.3). Strict adherence to one of the classical radium-based brachytherapy systems has diminished over time and hybrid approaches, using various elements from different classical systems, have now become predominant. Institutionally, prescription and reporting are frequently based on links to several classical traditions.

The volume-reporting approach, as recommended in ICRU Report 38 with the 60 Gy reference volume for the target volume, has not been widely accepted (Pötter *et al*., 2001a). Inherent in this approach was a target-volume concept, based on the clinical assessment of tumor extent at diagnosis through digital examination. Corresponding imaging was not available at that time, as 3D sectional and volumetric imaging were just evolving.

With the advent of volume-based imaging, useful information about tumor volume and location, as well as the adjacent normal organs, makes the limitations of a point-dose system apparent. The 60 Gy reference volume defined in ICRU Report 38 (ICRU, 1985) can currently be better understood by the relationship of this 60 Gy reference volume to the volume and location of the tumor imaged at diagnosis, prior to external-beam irradiation. This is similar to the newly defined Intermediate Risk CTV (CTV IR) using an image-guided adaptive-brachytherapy approach (see Sections 5.2.1.6, 5.4.5, 8.7, and 10.1.3.). However, this reference-volume approach as recommended in ICRU Report 38 for target assessment is not recommended in this report but is replaced by the individualized target and target dose-volume (see Sections 1.2.4, 1.2.7, 5.3, 5.4, and 8.3.2) and the isodose-surface-volume concept (see Section 8.7).

3.5.4 Developments in regard to New Absorbed-Dose Rates

When moving from radium to artificial radionuclides, not only were the application techniques adapted, but also the absorbed-dose rates. As the effects of different absorbed-dose rates were not well understood *a priori* (neither for tumor nor for normal-tissue effects), the clinical implementation of changes in absorbed-dose rate presented a major clinical problem for MDR ^{137}Cs, HDR ^{60}Co, and ^{192}Ir (Guerrero and Li, 2006; Kucera *et al*., 1984; Leborgne *et al*., 1996; Roberts *et al*., 2004). Absorbed-dose prescription based on the long-standing clinical radium experience could not be directly applied when using these new absorbed-dose rates (Roberts *et al*., 2004).

In ICRU Report 38, no specific considerations were given to absorbed-dose-rate effects, as the major frame of clinical and experimental experience was still the classical LDR (ICRU, 1985). A recommendation was given, however, how to differentiate the various absorbed-dose rates into LDR, MDR, and HDR, and these designations are to be reconsidered based on the clinical experience accumulated (see Section 7.3). With the further evolution of HDR and PDR applications, the issue of finding and applying a common language reflecting the various absorbed-dose-rate and dose-per-fraction effects has become essential. The diversity of dose prescription and reporting is a challenge that requires a practical solution to implement and to blend diverse practices. The use of equi-effective doses (EQD2) as defined in Section 7.6.4 will provide a model for a common language.

3.6 Modern Applications in the Volume-Based Imaging Era with HDR and PDR Brachytherapy

Low-dose-rate applicators carrying ^{226}Ra have evolved over many decades and have been modified for the artificial radionuclides such as ^{137}Cs and ^{60}Co, and more recently into models for PDR and HDR applicators based on ^{192}Ir. Many of these applicators are CT and MR compatible, which allows for imaged-based brachytherapy. All applicators have an intra-uterine tandem and a vaginal applicator that, in the majority of cases, has sources in close proximity to the cervix and the vaginal fornices (Gerbaulet *et al*., 2002b; Hellebust *et al*., 2010a). Due to the reduced size of the artificial HDR and PDR sources, the dimensions of the carriers (*e.g*., diameter of the tandem and vaginal applicators) have become smaller. This report does not provide absorbed-dose distributions for all available contemporary applicators, but several typical examples are given (see Appendix). To date, no comprehensive analysis has been reported comparing application techniques, loading patterns, absorbed-dose distributions, and their impact on absorbed dose in the CTV and the organs at risk, as outlined in the forthcomings Sections (5–8), which represents a major

future research challenge (Jürgenliemk-Schulz *et al*., 2010; Nomden *et al*., 2013a). Therefore, the following is meant as a description of the major various application techniques currently available.

3.6.1 Quality of an Application

It is important that applicators be inserted with care and precision in order to achieve a high-quality implant. This has been facilitated by afterloading techniques. The 1978 and 1983 Patterns of Care study (Corn *et al*., 1994) showed that high-quality implants correlated significantly with improved local control and a trend toward improved survival. This has been confirmed in several large retrospective reviews, both with respect to local control and complications (Katz and Eifel, 2000; Perez *et al*., 1983; 1984; Viswanathan *et al*., 2012a). Radiographic checks of application quality are now being replaced by volumetric imaging with the applicator in place. The use of ultrasound to guide tandem insertion can be extremely helpful in negotiating a narrowed or obliterated endo-cervical canal and preventing perforation (Davidson *et al*., 2008). Transrectal ultrasound can additionally provide online information about the position of the intracavitary applicator in relation to the tumor topography and can facilitate focused needle insertion. Furthermore, the use of CT and MR imaging following applicator insertion enables a check of the geometrically appropriate relationship between the applicator, the target, and the organs at risk. This also applies to the quality of the vaginal packing, which can be checked by sectional imaging, in particular by MRI (see Figures 4.11, 5.2 and 5.4 and Examples in the Appendix).

3.6.2 Tandem and Ovoids

The tandems and the ovoids used with HDR and PDR approaches are variations of the traditional Manchester, Fletcher, and Henschke applicators but are lighter, narrower, and smaller due to the smaller Ir^{192} sources used. The ovoids with and without shielding are 2.0 cm, 2.5 cm, and 3.0 cm in diameter. The availability of shielding can lead to different absorbed-dose distributions and resultant absorbed doses to the bladder, rectum, and upper vagina. The ovoids are placed taking into account the vaginal topography and the specific tumor spread. The angle on the HDR and PDR ovoids is different from that on LDR applicators so that the source can negotiate the angle between the handle and the ovoid. This can lead to a different relationship between the tandem and the ovoids and between the ovoid and the cervix compared with the classical techniques. The tandem angles in the HDR and PDR models also can be somewhat different from that for the LDR models.

The Henschke tandem and ovoid applicator was initially unshielded (Henschke, 1960; Perez *et al*., 1985) but later modified with rectal and bladder shielding (Hilaris *et al*., 1988; Mohan *et al*., 1985). It consists of hemi-spheroidal ovoids, with the ovoids and tandem fixed together. Sources in the ovoids are parallel to the sources in the uterine tandem (Hilaris *et al*., 1988). The Henschke applicator can be easier to insert into shallow vaginal fornices in comparison to ovoids/colpostats.

3.6.3 Tandem and Ring

The ring applicator is an adaptation of the Stockholm system (Björkholm, 1997; Erickson *et al*., 2000). Variable ring sizes, tandem lengths, and ring-tandem angles are available. The ring is always perpendicular to the tandem. This applicator is often referred to as a fixed applicator because the tandem is fixed in the middle of the ring, making for a predictable geometry. The ring applicator has been regarded as ideal for patients with shallow or obliterated vaginal fornices and with non-bulky disease, but also allows for larger tumors. Its predictable geometry makes it a popular alternative to tandem and ovoids. CT- and MRI-compatible variations of the tandem and ring are available. With the PDR and HDR applications, there are dwell locations all around the ring where the moving source will stop and dwell to deliver absorbed dose, which can be activated as needed. The classical Stockholm loading patterns can be reproduced, and other loading patterns can be used according to the specific needs of the individual clinical situation. The shape of the resulting isodose curves and the volume of tissue irradiated can therefore vary significantly depending on institutional practice and individual patient adaptation. The ring-tandem angle can push absorbed dose closer to the bladder or rectum depending on the angle chosen. The short distance from the ring to the vaginal mucosa can result in very high surface absorbed doses in small areas (Berger *et al*., 2007; Erickson *et al*., 2000; Noyes *et al*., 1995).

3.6.4 Tandem and Mold

At the Institut Gustave-Roussy in Paris, there has been a long tradition of use of a personalized applicator adapted to each patient, fabricated from individual vaginal impressions (Albano *et al*., 2008; Gerbaulet *et al*., 2002a; Magne *et al*., 2010). This mold technique was used previously for LDR brachytherapy (see Section 3.4.5) and is used currently for PDR and HDR brachytherapy with the appropriate adaptations.

3.6.5 Tandem and Cylinder

Tandem and cylinder applicators have been used systematically in some institutions for cervical

cancer brachytherapy (Tan *et al*., 1997a; 1997b). The cylinders are available with different sizes and lengths and with various tandem lengths and angles (Gerbaulet *et al*., 2002a; Pötter *et al*., 2002a). They can be especially helpful when there is vaginal spread of disease because the cervix and the vagina can be treated with one brachytherapy application. In addition to the classical cylinder applicators, shielded and multi-channel HDR and PDR tandem and cylinder applicators have been devised to better customize the absorbed-dose distribution in accordance with the location and volume of disease within the cervix and vagina and to spare the adjacent bladder and rectum.

Cylindrical applicators are also appropriate for patients with a narrow vagina. Great care must be taken when using these applicators because they may lead to a higher rate of local failure as the absorbed dose in the lateral cervix and pelvic sidewall is reduced in the absence of the ovoids or ring. Additionally, a higher rate of complications can occur due to the increased length of vagina treated and the proximity of rectum and bladder to the high-dose area. Packing cannot be used with cylinders as this would displace the targeted vaginal walls from the necessary absorbed dose (Crook *et al*., 1987; Cunningham *et al*., 1981; Esche *et al*., 1987a; 1987b). As an alternative, interstitial implantations have been proposed for patients with a narrow vagina or with distal vaginal disease, in particular for advanced disease that extends into the parametria.

3.6.6 Interstitial Applicators with and without a Tandem and Colpostats

Interstitial implantation is helpful in patients with bulky infiltrative extensive disease, anatomical unfavorable topography such as asymmetrical tumor growth, narrow vagina or an obliterated endo-cervical canal, vaginal spread of disease, or recurrent disease. Tumor volume and patient anatomy are key in the decision of whether or not to use intracavitary or interstitial brachytherapy. The appropriate applicator must be selected to match the disease and to shape the associated absorbed-dose distribution to encompass the disease (Dimopoulos *et al*., 2006a; Erickson and Gillin, 1997; Haie-Meder *et al*., 2002; Kirisits *et al*., 2006a; Viswanathan *et al*., 2011a).

The development of prefabricated perineal templates, through which needles are inserted and afterloaded, was pivotal in advancing interstitial techniques for the treatment of cervical and vaginal cancers in the early era of afterloading techniques. The template concept allows for a predictable distribution of needles inserted across the entire perineum through a perforated template according to a chosen pattern. Commercially available and institution-specific templates can be used to accommodate varying disease presentations. The MUPIT (Martinez Universal Perineal Interstitial Template, Beaumont, Hospital, Royal Oak, Detroit, MI, USA) template accommodates implantation of multiple pelvic-perineal malignancies and is available for both LDR and HDR applications (Martinez *et al*., 1984). The Syed-Neblett (Best Industries, Springfield, VA, USA) is the other well-known, commercially available template system (Fleming *et al*., 1980; Syed *et al*., 1986). Currently, there are three LDR Syed-Neblett templates of varying size and shape for use in implantation of gynecologic malignances (Best industries: GYN 1–36 needles; GYN 2–44 needles, GYN 3–53 needles). There are also commercially available templates that accommodate HDR and PDR needles. Stainless steel, titanium, and plastic needles are available and afford different imaging options. Free-hand interstitial implantation is also used selectively for small volume vaginal and parametrial disease and is especially helpful in treating peri-urethral disease (Frank *et al*., 2005).

The Vienna applicator (Nucletron, Veenendaal, The Netherlands; Varian, Palo Alto, USA) is a modified ring applicator with holes in the ring for needle guidance parallel to the uterine tandem and the ring fixed to the cervix through the tandem and vaginal packing. The Vienna applicator is used for treating parametrial residual disease after radio-chemotherapy with unfavorable topography (Dimopoulos *et al*., 2006a; Kirisits *et al*., 2006). Additional absorbed dose in residual disease can be provided with the addition of a number of needles implanted in those parts of the lateral tumor extension not covered by the intracavitary pear-shaped absorbed-dose pattern. There are also modified ovoid applicators (Utrecht applicator, Nucletron) using needles that are guided through holes in the ovoids, enabling better coverage of disease in the parametrium (Jürgenliemk-Schulz *et al*., 2009). These applicators can be used to extend and improve lateral and superior coverage of the target volume by approximately 10 mm. A "Vienna II" applicator has been suggested for distal parametrial disease with an add-on to the ring, providing holes for additional oblique needles (Berger *et al*., 2010).

The Syed-Neblett system and MUPIT are particularly suited for treatment of extensive vaginal disease as they are combined intracavitary and interstitial systems. The vaginal obturators that accompany the template are used to treat the vaginal surface, and the vaginal obturator needles can be strategically loaded to encompass disease from the fornices to the introitus. Along with the intracavitary uterine tandem, the obturator needles can also be advanced directly into the cervix as an interstitial application,

and can be essential in delivering high absorbed doses to the cervix thereby preventing a central low-dose region, especially in those circumstances in which an intra-uterine tandem cannot be inserted. Whenever possible, it is important to use a tandem along with the needles when there is an intact uterus. The tandem can extend absorbed dose superiorly throughout the uterine cavity, provide additional absorbed dose to the parametria, and increase the absorbed dose centrally in the implant where it is most needed (Viswanathan *et al*., 2009).

Modifications of these standard templates have evolved and other innovative templates developed for vulvar, vaginal, and cervical carcinomas (Erickson and Gillin, 1997; Viswanathan *et al*., 2011a). Optimal catheter placement in regard to tumor-tissue spread is pivotal with all these various implantation techniques. Absorbed-dose optimization is often beneficial, but can only partly compensate for poor implantation quality.

3.6.7 Insertion and Planning Techniques based on Volumetric Imaging

Brachytherapy insertions are performed according to the volume of disease present. In some patients with small-volume disease, brachytherapy might be possible from the beginning or can be used early during the course of external-beam irradiation and chemotherapy. Patients with more bulky and extensive disease require the completion of 5 weeks of concurrent external-beam and chemotherapy, producing sufficient disease regression to facilitate optimal applicator geometry in relation to target and organs at risk.

A classical cervical-brachytherapy application can be described in the following, using general terms. For brachytherapy to be optimal, patients must have proper sedation and analgesia to facilitate applicator placement and treatment planning. Various options for sedation and analgesia exist, ranging from general anesthesia to monitored sedation-analgesia and to regional anesthesia.

Insertions can take place in an operating room or departmental brachytherapy suite. To begin the process, the patient is evaluated for anesthesia options prior to the actual procedure. Once cleared, the procedures can begin. A bladder catheter is inserted and a vaginal and perineal preparation performed. A pelvic examination is performed under anesthesia. The endo-cervical canal is localized, measured, and dilated and a tandem inserted with a given length (flange) and angle. At the time of the first fraction, an endo-cervical stent can be inserted to maintain patency of the endo-cervical canal. Ultrasound guidance is useful, especially if there is difficulty finding the canal or if there is concern over perforation. Gold seeds or other appropriate CT- and MR-compatible markers can be placed into the anterior and posterior cervical lips. The largest-diameter vaginal applicator that will fit through the vaginal introitus and fill appropriately the upper vagina is chosen (threaded over the tandem in the case of ring or cylinder) and inserted through the introitus with care to avoid a vaginal tear. The vaginal-ring applicator or the colpostats are pushed against the cervix or into the lateral vaginal fornices, respectively. The utero-vaginal applicator is clamped together, and care is taken to avoid pinching of the vaginal mucosa between the vaginal applicator and tandem interlock system. Palpation of the interface between the vaginal applicator and the cervix follows to assure close approximation, and then insertion of the saline and/or gadolinium-soaked (if using MR imaging) vaginal packing to fix the applicator against the cervix and push away the bladder and rectum as much as possible. A rectal retractor can be used in addition to packing. C-arm fluoroscopy or online ultrasound examination can be helpful if there is concern over the position of the applicator relative to the cervix, uterus, or other pelvic organs. An external fixation device, such as a perineal bar, is used by some institutions to limit applicator movement, especially if no intensive vaginal packing is applied. A rectal catheter is inserted for image contrast and for rectal *in vivo* dosimetry if used. The patient is carefully taken from the dorsal lithotomy position and insertion stirrups into the legs-down position. The applicator can be readjusted to ascertain that it is in close proximity to the cervix, particularly if there is no intensive packing. Localization imaging is then performed. Such a classical cervical cancer brachytherapy insertion procedure has changed very little over the decades, even within the context of advanced image-guided planning procedures.

A large variety of planning strategies has been developed recently and will further evolve in the future with the full implementation of volumetric imaging in the planning process. The insertion procedure itself is not directly influenced by these strategies, as no direct interactive image-guided insertion technique has been developed at the time of writing (ultrasound is under consideration). However, more precise planning has become possible with repetitive clinical examination and imaging (4D imaging), which results in the upfront decision if intracavitary brachytherapy alone or intracavitary brachytherapy combined with an interstitial implant has to be performed. The classical post-implant imaging with radiographs is being replaced by volumetric imaging with the applicator in place, guiding the treatment–planning process, target and OAR contouring, and DVH calculation. The decision on the treatment plan takes into account both constraints for target coverage and the OAR (Pötter *et al*., 2008) (see Section 12).

3.7 External-Beam Radiotherapy

Just as changes and advances have been made in gynecologic brachytherapy, so also have they been made in gynecologic external-beam techniques, incorporating image-based planning and treatment-delivery systems. After a long period of opposed megavoltage beams, rotational techniques and four-field box techniques, three-dimensional conformal-radiation techniques, as well as intensity-modulated-radiation techniques (including arc techniques) have become and are becoming increasingly the standard of care for the treatment of gynecologic cancers (Erickson *et al*., 2011). These techniques are based on full 3D cross-sectional, image-based treatment planning with contouring of the various targets and OARs, and evaluated using DVHs. The goal with this advanced technology is to improve the coverage of image-defined targets while sparing as much as possible adjacent critical organs, such as the small bowel, bladder and recto-sigmoid in the pelvis, and the liver, kidneys, and upper GI tract in the upper abdomen. The impact of the most advanced techniques has not been fully assessed.

These developments parallel the evolving tumor and target concepts, as well as dose-point and dose–volume reporting for external-beam radiotherapy, with continuous adaptations over the last decades from original point assessments (ICRU point, maximum, minimum dose) for tumor and target, to volumetric absorbed-dose assessment (using $D_{50\ \%}$, $D_{98\ \%}$, and $D_{2\ \%}$) for various CTVs (ICRU, 1978; 1993b; 1999; 2010). Comprehensive integration of these different techniques of absorbed-dose planning and delivery in external-beam radiotherapy and brachytherapy is the ultimate aim of a high-quality application of therapeutic radiation.

This report discusses the image-guided approach for cervical-cancer brachytherapy in regard to terms and concepts as necessary to gain a full understanding, however not forgetting the link to the previous approaches that are still the most widely utilized in cervical-cancer radiotherapy worldwide. Links will be given to the corresponding areas of external-beam therapy as appropriate. However, a full understanding of these two worlds within the framework of their most advanced forms is only in its infancy at present.

3.8 Concluding Remarks

The history of gynecologic brachytherapy is a century of success, innovation, and progress. Cancer of the cervix has been cured for decades by radiotherapy alone because of the judicious use of both brachytherapy and external-beam radiotherapy. Despite excellent local control in many patients, there are numerous recurrences and complications that defy understanding and indicate also the limitations of TRAK and point-dose specification and prescription that apply to a reference-volume approach. There is certainly a need to move from the conventional dosimetry to a volume-based, image-guided dosimetry. Useful tools have been developed to define the tumor and normal tissues through volume-based imaging, which are described in this report (see Sections 5 through 9). Given the evolving variety of innovative CT, MR, and US imaging, beam-delivery systems and treatment-planning systems, cervical-cancer radiotherapy, and in particular brachytherapy, will change dramatically during the next decade, first at institutions with advanced technology, then also beyond. Future clinical and translational research based on a more comprehensive understanding of the overall complex situation will guide the further development of the necessary systems and techniques to be applied for cervical cancer brachytherapy in regard to tumors, CTVs, and normal tissues within the multi-disciplinary treatment approach.

3.9 Summary

A combination of external-beam irradiation and brachytherapy, often concurrently with chemotherapy, is administered to cure locally advanced cervical cancer. “Brachytherapy” is a pivotal component of this treatment. The quality of the brachytherapy implant (optimal applicator insertion) as well as the absorbed dose delivered are essential in achieving cure with an acceptable rate of complications.

“Intracavitary brachytherapy” for cervical carcinoma has been profoundly impacted by the historic development of various systems with regard to total absorbed doses, absorbed-dose rates, and application techniques. Brachytherapy “dosimetric systems” refer to specific, comprehensive sets of rules, adjusted for applicator type and radioactive isotope, distribution of sources in the applicator, and the consequent absorbed-dose distribution in a defined target. The systems established in the early 1900s include the “Stockholm System, the Paris Method,[2] and the Manchester System.” The *Manchester System*, pervasive in current brachytherapy, includes dose specification at Point A, vaginal packing, and rectum and bladder dosimetry to limit the absorbed doses to the latter organs.

In the *Fletcher System,* also pervasive in contemporary brachytherapy, ideal applicator geometry is key as is consideration of the absorbed-dose distribution relative to tumor volume.

[2]The “Paris method” refers to an intracavitary application and is called a “method” as the so-called “Paris System” refers to an interstitial brachytherapy system (Dutreix and Marinello, 1987).

In current gynecologic brachytherapy, LDR, PDR, and HDR techniques are available, with a large "variety of applicators and planning and treatment-delivery methods." This has resulted in dosimetric approaches combining elements from different systems in order to achieve appropriate and highly patient-specific treatment plans.

The "applicators" can be selected depending on the vaginal, uterine, and tumor topography, dimensions, and spread of disease at the time of brachytherapy. The variety of applicators currently available is described in this section and include tandem and ovoids, tandem and ring, tandem and mold, and tandem and cylinder, as well as variations which allow for additional interstitial needles.

The "ICRU Report 38 recommendations" are frequently used for assessment and reporting of absorbed dose to the ICRU bladder and rectal points. Historic applications were based on the normalized product of radium mass and application time (mg h) or on Point A, lymph-node points, and organs at risk absorbed-dose points. Their limitations have become increasingly apparent. However, the new ICRU/GEC ESTRO recommendations as presented in this report still refer to these points because of their wide-spread use and their representation of a huge clinical experience.

With the development of advanced 2D- and, more importantly, 3D-imaging techniques, volumetric information about tumor volume and location, as well as the adjacent normal organs at risk are available, allowing for an evaluation of the relationship between the applicator and the target and the organs at risk, and thus sophisticated dosimetric procedures to assess the absorbed doses to the target volumes and organs at risk. For external-beam-irradiation techniques, the use of 3D planning is currently considered the standard of care in the treatment of gynecologic malignancies.

3.10 Key Messages

(1) Modern brachytherapy has evolved from historical brachytherapy systems with many key elements of these systems still woven into contemporary methods in regard to applicators, loading patterns, treatment planning, absorbed-dose specification, total absorbed dose, and fractionation.
(2) A multitude of applicators and absorbed-dose rates are now available to customize treatment to the clinical situation and adhere to institutional traditions. Choice of the proper applicator based on the volume and spread of disease is an important first step in successful brachytherapy, as is the quality of the brachytherapy insertion.
(3) Prior 2D- and now 3D- and 4D-based treatment-planning strategies are essential to successful brachytherapy within the framework of various clinical scenarios. Volumetric CT- and MR-based brachytherapy planning provides better understanding of the relationship between the applicator and the absorbed-dose distribution in the tumor and the organs at risk.
(4) External-beam techniques are as essential as brachytherapy in the curative treatment of cervical cancer and are best actualized with 3D-imaging techniques.
(5) The evolution of 3D-image-based treatment of cervical carcinoma is expected to continue and ultimately lead to fewer complications and better local control.

Journal of the ICRU Vol 13 No 1–2 (2013) Report 89
Oxford University Press
doi:10.1093/jicru/ndw007

4. Brachytherapy Imaging for Treatment Planning

Various imaging modalities have been used to stage patients with gynecologic cancers and are invaluable in assessing local, regional, and metastatic spread of disease. As cervical cancer is directly accessible on pelvic examination, clinical findings based on visual and digital examination, and documented on clinical diagrams, also remain essential. Plain radiographs, including chest x rays, barium enemas (BE), intravenous urography (IVU), skeletal surveys, and lymphangiography (LAG), as well as cystoscopy and rectal endoscopy, have long been mainstays of staging of cervical cancer and remain so in many parts of the world. Radiographs to guide both external-beam therapy and brachytherapy have been used nearly universally, but are limited by their inability to demonstrate the tumor and its extensions to many of the critical, adjacent abdomino-pelvic organs. Reliance on bony anatomy is not sufficient for treatment planning for cervical cancer (Finlay *et al*., 2006; McAlpine *et al*., 2004). More recently, three-dimensional (3D)-imaging methods such as computed tomography (CT) and magnetic resonance imaging (MRI) have become the techniques of choice for external-beam and brachytherapy treatment planning, for monitoring response during treatment, and for post-treatment surveillance. Functional imaging, in particular positron-emission tomography (PET) combined with CT, and, recently functional MRI, play increasingly important roles. Ultrasound (US) has been replaced by MRI in the last two decades in the initial staging of patients, but it might have an essential role for image-guided intracavitary and interstitial gynecologic brachytherapy.

The focus in the following will be on the role of clinical diagrams and imaging in treatment planning and response monitoring leading to adaptive therapy.

4.1 Clinical Gynecologic Examination and Clinical Diagrams

From the beginning of cervical cancer treatment, and in particular radiotherapy, clinical examination has played the dominant role in assessing macroscopic tumor morphology and the local spread of disease, and monitoring of response during and after treatment. Additionally, the growth pattern can be further characterized as exophytic or infiltrative (see Figure 4.1). Clinical examination still remains the principal method for assessment of local disease in the FIGO staging system (Pecorelli, 2009).

For decades, diagrams depicting the clinical findings have been widely used in gynecologic disease assessment and radiotherapy treatment planning and monitoring. These serve as an initial baseline prior to external-beam radiotherapy (EBRT), with or without chemotherapy, and are reassessed at the time of brachytherapy. The Fletcher diagrams showing sagittal, coronal, transverse oblique, and vaginal speculum views (Eifel and Levenback, 2001; Fletcher *et al*., 1953) have become a universal recording tool (Burke, 2008) (see also Figure 3.4). Even with the advent of sophisticated 3D and 4D imaging, these clinical diagrams contain essential information and are regarded as a cornerstone of disease assessment and monitoring before, during, and after treatment (Figure 4.1) (Haie-Meder *et al*., 2005; Pötter *et al*., 2006).

The most recent version of the GEC ESTRO recommendations, containing these clinical diagrams, have been implemented in the first multi-center study on MRI-guided brachytherapy (www.embracestudy.dk) (EMBRACE, 2015) and are also included in this report.

4.2 Magnetic Resonance Imaging

Pelvic MRI has become the new standard for imaging of gynecologic cancers. Its strengths reside in its excellent soft-tissue contrast resolution, its multiplanar capability, and its lack of ionizing-radiation exposure. In cancer of the cervix and vagina, MRI is especially helpful in assessing parametrial, vaginal, uterine, bladder, and recto-sigmoid invasion (see Figure 4.2). The accuracy of staging of cervical cancer by MRI has been reported to be in the range of from 75 % to 96 % (Sala *et al*., 2007). Hricak *et al*. (1988) correlated pre-operative MRI with the surgical specimens and found the accuracy of MRI to be 81 % when comparing imaging *versus* histo-pathologic spread of disease, especially when assessing parametrial and

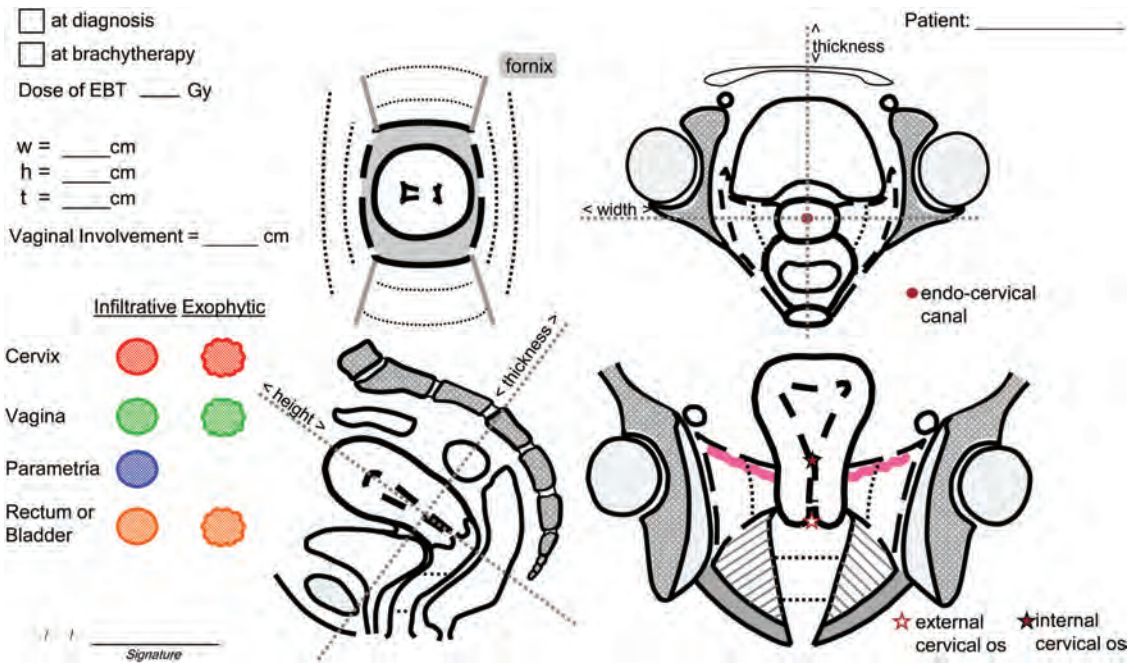

Figure 4.1. Clinical diagram template taken from the EMBRACE protocol (www.embracestudy.dk) (see also Supplementary appendix) (EMBRACE, 2015). Tumor delineation is done at the time of diagnosis, during treatment for response monitoring, and at the time of brachytherapy insertion.

vaginal spread. Cervical and vaginal malignancies are best imaged on T2-weighted images. Cervical and myometrial invasion of endometrial cancer is readily assessed on MRI; however, MRI is used less frequently because of the preference for initial-staging surgery for endometrial cancer. MRI is very helpful in the assessment of inoperable endometrial cancer prior to definitive irradiation, as tumor size, cervical involvement, and uterine wall invasion are easily seen. MRI is equivalent to CT in lymph-node assessment.

MRI has been especially helpful in monitoring treatment response (see Figure 4.3), even during the early weeks of treatment (Beadle *et al*., 2009; Dimopoulos *et al*., 2009a; Lim *et al*., 2008; Taylor and Powell, 2008; van de Bunt *et al*., 2006; 2008; Wang *et al*., 2010) (see also Section 5.3.4). Correlation of MRI-perfusion studies with volume reduction and diffusion-weighting imaging exams were subsequently found to be predictors of primary tumor control and disease-free survival (Mayr *et al*., 2010a; 2010b). Repetitive morphologic MRI has been crucial for the development of image-guided adaptive-brachytherapy treatment planning and monitoring (see Figure 4.3), but has not played a major role in external-beam treatment planning for gynecologic cancers.

In the future, functional MRI might help to more accurately delineate the residual GTV and any residual pathologic tissue (Haack *et al*., 2010) (see also Section 5.3.2). Furthermore, there seems to be considerable potential for defining prognostic sub-groups based on specific parameters derived from functional MRI at diagnosis (Andersen *et al*., 2011).

4.3 Computed Tomography

CT with oral and intravenous (IV) contrast is used routinely in the staging of patients with gynecologic cancers. CT is useful in screening for and defining distant metastases in the lungs, liver, peritoneal cavity, and at any other suspicious site. It is also used to assess the status of lymph nodes, which are considered abnormal when larger than 1 cm on the short axis (Hricak and Yu, 1996) (see Figure 4.4). Invasion of adjacent organs can also be assessed with CT when there is contrast opacification of the bladder and bowel. CT is inferior to MRI in tumor visualization and imaging of the local spread of tumor into the vagina, parametria, and uterine body cavity (compare in Figure 4.2), as reported in the ACRIN/GOG study (Hricak *et al*., 2007), but is equivalent in the assessment of enlarged lymph nodes.

Whereas CT has been widely implemented for 3D treatment planning for 3D conformal radiotherapy and for intensity-modulated radiotherapy (IMRT), it has only recently been implemented in brachytherapy treatment planning (Fellner *et al*., 2001). CT is useful for delineating the borders of the intact cervix (and the uterus) but of limited use for image-guided assessment of the boundaries of the tumor

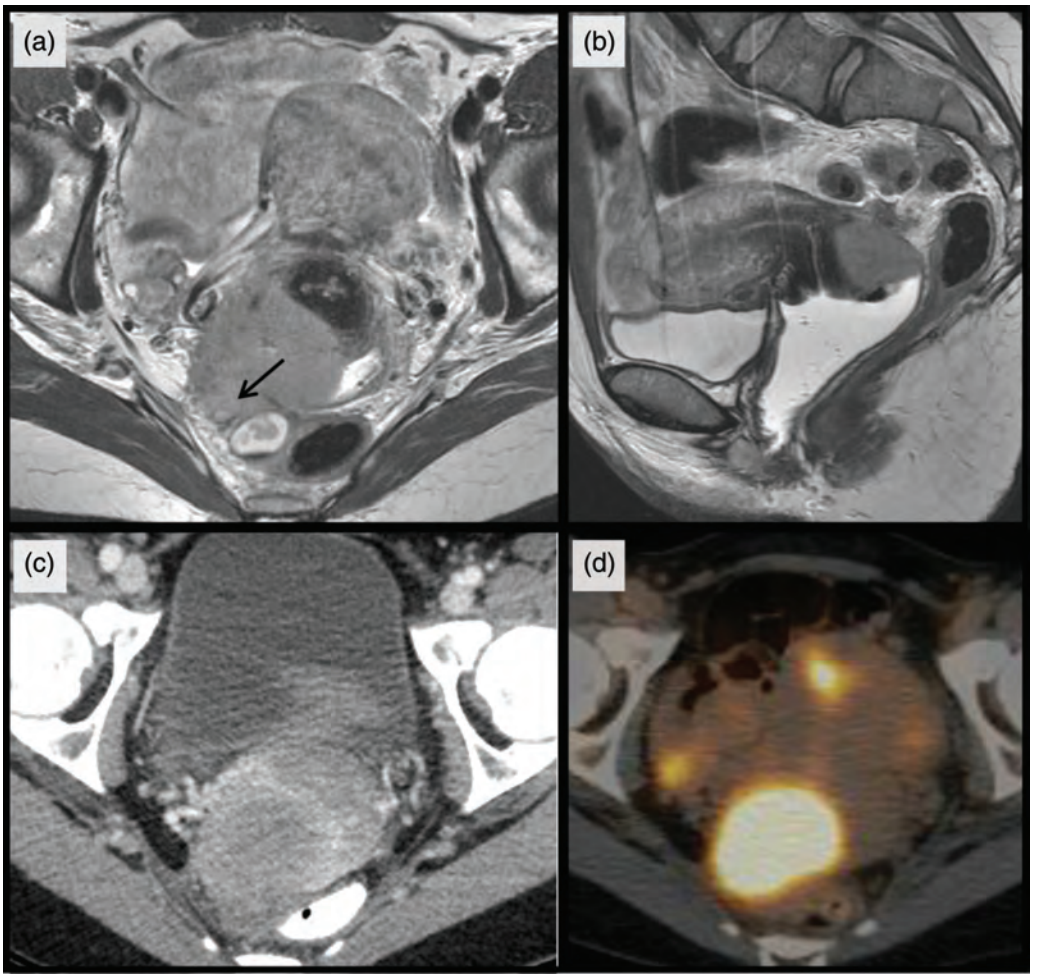

Figure 4.2. Axial MRI (a), sagittal MRI (b), CT (c), and FDG PET (d) showing a large cervical mass with extension toward the right parametrium (black arrow) and close to the rectum along the right utero-sacral ligament.

versus the cervix and the uterus and of parametrial invasion (see Section 5.4.5) (Hegazy *et al*., 2013). CT is, however, useful for the contouring of organs at risk (OAR) (Viswanathan *et al*., 2007).

4.4 Positron-Emission Tomography (PET–CT)

The role of PET-CT has been investigated for EBRT planning, in particular for assessing lymph nodes with increased uptake for possible boost therapy by conventional 3D-conformal techniques or by IMRT. The use of 2-(fluorine-18) fluoro-2-deoxy-D-glucose (FDG) in PET combined with CT is presently considered standard in the initial work-up of patients with cervical cancer (see Figure 4.2d) (Amit *et al*., 2011; Grigsby, 2009; Maffione *et al*., 2009). The FDG tracer is a glucose analog that is taken up by rapidly metabolizing cells. Uptake in the primary tumor and its extensions confirms the CT and MRI findings. Additionally, lymph nodes as small as 6 mm can show FDG positivity and hence be considered abnormal, rather than demanding the 1 cm size criterion used in traditional CT imaging (see Figure 4.5). Especially important are areas of uptake in the para-aortic and supra-clavicular lymph nodes, which, if identified, would alter the treatment and prognosis of these patients (Kidd *et al*., 2012). Bone metastases can also be detected through the use of PET rather than of bone scans. Positron-emission tomography scanning is also an important tool to assess treatment response and is especially helpful at 3 months following completion of radiation therapy when residual uptake is indicative of residual disease and poor prognosis (Grigsby, 2007). Positron-emission tomography is also useful in detecting asymptomatic recurrences, which can be capable of salvage if found prior to symptom development (Brooks *et al*., 2009). Positron-emission tomography is not particularly effective for the liver due to the background uptake of FDG, and might also be non-diagnostic in lung nodules less than 6 mm in size.

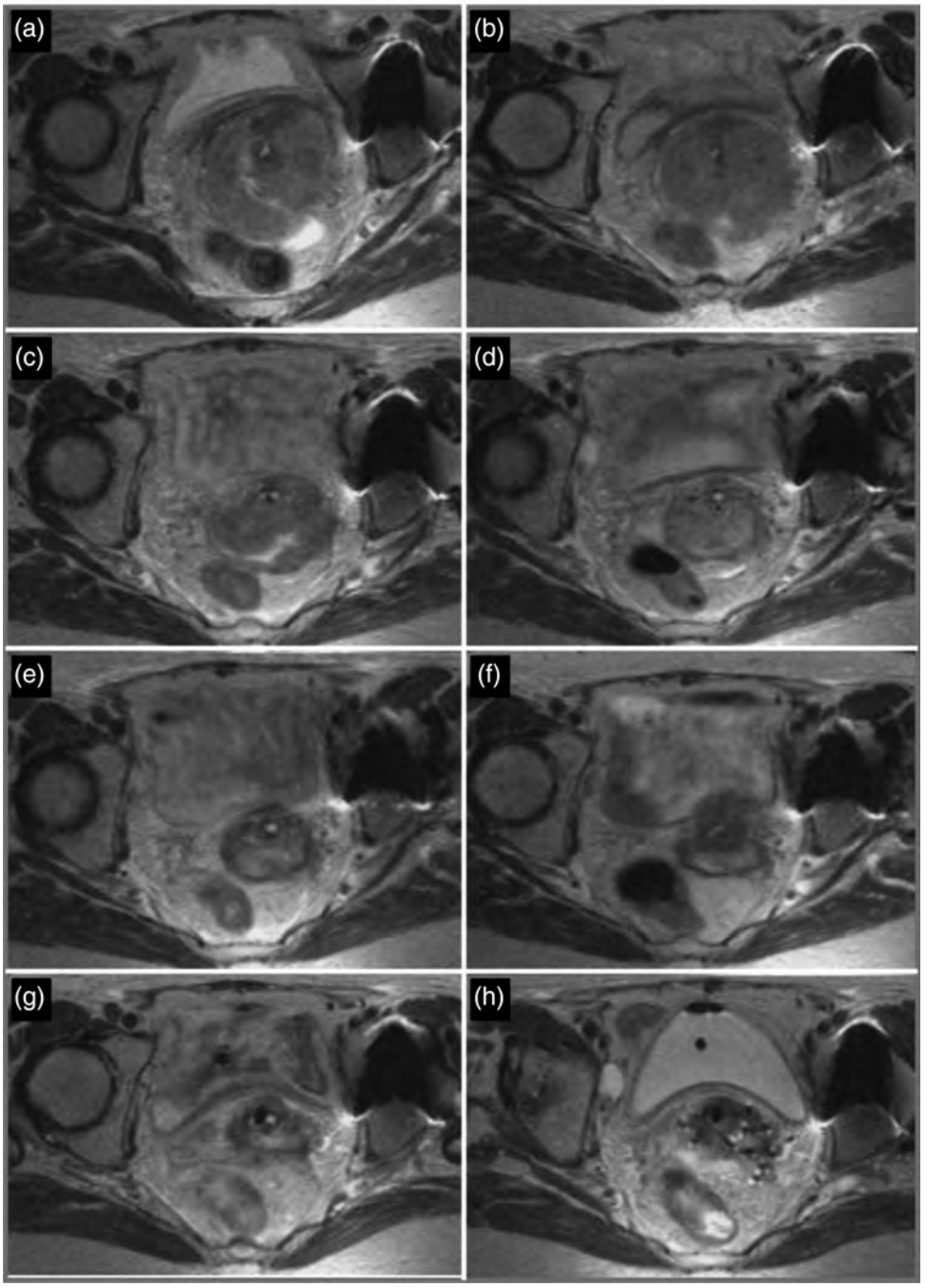

Figure 4.3. Magnetic resonance images revealing tumor regression in a patient with Stage IIIB cervical cancer during radio-chemotherapy (1.8 Gy EBRT per fraction and weekly cisplatin, 40 mg/m^2): (a) at the time of diagnosis; (b) after first week of EBRT (9 Gy)/first cisplatin; (c) after second week of EBRT (18 Gy)/second cisplatin; (d) after third week of EBRT (27 Gy)/third cisplatin; (e) after fourth week of EBRT (36 Gy)/fourth cisplatin; (f) after fifth week EBRT (45 Gy)/fifth cisplatin; (g) first intracavitary brachytherapy insertion ($D_{90\ \%}$: 2 × 7 Gy CTV_{HR}); and (h) second intracavitary/interstitial brachytherapy insertion (D90: 2 × 8 Gy CTV_{HR}). The total absorbed dose in the CTV_{HR} is 90 Gy ($EQD2_{10}$) (see Sections 2, 5, 7, and 8 for explanation of terms).

Positron-emission tomography–CT has limited applicability in image-guided adaptive brachytherapy, as the tracer uptake is limited following simultaneous radio-chemo-therapy, and thus provides limited information on residual disease (Kidd and Grigsby, 2011).

4.5 Ultrasound

The appeal of US lies in its widespread availability, low cost, reasonable soft-tissue contrast sensitivity, and absence of ionizing radiation. It is used frequently by gynecologists to assess the etiology of

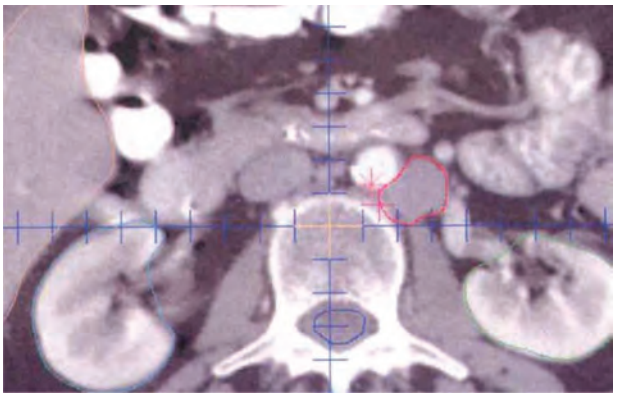

Figure 4.4. Enlarged para-aortic node, contoured in red, visible on an axial CT slice.

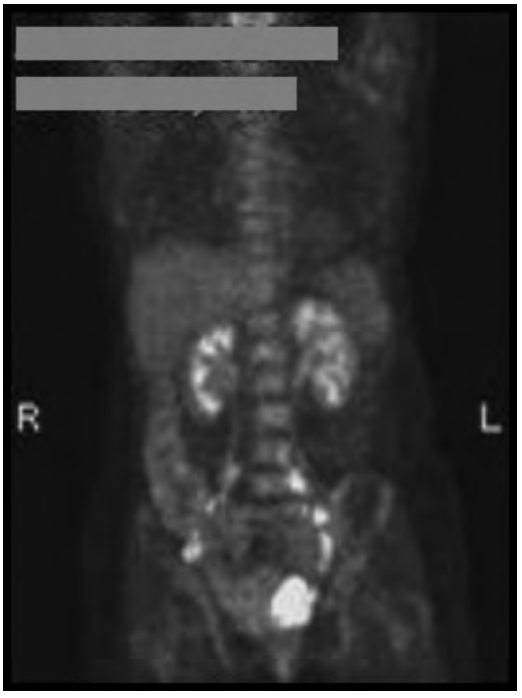

Figure 4.5. 2-(Fluorine-18) fluoro-2-deoxy-D-glucose PET-CT exam revealing a large cancer of the cervix on the left and multiple internal and common iliac nodes with increased FDG activity.

vaginal bleeding prior to surgery, often with findings of an endometrial cancer. In the context of radiation-therapy planning, however, there is limited recent literature on the use of US for cervical cancer brachytherapy (Narayan *et al.*, 2011; Schmid *et al.*, 2013a). Trans-abdominal, trans-rectal, and trans-vaginal US imaging might be performed (see Figure 4.6). Trans-vaginal US appears to be of less value due to its limited view of the parametria for delineation of extra-cervical disease and due to the limited space in the vagina after applicator insertion. For the assessment of the uterine body and cervical dimensions, a strong correlation between trans-abdominal US and

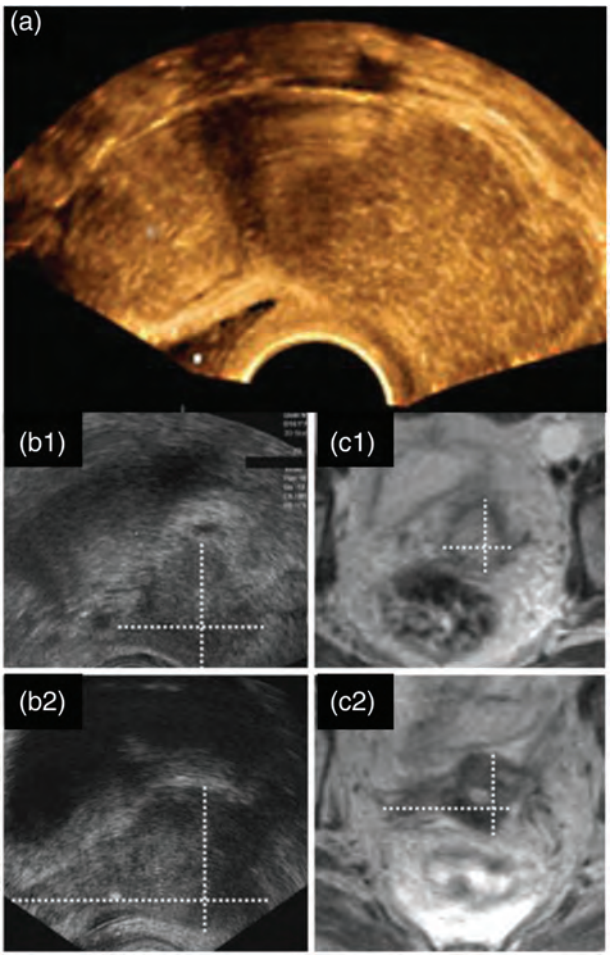

Figure 4.6. Ultrasound of cervical cancer: vaginal 3D endosonography of bulky cervical cancer infiltrating into the uterine corpus [from Figure 1.1. (Olpin and Tempany, 2011)]; trans-rectal US (b) and MRI (c) of advanced cervical cancer with bilateral proximal (1) and right distal (2) parametrial involvement at the time of brachytherapy without the applicator in place (Schmid *et al.*, 2013a).

MRI has been reported, indicating a potential for US-based treatment planning (Mahantshetty *et al.*, 2012; Van Dyk *et al.*, 2009). Furthermore, it has been shown that tumor size measured by trans-rectal US is a prognostic factor for relapse of cervical cancer (Magee *et al.*, 1991). The accuracy of trans-rectal ultrasound (TRUS) for staging cervical cancer, compared with the surgical findings, was reported in one study as 83 % (Innocenti *et al.*, 1992). Comparisons between TRUS and MRI in the assessment of tumor dimensions and tumor volume are currently being debated (Fischerova, 2011; Fischerova *et al.*, 2008; Hawnaur *et al.*, 1998; Schmid *et al.*, 2013a).

4.6 Radiography

Radiographic imaging has been used for local FIGO staging by assessing ureteral obstruction by

IVU (Stage IIIB), bowel invasion by BE (in addition to rectal endoscopy) (Stage IVA), bladder invasion by cystograms in addition to cystoscopy (Stage IVA). Bipedal LAG has been widely performed to assess lymph-node involvement (N category in the TNM classification) along the inguinal, iliac (external/common), and para-aortic regions.

Chest x ray and skeletal films have been used to assess lung metastases (M category in the TNM system) and to confirm bone metastases in suspicious lesions found through bone scintigraphy.

Treatment-planning radiographs have been used to document the position of the applicator in relation to the bony anatomy and the position of the rectosigmoid and the bladder (ICRU, 1985). Due to the difficulty of identifying the same points in each structure on both the anteroposterior and lateral radiographs, the role of contrast-enhanced 2D imaging of the rectosigmoid, bowel, bladder, and for point-based dosimetry is not established. Some institutions use clips to mark the cervix or vaginal extensions of disease.

With the advent of computerized treatment planning, radiographs have been taken in two (orthogonal) orientations with a 3D reference system (*e.g.*, reference box) to create individualized point-based dosimetry based on key applicator and reference point(s), including Point A, Point B, and ICRU bladder and rectum points, for a treatment plan (ICRU, 1985). This can be aided by drawing the tumor extension and/or the tumor width, thickness, and height in relation to the applicator onto the radiograph and/or the treatment plan (see Figure 4.7, lateral radiograph). This radiography-based 3D treatment planning, relying on bony landmarks and reference points (see

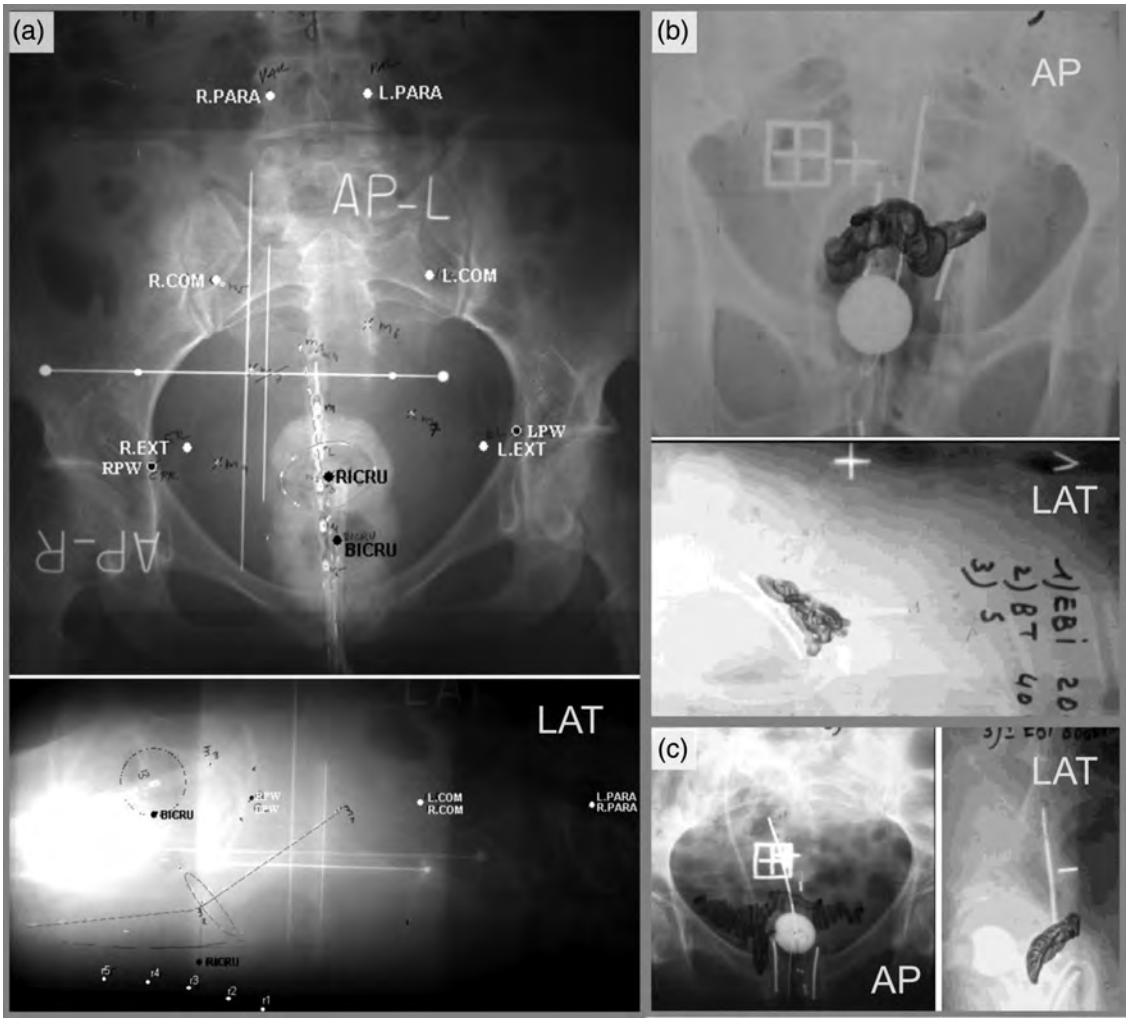

Figure 4.7. Anteroposterior and lateral radiographs with tandem-ring (a) and tandem-mold (b and c) applicator in place with bladder balloon, vaginal contrast [contrast medium (a); air (b) and (c); rectal probe in the rectum (a)] as basis for radiographic approximation of target dose [from the GEC ESTRO Handbook of Brachytherapy 2002 (Gerbaulet *et al*., 2002a)]. (a) Bladder (BICRU) and rectum (RICRU) reference points (compare with Figure 10.6), rectal probe points, pelvic wall points, and lymphatic trapezoid (compare with Figures 10.4 and 10.5); (b and c) Delineation of the tumor extension based on gynecologic examination at diagnosis (IIB and IIIB) for radiographic approximation of target dose (see also Section 10.3, Figure 10.3).

Section 10 and Appendix Examples A.4, A.7, A.9), has to be differentiated from volumetric-imaging-based "full" 3D treatment planning relying on soft-tissue information from CT or MRI (see Sections 8.3 and 8.4 and Appendix Examples A.1-3, A.5, A.6, A.8).

4.7 Imaging in Treatment Planning

The adoption of advanced, 3D volumetric-imaging tools has enabled improved treatment of gynecologic cancers. CT simulators are standard in many centers, and the number with MRI and positron-emission tomography (PET-CT) capabilities are increasing. These tools aid in improving external-beam therapy and customized brachytherapy absorbed-dose distributions. In addition, daily image-guided radiotherapy (IGRT) techniques can reveal any organ and target motion/regression relative to the beam, to confirm beam placement, potentially reducing morbidity, or allowing for absorbed-dose escalation (Erickson *et al*., 2011).

4.7.1 Imaging in external-beam radiotherapy

Rather than using just bony anatomy for treatment-field delineation, the use of CT or MR images to accurately define the targets of interest, as well as the OAR, has become increasingly standard, and allows for better absorbed-dose coverage of the defined targets and better sparing of the normal tissues (Finlay *et al*., 2006; McAlpine *et al*., 2004) (see Figure 4.8). This is true for traditional 3D conformal-radiation techniques (3D CRT) and increasingly true for the use of IMRT. A crucial prerequisite for the successful application of IMRT plans is a critical assessment of the anatomy of each individual patient based on volumetric CT or MR imaging (Erickson *et al*., 2011). Ideally, the MRI should be done immediately before or after the planning CT in order to minimize discrepancies in organ size and position due to factors such as bladder and rectal filling. With such imaging, the target tissues and OARs can be contoured to direct the creation of an IMRT plan (3D CRT) (Erickson *et al*., 2011). Consensus guidelines have been developed both for post-operative and intact-pelvis CTV contouring, providing a framework for standardization of volumes and absorbed doses (Erickson *et al*., 2011; Lim *et al*., 2011; Small *et al*., 2008). Important variables such as organ filling, organ and tumor motion, and tumor regression over time continue to pose a challenge and have led to the use of daily IGRT. With IGRT, either kilo-voltage or mega-voltage CT images are used to align the pre-treatment CT plan with the daily pre-treatment CT to improve the accuracy of field placement. MR-based-treatment-imaging and delivery-system developments are beginning to appear in clinical research projects (Raaymakers *et al*., 2009). Immobilization of patients as well as control of organ filling is particularly important for reproducibility.

Various image-fusion techniques are now in use to help delineate the targets of interest with greater accuracy. Treatment-planning CT images can be fused with a PET-CT images, also performed in the treatment position to help better define the metabolically active components of the cervical mass as well as the lymph nodes seen on CT. Imaging the metabolically active primary cervical tumor can improve target delineation (Kidd and Grigsby, 2011). The use of MRI simulation, or MRI fusion with CT, especially when using IMRT, is particularly appealing in patients with cervical and vaginal cancers.

4.7.2 Imaging in brachytherapy

Three-dimensional imaging enables the delineation of both the tumor at diagnosis (GTVinit) and at

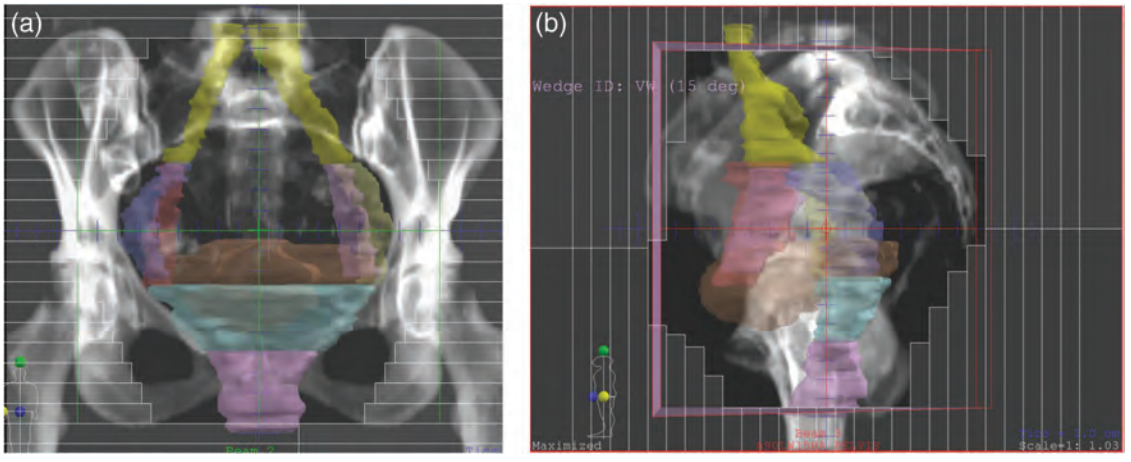

Figure 4.8. Anteroposterior (a) and lateral (b) pelvic fields defined by multi-leaf collimation (MLC) after contouring the targets and OAR.

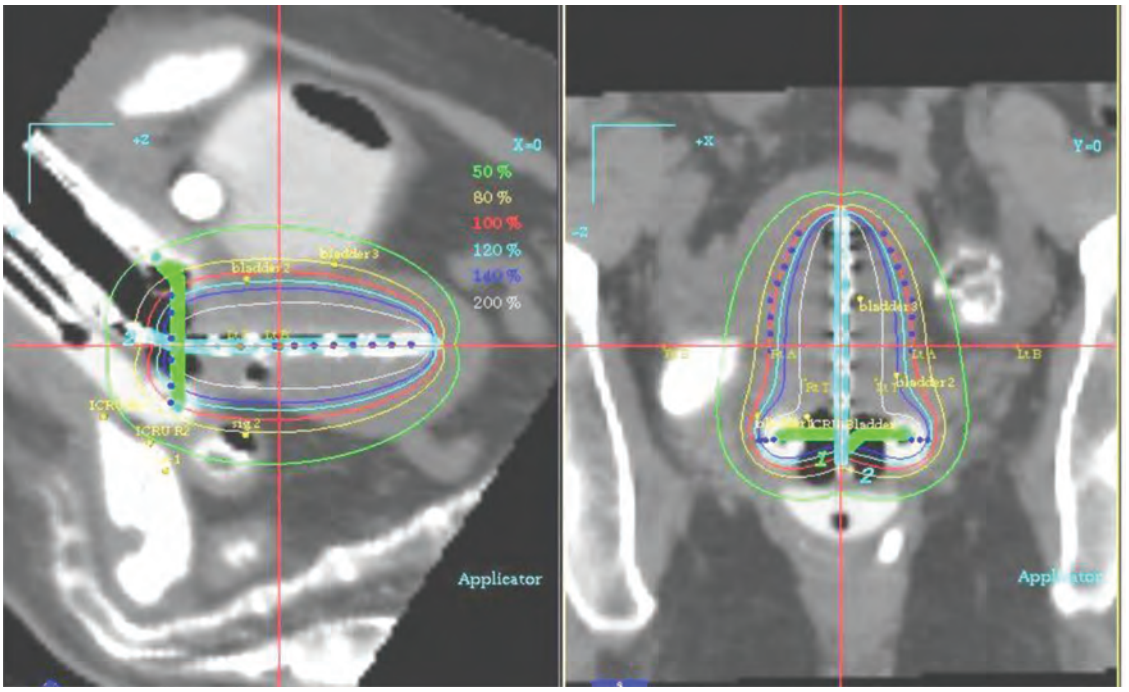

Figure 4.9. Computed tomography-based computerized treatment planning with the applicator in place, with associated isodoses in sagittal and coronal planes.

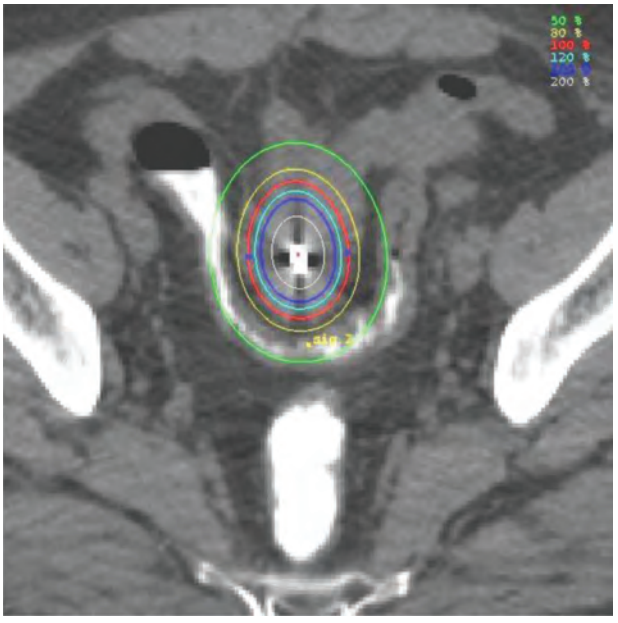

Figure 4.10. Axial CT slice showing a contrast-filled loop of sigmoid in close proximity to the high-absorbed-dose–volume from the intrauterine applicator, necessitating a change in loading pattern.

the time of brachytherapy (GTV_{res}), the high risk CTV [cervix, residual GTV, residual pathologic tissue (see Section 5.2)], and the OAR (see Section 6.3) and thus provides the basis for optimization of the absorbed-dose distribution within an adaptive approach. CT imaging following applicator placement allows immediate confirmation of the position of the applicator relative to the cervix and adjacent OAR (see Figures 4.9 and 4.10).

The greatest value of CT has been in gaining a better understanding of topographic relationships of OAR and subsequently absorbed doses in organs close to the applicators (see Figures 4.9 and 4.10). Point doses, isodose curves, and dose–volume histograms can be generated and used to define treatment.

The sigmoid, which might be subject to late ulceration and strictures, can weave much closer to the applicator with time between imaging and irradiation or during fractionated PDR brachytherapy than the displaced rectum located near the rectal ICRU Report 38 point. The sigmoid has typically been ignored because of the difficulty in opacifying and localizing it on plain-film images but is at considerable risk as it is above the vaginal packing or retractors and can weave very high around the uterine tandem (see Figure 4.10) or dip very low, close to the vaginal applicators (see Appendix). CT is excellent at visualizing these organ locations (Erickson *et al*., 2011; Lim *et al*., 2011; Shin *et al*., 2006). CT-based generation of dose–volume histograms for OAR (see Section 8.4) allows for a more reliable estimation of absorbed doses in the OAR and is currently regarded as the minimum requirement in image-based cervical cancer brachytherapy.

Even with CT-compatible applicators, the boundaries between structures of interest can be poorly defined using CT. The value of MRI in the imaging

of gynecologic cancers lies in its multi-planar capability and superior soft-tissue resolution compared with CT, enabling delineation of tumor within the cervix and uterus as well as within the parametrial and vaginal tissues (Erickson, 2003; Erickson *et al*., 2011; Wachter-Gerstner *et al*., 2003); this is true even for the residual tumor after external-beam therapy. Furthermore, residual pathologic tissue can become visible in areas occupied by the initial tumor. Tumors of the cervix display moderately increased signal on T2-weighted images relative to normal cervical stroma, permitting definition of tumor volume. This is an advantage during brachytherapy as it is possible to assess the proximity of the tumor to the applicator and the subsequent absorbed-dose distribution throughout the tumor volume, permitting accurate determination and better control of the absorbed dose in the adjacent normal organs (Dimopoulos *et al*., 2012a; Erickson *et al*., 2011; Lim *et al*., 2011).

The GEC ESTRO working group developed recommendations for recording and reporting 3D-image-based treatment planning for cervical cancer brachytherapy. These discussions began in 2000 and were based on evaluations of repeated MRI and gynecologic examinations, and resulted in recommendations published in 2005 (Haie-Meder *et al*., 2005), which described a methodology using morphologic MRI [fast spin-echo sequences (FSE)] at the time of diagnosis and at brachytherapy to define the GTV_{init}, the GTV_{res}, and the CTV_{HR} (see Sections 5.3 and 5.4).

More detailed recommendations based on the GEC ESTRO recommendations for target delineation from 2005 were published recently (Dimopoulos *et al*., 2012a). These recommendations include performing pelvic MRI (T2-weighted) prior to radiotherapy and at the time of brachytherapy using preferably the same MR scanner. Correlation with the images from the pelvic examination and with gynecologic examination at each of these points is essential. Multi-planar T2-weighted images (FSE) obtained parallel and orthogonal to the uterus (applicator) axes in (para-) transverse, (para-) sagittal, and (para-) coronal orientation are considered the gold standard for visualization of the tumor, the uterus, the parametria, and the critical organs (Dimopoulos *et al*., 2012a). Dedicated MRI protocols tailored to the institution-specific magnet strength and scanner are crucial. Attention to bladder/bowel filling is important, as is reduction in bowel motion through the use of IV or intramuscular antispasmodic agents. Applicator MRI compatibility, applicator immobilization, and minimization of patient movement are key. The spatial accuracy of MR images is essential for precise absorbed-dose planning and applicator reconstruction, and minimization of susceptibility artifacts is of special importance. A slice thickness less than or equal to 5 mm is recommended to minimize reconstruction errors. Delineation of the source channel is key in generating an MRI-based dosimetry plan and can be achieved using MR-compatible markers, fusion techniques, or a vendor-provided library of applicators that can be brought into the planning system (Hellebust *et al*., 2010a). It is recommended that the MR images be viewed and interpreted on dedicated DICOM-viewer workstations. In conjunction with the schematic diagrams from the gynecologic examination, this provides the basis for the contouring procedure. Window and level settings can be key in the definition of the GTV and CTV_{HR} (see Sections 5.3.4 and 5.4.5). The accuracy of delineating contours improves with practice, image quality, and sequences tailored specifically to brachytherapy. Inter-observer and intra-observer variabilities exist, but can be minimized with optimal imaging and experience (see Section 5.4.6).

Positron-emission tomography–CT-guided brachytherapy was pioneered by Grigsby and his group (Kidd and Grigsby, 2011). The volume created by the 40 % threshold of the maximum standardized uptake value (SUV) is used to define the metabolically active (residual) cervical tumor following external-beam therapy, and can be used for delineation of the metabolically active (residual) tumor in relation to the brachytherapy applicators and the surrounding OAR, enabling optimization of the absorbed-dose distribution.

For brachytherapy, US can be used to ensure optimal positioning of applicators and needles within the target volume and to assist in detecting and contouring the target volume and OAR (Petric *et al*., 2011). Real-time US can be used during insertion of the intrauterine tandem to achieve optimal placement, for example, in patients with an obliterated endo-cervical canal or with complex pathology, and to prevent inadvertent uterine perforation (see Figure 4.11). Both trans-rectal and trans-abdominal US have been used in interstitial treatment to guide the depth of needle insertion. Post-insertion US can be used to measure the diameter of the cervix, the thickness of the uterine wall, and the thickness of the vagina at the time of brachytherapy to aid in absorbed-dose specification (Narayan *et al*., 2011; Schmid *et al*., 2013a; Van Dyk *et al*., 2009).

4.8 Summary

Assessment of disease in cervical-cancer staging is achieved by clinical examination, various imaging techniques, and laparoscopic procedures. Gynecological examination and imaging are repeated during treatment to monitor response and to guide additional boost treatment by brachytherapy.

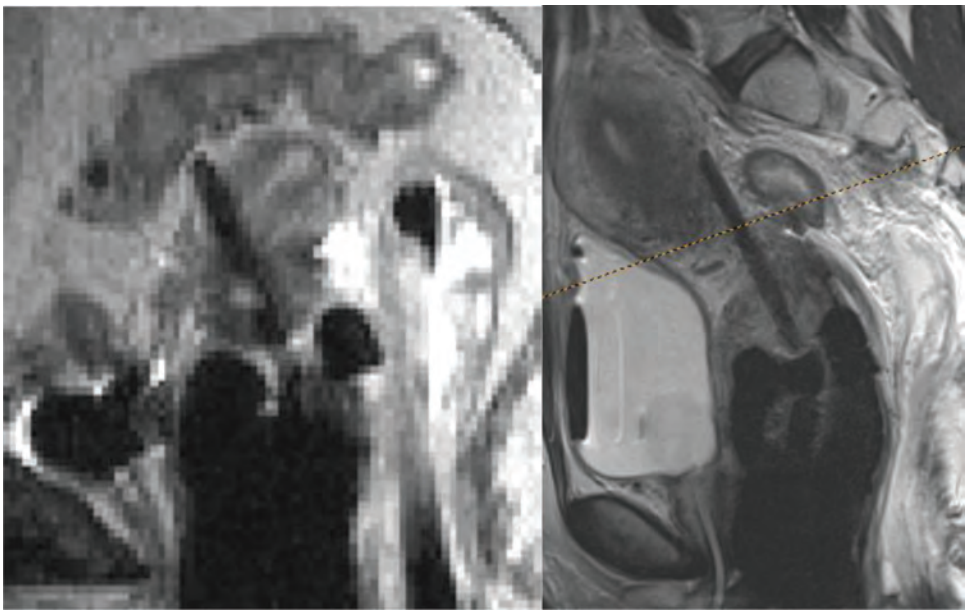

Figure 4.11. Examples of sagittal MRI with uterine tandem perforation. (Left) Patient with a retroflected small uterus, a large residual GTV, and an anterior perforation. (Right) Patient with large and hard residual GTV, no visible cervical os, a false posterior uterine pathway, and a posterior perforation.

Clinical gynecological examination remains essential, with detailed documentation on specific clinical diagrams both at diagnosis and following external beam at the time of brachytherapy.

Computed tomography, MRI, PET, and US are regarded as reliable and accurate tools with complementary capabilities in defining local, regional, and distant spread of disease.

Magnetic resonance imaging, with its excellent soft tissue resolution, is recognized as the most-accurate tool for the initial assessment of the tumor, monitoring of treatment response, and for brachytherapy treatment-planning guidance.

Computed tomography is regarded as a valuable tool for the initial staging of disease to exclude distant metastases and to detect enlarged lymph nodes but lacks the excellent soft-tissue resolution of MRI, and is therefore poor in local-disease assessment. Computed tomography is used routinely in the planning of external-beam radiotherapy. It is also useful for brachytherapy treatment planning for delineation of OAR, but is inferior to MRI in defining the cervix and extra-cervical soft-tissue extensions of disease at the time of brachytherapy.

Positron-emission tomography–CT is seen as the most-accurate imaging method for assessment of lymph-node and distant disease. Its role in brachytherapy treatment planning has not been clarified.

Ultrasound can be used for local-disease assessment and monitoring, and has a great potential to guide the brachytherapy application and treatment planning.

Radiography (IVU, chest radiographs, BE, skeletal survey) still forms the basis of the FIGO staging system and is useful in centers with limited resources for the initial staging of disease and plays an essential role in radiographic, point-based brachytherapy treatment planning.

4.9 Key Messages

- The initial evaluation of cervical cancer begins with clinical gynecologic examination and documentation and by drawing of the findings on clinical diagrams. This procedure is also used for monitoring tumor response.
- Initial staging involves MRI, CT, or PET-CT, where available, to establish a baseline comprehensive evaluation prior to treatment. The use of US, radiography (chest, IVU, skeletal), and scintigraphy can also be helpful, but the information they provide is more limited.
- Monitoring of disease regression during radiation treatment is important and is done through the use of repeated gynecologic examinations and imaging studies, before and at the time of brachytherapy to document disease regression and to plan brachytherapy.
- Magnetic resonance imaging and/or CT at the time of brachytherapy are essential—together with the information from gynecologic examination—to define a 3D target and the OAR in relationship to the applicator and the absorbed-dose distribution. Magnetic resonance imaging offers

superior soft-tissue resolution compared with CT and is essential for accurate assessment of local-tumor extension.

- If volumetric imaging is not available, clinical gynecologic examination alone can serve for definition of the target for brachytherapy (2D) with assessment and definition in particular of CTV width and thickness. Clinical drawing on a schematic diagram is essential. Radiography-based treatment planning can utilize such target dimensions. Information from clinical examination can be improved by additional information from any form of sectional or volumetric imaging, even if full imaging information with the applicator in place is not available.
- Treatment planning relying on 3D image-based techniques is superior to the use of bony anatomical reference structures.

Journal of the ICRU Vol 13 No 1–2 (2013) Report 89
Oxford University Press
doi:10.1093/jicru/ndw017

5. Tumor and Target Volumes and Adaptive Radiotherapy

5.1 Introduction and Overview

A series of ICRU Reports (ICRU, 1993b; 1999; 2004a; 2007; 2010) on prescribing, recording, and reporting several external-beam radiotherapy (EBRT) techniques, *viz*. photon-, electron-, and proton-beam radiotherapy and IMRT, provide fundamental and widely accepted terms and concepts that have had a significant impact on the clinical, scientific, and educational practice of radiation oncology. Reports on dose and volume specification for intracavitary therapy in gynecology (ICRU, 1985) and interstitial therapy (ICRU, 1997) have also been published. However, since these publications, important changes in brachytherapy practice have resulted from developments in engineering, computer technology, imaging, radionuclide, and dose rates, combined with an overall improved radio-oncological and radiobiological understanding in the field (Haie-Meder *et al*., 2011; Pötter, 2009). Many of these developments have been incorporated in the GEC-ESTRO recommendations for image-guided adaptive brachytherapy (IGABT) in cervical cancer (Dimopoulos *et al*., 2012a; Haie-Meder *et al*., 2005, Hellebust *et al*., 2010a, Pötter *et al*., 2006).

Radiotherapy for locally advanced cervical cancer is a prototypical example of adaptive radiotherapy that takes into account changes in tumor configuration, volume, and topography during the course of treatment (Tanderup *et al*., 2010b). The current report emphasizes the adaptive, four-dimensional (4D: three spatial dimension and time) treatment approach that aims to improve the efficacy:toxicity ratio by exploiting the tumor-volume regression often seen in cervical cancer after the first phase of treatment, a theme that is gaining prominence in (radiation) oncology in general (Yan, 2010). The concept of residual gross tumor volume (GTV_{res}) refers to the reassessed GTV after a significant part of the overall treatment has been completed (see Section 5.2.1.3); in cervical cancer treatment after external beam therapy with or without chemotherapy, it is often defined before boost brachytherapy (see Section 5.3.4). Correspondingly, an adaptive clinical target volume (CTV_{adapt}) can be delineated. In the case of brachytherapy for cervical cancer, CTV_{adapt} is often referred to as the high-risk CTV, CTV_{HR} (see Section 5.2.1.5).

For cervical cancer brachytherapy, the complex approach to adaptive radiotherapy has only recently been systematically described, especially for the combination of EBRT with boost brachytherapy (Haie-Meder *et al*., 2005; Pötter *et al*., 2006; 2008a). A rigorous description of adaptive radiotherapy for this disease requires the introduction of specific target volume concepts such as CTV_{HR} and the intermediate-risk CTV, the CTV_{IR}. These are illustrated in a set of clinical cases of cervical cancer of varying stage of disease (see Figures 5.7–5.14 and the Appendix).

Finally, this section briefly addresses the issue of adding margins to allow for geometric and dosimetric uncertainties (the planning target volume, PTV) for the specific situation of intracavitary brachytherapy (see Section 5.5).

5.2 Volume Definitions in Adaptive (Gynecological) Radiotherapy

GTV, CTV, and PTV are concepts defined for EBRT in ICRU Reports 50, 62, 71, and 78 (ICRU, 1993b; 1999; 2004a; 2007). Most recently, these concepts were discussed and expanded for use in IMRT in ICRU Report 83 (ICRU, 2010). Important recommendations of ICRU Report 83 on target volumes relevant to this report included:

- subdividing target volumes into primary tumor (-T), lymp node (-N), and distant metastasis (-M) volumes;
- specifying the method used for target selection and delineation {*e.g*., GTV-T (MRI, clinical examination) or GTV-T [FMISO positron-emission tomography (PET)/CT]}. These volumes might be nested or could be combined into a composite "clinical" GTV-T;
- specifying the accumulated dose (and the method used) at the time of target-volume assessment in adaptive treatment [*e.g*., CTV-N (26 Gy, CT)].

These recommendations are also relevant to adaptive gynecological radiotherapy, in particular when combined with brachytherapy as in cervical cancer treatment. These concepts are therefore translated, merged, and further developed for the currently established terminology of gynecological brachytherapy.

The initial gross tumor volume (GTV_{init}) is the macroscopically demonstrable extent and location of the tumor before any treatment. It can consist of a primary tumor (GTV-T_{init}), involved regional node(s) (GTV-N_{init}), or known distant metastases (GTV-M_{init}).

5.2.1 Tumor and Target Volume Definitions for the Primary Tumor

5.2.1.1 GTV for the Primary Tumor (GTV-T). The GTV-T is the basis for treatment prescription and planning. It is assessed by clinical, imaging, and/or pathology investigations and represents macroscopic demonstrable disease for the primary tumor according to the UICC TNM terminology (Sobin *et al*., 2009). Clinical and imaging investigations might yield different volumes. It is then the responsibility of the radiation oncologist in charge of the treatment to delineate a composite GTV-T in these situations (see Section 5.3.2). In the context of adaptive radiotherapy, it can be helpful to denote the initial GTV-T as GTV-T_{init} to distinguish this from the residual GTV-T as GTV-T_{res} (see Section 5.3.3).

5.2.1.2. CTV for the Primary Tumor (CTV-T). The CTV-T includes the GTV-T and a volume of surrounding tissue in which the risk of microscopic disease is deemed so high that this region should be treated with a dose sufficient to control microscopic disease (see Section 5.4). In early treatment of limited disease with brachytherapy, current practice often specifies a set of CTVs as described in Sections 5.2.1.9 and 5.4.4.2.

5.2.1.3 Residual GTV-T (GTV-T_{res}). The GTV-T_{res} is defined as the residual tumor *at the time of brachytherapy application* after treatment assumed sufficient to control microscopic disease. The GTV-T_{res} still has the clinical and/or imaging characteristics similar to the GTV-T_{init} and can likely represent macroscopic and/or microscopic disease, but might also be without residual disease. Using the terminology of ICRU Report 83 (2010), if 45 Gy has been delivered before the brachytherapy, the GTV-T_{res} could also be denoted GTV-T_{res} (45 Gy).

5.2.1.4 Adaptive CTV-T (CTV-T_{adapt}). The CTV-T_{adapt} can be defined after any treatment phase and includes the GTV-T_{res} and the residual pathologic tissue that might surround the residual GTV-T. The CTV-T_{adapt} bears different clinical and/or imaging characteristics (*e.g*., edema, fibrosis) compared with the GTV-T_{res}. It is located within the region of the initial CTV-T except in cases progressing locally during therapy. Furthermore, the CTV-T_{adapt} can also take into account anatomical compartments with a significant risk for residual tumor cells.

5.2.1.5 High-Risk CTV-T (CTV-T_{HR}). According to the GEC ESTRO recommendations for cervixal cancer radiotherapy, the CTV-T_{HR} is defined as the CTV-T_{adapt} that includes the GTV-T_{res}, the whole cervix, and adjacent residual pathologic tissue, if present. It is the volume bearing the highest risk for recurrence and is selected by clinical examination and imaging at the time of brachytherapy, *i.e*., after 40–45 Gy EBRT plus chemotherapy in locally advanced cervical cancer.

5.2.1.6 Intermediate-Risk CTV-T (CTV-T_{IR}). The CTV-T_{IR} represents the GTV-T_{init} as superimposed on the topography at the time of brachytherapy, together with a margin surrounding the anatomical cervix border (CTV-T_{HR}) in areas without an initial GTV-T_{init}. By definition, the CTV-T_{IR} therefore includes all of the CTV-T_{HR} and margins as appropriate.

5.2.1.7 Low-Risk CTV-T (CTV-T_{LR}). The CTV-T_{LR} represents compartments at risk for potential contiguous or non-contiguous microscopic spread from the primary tumor. In locally advanced cervical cancer, the CTV-T_{LR} comprises the whole parametria, the whole uterus, the upper part of the vagina, and the anterior/posterior spaces toward the bladder and rectum. This CTV-T_{LR} always includes the $CTV_{HR/IR}$. The CTV-T_{LR} is defined at the start of treatment (initial CTV-T_{LR}) and can be adapted according to the topographic and volumetric changes during EBRT and also at brachytherapy (adaptive CTV-T_{LR}).

5.2.1.8 Planning Target Volume (PTV-T). The PTV-T is a dosimetric concept determined by geometrical expansion of the CTV (*i.e*., by adding a "PTV margin") to account for geometric and dosimetric uncertainties. The PTV-T is essential in EBRT to ensure that the delivered dose to the CTV is within the limits defined in the dose prescription. The dosimetric uncertainties in brachytherapy differ from those in EBRT and in general would not be accommodated by defining a PTV by adding margins as in EBRT. Such margins will effectively escalate the dose throughout the target volume (see Section 5.5). Thus, addition of PTV margins after applicator insertion is not recommended in general. On the other hand, internal motion of the CTV-T_{HR} relative to the applicator will be minimal if the applicator is fixed (*e.g*., by an intra-vaginal tamponade). However, geometric uncertainties can occur (Tanderup *et al*., 2013), in particular in the direction

of the longitudinal axis of the tandem. As margins along the longitudinal axis of the tandem have very limited impact on the dose throughout the target, longitudinal margins can be added to compensate in part for set-up variations, even after application.

5.2.1.9 Initial Treatment based on Different CTV-Ts. In treatment of limited disease with early brachytherapy, current clinical practice of IGABT often defines three CTV-Ts at the time of diagnosis: CTV-T_1 is the GTV-T and adjacent tissue, always including the whole cervix; CTV-T_2 includes the CTV-T_1 plus margins; CTV-T_3 includes the CTV-T_2 plus sub-volumes of adjacent compartments at risk for potential contiguous or incontiguous microscopic invasion (see Section 5.2.1.7). Such concept is also considered for adaptive EBRT in locally advanced disease based on these definitions.

The terms initial CTV-T_{HR}, initial CTV-T_{IR}, and initial CTV-T_{LR} can be used also for CTV-T_1, CTV-T_2, and CTV-T_3 in limited disease treated with brachytherapy at the beginning of EBRT. It can be used in addition for any other clinical scenarios and treatment techniques that ask for an upfront definition of these CTV-T volumes, as, for example, in adaptive EBRT of locally advanced cervical cancer. CTV-T_1, CTV-T_2, and CTV-T_3 can then also be called "Initial CTV-T_{HR}," "Initial CTV-T_{IR}," and "Initial CTV-T_{LR}," respectively.

5.2.2. Target Volume Definitions for Nodal and Metastatic Disease

The recommended terminology for nodal and metastatic target volume definitions—except for the primary-tumor-related volumes—are in principal those of ICRU Report 83, as these volumes are mainly treated with EBRT. However, the concepts and terms for adaptive radiotherapy as elaborated in this report can be further developed and adopted also for nodal and metastatic disease (see Section 5.4.4.4).

5.3 Clinical Aspects of Selecting and Contouring the Initial (GTV-T_{init}) and Residual (GTV-T_{res}) GTV-T

5.3.1 Concept of the GTV

Complete and accurate staging and delineation of the GTV for cervical cancer requires specification of the tumor location and its extent in all dimensions (in particular the width as the most important tumor-related prognostic factor), its volume, and its growth pattern (expansive/infiltrative). The dimensions and anatomical location of the GTV still form the major basis of the FIGO and TNM classification systems (see Table 2.1 in Section 2) (Pecorelli, 2009; Sobin *et al*., 2009) and the WHO International Code for Disease in Oncology (ICD-O-3) (WHO, 2000). The stage classification, including nodal disease, represents the major prognostic factor. The GTV-T should be described in relation to the cervix, parametria, and pelvic wall, as well as the uterine corpus, the vagina, and the adjacent organs. As a minimum requirement, the GTV-T size should be specified in terms of maximum width (latero-lateral dimension) and thickness (dorso-ventral dimension, in a plane perpendicular to the cervix axis). In locally advanced disease, height (cranio-caudal dimension in a plane parallel to the cervix axis) can be assessed only if appropriate imaging is available (see Figures 5.1 and 5.2).

Although the concept of the GTV itself is straightforward, accurate delineation of any GTV relies on discrimination between malignant tumor and normal tissue, which is dependent on the physician and the diagnostic tools used.

In general, separate GTVs are delineated for the primary tumor (GTV-T) and the regional node(s) (GTV-N). In some clinical situations, however, the metastatic node is not easily distinguishable from the primary tumor at diagnosis [*e.g*., in cervical cancer infiltrating the pelvic side wall (Stage IIIB) with enlarged internal iliac nodes present]. In this case, a single GTV encompassing both the primary tumor and the node(s) might be delineated for planning the primary chemo-radiotherapy. This can be adapted during the course of treatment according to the volume regression of the macroscopic primary or nodal tumor.

5.3.2 GTV-T Selection and Delineation

The GTV-T_{init} includes macroscopic tumor extension at diagnosis as detected by clinical examination (GTV-$T_{init/clin}$) or as visualized on MRI as a mass with high signal intensity using T2-weighted, fast spin-echo sequences (FSE) (GTV-$T_{init/MRI}$, or as composite GTV-$T_{init/MRI+clin}$) (see Figures 5.2a, 5.4.1a, and 5.4.2a). As for cervix cancer the GTV-T_{init} is difficult to visualize directly on CT; it can be superimposed on CT from clinical examination, GTV-$T_{init/clin: CT}$, or more accurately from MRI, GTV-$T_{init/MRI: CT}$.

5.3.2.1 GTV-T Selection and Investigation Technique. In radiation oncology in general, CT and MRI are the most commonly used imaging modalities for delineating the GTV-T and serve as a complement to clinical examination for tumors that are clinically accessible. Increasingly, PET–CT and functional MRI are being introduced to improve the evaluation of the GTV. The delineated GTV-T

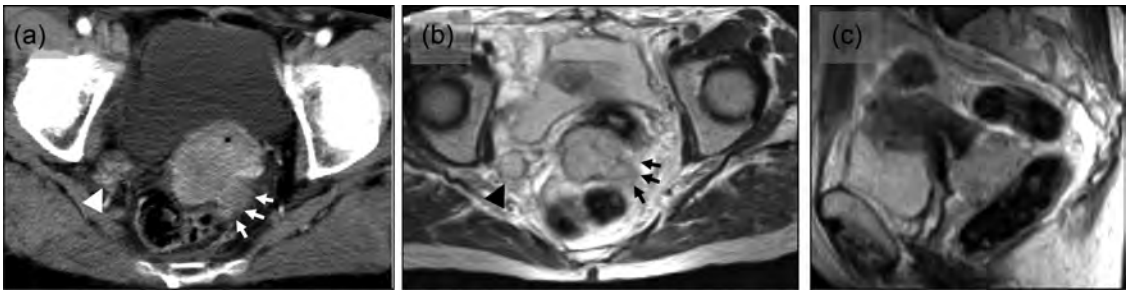

Figure 5.1. Intravenous-contrast-enhanced pelvic CT and T2-weighted FSE MRI of a patient with locally advanced cervical cancer, illustrating superiority of MRI in imaging the local-tumor extent and the muscular walls of the organs at risk. (a) An irregular, contrast-enhanced large cervical mass (white arrows) is seen on CT with transposition of the cervix to the left side (lumen visible). Irregular border between the cervix and the parametrium on the left suggests tumor invasion (white arrows). Contrast enhancement at the posterior aspect of the right internal obturator muscle is indicative of a pathologically enlarged lymph node (white arrow-head). The outer contours of the rectum and bladder are well visualized. (b and c) T2-weighted FSE MRI of the same patient offers improved soft-tissue visualization. Transverse and sagittal projections reveal a high-signal intensity lesion in the postero-inferior aspect of the cervix, representing the GTV (black arrows). The tumor exhibits a combined infiltrative and exophytic growth pattern with protrusion into the vagina, invasion of the posterior and left vaginal fornix, and infiltration into the left parametrium (black arrows). Anterior and superior to the lesion, the cervical tissue demonstrates its normal low-signal intensity, with a hyper-intensive signal of the mucus-containing cervical canal. A pathologically enlarged lymph node at the posterior aspect of the right internal obturator muscles (black arrow-head) shows high signal intensity, resembling the appearance of the primary tumor. In addition to their outer contours, hypo-intensity-signal walls of the rectum and bladder are clearly seen.

can vary significantly depending on the assessment method (see Figure 5.1); therefore, the method(s) used to delineate the GTV must be specified and reported [*e.g.*, GTV_{clin}, GTV_{CT}, GTV_{MRI}, $GTV_{PET\ CT}$, as proposed in ICRU 83 (Geets *et al.*, 2006; 2007; ICRU, 2010)]. For locally advanced disease, MRI is widely accepted as the gold standard for clinical staging, radiotherapy planning, and assessment of treatment response and recurrent disease (Hricak *et al.*, 1993). Magnetic resonance imaging is regarded superior to CT and Ultrasonography (US) for primary-tumor assessment, except for small-volume disease in stage IB (Epstein *et al.*, 2013; Hricak *et al.*, 2007; Mitchell *et al.*, 2006) (see Figure 5.1). However, clinical examination remains a valid and useful primary method of assessment. Topographical descriptions, indicating dimensions (width, thickness, height) and the overall volume, should be given as accurately as possible, always stating the method of evaluation (see Figures 5.1, 5.2a, 5.4.1a, and 5.4.2a).

Computed tomography has limited value for delineating the GTV-T in cervical cancer because of poor discrimination between normal soft tissues and tumor in most cases (see Figure 5.1). Ultrasonography provides good discrimination between the hypo-echogenic tumor and, for example, the hyper-echogenic (fatty) parametrial tissue as the echogenicity is different (see also Figure 4.6) (Schmid *et al.*, 2013a).

The information from different assessment methods is often complementary (see Section 4). For evaluation of vaginal disease, clinical examination with inspection and palpation, possibly supported by a vaginal impression (Magne *et al.*, 2010), is of major value. Magnetic resonance imaging following a specific protocol (*e.g.*, vaginal filling with ultrasound gel to visualize vaginal walls) provides additional information on vaginal infiltration depth, but limited information on superficial mucosal infiltration (Dimopoulos *et al.*, 2006b; 2012a; Van Hoe *et al.*, 1999). For assessing the tumor width, with or without infiltration into the parametrium, as well as tumor thickness, MRI, US, and vaginal and rectal clinical examination provide essential and comparable information. In most cases, tumor height is difficult or impossible to assess by clinical examination or CT, whereas it appears to be precise with MRI. Positron-emission tomography/CT for primary-tumor delineation appears promising, but more data are needed (Kidd and Grigsby, 2011).

5.3.2.2 Identification of Sub-GTV-T(s). The use of functional imaging with PET using various tracers or with functional MRI can add to the delineation of the GTV by showing, for example, cellular functionality such as hypoxia, which is likely to have impact on the treatment outcome (Gregoire *et al.*, 2003; Kidd *et al.*, 2013; Schuetz *et al.*, 2010). The identification of functional sub-GTV(s) by a suffix (*e.g.*, $GTV_{Faza\text{-}PET\ CT}$ for a hypoxic sub-volume) will avoid the introduction of new or potentially confusing terminology [*e.g.*, biological target volume, metabolic target volume, or hypoxic target volume (Kidd *et al.*, 2013; Ling *et al.*, 2000)]. The sub-GTV approach is able to cover all the different situations that might be encountered (Ling *et al.*, 2000). Functional imaging can be used repetitively indicating changes in functional (sub)-GTV during the course of treatment (residual sub- GTV) (Haack *et al.*, 2010). It is important that the method used to

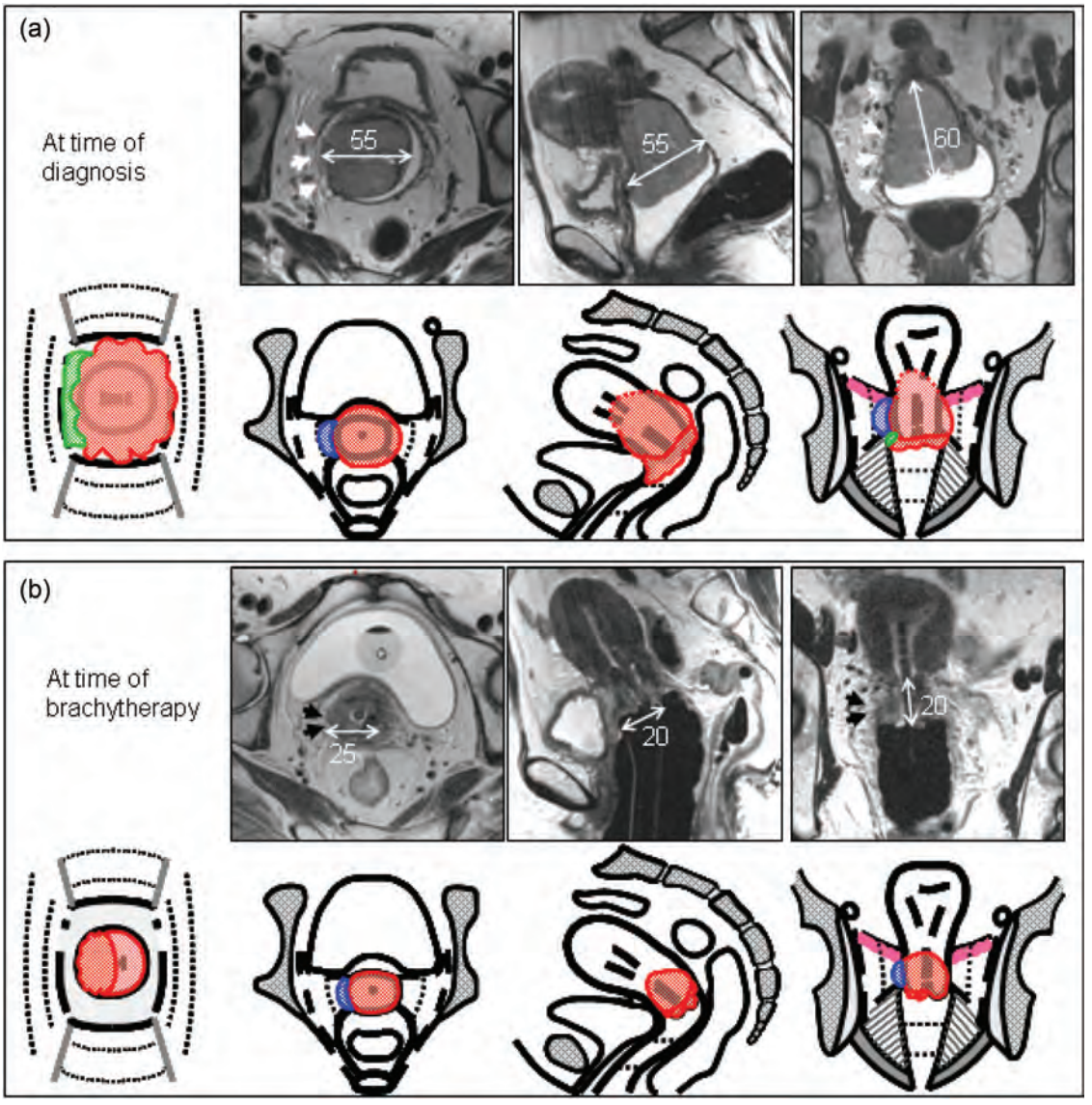

Figure 5.2. Magnetic resonance imaging and clinical findings at diagnosis (a) and at the start of brachytherapy (b), following EBRT (45 Gy in 25 daily fractions) with concomitant weekly cisplatin, 40 mg/m^2. FIGO and MRI Stage: IIB. Good response to treatment. (a) Initial T2-weighted FSE MRI in transverse, sagittal, and coronal planes reveal hyper-intensity-signal tumor mass in the caudal part of the cervix, distorting the cervico-uterine canal. Predominantly, expansive growth is seen in its cranial and left extent, with a preserved rim of hypo-intensive cervical stroma. Proximal parametrial infiltration is present on the right side, as demonstrated by the disappearance of the normal cervical stroma and spicular tumor projections in the parametrium (white arrows). Vaginal walls and fornices were unfolded by intra-vaginal injection of gel, revealing right parametrial infiltration of approximately 5 mm. The composite clinical/radiological drawings demonstrate in a systematic way the dimensions (width, height, and thickness) of the initial GTV and its relations to the normal tissues as assessed by the clinical and MRI examination. Invasion into the uterine cervix and corpus (red), the parametria (blue), and vagina (green), and its relations to the bladder, rectum, and pelvic wall are outlined. The dotted red line in the direction of the uterine corpus reflects the difficulty in clinical assessment of tumor height, which is identified mainly from the MRI. Speculum view of the tumor is shown in the inset. (b) T2-weighted FSE MRI at the time of brachytherapy in para-transverse (perpendicular to cervical canal), para-sagittal, and para-coronal (parallel to cervical canal) planes. The applicator (intrauterine tandem and vaginal ring) is inserted. The vagina is distended by vaginal packing, producing a signal void. Magnetic resonance imaging reveals residual high-signal-intensity tissue, the GTV_{res}, located mainly in the caudal and right parts of the cervix. The width, thickness, and height of the GTV_{res} are shown (see Section 5.3.3). Residual intermediate-signal pathological tissues (the grey zones) are present in the right parametrium, corresponding to the location of the initial tumor infiltration (black arrows). The drawings demonstrate clinical and MRI findings in a composite, systematic way, including the dimensions of residual GTV and the residual pathological tissues in the right parametrium. Disappearance of vaginal infiltration is documented.

evaluate the size and shape of the sub-GTV be specified, as different imaging methods can result in different delineated sub-GTVs.

At present, there is no clear indication on how to use functional imaging for cervical cancer sub-GTV assessment, leaving this field open for future research.

5.3.2.3 The Composite GTV: The GTV-T. The GTV-T is the volume finally chosen by the oncologist for treatment planning, and this is the result of considering information from different clinical and imaging investigations. This final GTV-T used for treatment planning is called the composite GTV-T. The dimensions and the volume of this composite GTV-T should be reported as comprehensively as possible, together with its topographical relationships.

It is essential that the methods used for defining the composite GTV-T are clearly described as pointed out here (see Figures 5.1, 5.2, and 5.4) and in the clinical examples in the Appendix. In cervical cancer, the GTV-T assessment is at present recommended to be based both on MRI and clinical examination. Together they are regarded as the gold standard for the decision on the composite GTV-T, which is then a GTV-$T_{clin+MRI}$ (see Figures 5.2 and 5.4, and the clinical examples in the Appendix).

5.3.3 Change of Primary Tumors during Treatment: The Initial GTV-T (GTV-T_{init}) and the Residual GTV-T (GTV-T_{res})

(Chemo-)radiotherapy is delivered over a period of several weeks, often causing changes of tumor characteristics, dimensions, volume, and topography, and allowing treatment adaptation according to tumor response (Yan, 2010). Many tumors show significant volume regression during the first weeks of radiotherapy, and the regression is generally more pronounced after combined chemo-radiotherapy. Tumor regression during treatment has long been recognized, but can now be better visualized and quantified by state-of-the-art 3D and 4D repeated CT, MRI (US), and functional imaging.

The change of the tumor during treatment can impact treatment strategies at any time. The GTV-T_{res} as defined in this report should be used only for adapting the target volume after delivery of a radiation dose (*e.g.*, 45–50 Gy) regarded as sufficient to control microscopic disease. For any other situation, the radiation dose delivered should be indicated (*e.g.*, GTV-$T_{res\ 25\ Gy}$). There is evidence from other tumor histologies, in particular rectal cancer, that the visualized residual GTV-T after 50 Gy of preoperative radiotherapy or chemo-radiotherapy might contain macroscopic, microscopic, or no disease at the time of surgery (Dresen *et al.*, 2009).

Analogous to the GTV-T_{init}, the GTV-T_{res} represents remaining macroscopic disease, determined using the same clinical or imaging investigations as used initially, at a specific point during the course of treatment. This makes an assessment of macroscopic tumor response possible. However, the pathologic nature of the GTV-T_{res} is less well defined than that of the GTV-T_{init}, which is proven by (representative) biopsy at diagnosis. As stated above, there may or may not be macroscopic and/or microscopic disease within GTV-T_{res}. The GTV_{res} is used for defining an adaptive CTV-T (see Figure 5.3). Analogous to the specification of the initial GTV-T (see Figure 5.2A), the location, size, growth pattern, and investigation techniques should be specified for the residual GTV-T (see Figure 5.2B). The GTV-T_{res}-related (boost) CTV-T can be defined as an adaptive target volume (see Figure 5.3).

The initial GTV-T can completely disappear or can shrink and/or change in appearance due to the initial part of the treatment (see Figure 5.3). The GTV-T_{res} can have undergone inflammatory reactions with edema and fibrotic remodeling and thus not reflect the tumor tissue at diagnosis. Such changes can be detectable by clinical means, endoscopy, or various imaging procedures. One typical MRI finding is termed "gray zones," zones that were signal intensive on the initial MRI depicting the GTV-T but became gray indicating pathologic residual fibrotic tissue (Schmid *et al.*, 2013b), which might or might not contain macroscopic or microscopic tumor (Dresen *et al.*, 2009; Vincens *et al.*, 2008) (see Section 5.4.3). Observations from morphologic imaging might be supplemented in the future by repeated functional-imaging studies [see Figures 4.2 and 4.3 in ICRU Report 83 (ICRU, 2010)] or by biomarkers for tumor oxygenation (Haack *et al.*, 2010), for permeability, or a certain receptor status (Noordhuis *et al.*, 2011). At present, such approaches are investigational.

5.3.4 Initial GTV-T (GTV-T_{init}) and Residual GTV-T (GTV-T_{res}) in Cervical Cancer Radiotherapy (at the Time of Brachytherapy)

For cervical cancer, clinical examination and repeated imaging studies have shown large volumetric and topographic changes during EBRT, with or without chemotherapy, with an average volume reduction of from 60 % to 80 % after 4 to 5 weeks (see Figures 5.2 and 5.4), *i.e.*, from a mean of 59 cm^3 to 13 cm^3 assessed on MRI (Schmid *et al.*, 2013b). It has also been shown that the position of the uterus can vary by from 0.5 cm to 3.5 cm (Beadle *et al.*, 2009; Dimopoulos *et al.*, 2009a; Lim *et al.*, 2008; Taylor and Powell, 2008; van de Bunt *et al.*, 2006; 2008). Furthermore, there is evidence that the response pattern is dependent on certain tumor characteristics, such as the initial growth pattern (Dimopoulos *et al.*, 2009b; Schmid *et al.*, 2012). In predominantly expansive tumors (cervix/parametria/vagina/uterine corpus), there is often a huge

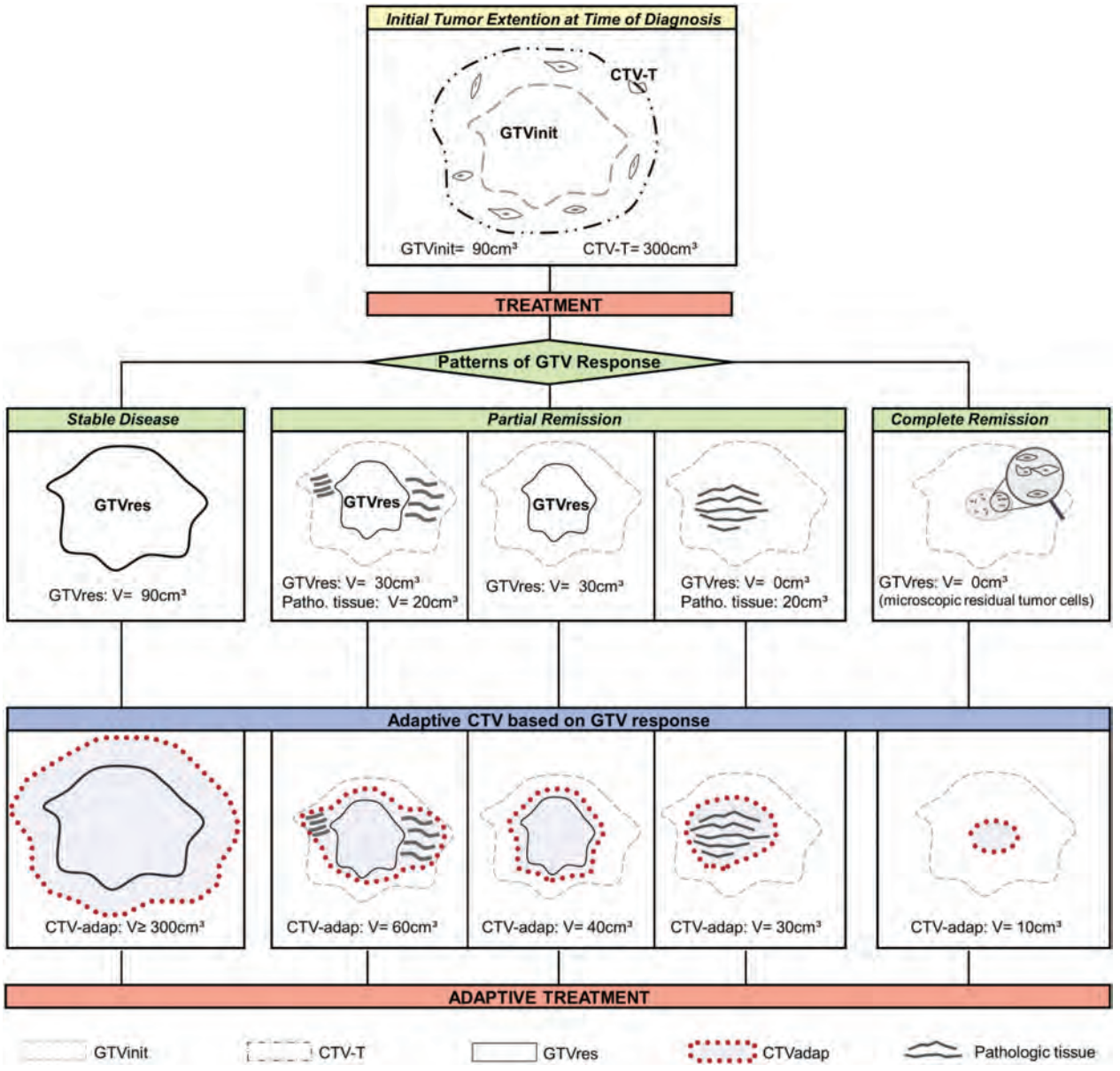

Figure 5.3. Schematic diagram indicating various forms of response of the initial GTV to treatment, resulting in various forms of residual GTV, pathologic and normal residual tissue, and an adaptive CTV that takes into account the GTV_{res} and adjacent residual pathologic tissue. A tumor-bearing organ is not included in this schematic diagram (compare with Figures 5.6–5.11 for cervix cancer, where the tumor-bearing cervix is always included, see also the examples in the Appendix). Progressive disease is not demonstrated.

volume reduction toward the central uterine cervix, resulting in a limited residual tumor volume at the time of brachytherapy (approximately 2 cm^3 to 20 cm^3). In predominantly infiltrative tumors, on the other hand, particularly those spreading far into the parametria, there is typically major residual tumor volume (approximately 30 cm^3 to 60 cm^3).

5.3.4.1 Initial GTV (GTV-T_{init}). The GTV-T_{init} represents macroscopic tumor extension at diagnosis, proven by histology as detected by clinical examination (GTV-$T_{init/clin}$) and as visualized as a high-signal-intensity mass using FSE T2-weighted MRI, GTV-$T_{init/MRI}$ or as composite $GTV_{init/MRI+clin}$ (see Figures 5.2a, 5.4.1a, and 5.4.2a). As the GTV-T_{init} can rarely be precisely visualized with CT, it can be superimposed on CT from clinical examination, $GTV_{init/clin:\ CT}$, or rather by additional MRI, $GTV_{res/clin+MRI:\ CT}$.

5.3.4.2 Residual GTV (GTV-T_{res}). The GTV-T_{res} represents the residual GTV at the time of brachytherapy, assessed clinically and/or by imaging, and then classified as the GTV-$T_{res/clin}$ and the GTV-$T_{res/MRI}$ or as the composite GTV-$T_{res/MRI+clin}$ (see Figures 5.2b, 5.4.1b, and 5.4.2b). If only CT is available, the same procedure can be followed for

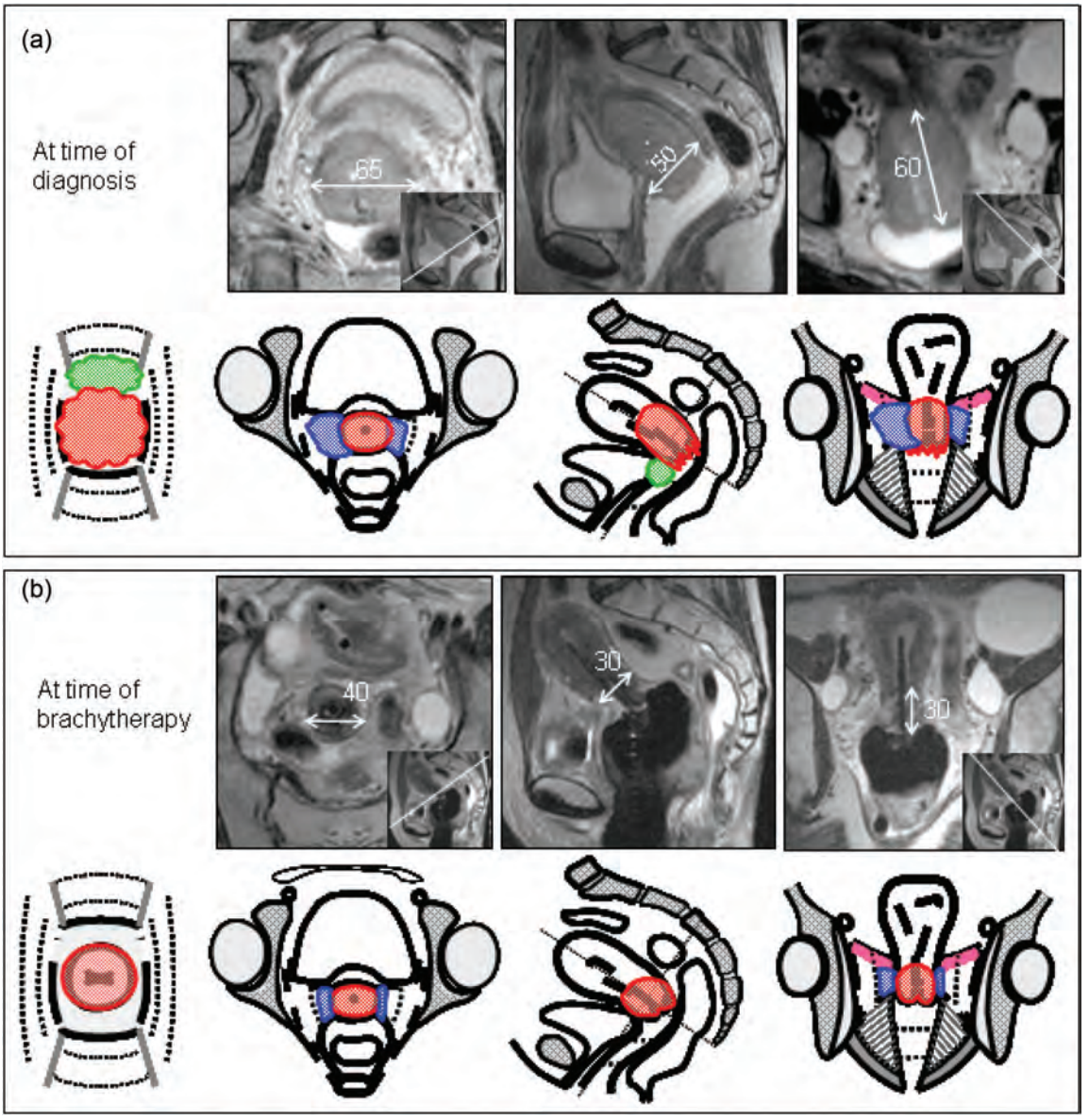

Figure 5.4.1. Cervical cancers with expansive and infiltrative growth patterns and different treatment responses.

the GTV-T_{res} as for the GTV-T_{init} with superimposition on CT of the residual tumor assessed by clinical examination, $GTV_{res/clin:\ CT}$, or rather by additional MRI, $GTV_{res/clin+MRI:\ CT}$.

The GTV-T_{res} as defined here should be used only after delivery of a radiation dose sufficient to control microscopic disease (40 Gy to 45 Gy). For any other situation, the radiation dose delivered should be indicated (*e.g.*, GTV-$T_{res\ 25\ Gy}$).

It is important to emphasize the following:

- When using clinical drawings and CT images for treatment planning in locally advanced disease, the GTV can be reliably described only based on clinical examination with regard to cervical, parametrial, and vaginal extension (not for infiltration into the uterine corpus), as CT at present is not recognized as a reliable and valid method to assess the advanced macroscopic tumor of the cervix (see Section 5.4.5).
- In patients treated initially with brachytherapy or with brachytherapy alone, there is the initial GTV at first brachytherapy (see Section 5.4.4).

5.3.5 Uncertainties in GTV-T Selection and Contouring

Various clinical, imaging, and pathohistologic methods give rise to varying uncertainties in defining the GTV. To limit these uncertainties, standardized imaging and pathologic protocols are increasingly used and refined to accommodate new developments in anatomic and functional imaging, as well as pathologic assessment. The least variations in overall

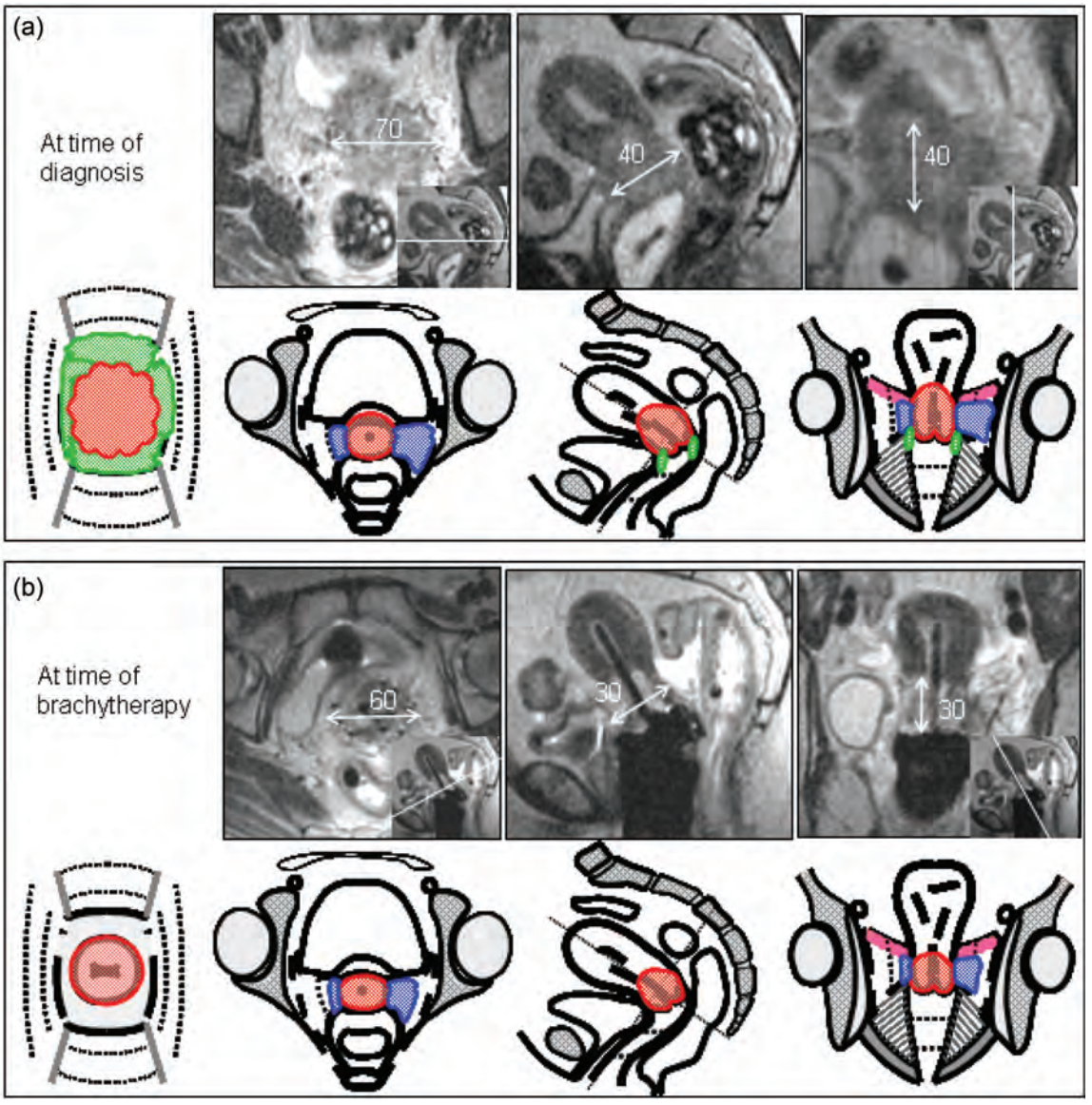

Figure 5.4.2. Large cervical mass in Stage IIIB cervical cancer with predominantly infiltrative tumor growth at diagnosis (a). Moderate response after chemo-radiotherapy with significant GTV_{res} and large amount of residual pathologic tissue (b).

assessment are seen in patho-histologic assessments (Daisne *et al*., 2004). The degree of certainty is indicated in the TNM classification (Sobin *et al*., 2009): pathologic staging is indicated with a preceding "p," for example, as pT2; any other form of clinical and imaging assessment results in greater variations, and is indicated with a "c," as in cT2. In the context of head-and-neck oncology, the variations for GTV assessment have been shown comparing CT, MRI, and PET–CT with pathologic findings (Fiorino *et al*., 1998; Giraud *et al*., 2002; Van de Steene *et al*., 2002; Weiss *et al*., 2010; Wong *et al*., 2006). Past ICRU reports have referred to differences resulting from assessment methods at diagnosis when, for example, comparing pathologic specimen and radiologic imaging for breast cancer (Figure 2.3 in ICRU Report 62 (ICRU, 1999);(Dresen *et al*., 2009; Lambrecht *et al*., 2010; Muschitz *et al*., 2004; Vincens *et al*., 2008). In concordance with ICRU Report 83, it is recommended to indicate the imaging method used for determination of the GTV-T.

With regard to defining the $GTV\text{-}T_{res}$ during or after chemo-radiotherapy, the validity and reliability of clinical imaging is probably less than at the time of diagnosis (Vliegen *et al*., 2008). For histo-pathologic assessment (staging) of the residual GTV after neo-adjuvant treatment, a preceding "y" has been introduced, for example, as yT1, which has already become widespread in oncology. There is limited consensus on what should be regarded as the residual GTV in the case of imaging. Even greater uncertainties exist with regard to residual microscopic disease

in the area of adjacent "residual pathologic tissue" (region of the intial GTV) (Hricak *et al*., 2007), and more research is needed, including morphologic and functional imaging and histo-pathologic evaluation.

In order to minimize the uncertainties of GTV selection and contouring, the GEC ESTRO recommends MRI and clinical examination as the standards for contouring the GTV-T_{init} for cervical cancer, and detailed imaging protocols have been proposed (Dimopoulos *et al*., 2012a; Schmid *et al.*, 2013b), which also include the definition of the GTV-T_{res} as the volume of high-signal-intensity and clinically detectable residual mass and the definition of residual pathologic tissue as fibrotic areas within the volume of the initial GTV. Systematic clinical investigations of patterns of spread at diagnosis and after chemo-radiotherapy, at the time of brachytherapy, support these recommendations (Dimopoulos *et al*., 2009a; Lang *et al*., 2007; Petric *et al*., 2008; Petrič *et al*., 2013; Weiss *et al*., 2003, Wu *et al*., 2005). The use of standards for imaging, appropriate image quality, adequate training, and adherence to contouring recommendations are the main strategies to minimize inter-observer variations for contouring both the GTV-T_{init} and the GTV-T_{res} (Petrič *et al*., 2013).

For the further development of adaptive-radiotherapy approaches, the investigation and reporting of uncertainties in GTV assessment is needed. The evaluation and reporting of systematic and random variations of GTV-T_{init} and GTV-T_{res} contouring are therefore encouraged. These uncertainties should be reported separately from those related to the CTV-T or the PTV-T (ICRU, 2010).

5.4 CTV and Adaptive CTV

5.4.1 Concept of CTV

The CTV is a volume containing a demonstrable GTV and assumed sub-clinical malignant disease considered to require therapy to achieve the treatment aim. Following surgical resection, the CTV may contain sub-clinical disease only. For well-defined types and stages of tumors, available guidelines for CTV delineation should be followed if applicable to the clinical case.

CTV-T encompasses the microscopic tumor spread at the boundary of the primary tumor GTV; CTV-N encompasses the potential microscopic tumor spread into lymph nodes and around a macroscopically involved node (GTV-N). A CTV-M, *i.e.*, the potential metastatic involvement of other organs (*e.g*., the lung), may in general also be considered, including possible management with radiotherapy.

As this report focuses on brachytherapy for cervical cancer, the following discussion concentrates on CTV-T, only partly covering issues related to CTV-N.

5.4.2 CTV-T Selection and Delineation

The selection of the CTV-T is based on a probabilistic assessment integrating the biological and clinical behavior of the individual tumor, and the knowledge of the surrounding anatomy, including structures that are barriers to tissue infiltration or structures that are conduits allowing easy passage for tumor dissemination (Figure 5.5).

The probability for the presence of malignant cells and their density in the margin around the GTV often decreases with the distance from the border of the GTV which may be symmetrical or asymmetrical. In addition, there may be local routes of spread giving specific adjacent locations a higher probability for malignant cells to be present.

For primary cancer of the cervix, the selection of CTV-T is guided by the assumed decrease in the density of cancer cells with distance from the GTV and by typical routes of microscopic spread into the adjacent tissues. Tumor spread follow anatomical compartments, for example, into the lateral and posterior parts of the parametrium, and the risk of spread is reduced by anatomical barriers [*e.g*., the posterior sacro-uterine ligament effectively preventing spread into the adjacent para-rectal space (Figures 5.4 and 5.5; see also Section 5.2.1.4)]. One practical consequence is that different CTV-Ts may be selected according to their assumed tumor burden (ICRU, 2004a; 2010). The probability of pathologic lymph node involvement depends mainly on histology, stage, and primary tumor location.

The size and configuration of the CTV-T result from the selection of the width of the margin around the GTV but may include the whole tumor-bearing organ (c.f., the whole prostate in cancer of the prostate, the whole breast in cancer of the breast).

In cervical cancer, the whole cervix is regarded as CTV-T_1, even if the GTV occupies only part of it. A second CTV-T_2 is defined with margins around the cervix indicating adjacent areas of suspected tumor spread with a significant probability of tumor cells which require treatment. A third CTV-T_3 is defined as covering the well-known areas of potential spread; for example, for advanced cervix cancer the whole uterus, the whole parametria, and the upper vaginal third (if the vagina is not involved) (see Figures 5.7–5.9; Sections 5.2.1.7 and 5.2.1.9).

The CTV selection should take into account target selection and contouring uncertainties (see Section 5.4.6). However, the CTV does not include the range of motion of internal anatomy (see PTV Section 5.5).

Selection of the CTV(s) is the responsibility of the radiation oncologist and is currently based on different levels of evidence derived from personal or departmental clinical experience and on exchanged or

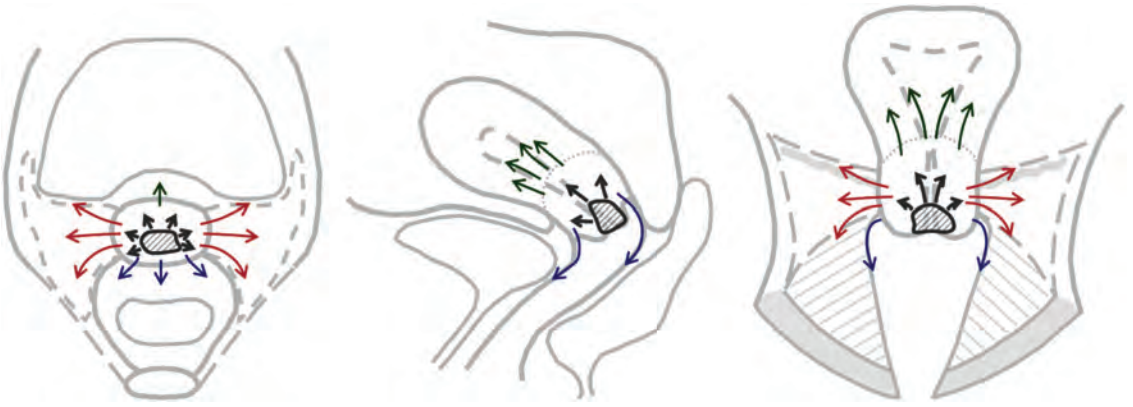

Figure 5.5. Schematic axial (left) mid-sagittal (middle) and mid-coronal (right) views of typical cervix cancer growth in—and outside—the cervix with extra-cervical infiltration into adjacent structures such as parametria, uterine corpus, vagina [see also electronic appendix Gyn GEC ESTRO Rec II (Lim *et al*., 2011; Pötter *et al*., 2006)].

published information. Such decision may be linked mainly to one imaging or clinical investigation modality showing a certain GTV size and morphology or may represent a composition of information from different imaging and clinical investigations which show variations in GTV [compare the composite GTV (Section 5.3.2)]. The 3D delineation of the CTVs for both the primary tumor and the nodal site will often follow published guidelines, which aim to describe the regions at risk for microscopic spread (both at the primary tumor site and at lymph node areas) and relate them to boundaries identifiable on planning CT or MRI (Castadot *et al*., 2010; Haie-Meder *et al*., 2005; Lim *et al.*, 2011; Small *et al*., 2008; Taylor *et al*., 2005).

5.4.3 Change of Primary Tumor CTV-T during Treatment: The Adaptive CTV

The adaptive CTV-T (CTV_{adapt}) is based on the size and the configuration of the GTV-T_{res}. For the purpose of this report with two distinct treatment steps (EBRT and brachytherapy), the GTV-T_{res} is further specified as it presents at the time when the delivered dose is considered sufficient to control microscopic disease (see Section 5.2.1.3 and 5.3.4). Around this GTV-T_{res}, residual microscopic tumor cells may or may not be suspected depending, for example, on the initial growth (exophytic/infiltrative) and the response pattern (central/non-central). In the case of infiltrative tumors, multiple areas with residual (macroscopic) pathologic tissue may be observed adjacent to the GTV_{res}. On MRI, such areas may appear as gray zones, indicating residual fibrotic tissue. Such residual pathologic tissue is located by definition in the volume of GTV_{init}. Therefore, the selection of CTV_{adapt} must also take into account the morphology and topography of GTV_{init} and the morphologic and/or functional response to treatment. CTV_{adapt} may or may not include a margin around GTV_{res} depending on the growth and response patterns and the suspected presence of residual tumor cells (Figure 5.3). Even a sub-volume of GTV_{res}, considered likely to bear a specific tumor burden, may be selected as the CTV_{adapt} (Figure 5.6).

The adaptive radiotherapy paradigm assumes that, after the first treatment phase, additional treatment is needed to the CTV_{adapt}. This additional treatment may be a radiotherapy boost, chemotherapy, surgery, or some combination of these modalities. Whereas traditional radiotherapy practice has mainly focused on providing additional treatment to the GTV_{init} related CTV-T, there is increasing evidence from analyses of pattern of recurrence, for example, in anal cancer or in head and neck cancer, that some situations may require additional treatment only to an adaptive CTV based on GTV_{res}. More aggressive treatment may be considered for such—significantly smaller—volumes in an attempt to improve local control. Treatment-related morbidity could be minimized, either due to less radical surgery or to less toxic high-dose radiotherapy focused on small volumes (Figure 5.6).

The radiotherapy target boost concept, as the target for most types of radical surgery after treatment for remission induction, has so far been mainly related to the initial GTV plus margins for potential microscopic spread. This is in contrast to the so far rarely applied response-related adaptive boost concept, which implies an adaptive CTV-T and which focuses on the situation as it presents after initial treatment with often significant changes of GTV, topography, and geometry, the residual GTV-T. The geometrical changes during fractionated radiotherapy may lead to considerable dosimetric changes and have received major attention in the recent period of repetitive imaging (Yan, 2010). "Adaptive radiotherapy" so far has mainly addressed these geometric and dosimetric changes. In the tumor-response-related, adaptive approach as presented here, the individual tumor response is the

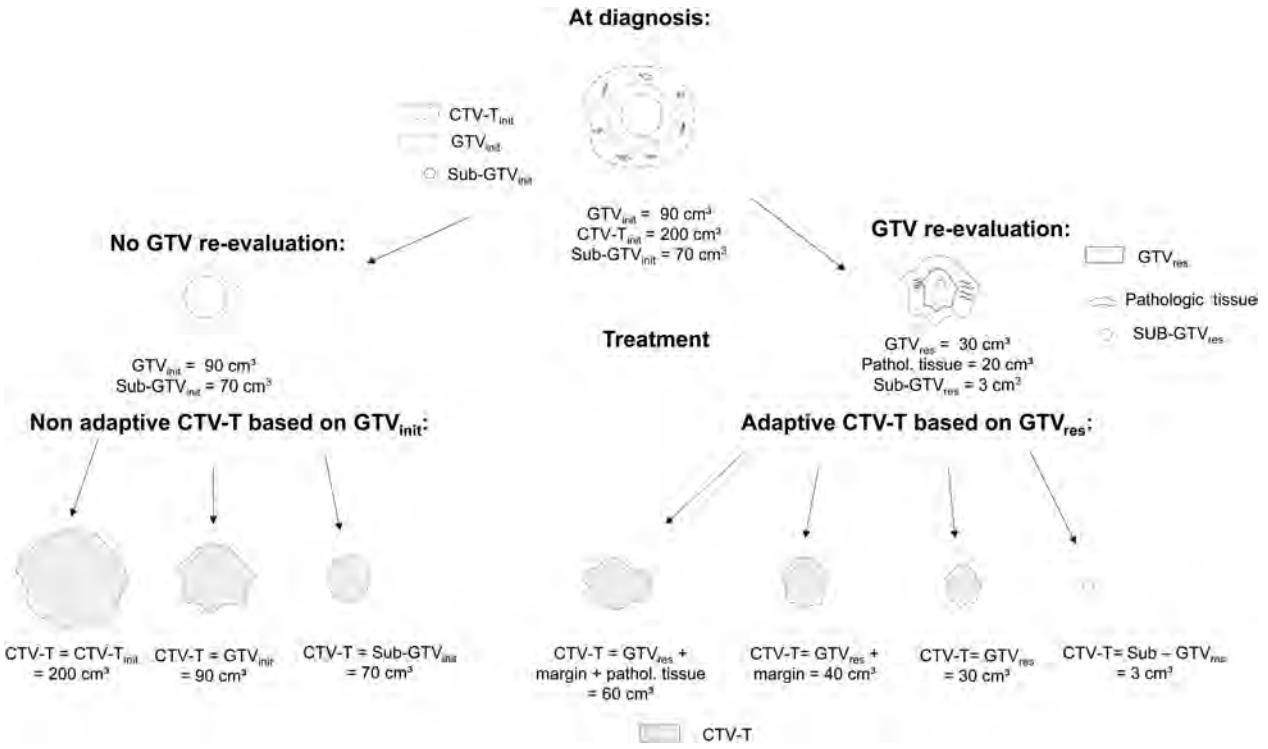

Figure 5.6. Schematic diagram indicating one typical response pattern of the initial GTV to treatment resulting in a typical residual GTV and adjacent pathologic residual tissue (compare Figure 5.3). Various forms of CTVs are shown for boost treatment, referring either to the initial or to the residual GTV with non-adaptive and adaptive CTV. Initial findings of tumor configuration and spread, or findings after a first phase of treatment are taken into account (see text).

frame into which the adaptive boost for radiotherapy is integrated. This is accomplished through morphologic repetitive imaging that provides major information about the change of GTV. In future, such adaptation may additionally be guided by various forms of imaging including functional imaging as, for example, shown for lung cancer (van Elmpt *et al*., 2012) or for Hodgkin's disease (Eich *et al*., 2008; Lutgendorf-Caucig *et al*., 2012; Specht *et al*., 2014).

The examples below illustrate the adaptive CTV-T approach (see also one example as shown in Figure 5.3). Notice that the tumor-response concept of adaptive CTV-T can also be applied to macroscopic nodal and metastatic disease, which would then become a CTV-N_{adapt} or a CTV-M_{adapt}.

There are two basic approaches to selecting the CTV-T for additional radiotherapy. One approach is to select the boost CTV-T based on the GTV-T_{init} (Figure 5.6):

- initial GTV plus margins for microscopic spread (traditional CTV-T concept);
- initial GTV alone (CTV_{IR}; Section 5.2.1.6)
- initial sub-GTVs [*e.g*., based on functional imaging (Geets *et al*., 2007, van Elmpt *et al*., 2012; Viswanathan *et al*., 2007)]

Alternatively, a CTV-T_{adapt} approach may be used based on the GTV-T_{res}, which may again give rise to multiple possible boost CTV-Ts (Figures 5.3, 5.6):

- residual GTV plus residual pathologic tissue in the area of the initial GTV (*e.g*., gray zones) plus tumor-bearing organ (CTV_{HR}; Section 5.2.1.3); (compare Figure 5.3)
- residual GTV plus residual pathologic tissue in the area of the initial GTV (*e.g*., gray zones) (as demonstrated in Figure 5.3);
- residual GTV alone plus margins for suspected microscopic spread (Figure 5.6);
- residual GTV alone (*e.g*., SRT boost for brain metastases after whole-brain RT) (Figure 5.6);
- residual sub-GTVs (*e.g.*, based on functional imaging) (Figure 5.6).

GTV-T_{res}-related CTV-T_{adapt} selection is currently based on morphologic repeat imaging, such as CT, MRI, US, or endoscopy, and clinical examination, whereas the selection of the (initial) CTV-T is based on the GTV_{init} as represented on imaging at diagnosis. The resulting selection of adaptive target volumes depends on the imaging modality applied (Daisne *et al*., 2004). Functional imaging is being investigated for defining volumes with specific

biological characteristics and these are often smaller than those defined from morphologic imaging alone (Daisne *et al*., 2004). In order to fully exploit the adaptive approach, a more thorough understanding of tumor spread at diagnosis [cervix cancer (Burghardt *et al*., 1989)] and regression pattern during treatment [cervix cancer (Kidd *et al*., 2013; Schmid *et al*., 2012)] is essential which requires major research and development.

Response-related adaptive target concepts for defining boost treatments in radiotherapy alone or in multimodality approaches have been successfully used, for example, in Hodgkin's disease (lymph nodes), small cell lung cancer (tumor and lymph nodes), anal cancer (tumor), Ewing Sarcoma (tumor), and in selected cases of head and neck cancer (tumor/lymph nodes).

5.4.4 Initial CTV-T and Adaptive CTV-T in Stage-Related Treatment of Cervical Cancer

The initial and adaptive CTV-T concepts are described below for the various stages of cervical cancer with special emphasis on brachytherapy. Whereas FIGO stage-adapted treatment has been the standard of care in local treatment of cervical cancer for decades [stage adapted dose prescriptions to Point A (Perez *et al*., 1998)], systematic GTV-related CTV-T concepts have only been recently introduced, mainly due to the progress in volumetric imaging (Pötter *et al*., 2008a).

The typical pattern of spread of cervical cancer is well known from observation of clinical behavior and pathological examination of cervical cancer, thus allowing a probabilistic assessment of tumor involvement and spread, lymph node involvement, and potential recurrence patterns (Dimopoulos *et al*., 2006b; Eifel and Levenback, 2001) (Figure 5.5). According to the primary route of tumor spread within the cervix, the whole cervix forms the basis for the CTV-T_1. The second route of tumor spread is the adjacent uterine corpus, the adjacent parametria, the adjacent vagina, and the adjacent anterior and posterior spaces toward the bladder and rectum, respectively, which form the CTV-T_2. Furthermore, the whole or major parts of these structures are regarded as the areas of possible microscopic tumor spread [Figure 5.5 (Hertel *et al*., 2006)]. Therefore, the whole uterine corpus, the whole parametria, the upper half of the vagina, and the utero-bladder and cervico-rectal spaces are generally regarded as a CTV-T_3. The anterior, posterior, and cranial uterine surfaces form strong barriers for tumor infiltration into adjacent structures and spaces such as the rectum, sigmoid, bladder, and bowel. The sacro-uterine ligaments are at the same time barriers against infiltration into adjacent structures and spaces such as the para-rectal space and the lateral rectum and routes of spread as they form the posterior border of the parametrial space (Figure 5.5).

5.4.4.1 Uterine Cervix: The Primary CTV-T for Any Invasive Cervical Cancer. In invasive cervical cancer, the whole uterine cervix is included into any GTV-related CTV-T for any stage of disease and at any time of treatment (Haie-Meder *et al*., 2005; Viswanathan and Thomadsen, 2012; Viswanathan *et al*., 2012b).

In early disease, such as FIGO IA2 and low-risk IB, the whole cervix is the only CTV-T to be treated, most often by surgery alone but treatment may also include small-volume brachytherapy focused on the uterine cervix. Specific surgical procedures (trachelectomy) have been developed to spare the uterine corpus—an approach that is mainly applied in young women to retain their ability to give birth. Local recurrences in the remaining uterine corpus and the adjacent parametria have rarely been reported (Hertel *et al*., 2006).

5.4.4.2 Peri-Cervical Areas at Risk in Tumors with an Intact Cervix (Stage IB, IB1, IB2). Invasive cervical cancer with an intact cervix presents with a wide range of tumors that vary in size and risk from limited ($<$4 cm, IB1) to bulky ($\geq$4 cm, IB2) disease (see Table 2.1). Treatment may consist of definitive radiotherapy (including brachytherapy) with or without chemotherapy, definitive surgery, or a combination of these (see Section 2.7.3).

For the selection of CTV-T, two clinical scenarios and treatment strategies should be distinguished. For IB1 tumors, radiotherapy alone may be chosen, including early brachytherapy during initial treatment. The large IB2 tumors require more intensive treatment with upfront chemo-radiotherapy and late brachytherapy that is adaptive in the case of significant tumor shrinkage.

The appropriate CTV-Ts based on initial GTV-T assessment (Stage IB1) are the following (Figures 5.7 and 5.8):

- CTV-T_1: the area adjacent to the GTV-T not separated by any anatomical borders and the whole cervix where the risk of microscopic tumor spread is high;
- CTV-T_2: potential significant microscopic tumor spread beyond the cervical borders in adjacent tissues: parametria (10 mm margin), uterine corpus (10 mm), vagina (10 mm), anterior cervix–bladder, and posterior cervix–rectum space (5 mm);
- CTV-T_3: potential minimal tumor cell load, spread contiguously or incontiguously within anatomical

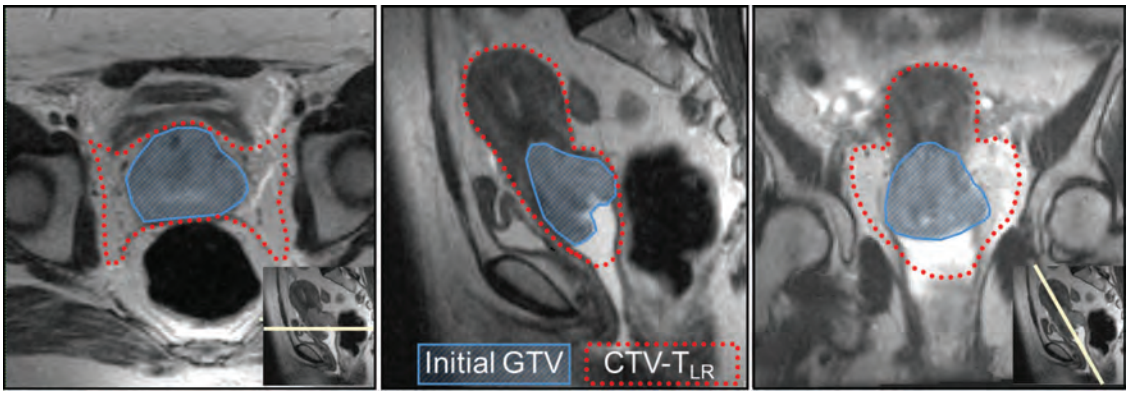

Figure 5.7. Magnetic resonance imaging at diagnosis of Stage IIB cervical cancer infiltrating both parametria with GTV-T_{init} and CTV-T_{LR} (CTV-T_3) including both parametria, uterine corpus, and upper vagina, contoured for treatment planning of EBRT.

compartments adjacent to the CTV-T_2 and not separated by anatomical borders: parametria, uterine corpus, upper vagina, anterior uterus–bladder, and posterior cervix–rectum space.

For early brachytherapy (limited Stage IB1), the CTV-T_{1-3} is recommended, for late brachytherapy (IB2), the use of CTV-T_3 is recommended for designing the initial CTV-T_3 for EBRT (CTV-T_{LR}).

The margins above for CTV-T_2 have been defined at a certain distance around the cervix based on pathologic evidence from surgical specimens and on clinical experience from patterns of recurrences by GEC ESTRO in Europe and American Brachytherapy Society in the USA (Haie-Meder *et al*., 2005; Viswanathan *et al*., 2012b). The GEC ESTRO Recommendations on margins were mainly based on the long French clinical tradition in CTV definition in limited disease (Gerbaulet *et al*., 1995; 2002a) (Figures 5.7 and 5.8). An extra 5 mm margin may be applied for the CTV-T_2 in the assumed direction of potential spread in the case of specific risks (*e.g*., macroscopic tumor growth close to a uterine border).

The selection and the contouring of CTV-T_3 are based on the assumed risk of tumor cell spread within the compartments at risk (see above). Within the long-standing traditions, this target includes at present: the whole uterus, the whole parametria, and the upper part, the upper third or the upper half, of the vagina (Gerbaulet *et al*., 2002a). More evidence on appropriate and individualized margins will have to come from clinical and imaging studies relating margins to clinical outcome.

Three different CTV-Ts have been defined in the GEC ESTRO recommendations: "High Risk CTV," "Intermediate Risk CTV," and "Low risk CTV" (see Section 5.4.5). If this terminology is used for the initial CTV-T concept as suggested also in this ICRU/GEC ESTRO report, a clear distinction must be made to the corresponding risk definitions based on the adaptive CTV-T target concept. The volumes of the adaptive concept refer to the clinical situation after chemo-radiotherapy which implies the treatment response as a major factor. The volumes of the initial CTV-T concept, however, refer to the initial clinical situation without any treatment. Ideally, the GEC ESTRO terminology, widely spread during the last decade, should be merged with the terms CTV-T_{1-3} developed in this ICRU/GEC ESTRO report.

For clarity, it is therefore recommended to use the terms "initial CTV_{HR}" and "initial CTV_{IR}" for the terms "CTV-T_1" and "CTV-T_2", respectively, if these targets are selected and contoured at the beginning of EBRT with or without chemotherapy.

The terms "CTV_{LR}" and "CTV-T_3" are interchangeable as the underlying volume concept is identical with the same anatomical compartments needing treatment. Some changes may be observed in specific volumes, as, for example, the shape and volume of the parametria and the uterine corpus may change with treatment.

CTV-T_{LR} (CTV-T_3) is recommended in any case as the tumor-related CTV for the treatment planning of EBRT. This applies to limited disease Stage IB1 treated with EBRT and brachytherapy from the beginning and extensive disease treated with EBRT first and brachytherapy as a boost after EBRT with or without chemotherapy. The other target concepts can be used in addition: the one related to the initial GTV-T as, for example, "initial CTV-T_{HR}" and the "initial CTV_{IR}" for tumor-related CTV margins at diagnosis. These terms can be used in more advanced stages requiring an adaptive CTV for EBRT (Figures 5.9 through 5.12). In advanced disease, CTV-T_{LR}, CTV-T_{HR}, and CTV_{IR} may be defined at the start of treatment (initial CTV-T_{LR}, initial CTV-T_{HR}, initial CTV-T_{IR}) and may be adapted according to the topographic and volumetric changes during EBRT and also at brachytherapy.

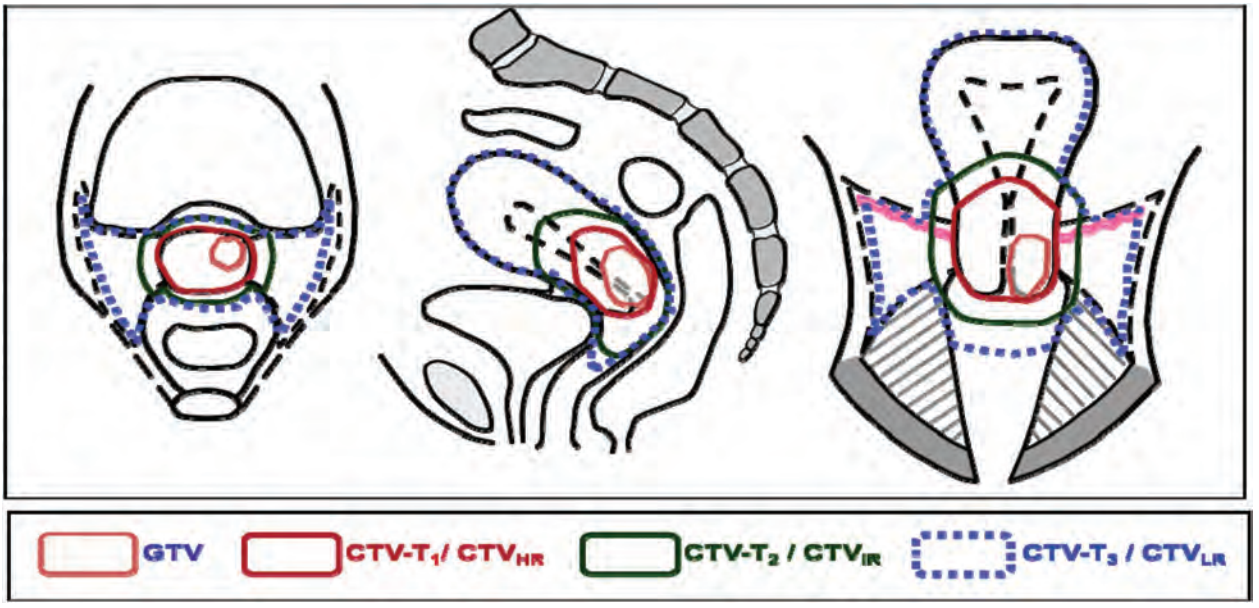

Figure 5.8. Schematic diagram for cervical cancer, limited disease, Stage IB1, with initial GTV, initial CTV_{HR} (cervix) (CTV-T_1) and initial CTV_{IR} (margins around cervix) (CTV-T_2) and initial CTV_{LR} (margins for whole parametria, whole uterine corpus, upper third of vagina, utero-bladder ,and cervix–rectum space) (CTV-T_3) for initial brachytherapy combined with EBRT: coronal, transversal, and sagittal view [see also Appendix example 1].

The overall CTV-T (including CTV-$T_{1/2/3}$ as necessary) may be treated by either surgery or radiotherapy, taking into account the volumes at risk. External-beam radiotherapy is selected to treat all CTV-Ts—usually together with the CTV-N—to a certain dose sufficient to control microscopic disease. Brachytherapy mainly contributes high doses to the CTV-T_{1+2} intermediate doses to CTV-T_3 and for doses to CTV-N.

In the case of large bulky cervical disease (IB2), the CTV-T for brachytherapy is adapted to allow for tumor shrinkage following EBRT and concurrent chemotherapy. The adaptive target concept is applied with two additional CTV-Ts, the CTV_{HR} and the CTV_{IR} (see the following paragraphs whereas the compartments of potential tumor spread remain the same—maybe with some topographic changes—, therefore the adaptive CTV_{LR} remains comparable to the initial CTV-T_3).

5.4.4.3 Peri-Cervical Areas at Risk in Tumors Infiltrating beyond the Cervix (Stage II–IVA). Tumor infiltration beyond the cervix represents the third clinical scenario relevant for CTV-T determination. In particular, the parametria, uterine corpus, vagina, and the adjacent anterior and posterior spaces with the limiting bladder and rectum organ walls present volumes with assumed high risk of microscopic infiltration. The risk depends on the individual extent and biology of disease and the topographic relation to the potential routes of spread in the peri-cervical areas and the barriers of spread (see Sections 5.4.2 and 5.4.4.2; Figure 5.5). The major routes of spread are reflected in the FIGO classification, except for uterine corpus infiltration. In Stage IIB, a sub-division into proximal and distal infiltration has proven useful for further categorization of the parametrial disease spread (Gerbaulet *et al*., 1995; 2002a). For uni- and bilateral parametrial infiltrations up to the pelvic wall, a subdivision of Stage III has been proposed as IIIA and IIIB, respectively (Eifel and Levenback 2001; Fletcher, 1980).

The CTV-T for any infiltration beyond the cervix has been related in the past to the extent of tumor infiltration at diagnosis [*e.g.*, ICRU 38 (1985); Gerbaulet *et al*. (2002a), see Figure 4.7].

The initial external chemo-radiotherapy, the standard treatment for any patient with extracervical disease (see Section 2.7.4), typically causes significant tumor shrinkage and consequently a major change in topography. The CTV-T determination for the brachytherapy boost at the end of external therapy takes these changes into account by applying the adaptive CTV-T concept with CTV-T_{HR} and CTV-T_{IR} as described in detail in the following section for the various clinical scenarios (Figures 5.9 through 5.12).

5.4.4.4 Regional Lymph Nodes Involved and at Risk. CTV-N is defined from nodal staging as nodes with proven macroscopic, microscopic, or

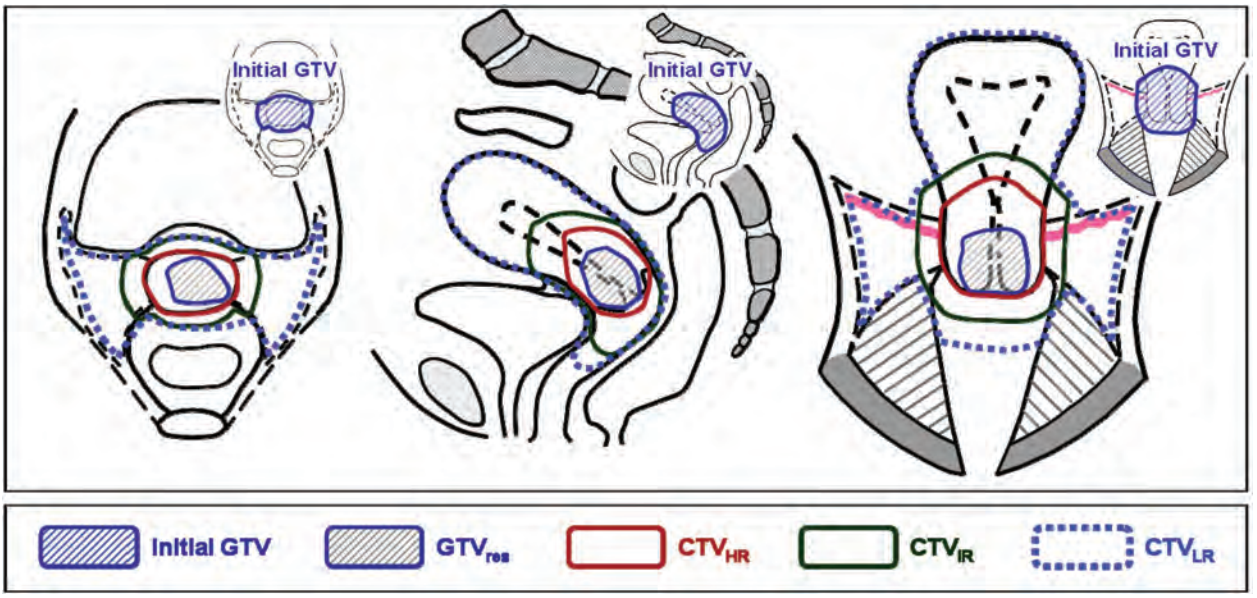

Figure 5.9. Schematic diagram for cervical cancer, Stage IB_2 (bulky disease), good response after chemo-radiotherapy: residual GTV-T (GTV-T_{res}), adaptive CTV-T (CTV-T_{HR}), initial GTV-T (GTV-T_{init}), intermediate risk CTV-T (CTV-T_{IR}) (GTV-T_{init} plus margins around the CTV-T_{HR}), and CTV-T_{LR} for adaptive brachytherapy: coronal, transversal, and sagittal view (see also Appendix Example 2 and 9).

suspected involvement. Nodal boost volumes may be additionally defined, for example, for suspected or proven disease. The probability of lymph node involvement increases with stage [15 % to 20 % in Stage IB, 30 % in Stage IIB, 40% to 50 % in IIIB (see Sections 2.5 and 2.6)] and is also dependent on pathologic characteristics. Morphologic and functional volumetric imaging (CT, MRI, PET–CT, US) has been used for nodal staging of cervical cancer (not included in FIGO but in TNM classification) and assessment of the CTV-N. However, due to the risk of false-negative imaging results, laparoscopic lymph node sampling and radical lymph node dissection play an important role in assessing the nodal status: selected para-aortic lymph and/or pelvic node areas are sampled according to tumor stage, imaging findings, and the estimated risk of involvement (see Section 2.5). The areas of macroscopic involvement (GTV-N) and proven or suspected microscopic involvement (CTV-N) are considered for EBRT. Recommendations have been published on the delineation of such nodal targets with suggested margins to vessels in regions of suspected microscopic disease for the elective CTV-N and margins around the GTV-N for the CTV-N (Haie-Meder *et al*., 2005; Lim *et al.*, 2011; Small *et al*., 2008; Taylor and Powell, 2008). Areas of macroscopic involvement and/or poor response may be selected for a boost CTV-N that is considered to require higher radiation doses (*e.g*., CTV-N_1, CTV-N_2, *etc*.). If such a boost is related to response at the end of chemo-radiotherapy, an adaptive CTV-N concept may be applied.

5.4.5 High-Risk CTV (CTV_{HR}), Intermediate-Risk CTV (CTV_{IR}), Low-Risk CTV (CTV_{LR}) in Combined Radiotherapy of Cervical Cancer

The high risk, CTV-T_{HR}, and intermediate risk, CTV-T_{IR}, as defined in Sections 5.2.1.5 and 5.2.1.6, respectively, are GTV-T-related concepts representing areas of initial macroscopic disease (GTV-T_{init}) and microscopic disease ("the whole cervix") while taking into account the change of these areas during treatment (GTV-T_{res} $\pm$ pathologic residual tissue). These areas have the highest risk of recurrence within the overall CTV-T. The adaptive concept with CTV-T_{HR} and CTV-T_{IR} has been developed since 2000 with upcoming volumetric imaging in cervical cancer brachytherapy based on the ICRU 38 tradition and within the Point A-related tradition (Nag, 2006) to define volumes during the course of treatment that may be considered to require additional boost treatment (*e.g*., by brachytherapy). CTV_{IR} is related to the GTV_{init}, and CTV_{HR} to the GTV_{res}, any adjacent residual pathologic tissue and the whole uterine cervix.

CTV-T_{LR} is defined for adjacent compartments with potential microscopic disease such as parametria, uterine corpus, and vagina analogous to CTV-T_3 at diagnosis but may be redefined according to the topography as it presents at the time of brachytherapy (adaptive CTV-T_{LR}, see Section 5.4.4.2). CTV-T_{LR} is mainly treated by EBRT with less contribution from brachytherapy.

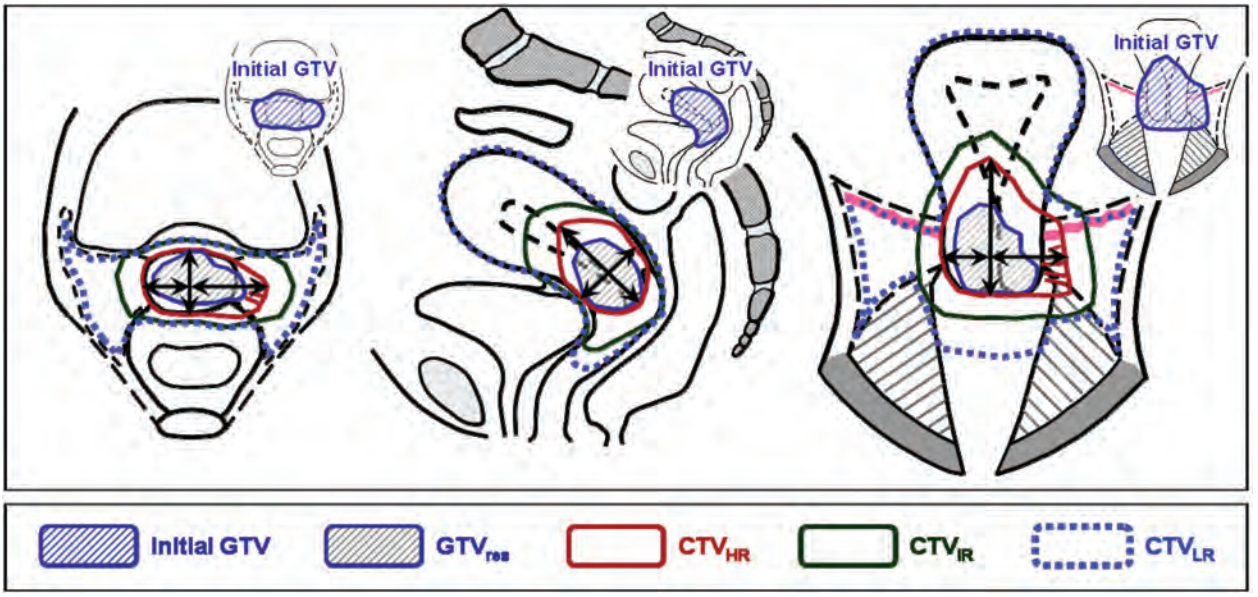

Figure 5.10. Schematic diagram for cervical cancer, Stage IIB bulky disease, and good response after chemo-radiotherapy: GTV-T_{init}, GTV-T_{res}, and extra-cervical gray zones, adaptive CTV-T_{HR}, CTV-T_{IR} (GTV-T_{init} plus margins around the CTV-T_{HR}), and CTV-T_{LR} for adaptive brachytherapy: coronal, transversal, and sagittal view. Maximum width, thickness, and height of the CTV-T_{HR} are indicated (see also Example 5 and 7 in the Appendix).

The CTV_{HR} and CTV_{IR} concepts were introduced for image-guided, adaptive cervical cancer brachytherapy in the 2005 GEC ESTRO recommendations (Haie-Meder *et al*., 2005) and have become widely accepted in the international gynecological-radio-oncological scientific community (Nag, 2006), scientific and educational communications and teaching activities [ESTRO, ABS, Association of Radiation Oncology of India (AROI), Chinese Society of Thereapeutic Radiology and Oncology (CISTRO), South-East Asian Society of Radiation Oncology (SEAROG), Association of Latin American Therapeutic Radiology and Oncology (ALATRO) and International Atomic Energy Agency (IAEA)], international treatment guidelines [ABS Guidelines (Viswanathan and Thomadsen 2012; Viswanathan *et al*., 2012b)], International Atomic Energy Agency technical reports (IAEA, 2013), and national guidelines [United Kingdom (Tan *et al*., 2009)].

In the following, the general concept for tumor-response related adaptive-CTV selection (see Sections 5.4.3 and 5.4.4) is specified according to the situation at diagnosis, and during treatment planning and treatment for the different advanced stages of cervical cancer.

The overall concept of the Gyn GEC ESTRO Recommendations (I), linked to MRI, is maintained (Haie-Meder *et al*., 2005) with some minor adaptations: terminology for initial brachytherapy (CTV-$T_{1,2}$/initial CTV-$T_{HR/IR}$), imaging requirements (allowing now also for CT and US), specification of the CTV_{IR} in specific clinical settings (*e.g*., poor response, stable disease). As CTV_{HR} and CTV_{IR} have become a widely accepted terminology in this field, these terms are further recommended for adaptive brachytherapy in gynecology.

The GEC ESTRO Recommendations were originally intended for recording and reporting only as no clinical target concept was supported by major clinical evidence at the time. This situation has gradually improved with accumulating single- and multi-institutional experience supporting the clinical value of these recommendations (Chargari *et al*., 2009; Haie-Meder *et al*., 2010b; Pötter *et al*., 2007, 2011; Sturdza *et al*., 2012) leading to their implementation into international treatment guidelines (see above) and into large international studies [STIC (Charra-Brunaud *et al*., 2012); EMBRACE 2015 (I and II) (www.embracestudy.dk), RETRO EMBRACE (Sturdza *et al*., 2016)].

Tumor volume and pelvic anatomy change significantly during EBRT with or without chemotherapy (see Section 5.3.4) which indicates the need for systematic assessment of volume and configuration of GTV-T_{init} and GTV-T_{res}, residual pathologic tissue and the adjacent OAR.

The assessment and the final volume contouring are based on the following:

- clinical examination with subsequent clinical drawings at diagnosis, during radiotherapy (if possible at weekly intervals) and at the beginning of brachytherapy;

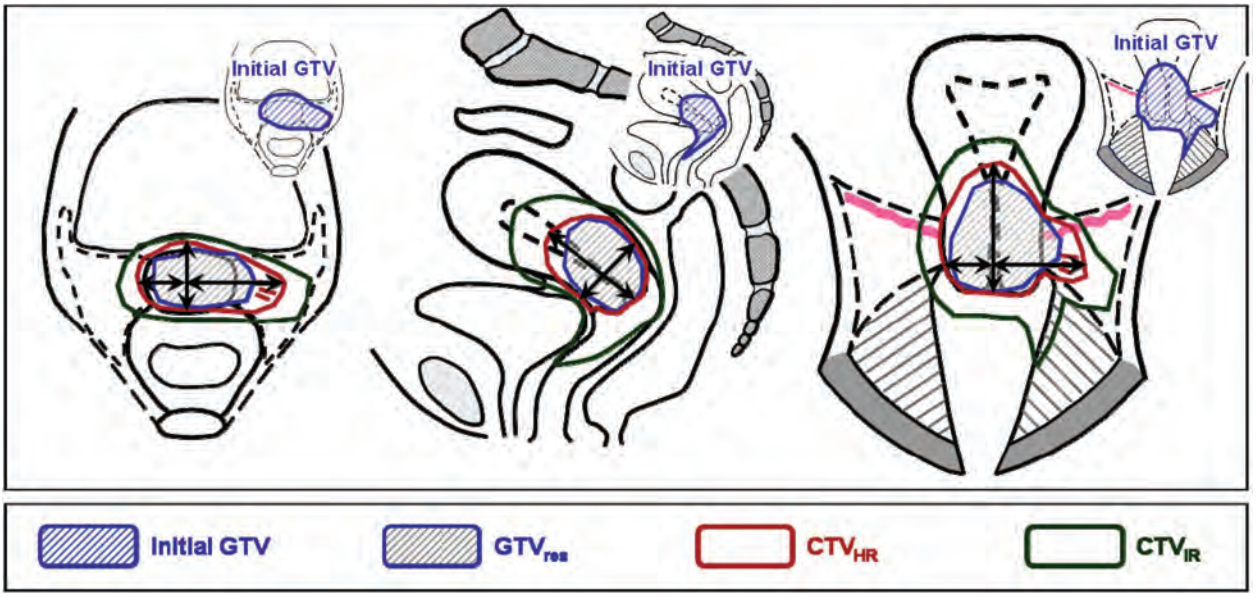

Figure 5.11. Schematic diagram for cervical cancer, IIIB, extensive disease, poor response after chemo-radiotherapy: large initial and residual GTV-T (GTV-T_{init}, GTV-T_{res}), extensive gray zones, adaptive CTV-T_{HR}, CTV-T_{IR} (GTV-T_{init} plus margins around the CTV-T_{HR}), and CTV-T_{LR} for definitive treatment: coronal and transversal view. Maximum width, thickness, and height of the CTV-T_{HR} are indicated (see also Examples 6 and 8 in the Appendix.).

- volumetric images, preferably MRI, taken at diagnosis, and as a minimum at beginning of brachytherapy, preferably with the applicator in place.

5.4.5.1 The High-Risk CTV-T: The Adaptive CTV-T for Cervical Cancer Brachytherapy. The adaptive high-risk CTV-T, the CTV-T_{HR}, is assumed to carry the highest residual tumor burden after chemo-radiotherapy. CTV-T_{HR} consists of the whole cervix and the GTV-T_{res} which is composed of any manifest intra- and extra-cervical residual tumor extension at the time of brachytherapy and of residual pathologic tissue as defined by clinical examination and by MRI at that point in time, and taking into account the tumor extent at diagnosis. The residual (extra-cervical) pathologic tissue is defined as one or more of the following:

- residual palpable mass;
- residual visible mucosal change;
- pathologic induration;
- residual gray zones (MRI);
- any other residual pathologic tissue on MRI or clinical examination.

To be included as residual pathology, these regions must be located inside the GTV-T_{init} and have characteristics that are consistent with residual disease. If there is disease outside GTV-T_{init}, this would indicate local progressive disease and the patient should be managed accordingly. Such pathologic tissues may include parts of the cervix, parametria, uterine corpus, vagina, rectum, or bladder, according to the initial spread of disease. All suspect areas of residual disease are included in the selection and delineation of CTV-T_{adapt}, the CTV-T_{HR}, with no margins added. The target delineation has to take uncertainties in target selection and contouring into account (see Section 5.4.6).

Figures 5.9–5.12 demonstrate the typical clinical scenarios for adaptive, stage-related CTV-T selection in gynecologic brachytherapy for advanced cervical cancer, applying the concepts of GTV-T_{init}/GTV-T_{res} as well as CTV-T_{HR}/CTV-T_{IR}/CTV-T_{LR} (see also Sections 5.3.3, 5.4.3, 5.4.4).

5.4.5.1.1 Alternative Imaging Modalities for Selection of CTV$_{HR}$. Magnetic resonance imaging together with clinical examination is considered the standard for repeat tumor assessment and for selecting CTV-T_{adapt}. However, the limited availability of MRI, in particular in radiotherapy departments in the developing world, means that alternative volume-imaging modalities have to be considered (see Sections 4.3, 4.5, and 4.6).

Presently, the most widely available imaging modality with the best discrimination potential for assessment of cervical tumors compared with MRI is US (Schmid *et al.*, 2013a). Ultrosonography may become essential—even competitive with MRI—if its potential can be further developed and if it becomes widely available in clinical practice for cervical

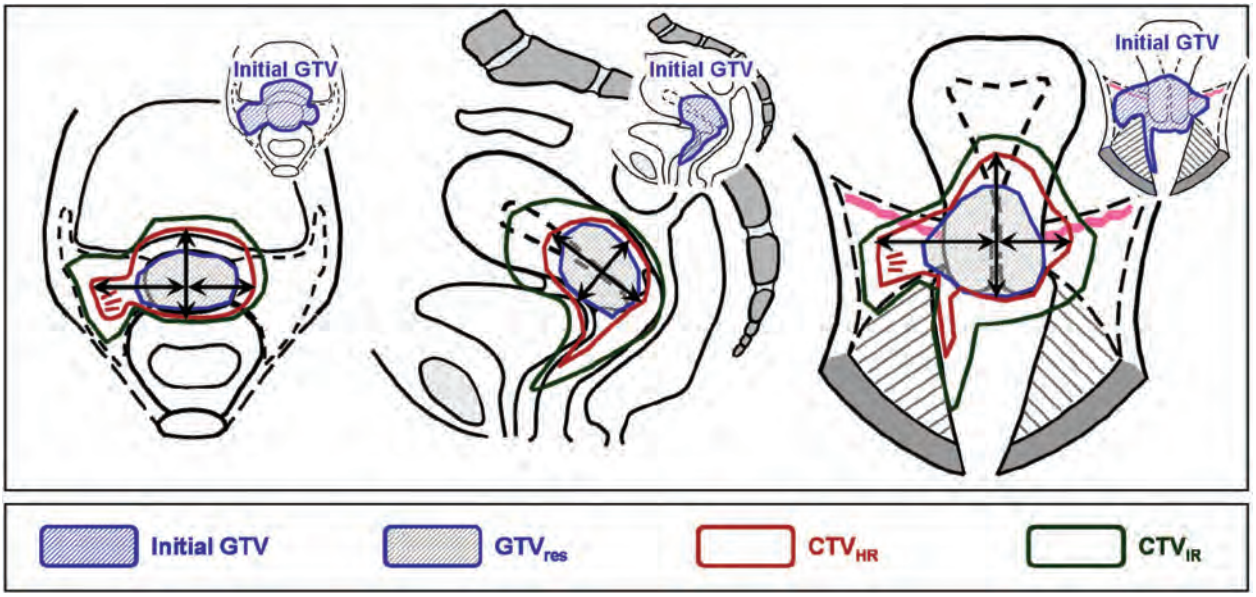

Figure 5.12. Schematic diagram for cervical cancer, with bladder infiltration, Stage IVA, and good response after chemo-radiotherapy: large initial and residual GTV-T (GTV-T_{init}, GTV-T_{res}), extensive gray zones, residual infiltration in the posterior bladder wall; adaptive CTV-T_{HR}, CTV-T_{IR} (GTV-T_{init} plus margins around the CTV-T_{HR}), CTV-T_{LR} for adaptive brachytherapy: coronal, transversal, and sagittal view. Maximum width, thickness, and height of the CTV-T_{HR} are indicated.

cancer diagnostic assessment and for adaptive brachytherapy treatment planning.

The adaptive volumetric CTV-T_{HR} concept can also be applied if only CT images and clinical examination are available for treatment planning. However, in this case, GTV-T_{res} can only be defined based on the clinical examination, which provides information on cervical, parametrial, and vaginal extension but not on uterine extension (tumor height). Drawings of the clinical findings may be used for delineating tumor spread. Tumor contours have to be transferred and superimposed onto the planning CT images (Hegazy *et al*., 2013). Due to uncertainties in clinical assessment, Hegazy *et al*. (2013) suggest inclusion of at least two-thirds of the uterus for advanced disease (IB2-IVA). For limited cervical disease (IB1), they recommend inclusion of only half of the uterus in the CTV-T. These suggestions, based on a large patient cohort, apply to clinical situations in which informations on tumor height are not available due to missing MRI information and seem to be more safely applicable compared with other recommendations (Viswanathan *et al*., 2007). CTV definition based on clinical examination and CT is feasible but results in many cases in less precise target selection and contouring, and consequently larger target volumes (Hegazy *et al*., 2013; Viswanathan *et al*., 2007). Major shortcomings of this approach may exist in advanced disease (Pötter *et al*., 2016). Further research is needed to evaluate the applicability of these approaches.

The role of functional imaging for defining CTV-T_{adapt} is not clear. The vast majority of tumors do not provide any residual uptake signal after combined chemo-radiotherapy (Kidd *et al*., 2013), which would be required to use these imaging modalities for defining CTV-T_{adapt}.

If treatment planning is based exclusively on radiographs, the adaptive approach can still be followed, but with more limited accuracy. The information from repeat gynecologic examination with regard to tumor configuration and tumor dimensions and any adjacent residual pathologic tissue as documented on a 3D drawing is transferred onto the radiographs (Figure 4.7) and onto the 3D treatment plan in relation to the applicator (see Section 10 and Figure 10.3). If additional information from volumetric or sectional imaging is available, this can also be used to define the GTV-T and the CTV-T following the radiographic approach. Based on this information, the adaptive CTV_{HR} or the CTV-T_{IR} may be selected in particular focusing on maximum width, and thickness (height) as available. Specific attention is necessary to assess the maximum target dimensions and their distance from the tandem (vaginal sources) for the various directions of interest such as left–right, anterior–posterior (along the uterine axis) (see Figures 5.9–5.12, 5.14, 5.16 and 10.3).

5.4.5.2 The Intermediate-Risk CTV-T (CTV-T_{IR}). GTV-T_{init} carries the highest density of tumor cells at the start of treatment. Even after

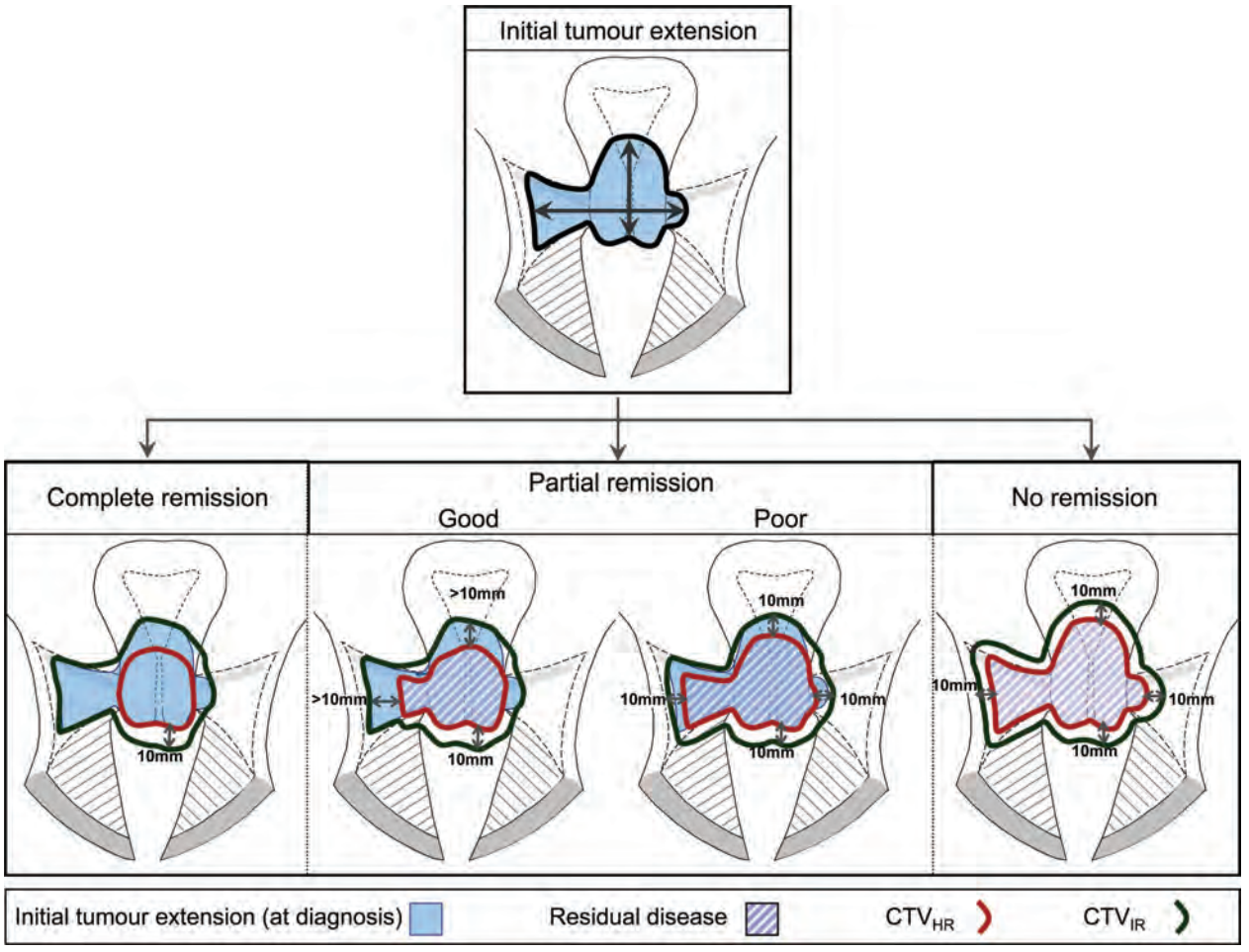

Figure 5.13. Schematic diagram for cervical cancer, with parametrial infiltration (IIB distal) and various level of remission (response): selection of different CTV-T_{HR} and CTV-T_{IR} dependent on GTV-T_{init} and GTV-T_{res} applying various margins for the CTV-T_{IR} in adaptive brachytherapy (see also examples in the Appendix).

considerable treatment and volume change, GTV-T_{init} retains importance. It can be assumed that residual tumor cells remain at various locations in this volume, even if the tissue has changed to a macroscopic normal appearance on clinical and imaging examination. Therefore, in the adaptive target concept for cervical cancer, special attention is paid to GTV-T_{init}. To this end, the CTV-T_{IR} is defined, which includes GTV-T_{init} [and in any case, a margin around the CTV-T_{HR} (see next paragraph)]. The concept of CTV_{IR} can be applied, for example, if patients are treated with EBRT and chemotherapy to be followed by brachytherapy (common for Stage IB2 to Stage IVA disease). The selection and contouring of CTV-T_{IR} is based on macroscopic tumor extension at diagnosis (GTV-T_{init}), which is superimposed on the topographic situation at the time of brachytherapy. This usually also leads to a margin around the CTV-T_{HR} in areas of the initial GTV-T due to tumor shrinkage. This definition is sufficient if the GTV-T_{init} covers the whole cervix as a minimum.

For areas of GTV-T_{init} located within the borders of the whole cervix, the concept of the GTV-T_{init} is alone not sufficient to define an intermediate risk CTV-T. CTV-T_{HR} then serves as (additional) criterion for the selection of CTV-T_{IR} as it always includes the whole cervix, independent of the size and configuration of the GTV-T. In order to account for suspected microscopic residual disease in the regions outside the CTV-T_{HR} borders, a margin around CTV-T_{HR} is added to produce CTV-T_{IR}.[1] This margin should be large enough to include the suspected residual microscopic disease and is decided by the radiation oncologist. The GEC ESTRO Recommendations suggest a 10 mm margin in the lateral and cranio-caudal directions and 5 mm in the anterior–posterior direction (Haie-Meder

[1]The authors are aware that the area of significant microscopic tumor burden is situated around the CTV-T_{HR} (and partly inside the CTV-T_{HR}). Therefore the CTV-T_{IR} should be a volume surrounding the CTV-T_{HR} like a shell according to the dimensions and the configuration of the GTV-T_{init} and should include a margin at the borders of the CTV-T_{HR} where there was no initial GTV-T.

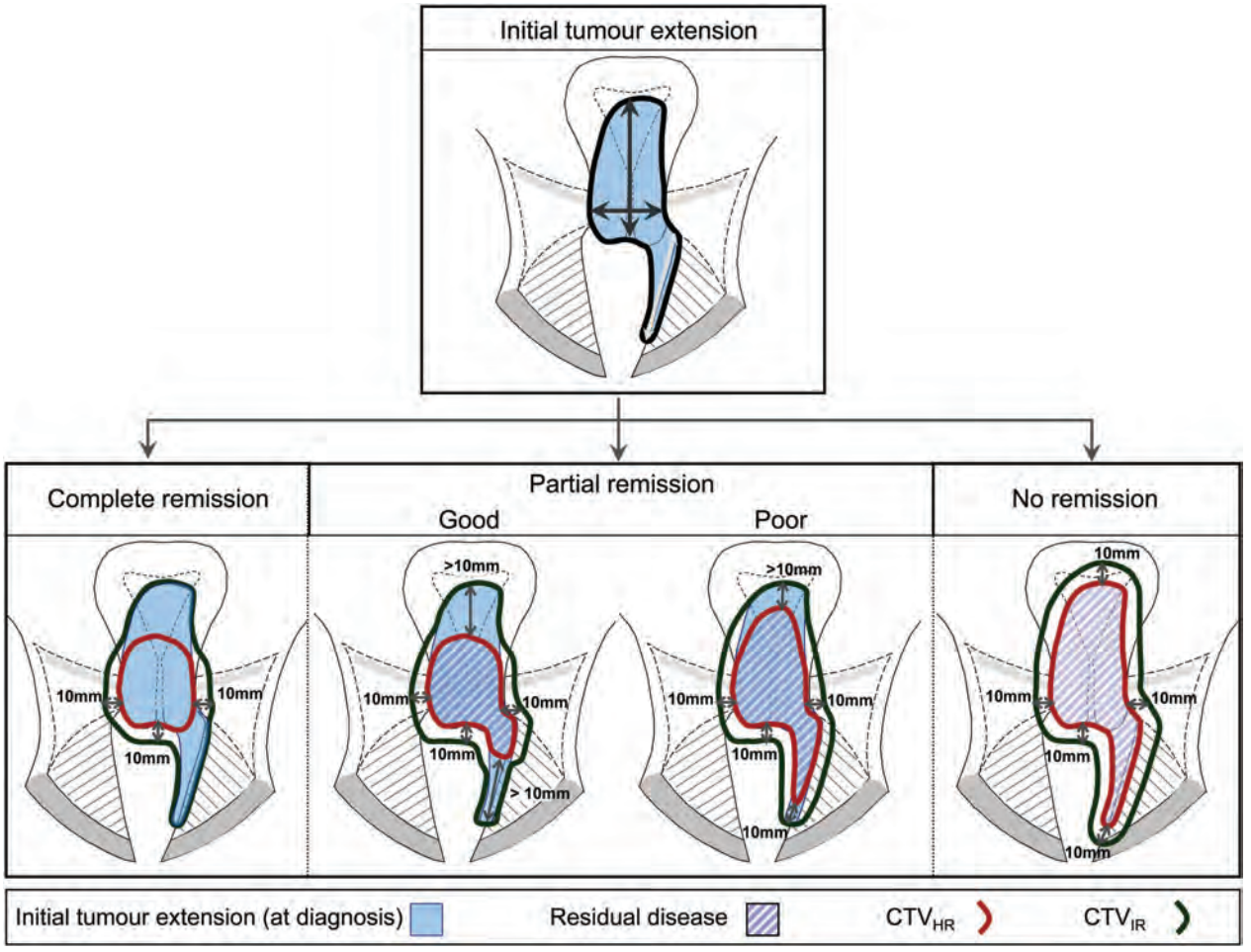

Figure 5.14. Schematic diagram for cervical cancer, with uterine and vaginal infiltration (IIIA) and various levels of remission (response): selection of different CTV-T_{HR} and CTV-T_{IR} dependent on GTV-T_{init} and GTV-T_{res} applying various margins for the CTV-T_{IR} in adaptive brachytherapy (see also examples in the Appendix).

et al., 2005), which has been widely accepted in clinical practice (see introduction to 5.4.5). Further clinical research may provide more clinical evidence for defining the necessary width of such margins.

5.4.5.2.1. Selection of the CTV-T_{IR} for Various Patterns of Tumor Response after EBRT ± Chemotherapy.

For *complete response*, CTV-T_{IR} includes the CTV-T_{HR} and the initial macroscopic tumor extension (GTV-T_{init}) as superimposed on the anatomy at the time of brachytherapy. Margins must be applied around the (other) CTV-T_{HR} borders (not included in GTV_{init}), as appropriate (Figures 5.13 and 5.14).

For *good response* (≥70 % to 75 % GTV-T volume reduction, limited residual pathologic tissue), CTV-T_{IR} includes the CTV-T_{HR} and the initial macroscopic tumor extension as superimposed on the anatomy at the time of brachytherapy. Margins must be applied around the (other) CTV_{HR} borders (not included in GTV_{init}), as appropriate (Figures 5.13 and 5.14).

For *poor response* (<70 % to 75 % GTV volume reduction and significant residual pathologic tissue), CTV-T_{IR} includes GTV_{res} and the residual pathological tissue as starting point. Margins are added for suspected adjacent residual microscopic disease in the direction of potential residual microscopic spread taking into account natural anatomical borders [according to GEC ESTRO recommendations (Haie-Meder *et al*., 2005)]. The margins have to include as minimum the initial macroscopic tumor extension as superimposed on the anatomy at the time of brachytherapy. In addition, margins must be applied around the other borders of the CTV_{HR} not included in GTV_{init}, as appropriate (Figures 5.13 and 5.14).

For *stable disease*, CTV-T_{HR} becomes similar to the GTV-T_{init}. Margins [according to GEC ESTRO recommendations (Haie-Meder *et al*., 2005)] are added to this CTV-T_{HR} analogue to those applied at

diagnosis (Figures 5.13 and 5.14, compare also Figure 5.3). In addition, margins must be applied around the other borders of the CTV_{HR} not included in GTV_{init}, as appropriate.

In the case of rectal/bladder invasion, CTV-T margins should not go into the organ lumen but should just include the tumor invasion into the organ wall (Figure 5.12).

The GEC ESTRO Recommendations suggest margins around the CTV-T_{HR} in the range of 5–10 (15) mm [10 mm in all directions except anterior/posterior with 5 mm (Haie-Meder *et al*., 2005)], which corresponds to the guidelines in the EMBRACE studies (EMBRACE, 2015). These margins must not include any OAR besides the vagina, except in Stage IVA disease. Prospective studies of current clinical practice may be helpful to better understand which margins are relevant in specific clinical situations.

5.4.6 Uncertainties in Target Selection and Contouring

Uncertainties in target selection and contouring are inherent to the CTV concept, as assumptions about microscopic tumor spread have to be made and decisions taken (Petrič *et al*., 2013). Such uncertainties have also been recognized for other tumor sites (Buijsen *et al*., 2012; Nijkamp *et al*., 2012; Steenbakkers *et al*., 2006; Wang *et al*., 2011) and have been discussed in ICRU reports for EBRT (ICRU, 1999; 2004a; 2007; 2010). In high-precision treatment planning and delivery, the uncertainties in target selection and delineation represent one of the weakest parts of the chain of image-guided adaptive radiotherapy (Kirisits *et al*., 2014; Njeh, 2008) and this seems also to be true for brachytherapy in cervical cancer (Tanderup *et al*., 2013). There is emerging evidence (Kirisits *et al.*, 2014) that CTV-related uncertainties may even overshadow the so-called motion and set-up geometrical uncertainties considered in the PTV concept (van Herk *et al*., 2000).

In the adaptive CTV-T definition, the operator-related uncertainties may be even more significant compared with CTV-T definition at diagnosis, since the relevant empirical base is still developing. The adaptive approach implies that GTV-T_{res} and the residual pathologic tissue after tumor shrinkage are considered in target selection. Knowledge about the validity and reliability of imaging and clinical findings after chemo-radiotherapy with regard to residual GTV-T and residual pathologic findings remain sparse, supported by only limited pathologic and/or clinical evidence (Lambrecht *et al*., 2010; Vincens *et al*., 2008).

Several inter-observer studies of MRI-based contouring of target volumes have shown reasonably high conformity indices (0.6–0.7); however, with some variation in certain regions, particularly the parametria, vagina, and uterine corpus (Dimopoulos *et al*., 2009a; Lang *et al*., 2006; Petric *et al*., 2008; Petrič *et al*., 2013). Uncertainties are much more pronounced for CT compared with MRI due to the limited soft tissue contrast obtainable. These uncertainties result in relatively larger target volumes when CT is used for target delineation (Hegazy *et al*., 2013; Pötter *et al*., 2016; Viswanathan *et al*., 2007). Due to the significant dose gradients in brachytherapy, the impact of contouring uncertainties on dose reporting can be significant (Hellebust *et al*., 2013) and may result in different CTV-T doses when reporting either MRI or CT-based target definitions. Therefore, dose reporting must specify the imaging modality used (see Section 5.3.2 and 5.4.2).

In the process of treatment planning, the prescription isodose is at present—in the era of transition from 2D to 3D—frequently chosen larger than the contoured CTV-T_{HR}. This expansion reflects that CTV-T uncertainties are taken into account by prescribing a treatment that is not completely conformal to the delineated CTV-T (Figure 5.15). This clinical practice includes a CTV-T-related non-conformality region that takes uncertainties in both target selection and contouring into account.

The definition for CTV-T_{HR} according to the GEC ESTRO recommendations was primarily intended only for reporting and not for prescription, as no clinical experience was available to justify these definitions (Chargari *et al*., 2009; Lindegaard *et al*., 2013; Nomden *et al*., 2013a; Pötter *et al*., 2007, 2011). Therefore, due to limited clinical validation of this new adaptive CTV-T_{HR} concept, traditional prescription and target concepts have been and may continue to be used—in particular in a transition period from radiography to volumetric-imaging-based treatment planning and prescription. One hundred years of successful experience in cervical cancer brachytherapy with overall excellent clinical results have to be recognized when considering the implementation of new prescription and target concepts within the frame of IGABT. Traditional brachytherapy of cervical cancer has, for example, always included large parts of the uterine corpus and of the upper vagina [traditional pear-shaped isodose (Erickson, 2003; Nkiwane *et al*., 2013; Sapru *et al*., 2013; Tanderup *et al*., 2010a)]. Therefore, the planning aim and the prescription isodose according to institutional guidelines (see also Section 8.6) may (still) involve margins outside the contour of CTV-T_{HR} (Figure 5.15). This practice is likely to change gradually with the accumulation of clinical evidence for

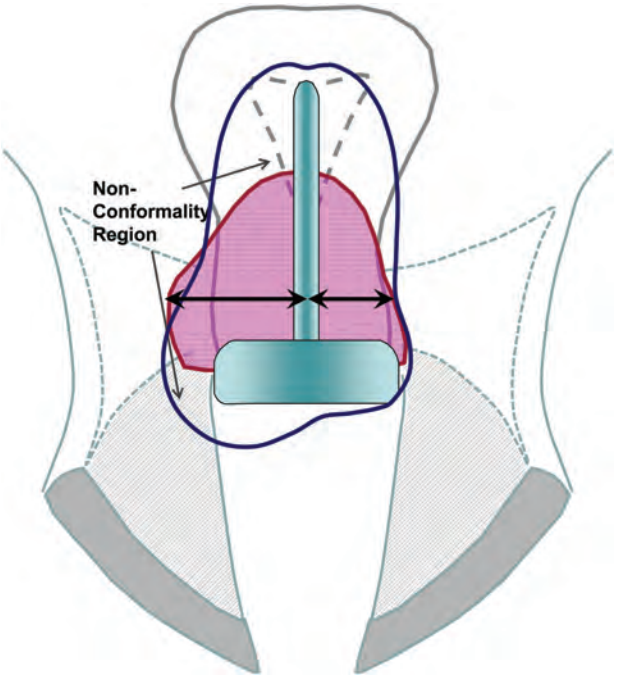

Figure 5.15. Schematic illustration of a cervical cancer Stage IIB after EBRT and chemotherapy with the ring applicator in place: CTV-T_{HR} and prescription isodose (black line) are shown in the cervix, uterus, parametria, and vagina in the coronal view. The size of the cranial uterine non-conformality region reflects the target contouring uncertainty mainly due to the lack of discrimination in the uterine stroma between the cervix and uterine corpus, whereas the caudal vaginal non-conformality region reflects uncertainties in target selection for the upper vagina, following older traditions. Toward the lateral parametria, there is almost no non-conformality-region included [modified from Tanderup *et al*. (2010c)].

the use of prescription isodoses more tailored to the adaptive clinical target contours (Mohamed *et al*., 2014; Nkiwane *et al*., 2013; Tanderup *et al*., 2010a).

Evidence is emerging, that with IGABT, very high local control rates can be achieved using the new target concept based on for CTV_{HR} and CTV_{IR} (Chargari *et al*., 2009; Lindegaard *et al*., 2013; Nomden *et al*., 2013a; Pötter *et al*., 2007; 2011) and joining this with the past *pear concept* for intracavitary brachytherapy (Lindegaard *et al*., 2008, 2013; Pötter *et al*., 2008b; Tanderup *et al*., 2010a). This new approach includes extension of the dose into the parametria as appropriate and feasible in the case of Stage IIB and IIIB tumors and typically a decrease in the dose toward the tip of the tandem (upper uterine corpus) tailored to primary tumor spread and response (Figure 5.15, see examples in the Appendix (Jürgenliemk-Schulz *et al*., 2009; 2010; Kirisits *et al*., 2005; 2006a; Nomden *et al*., 2013a). So far, the isodose in the vagina has been kept quite similar to the traditional pear shape in many institutions. This pear-shaped isodose still implies a large non-conformality region when compared with the CTV-T_{HR} definition (Figure 5.15).

Specific considerations for target selection are discussed in the following (Figure 5.15). They reflect the situation as outlined above reflecting the time when this report is written:

(a) In the cranial uterine direction, there is a smooth transition between the uterine cervix and uterine body without natural borders. The internal uterine os indicates the beginning of the uterine cavity and the end of the endo-cervical canal. There is no clear border visible on images between the uterine cervix and corpus stroma in many women. Traditional experience included major parts of the uterine corpus in the target since applicator loading through the tip of the tandem was standard (Gerbaulet *et al*., 2002a; ICRU, 1985). This traditional approach for non-volumetric image-based target definition was significantly different from the present MRI-based practice of often including only the cervix in the CTV-T_{HR} volume for tumors not infiltrating the uterine corpus [such approach is not appropriate, if only CT is available (Hegazy *et al*., 2013)].

(b) In the caudal vaginal direction, the upper vagina, taken as approximately the upper third, about 2 cm to 3 cm, has been included in the prescribed isodose contour since the early days of intracavitary brachytherapy, resulting in exposure of a significant vaginal volume (Gerbaulet *et al*., 2002a; ICRU, 1985). Furthermore, due to the loading of the vaginal part of the applicator, the upper third of the vagina has always received high radiation doses. The large non-conformality region in the upper vagina associated with the traditional pear-shaped isodose has not changed significantly with the implementation of IGABT so far. This caudal margin is also large compared with that at the cranial part of the high-risk CTV at the uterine cervix–corpus transition (Mohamed *et al*., 2014; Sapru *et al*., 2013; Westerveld *et al*., 2013).

(c) For the lateral parametrial extensions, the cervical border in the case of an intact cervix and the residual GTV and the gray zones indicating residual pathologic tissue in the case of infiltrative extra-cervical growth have been introduced for target delineation. The outer cervical border represents the border of potential spread within the tumor-bearing organ (intact cervical rim). Residual GTV and adjacent gray zones represent areas with a high risk of residual disease. Such gray zones must be located in areas where gross disease was seen before initial treatment

($GTV\text{-}T_{init}$). The pear-shaped isodose may not have covered these borders in the past. For tumors with a large width after EBRT, the target width delineated according to the $CTV\text{-}T_{HR}$ definition would often be outside the width of the pear-shaped prescription isodose. Following the high-risk CTV-T recommendations, it is straightforward to contour the cervical border for the intact cervix; however, it is not so clear how to define the borders of such gray zones in the case of extra-cervical growth. These borders are by definition not very well defined which may lead to large inter-observer variations. Nevertheless, the existing evidence shows that contouring uncertainties for the $CTV\text{-}T_{HR}$ seem to be less pronounced than for the $GTV\text{-}T_{res}$ and the $CTV\text{-}T_{IR}$ (Dimopoulos *et al*., 2009a; Lang *et al*., 2006; Petric *et al*., 2008; Petrič *et al*., 2013).

(d) Similar considerations as described in (c) apply to the anterior and posterior borders in the case of very advanced disease infiltrating these regions. However, in the majority of cases, these areas are not involved and therefore the borders are clearly visible and no major uncertainties are to be expected.

In summary, $CTV\text{-}T_{HR}$ selection and contouring uncertainties may at present be taken into account during dose planning by application of dose distributions that are not completely conformal in particular in the cranio-caudal direction. Systematic application of uniform margins to compensate for target selection and/or contouring uncertainties is strongly discouraged, since this leads to an overall dose escalation in the entire target volume [the same applies for PTV margins, see Figure 5.16 and Section 5.5 (Tanderup *et al*., 2010c)].

When the image-guided approach and the high-risk CTV definitions become more clinically validated and with improvements in imaging technology, uncertainties in target selection and contouring are expected to decrease and the conformality of the planning aim and the prescribed isodose is likely to improve significantly. Every effort should be undertaken to reduce these uncertainties through the use of adequate imaging, delineation guidelines, education and training, and continuous clinical research.

To this end, it is suggested to describe these uncertainties and the applied regions of non-conformality in order to provide evidence-based guidelines on imaging, target selection, and contouring in different clinical situations (tumor stage, tumor response) and their effect on clinical outcome.

5.5 Planning Target Volume (PTV-T)

5.5.1 Concept of PTV-T. The PTV is defined as the volume that includes the CTV with a margin that accounts for organ motion and geometrical uncertainties in dose delivery. The PTV is a geometrical concept, designed so that the CTV receives the prescribed dose with a clinically acceptable probability (ICRU, 1993b). The PTV may be equal to or larger than the CTV.

A PTV is defined each time radiotherapy of a CTV is planned for curative, postoperative, or palliative intent.

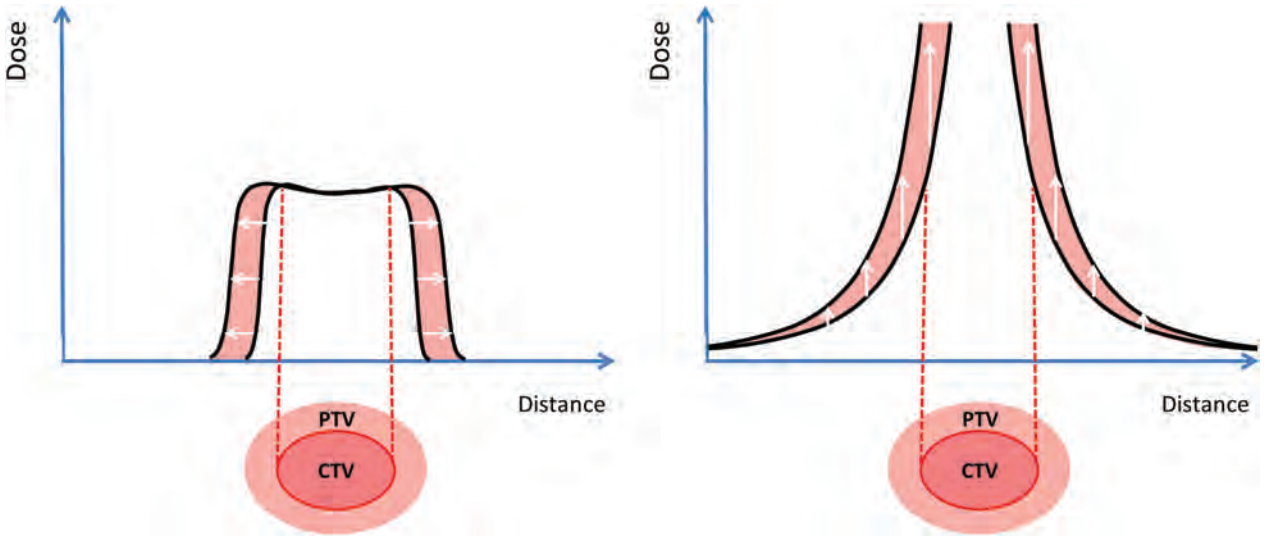

Figure 5.16. Dose profiles comparing the effects of adding margins on dose distribution in the CTV and PTV in external beam therapy (left panel) and in intracavitary cervical cancer brachytherapy (right panel). In external beam radiotherapy, adding a PTV margin increases the volume irradiated to a high dose, but the magnitude of the CTV dose remains roughly unchanged. In contrast, application of a PTV margin in the lateral and anterior–posterior directions in brachytherapy and a re-normalization of dose to the PTV will result in a systematic increase of the dose throughout the CTV and organs at risk. Modified from Tanderup *et al*., (2010c) with permission.

However, the approach to delineate the PTV, its size and shape depend on the radiotherapy technique.

The concept of PTV was initially introduced for external photon-beam therapy in ICRU Report 50 (ICRU, 1993b). It was developed and slightly adapted in successive ICRU Reports (ICRU, 1999; 2004a; 2007; 2010). It has not been specified for brachytherapy explicitly (ICRU, 1985; 1997) except for endovascular brachytherapy (ICRU, 2004b; Pötter *et al*., 2001).

5.5.2 Geometric Uncertainties in EBRT and Brachytherapy

Delivery of the appropriate dose distribution to a CTV leads inevitably to irradiation of normal tissue. In earlier ICRU documents, the possibility of compromising margins of the PTV was suggested if they encroached on an OAR (ICRU, 1999). It is now recommended (ICRU, 2007; 2010) that the delineation of the primary PTV should not be compromised. Alternatively, subdivision of the PTV with different prescribed doses or the establishment of appropriate dose gradients sufficient to protect the OAR is now recommended. Regardless of the chosen approach dose reporting should include the entire primary PTV in order to indicate the existence of regions of under-dosage in the PTV and possibly the CTV.

The delineation of a PTV has to take into account two types of uncertainties:

- The CTV's movements within the patient,
- irradiation delivery, which depends largely on the irradiation technique.

The margin taking movement into account surrounds the CTV like a shell and is called the internal margin and defines the internal target volume (ITV). The second set of uncertainties related to beam delivery conditions leads to the definition of the set-up or external margin which is again added to the CTV. The combination of these two types of margins around the CTV forms the PTV. ICRU Report 62 (ICRU, 1999) recommended that, for EBRT, internal and external margins should be added in quadrature. The additional volume irradiated when adding a PTV margin to a CTV depends on tumor location and radiation treatment technique. In some cases, such margins may be small, such as in high-precision radiation application techniques like IGRT or where the radiation applicator is fixed relative to the target, as in intracavitary and interstitial brachytherapy.

5.5.3 Geometric Uncertainties and PTV Margins in Brachytherapy

In brachytherapy, dose distribution is different from EBRT due to source characteristics with a steep dose fall off near the sources resulting in a very inhomogeneous dose distribution inside the GTV and CTV and in adjacent areas. In cervix cancer brachytherapy, the tandem and needles as source carriers are inside the CTV. The ability to modify the brachytherapy dose distribution differs in the direction of the axis of source catheters [longitudinal direction—(*e.g*., along tandem and needles)] *versus* in the direction perpendicular to these (orthogonal direction).

In the longitudinal direction, the dose distribution may be elongated by loading source positions just at the edge or outside the target. In this way, a dose distribution can be obtained which extends beyond the CTV. This approach will make the dose distribution more robust with respect to uncertainties in the direction along source catheters. Such an arrangement of source positions has little effect on the dose distribution in the central region of the application.

In the orthogonal direction, the dose distribution cannot be elongated in a similar way. The orthogonal dose fall off is almost exclusively determined by the inverse square law and cannot be manipulated to become less steep by modifying the loading pattern without introducing additional catheters or needles. The isodose lines can be pushed further away from the source in the orthogonal plane only by escalating the dose. Therefore, defining a PTV for brachytherapy with a fixed margin uniformly around the CTV and prescribing to that PTV significantly increases the dose within the whole CTV [Figure 5.16 (Tanderup *et al*., 2010c)]. This is fundamentally different from the situation in EBRT where the dose plateau is increased in size by application of a margin with no accompanying dose escalation (Figure 5.16).

For endovascular brachytherapy, a detailed PTV concept was developed (ICRU, 2004a; Pötter *et al*., 2001), which includes adding a margin in the direction of the catheter axis compensating for movements relative to the defined target. This longitudinal-margin concept has also been applied for intra-luminal brachytherapy for other malignancies (Pötter *et al*., 2002b) and specifically for esophageal cancer (Pötter and Van Limbergen, 2002). Again, margins in the orthogonal direction are not included. The longitudinal-margin approach for intra-luminal brachytherapy has been reported to be relevant for clinical outcome (Schmid *et al*., 2004) and represents an approach similar to what is proposed here for intracavitary brachytherapy.

5.5.4 Internal Margin and the ITV

The ITV is defined as the CTV plus a margin which takes into account uncertainties and variations in

size and shape of the CTV and its position/movements within the patient (ICRU, 1999).

These uncertainties in the position of the CTV result essentially from expected physiological movements (*e.g.*, respiration, organ movement) and variations in site, size, shape, and position of the GTV, the CTV, and organs in or adjacent to the CTV (uterine and vaginal movement resultant from different filling of the bladder, rectum, movements of the bowel, *etc.*) (Beadle *et al.*, 2009; Lim *et al.*, 2008; Taylor and Powell, 2008; van de Bunt *et al.*, 2006; 2008).

As a result, the additional normal tissue volume that needs to be irradiated constitutes the basis for the internal margin (Aaltonen *et al.*, 1997; Ekberg *et al.*, 1998).

5.5.4.1 External Beam Radiotherapy. In gynecologic EBRT, there are significant spatial variations both for the uterus as a tumor-bearing organ and for the adjacent organs at risk during the course of external beam radiotherapy and even within fractions (Beadle *et al.*, 2009; Lim *et al.*, 2008; Taylor and Powell, 2008; van de Bunt *et al.*, 2006; 2008). These variations require consideration of margins to compensate for the internal movements of the CTV-T and adjacent OARs, in particular when applying advanced conformal techniques like IMRT.

5.5.4.2 Brachytherapy. There may be variations in the relation between applicator and organs/target during delivery of brachytherapy and/or between brachytherapy planning and delivery, which have to be addressed as intra-fraction, inter-fraction, and/or intra-application and inter-application variation. These variations may be different for one HDR brachytherapy application with one or two fractions and for a protracted course of PDR/LDR brachytherapy, which may last from 10 h to 120 h. Furthermore, there may be more than one application for the full course of brachytherapy, such as in fractionated HDR brachytherapy or in 2 fractions of PDR/LDR brachytherapy leading to inter-application variation. Clinical research addressing this type of uncertainties is ongoing [see Section 9.6 (Andersen *et al.*, 2013; De Leeuw *et al.*, 2009; Hellebust *et al.*, 2001; Jamema *et al.*, 2013; Kirisits *et al.*, 2006b; Lang *et al.*, 2013; Mohamed *et al.*, 2013, Morgia *et al.*, 2013; Nesvacil *et al.*, 2013a)].

In intracavitary brachytherapy, a tandem combined with a vaginal applicator is inserted into the narrow cervical canal and the uterine cavity and additionally fixed toward the cervix with a vaginal tamponade or a vaginal mould. As a result, the uterine cervix and the tumor have a fixed relationship with the source carrier system (the applicator). Studies of the CTV-T_{HR} for cervical cancer showed no, or very limited, motion of the cervix and the adjacent target structures relative to the applicator (Petrič *et al.*, 2013). These findings imply that internal margins as recommended for external beam radiotherapy need not be applied for intracavitary cervical cancer brachytherapy.

There may be clinical situations in brachytherapy, where the applicator is not sufficiently fixed within one fraction or within several fractions using the same applicator implantation and treatment plan. This could result in different positions of the applicator in relation to the target. Nevertheless, such an application technique is regarded as clinically inappropriate and should not be compensated for by additional margins. Specific measures for quality control such as re-imaging are more appropriate. The possible development of edema or swelling of the cervix during a protracted course of high-dose intracavitary radiotherapy, potentially leading to some volume changes (Morgia *et al.*, 2013), requires specific attention. The most appropriate way to deal with this problem may be repeated imaging and re-contouring and subsequent adaptation of the treatment plan as appropriate.

When imaging, target definition and dose planning is performed for each brachytherapy fraction or for each application (applicator insertion), the inter-application and/or inter-fraction uncertainties are taken into account by the repeated target definition for each fraction or application, respectively.

In summary, according to current knowledge internal margins need not be applied to compensate for variations in target position from treatment to treatment in the vast majority of cervical cancer cases treated with intracavitary brachytherapy. On the other hand, application of an internal margin is needed to compensate for variations of the CTV during the course of EBRT, in particular when applying advanced conformal techniques like IMRT with delineation of a CTV-T which may require extra PTV margins due to uterine movements or to variations in rectum and bladder filling.

5.5.5 Set-up Margin (External Margin)

The set-up margin is related to uncertainties in aligning the patient relative to the radiation source, mechanical uncertainties of the treatment delivery equipment, as well as uncertainties introduced during the treatment planning procedure such as image transfer and fusion.

5.5.5.1 External Beam Radiotherapy. To account for uncertainties in patient positioning and alignment of therapeutic beams during treatment

planning and through treatment, an additional volume of normal tissue may need to be irradiated. For this purpose, the concept of set-up margin has been introduced within EBRT (ICRU, 1999). The size and shape of the margins depend on the irradiation technique and on daily uncertainties in positioning. For some tumor locations, the margins can be reduced by special techniques (*e.g.*, fixation devices for pelvic tumors or for head and neck tumors, tumor tracking or gating for respiration-related motion management. However, in general, these uncertainties cannot be totally avoided, only reduced under high-precision radiotherapy conditions.

5.5.5.2 Brachytherapy. The set-up uncertainties, as defined for EBRT, may not apply in the context of brachytherapy. In principle, the uncertainties for brachytherapy depend on the reconstruction of the applicator on the images (see Section 9.1), image fusion uncertainties (see Section 9.3), as well as afterloader source positioning. These uncertainties have recently been elaborated in detail for the whole field of brachytherapy (Kirisits *et al*., 2014) and for image-guided cervical cancer brachytherapy in particular (Hellebust *et al*., 2010a; Tanderup *et al*., 2013). There are systematic and random components of these uncertainties. Applicator reconstruction uncertainties are dependent on imaging modality, image quality, and on the procedure used for reconstruction. Under the condition of appropriate applicator commissioning and reconstruction, the uncertainties are limited (SD$<$ 1–2 mm) and occur mainly along the axis of the source catheters (Haack *et al*., 2009; Hellebust *et al*., 2007; 2010a; Tanderup *et al*., 2010b). The geometric uncertainties related to the afterloader source positioning are also mainly present in the direction along source catheters, and have been reported to be limited to about 1 mm in straight catheters, but may be larger in curved catheters such as the ring (Hellebust *et al*., 2007; 2010a). When image fusion is used during the patient preparation phase, this will also contribute to set-up uncertainties. Image fusion uncertainty tends to be more pronounced in the direction orthogonal to image slice orientation, which is along the tandem in the case of para-transversal imaging.

For set-up uncertainties, which may have to be regarded as the major contributor to geometric uncertainties, it is not possible to apply in general the PTV margin concept as developed for EBRT (see Section 5.5.3). However, in the direction along source catheters, it is possible to apply a PTV margin and to expand the dose distribution by application of additional source positions (Figure 5.17).

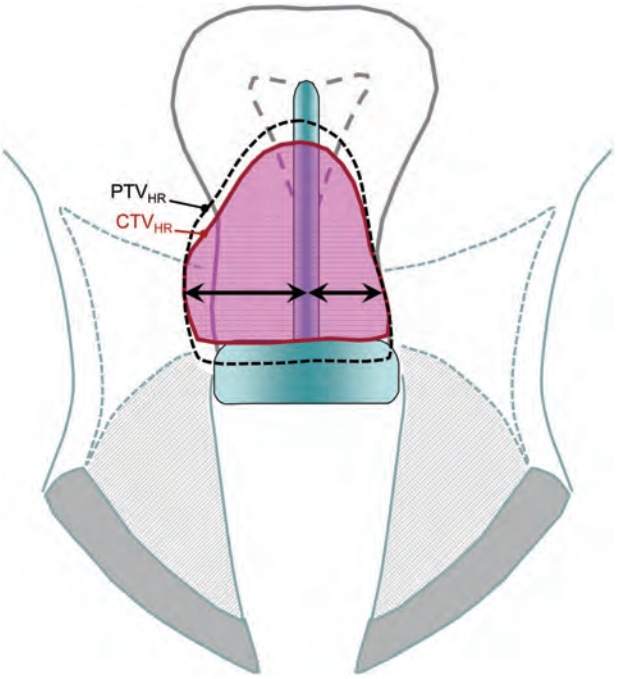

Figure 5.17. Longitudinal margins for set-up uncertainties in intracavitary IGABT. Margins are added to compensate for uncertainties only in the longitudinal direction, whereas no margins can be added in the orthogonal direction. Therefore, a PTV$_{HR}$ may be delineated in the cranio-caudal direction. This may also apply within a planning procedure before the applicator insertion, resulting in a guiding PTV, which may guide the necessary length of the tandem to compensate for set-up uncertainties.

5.5.6 Preimplantation PTV

Within the setting of intracavitary brachytherapy, the major approach to account for uncertainties in the application is to adapt the application itself to the specific issues caused by uncertainties. These have to be clearly defined before the application is performed to ensure the appropriate choice and positioning of the applicator. A systematic planning procedure is recommended that includes pre-implantation PTV contouring with a margin added to the CTV in any directions as appropriate. Such pre-implantation concept avoids the need to draw a shell margin around the CTV after application. In the case of contour extensions necessary in the longitudinal and/or orthogonal direction of the source axes, the application has to be adapted by lengthening and/or widening the applicator to ensure that the dose can be appropriately delivered to the CTV. Such a pre-planning procedure has long been practiced for interstitial brachytherapy, even before 3D imaging was used. Pre-implant planning and dosimetry was based on clinical examination, drawings, radiographs, tumor measurements in all directions, and CTV margin determination (ICRU,

1997; Pierquin and Marinello, 1997) and was applied for accessible cancer sites such as skin, head, and neck. PTV margins to compensate for geometrical uncertainties were not explicitly taken into account (ICRU, 1997).

Another more advanced 3D image-based pre-planning procedure has been developed for US-based prostate brachytherapy with a 3D image-based target concept and the application of upfront margins for uncertainties and 3D dose planning. This prostate pre-procedure planning has become widely used in clinical practice (Blasko *et al*., 1993; Polo *et al*., 2010) and is now increasingly replaced by on-line 3D-based planning (Hoskin *et al*., 2013; Polo *et al*., 2010).

An image-based pre-planning procedure had not been implemented routinely in gynecologic brachytherapy in the past. However, application adaptation has been a common procedure. The MD Anderson and Paris school took into account individual anatomy and spread of disease based on clinical examination (Fletcher, 1980; Gerbaulet *et al*., 2002a). The individual mould fabrication was developed in the Paris school long ago (Chassagne and Pierquin, 1966; Magne *et al*., 2010). The introduction of the combined intracavitary and interstitial applicators [*e.g*., MUPIT-applicator (Martinez *et al*., 1985)] followed later for advanced disease. Their further development has been based on clinical and imaging information and resulted in applicators which used the vaginal source carriers (ring/ovoids) as a parametrial needle template(Dimopoulos *et al*., 2006b, Jürgenliemk-Schulz *et al*., 2009; Kirisits *et al*., 2006a). A systematic pre-application planning strategy, including a pre-procedure PTV, is now considered important to account for the specific clinical situation, the selection and contouring uncertainties in CTV and adaptive CTV, and the expected geometrical and dosimetrical uncertainties for the PTV (Fokdal *et al*., 2013; Petric *et al*., 2009; Tanderup *et al*., 2010c). However, the logistics of such pre-planning procedures remain challenging and therefore they have not become widespread. Pre-planning may in future be replaced by a 3D image based on-line approach comparable to the developments in prostate brachytherapy as outlined above.

The quality of applicator positioning, particularly the implantation procedure itself and how the implantation provides adequate dose coverage, is another important issue. The quality of the applicator positioning should not be confused with the geometric uncertainties as described. Quality of applicator positioning can in general not be compensated by margins but has mainly to be optimized through clinical experience and expertise, image guidance, and appropriate applicator availability.

5.6 Recommendations

Level 1: Minimum standard for reporting

FIGO/TNM stage
Tumor assessment is always based on initial and repeat clinical gynecologic examination and on additional volumetric or sectional imaging (MRI, CT, US, PET CT) as available

Initial and residual GTV:
GTV_{init} before any treatment
GTV_{res} at brachytherapy
Schematic 3D documentation on a clinical diagram of the findings on initial and repeat clinical gynecologic examination
- (transverse, mid-sagittal, mid-coronal sections; speculum view):
- location of GTV_{init} and GTV_{res} plus residual pathologic tissue
- dimensions of GTV_{init} and GTV_{res} plus residual pathologic tissue
  - maximum width and thickness, height as available (in mm) related to the endo-cervical canal (left, right, anterior, posterior)
- related to the upper vagina (fornices) (height) as appropriate
- configuration of GTV_{init} and GTV_{res} plus residual pathologic tissue

spread and growth pattern of GTV_{init} (exophytic/infiltrative)
High-risk CTV
CTV_{HR}: GTV_{res} at the time of brachytherapy (after response to chemo-radiotherapy) $\pm$ any pathologic residual tissue (CTV_{IR} in the case of prescription to CTV_{IR}) and the whole cervix

Schematic 3D documentation on a clinical diagram for clinical gynecologic examination
- (transverse, mid-sagittal, mid-coronal sections; speculum view):
- location of CTV_{HR}
- dimensions of CTV_{HR}
  - maximum width and thickness, height as available (in mm)/ standard height
  - related to the endo-cervical canal (left, right, anterior, posterior)
  - related to the upper vagina (fornices) (height) as appropriate
- configuration of CTV_{HR}
- volume is calculated by ellipsoid formula (optional) except for extensive vaginal involvement

Level 2: *Advanced standard for reporting*
All that is reported in Level 1 plus:

Volumetric imaging-based management	Radiography/treatment plan-based management
based on MRI (CT, US) and clinical drawing	based on clinical drawing $\pm$ volumetric imaging (2D information)
GTV_{init} and GTV_{res} (MRI + clin):	GTV_{res} (treatment plan/radiograph + clin $\pm$ volume image):
Volumetric imaging-based spread and topography (3D) for GTV_{init} and GTV_{res} + pathologic residual tissue	Clinical $\pm$ volumetric imaging (2D information)-based spread and topography for GTV_{init} and GTV_{res} + pathologic res. tissue
maximum width, thickness, height, and volume related to the endo-cervical canal (left, right, anterior, posterior) at diagnosis and at brachytherapy without applicator in place and with applicator in place and/or	maximum width, thickness, height, and volume related to the endo-cervical canal (left, right, anterior, posterior) at diagnosis and at brachytherapy without applicator in place and with applicator in place on radiograph/treatment plan
CTV_{HR} (MRI + clin; (CT + clin/US + clin)): (imaging modality to be specified)	CTV_{HR} (treatment plan/radiograph + clin $\pm$ volume image):
CTV_{HR} and CTV_{IR} (in the case of CTV_{IR} prescription) Volumetric imaging-based location of CTV_{HR} in 3D: CTV_{HR} includes GTV_{res} (if present) plus residual pathologic tissue plus whole cervix in relation to the applicator;	CTV_{IR} and CTV_{HR} in the case of CTV_{IR} prescription Radiography/treatment plan-based location of CTV_{HR} in relation to the applicator standard length defined as 2/3 up to full length of the uterine cavity;
maximum width, thickness, height, and volume; related to the endo-cervical canal (left, right, anterior, posterior)	maximum width, thickness, and standard height (tandem or 2/3 of uterine cavity length) and the estimated volume; related to the endo-cervical canal (left, right, anterior, posterior)

Level 3: *Research-oriented reporting*
All that is reported in Level 1 and 2 plus:

Volumetric imaging approximation based on:

GTV, HR CTV:
Functional imaging for additional information at diagnosis, during treatment, and at brachytherapy;

PTV
• Margins along the tandem

5.7 Summary

GTV, CTV, and PTV concepts as developed for EBRT in ICRU reports 50, 62, 71, 78, 83 are translated, merged, and further elaborated for adaptive radiotherapy in general and specified for adaptive brachytherapy in cervix cancer. The focus is on volumes related to the primary tumor.

GTV for the primary Tumor (GTV-T) is defined at diagnosis as macroscopic demonstrable disease assessed through various clinical, imaging, and/or pathologic investigations. A "composite GTV-T" is additionally introduced, which is the GTV finally delineated by the radiation oncologist responsible for the treatment. In the context of adaptive radiotherapy, the initial GTV-T is denoted as $GTV\text{-}T_{init}$.

CTV for the primary Tumor (CTV-T) includes the GTV-T and an area of surrounding tissue with potential contiguous and/or incontiguous microscopic disease. At diagnosis three CTVs-T may be defined for cervix cancer treatment, mainly in the case of limited disease treated with early brachytherapy: $CTV\text{-}T_1$ is the GTV-T and adjacent tissue, always including the whole cervix (initial CTV_{HR}); $CTV\text{-}T_2$ includes the $CTV\text{-}T_1$ plus margins (initial CTV_{IR}); $CTV\text{-}T_3$ includes the $CTV\text{-}T_2$ plus areas in adjacent compartments at risk for potential contiguous or incontinguos microscopic spread (initial CTV_{LR}) (see also below).

Change of GTV-T and CTV-T during treatment is emphasized in this report as it occurs regularly during an oncological treatment involving multiple treatment steps and modalities.

Residual GTV-T ($GTV\text{-}T_{res}$) is defined as the residual macroscopic tumor at the time of (brachytherapy) boost after treatment assumed sufficient to control microscopic disease. $GTV\text{-}T_{res}$ still bears clinical and/or imaging characteristics similar to the initial $GTV\text{-}T_{init}$ and may represent macroscopic and/or microscopic and/or even no residual disease.

Residual pathologic tissue may surround the residual GTV-T and bears different clinical and/or imaging characteristics (*e.g.*, edema, fibrosis)

compared with the initial GTV-T. It is always located within the region of the initial GTV-T.

Adaptive CTV-T (CTV-T_{adapt}) can be defined after any treatment phase and includes in any case the GTV-T_{res} and the residual surrounding pathologic tissue, if present. The adaptive CTV-T is a sub-volume of the initial CTV-T, except in the case of tumor progression.

High-Risk CTV-T (CTV-T_{HR}) is defined as a specific form of the adaptive CTV-T for "cervix cancer radiotherapy" following the GEC ESTRO recommendations. CTV-T_{HR} includes the GTV-T_{res} and the whole cervix and adjacent residual pathologic tissue, if present. It is the volume bearing the highest risk for recurrence. The CTV-T_{HR} for cervix cancer is selected by clinical examination and imaging at the time of brachytherapy, after 40 Gy to 45 Gy EBRT plus chemotherapy in advanced cervical cancer.

Intermediate-risk CTV-T (CTV-T_{IR}) represents the area of the GTV_{init} as superimposed on the topography at the time of brachytherapy and a margin surrounding the anatomical cervix borders (CTV-T_{HR}) in areas without an initial GTV. The CTV-T_{IR} therefore always includes the CTV-T_{HR} and margins as appropriate.

The terms "initial CTV-T_{HR}/initial CTV-T_{IR}" may be also used for CTV-T_1/CTV-T_2 as defined at diagnosis.

Low-risk CTV-T represents compartmental areas at risk for potential contiguous or incontiguous microscopic spread from the primary tumor (identical to CTV-T_3). CTV-T_{LR} comprises in advanced cervix cancer the whole parametria, the whole uterus, the upper part of the vagina, and the anterior/posterior spaces toward the bladder and rectum. This CTV-T_{LR} always includes the $CTV_{1/2}$ and the $CTV_{HR/IR}$, respectively. The CTV-T_{LR} is defined at diagnosis (initial CTV-T_{LR}) and maybe adapted during EBRT and also at brachytherapy (adaptive CTV-T_{LR}).

Examples, variations, and uncertainties for selection and contouring of the "initial and residual GTV-T and the initial and adaptive CTV-T" are described. Uncertainties vary with method of investigation (*e.g.*, imaging modality such as MRI, CT, US) with MRI and clinical examination at present regarded as gold standard.

Planning target volume (PTV-T) assures that the dose prescribed to the CTV-T is actually applied and has been developed within the frame of EBRT. The PTV-T margin around the CTV-T takes into account geometric and dosimetric uncertainties and is considered essential in EBRT. In brachytherapy, the dosimetric characteristics with sources inside the target volume, the variations, and the uncertainties are different from those in EBRT. A PTV-T margin in brachytherapy, selected after application, would contribute to dose escalation throughout the target. This applies to intracavitary and interstitial brachytherapy in cervix cancer. "Therefore, PTV margins are not recommended in general after applicator insertion." They may be considered within a Pre-Planning PTV selection procedure, as the application can then be adapted as appropriate. On the other hand, "internal target motion" of the CTV-T_{HR} in relation to the applicator can be regarded as minimal, if the applicator is fixed (*e.g.*, by an intravaginal tamponade). However, "geometric uncertainties" may occur, in particular in the longitudinal direction along the tandem. As margins along the longitudinal axis of the tandem have very limited impact on the dose throughout the target, "longitudinal margins" along the axis of the tandem maybe used to some degree to compensate for these set-up variations, even after application. Addition of margins orthogonal to the tandem axis leads to a dose increase throughout the entire target and are therefore not recommended.

Journal of the ICRU Vol 13 No 1–2 (2013) Report 89
Oxford University Press
doi:10.1093/jicru/ndw010

6. Organs at Risk and Morbidity-Related Concepts and Volumes

6.1 Treatment-Related Morbidity and Health-Related Quality of Life

Any oncological treatment impacts normal tissues within the tumor (blood vessels, connective tissue), in the vicinity of the tumor, or elsewhere (*e.g.*, systemic toxicity after chemotherapy). An effective curative treatment is therefore associated with a certain risk of side effects. Hence, treatment-related morbidity and associated impairment of health-related quality of life are essential considerations in cancer treatment.

There are typical patterns in the incidence and time course of early and/or late morbidity for any treatment modality. Different treatment modalities can interact and further increase the risk of toxicity. Therefore, the choice of a certain treatment strategy must be based on balancing the curative (or palliative) potential of each individual modality and their combination(s) and the probability of inducing early or late adverse effects, based on the available evidence.

For localized cervical cancer management, the well-established curative options are surgery or radiotherapy alone or in combination. Adding concurrent cytotoxic chemotherapy to external-beam pelvic radiotherapy significantly increases the probability of local control and survival, in particular in locally advanced disease according to several randomized controlled trials [see Section 2 (Vale *et al.*, 2008)].

Cervical cancer surgery has a typical morbidity pattern, which is dependent on the extent of the procedure. Adequate surgery [*e.g.*, Piver I, II, III (modified Wertheim)] is dependent on the spread and stage of disease. The potential for cure is very high for Piver I surgery in early and limited-stage disease (IA, IB1, IIA) with low associated morbidity; hence, surgery plays an essential role in the management of these disease stages. Radiotherapy also has a very high curative potential in these stages of disease, with low associated morbidity, and therefore, radiotherapy is a clear alternative to surgery, arguably with less treatment-related morbidity according to a randomized trial (Landoni *et al.*, 1997). For more extensive locally advanced disease (*e.g.*, stage IB2, IIB, III), combined EBRT plus brachytherapy and concurrent cytotoxic chemotherapy provides a high potential for cure with moderate and acceptable late morbidity involving the bowel, bladder, or vagina (Eifel *et al.*, 1995; Perez *et al.*, 1983; 1984; Vale *et al.*, 2008). On the other hand, the potential of cure even with very radical surgery (*e.g.*, Piver III) in extensive locally advanced disease is low, and the treatment-associated complications and morbidity are high, particularly the rate of bladder incontinence. Therefore, surgery is not regarded as a standard treatment option for these disease stages [European Society of Medical Oncology guidelines (Haie-Meder *et al.*, 2010b)]. If surgery is combined with radiotherapy, there is evidence that treatment-related morbidity becomes more pronounced, particularly for lymphatic tissues (*e.g.*, lymph edema) and urinary bladder (Touboul *et al.*, 2010).

Chemotherapy, particularly cisplatinum and 5-Fluoruracil, has been shown to be effective in cervical cancer if applied concurrently with radiotherapy (Vale *et al.*, 2008). The typical morbidity patterns are early transient hematological toxicity, renal-function impairment (cisplatinum), and gastro-intestinal symptoms (5-FU) and dose-dependent chronic nerve pain, chronic kidney function impairment and hearing loss (cisplatinum), and reduced bowel function (5-FU). With combination treatment, there is added early morbidity, and there can also be increased late side effects (*e.g.*, gastrointestinal morbidity with 5-FU, vaginal changes, skeletal toxicity) (Gondi *et al.*, 2012). The mechanism underlying treatment-related morbidities can be different for the different treatment modalities and are currently not fully understood (Dörr, 2009; 2011; Trott *et al.*, 2012).

Impairment of quality of life in relation to treatment-related morbidity becomes an increasingly important concern when choosing oncological-treatment strategies (Kirchheiner *et al.*, 2012a). As knowledge in this field is still limited, substantial research efforts are required to understand the association between typical treatment-related clinical morbidity patterns and/or individual endpoints, and quality of life issues. Also in radiotherapy of cervix cancer, quality-of-life research is essential and must be based on patient-reported symptoms, for example, in major domains such as physical, social, and emotional quality of life, and in sexuality and body image.

In the following sections, the focus will be on the radiation oncology-related concepts for the assessment of treatment sequelae in organs at risk (OAR).

6.2 Radiation-Related Morbidity Endpoints

Organs at risk or critical normal structures are tissues that if irradiated could suffer significant morbidity and thus influence the treatment planning and the dose prescription (ICRU, 2010). In principle, all non-target tissues might be considered organs/tissues at risk. In clinical practice, however, the consideration of normal tissues as OARs usually depends on their radio-responsiveness and the dose to which their total or fractional volume is exposed for a given dose prescribed to the target.

In cervical cancer radiotherapy (EBRT with or without chemotherapy, brachytherapy), there are some relevant normal structures such as rectum and anus, sigmoid colon, large and small bowel, ureter, bladder, urethra, and vagina directly adjacent to CTV_{HR}, CTV_{IR}, and CTV_{LR}, and partly to the nodal CTV (CTV-N). The vagina and other organs might even be part of the CTV in advanced disease. Furthermore, there are structures adjacent to the tumor-related CTV, such as nerves (*e.g.*, for bladder, vagina, or rectum), vessels (such as in the parametria), and connective tissue. Finally, there are additional important normal structures in the pelvis (and beyond) (*e.g.*, ovaries, kidneys, bones, bone marrow, lymphatic structures, vessels, and nerves, some of which are of particular relevance for external-beam radiotherapy).

There are OAR-specific or OAR-sub-volume-specific types of morbidity, some of which are listed here only as examples. For bladder morbidity, urgency and incontinence can be related to the absorbed dose to the bladder trigone and neck, which are involved in bladder emptying and sphincter function. Increased bladder detrusor muscle tone, bladder fibrosis, and volume shrinkage, causing urinary frequency, can occur when larger parts or the entire bladder (wall) are in the moderate-to-high-dose volume. For rectal and sigmoidal morbidity, bleeding is linked to different grades of telangiectasia occurring even in small volumes. A change in bowel habits is rather a consequence of the circumferential absorbed dose. Rectal urgency and continence problems appear to be a consequence of damage to the overall recto-anal wall, with the relevant muscle and nerve plexus structures regulating the recto-anal discharge (Smeenk *et al.*, 2012).

The dose to certain specific anatomically defined OAR sub-volumes, as defined at specific points, can also predict morbidity [*e.g.*, rectal bleeding, ulceration, vaginal stenosis/shortening (see Figures 6.1–6.4)]. The ICRU rectal and bladder reference points have been used in the past in this respect (see Sections 8.4.1 and 10.3). For the vagina, new reference points are suggested in this report in the upper, middle, and lower part of the vagina as defined on radiographs or on volumetric images {*e.g.*, at the level of posterior-inferior border of the symphysis (PIBS) [see Sections 8.4.3 and 10.2, and Figures 6.1, 6.4, and 8.12 (Westerveld *et al.*, 2013)]}. Also the traditional ICRU rectum point as defined on radiographs (see Section 10.3) or on volumetric images (see Section 9.2) can serve as a recto-vaginal reference point correlating with vaginal stenosis/shortening (Kirchheiner *et al.*, 2016). Other points might be of interest, such as an anal reference point at the anal verge (see Figure 6.4). These anatomical reference points have patho-physiological or dosimetric relevance for the endpoint in question (compare rectum and bladder in Figure 6.4 and in Section 8.4.1; vagina in Figures 6.4 and 8.10–8.12 and in Section 8.4.3). Such anatomical reference points have the advantage of being located at a defined position within the organ (*e.g.*, as the bladder point in the bladder neck and the vaginal points in the upper, middle, and low vagina). The bladder reference point, for example, may be combined with the volume of interest (*e.g.*, as ratio of dose) in order to locate the high dose–volume within the bladder [posterior bladder wall/bladder neck (Nkiwane *et al.*, 2015)] which may help to find out a correlation between dose, volume, location, and a certain endpoint specific for a location of the high dose–volume (Mazeron *et al.*, 2015a).

Traditionally, tissue organization has been characterized as serial, parallel, or serial–parallel (ICRU, 1993b; 2010; Withers *et al.*, 1988). Serial organs or serial-like organs, such as the recto-sigmoid colon, bowel, and vagina, consist of a chain of functional units, which all need to be preserved to guarantee the functionality of the tissue. In contrast, in organs with a parallel organization, the functional sub-units are functioning independent of each other, and clinical symptoms are observed only if a certain (threshold) number of units are inactivated. However, more recently, this concept has been further developed to address the tissue organization also within certain organs that are a mixture of parallel and serial organization (Dörr and Van der Kogel, 2009). For example, the vasculature and neural network of any "parallel" organ represent serial targets. Also, in the lung, traditionally considered a parallel-organized organ, the airway network is organized serially, and damage to large bronchi might result in loss of function of the downstream bronchioli and alveoli. Kidneys also have a mixed serial and parallel organization, with the glomerula considered to be parallel structures, while the distal tubules exhibit a more serial organization.

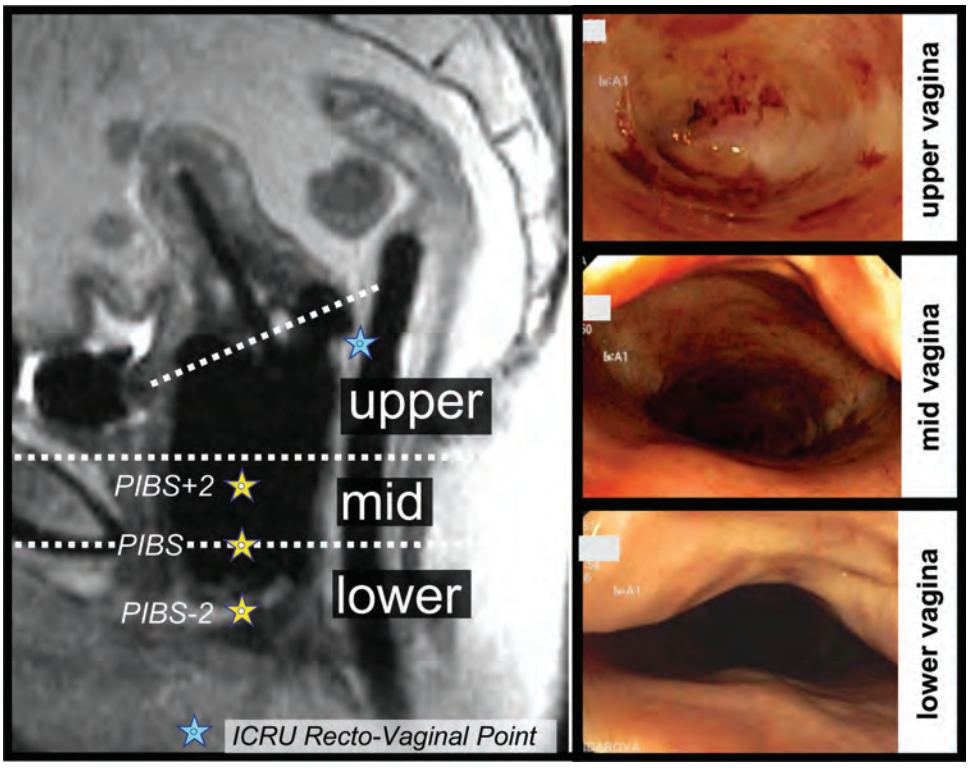

Figure 6.1. MRI sagittal view of the vagina with applicator, rectal probe, and bladder balloon in place. Lines indicate the cranial borders of the upper, mid, and lower portion of the vagina. The lower vaginal line, as the transition between lower and mid-vagina, is defined at the level of the posterior-inferior border of the symphysis (PIBS, as denoted by asterisk, together with the other vaginal points in Figure 6.4). Endoscopic views of typical vaginal morbidity in the upper, mid, and lower portion: dome shape indicative of fibrosis, multiple telangiectasia, and mucosal pallor in the upper vagina; telangiectasia, mucosal pallor, and reduced rugae in the mid vagina; some pallor in lower vagina.

In gynecologic brachytherapy, the serial-organ concept would apply to the transport function of the rectum, sigmoid colon, bowel, ureter, urethra, nerves, and vessels. Parallel structures, in contrast, include the ovaries, kidneys, and connective tissue. Rectal bleeding or circumscribed ulceration or fistula could reflect a parallel organization of vessel and wall architecture. Yet, ulceration and fistula could lead to a clinical breakdown of the (serial) rectal transport function. The bladder and vagina are difficult organs to clearly categorize. The bladder has two main functions, first as an elastic reservoir for urine with the filling capacity as an indicator of the functionality of the bladder wall, and second as a closing and opening mechanism allowing for controlled emptying of urine, which would be related to the condition of the bladder neck and trigone. The vagina plays a role in sexuality, with patient satisfaction related to the whole or parts of the vagina/vulva; this may therefore be considered a parallel function. The vagina as an organ displays a variety of different symptoms and endpoints; morphological changes include pallor and reduced rugae, telangiectasia, fragility, ulceration, and adhesions/occlusions in varying degrees (Kirchheiner *et al*., 2012b), in combination with palpable fibrosis and stenosis. For "natural" delivery through the vaginal birth channel, the vagina must be considered a serial structure, with fibrosis and stenosis (*e.g.*, as morbidity endpoints). Depending on the organization of these tissues and the related morbidity endpoints, gynecologic brachytherapy and the radiation dose–volume distribution in these tissues may lead to different adverse side effects.

Typical brachytherapy-related morbidity, such as ulceration (Figure 6.3), fistula, or circumscribed telangiectasia (Figures 6.1 and 6.3), is usually linked to small volumes receiving high absorbed doses. In order to be able to assess such volumes and doses appropriately, a reference-volume approach, such as 0.1 cm^3 and 2 cm^3, for limited organ-wall volumes to the sources has been suggested (Pötter *et al*., 2006) and is also recommended in this report (see Figures 6.2–6.4, and Section 8.4.1). These represent the very small (0.1 cm^3) and small (2 cm^3) wall areas/volumes that receive the highest absorbed doses. As these volumes are of limited size, they are always linked to a certain location within the respective OAR near the sources, such as anterior rectal wall, posterior-caudal bladder wall, or upper vaginal wall. It must be emphasized that the absorbed doses in these very small and small areas (0.1 cm^3 and 2 cm^3) are significantly different

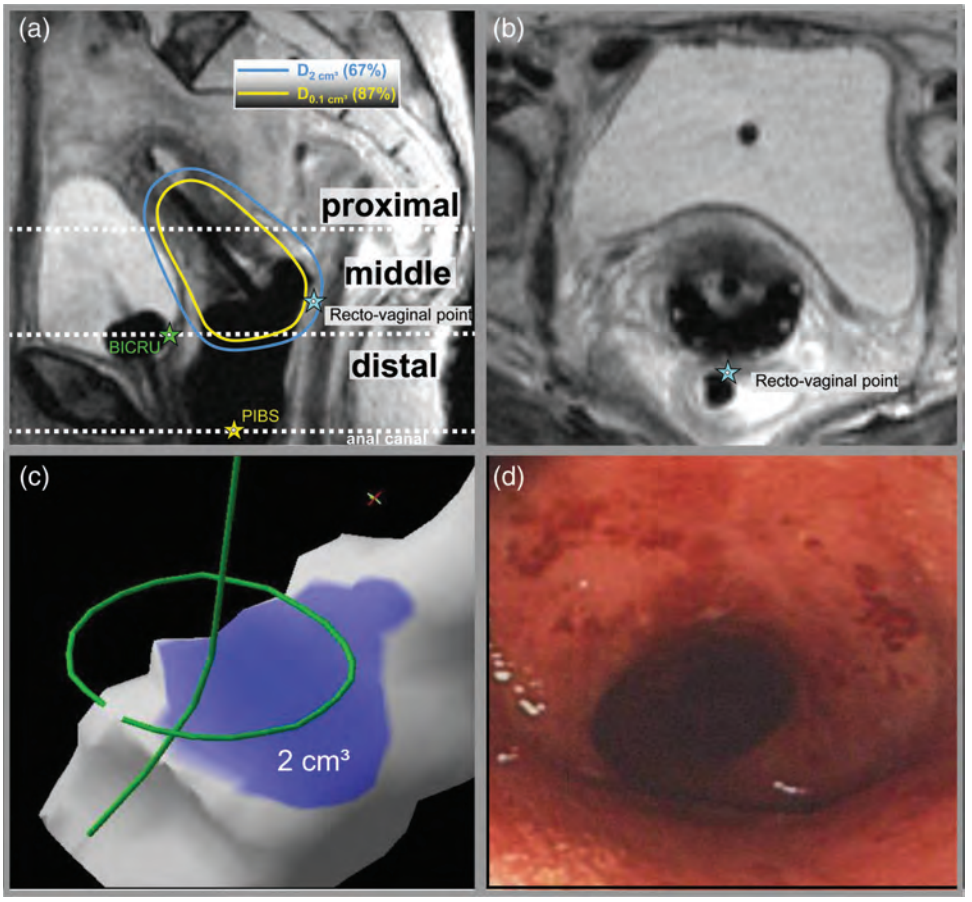

Figure 6.2. MRI sagittal and transversal views with utero-vaginal applicator in place and probe in the rectum with three transverse lines, indicating the distal, middle, and proximal third of the rectum (a) and the ICRU recto-vaginal point (RVICRU, blue star in a and b). Lower line is at the level of the pelvic diaphragm, which is indicated by the PIBS (yellow star) and also shows the beginning of the anal canal (see Figure 6.4). The highest absorbed dose is at the level of the vaginal sources above the middle line in the mid-rectum. The 2 cm^3 rectal volume is shown on the anterior wall (c). The D_{2cm^3} and the $D_{0.1cm^3}$ for the rectum and the corresponding isodose lines (67%/87% of the prescribed absorbed dose) are shown and correspond to 71 and 103 Gy $EQD2_3$, respectively (a) (see Section 8.4.1; compare examples in the Appendix). Endoscopic images of multiple teleangiectasia/petechiae related to the anterior wall 2 cm^3 volume after 18 months (d). Note also the bladder ICRU reference point (BICRU, green star) (modified from Georg *et al*., 2009).

(see Section 8.4.2 and examples in the Appendix) and therefore can be associated with different patterns of morbidity (see Figures 6.2 and 6.3).

It will be essential for future clinical research and practice to define and discriminate the different biological targets (sub-volumes/points) for different functional and/or morphological endpoints and their associations with the various treatment modalities, particularly radiotherapy dose–volume/point relations. This is important also when different treatment modalities such as EBRT, brachytherapy, and chemotherapy are combined with their respective targets (CTV-Ts, CTV-Ns) and absorbed-dose distributions.

The recommended dose–volume constraints in the OAR will evolve further with time, based on clinical research and based on better understanding of underlying biological mechanisms. Such progress will be associated with the development of experimental, (bio-) imaging, and treatment techniques.

6.3 Volume Selection and Contouring Uncertainties for the OAR in brachytherapy

For the OARs in gynecologic brachytherapy representing mainly hollow organs, organ walls are the essential structures to be contoured. The organ walls have to be delineated slice by slice in CT or MR images. It must be emphasized that for hollow organs, a reproducible filling status at delineation and at each irradiation is desirable, which will reduce uncertainties in absorbed-dose distributions.

Practical difficulties, however, have to be overcome in regard to the manual contouring procedure because of the small wall thickness (in the range of millimeters), which may cause substantial intra- and inter-observer variations. Such variations can result in significant uncertainties, as clearly shown for vaginal-wall contouring for volumes ranging from 0.1 cm^3 to 2 cm^3 (Berger *et al*., 2007) that are recommended for

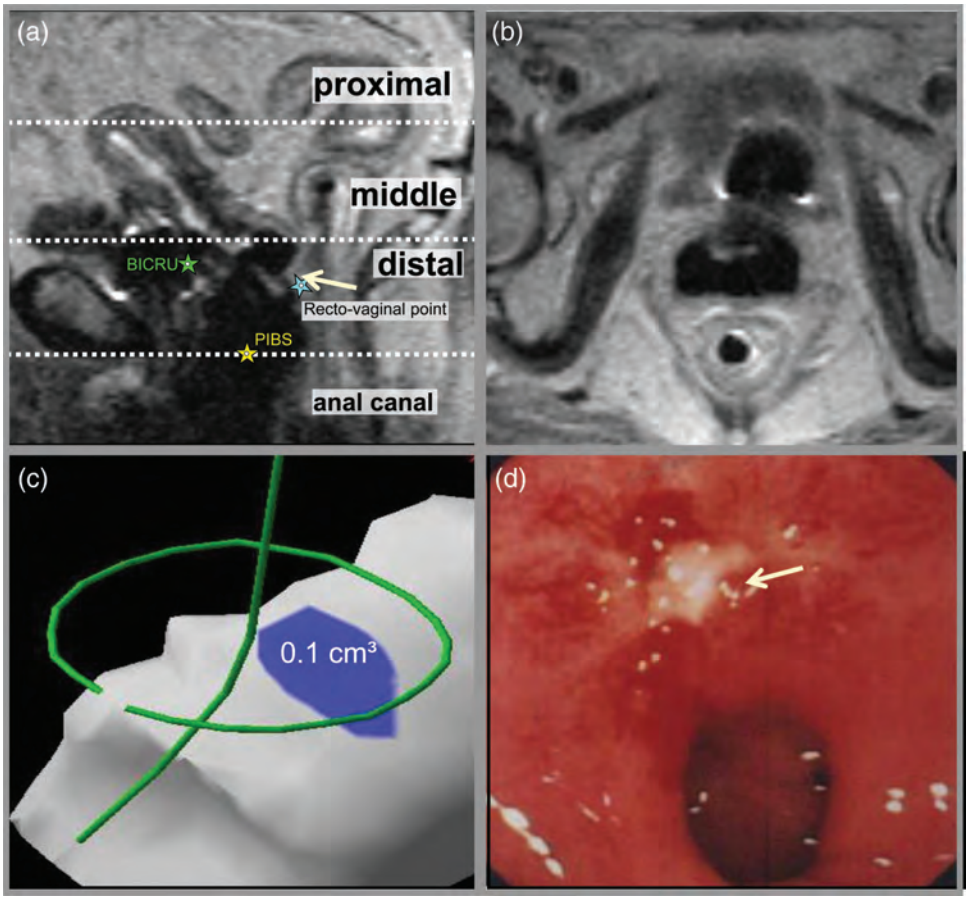

Figure 6.3. MRI sagittal and transversal views with utero-vaginal applicator in place and a rectal probe with three transverse lines, indicating the distal, middle, and proximal third of the rectum (a and b) and the ICRU recto-vaginal point RVICRU (a and b, blue star). Lower line is at the level of the pelvic diaphragm, which is indicated by the PIBS (yellow star) and demonstrates also the beginning of the anal canal (see Figure 6.4), which for this patient is not far from the vaginal sources (compare Figures 6.2 and 6.4). The 0.1 cm^3 rectal volume is shown on the anterior wall (c). The highest rectal absorbed dose is at the level of the vaginal sources below the middle line in the distal rectum. The $D_{0.1cm^3}$ for the rectum (arrow) is 108 Gy $EQD2_3$ and D_{2cm^3} is 80 Gy $EQD2_3$ (see Section 8.4.1; compare examples in the Appendix). Endoscopic images of transient, asymptomatic ulzeration (G2) of the anterior wall after 24 months (d) (modified from Georg *et al*., 2009).

the other hollow organs. Furthermore, there has been limited availability of automatic-contouring support in the past, making contouring of the organ wall time-consuming. There is also some concern, based on consistent clinical observations, with respect to certain clinical scenarios about the applicability of automatically generated second contours at selected distances from the primary contour to indicate the organ wall. These practical difficulties in contouring organ walls with variations in thickness can still lead to major uncertainties and consequent inaccuracies.

Small organ-wall volumes up to 2 cm^3–3 cm^3 represent typical targets for brachytherapy-related morbidity (see Section 6.2, Figures 6.2 and 6.3). For these, outer contour delineation (one contour) and wall delineation (two contours), lead to very similar numerical absorbed-dose values (Olszewska *et al*., 2001; Wachter-Gerstner *et al*., 2003b). Hence, this allows organ outer-wall contouring using only one line, which has been a major recommendation for OAR volume reporting from the GEC ESTRO group (Pötter *et al*., 2006). This is feasible, valid, and reliable in clinical practice according to published experience (Chargari *et al*., 2009; Charra-Brunaud *et al*., 2012; Georg *et al*., 2009; 2011; 2012; Haie-Meder *et al*., 2009; 2010b; Jürgenliemk-Schulz *et al*., 2010; Kang *et al*., 2010; Koom *et al*., 2007; Lindegaard *et al*., 2008; Tanderup *et al*., 2013). This procedure is therefore also recommended in this report. In the case of other morbidity endpoints linked to larger biological targets (*e.g*., sigmoid stricture), larger organ-wall volumes [>2 cm^3–3 cm^3 (*e.g*., representing the whole circumference over a considerable length)] might have to be considered. In such cases, the precise organ-wall definition using the inner plus the outer contour should be performed (Olszewska *et al*., 2001, Wachter-Gerstner *et al*., 2003b).

The tissue organization and the topographic distribution of absorbed dose and the location of the

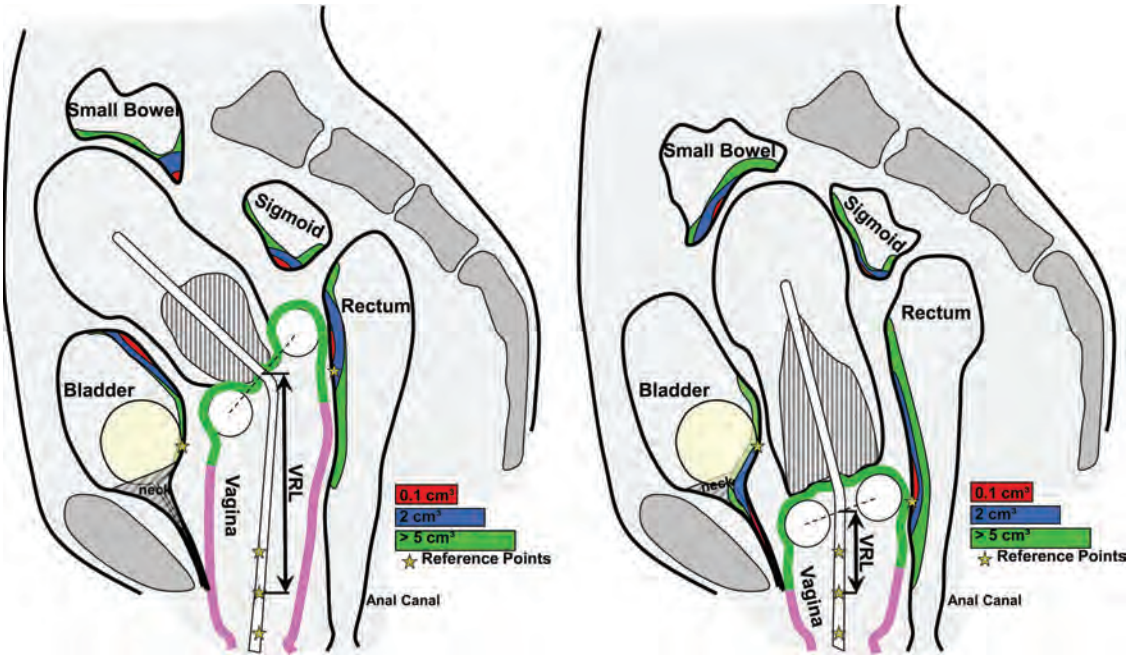

Figure 6.4. Schematic anatomical diagrams (sagittal view) showing two different positions of the vaginal part of the utero-vaginal applicators, the cervix tumor, the uterus, and the reference volumes of OARs in two different patients. The most irradiated-tissue volumes adjacent to the applicator, *i.e.*, the reference volumes 0.1 cm^3, 2 cm^3, and 5 cm^3, are illustrated for the various adjacent organs such as the bladder (neck), rectum (anus), sigmoid, and small bowel (see Section 8.4.1). The two panels show the different locations of the 0.1 cm^3 and 2 cm^3 reference volumes in the adjacent OARs [modified from GEC ESTRO Recommendations II; see also Westerveld *et al*. (2013)]. Reference points are indicated for the bladder (ICRU, 1985), the rectum and upper vagina (ICRU, 1985), and the mid- and lower vagina (PIBS $\pm$ 2 cm). The vaginal reference length (VRL) (PIBS to midpoint between the vaginal sources) can serve as an indicator to assess the varying position of the vaginal sources relative to the surrounding normal-tissue structures (Westerveld *et al*., 2013).

high absorbed-dose regions, also have to be taken into account in the delineation of OARs when addressing different morbidity endpoints. For the transport function of a tubular-type organ such as the rectum or sigmoid colon (morbidity endpoint: stenosis), it is preferable to delineate the entire circumferential wall or surface. For the assessment of mucosal/submucosal local function (telangiectasia, ulceration), small wall volumes adjacent to the radiation sources should be delineated (*e.g.*, posterior bladder wall, anterior rectum wall, sigmoid colon, small bowel, lateral vaginal walls). For the bladder, this would imply separate posterior bladder-wall and bladder-trigone/neck contouring in order to assess hematuria and incontinence, respectively.

To allow for comparative studies among centers, it is essential to follow similar accepted protocols (including strategies for a defined filling status in hollow OARs) and contouring guidelines for OARs. These have only been suggested, in general, within the GEC ESTRO recommendations (Dimopoulos *et al*., 2012a, Pötter *et al*., 2006). They have, however, been more specifically recommended, for example, within the prospective EMBRACE study (www.embracestudy.dk).

For bladder filling, various clinical protocols have been suggested (Buchali *et al*., 1999; Lang *et al*., 2013), without proven superiority of one over the other. In any case, one of these protocols should be selected and consistently followed, as they all provide a constant limited bladder filling. For example, one protocol is to keep the transurethral catheter open, which provides an "empty" bladder (Mazeron *et al*., 2014). Such an "empty" bladder usually includes some residual urine in the inferior-posterior part of the organ. Low-dose rate brachytherapy has a long tradition using this protocol, which is also often applied for PDR brachytherapy. Another clinical protocol is frequently used to adjust a defined, limited filling status (*e.g.*, 50 cm^3) after emptying of the bladder (Georg *et al*., 2012). This protocol provides a certain specific distance between anterior and posterior bladder wall, but does not lead to major filling of the lateral bladder recesses.

For the recto-sigmoid and the other bowel, the filling status is similarly important. An empty recto-sigmoid is usually accomplished by a pre-interventional enema and a rectal tube allowing emptying, which is mainly used in PDR brachytherapy, but can also be suitable for high-dose rate. In any case, gas and feces accumulation has to be avoided as much as possible, during both imaging and irradiation, as this can lead to large variations in the luminal volume and consequently in the wall location relative to the applicator and the radiation sources.

The vaginal applicator together with the packing should be well visualized in the imaging study (*e.g.*, gauze packing with diluted gadolinium for MRI) (see Figures 6.1–6.3) and provide a constant distension of the vaginal wall throughout the imaging procedure and the subsequent irradiation. Another possibility is the individual mould applicator.

For the assessment of small OAR volumes for brachytherapy planning and reporting (0.1 cm^3 and 2 cm^3), it seems sufficient to delineate the regions adjacent to the applicator with one outer contour. For the rectum, this would imply a contouring area about 5 cm in the cranio-caudal direction related to the vaginal sources and its circumference. If the recto-sigmoid junction is in this area, then it should be included in the rectum contour. The sigmoid colon should be clearly identified, and the whole structure should be contoured, with specific focus on the areas adjacent to the uterus. Similarly, small-bowel loops have to be identified and areas (*i.e.*, wall or organ volumes) near the uterus need to be contoured with their entire circumference. For bladder small-volume assessment, the whole posterior, posterior-caudal (trigone), and posterior-cranial bladder wall should be included. For the vagina, the whole vagina may be contoured, perhaps with specification of upper, mid, and lower vagina (see the second paragraph of Section 6.3). Other volumes (*e.g.*, anus, urethra, and ureter), which have typically not been contoured so far might become relevant depending on the outcome of future research.

As stated above, for the assessment of absorbed doses to OAR volumes larger than 2 cm^3–3 cm^3 for brachytherapy planning and reporting, the whole organ wall has to be contoured. For the rectum, this implies the entire length from the ano-rectum to the recto-sigmoid junction and—for the sigmoid colon—its length up to the junction with the descending colon. Also the anal canal can be contoured as a whole. For colon and small bowel, large-volume protocols should be followed and modified according to available evidence from clinical observations in external-beam radiotherapy as appropriate (see Section 8.4.2).

The most appropriate 3D imaging system for OAR delineation remains to be defined. While there is evidence that MRI provides the most reliable discrimination between initial and residual GTV and adjacent normal (uterine) tissue (see Sections 5.3.3 and 5.3.4), there is also some evidence that OAR delineation is improved based on the superior soft-tissue contrast of MRI over CT (Dimopoulos *et al.*, 2006b). This, however, was not demonstrated in other contouring studies, which showed CT to be comparable to MRI (Viswanathan *et al.*, 2007). Computed tomography technology might provide sufficient information for a valid and reliable delineation of OARs. Protocols applying contrast media *via* different routes (*e.g.*, intravenous, intraluminal) might help to further improve CT-imaging quality, in particular for OARs.

Overall contouring uncertainties in brachytherapy are of major importance because variations in delineation of only a few millimeters lead to significant variations in absorbed dose and absorbed-dose distribution due to the steep absorbed-dose gradient (Hellebust *et al.*, 2013). This also applies for point definitions (Tanderup *et al.*, 2013). Therefore, identification of the most appropriate contouring approach must be a major aim for future clinical research.

6.4 Geometrical Uncertainties in OAR Assessment

Variations in the position of the OAR during treatment must be considered in order to avoid serious complications. The major determinant seems to be variation in organ geometry (*e.g.*, filling status and motion in relation to the radiation sources). These can occur during or between fractions in external radiotherapy, but may be even more significant in brachytherapy due to steep absorbed-dose gradients and can result in considerable variations in the absorbed dose and the absorbed-dose distribution within the overall irradiated volume. These uncertainties are in addition to contouring uncertainties, in particular for organs such as the mobile bowel, the urinary bladder, or the rectum.

For EBRT, the concept of the planning organ-at-risk volume (PRV) has been developed (ICRU, 1998; 2004a; 2007; 2010) using shell-like margins that have to be added to the OARs to compensate for variations and uncertainties, using similar principles as for the PTV. A margin around an OAR with a predominantly serial-like structure and endpoint (*e.g.*, rectum, in which the maximum absorbed dose to a small circumferential volume determines tolerance to stenosis) is more clinically relevant than around OARs with a largely parallel-like structure (*e.g.*, liver, lung, parotid gland). For the latter, it is more important to delineate the entire organ, as tolerance, for most endpoints, depends more on the fraction of the total volume irradiated to a certain absorbed dose. This, however, overlooks variations in tissue tolerance within the organ.

For reporting OAR absorbed doses in EBRT, ICRU Report 83 (ICRU, 2010) recommended that, similar to the PTV, the PRV be described by including the size of the margins applied to the OAR volume in different directions. As for the PTV, several authors have proposed approaches to calculate the OAR–PRV margins on the basis of systematic and random uncertainties (McKenzie *et al.*, 2000; ICRU, 2010; van Herk *et al.*, 2000). Planning organ-at-risk volume margins are used mainly for serial organs in which damage could be dramatic [*e.g.*, the spinal cord (Castadot *et al.*, 2011; Mongioj *et al.*, 2011)].

A major new direction for more accurate dose–volume assessment for the OAR during the overall EBRT and brachytherapy treatment is repetitive imaging in the framework of IGRT, in combination with advanced image-registration methods [*e.g.*, rigid registration (see Section 9.3)].

For brachytherapy, and in particular for the image-guided approach, no systematic margin concept has been developed so far to compensate for organ motion and uncertainties in the precise location of OAR. In principle, the same basic difficulties arise with applying shell margins for OARs as outlined for the PTV (Section 5.5.3). Even with small millimeter-size margins in adjacent OAR within the steep absorbed-dose gradient, the reported absorbed doses would significantly overestimate the absorbed dose actually received. For these reasons, no planning shell margins around the OAR contour are recommended at present for image-guided gynecologic brachytherapy.

In brachytherapy, intra-fraction and inter-fraction variations of OAR topography can be significant and lead to uncertainties in dose reporting (Anderson *et al.*, 2013; De Leeuw *et al.*, 2009; Hellebust *et al.*, 2001; Lang *et al.*, 2013; Mohamed *et al.*, 2013). If OARs and thus the high-absorbed-dose regions move closer to the applicator between imaging and absorbed-dose delivery, the delivered absorbed dose will be higher than planned. These uncertainties are highly related to the mobility of the organs, and—in particular—the sigmoid, small bowel, and bladder are prone to significant organ motion. The amount and the clinical impact of such variations have been under investigation in multi-center GEC ESTRO network-related activities (Kirisits *et al.*, 2013; Nesvacil *et al.*, 2013a; Tanderup *et al.*, 2013).

For assessment of accumulated dose after several brachytherapy fractions, it is assumed in the GEC ESTRO Recommendations II (Pötter *et al.*, 2006) that the same volume of a certain organ is irradiated to the highest absorbed dose (hotspot) in each fraction of the entire brachytherapy process. The "assumption of a static hotspot" location enables the calculation of the highest possible dose to the defined location under a given topographical situation. The term "worst-case assumption" (Pötter *et al.,* 2006) should be avoided as this might cause misunderstanding, because the highest possible hotspot absorbed dose estimated from static images might still represent an underestimation of delivered absorbed dose in case the organ moves closer to the applicator in between imaging and absorbed-dose delivery. The validity of this assumption of a static hotspot position depends on the uncertainties in organ movement and deformation, as well as on the applicator position (see Section 9.5), which can vary for different organs according to their anatomical structure and fixation, and can also vary with different treatment techniques. There is some clinical evidence demonstrating the practical usefulness of this simplifying model [*e.g.*, for the rectum (Georg *et al.*, 2009; 2011; 2012)], but there is also evidence to question this model [*e.g.*, for the sigmoid colon (Jamema *et al.*, 2013; Mahantshetty *et al.*, 2011a)]. Mono-institutional data suggest that bladder $D_{2\text{cm}^3}$ hotspot distribution might fulfill the static assumption, whereas $D_{0.1\text{cm}^3}$ is more prone to variations (Lang *et al.*, 2013; Mohamed *et al.*, 2013). However, this conclusion might be critically dependent on the control of bladder filling. Further clinical research is necessary to evaluate the validity and the limitations of this pragmatic model.

As for IGRT in EBRT, a major clinical-research question in image-guided brachytherapy is the value of repetitive imaging and advanced image-registration methods. For gynecologic image-guided adaptive brachytherapy, this implies evaluation of the impact of intra-fraction motion and thus shortcomings of the "static hotspot assumption" approach for the various morbidity endpoints and corresponding target structures in the OAR, and the specific uncertainties of each "system," such as rectum and sigmoid colon. The overall aim is to minimize such geometric uncertainties as much as possible (Tanderup *et al.*, 2013).

6.5 Remaining Volumes at Risk

The volume that is within the imaged region of the patient, but outside all delineated OARs and CTVs should be identified as the "remaining volume" at risk (RVR). Absorbed doses to the RVR should be reported in addition to, and in the same way as, the absorbed doses to specifically delineated volumes of interest are documented (*e.g.*, as dose–volume histograms), in order to ensure that attention is paid to all tissues, and not just a selected subset. This recommendation refers not only to a risk of second cancers, but also to morbidity endpoints, which may potentially become relevant if others are avoided or become less frequent. In the context of brachytherapy, such a recommendation might apply for the various tissues as mentioned in Section 6.2 (*e.g.*, ureter, vessels, nerves, ovaries, kidneys) which are not specifically addressed by the current recommendations for OAR and volume selection. The outer body contour would delineate such an overall volume of interest and has been utilized, in particular, in regard to external-beam radiotherapy. There could be, for example, unsuspected regions of high absorbed dose within the patient that would go undetected if RVRs were not explicitly evaluated, particularly when IMRT is used.

6.6 Recommendations on Morbidity-Related Volumes and Points

Level 1: *Minimum standard for reporting*

Volumetric imaging approximation based on:	Radiographic approximation based on:
Baseline morbidity and QoL assessment according to international classification systems	Baseline morbidity and QoL assessment according to international classification systems
Reference volumes on 3D images:	Reference point location on radiographs or on a treatment plan:
Assessment of small organ volumes (0.1 cm^3 and 2 cm^3) for brachytherapy-related morbidity through outer-wall contouring on volumetric images in the treatment planning system:	
(1) bladder contour/volume; (2) Rectum contour/volume.	(1) Bladder reference point (2) Recto-vaginal reference point
Recto-vaginal reference point (positioned on volumetric images)	

Level 2: *Advanced standard for reporting*
All that is reported in level 1 plus:

Volumetric-imaging approximation based on:	Radiographic approximation based on:
Bladder reference point (positioned on volumetric images)	Vagina reference points (on radiographs):
	Upper-vagina points (5 mm lateral from vaginal applicator surface, right and left) for brachytherapy-related morbidity
Assessment of small organ volumes (0.1 cm^3 and 2 cm^3) for brachytherapy-related morbidity through outer-wall contouring on volumetric images in the treatment-planning system:	Anatomical points for lower and mid vagina (PIBS, PIBS $\pm$ 2 cm), for morbidity from EBRT and brachytherapy (on radiographs)
(1) Sigmoid-colon contour/volume;	
(2) Bowel contour/volume (adjacent, fixed)	
Assessment of intermediate- and large-organ volumes for EBRT- and brachytherapy-related morbidity through outer-wall contouring on volumetric images in the treatment-planning system:	
(1) Bladder contour/volume (2) Rectum contour/volume (3) Sigmoid-colon contour/volume (4) Bowel (adjacent) contour/volume	
Vagina reference points (all contoured on volumetric images):	
(1) Upper-vagina points (5 mm lateral from vaginal applicator surface, right and left) for brachytherapy-related morbidity;	

Level 3: *Research-oriented reporting*
All that is reported in Level 1 and 2 plus:

Volumetric-imaging approximation based on:	Radiographic approximation based on:
(1) Volumes or surface for vagina; (2) Vaginal reference length/volume (3) Bladder sub-volumes, for example, the neck or wall; (4) Small volumes for anus; anal reference point; (5) Remaining volume of interest: body outline; (6) Other sub-volumes of potential interest	(1) Other bladder points; (2) Anatomical anal reference point; (3) Sigmoid-colon and small/large bowel reference points; (4) Vaginal reference length

6.7 Summary

Radiotherapy-related morbidity endpoints and (sub-) volumes of OAR are selected based on the typical morbidity profiles as known from clinical experience in cervical cancer radiotherapy. Certain targets in the OAR are selected that correspond to the typical pathology and morbidity patterns [*e.g.*, rectal-wall area (vasculature), telangiectasia/bleeding]. This selection implies multiple targets within one organ according to different morbidity endpoints (*e.g.*, bleeding *versus* urgency/frequency in the rectum). Small absolute volumes (*e.g.*, 2 cm^3, 0.1 cm^3) correspond to

typical brachytherapy-related morbidity, such as teleangiectasia and ulceration/fistula. These volumes can have different locations in the OARs depending on the application technique. The location of such volumes within a given organ can be reflected by anatomically defined points in OARs (*e.g.*, ICRU bladder point at the bladder floor, mid- and inferior vaginal points) and/or by application-related points (upper vaginal points, ICRU recto-vaginal point). Larger volumes are also of interest for morbidity, including the whole circumference of a hollow organ (*e.g.*, for stenosis, shrinkage).

Volume selection and delineation of the hollow OARs adjacent to the CTV, such as rectum, sigmoid colon, adjacent small bowel, bladder (vagina, anus, ureter, and urethra) is performed along their walls, either as outer contour or as wall contour. For small absolute volumes, outer contour delineation is sufficient, whereas organ-wall contouring is recommended for volumes larger than 2 cm^3. Due to contouring uncertainties, the latter approach is at present not recommended for the vagina. Protocols to ascertain a particular organ-filling status, as well as specific delineation protocols, are essential.

Variations and uncertainties due to internal motion are known for OARs but should not be compensated for by adding shell margins around the OARs as suggested for EBRT. Organ motion in between imaging and absorbed-dose delivery leads to discrepancies between prescribed and delivered absorbed dose. Rather, these variations should be assessed through repetitive imaging and corrected for as appropriate. The assumption of static anatomical location of hotspots is recommended for small volumes in fractionated brachytherapy to assess the accumulated high-absorbed-dose region for a certain treatment. There is some evidence that such an approach is valid and reliable within reasonable confidence intervals.

Journal of the ICRU Vol 13 No 1–2 (2013) Report 89
Oxford University Press
doi:10.1093/jicru/ndw011

7. Radiobiological Considerations

7.1 Introduction

7.1.1 Dose Distributions

Historically, variation in dose is kept to a minimum inside each CTV and planning target volume (PTV) in external-beam treatments, with the aim of achieving a homogeneous dose distribution with the dose varying between 95 % and 107 % of the prescribed dose (ICRU, 1993b; 2000). However, with new techniques [such as intensity-modulated radiation therapy (IMRT)], some dose inhomogeneity (dose painting) may be specifically planned (ICRU, 2010).

For intracavitary brachytherapy (ICBT), the dose may be prescribed to a point but more typically to a CTV with a volume of 10 cm^3 to 200 cm^3 (Pötter *et al.,* 2006). Dose to a CTV may be prescribed as a D98 or other dose–volume value or to other clinical volumes as discussed in Sections 5 and 6. Even in the smaller CTVs, the dose distribution is heterogeneous with relatively low doses near the margin of the CTV and two to three times greater dose rates and doses delivered immediately adjacent to the radioactive sources. The average dose and dose rate within the CTV is consequently much higher than the dose and dose rate at the periphery. In external beam therapy, because of dose–volume–effect relationships, these high doses would not be tolerated by normal tissues, given the larger volumes commonly exposed. A study by De Brabandere *et al.* (2008) shows that the GTV receives on average 146 % (108 % to 273 %) of the dose to the periphery of the CTV. Outside of the CTV, there is a steep decrease in dose rate and dose.

7.1.2 Time-Dose Patterns

In addition to the difference in the spatial dose distribution, the second major difference between brachytherapy and external-beam radiation therapy (EBRT) is the time–dose characteristics: dose per fraction, dose rate, and the overall treatment duration (Joiner, 2009; van der Kogel, 2009).

In conventional EBRT, the treatment is typically delivered with many (25 to 35) fractions of 1.8 Gy to 2.0 Gy. Each fraction is delivered in a few minutes and fractions are usually separated by sufficient time to allow for (near) full normal tissue recovery between fractions. The overall duration of treatment usually extends over 4 to 7 weeks. Hypofractionated treatment schedules deliver the total dose in fewer larger fractions (>2.2 Gy) and are used e.g. for the curative treatment of melanoma (Bentzen *et al.*, 1989a) and liposarcoma (Thames and Suit, 1986), and more recently for prostate (Vogelius and Bentzen, 2013) and sub-clinical breast cancer (Bentzen *et al.*, 2008). Hypofractionation is increasingly used in IMRT and stereotactic photon or hadron therapy, and in some palliative treatments. Hyperfractionated radiotherapy applies doses per fraction <1.8 Gy, mostly in the range of 1.2–1.5 Gy. Accelerated protocols deliver the total dose with a rate of dose accumulation exceeding an EQD2 of 10 Gy $week^{-1}$. In some instances, combination protocols, *i.e.*, accelerated-hyperfractionated schedules, are applied.

Currently, in brachytherapy, the dose is delivered either at a continuous low-dose rate (LDR), typically 0.5 Gy h^{-1}, or a pulsed-dose rate (PDR), typically of 0.5 Gy to 1 Gy h^{-1}, in an overall treatment time of a few days, or in a few large (*e.g.*, ~7 Gy), high-dose rate (HDR) fractions delivered over a few days or weeks.

ICRU Report 38 (ICRU, 1985) was written in the context of classical LDR brachytherapy. As a result of new technological developments such as stepping-source brachytherapy, different time–dose patterns have been introduced into clinical practice. Hence, agreement is necessary on definitions of terms such as dose, dose rate, fraction (or pulse) size, overall treatment time relevant for biological effects, how to report these treatment parameters, the predicted tumor response, and the incidence of normal tissue reactions for different treatment conditions.

7.2 Time–Dose Patterns: Definitions

Different time–dose patterns are used in clinical brachytherapy practice; these different patterns evolved with the introduction of various kinds of remote afterloading devices (Section 3.6). Some definitions of time–dose parameters are given in ICRU Report 58 (ICRU, 1997). The specifics of the time–dose pattern used should always be clearly and completely

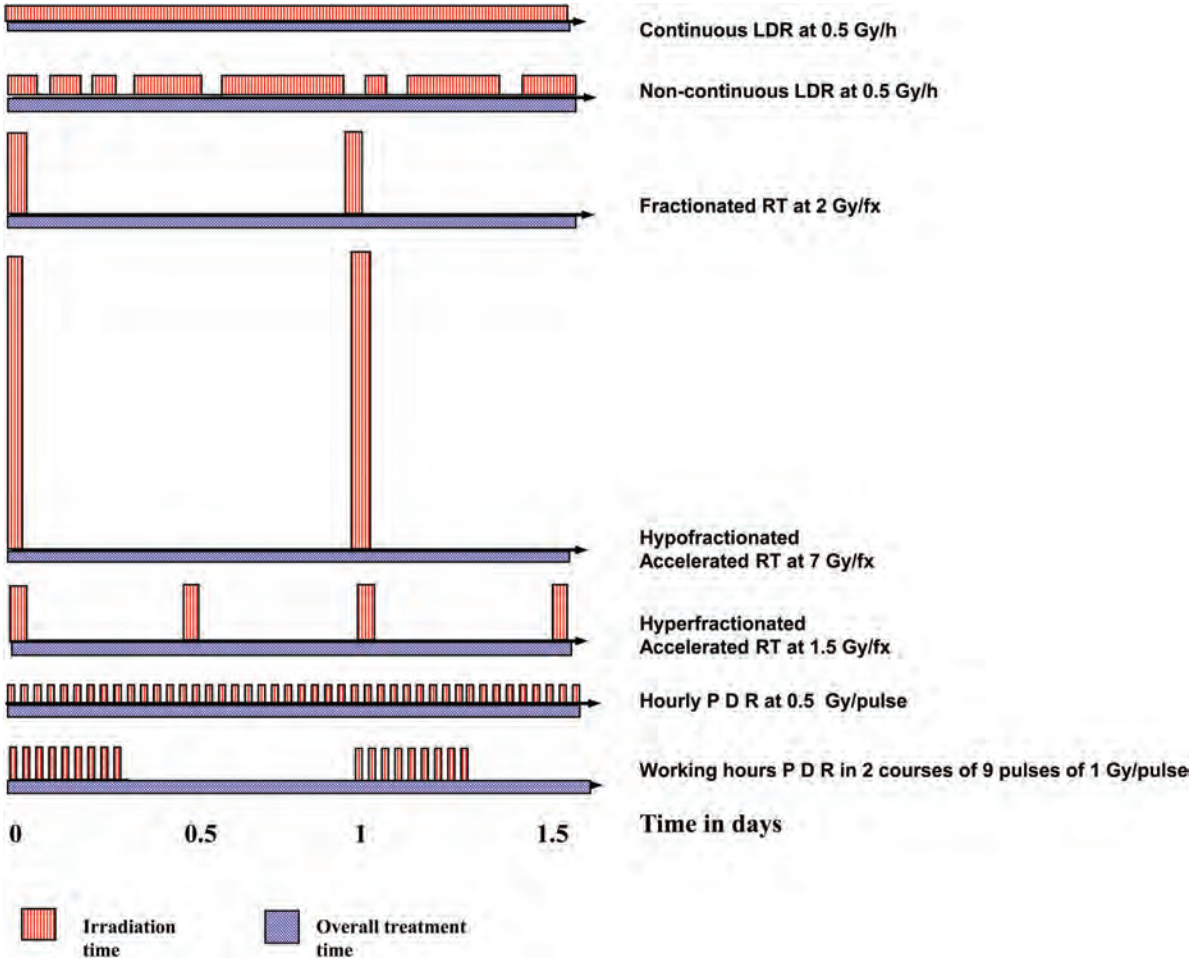

Figure 7.1. Definitions are shown of the time–dose patterns used in brachytherapy for cervix treatment. Overall treatment times (blue) and irradiation times (red) are presented for different types of treatment.

reported (see, for example, Figure 7.1). Below we define the more critical concepts and parameters.

7.2.1 Application

An application consists of one insertion of the applicator. A brachytherapy regime generally consists of one to four applications. One or many fractions (or pulses—see below) can be delivered within one application.

7.2.2 Fraction

A fraction is a specified absorbed dose delivered in one continuous irradiation. It is characterized by the absorbed dose delivered, the dose rate, and the resulting duration.

7.2.3 Fractionated Irradiation

In brachytherapy, as in external beam therapy, the treatment is generally delivered in a number of fractions. The fraction duration can range from minutes in PDR and HDR brachytherapy to hours in LDR brachytherapy. The biological effect of fractionated therapy depends on dose per fraction, total absorbed dose, dose rate (particularly important in LDR and MDR brachytherapy), and the time interval between fractions.

7.2.4 Pulse

When the interval between the fractions is shorter than the time needed to accomplish complete recovery between fractions, in brachytherapy, these are called pulses (although still defined as fractions in EBRT). A pulse is characterized by the absorbed dose delivered (pulse size), its duration, and dose rate.

7.2.5 Hypofractionation

A treatment is called hypofractionated when the fraction size is larger than 2.2 Gy per fraction.

7.2.6 Hyperfractionation

An irradiation is called hyperfractionated when it is delivered using fractions of less than 1.8 Gy.

7.2.7 Accelerated Fractionation

Treatments of more than 10 Gy per week are called accelerated.

7.2.8 Fractionated HDR Irradiation

The introduction of the single-stepping source HDR afterloading technique (see Section 3) resulted in short irradiation times. The initial reference air kerma rate (RAKR) of a typical ^{192}Ir source used for such treatments is 40 mGy h^{-1} at a distance of 1 m, which corresponds to a source activity of about 370 GBq (or about 10 Ci) of ^{192}Ir. A dose of 10 Gy at 1 cm distance is typically given in a few minutes. When a time interval between short HDR fractions exceeds approximately 6 h, complete recovery between fractions is usually assumed. High-dose rate treatments with curative intent for a cervix tumor are usually given in a hypofractionated-accelerated schedule of a few fractions (*e.g.*, 4 × 7 Gy, 2 fractions per week).

7.2.9 PDR Irradiation

Pulsed-dose-rate treatment is currently delivered at the prescription isodose, in one or two applications each consisting of a large number (∼40–80) of small pulses of ∼0.5 Gy to 1 Gy (with a duration of minutes) separated by short time intervals up to ∼1.5 h.

The clinical introduction of PDR brachytherapy aimed to simulate the biological effects of continuous LDR irradiation. It results in even more variation in treatment time schedules. As in HDR treatments, a single source but with a lower RAKR of typically 4 mGy h^{-1} at 1 m is used. Pulsed-dose rate irradiation is a combined accelerated-hyperfractioned treatment but with incomplete recovery in the short intervals between irradiations.

7.2.10 Continuous LDR Irradiation

The conventional LDR treatment is a continuous irradiation delivered in one or two applications at a low dose rate at the point or isodose surface of the prescription.

7.2.11 Non-Continuous LDR

The introduction of remote-controlled afterloading devices allowed for the interruption of LDR treatments according to the treatment plan or for logistic reasons. The overall treatment time then becomes longer than the irradiation time. When the duration of at least one interruption is longer than 6 h, a LDR irradiation should be considered as fractionated (ICRU, 1985). The total dose in LDR or PDR treatments is often delivered in one or two applications.

7.2.12 Overall Treatment Time

The overall treatment time or duration is the time elapsed from the beginning of the first fraction to the end of the last fraction.

7.2.13 Mean Dose Rate

The mean dose rate in a fraction or pulse from a stepping source is the ratio of the absorbed dose given in that fraction or pulse to the actual pulse time. This quantity has little biological significance. The biological effects are much more dependent on the instantaneous HDR at which the dose is delivered while the source is stepping through the catheters, the stepping PDR source creates an area of instantaneous HDR ($>$12 Gy h^{-1})—the size of a golf ball—traveling through the applicators (Fowler and Van Limbergen, 1997). This means that more than two-third of the doses delivered by PDR sources to the target and OAR are delivered at dose rates above 12 Gy h^{-1} and thus at HDR.

7.3 Dose-Rate Effects on Recovery

Experimental and clinical data have characterized the effects of dose rate on biological endpoints and clinical outcome. With decreasing dose rate $<$12 Gy h^{-1}, there is increasing recovery of biological damage during irradiation (Figure 7.2). In return, the radiobiological effect of a given dose typically increases as a sigmoid function with increasing dose rate as a result of an increasing amount of accumulated non-recoverable damage (see Figure 7.3). At very low dose rates $<10^{-3}$ Gy h^{-1}, repopulation may occur during irradiation, further reducing the effect of irradiation.

Somewhat arbitrarily, dose rates can be divided into three ranges, *viz*, LDR (below 1 Gy h^{-1}), MDR (between 1 Gy h^{-1} and 12 Gy h^{-1}), and HDR (above 12 Gy h^{-1}) (Figure 7.3). The dose rate ranges specified here are slightly different from those in ICRU Report 38 (ICRU, 1985).

A change in dose rate has the most pronounced effect at MDR, while it has less consequence on outcome at LDR or at HDR (Steel, 1991).

7.3.1 Low-Dose-Rate Brachytherapy

According to ICRU Report 38 (ICRU, 1985), the dose range defining LDR is between 0.4 Gy h^{-1} and 2 Gy h^{-1}. However, it seems preferable to limit the definition of LDR to a maximum of 1 Gy h^{-1} since clinically relevant differences in effects were seen at

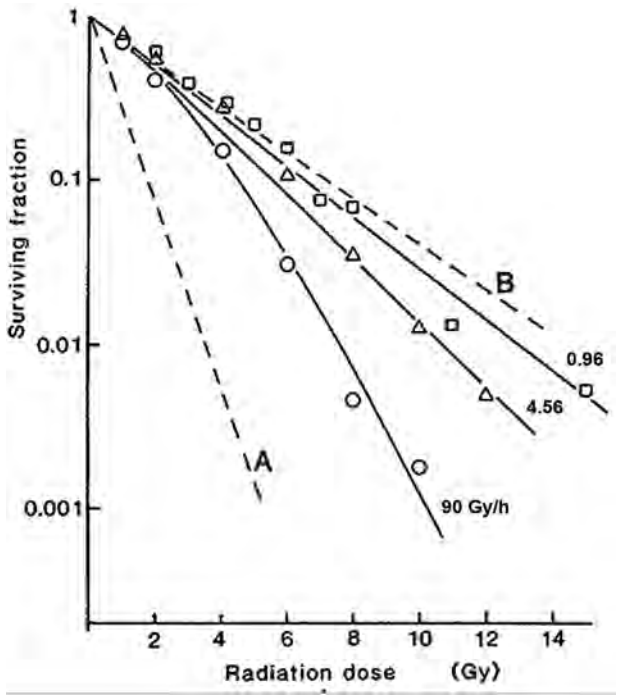

Figure 7.2. Cell survival data for a human melanoma cell line irradiated at three different dose rates. Data are fit by a mathematical model from which the survival is derived in the complete absence of recovery (Line A) or for complete recovery (Line B) (Steel, 1991).

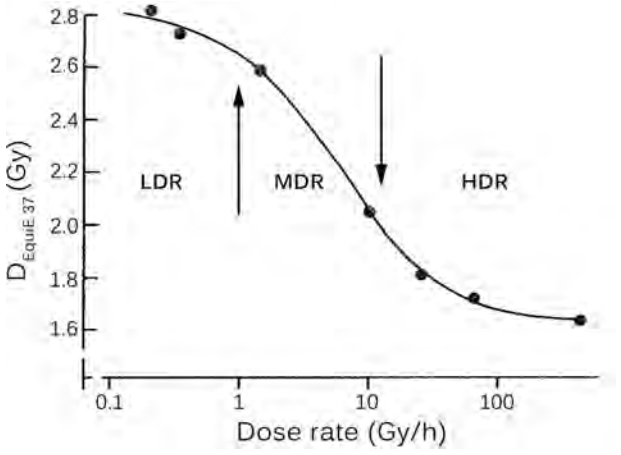

Figure 7.3. Schematic diagram of total absorbed dose producing a given biological effect as a function of dose rate based on the incomplete repair model (Thames, 1985) $D_{EquiE37}$ is the dose that in the experiments led to a 37 % cell survival rate. [Figure modified after Hall (1972).]

dose rates above 1 Gy h^{-1} in head and neck cancers (Mazeron *et al.*, 1991; Pernot *et al.*, 1994; 1997) as well as in gynecological brachytherapy (Haie-Meder *et al*., 1994; Leborgne *et al*., 1996; Rodrigus *et al*., 1997). At higher dose rates and depending on the clinical situation, a reduction in total dose or use of fractionated MDR should be considered (Hunter and Davidson, 2002; Leborgne *et al*., 1999; Mazeron *et al*. 2002; Newman, 1996; Patel *et al*., 1998, Stout and Hunter, 1989; Wilkinson *et al*., 1980).

7.3.2 Medium-Dose-Rate Brachytherapy

According to ICRU 38, MDR is defined as lying between 2 and 12 Gy h^{-1} but, as discussed above, it is in this report redefined as ranging between 1 and 12 Gy h^{-1}. Again it has to be stressed that the biological effects of a given dose change gradually from the LDR to the MDR region, as well as from the MDR to the HDR region and that these boundaries are defined by convention. Medium-dose rate is delivered as fractionated or hypo-fractionated irradiation.

7.3.3 High-Dose-Rate Brachytherapy

High-dose rate has been and is now defined as a dose rate higher than 12 Gy h^{-1} which is delivered as accelerated hypo-fractionated irradiation. Again the boundary with MDR is set arbitrarily. But when the dose rate decreases below 12 Gy h^{-1}, for example, due to decaying sources that are not replaced in time (*e.g*., in developing countries), estimation of the loss in biological effect should take account the recovery processes during the prolonged irradiation time (see Section 7.6.2).

7.4 Other Time–Dose Pattern-Related Radiobiological Processes

In addition to recovery processes (dose-rate or fractionation effects), repopulation, reoxygenation, and redistribution in the cell cycle may influence the outcome of a radiation schedule.

7.4.1 Repopulation

For a 6 to 7-week irradiation protocol, repopulation does not depend on overall treatment time with the exception of late effects that may arise as a consequence of very pronounced early side effects (Dörr, 2009; Dorr and Hendry, 2001). But overall treatment time does play a role for early reactions and tumor control. Repopulation has little effect in many tumors—as studied so far—for treatment times shorter than 3 to 4 weeks, but beyond this time, accelerated repopulation can be observed (Bentzen and Thames, 1991). Total treatment times exceeding 52 to 60 days have been correlated with decreased tumor control in cervix cancer with a decline of 0.7 % to 1 % per day when exceeding 55 days (Chen *et al*., 2003; Girinski *et al*., 1989; Mazeron *et al*., 2015b; Perez *et al*., 1995; Petereit *et al*., 1995; Tanderup *et al.*, 2016).

For early normal tissue responses, a similar time course of repopulation has been described. The lag time before the onset of repopulation, however, is dependent on the tissue (Dörr, 2009). An effect of overall treatment time may also be seen in late responding tissues with a strong consequential component, *i.e.*, when the early response results in additional trauma to the target structures of the late endpoint (Dörr, 2009; Dorr and Hendry, 2001).

Interruption of treatment may occur during a planned continuous irradiation of several days, notably if an afterloading device is used. In most cases, it is due to a short interruption such as when staff enters the room, but this will have no effect on repopulation.

Total treatment time should always be taken into account when estimating efficacy of radiation therapy for cervix cancer (Bentzen and Joiner, 2009).

7.4.2 Reoxygenation

Reoxygenation of hypoxic cells takes hours to weeks. Several short- and long-term mechanisms are involved (Horsman *et al.*, 2009). Reoxygenation that takes place over a longer time is probably due to tumor shrinkage or cell killing leading to lower oxygen consumption. This will reduce diffusion-limited chronic hypoxia. In the case of perfusion-limited hypoxia, other mechanisms are probably involved, such as reopening of transiently closed vessels leading to acute reoxygenation. The oxygen enhancement ratio (OER) associated with LDR irradiation has been estimated to be as low as 1.6 to 1.7 (Bedford and Hall, 1966; Horsman *et al.*, 2009; Ling *et al.*, 1985).

7.4.3 Redistribution

Below 10 cGy min^{-1}, cell cycle effects may be the most important process in LDR brachytherapy (van der Kogel, 2009). Preferential killing of cells in radiosensitive phases will result in a general decrease in radiation sensitivity. The surviving cells will progress synchronously through the subsequent cycle phases. In addition, cell cycle blocks (G2) will contribute to these synchronization processes. Redistribution over all phases of the cell cycle in a population of cells occurs due to slight differences in cell cycle times. However, while there is experimental evidence for the process of re-sensitization due to progression of synchronized cells through the cell cycle, mainly from *in vitro* studies, it has not been possible to exploit this phenomenon clinically to achieve a therapeutic gain.

7.5. Dose–Time Patterns and Dose Rates

As indicated in the previous section, the dose–time relationships in brachytherapy differ from those in external beam therapy. In addition, they vary among centers and depend to a large extent on the local technical resources and equipment (LDR *versus* PDR or HDR).

Low-dose-rate irradiations using radium sources were delivered at dose rates of about 0.5 Gy h^{-1} leading to overall times of several days in a single or fractionated application. Historically, 0.5 Gy h^{-1} was commonly used as the reference dose rate because of the extensive experience accumulated with radium sources (IAEA and ICRU, 2007, 2008). Today other radionuclides and new methods of application cause a broader range of dose rates. Stepping sources are increasingly used in HDR and PDR applications. These applications can be considered as fractionated irradiations.

Five typical dose–time patterns are presented in Figure 7.1. These examples typify protocols in current use in the treatment of cervix cancer and illustrate the integration of EBRT with brachytherapy and chemotherapy. In all cases, the assumed treatment starts with 5 weeks of conventional EBRT delivered in 5 daily fractions of 1.8 Gy. External-beam radiation therapy is currently often delivered in combination with chemotherapy (*e.g.*, 40 mg cisplatinum m^{-2} each week). This combination is assumed to be "clinically equieffective" to daily radiation fractions of 2 Gy (Green *et al.*, 2005).

7.6 Radiobiological Consequences of Different Dose–Time Patterns

7.6.1 From Absorbed Dose to Biologically Equieffective Dose

Absorbed dose is an essential quantity when evaluating the effects of an irradiation. Therefore, the clinical outcome is always closely related to the total absorbed dose. Therefore, the ICRU has recommended that both spatial absorbed dose distribution and the associated temporal information be reported in an accurate and complete way in order to allow an understanding of the biological effects of radiation (IAEA and ICRU, 2007; 2008; ICRU, 1999, 2004).

However, the same absorbed dose may give rise to very different biological or clinical effects depending on the irradiation conditions such as:

- average (and instantaneous) dose rate
- dose per fraction or dose per pulse
- interval between fractions or pulses
- overall time

- dose and dose rate distribution
- radiation quality (linear energy transfer, LET)
- other Therapeutic Interventions (*e.g.*, chemotherapy, hyperthermia, etc.)
- Patient-related factors (*e.g.*, comorbidities)
- Tumor-related factors (*e.g.*, hypoxia)

Therefore, in radiation therapy, when exchanging clinical information, comparing or combining (adding) treatments performed under different technical conditions (*i.e.*, when altering treatment protocols or designing new protocols), the transformation of absorbed dose into biologically equieffective dose is necessary to estimate the probability of a given biological effect. The transformation function should in principle take into account all factors that could influence the clinical outcome of the treatments compared. It is very important to note that the numerical values of parameters used in these transformation functions may vary significantly with tissue type and with the endpoint considered (individual early or late effects, cancer induction, etc.). They may also be influenced by physico-chemical conditions such as oxygenation, temperature, previous and/or concomitant chemotherapy, and patient factors (*e.g.*, anemia, comorbidities).

In general, late-responding tissues are more sensitive than early-responding tissues or tumors to a change in dose per fraction, dose rate, or LET. The overall treatment time is less important in these tissues with the exception of consequential late effects.

7.6.2 Mathematical Modeling of the Effects of Dose Rate and Dose per Fraction, Recovery Capacity, and Half-Time of Recovery

Mathematical models have been developed to compare the effects of different doses, dose rates, and fraction sizes and inter-fraction intervals. In EBRT, the linear-quadratic (LQ) model is commonly used. The LQ model assumes that the effect of a single irradiation is determined by absorbed dose and two parameters, α and β, and their ratio α/β [see Equations (7.1 and 7.2)] that depend on tissue, endpoint, and radiation quality and are usually determined at HDRs. In EBRT with fractionation intervals greater than 6 h to 8 h, it is usually assumed that there is recovery between fractions and that the LQ feature of the response curve repeats for each fraction [see n in Equation (7.1)]. The α/β value [see Equation (7.2)] quantifies the sensitivity to changes in fraction size, with low α/β (1 Gy to 6 Gy) indicating a high sensitivity to fractionation typical of many late effects, while higher α/β values (7 Gy to 20 Gy) are typical of early effects and tumor control showing lower effects of fractionation. These concepts are shown mathematically as:

$$E = n\,(\alpha\,\mathrm{d} + \beta\,\mathrm{d}^2) \tag{7.1}$$

Where E is a measure or predictor of biological effect that requires a dose–response relationship, n the number of fractions, and d the dose per fraction. Note that D is the total dose and is equal to $n \times d$. The dependence on α/β is more explicitly shown as:

$$E = nd\,\beta\left(\frac{\alpha}{\beta} + d\right) = \beta D\left(\frac{\alpha}{\beta} + d\right) \tag{7.2}$$

In brachytherapy using LDRs, the LQ model needs to be modified, by addition of a recovery factor g [see Equation (7.3) based upon a recovery time constant $T_{1/2}$ to take into account incomplete mono-exponential recovery of sublethal damage during irradiation (Thames, 1985)].

It must be pointed out that E in Equations (7.1) and (7.2) is a mathematical construct, easily related to cell survival studies, but it may not be easily related to the severity of clinically observable phenomena such as erythema, stenosis, fibrosis, necrosis, etc. It is assumed, however, that protocols giving rise to equal values of E, *i.e.*, equieffective doses, for a given tissue will lead to equivalent biological or clinical outcomes.

Reasonable estimates of fractionation sensitivity (α/β values) of many normal tissue endpoints are available (Bentzen and Joiner, 2009). Values of 7 Gy to 10 Gy have been reported for early responding normal tissues and between 1 Gy and 6 Gy for late responding normal tissues. The α/β values for human tumors vary considerably among tumor histologies and have been reported as similar to early responding tissues or higher (7 Gy to 20 Gy) for many tumors, but to be much lower in melanoma, sarcomas, breast, and prostate cancer.

Less is known of the recovery kinetics, *i.e.*, the time frame in which recovery takes place ($T_{1/2}$ of recovery) (Bentzen and Joiner, 2009).

7.6.2.1 HDR Irradiation. Except for effects related to their inhomogeneous dose distributions, the radiobiological effects of HDR brachytherapy are similar to those in fractionated EBRT.

No correction need be made for dose-rate effects. Total dose and fraction size determine the radiobiological effect, when full recovery is assumed to occur between fractions (an interval of at least 6 h to 8 h). Hence Equations (7.1) and (7.2) apply.

Although there is some controversy of the validity of the LQ formalism at large doses per fraction (Brenner, 2008; Kirkpatrick *et al.*, 2008), it is believed to quantify adequately the biological effects

in most tissues in the dose range of 0.5 Gy to 6 Gy. At dose per fraction exceeding 6 Gy to 10 Gy, the LQ formalism may overestimate the biological effect (Bentzen *et al*., 2012; Joiner, 2009).

7.6.2.2 LDR Irradiation. The biological effect of a given absorbed dose will decrease with decreasing dose rate to an extent depending on the α/β value and the half-time of recovery, $T_{1/2}$, for a specific endpoint.

An incomplete recovery model was proposed (Thames, 1985) based on an earlier idea (Oliver, 1964). With this, the biological effect E of total absorbed dose, D, delivered in time, t, can be described as

$$E_{\mathrm{LDR}} = n(\alpha d + g\beta d^2) = D\beta\left(\frac{\alpha}{\beta} + g\,d\right) \qquad (7.3)$$

where g is the Lea–Catcheside factor (Thames, 1985), that depends on the overall time, t, and the recovery half-time, $T_{1/2}$. as follows:

$$g(\mathrm{LDR}) = \frac{2}{\mu t}\left[1 - \frac{1 - \mathrm{e}^{-\mu t}}{\mu t}\right] \qquad (7.4)$$

where $\mu = \ln 2/T_{1/2}$ is the recovery rate constant. If $t << T_{1/2}$, then $\mathrm{g} \approx 1$; if $t >> T_{1/2}$, then $\mathrm{g} \approx 0$.

The recovery half-time is an important tissue and endpoint-specific radiobiological parameter in analyzing radiation responses to LDR irradiation. Unfortunately, values of $T_{1/2}$ are less well established than values of α/β. Some $T_{1/2}$ estimates come from small animal model studies and are usually shorter than those derived from clinical data and cannot be translated from species to species (Bentzen and Joiner, 2009; Joiner and Bentzen, 2009). Moreover, little data exist at dose rates lower than 1 Gy h^{-1} (Scalliet *et al*., 1989). The few values published from studies in humans have been derived from external irradiation of breast cancer or from clinical brachytherapy data (Fowler and Van Limbergen, 1997; Guerrero and Li, 2006; Leborgne *et al*., 1999; Mazeron *et al*., 1991; Patel *et al*., 1998; Roberts *et al*., 2004; Thames *et al*., 1990; Turesson, 1990; Turesson and Thames, 1989). Estimated half-times of recovery for late effects are long: >5 h for myelopathy (Dische and Saunders, 1989), 4.4 h for subcutaneous fibrosis (Bentzen *et al*., 1999), >4 h for temporal lobe necrosis (Lee *et al*., 1999), and 3.8 h for skin teleangiectasia (Bentzen *et al*., 1999). For late effects in the bladder and rectum in patients treated for cervix cancer, both long (1.5 h to 2 h) (Fowler, 1997; Leborgne *et al*., 1999) and short (0.3 h to 1 h) (Guerrero and Li, 2006; Roberts *et al*., 2004) recovery half-times have been reported. Two comparisons between LDR (at 0.5 Gy h^{-1} to 0.6 Gy h^{-1}) and MDR (1.4 Gy h^{-1} to 2.2 Gy h^{-1}) treatments resulted in different but differently calculated values of $T_{1/2}$ for recovery of normal tissues (bladder and rectum) (Fowler and Van Limbergen, 1997; Roberts *et al*., 2004).

Fowler (1997) based his calculation on the clinical data from Bristol, reported by Newman (1996) and on the prescription doses to Point A. He estimated that, when assuming an α/β value of 2 Gy to 4 Gy, the $T_{1/2}$ for recovery of normal tissues most probably lies between 1.5 h and 2.5 h. On the other hand, Roberts *et al.* (2004) based on the analysis of the Manchester trials (Hunter, 1994; Hunter and Davidson, 2002; Stout and Hunter, 1989), in which different dose levels of ^{137}Cs were compared with the older radium brachytherapy implants found shorter recovery half-times for late effects. These calculations were not based on doses to point A but on estimated absorbed doses to the rectum and bladder. These doses are lower than the doses to Point A by a ratio, f, defined as the ratio of the estimated rectal and bladder dose to the prescribed dose to Point A. Using a value of $f = 0.6$, which is a reasonable estimate of the average ratio in a patient group, they obtained a $T_{1/2}$ for recovery of 0.5 h with a 95 % confidence interval of 0.32–1.1 h. if $\alpha/\beta = 3$ Gy.

Guerrero and Li (2006) were able to eliminate the inconsistency between the previous studies (Fowler, 1997; Roberts *et al*., 2004) by introducing the sparing factor f in the older studies. Calculating the biological equieffective dose values for different treatment schedules, they estimated that, assuming an α/β value of 2 Gy to 4 Gy, the most likely value of the recovery half-time for bladder and rectum is short, 0.2 h to 0.4 h, which is almost identical to that of Roberts *et al*. (2004). These estimates are also in the same range as estimated by an independent study comparing LDR and MDR treatments (Patel *et al*., 1998). In this study, an average sparing factor of $f = 0.75$ was used for the rectum and bladder. Guerrero and Li (2006) concluded that according to their simple calculation of the biological equieffective dose values a short recovery time for cervical cancer treatment complications is supported.

It is not clear if a simple single-exponential recovery kinetics model is a good approximation in all clinical situations. Two-component recovery models, with a fast and a slow recovery component, appear to give an improved fit to experimental results in many normal tissue tolerance studies in animals (Joiner and Bentzen, 2009) as well in the tolerance study on skin telangiectasia in breast cancer patients where a fast component of 0.4 h and a slow component of 3.5 h was estimated (Turesson and Thames, 1989). Guerrero and Li (2006) calculated from the cervix cancer data of Fowler (1997) and

Roberts *et al*. (2004), that when a second component is considered, there is a possibility of a longer recovery half-time co-existing with the short one. However, with an assumed α/β value of 3 Gy, this longer recovery half-time could not be longer than about 1 h.

For tumor control in cervical cancer, a short recovery half-time of 0.25 h was calculated by Roberts *et al.* (2004). These short half-times that were found in comparisons between LDR and MDR series are probably not applicable to larger HDR fractions, if the repartition coefficient (being the relative amount of the fast to slow components of the recovery process) is fraction size-dependent.

7.6.2.3 PDR Irradiation. Pulsed dose rate brachytherapy was developed to mimic the biological effects of continuous LDR brachytherapy, using the stepping-source equipment developed for HDR brachytherapy but with an initial source strength of about 37 MBq (instead of 370 MBq for HDR). Total dose is delivered in the same total time as with continuous LDR treatment, but with a large number of "pulses" (see definitions in Section 7.2), typically one per hour, with incomplete recovery assumed during and between pulses.

The stepping PDR point source irradiates a volume the size of a golf ball (3 cm^3) (Fowler and Van Limbergen, 1997) at instantaneous dose rates higher than 10 Gy h^{-1} in the target. Twenty gray per hour is delivered at 14.6 mm by a 37 GBq ^{192}Ir source and still at 10 Gy h^{-1} at the same distance at the time the source decayed to 18.5 GBq (1 half-time of decay). Most of the target dose is thus delivered as accelerated HDR, with incomplete recovery between pulses. The biological effect of a PDR schedule can be expressed as:

$$E_{\mathrm{PDR}} = n(\alpha d + g\beta d^2) \qquad (7.5)$$

where the incomplete recovery function g for PDR [note that this "g" is different from g in Equation (7.4)] is calculated as:

$$g(\mathrm{PDR}) = \frac{2}{\mu t}\left[1 - \frac{\mathrm{NY} - \mathrm{SY}^2}{\mathrm{N}\,\mu t}\right] \qquad (7.6)$$

where $Y = 1 - \mathrm{e}^{-\mu t}$ and $K = \mathrm{e}^{-\mu x}$. Thus

$$S = \left[\frac{NK - K - NK^2\mathrm{e}^{-\mu t} + K^{N+1}\mathrm{e}^{-N\mu t}}{(1 - K\mathrm{e}^{-\mu t})^2}\right] \qquad (7.7)$$

where t is the time of duration of each pulse, x the time between pulses without irradiation and N the total number of pulses.

The lack of knowledge about $T_{1/2}$ values for human tissues *in situ* is probably the largest source of uncertainty in PDR brachytherapy biological effect estimations. However, treatment schedules with pulse sizes of 0.5 Gy to 1.5 Gy repeated every 1 h to 3 h have been estimated to reproduce the effects of an LDR irradiation with an increase in biologic effect not exceeding 10 %, except for very short values of $T_{1/2}$ in late reacting normal tissues (see Figure 7.4) (Fowler and Van Limbergen, 1997).

Figure 7.4 shows the biological effects of four different PDR schedules (0.5 Gy every hour, 1 Gy every 2 h, 1.5 Gy every 3 h, and 2 Gy every 4 h) calculated as the ratio to the effect of a continuous LDR schedule (CLDR) at 0.5 Gy h^{-1}. It demonstrates that at small pulse sizes (0.5 Gy every hour), the PDR/CLDR ratio (when the instantaneous HDR is taken into account), the ratio is maximally 1.1 (*i.e*., maximum 10 % more toxic for PDR in a broad range of assumed half-times of recovery). The ratio increases, however, strongly with increasing pulse sizes and decreasing half-times of recovery. This leads to high PDR/CLDR ratios when the pulse size increases from 0.5 Gy to 2 Gy and $T_{1/2}$ decreases from 1.5 h to less than 6 min.

Since pulse sizes can easily be changed, PDR allows easy "biological optimization" of a treatment plan. Pulse sizes to organ at risk can be decreased below 0.6 Gy per pulse to lower the risk for late bladder and bowel complications. It can be assumed that for organs with a low α/β value, the pulse size reduction will result in a reduced rate of complications, with a smaller decrease in efficacy for a tumor with a higher α/β value (De Brabandere *et al*., 2008). To reach a similar biological optimization effect within an HDR schedule, by lowering the fraction size, extra fractions (and possibly applications) have to be administered.

7.6.3 The Equieffective Absorbed Dose Concept, EQDX

The "equieffective" absorbed dose concept has been developed exclusively for radiation-therapy applications for comparing the clinical effects of physical doses delivered to the PTV and organs at risk using two or more different fractionation schedules (Bentzen *et al.*, 2012). Equieffective doses are defined as absorbed doses that, when delivered under specified but different conditions produce the same probability of a specific radiation effect or endpoint.

In brachytherapy, total dose, dose rate, fractionation, overall time, and temporal dose distribution, as currently used, are the main factors that have to be taken into account (Figure 7.5). Separately, spatial dose distribution of the absorbed dose may need to be considered in the form of dose–volume relationships.

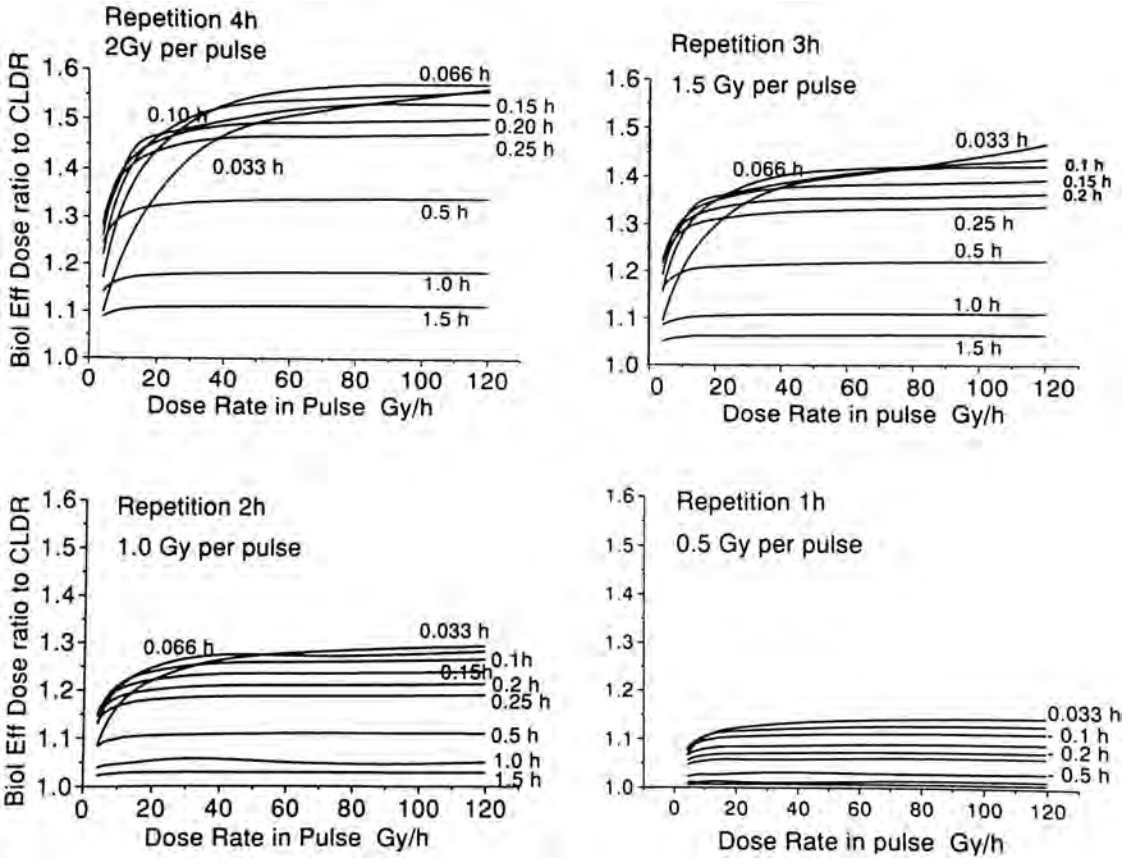

Figure 7.4. Biological effect ratio when compared with a CLDR at 0.5 Gy h^{-1} of four different PDR schedules (0.5 Gy h^{-1}, 1 Gy every 2 h, 1.5 Gy every 3 h, and 2 Gy every 4 h) and $T_{1/2}$ values ranging from 0.033 to 1.5 h. The PDR/CLDR ratio is strongly dependent on pulse sizes and half-times of recovery leading to high values when pulse size increases from 0.5 to 2 Gy and $T_{1/2}$ decreases from 1.5 h to less than 6 min. When pulse doses exceed 1 Gy equieffectiviness to CLDR (ratio between 1 and 1.1) is only present when half-time of recovery is more than 1 h. These calculations were done for late responding tissues assuming an α/β ratio of 3 Gy. Modified from Fowler and Van Limbergen (1997).

Using the LQ model, the mathematical underpinnings of the equieffective dose concept can be seen from the following.

For the two protocols, from Equation (7.2), the biological effects are given by

$$E_1 = n_1\, d_1\, \beta_1 \left(\frac{\alpha_1}{\beta_1} + d_1\right) \quad \text{and} \quad E_2 = n_2\, d_2\, \beta_2 \left(\frac{\alpha_2}{\beta_2} + d_2\right) \tag{7.8}$$

And substituting $D_1 = n_1 \times d_1$ and $D_2 = n_2 \times d_2$,

$$E_1 = D_1\, \beta_1 \left(\frac{\alpha_1}{\beta_1} + d_1\right) \quad \text{and} \quad E_2 = D_2\, \beta_2 \left(\frac{\alpha_2}{\beta_2} + d_2\right) \tag{7.9}$$

Since the goal is to find two doses, D_1 and D_2 that produce equal effects, $E_1 = E_2$, hence

$$D_1\, \beta_1 \left(\frac{\alpha_1}{\beta_1} + d_1\right) = D_2\, \beta_2 \left(\frac{\alpha_2}{\beta_2} + d_2\right) \tag{7.10}$$

It is convenient to define a dose EQDX as a total dose given where $d_2 = X$ Gy that produces an effect equal to a dose D_1 given using a different fraction size, d_1. In this case, the result is

$$D_1\, \beta_1 \left(\frac{\alpha_1}{\beta_1} + d_1\right) = \text{EQDX}\, \beta_2 \left(\frac{\alpha_2}{\beta_2} + X\right) \tag{7.11}$$

Because of the large body of clinical experience gathered with fractions of 2 Gy, it is common to assume a reference protocol using photons in 2 Gy fractions in the EQDX formula and define EQD2 as

$$\text{EQD2} = D_1 \left| \frac{\beta_1(\alpha_1/\beta_1 + d_1)}{\beta_2(\alpha_2/\beta_2 + d_2)} \right| \tag{7.12}$$

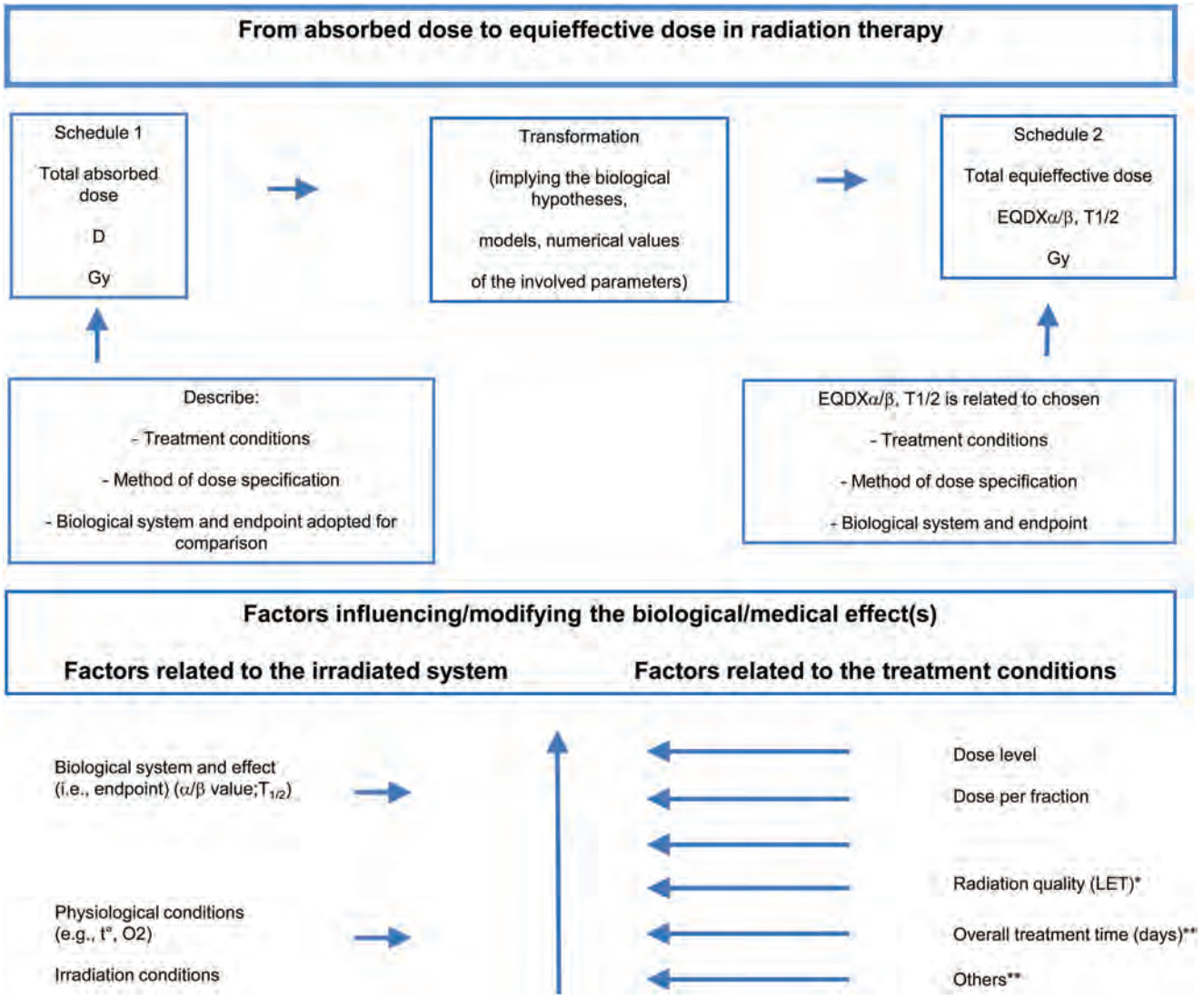

Figure 7.5. Transformation of the absorbed dose, D, to equieffective dose, EQDX, applicable to all types of radiation therapy techniques. The concept of EQDX includes the combined effects of recovery capacity and recovery kinetics. *The effect of radiation quality or LET is indirectly included via the α/β-value for a given endpoint. **The treatment conditions selected for the comparison,—including overall treatment time or other factors—have to be specified in the context; however, their effects are not currently factors included in the equieffective dose formalism (Bentzen *et al.*, 2012).

where $d_2 = 2$ Gy per fraction. In the common case when both radiations are photons given at similar dose rates, $\beta_1 = \beta_2$ and $\alpha_1/\beta_1 = \alpha_2/\beta_2$. Equation (7.12) becomes

$$\mathrm{EQD2} = D\left[\frac{\alpha/\beta + d}{\alpha/\beta + 2}\right] \qquad (7.13)$$

The values of α/β used in the calculations should be given in subscript, $\mathrm{EQD2}_{\alpha/\beta}$. In the case of an EQD2 of a radiation schedule carried out with a radiation quality other than photons, the appropriate α/β and β values for that particular radiation quality have to be used in the EQD2 formalism. [See Equation (7.12).]

The LQ approach is assumed to give an adequate estimate of equieffective doses of fractionated EBRT and HDR brachytherapy in fractions up to 5 Gy to 6 Gy, assuming that all sublethal damage is recovered between fractions and repopulation and redistribution processes are similar between the different protocols.

For translating continuous LDR into an equieffective fractionated HDR dose, the use of the Liversage formula (Liversage, 1969) has been suggested:

$$N = \frac{\mu t/2}{1 - (1/(\mu t(1 - e^{-\mu t})))} \qquad (7.14)$$

where N is the number of fractions into which the HDR treatment must hypothetically be divided in

order to have an effect equivalent to the LDR treatment lasting t hours if both total time and total dose are kept constant for both approaches when t considerably exceeds the recovery half-time, the exponential term becomes negligible and the formula reduces to:

$$N = \frac{\mu t/2}{1 - (1/\mu t)} \tag{7.15}$$

When t approaches 100 h, the last term in the denominator becomes negligible and the formula can be simplified again such that:

$$N \approx \mu t/2 \text{ and } d \approx 2.9\ T_{1/2}\text{DR} \tag{7.16}$$

where DR is the dose rate in Gy h^{-1}.

The EQD2 value of this LDR treatment then corresponds to:

$$\text{EQD2} = D\,\frac{\alpha/\beta + 2.9\ T_{1/2}\text{DR}}{(\alpha/\beta) + 2} \tag{7.17}$$

The value of α/β and $T_{1/2}$ used in the calculations should be given in subscripts, $\text{EQD2}_{\alpha/\beta}$, $T_{1/2}$.

EQD2 values computed for external beam therapy and brachytherapy can be added assuming that the volumes or points of interest for brachytherapy receive the stated external beam dose. This estimate serves as a static hotspot assumption for organs at risk. It is reasonable for the target volume of brachytherapy, which is a boost volume within the PTV of external beam treatment.

In practice, the calculation of EQD2 values of a given treatment plan can be facilitated by the use of the GEC-ESTRO EQD2 spread sheet (http://icru.org/content/reports/prescribing-recording-and-reporting-brachytherapy-for-cancer-of-the-cervix-report-no-89). In the spread sheet, the effects due to the total dose and fraction size administered by EBRT can easily be combined with the effects due to the total dose and fraction size administered by HDR, or pulse size of PDR or dose rate using LDR or MDR delivered using brachytherapy, using appropriate α/β ratios and $T_{1/2}$ values for tumor control and organs at risk. However, the uncertainties in these endpoint-specific parameters should always be carefully considered. Bioeffect calculations may be useful for decision support but should not replace sound clinical judgment.

Numerical values of equieffective doses are meaningful only to the extent that the following conditions are fulfilled:

- the irradiation conditions selected for comparison are accurately and completely specified. This includes in particular: fractionation, dose rate, time between fractions, overall time, radiation quality.
- the biological systems and endpoints for which equieffective doses are estimated, are specified. Different numerical values for equieffective doses could be obtained for different biological systems or effects and endpoints (*e.g.*, late *versus* early effects).
- the tissue volume [*e.g.*, GTV, HR CTV, IRCTV, PTV, (see Section 5)] selected for evaluation of the equieffective doses should be the same for the compared techniques and should be specified. Comparison of equieffective doses in a PTV or OAR may be relevant for comparing the efficacies of two treatments.
- the method used for prescribing or reporting the dose is the same for the compared techniques and is specified [*e.g.*, the dose at a reference point or a dose value specified on the DVH curve (*e.g.*, D_{50}, D_{90}, D_{98}, or others)].
- the biological model used is valid for the dose and fractionation schedule that is evaluated.

The assumption and methods used to fulfill these five conditions should be clearly, precisely, and completely specified and reported, thus permitting the evaluation of equieffective doses using different biological and clinical hypotheses.

The determination of equieffective doses should ideally include the effects of ALL treatment parameters and conditions (see Figure 7.5). When the treatment is delivered using X Gy per fraction, the formalism EQDX is adopted (Bentzen *et al.*, 2012).

At present, the effects of fraction size, dose rate, and, with higher uncertainties, interval between pulses or fractions, and radiation quality are considered in the EQDX formalism. Even more uncertainties become present, when the overall treatment time is significantly changed since overall treatment time is not included in the EQDX formalism; hence this must be corrected for independently of the EQDX formalism (Bentzen *et al.*, 2012). The effect of radiation quality is indirectly included *via* the α/β value for a given endpoint.

Chemotherapy and biologically targeted response modifiers may have an additive, synergistic, or protective effect and may have a differential effect on tumors, early and late responding tissues and endpoints. These effects are not independent from each other and their impact depends on the biological system and endpoint under consideration. Although attempts to include chemotherapy have been published, none of these methods are currently safely to be used in clinical practice (Bentzen *et al.*, 1989b; Jones and Dale, 2005).

7.6.4 Equieffective Dose and EQD2

Historically, the majority of patients treated curatively with external photon beams receive fractions

of 2 Gy, 5 times a week. Considerable clinical experience has been accumulated with this schedule. It is widely accepted as a reference by the radiation-oncology community. Many relationships between dose and the probability of a specific clinical outcome are well established. This broad clinical experience should not be neglected. Therefore, in external photon-beam therapy for the majority of patients, 2 Gy photon fractions, 5 fractions per week has been recommended (IAEA and ICRU, 2008) as a relevant universal reference treatment schedule. However, the use of the historical term iso-effective dose should be discouraged and replaced by Equieffective Dose at 2 Gy per fraction or EQD2 (Bentzen *et al*., 2012).

EQD2 implies that when comparing two or more radiation schedules, the reference treatment is delivered using 2 Gy per fraction. It also presumes that the LQ model (7.6.5) can be used safely to calculate EQD2. For instance, for doses in excess of 6 Gy to 10 Gy per fraction, the LQ model might not be applicable.

The potential effect of variations in the overall time is not taken into account in the EQD2 concept, *i.e.*, near similar overall treatment times are assumed.

When equieffective doses are calculated, it is always necessary to indicate apart from physical time-absorbed dose pattern also the parameters (such as α/β values and $T_{1/2}$) used for the mathematical modeling (see Section 7.6.5).

Absorbed dose D, equieffective dose, EQDX, and EQD2 are all parameters expressed in Gy. Therefore, when a dose is reported, the corresponding quantity, unit, and parameters have all to be clearly specified to avoid possible confusion (*e.g.*, 10 Gy $EQD2_{\alpha/\beta,\, T1/2}$).

7.6.5 Combination of EBRT and brachytherapy

Except for preoperative ICBT of cervix cancer Stage Ib–IIb and radical ICBT in inoperable Stage Ia, ICBT is always used as a boost treatment combined with EBRT to the pelvis. Time–dose patterns of both treatments should be taken into account to calculate the combined effects to the tumor and organs at risk. The EQD2 or EQDX formalism allows for the addition of the effects of both techniques.

Figure 7.6 shows examples of the integration of various HDR, LDR, and PDR ICBT schedules with EBRT to the pelvis. The five examples that are presented are typical time–dose patterns used for the treatment of locally advanced cervix carcinoma. In all cases, the treatment includes 25 fractions of 1.8 Gy delivered in 5 fractions per week. The total absorbed dose of 45 Gy delivered using 1.8 Gy fractions corresponds to an EQD2 of 43.2 Gy assuming $\alpha/\beta = 3$ Gy and 44.3 Gy assuming $\alpha/\beta = 10$ Gy.

External-beam radiation therapy is followed by or mixed with different schedules of ICBT.

In two examples [Figure 7.6a and b], four ICBT fractions of 7 Gy are delivered; they correspond to an EQD2 of 56 Gy assuming $\alpha/\beta = 3$ Gy and 39.7 Gy assuming $\alpha/\beta = 10$ Gy, respectfully.

In two examples [Figure 7.6c and d], PDR brachytherapy delivers 40 Gy in 80 pulses of 0.5 Gy in one or two fractions. When two PDR courses of 40 pulses are given (Figure 7.6c), the EQD2 values are 40.6 Gy for $\alpha/\beta = 3$ Gy, and 40.2 Gy for $\alpha/\beta = 10$ Gy and $T_{\frac{1}{2}}^{1} = 1.5$ h. When only one course of 80 pulses is given (Figure 7.6d), the EQD2 of the single PDR is 41 Gy assuming $\alpha/\beta = 3$ Gy and 40.4 Gy assuming $\alpha/\beta = 10$ Gy. This small increase in EQD2 when compared with the 2 PDR course schedule is due to the fact, that there is no full repair after pulse 40, while this is the case after the first PDR course when two courses are given.

In the fifth example (Figure 7.6e), continuous LDR brachytherapy delivers 40 Gy at 0.5 Gy h^{-1}. This corresponds to an EQD2 of 40.8 Gy for $\alpha/\beta =$ 3 Gy and 40.4 Gy for $\alpha/\beta = 10$ Gy, the same $T_{\frac{1}{2}}^{1} =$ 1.5 h value being assumed. The EQD2 values for PDR and LDR are thus very close to each other if the same $T_{\frac{1}{2}}^{1}$ value is assumed.

As the EQD2 delivered by EBRT and brachytherapy are additive, when 4 fractions of 7 Gy are delivered, the total EQD2 is 99.2 Gy assuming $\alpha/\beta =$ 3 Gy and 84 Gy assuming $\alpha/\beta = 10$ Gy. For PDR, in two courses, the total EQD2 is 83.8 Gy assuming $\alpha/\beta = 3$ Gy, 84.5 Gy assuming $\alpha/\beta = 10$ Gy and for PDR in 1 course, the total EQD2 is 84.2 Gy assuming $\alpha/\beta = 3$ Gy, 84.7 Gy assuming $\alpha/\beta = 10$ Gy with $T_{\frac{1}{2}}^{1} = 1.5$. For LDR, the EQD2 are 84 and 84.7 Gy, respectively.

The total EQD2 doses are thus similar for the five schedules that are compared. The numerical values of the EQD2 however strongly depend on (1) the assumed α/β values and (2) in PDR and LDR also on the assumed $T_{\frac{1}{2}}^{1}$ value.

7.7 Recommended Common Terminology for Reporting Dose–Time Parameters of Combined EBRT and ICBT

In order to compare the biological effects of the different dose rate and fractionation schedules that are used in HDR, PDR, and LDR brachytherapy, and also to make possible the comparison of the absorbed doses delivered with brachytherapy and external beam radiotherapy and allow them to be simply added, the GEC-ESTRO recommendations (Pötter *et al.*, 2006) promote the use of the EQD2 formalism proposed by Steel (Bentzen and Baumann, 2002; Joiner and Bentzen, 2002; Steel,

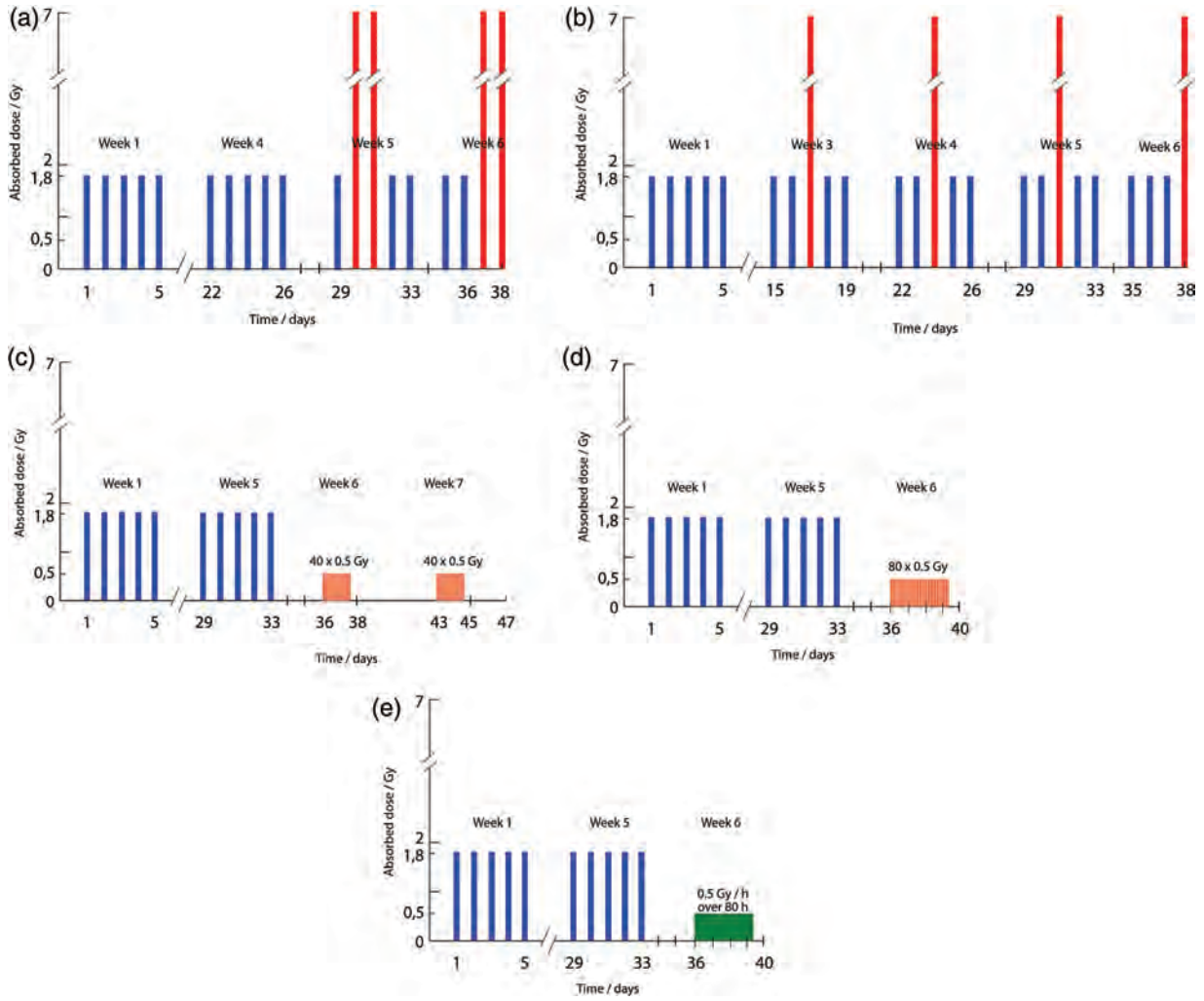

Figure 7.6. (a) An example is shown of the integration of external beam (EBRT) and HDR brachytherapy for the treatment of a locally advanced cervix carcinoma. The treatment includes 5 to 6 weeks of EBRT, which delivers 25 fractions of 1.8 Gy five times a week. External-beam radiation therapy is followed by 28 Gy of brachytherapy delivered in 4 fractions of 7 Gy; 2 fractions are given in Week 5; and 2 fractions in Week 6. The total absorbed dose of 45 Gy delivered with EBRT corresponds to an EQD2 of 43.2 Gy assuming $\alpha/\beta = 3$ Gy and 44.3 Gy assuming $\alpha/\beta = 10$ Gy. The 4 fractions of 7 Gy correspond to an EQD2 of 56 Gy assuming $\alpha/\beta = 3$ Gy and 39.7 Gy assuming $\alpha/\beta = 10$ Gy. As the EQD2 delivered by EBRT and brachytherapy are additive, the total EQD2 is thus 99.2 Gy assuming $\alpha/\beta = 3$ Gy, and 84 Gy assuming $\alpha/\beta = 10$ Gy. (b) Treatment schedule similar to Figure 7.6a but one brachytherapy fraction (or application) of 7 Gy is delivered per week. As the calculation of EQD2 takes into account only the dose per fraction, the EQD2 is the same as in (a). (c) The 5 weeks of EBRT are followed by brachytherapy delivered using two PDR applications of 20 Gy each, 1 week apart. Each PDR course consists of 40 pulses of 0.5 Gy delivered per hour (the pulse duration is 5 min to 10 min). The duration of each PDR course is 1.7 days. The EQD2 corresponding to the 45 Gy of EBRT is 43.2 Gy assuming $\alpha/\beta = 3$ Gy, and 44.3 Gy assuming $\alpha/\beta = 10$ Gy as in (a) and (b). The total absorbed dose of 40 Gy (2×20 Gy) delivered with PDR corresponds to an EQD2 of 40.6 Gy assuming $\alpha/\beta = 3$ Gy, and 40.2 Gy assuming $\alpha/\beta = 10$ Gy. A $T_{1/2}$ value of 1.5 h is used for the computation. As the EQD2 delivered by EBRT and brachytherapy are additive, the total EQD2 is 83.8 Gy assuming $\alpha/\beta = 3$ Gy, and 84.5 Gy assuming $\alpha/\beta = 10$ Gy. (d) Similar schedule as in (c), but PDR is given in only one application delivering 40 Gy in 80 pulses of 0.5 Gy. The duration of the single PDR course is 3.5 days. As in the calculation of EQD2, only the dose per fraction and $T_{1/2}$ are taken into account, the EQD2 of the single PDR is 41 Gy assuming $\alpha/\beta = 3$ Gy and 40.4 Gy assuming $\alpha/\beta = 10$ Gy. A $T_{1/2}$ value of 1.5 h is used for the computation. This small increase in EQD2 is due to the fact that there is no full repair after pulse 40, while this is the case after the first PDR course when two courses are given. As the EQD2 delivered by EBRT and brachytherapy are additive, the total EQD2 is 84.2 Gy assuming $\alpha/\beta = 3$ Gy and 84.7 Gy assuming $\alpha/\beta = 10$ Gy. (e) The 5 weeks of EBRT are followed by brachytherapy, which is delivered with continuous LDR irradiation: 40 Gy is delivered at 0.5 Gy h^{-1} (over 80 h). This corresponds to an EQD2 of 40.8 Gy assuming $\alpha/\beta = 3$ Gy and 40.4 Gy assuming $\alpha/\beta = 10$ Gy. $T_{1/2}$ is taken = 1.5 h. As the EQD2 delivered by EBRT and brachytherapy are additive, the total EQD2 is 84 Gy assuming $\alpha/\beta = 3$ Gy and 84.7 assuming $\alpha/\beta = 10$ Gy.

2002). This use is also supported by ICRU Report Committee 25 (Bentzen *et al.*, 2012). This common terminology has been shown to be practical and useful when HDR, PDR, or LDR brachytherapy and external beam therapy are combined for cervix cancer treatments.

The advantage of the EQD2 concept is that it is a simple approach based on the LQ model. It includes

the recovery parameters α/β and $T_{1/2}$. Equivalence can be calculated for each tissue and endpoint of interest using the appropriate relevant parameters, if they are known. In practice, consensus α/β and $T_{1/2}$ values are most often used (and recommended in protocols), *i.e.*, 10 Gy and 1 h for early endpoints and 3 Gy and 1.5 h for late endpoints, respectively.

An important caution is necessary when considering mathematical bioeffect models. There are almost no human data exploring the dose rate effect beyond 24 h to 30 h of continuous irradiation. Therefore, the models, and more particularly the incomplete repair model, have not yet been properly validated at dose rates relevant to classical LDR brachytherapy.

Moreover, the estimated equieffectiveness varies widely with the selection of α/β and $T_{1/2}$. Thus, a simple "magical" formula equating HDR with LDR probably does not exist. The clinician always has to proceed with caution. Moreover, calculations have been made with the LQ model assuming first order (mono-exponential) recovery kinetics. If mathematically more complex models of recovery are shown to be required in the future, then equieffectiveness might have to be recalculated with the appropriate formulae.

Of course, the values of any parameters can be changed if and when new data and insights lead to another consensus. For that reason, the ICRU recommends that the total absorbed dose, dose distribution, dose rate, pulse, and fraction sizes always be reported in Gy with no biological correction. This should allow calculation or re-calculation if needed of the EQD2 as new radiobiological data become available.

7.8 Uncertainties Related to the Dose–Time Modeling

Although the LQ formalism can help to provide a common language that allows translation and addition of different LDR, PDR, HDR brachytherapy schedules to the estimated effects of EBRT, it must be pointed out that many uncertainties remain.

- The calculation of EQD2 with a mono-exponential recovery model might be too simplistic, since some newer data suggest rather that a more complex recovery pattern such as a bi-exponential, with a fast and a slow component, would better fit the data. The repartition coefficient between fast and slow component might be dose rate and fraction size-dependent making EQD2 calculations between LDR/PDR/HDR even more complex.
- The values of α/β and $T_{1/2}$, as proposed for model parameters in the GEC-ESTRO recommendations (Pötter *et al.*, 2006), are estimates with large uncertainties. The GEC-ESTRO has recommended in cervix cancer an assumed $\alpha/\beta = 10$ for the target volumes and $\alpha/\beta = 3$ Gy for the late effects in the organs at risk, including the bladder, rectum, sigmoid, and small bowel.
- As far as the half-time for recovery, $T_{1/2}$, is concerned, in the original GEC-ESTRO paper, a half-time of 1.5 h for late effects and for tumor control was proposed (Pötter *et al.*, 2006). Based on the revision of the published data (see Section 7.6.2.2), it could be more appropriate to assume a $T_{1/2}$ of 0.5 h for late effects and 0.25 h for tumor control. However, these data should be considered with extreme care, since all other human data on late normal tissue tolerance suggest much longer half-times of recovery. Therefore, as long as improved data from ongoing trials on local control and late complications are not available, it seems prudent to stay with the original assumptions.

7.9 Equivalent Uniform Dose, EUD

The dose distribution in ICBT is heterogeneous with a minimal target dose encompassing the CTV, and much higher doses (and thus dose rates) delivered in the immediate surroundings of the radioactive sources. Variation in dose and dose rate leads to major differences in biological effect.

To attempt to account for these variations, the concept of equivalent uniform dose (EUD) was introduced (Niemierko, 1997). The EUD is intended to be a dose that, if delivered homogeneously, would produce the same biological effect as that achieved by the actual inhomogeneous delivery.

For brachytherapy, the EUDs are consistently higher than the doses calculated at the prescription isodose. Equivalent uniform dose is thus a function of the choice of the prescription isodose. Because of the steep dose fall off close to the central sources, the calculated EUD will be larger when the prescription isodose is chosen closer to the source. Comparing EUD weighing factors of different intracavitary applications is thus only valid when compared at the same prescription dose levels. For typical radical gynecological treatments, the EUD weighting factors are in the approximate range of 1.15 to 1.30 (Dale *et al.*, 1997). The lower numbers apply to LDR brachytherapy, the higher for HDR brachytherapy (6 Gy per fraction). The dependence of calculated EUDs on the assumed radiobiological parameters (radiosensitivity and α/β) is less important (Dale *et al*., 1997). The weighting factor for 6 Gy per fraction is 1.3 for an $\alpha/\beta = 10$ Gy and 1.4 for 3 Gy.

What would be the benefit of applying EUD weighting factors in ICBT for the doses calculated for target and OAR? Due to the exponential dose fall-off around the intracavitary sources, the highest doses will be present in the central area: either in

the applicators themselves, in the central part of the tumor, or in the more radio-resistant tissues of the cervix or the uterine muscle. Multiplying the doses in that area has no meaning for tolerance. The doses to the organs at risk, which are at a larger distance from the sources, are usually lower than the prescription isodose. The dose gradients in the relevant volumes of the organs at risk are not as steep, and the need for EUD correction will be smaller.

Because of the large uncertainty of parameter estimates and the unproven validity of the EUD formalism, it is not recommended to use EUD for the OAR.

7.10 Recommendations for Reporting Dose–Time Parameters

Level 1: *Minimum standard for reporting*

Dose delivery pattern:

1. A. LDR
   - (a) Absorbed dose (Gy)
   - (b) Dose rate (Gy h^{-1})
   - (c) Number of fractions
   - (d) Time between fractions (h)

   B. HDR
   - (e) Absorbed dose per fraction (Gy)
   - (f) Number of fractions
   - (g) Time between fractions (h)

   C. PDR
   - (h) Absorbed dose (Gy)
   - (i) Number of fractions, interval between fractions
   - (j) Pulse size (Gy)
   - (k) Number of pulses
   - (l) Time between pulses (h)
2. Total treatment time (TT) in hours or days of EBRT, brachytherapy, and overall TT of combined modality
3. EQD2 values where available

Level 2: *Advanced standard*

All that is reported in Level 1 plus:

1. EQD2 values for target and OAR biological endpoints
2. Respective α/β values for the target and OAR,*
3. Respective $T_{1/2}$ of recovery*
4. Applied recovery model, mono- or bi-exponential

*For the moment, the advice is to follow the GEC-ESTR0 recommendations $\alpha/\beta = 3$ Gy for late effects in OAR and 10 Gy for tumor response, and a $T_{1/2}$ of 1.5 h for both

Level 3: *Research-oriented reporting*

All that is reported in Level 2 plus:

1. Detailed DVH parameters for target or OAR biological endpoints
2. NTPC and TPC calculations, with the model explicitly stated

7.11 Summary

Brachytherapy differs from external beam therapy (EBRT) in two main ways: the distribution of the absorbed dose and the time–dose patterns.

Dose distribution: Total dose and dose rate in brachytherapy decrease dramatically with the distance from the sources. The dose is prescribed to a CTV, *i.e.*, an isodose surface often encompassing a volume of $\sim$10 cm^3 to 200 cm^3. The GTV receives about >150 % of the prescribed dose.

For brachytherapy dose rates are divided, somewhat arbitrarily, into three ranges: LDR < 1 Gy h^{-1}, MDR between 1 and 12 Gy h^{-1}, and HDR >12 Gy h^{-1}. Changing dose rate in the MDR range causes the most pronounced changes in biological effect. In the present report, terms describing dose–time distributions specific to cervix brachytherapy, including (mean) dose rate, fractionation, pulse, application, and overall treatment time are defined. Moreover, biological mechanisms potentially impacting on effectiveness of the treatment, such as repopulation, re-oxygenation, and redistribution, are discussed. The large decrease in dose with distance and the large variation in dose rate and fraction size require a common concept and a joint terminology to facilitate biological comparison between the different brachytherapy schedules.

The LQ formalism and EQDX: allows comparison of the predicted effects of a particular brachytherapy schedule with other brachytherapy and external beam schedules, with regard to both tumor control and normal tissue effects. With a set of assumptions, even the additional effect of chemotherapy may be quantified, but with large uncertainties. This formalism can be safely applied within a range of doses per fraction from 0.5 Gy to 6–10 Gy; it might, however, potentially overestimate the effects at higher doses per fraction.

For all dose rates, the calculations of the effects are strongly dependent on the recovery capacity (related to the α/β values) and half-times for recovery $T_{1/2}$ that are assumed in the modeling. Uncertainties in the estimates of these values need to be considered. This applies to tumors as well as to normal tissues.

For photon irradiations, an α/β value of 10 Gy and a recovery half-time of 1.5 h for cervix tumor tissue is generally assumed and of 3 Gy and 1.5 h for late effects in the OAR. For more specific and precise calculations, tissue-specific recovery parameters should be used where available.

The equieffective absorbed dose concept, EQDX: has been developed for comparing different irradiation protocols and techniques. Equieffective doses delivered in X Gy fractions (EQDX) are

defined as total doses that—delivered under different conditions, which have to be specified in the context, are assumed to produce the same probability of a specific effect (endpoint), as the resultant total dose given in X Gy fractions. For protocols involving only one type of radiation equieffective doses can be calculated using the LQ formalism; and assumed values of α/β well as the $T_{1/2}$ of recovery if required for the EQDX calculations have to be specified by subscripts: $EQDX_{\alpha/\beta,\ T1/2}$. Because recovery is often assumed to be complete between fractions, the reference to $T_{1/2}$ may be omitted, depending on the details of the dose delivery. Because of historical precedents and clinical experience EQD2 referring to photon doses of 2 Gy/fraction is commonly used. For protocols involving different radiations, assumed values of β are required for both radiation types and must be specified. This ICRU/GEC-ESTRO report recommends the use of the equieffective formalism, particularly EQD2, for addition of absorbed doses to report doses for planning aims, prescriptions, and doses delivered.

Journal of the ICRU Vol 13 No 1–2 (2013) Report 89
Oxford University Press
doi:10.1093/jicru/ndw009

8. Dose and Volume Parameters for Prescribing, Recording, and Reporting Brachytherapy, Alone and Combined with External-Beam Radiotherapy

8.1 Brief Historical Survey of Dose Effects and Reporting

There are large amounts of accumulated data on the effects of radiation on both tumors and normal tissues. There has been a long and successful record of curative treatment of cervical cancer applying brachytherapy alone for limited disease, or combined with external-beam radiation therapy (EBRT) for more advanced disease (see Section 2.9). In the radium era, absorbed dose in brachytherapy was specified mainly in terms of the product of the radium mass and the treatment time, in units of milligram hours (mg h) (later TRAK) or as absorbed dose to Point A (see Sections 3.2–3.5, 10.1, and 11.3). An amount of radium mass times treatment time, specified in terms of mg h, or absorbed dose to Point A, applied under certain conditions, resulted in predictable levels of tumor control, survival, and adverse side effects.

The rectum, bowel, and bladder were identified as organs at risk (OAR) of major importance and often suffered severe radiation-induced inflammatory or ulcerative disease, sometimes resulting in the development of fistulae and stenosis. Absorbed-dose assessment for the rectum and the bladder was based mainly on reproducible anatomic or applicator-related points, which could be defined on orthogonal radiographs with the applicator in place (see Section 10.3). Some of these points were later defined as ICRU reference points (ICRU, 1985). In particular, the rectum dose–effect relations using these reference points defined 30 years ago are based on large multi-center experience (Pötter *et al*., 2001a; Pourquier *et al*., 1982).

Attempts to relate the more than 50 years of experience using LDR brachytherapy to the newer modalities of high-dose rate (HDR) and low-dose rate (PDR) brachytherapy required new radiobiological models for predicting tumor and normal-tissue effects (see Sections 7.6 and 7.7). Radiobiologists investigated absorbed-dose-rate effects and tried to interpret new experimental and clinical information with bio-mathematical models while striving to establish a common terminology and predictors for outcome. Biological models, applicable to the complexity of brachytherapy of the cervix, have been implemented in a pragmatic way (see Sections 7.6–7.8). Current planning aims are based on clinical experience combined with models to define dose constraints. With the introduction of image-guided adaptive brachytherapy, communication of information about absorbed dose, absorbed dose per fraction, and absorbed-dose rates to defined volumes in a valid way has become more reliable, thus facilitating a better understanding of the relationships between absorbed dose and volume (Pötter *et al*., 2006).

First published experiences with a considerable number of patients treated in a single institution have shown dose–volume effects based on a volumetric representation of absorbed dose to the target and OARs, and local control, and normal-tissue morbidity (Dimopoulos *et al*., 2009; Georg *et al*., 2009; 2012; Koom *et al*., 2007) (see Figure 8.1).

8.2. Dose Distribution and DVH for Targets and OARs

The heterogeneous absorbed-dose distribution in highly variable volumes, typical of intracavitary brachytherapy, requires comprehensive assessment. Absorbed doses delivered to different volumes in different locations within different biological systems over different time intervals lead to very different biological effects. Integrated absorbed-dose assessment for brachytherapy and for EBRT within a complex 4D registration system (volume and time) is an enormous challenge (see Section 8.5) and should ideally take into account effects at the cellular level. Simple, voxel-based registration methods that do not take into account spatial volume changes of tumor and organs are not sufficient.

The overall aim of dose prescription and reporting is to describe the dose distribution related to target volumes and to OARs as completely and precisely as

possible. The typical heterogeneity of the brachytherapy absorbed-dose distribution complicates achievement of this goal. In the hypothetical case of a completely uniform absorbed-dose distribution over the target volume, there would simply be one dose value prescribed and reported. Absorbed-dose homogeneity in the target volume has been the major aim of most traditional EBRT techniques. However, even with external photon beams, it is not possible to achieve completely uniform absorbed-dose distributions. The mean, median, near maximum, and near minimum absorbed-dose values serve for reporting realistic absorbed-dose distributions. More information is conveyed through the entire cumulative dose–volume histogram (DVH), which provides information about volume irradiated as a function of absorbed dose.

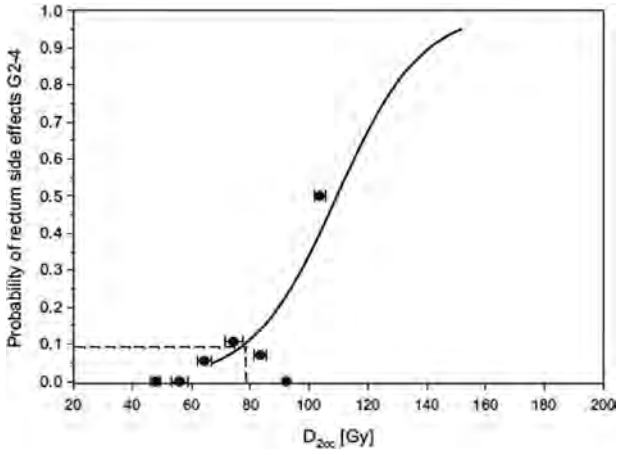

Figure 8.1. Example of a dose–volume response curve for rectum late effects in 141 patients treated with definitive radio-chemotherapy for advanced cervical cancer and image-guided adaptive brachytherapy (from Georg *et al*., 2012). Note that D_{2cc} was a symbol previously used for D_{2cm^3}.

Recording and reporting the entire DVH for each patient might not be practical in summarizing a series of patients, and methods to compare different DVHs and link them to dose–volume effects are not straightforward. Therefore, single parameters derived from a cumulative DVH are often used in an attempt to predict a certain biological effect. Parameters in the form of D_V are defined as dose received by at least a volume V, where V is given as a percent of a defined region or in units of cm^3. Parameters V_D are the volume receiving doses greater than or equal to the absorbed dose D specified either as the absorbed dose, the EQD2, or a percent of a defined absorbed-dose value. The DVH parameters should be chosen to predict outcome with high accuracy.

Examples of DVH are shown in Figure 8.2. The DVH has a plateau until it reaches the minimum absorbed dose (the near minimum dose $D_{98\%}$) in the specified volume. There is then a region of declining absorbed dose until it reaches the highest absorbed dose shown on the plot. With brachytherapy, the absorbed dose near the sources becomes very high, as shown in Figure 8.2. Organs at risk not containing sources will fall to zero volume at the maximum absorbed dose received by that organ.

In situations in which the final slope of the DVH approximates a straight line, only two numerical values as $D_{98\ \%}$ and $D_{2\ \%}$ would be needed to describe adequately the DVH. However, for realistic dose distributions within clinically relevant volumes, more points are needed for a description that conveys the shape. Sometimes a third point adds the necessary

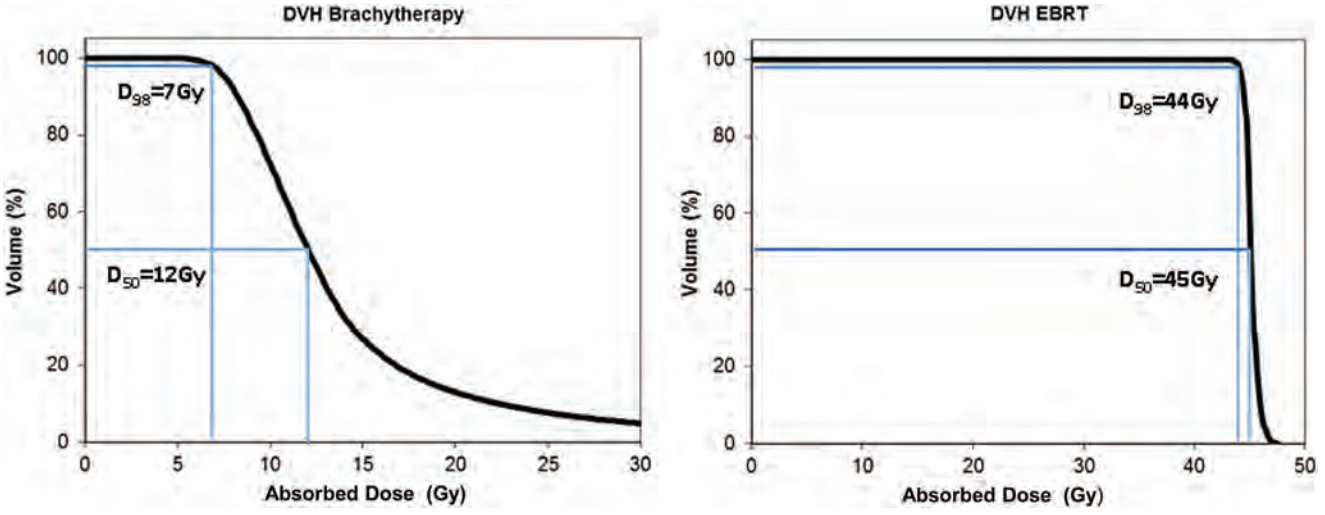

Figure 8.2. Example of two target DVHs based on typical brachytherapy and EBRT absorbed-dose distributions. The intracavitary brachytherapy DVH indicates a highly heterogeneous absorbed dose with 98 % of the volume being covered by 7 Gy, and a significantly higher median absorbed dose of 12 Gy. The EBRT DVH shows an almost flat absorbed-dose profile followed by a steep fall. In this case, 98 % of the volume is covered by 44 Gy, and the median absorbed dose is 45 Gy.

information. However, if more points are needed, the entire curve should probably be provided.

Because intracavitary brachytherapy is most often combined with EBRT, when assessing dose to the target and OARs, the integrated EBRT and brachytherapy dose must be taken into account (see Figure 8.3) (in case of midline block see Tamaki *et al.*, 2015). The weighting of EBRT and brachytherapy doses has major impact on the accumulated dose distribution and dose gradients. The dose heterogeneity is substantially increased when an increased fraction of the total EQD2 is delivered by brachytherapy.

As discussed above, the dose heterogeneity in various volumes will not be fully reflected if only a single point on the DVH is reported, and therefore, heterogeneous doses are more adequately described by choosing a number of appropriate points. In the case of similar steepness and bending of the DVH, which occurs for the same combination of EBRT and brachytherapy EQD2, a variety of points on the DVH for a patient are surrogates for proper estimation of the full curve. It remains difficult to determine exactly which of the DVH parameters is most directly related to a particular clinical effect (*e.g.*, is rectal toxicity related to a high-dose region as described by the minimum dose to 0.1 cm^3, 2 cm^3, or 5 cm^3). However, in order to compare DVH parameters for combined EBRT and intracavitary brachytherapy with DVH parameters from other RT techniques, such as interstitial brachytherapy or external-beam radiotherapy, stereotactic radiotherapy, proton, and other particle therapy, it may be necessary to report a set of parameters that are believed to be most logically linked to a certain clinical effect, for example, high-dose levels in small volumes for bleeding and ulceration. Dose–volume histograms reduce spatial three-dimensional (3D) information into a 2D dose and volume representation.

The specific spatial location(s) within a certain volume of interest is not indicated on the DVH. However, both targets and OARs often are composed of sub-volumes that have different biological characteristics, function, and response to dose. For example,

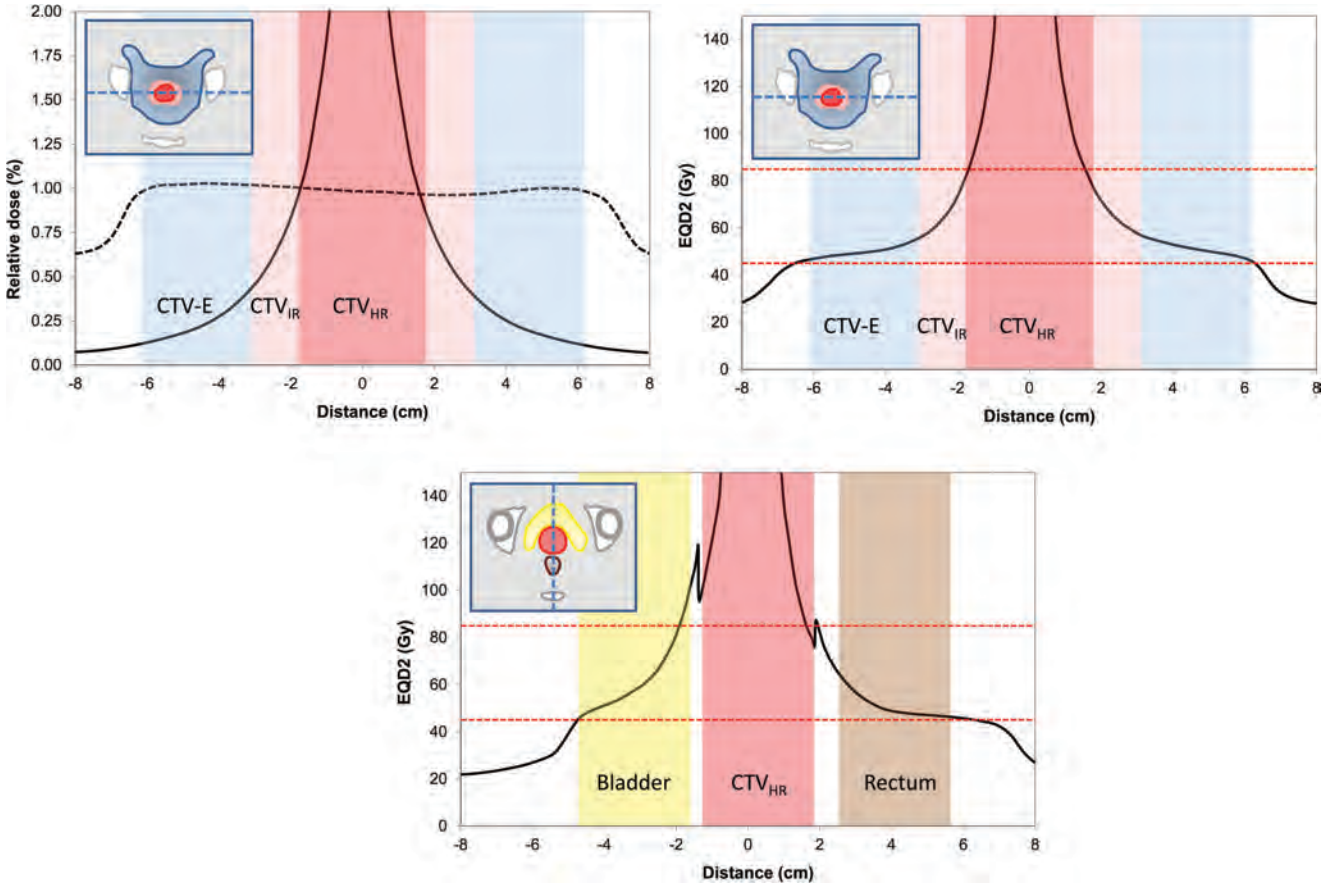

Figure 8.3. Dose profiles from intracavitary brachytherapy and whole-pelvis EBRT. (Upper left) The EBRT covers the elective CTV-E with a homogeneous absorbed dose, whereas the brachytherapy boost presents with the typical inhomogeneous absorbed dose; lateral EBRT (dashed line) and brachytherapy (solid line) absorbed-dose profiles (relative absorbed dose normalized to prescribed EBRT and brachytherapy dose, respectively). (Upper right and lower panel) Accumulated EBRT+brachytherapy dose in EQD2 ($\alpha/\beta = 10$ Gy inside the CTV, and $\alpha/\beta = 3$ Gy outside the CTV) in lateral and anterior–posterior directions, respectively. In the anterior–posterior direction, the steep dose increase at the border of the CTV_{HR} is due to the change in α/β from tumor to normal tissue. Red dashed lines indicate EQD2 dose levels of 85 Gy and 45 Gy.

certain regions of the tumor are likely to benefit from a higher dose because of clonogenic cell density or a specific micro-environment (*e.g.*, hypoxia). Similarly, the functionality of OAR has some spatial distribution, such as for the bladder where the trigonum/bladder neck has a specific bladder emptying function. Therefore, a specific dose distribution in a specific volume is expected to influence the outcome, and there will be an inherent limitation in the use of DVH alone. Sub-volumes can be delineated to focus on a certain biological target and clinical effect, and consequently, the calculation of DVHs for such sub-volumes might be used for further characterization of the dose distribution. However, the most appropriate method remains the study of the entire spatial absorbed dose and EQD2 distribution within the target and OAR volumes, usually performed by displaying the isodose distributions slice-by-slice.

8.3. Point Doses and Dose–Volume Parameters for the Target

8.3.1 TRAK and Dose to Point A

In the past, dose assessment for brachytherapy was mainly based on the amount of radiation incident on the patient (TRAK) and/or the absorbed dose at specified points, such as Point A (see Sections 3.2, 3.4, 10.1.1, and 11.3). A large clinical experience has and is still being accumulated with these metrics worldwide. The continuation of their use makes it possible to build upon previous experience and to facilitate communication between current radiographic-based and the volume-image-based radiotherapy approaches.

The TRAK is the integral of the reference air-kerma rate from all sources at a distance of 1 m from the source over the treatment duration (for details, see Section 11.3). The concept of a product of source strength and treatment time is, in principle, very similar to reporting radium treatments in units of mg h. It is linked approximately to the integral absorbed dose delivered to the patient. TRAK is a purely physical parameter and cannot be directly associated with a given biological effect because TRAK does not take into account the absorbed-dose distribution, fraction size, and absorbed-dose rate. For example, the TRAK required for a PDR treatment schedule will be higher than for an HDR treatment because a PDR treatment usually produces lower biological effects per unit TRAK than does an HDR treatment. TRAK, without any further radiobiological normalization, can be used only for comparisons among treatments with similar equieffective fractionation schedules (see Section 7).

Absorbed dose to Point A is related to the absorbed dose within or close to the target structures (see Section 10.1.2 and Figure 10.2). Point A is now defined in a fixed relationship to the applicator, 2 cm cranial to the upper surface of the vaginal applicator part (see Section 10.1.1) and at a distance of 2 cm left and right lateral to the intrauterine tandem applicator. Dose to Point A is a surrogate for the minimum target dose in a symmetrical cylindrical target volume with a diameter of 4 cm and a height less than the loaded part of the tandem. The total equieffective dose at Point A delivered through EBRT and brachytherapy can be calculated using the EQDX concept. Reporting of the dose to Point A is not dependent on target-volume contouring, and therefore is a key parameter that allows a direct comparison of the effects of dose delivered to different patients in different departments with different fractionation schedules and absorbed-dose rates.

For intracavitary brachytherapy, isodose lines at distances of 2 cm from the tandem already exhibit smooth contours. This is substantially different from the situation in which intracavitary brachytherapy is combined with interstitial implants. In this case, Point A is located within a region of a very heterogeneous absorbed-dose distribution, depending on each single dwell position within a needle. A dwell position could even be exactly at Point A, resulting in an indefinable absorbed-dose value. For such cases, the absorbed dose to Point A does not represent a relevant target absorbed dose, and Point A cannot be used for reporting. If the interstitial component is limited to one lateral part of the implant, the absorbed dose to Point A on the contralateral side can be used for dose evaluation during treatment planning (see clinical examples in the Appendix).

8.3.2 CTV_{HR} and CTV_{IR} ($D_{98\ \%}$, $D_{90\ \%}$, $D_{50\ \%}$)

The GEC ESTRO report recommended the reporting of $D_{100\ \%}$ and $D_{90\ \%}$, defining the minimum doses delivered to 100 % and 90 % of the target volume, respectively. These DVH parameters reflect the dose in the outer region of the target. $D_{90\ \%}$ is more stable with respect to random uncertainties when compared with an absolute minimum target dose, $D_{100\ \%}$. However, due to the significant absorbed-dose gradients, $D_{90\ \%}$ might look favorable even though 10 % of the target volume receives a much lower dose. The minimum target absorbed dose is very dependent on volume reconstruction and absorbed-dose sampling in the treatment–planning system (ICRU, 2010; Kirisits *et al.*, 2007). A more robust metric is the near-minimum dose $D_{98\ \%}$, in which 2 % of the target volume receives less than this dose. $D_{98\ \%}$ is also proposed for IMRT treatments in ICRU Report 83 (ICRU, 2010). Because of the absorbed-dose gradients in brachytherapy, there can be considerable differences between $D_{98\ \%}$ and $D_{100\ \%}$

(Schmid *et al*., 2012), and therefore, care must be taken when comparing previously reported $D_{100\ \%}$ values with new $D_{98\ \%}$ values. The use of $D_{98\ \%}$ and $D_{90\ \%}$ parameters is recommended for reporting dose to the CTV_{HR}. If the CTV_{IR} is used for prescription and in the case of clinical trials, these two parameters are also recommended for the CTV_{IR}.

High-dose volumes for intracavitary brachytherapy are regarded as important because they probably contribute to the excellent local control observed, even for large-volume disease (Viswanathan *et al*., 2011a). The brachytherapy dose heterogeneity is substantial in the target region, with typical absorbed-dose gradients of from 5 % to 25 % mm^{-1}, which means that a considerable part of the tumor will be irradiated to more than 200 % of the absorbed dose to Point A. When taking into account fraction size and absorbed-dose rate, the heterogeneity of the biologically equieffective dose in the target becomes even more pronounced, as the high absorbed doses near the applicator are even more effective because they are delivered at a higher absorbed-dose rate for LDR treatments and larger fraction size for HDR treatments (see Section 7.1.1). For the evaluation of these high-dose volumes, the DVH parameter $D_{50\ \%}$ is recommended. However, because of these high absorbed-dose values, substantial radiobiological uncertainties are inherent in calculating an EQD2 of $D_{50\ \%}$ (see Section 7.6.4)

In ICRU Report 83 (ICRU, 2010), the use of the near-maximum dose $D_{2\ \%}$ was recommended. A $D_{2\ \%}$ for intracavitary brachytherapy would represent the dose to tissue close to the source or even in the applicator itself and might not be relevant. The use of $D_{98\ \%}$, $D_{90\ \%}$, and $D_{50\ \%}$ for intracavitary brachytherapy alone could be seen as analogous to the ICRU Report 83 recommendations to report $D_{98\ \%}$, $D_{50\ \%}$, and $D_{2\ \%}$ for target structures treated with IMRT. However, the dose range described with these three parameters is very different for EBRT combined with brachytherapy. For IMRT treatment plans, the $D_{98\ \%}$ and $D_{2\ \%}$ are usually between ± 10 % of $D_{50\ \%}$. The situation is different for intracavitary brachytherapy combined with EBRT. The difference depends in particular on the tumor size and the implant, as well as on the weighting of EBRT and brachytherapy doses. For conventional treatment schedules in which about half of the total EQD2 to the primary target is delivered by brachytherapy, the dose heterogeneity is significant with $D_{50\ \%}$, in terms of total EQD2, being substantially higher than $D_{90\ \%}$ (see Figure 8.4).

8.3.3 GTV_{res} at the Time of Brachytherapy ($D_{98\ \%}$)

The brachytherapy applicator is generally placed inside or very close to the residual GTV, and the minimum absorbed dose in the GTV_{res} at the time of brachytherapy is often much higher than the minimum absorbed dose to the CTV_{HR}, which in turn is very much higher than the minimum absorbed

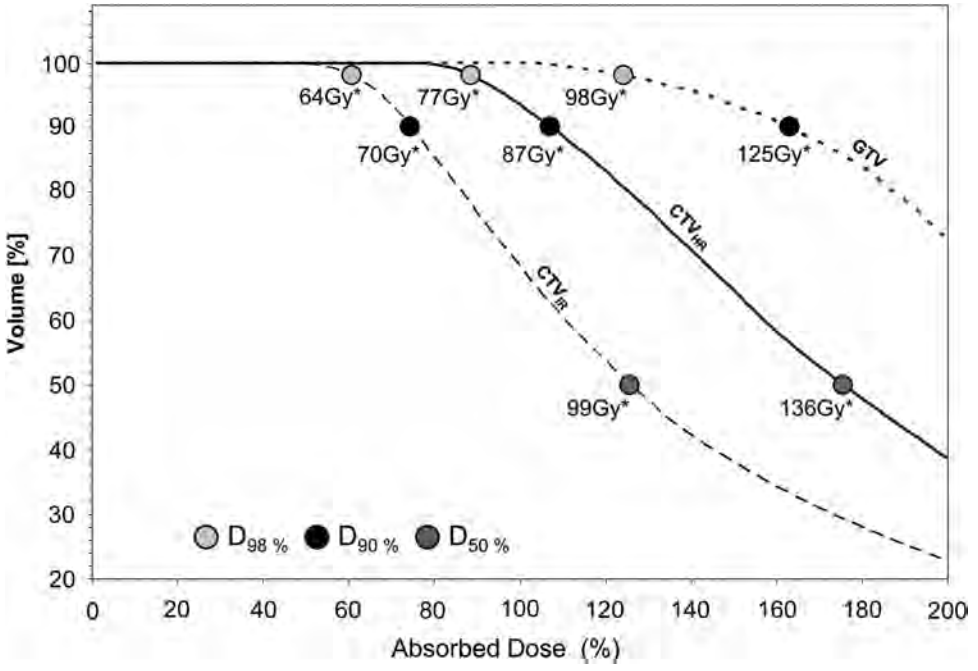

Figure 8.4. Dose–volume histogram for GTV_{res}, CTV_{HR}, and CTV_{IR}. The initial planning-aim absorbed dose was 25×1.8 Gy external-beam therapy (44.3 Gy EQD2) plus 4×7 Gy with HDR brachytherapy (40 Gy EQD2) for a total $D_{90\ \%}$ for the CTV_{HR} of $\geq$84 Gy EQD2 ($\alpha/\beta = 10$ Gy). The fraction on the x-axis illustrates the normalized absorbed dose per brachytherapy fraction. *Total EQD2 values ($D_{98\ \%}$, $D_{90\ \%}$, and $D_{50\ \%}$) are given.

dose to the CTV_{IR}. $D_{98\ \%}$ and $D_{90\ \%}$ are relevant dose parameters for the GTV_{res}. The equieffective dose calculations for $D_{50\ \%}$ for the GTV_{res} become unreliable because they exceed the limits of the models currently in use (see Section 7.6.4). As the experience with dose values reported for the GTV_{res} is limited, it is recommended to keep $D_{98\ \%}$ as the primary parameter and $D_{90\ \%}$ in the case of research-oriented analysis.

8.3.4 PTV for Brachytherapy

In photon EBRT, the common approach is to prescribe the absorbed dose to the PTV with the assumption that the margins included in the PTV will result in the CTV receiving the prescribed absorbed dose. In the case of homogeneous EBRT absorbed-dose distributions, the absorbed dose in the CTV will be similar to the absorbed dose in the PTV if CTV movements are within the PTV. However, in brachytherapy, the situation is different due to the very heterogeneous absorbed-dose distribution. If a PTV margin is used around a CTV in intracavitary brachytherapy, the absorbed dose would be systematically lower than the CTV absorbed dose because the PTV represents a larger volume, part of which is more distant from the sources (Tanderup *et al.,* 2010c). Also, uncertainties are different in intracavitary brachytherapy (see Sections 5.4.6 and 5.5). Currently, there appear no compelling reasons to introduce PTV dose reporting in routine brachytherapy practice.

On the other hand, a pre-implantation PTV concept could be used during implantation to ensure that the applicator geometry results in a dose distribution covering the entire brachytherapy CTV with the appropriate absorbed dose (see Section 5.5.6). A PTV in the cranio-caudal direction could also be used for prescription to avoid a too-tight coverage at the upper CTV_{HR}, which might result in a geographical miss due to applicator movements between imaging and during absorbed-dose delivery (see Figure 5.17). Further research might provide additional support to use the PTV concept for dedicated treatment situations. However, for reporting, the CTV and not the PTV is the primary target volume in intracavitary brachytherapy because it represents a better estimate of the dose delivered.

8.3.5 Lymph Nodes ($D_{98\ \%}$)

Lymph nodes can or cannot receive significant absorbed doses in brachytherapy, and that absorbed dose can be of particular interest for analysis of recurrences. There is a significant brachytherapy absorbed-dose gradient along the lymph-node chains, and therefore, the brachytherapy absorbed dose is variable within each lymph-node region (see also Section 10.1.5). It has been shown that the average absorbed dose to the obturator and internal iliac lymph-node regions is about from 15 % to 30 % of the absorbed dose to Point A, while it is about from 10 % to 20 % in the external iliac chain (Gebara *et al*., 2000; Lee *et al*., 2009). In terms of EQD2, this amounts to from 4 Gy to 8 Gy for obturator and internal iliac nodes and from 2 Gy to 6 Gy for external iliac lymph nodes in HDR brachytherapy schedules with four brachytherapy fractions, and total EQD2 dose of 85 Gy to the CTV_{HR}. If the CTV_{HR} is treated by increasing the TRAK, than this also leads to an increase in the dose in the lymph nodes. The current recommendation is to report the near-minimum dose, $D_{98\ \%}$, for pathological lymph nodes even if the relevance of such reporting has not been validated. The median dose, $D_{50\ \%}$, can be used for research purposes.

For radiographic approximation, the concepts of the lymphatic trapezoid and pelvic wall points can be used as described in Section 10.1.5.

8.4 OAR: Dose-Point and Dose–Volume Parameters

In the past, OAR dose constraints have often been based on relative fractions of a prescribed absorbed dose [*e.g.*, two-third of the prescribed absorbed dose at Point A allowed as maximum absorbed dose in the rectum (Stitt *et al*., 1992)], or 150 % to the lateral vaginal surface of the applicator (Nag *et al*., 2002). As noted by the authors of these reports, such relative absorbed-dose constraints cannot be used universally, as changing the total target absorbed dose or changing the fractionation schedule directly influences absorbed-dose constraints for OARs. To reach the most valid, reliable, and reproducible OAR dose assessment, dose-point, and dose–volume reporting of dose values to absolute volumes is strongly suggested in this report.

Analysis of the 3D dose distribution in an OAR has been based on two approaches: using a relative DVH in which the entire organ is contoured and the doses relate to the fraction of the contoured volume, and an absolute DVH in which the doses relate to absolute volumes. Local pathologic-tissue alterations in gynecologic brachytherapy, such as circumscribed inflammation and fibrosis, telangiectasia, ulceration, necrosis, or fistula, occur mainly in those volumes of hollow organs adjacent to the applicator and exposed to high EQD2 (> from 70 Gy to 80 Gy) to small volumes. Organ complications such as stricture, stenosis, and functional impairments occur mainly after irradiation of large organ volumes—predominantly those including the whole circumference of hollow organs—with intermediate-to-high EQD2 (from 40 Gy to 65 Gy, or more) (see Sections 6.2 and 6.3).

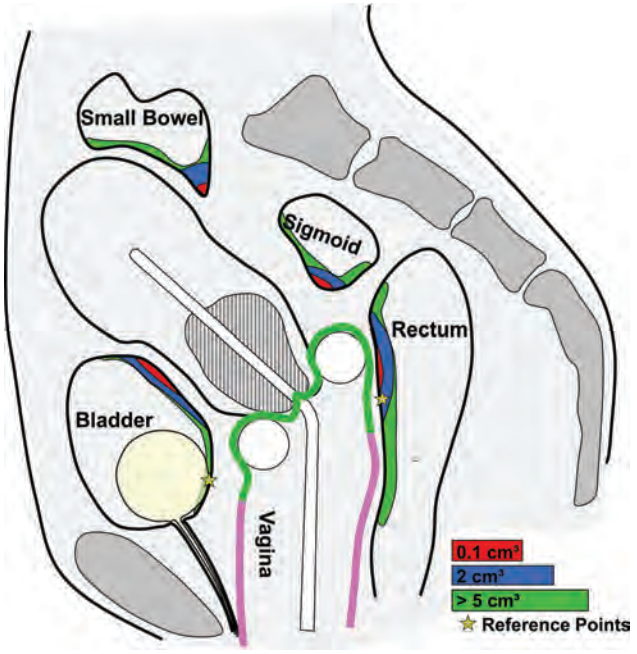

Figure 8.5. Sagittal view showing the volumes related to $D_{0.1\text{cm}^3}$, $D_{2\text{cm}^3}$, and a D_V with $V > 5\ \text{cm}^3$. Note that if the dose to large volumes should be evaluated, delineation of an organ wall is needed, while small volumes will be located mainly within the wall, even with whole-organ contouring. The location of the bladder and recto-vaginal reference points are also shown. For the vagina, heavily irradiated volumes of approximately 2 cm^3 and smaller are located adjacent to the lateral parts of the applicator not visible in this cross-sectional view (see Figures 8.12 and 10.1).

Bladder and rectal points delineated on radiographs (see Section 10.3) have been widely used (ICRU, 1985). However, the large absorbed-dose inhomogeneity in these adjacent organs results in poor characterization of the OAR dose when using point reporting only. Parts of the bladder, rectum, bowel, and vagina walls are irradiated with doses close to or higher than the minimum target doses. Wall segments, such as the posterior recto-sigmoid walls, the superior-anterior bladder wall, and the inferior vagina, receive much lower brachytherapy absorbed doses (such as 10 % to 20 % of prescribed CTV absorbed-dose values) that have to be added to the EBRT absorbed doses. In combined brachytherapy and EBRT, there is an enormous variation in the dose distribution in the adjacent OAR walls (see Figure 8.5).

Specific OAR volumes for treatment planning and dose reporting were introduced in the second GEC ESTRO recommendations (Pötter *et al.*, 2006). Addressing mainly brachytherapy-related morbidity, the analysis of doses in small volumes (0.1 cm^3, 1 cm^3, and 2 cm^3) adjacent to the applicator, which receive high doses, was recommended and has become widespread practice in centers using image-guided brachytherapy (Chargari *et al.*, 2009; De Brabandere *et al.*, 2008; Jürgenliemk-Schulz *et al.*, 2009; Kirisits *et al.*, 2005; 2006a; Levitchi *et al.*, 2012; Lindegaard *et al.*, 2008; Mahantshetty *et al.*, 2011b; Pötter *et al.*, 2011). However, due to the dose gradients throughout these organs and the complex pattern of overall acute and long-term morbidity, larger volumes are also of interest for a comprehensive assessment and reporting of morbidity. Therefore, in the following sections, both small and large volumes are discussed for the various OARs treated at high, intermediate, and low dose levels, and recommendations for dose reporting are given as based on current clinical evidence.

8.4.1. Bladder, Rectum, Sigmoid, and Bowel: High-Dose Regions, Points, and Small Volumes ($D_{0.1\text{cm}^3}$, $D_{2\text{cm}^3}$)

Typical brachytherapy-related adverse effects are bleeding, local fibrosis, ulceration, necrosis, and fistula, and—to some degree—urgency, frequency, and incontinence. The biological targets are small normal-tissue sub-volumes located mainly in the mucosa and sub-mucosa of the organ walls, and in the neural plexus and muscles that regulate specific functions of the bladder, rectum, and anus (see Section 6.2).

Due to absorbed-dose heterogeneity within the organ walls, it is recommended to report at least two dose–volume values in the high-dose region. The dose values $D_{0.1\text{cm}^3}$ and $D_{2\text{cm}^3}$ represent, respectively, the minimum doses to the 0.1 cm^3 and 2 cm^3 volumes of the OAR that receive the maximum dose. These OAR parameters were recommended by the GEC ESTRO GYN group in 2006 and seem to be useful in clinical practice, with first reports showing their validity for predicting morbidity (Georg *et al.*, 2009; 2012; Jürgenliemk-Schulz *et al.*, 2010; Koom *et al.*, 2007; Lang *et al.*, 2006). An intermediate value for $D_{1\text{cm}^3}$, appeared to add no additional information, as it can be interpolated from the two other values. No maximum point-dose reporting is recommended, especially because of the limitations of calculating a maximum absorbed dose by sampling algorithms, 3D reconstruction of volumes in treatment–planning systems, and contouring uncertainties (Kirisits *et al.*, 2007). Similar to the situation for the target, only a near maximum absorbed dose as represented by the $D_{0.1\text{cm}^3}$ can be based on a sufficient number of sampling points for reproducible calculation. The volumes for the $D_{0.1\text{cm}^3}$ and $D_{2\text{cm}^3}$ do not have a compact spherical shape. Rather, they have sizeable extensions of more than 10 mm and 30 mm in the width and height in the organ wall, respectively. As illustrated in Figures 8.5 and 8.6, it is evident that $D_{0.1\text{cm}^3}$ and $D_{2\text{cm}^3}$ do not represent point doses.

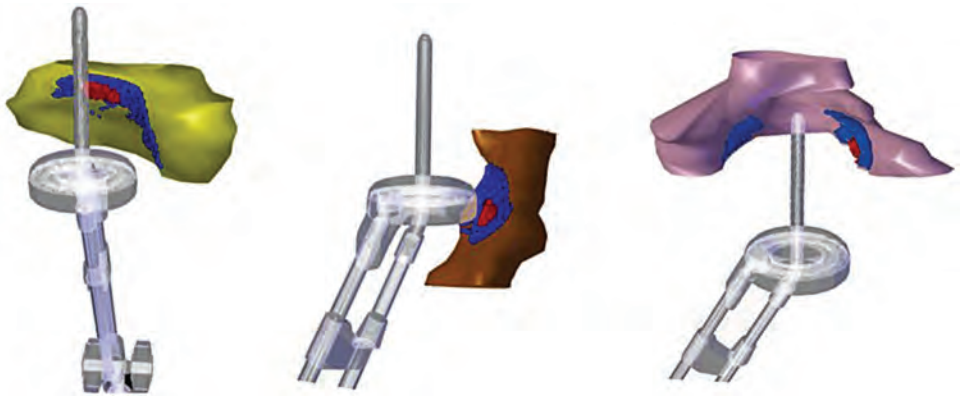

Figure 8.6. Three-dimensional reconstructed images showing contiguous 2 cm^3 volumes in blue for the bladder and rectum, while it is distributed in two parts for the sigmoid. The red-colored region receives at least the dose $D_{0.1cm^3}$.

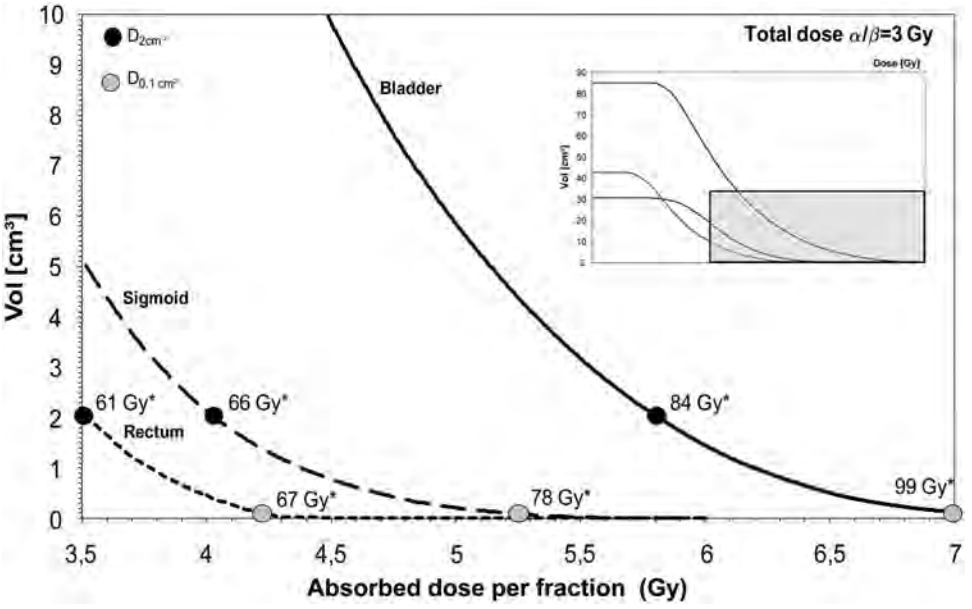

Figure 8.7. Cumulative DVHs of the bladder, rectum, and sigmoid, based on organ contouring indicating $D_{0.1cm^3}$ and D_{2cm^3}. *Total EQD2 values for these OAR are given assuming four identical HDR fractions and an additional 25 × 1.8 Gy of EBRT, assuming a α/β value of 3 Gy.

The clinical effects in hollow OARs are related to irradiation of the organ walls only, and not of the entire organ that would include the lumen. In principle, OAR doses should therefore be evaluated in dose-wall histograms. However, as the volumes of $D_{0.1cm^3}$ and D_{2cm^3} are of limited thickness and mainly located in the wall, it is possible to calculate these parameters with sufficient accuracy based on contours of the entire organs including the lumen (Olszewska *et al.*, 2001; Wachter-Gerstner *et al.*, 2003b). However, when evaluating dose in larger volumes, with parameters such as D_{5cm^3} and D_{10cm^3}, dose-wall histograms are relevant, because when calculating DVHs for the entire organ, the absorbed doses in those volumes can include absorbed doses in the organ lumen. A different type of uncertainty results when the reported volumes are not contiguous. If the D_{2cm^3} represents dose in two completely different parts of the sigmoid, it is believed to have less clinical effect than one contiguous volume in the same organ region. In practice, the D_{2cm^3} appears as contiguous in the bladder (with limited bladder filling resulting in no extensive lateral recessus) and rectum, whereas in the sigmoid and bowel, it can often be distributed into several hot-spots as illustrated in Figure 8.6.

Another important aspect is the underestimation of dose if the volume with the highest absorbed dose is directly located at the recto-sigmoid junction. In the worst case, a contiguous 2 cm^3 high-absorbed-dose volume could be distributed equally between both contoured volumes, 1 cm^3 per volume. However, as the DVH parameter is D_{2cm^3} for a single organ contour, it will report a lower value compared with the D_{2cm^3} for

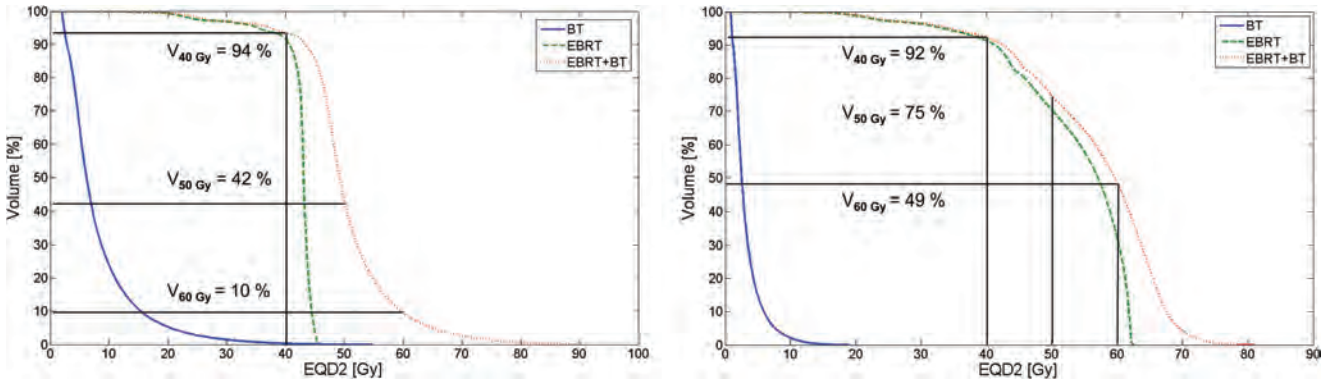

Figure 8.8. Rectum DVHs for two different schedules: (a in left panel) 45 Gy whole-pelvis EBRT plus 4 fractions of HDR brachytherapy boost (total target dose 85 Gy EQD2), and (b in right panel) 45 Gy whole-pelvis EBRT plus 15 Gy EBRT tumor boost plus 2 fractions of HDR brachytherapy boost (total target dose 85 Gy EQD2). The DVHs are given in terms of EQD2 for brachytherapy (blue), EBRT (green), and total EBRT plus brachytherapy (red). The D_{2cm^3} values are almost the same for the two scenarios, but the DVH shapes of total EQD2 are very different. In the scenario with a large brachytherapy contribution (a), the DVH in the high dose region is less steep than in the case of a small brachytherapy contribution (b). This means that the $D_{0.1cm^3}$ value is higher in (a), whereas the intermediate doses are much lower, with V60 Gy being 10 % in (a), and 49 % in (b).

the combined recto-sigmoid structure (see also Section 6.3) (Lang *et al*., 2008). This demonstrates the importance of examining isodose distributions anatomically, with which such a situation would be identified and the volumes combined.

The use of both $D_{0.1cm^3}$ and D_{2cm^3} allows characterization of only the high-dose part of the dose distribution in the organ at risk. The clinical effect and the D_{2cm^3} tolerance are likely dependent also on dose in adjacent intermediate- and low-dose regions visible in the entire DVH, as shown in Figures 8.7 and 8.8. If the contribution of EBRT is changed substantially (*e.g.*, absorbed doses higher than from 45 Gy to 50 Gy, as shown in Figure 8.8, or no EBRT contribution), the DVH is directly influenced and changes its shape considerably. Therefore, D_{2cm^3} cannot be expected to lead to identical effects across treatment schedules with very different combinations of brachytherapy and EBRT. Similarly, a source position very close to the organ wall generates a different dose distribution. These changes are reflected in different ratios $D_{0.1cm^3}/D_{2cm^3}$. Only by including reporting of $D_{0.1cm^3}$ in such situations can very inhomogeneous dose distributions with high values of $D_{0.1cm^3}$ be detected and their potential biological effects taken into account (see Figure 6.3).

Whereas the recommendation for reporting $D_{0.1cm^3}$ and D_{2cm^3} is straightforward for the rectum and bladder, the situation is different for the sigmoid colon and the small bowel and other parts of the colon as the position of these organs is not static. For the sigmoid colon, the assumption of a static absorbed-dose distribution across the organ wall for the summation of dose does not apply for the majority of clinical scenarios (see Sections 6.4 and 8.5). For all other portions of the bowel, high-dose assessment using $D_{0.1cm^3}$ and D_{2cm^3} is relevant if organ structures are near the high-dose area of brachytherapy for the duration of treatment (*e.g.*, if they are fixed to the uterus). However, in the normal clinical situation, as the bowel has to be assumed to be highly mobile, the spatial absorbed-dose distribution has to be studied and compared for each brachytherapy fraction. There is a high probability that these high-dose regions vary substantially between different fractions. Adding the high-dose DVH parameters without taking into account the varying spatial distribution of absorbed dose might substantially overestimate the total EQD2 to the bowel and might result in an unneeded compromise on tumor coverage. Further research on dose assessment and dose–effect relationships has to develop a more valid dose-summation model, in which a differentiation in effects among different anatomical parts of the bowel might become possible.

As discussed in Section 8.2, a DVH for an entire organ provides no information about the spatial distribution of dose within the organ. Individual doses to functional sub-units of organs must be assessed by contouring sub-volumes and analyzing the corresponding DVHs. A simple way for rough estimations is the delineation of volumes at reproducible locations that show representative absorbed-dose values for a functional sub-unit. For example the bladder-neck region and the trigone are of specific clinical relevance, as the emptying function is located mainly in this region, and it might be of interest for analysis to assess effects such as urinary urgency, increased frequency, and incontinence. During a transition period, the use of point doses (*e.g.*, the ICRU bladder point related to the balloon fixed to the bladder neck) as a surrogate for the 3D dose distribution in sub-volumes

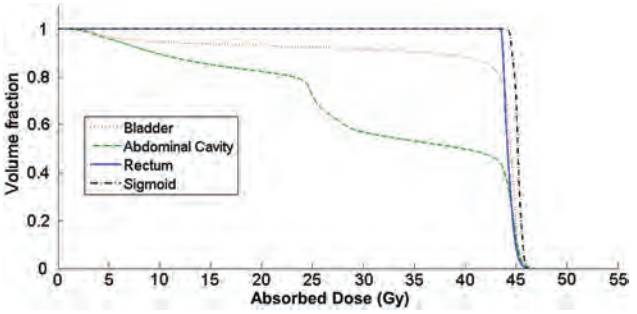

Figure 8.9. External-beam radiation therapy DVHs for the bladder, rectum, sigmoid, and abdominal cavity (bowel bag). It can be seen from the DVHs that almost the entire rectum and sigmoid are irradiated to the prescribed absorbed dose of 45 Gy when using conventional 3D conformal techniques, whereas part of the bladder may be outside the high-absorbed-dose region. The bowel (abdominal cavity) shows significant absorbed-dose variation over the organ.

might remain important (ratio of DVH volumes *versus* point dose as described in Section 6.2). A similar approach with point doses, which is currently under investigation, might be followed for the anorectal region, with the related morbidity pattern of anal urgency, stool frequency, and fecal incontinence. An anal reference point might be of interest (see Figure 6.4) as a surrogate for the 3D dose distribution in the anus or at the internal anal sphincter

8.4.2 Bladder, Rectum, Sigmoid, and Bowel: Intermediate- and Low-Dose and Non-Small Volumes

Assessment of the bowel, sigmoid, and rectum morbidity related to EBRT absorbed dose and volume has long been a major concern with pelvic and abdominal radiotherapy. The volume of small and large bowel included in the radiation fields is a predictor for morbidity (Haie *et al.,* 1988; Letschert *et al.,* 1990; 1994). Bowel morbidity related to irradiation of large volumes is variable, with stenosis, stricture, and obstruction leading to major clinical symptoms that often require surgical intervention. Other symptoms include chronic (intermittent) diarrhea, chronic inflammation, cramping, gas production, and mal-absorption.

Rectum morbidity is related mainly to transient bleeding, increased stool frequency and urgency, fecal incontinence, and also rectal stenosis. For bladder morbidity, the situation is complex. Global bladder-related symptoms include reduced flow and capacity, chronic inflammation, contracture, spasm, but also dysuria, increased frequency, urgency, and incontinence. Urgency and incontinence are assumed to have also a major component with regard to the bladder neck and the trigone. Other symptoms might be related to intermediate doses to volumes greater than 2 cm^3. However, even with 3D conformal radiotherapy and IMRT, only limited evidence has been provided that would enable a clear understanding of the relation of this type of morbidity to irradiated (sub-) volumes and thus facilitate recommendations for treatment planning and reporting. It is evident that doses from the EBRT component as illustrated in Figures 8.8 and 8.9 to large organ volumes have to be taken into account (see also clinical examples in the Appendix). In principle, combined dose distributions from both EBRT and brachytherapy should be considered. For practical reasons, outcomes related to larger volumes or doses close to or lower than the EBRT prescription might be assessed based on the EBRT plan only. The modeling of biological effects of irradiation for pelvic OARs becomes quite complex, and the use of a single dose to some part of an organ for characterizing a biological effect seldom completely captures the interrelationships of the effects of absorbed doses to sub-volumes of the organ. In the recent "Quantitative Analysis of Normal Tissue Effects in the Clinic" (Bentzen *et al*., 2010; Kavanagh *et al*., 2010), the use of a threshold model suggested that, at a certain absorbed-dose level in a certain volume, a significant increase in adverse side effects is observed.

For bowel morbidity, a $V_{15\ Gy}$ of 120 cm^3 is an estimate for such a threshold if individual bowel loops are delineated. If the peritoneal cavity is contoured, a $V_{45\ Gy}$ of 195 cm^3 was reported as threshold (Kavanagh *et al.,* 2010). Based on these findings, it is recommended to report the DVH parameters for bowel structures and state which anatomical parts (small-bowel loops, large-bowel structures, or entire peritoneal potential space of bowel) have been contoured. Specific parameters for intermediate absorbed-dose assessment still need to be validated. V_D parameters with D between 15 Gy and 50 Gy can be analyzed to define clinically relevant threshold levels. This V_D can refer to absolute or fractional bowel volumes. Another strategy to analyze single values of the entire DVH in the intermediate dose region would be a D_V, *i.e*., to report the dose for a defined absolute or fractional bowel volume (*e.g*., for a volume V between 10 cm^3 and 200 cm^3), or for a volume of 50 % or 98 % or 2 % of the organ (compare Tables A1.2–A9.2 in the clinical examples in the Appendix).

For rectal morbidity (in particular bleeding), it has been recommended, mainly based on experience with EBRT for prostate cancer (Fiorino *et al*., 2002; Gulliford *et al*., 2010; Michalski *et al*., 2010; Nguyen *et al*., 2010; Vargas *et al*., 2005) to refer to the amount of rectal volume receiving 60 Gy (V_{60Gy}). In cervical cancer, most of the whole rectum and sigmoid has been usually within the volume that is irradiated to the prescribed EBRT absorbed dose (if a midline block is not applied), which means that most of the organ receives 45 Gy or 50 Gy from the external-beam

portion of the treatment alone (Lim *et al.,* 2009). This might be true also even for IMRT. Therefore, the $V_{60\ \mathrm{Gy}}$ is then very limited (see Figure 8.8 at the 10 % volume level).

For strategies with inhomogeneous EBRT absorbed doses, such as with tumor boost, parametrial boost, or simultaneous integrated lymph-node boost, the sigmoid and rectum can receive significant additional EBRT absorbed dose, increasing the amount of the organ irradiated to intermediate doses [see Figure 8.8 and Fenkell *et al*. (2011)]. Irradiated volumes and intermediate absorbed-dose levels should then be reported, such as V_D starting from 45 Gy to 60 Gy and greater, or conversely to report D_V with V from 5 cm^3 to 30 cm^3 or as a fraction of organ volume. These volumes are often spread over the whole organ circumference and over a long part of the rectum or sigmoid.

For the bladder, the situation is even less clear, and the majority of studies have found no clear dose–volume relationship for intermediate doses of EBRT in bladder and prostate cancer (Viswanathan *et al.,* 2010). The bladder shape and volume is highly variable, with changes in position, volume, and shape occurring during a course of radiotherapy and even during administration of a single fraction. This causes uncertainties in the dose delivered, and the DVH from treatment planning cannot be assumed to represent accurately the absorbed dose delivered by EBRT (Lim *et al.,* 2009). However, in combinations of EBRT and brachytherapy in cervical cancer, certain volume levels V_D ($D \geq 40$ Gy) or certain dose levels D_V ($V \geq 10$ cm^3 or V as a fraction of the organ volume) can be indicated based on the treatment–planning CT and ignoring the daily changes during fractionated EBRT. This would at least allow the determination of the amount of dose, mainly from EBRT, given with some certainty to large bladder volumes in different treatment schedules with varying contributions from EBRT and brachytherapy. In the future, IGRT with repetitive imaging in combination with protocols for bladder filling and CT protocols simulating the potential bladder-volume changes (Ahmad *et al.,* 2012) will contribute to reduce uncertainties.

As there is limited evidence for the validity of most of these considerations with regard to intermediate dose- and volume-assessment for combined EBRT and brachytherapy in cervical cancer, the proposed dose–volume parameters should be used with great caution in routine clinical practice. They are elaborated here to suggest routes for future clinical research. It is desirable at present to report a variety of dose–volume parameters in the intermediate-dose regions and in larger organ volumes and to correlate them with specific morbidity endpoints in order to determine valid and predictive morbidity parameters for treatment planning.

8.4.3 Vagina High-, Intermediate-, and Low-Dose Regions, Points, Small and Large Volumes

Radiotherapy-associated vaginal morbidity has been investigated only to a limited extent. Recto-vaginal and vesico-vaginal fistula, extensive vaginal stenosis, and complete vaginal obliteration have represented the major Grade 3 and Grade 4 events occurring in a limited number of patients (Hintz *et al.,* 1980). Extensive stenosis and obliteration has been observed in patients mainly with extensive vaginal disease treated with brachytherapy to a large part of the vagina (Barillot *et al.,* 2000). On the other hand, in the upper vagina near the vaginal sources, morbidity such as adhesions, telangectasia, fragility (contact bleeding), mucosal pallor, fibrosis, shortening, and partial obliteration (Grade1 and 2 toxicity) have been described in a large proportion of patients (see Figure 6.1) (Kirchheiner *et al.*, 2012b; 2014).

The vagina points located at the lateral vaginal-applicator surface and at 5 mm depth into the lateral walls of the vagina have traditionally been used for vaginal-dose reporting. Dose–effect relationships based on these points have not been well established, and the points have served mainly as tools for prescribing absorbed-dose constraints (Lee *et al.,* 2012; Viswanathan and Thomadsen, 2012; Viswanathan *et al.,* 2012b). There is evidence from evaluations of patient cohorts from the EMBRACE trial that the ICRU rectal point can be reliably used for a dose–response analysis for vaginal shortening and therefore can serve as surrogate point (recto-vaginal reference point) to predict vaginal morbidity (Kirchheiner *et al.,* 2016).

Implementation and evaluation of valid and reliable dose–volume parameters for the high-absorbed-dose region in the vagina ($D_{0.1\mathrm{cm}^3}$ and $D_{2\mathrm{cm}^3}$) are challenging due to the very high absorbed-dose gradients near the vaginal sources and the difficulties of precisely delineating and reconstructing the thin organ walls on 3D images with the applicator in place, using the currently available treatment–planning systems (Berger *et al.,* 2007). No clear recommendations for dose–volume parameters relevant for morbidity in the vagina have been developed so far. The dose–volume parameter $D_{2\mathrm{cm}^3}$ does not correlate with vaginal side effects in individual patients with cervical cancer treated within a defined treatment protocol with very high brachytherapy doses (Fidarova *et al.,* 2010). Dose–volume parameters for larger vaginal volumes (*e.g.*, 5 cm^3 or 10 cm^3) have not been investigated so far.

Despite limited evidence and progress in vaginal-morbidity analysis so far, a dose–volume or a dose–surface concept for treatment planning and reporting is, in principle, suggested here based on contouring

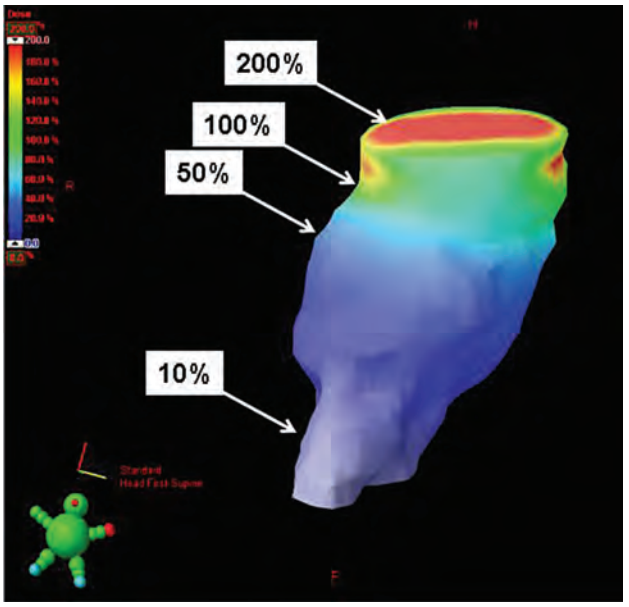

Figure 8.10. Plot of brachytherapy surface absorbed dose for the vagina using a ring applicator, frontal view. The absorbed-dose variation is high around the circumference at the level of the vaginal sources (ring: from 200 % to 100 % lateral in small areas, 50 % to 70 % anterior and posterior in large areas) and along the axis in the cranio-caudal direction, with from 30 % to 80 % in the mid-vagina and less than from 10 % to 30 % in the lower vagina (compare Figure 8.11).

the whole vagina as a wall structure with a certain thickness or as a surface structure. It can be assumed, for obvious reasons, that late vaginal morbidity is related to the different doses applied to different vaginal parts, areas, and volumes. Figure 8.10 shows an example of an absorbed-dose plot for the vaginal surface. As for other OAR, it is recommended that research should aim at the implementation of a dose–surface histogram (DSH) approach, with absolute values for planning and reporting vaginal dose based on an appropriate vaginal contouring, both for high doses in small volumes and intermediate and lower doses in larger volumes related to anatomical vaginal regions. V_D parameters with D from 5 Gy to 150 Gy EQD2, D_V parameters with V from 0.1 cm^3 to 10 cm^3, or certain fractions can serve to quantify the DVH. In cases in which DSHs are applied, D_A with A indicating representative areas can be reported.

Research and development have to provide the appropriate approaches to reduce relevant uncertainties both in contouring and in dose and volume assessment. Such approaches might be in the form of software-based methods to automatically delineate a surface around the vaginal packing, which can be used to calculate DSHs and dose maps, and which would then include the entire dose information for the vaginal wall.

Following a long tradition, it is recommended to report the absorbed dose at points at a 5 mm depth lateral at the level of the vaginal sources, identical to the approach recommended for dose reporting when using radiographic localization (see Section 10.2). A high correlation between absorbed dose to the surface and absorbed-dose points 5 mm deep and absorbed-dose parameters for limited volumes (*e.g.*, $D_{0.1cm^3}$ and D_{2cm^3}), has been described based on automatic contouring around the vaginal sources, assuming a certain thickness of the vaginal wall (Trnková *et al.*, 2014). Therefore, it is likely that these points will provide reasonable information for the high-dose area around the vaginal sources.

Because of the inhomogeneous absorbed-dose distribution around the vaginal sources, the absorbed dose to the lateral dose points is usually very different from absorbed doses to points located in the anterior or posterior direction from the vaginal sources (see Figure 8.10). For ring applicators, the absorbed dose at anterior and posterior points will usually be lower, due to the lateral loading. In ovoids, the absorbed dose on the anterior or posterior vaginal surface might be higher than in the lateral direction, depending on the contribution and position of the tandem and the distance from the active dwell positions to the anterior or posterior ovoid surface. Thus, points, while useful for dosimetric control, serve as poor surrogates for the entire vaginal-surface absorbed-dose distribution. This might explain the lack of definitive relations between the absorbed dose to vaginal points and toxicity endpoints.

In conclusion, future research should aim to develop automatically generated contours around the vaginal applicators and along the whole vaginal surface, excluding the packing, for DSH/DVH evaluation. Such methods would detect all locations of high and low dose throughout the vagina. The whole of this dosimetric and volumetric information, together with topographic correlation, might be critical for finding parameters to predict vaginal morbidity.

Based on radiographic localization, the length of the vagina irradiated to certain absorbed-dose levels has been shown to be a surrogate for the vaginal volume and has been reported to predict major vaginal morbidity (Barillot *et al.*, 2000). Therefore, it is recommended to analyze the dose profile from EBRT and brachytherapy along the vaginal axis. An example of such a dose profile is shown in Figure 8.11.

The length along the vaginal axis corresponding to a certain dose can be measured from such dose profiles. In order to further assess the intermediate- and low-dose regions in the vagina, anatomical reference points along the vaginal axis can serve as surrogates for the dose distribution in the vaginal wall: one at the mid-vagina [posterio-inferior border of the symphysis (PIBS) + 2 cm], one at the transition from mid- to lower vagina (PIBS), and one at the lower

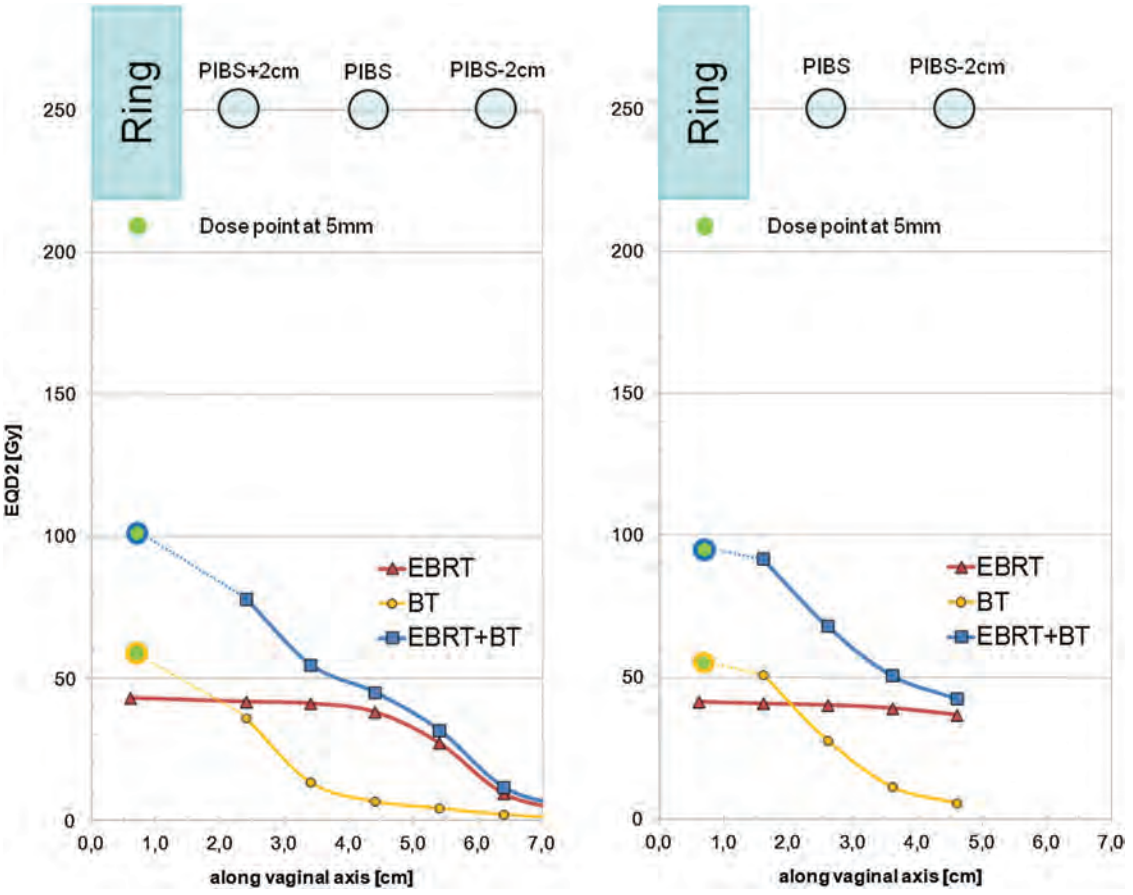

Figure 8.11. Illustration of vaginal dose profiles for two different cases, showing the contribution of EBRT and brachytherapy dose to the total EQD2. The *x*-axis starts at the upper vaginal surface and continues in the caudal direction along the central axis of the vagina. Posterio-inferior border of the symphysis (PIBS) and PIBS $\pm$ 2 cm points are shown. At the level of the ring-source path, a point (green) at 5 mm depth is indicated. The left case (PIBS) illustrates a representative situation with the lower field border of EBRT located close to PIBS. The right case shows a situation with PIBS very close to the ring applicator. Definition of PIBS+2 cm is not applicable anymore. External-beam radiation therapy dose is substantially higher at PIBS as well as PIBS−2 cm compared with the case at the left [from Westerveld *et al*. (2013)].

region of the vagina (PIBS – 2 cm) (Westerveld *et al*., 2013). These points have been defined anatomically and reproducibly both for EBRT and for brachytherapy. Figure 8.12 shows a schematic diagram for this approach. These points serve as anatomical reference points both for brachytherapy and for EBRT and should be reported separately, and the doses added. For the mid-vaginal point that is at from 3 cm to 5 cm into the dose profile (see Figure 8.11), the dose from EBRT is constant (prescribed dose), and variations are determined by the brachytherapy dose. The dose to the lower vaginal points (PIBS and PIBS−2 cm) depends mainly on the location of the lower field border of EBRT and inter-fraction variations, and is constantly low and almost independent of brachytherapy if the vaginal length during brachytherapy is $\geq$5 cm−6 cm and is not treated explicitly by brachytherapy. However, the impact of brachytherapy dose to the lower parts of the vagina can increase substantially if the vagina is short (see Figure 6.4), the vaginal source is not placed at the vaginal apex, or if the vagina is treated due to involvement of disease.

The situation is very different if the mid- and lower vagina form part of the CTV_{HR} due to suspected residual disease, and the usual vaginal applicators have to be replaced with cylinders. In these cases, while the target dose is included in CTV_{HR} dose reporting, the vaginal-surface dose along the applicator has to be given with much more detail in the spatial distribution, including high-dose regions along the circumference of the cylinder surface (see Figure 8.12, cross sections).

8.4.4 Other OAR

In addition to the OARs discussed above, there are other normal-tissue structures of interest, such as ureter, anal canal, ovaries, urethra, large vessels, large nerves, connective tissue, bone and bone marrow, lymph vessels, and lymph nodes. Due to limitations in imaging and knowledge, identifying and contouring and defining dose–volume constraints of these structures is not straightforward. Consequently, further imaging, contouring, treatment planning, and clinical research is needed to link potential dose–volume parameters to morbidity outcome.

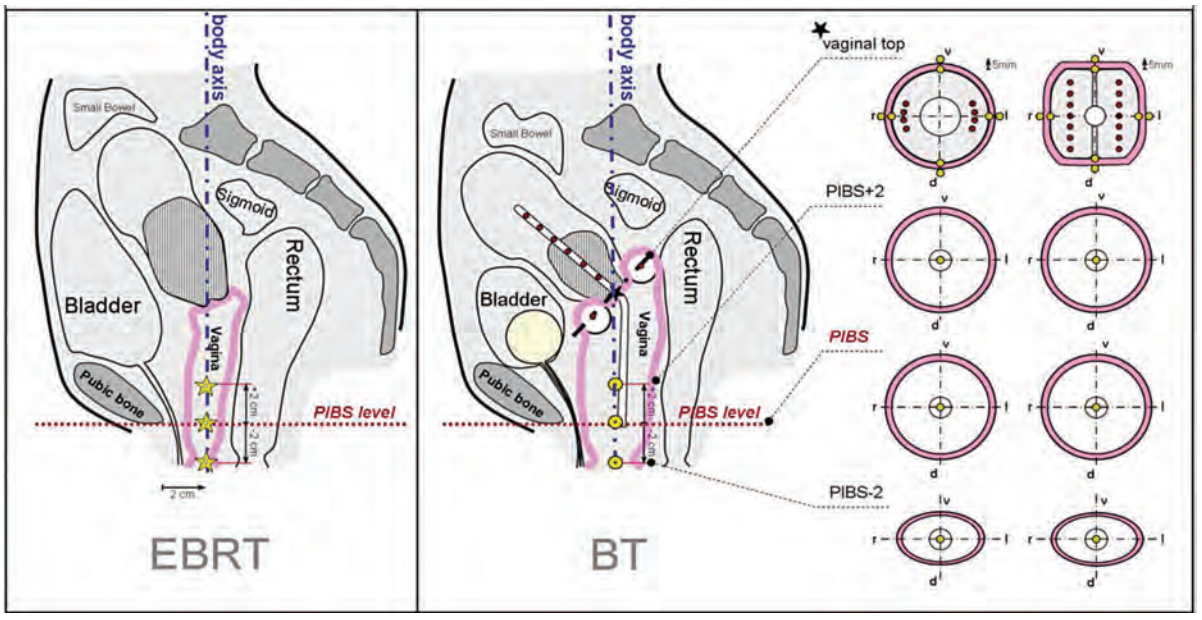

Figure 8.12. Sagittal views showing the vagina at the time of EBRT and at brachytherapy with an intracavitary applicator in place. At the level of the vaginal source, dose points lateral to the rings or ovoids can be defined at 0 mm and 5 mm from the applicator surface. Three additional points are defined along the central axis of the vagina in the cranio-caudal direction. The PIBS vaginal-dose point was defined 2 cm posterior from the posterior-inferior border of the pubic symphysis and for brachytherapy at the point of this line where it crosses the applicator tandem. From there, two additional points 2 cm up and down along the vaginal axis are defined with PIBS+2 representing the mid of the vagina and PIBS−2 representing the introitus level [from Westerveld *et al*. (2013)].

8.5 Specific Issues in Dose–Volume Reporting for the Combination of EBRT and Brachytherapy

The simple addition of absorbed doses from EBRT and from brachytherapy is not meaningful because of the different biological effectiveness associated with their delivery. Therefore, assessment of the total equieffective dose from EBRT and brachytherapy involves two steps: (1) the calculation of absorbed dose to points, volumes, voxels, or regions from each fraction of EBRT and brachytherapy; (2) the application of the EQD2 or some other appropriate formalism on a point-by-point basis for dose summation (see Section 7.6). In principle, deformable registration could match each tissue voxel irradiated by each fraction of external-beam radiation with the corresponding voxel irradiated by each fraction of brachytherapy (see Section 9.4). However, currently no deformable-registration program is capable of tracking the location and dose-exposure history of relevant biological structures within the target volumes and OAR. Currently, some simplifications and assumptions are therefore suggested, which can be replaced by more appropriate approaches as this becomes technically feasible. These assumptions are suited for several scenarios for typical treatment conditions. First, it can be assumed that the organ walls adjacent to the applicator receiving a high brachytherapy absorbed dose (such as $D_{0.1\text{cm}^3}$ and $D_{2\text{cm}^3}$) are irradiated with the full absorbed dose of external-beam therapy, if an EBRT technique is applied with a homogeneous absorbed-dose plateau (*e.g*., a four field box). Such an assumption is not necessarily valid for the parts of organ walls at a greater distance from the brachytherapy applicator. Furthermore, the assumption might be less valid for techniques such as IMRT or intensity-modulated arc therapy (IMAT or VMAT) that can produce more-pronounced absorbed-dose gradients in those regions of OARs irradiated to high absorbed dose during brachytherapy. It follows that care should be taken that hot spots from IMRT/IMAT treatment plans should not coincide with the high-dose regions from brachytherapy. If boosts are given as part of the EBRT, a specific analysis of possible overlap of brachytherapy and EBRT dose distributions must be performed, as additional dose to CTV_{HR}, CTV_{IR}, or OAR structures can be significant (Van de Kamer *et al*., 2010). Evaluation of total dose is particularly challenging when a midline block or parametrial boost is used, because large gradients in the absorbed dose from both the EBRT and brachytherapy are present in the same regions (Tamaki *et al*., 2015). It has been shown that midline-blocked fields do not predictably protect OARs ($D_{2\text{cm}^3}$), nor do they predictably contribute absorbed dose to the CTV_{HR} or CTV_{IR} (Fenkell *et al*., 2011).

A second assumption used for combining doses from EBRT and brachytherapy is related to accumulation of dose from succeeding brachytherapy fractions.

When adding doses for absolute OAR volumes (*e.g.*, D_{2cm^3} and $D_{0.1cm^3}$), it is assumed that the location of the given high-absorbed-dose volumes is identical for each brachytherapy fraction (Pötter *et al.,* 2006). With such an assumption, it is possible to calculate absorbed dose by crude addition of DVH parameters from each brachytherapy fraction. The assumption of such a static situation predicts the highest dose possible for the analyzed volume and the anatomical configurations observed with imaging. It is linked to uncertainties due to organ movement and deformation and the applicator position (see Sections 9.2 and 9.4), and uncertainties can vary for different organs according to their anatomical structure and fixation, which also can vary with different treatment techniques. For example, for the anterior rectal and posterior bladder wall $2\,cm^3$ volumes, there is some indication that the assumption of a static anatomical dose distribution can be regarded as a valuable approximation of the clinical situation in the patient (Andersen *et al.,* 2013). This is less clear for mobile organs such as the sigmoid. The static scenario is not a "worst case assumption," as the organs might, in addition, also move in relation to the applicator between imaging and absorbed-dose delivery, with the possibility to deliver higher doses than reported.

With regard to the target, the relation between the intracavitary applicator and the outer part of the target is often quite stable, and the lowest dose voxels are likely to be situated in the same region of the target for succeeding fractions. However, in cases with an interstitial component, there can be significant differences in the location of the lowest absorbed doses from implant-to-implant, which leads to an under-estimation of target near-minimum dose parameters $D_{98\ \%}$ and $D_{90\ \%}$. In contrast to the situation for the OAR, this means that for the target $D_{98\ \%}$ and $D_{90\ \%}$, a crude addition of DVH parameters will result in a "worst-case assumption" that assumes that the low-dose region is located in the same position for every fraction.

In clinical practice, it is of particular importance, to check the individual case as comprehensively as possible in case dose–volume outcomes exceed dose–volume constraints. Static scenarios might not be applicable for all cases.

8.6 From Planning Aims to Prescription

8.6.1 Traditional Terms for Dose Prescription

Concepts and terms for a common language in image-guided adaptive brachytherapy have been established for recording and reporting dose–volume parameters for the GTV and the CTV following the ICRU tradition (ICRU, 1993b; 1999; 2007; 2010) and that of the recent GYN-GEC ESTRO Recommendations (Haie-Meder *et al*., 2005). While prescription for the treatment of a given patient, and the process of prescription itself, is left to the discretion of the individual radiation oncologist, the use of the same concepts and terms originally recommended for recording and reporting has been adapted and recommended for prescription. Prescription in gynecologic brachytherapy has typically been based on an absorbed dose to a point (mainly Point A), an absorbed dose to a defined isodose surface (ICRU, 1985), an absorbed dose to a set of dose/volume parameters (Haie-Meder *et al*., 2005), or an absorbed dose defined in terms of TRAK (corresponding to the previously used product of radium mass and duration).

The definition of prescription as given in the GEC ESTRO recommendations did not clarify the prescription process, saying, "when prescribing to a target, the prescription dose is the planned dose to cover this target as completely as possible" (Haie-Meder *et al*., 2005). The term "as completely as possible" is then left to the discretion of the radiation oncologist responsible for the treatment. Another common method to prescribe the dose has been to relate the prescription to a 100 % isodose that "covers" the target volume (Viswanathan *et al*., 2011b). Here, also, the term "covers" remains unclear. If the underlying understanding is supposed to be full coverage, then the prescription should be related to the minimum target absorbed dose, the $D_{100\ \%}$. However, this is not the widespread practice in clinical brachytherapy, and the $D_{90\ \%}$ was recommended in the GEC ESTRO recommendations II (Pötter *et al*., 2006). In gynecologic brachytherapy, the delivery of a dose to the entire target according to the initially planned dose is not always possible due to size and configuration of the target volume or OAR in relation to the applicator. Optimization includes the individual shaping of the absorbed-dose distribution in order to reach a compromise among the dose constraints for the target and the OARs (see Figure 10.2) (Tanderup *et al.*, 2010a). Another scenario arises when the therapeutic window is sufficiently large: the target receives significantly more dose than defined in the initial planning aim, while the OARs are within the specified dose constraints. In both scenarios, the target dose of the approved treatment plan will be different from the initial planning aim (see Figure 10.2.)

In EBRT, a balance is struck between target- and OAR-absorbed-dose constraints during the treatment–planning process. The balance can be identical to or different from the initial planning aim. ICRU Report 83 defined the process from the initial planning aim to the prescription in a reproducible way with clearly defined terms. The concepts and terms for gynecologic brachytherapy will follow the same framework.

8.6.2 Concepts and Terms: From Planning Aim to Dose Prescription

Following ICRU Reports 78 and 83, the goal for treatment planning is the "planning-aim dose," which is determined before the treatment–planning process (ICRU, 2007; 2010). The "prescribed dose" is the achievable dose chosen for treatment to a specific volume of the target and approved by the radiation oncologist at the end of the treatment–planning process. The prescribed dose may or may not be equal to the planning-aim dose. In the clinical series reported so far, there is a significant difference between planning-aim dose and prescription dose (Chargari *et al.,* 2009; De Brabandere *et al.*, 2008; Jürgenliemk-Schulz *et al.,* 2009; Kirisits *et al.*, 2005; 2006; Levitchi *et al.,* 2012; Lindegaard *et al.*, 2008; Mahantshetty *et al.*, 2011; Pötter *et al.,* 2011). The new concepts for the terms "planning aim" and "dose prescription" take into account the stepwise brachytherapy planning procedure, starting with initial aims for treatment planning and ending with an approved treatment plan and a prescribed dose. The planning aim defines a set of intended dosimetric parameters and constraints for the target and the OARs that are used to develop the treatment plan. The dose–volume constraints for the OARs and target are defined initially according to clinical evidence, to institutional rules or according to patient-specific considerations. Through individual treatment planning, a finally accepted set of treatment parameters is achieved, balancing dose–volume constraints for the OARs and for the target, for example, a $D_{90\ \%}$ for the CTV_{HR} of 7.4 Gy, a D_{2cm^3} for the rectum, sigmoid, and bladder of 3.5 Gy, 3.2 Gy, 5.5 Gy, respectively, for one single fraction within an HDR schedule of four fractions. The set of these parameters derived from the planned treatment becomes the prescription, which is approved by the responsible radiation oncologist. For each brachytherapy fraction, a set of prescription parameters will be generated which might or might not vary.

Within this new definition of prescription, it is neither reasonable nor necessary, and probably not possible, for adaptive image-guided brachytherapy in cervical cancer to use the same prescribed dose for all patients in a specific patient cohort. Reporting prescribed doses for a patient group by one single value is then not appropriate; the report must include the mean or median value, standard deviation (SD), and range. The prescribed dose can also be reported in terms of the total dose from EBRT and brachytherapy using EQD2 as, for example, a $D_{90\ \%}$ of 92 Gy $\pm$ 13 Gy (1 SD), while the initial planning aim was to deliver at least 84 Gy (Pötter *et al.,* 2011). In EBRT, the situation is somewhat different because the prescription absorbed dose is usually very similar to the planning aim and becomes identical if the absorbed dose plan is normalized according to the planning aim. In cervical brachytherapy, the differences between planning-aim dose and prescribed dose are especially pronounced if the planning aims for small tumors are reached without the need to optimize for the OARs, resulting in very high prescription-dose levels.

8.7 Isodose Surface Volume

The volume encompassed by an isodose surface is called the isodose surface volume. The dose value for this volume can be chosen to be clinically relevant for tumor control or development of complications. Isodose surface volumes can be used for comparison among institutions, or they can be used within a single institution to follow the transition from institutional standard loading to optimized treatment plans. The term, "isodose surface volume," replaces the terms "volume of prescribed dose" or "100 % dose." As previously described, individualized dose prescription can be performed, and therefore the reporting of volumes related to a fraction of a prescribed absorbed-dose value as $V_{100\ \%}$, $V_{200\ \%}$, *etc*. becomes useless without stating the normalization value if the prescribed value is changing for each individual treatment plan. Therefore, it can be helpful to keep certain absolute dose levels fixed for reporting and for following the planning procedure from the initial standard plan to the optimized plan. An isodose surface volume should be linked to a dose that is judged as representative for a certain clinical effect. Typical dose values are the planning-aim dose per fraction for HDR or PDR treatments (*e.g.*, 7 Gy in an HDR treatment of 4×7 Gy), or the total absorbed dose given in LDR or PDR treatments of 60 Gy or 15 Gy.

For comparison of irradiated volumes among different institutions, it is of little relevance to report the volumes irradiated with the planning-aim dose because such volumes would be related to the individual institutional dose levels. It is necessary to choose common dose levels according to clinically relevant EQD2 values, such as 60 Gy, 75 Gy, or 85 Gy (Pötter *et al.*, 2002b). In order to evaluate such isodose volumes, the fractional brachytherapy absorbed dose must be calculated that corresponds to the total dose of interest. As an example, fractional absorbed doses of 7.1 Gy, 5.8 Gy, and 3.5 Gy correspond to an EQD2 ($\alpha/\beta = 10$ Gy) of 85 Gy, 75 Gy, and 60 Gy, respectively, assuming a schedule of 4 similar fractions of HDR brachytherapy with 45 Gy in 25 fractions of EBRT.

The isodose surface volume can be reported as a volume as well as by indicating the maximum dimensions of height, width, and thickness (ICRU 1985). It can be useful to compare the volume treated independent from the individual planning aims as a constancy check.

The volume encompassed by the planning aim isodose surface is of special interest. The location,

dimension, and shape of this volume when compared with the target are of interest because this information contributes to the assessment of conformality. In order to illustrate the use of the isodose surface volume concept, an example is given in Figure 8.13 for an HDR schedule with 4 fractions of brachytherapy and a planning-aim absorbed dose of 7 Gy for the CTV_{HR}. A similar example is the use of the 60 Gy volume for cases in which the planning aim and dose prescription is linked to the CTV_{IR}. (Compare tables for the clinical examples in the Appendix A.1.4-A.9.4.)

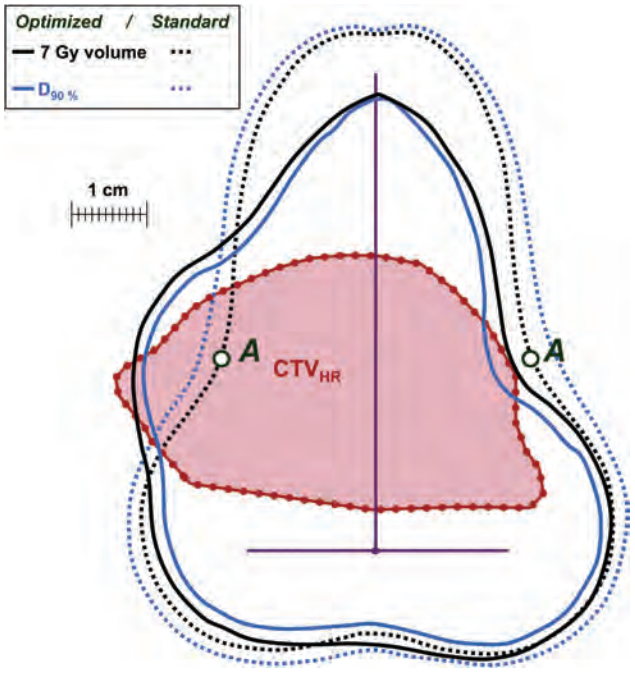

Figure 8.13. Schematic drawing illustrating the absorbed-dose distribution in relation to the CTV_{HR}. The dotted lines illustrate the situation for a standard loading intracavitary-only plan with normalization to Point A, while the solid lines are for an optimized combined intracavitary/interstitial plan. During the planning process, a planning-aim absorbed dose of 7 Gy is normalized to 100 %, which is also the dose to Point A in the standard plan. For this non-optimized plan, the $D_{90\ \%}$ reached only 6.1 Gy, while after optimization, the $D_{90\ \%}$ was increased to 8 Gy. The finally prescribed dose is related to the $D_{90\ \%}$, which is indicated in blue. It is important to note that, despite a large increase for the $D_{90\ \%}$, the overall isodose volumes that are achieved after optimization remain similar or can become even smaller than the volumes using standard loading. The geometrical configuration changes significantly with optimization, which is seen in this case as a larger right-lateral width at the level of the residual parametrial tumor (Point A) and a reduced length at the upper tandem according to the limited residual-tumor spread into the uterine corpus. On the other hand, the length and width was changed very little at the vaginal level, as no major optimization was performed in this region. The thickness might be less affected by these geometrical changes. The 7 Gy isodose surface volume was, by chance, in the standard and optimized case identical with 112 cm^3, because the optimization decreased the volume in the uterine direction and increased it in the right-lateral direction.

8.8 Recommendations for Reporting

Level 1: *Minimum standard for reporting*

Dose reporting
- TRAK
- Point A dose
- Recto-vaginal reference point dose
- $D_{0.1cm^3}$, D_{2cm^3} for the bladder, rectum

Level 2: *Advanced standard for reporting*
All that is reported in level 1 plus

Dose reporting for defined volumes
- $D_{98\ \%}$, $D_{90\ \%}$, $D_{50\ \%}$ for the CTV_{HR}
- ($D_{98\ \%}$, $D_{90\ \%}$ for the CTV_{IR} if used for prescription)
- $D_{98\ \%}$ for GTV_{res}
- $D_{98\ \%}$ for pathological lymph nodes

Dose reporting OARs
- Bladder reference-point dose
- $D_{0.1cm^3}$, D_{2cm^3} for the sigmoid
- D_{cm^3} for the bowel
- Intermediate- and low-dose parameters for the bladder, rectum, sigmoid, and bowel (*e.g.,* $V_{15\ Gy}$, $V_{25\ Gy}$, $V_{35\ Gy}$, $V_{45\ Gy}$, or $D_{98\ \%}$, $D_{50\ \%}$, $D_{2\ \%}$)
- Vaginal point doses at level of sources (lateral at 5 mm)[a]
- Lower and mid-vagina doses (PIBS, PIBS $\pm$ 2 cm)[a]

[a]Surrogate points for volumetric vaginal-dose assessment.

Level 3: *Research-oriented reporting*
All that is reported in Level 1 and 2 plus

Absorbed-dose reporting for the tumor:
- $D_{98\ \%}$, $D_{90\ \%}$ for the CTV_{IR} even if not used for prescription
- $D_{90\ \%}$ for the GTV_{res}
- DVH parameters for the PTV
- $D_{50\ \%}$ for pathological lymph nodes
- DVH parameters for non-involved nodes (ext/int iliac, common iliac)

OAR volumes and points
- Additional bladder and rectum reference points
- OAR sub-volumes (*e.g.,* trigonum or bladder neck, sphincter muscles)
- Vagina (upper, middle, lower)
- Anal canal (sphincter)
- Vulva (labia, clitoris)
- Other volumes/sub-volumes of interest (*e.g.,* ureter)

Dose–volume reporting for OARs
- Dose–volume and DSH parameters for additional OARs and sub-volumes
- Vaginal dose profiles, dose–volume, and DSHs
- Length of treated vagina

Isodose surface volumes
- 85 Gy EQD2 volume
- 60 Gy EQD2 volume

8.9 Summary

This section has given the relevant background and recommendations to prescribe, record, and report dose distributions for cervical cancer treatments. The complete information requires reporting the detailed spatial distribution of dose in relation to target structures and OAR, sometimes with specific parameters for their sub-structures. With volumetric imaging, defined volumes can be contoured, and consequently DVH parameters can be utilized to quantify dose distributions resulting from treatment planning. Although parameters such as $D_{90\ \%}$, D_{2cm^3}, and others are linked to fixed dose or volume values on the DVH, they lose spatial information. For that reason, reference points remain important.

For both the CTV_{HR} and the CTV_{IR}, the $D_{90\ \%}$ and the near minimum dose, $D_{98\ \%}$, are recommended, as they have been demonstrated to be representative clinically relevant-dose levels. In addition, the median dose, $D_{50\ \%}$, is also suggested . Together with $D_{98\ \%}$ and $D_{90\ \%}$, $D_{50\ \%}$ characterizes the large dose inhomogeneity within the CTV and, in particular, the dose to the high-dose volume, which is typical in intracavitary treatments. As the use of a PTV is not straightforward for intracavitary brachytherapy, reporting of DVH parameters for the PTV is currently limited to research. The $D_{98\ \%}$ is recommended for reporting absorbed dose to the GTV_{res} and to pathological lymph nodes.

For OARs, such as the bladder and rectum, the DVH parameters D_{2cm^3} and $D_{0.1cm^3}$ are recommended to describe the high-dose regions within these OARs. Furthermore, these parameters are regarded as being sufficient to assess brachytherapy-related morbidity if the relative contributions of EBRT and brachytherapy to the overall treatment dose remain constant.

Additional DVH parameters for the intermediate- and low- dose regions are important to characterize morbidity (*e.g.*, stenosis, stricture) related to larger irradiated volumes of the OAR. These parameters can be essential in situations in which larger contributions to the total absorbed dose are delivered with EBRT. In the case of brachytherapy-only treatments, the high-dose parameters D_{2cm^3} and $D_{0.1cm^3}$ are essential but not sufficient for comparison to treatments with a large component of EBRT (*e.g.*, 45 Gy).

The vagina, both as a potential target and an OAR, needs appropriate metrics for a comprehensive volumetric dose assessment covering high-, intermediate-, and low-dose regions. Due to inherent problems in dosimetric assessment of thin-wall structures in the vagina, alternative strategies are recommended, including a specific set of dose points. Other OARs such as urethra, ano-rectum, and ureter might also be considered.

In general, DVHs for gross OAR contours lack information on the spatial dose distribution within organ sub-structures, which are in turn responsible for various morbidity endpoints. This fact might substantially limit the current understanding of dose/volume-effect relations. The need for future research on sub-volume analysis is emphasized for specific morbidity endpoints together with reference points or volumes for these structures (bladder/vagina/anus).

Absorbed-dose reporting to Point A and TRAK remains a minimum standard requirement for any brachytherapy treatment, although volumetric assessment is recognized as the method of choice. Point A and TRAK reporting is reproducible and straightforward; moreover it enables comparisons among present, past, and future clinical practice and among different levels of complexity for dose reporting.

The use of "isodose surface volumes" is introduced to compare treatment strategies between Centers and during the planning process within Centers. These are volumes contained within an encompassing isodose surface. The term "reference volume," the volume receiving 60 Gy, as introduced for target-related reporting in ICRU Report 38 is no longer recommended in this report.

The whole process of treatment planning, dose prescription, and reporting as traditionally performed for cervical cancer brachytherapy is redefined and amplified by introducing "planning aims" and "final prescription." The planning aims are dose and volume values defined prior to treatment planning and might ultimately not be achievable. The prescription defines the finally accepted set of values, after treatment-plan acceptance. It can differ from the planning aims as a result of compromises among target and OAR doses.

Journal of the ICRU Vol 13 No 1–2 (2013) Report 89
Oxford University Press
doi:10.1093/jicru/ndw018

9. Volumetric Dose Assessment

Evaluation of three-dimensional (3D) absorbed-dose distributions in cervix brachytherapy has been performed for decades, even though it was initially not always related to volumetric CT or MR imaging. Even when based on radiographs or clinical investigation, the calculation of dose volumes, absorbed dose at target points (Point A), and organs-at-risk (OAR) points (ICRU bladder and rectal points) requires a 3D absorbed-dose calculation. Prescription, reporting, and recording of dose have therefore relied on 3D absorbed-dose evaluation in the major brachytherapy schools and according to ICRU Report 38 recommendations (ICRU, 1985). With the introduction of target definition and OAR contouring in sectional CT and MR imaging, 3D dose assessment and evaluation have become more advanced (Kirisits *et al.*, 2005). The new standard of prescription, reporting, and recording in volumetric-image-based brachytherapy relies to a large extent on dose–volume histogram (DVH) parameters (see Section 8). Assessment of uncertainties of 3D volumetric dose assessment has therefore become essential for the reproducibility and reliability of image-based brachytherapy in cervical cancer.

Volumetric dose assessment involves several procedures, including applicator reconstruction, image fusion, absorbed-dose calculation, and DVH calculation. When adding the fourth dimension of time, changes in anatomy can be taken into account with repeated imaging and adaptive treatment planning.

9.1 Applicator Reconstruction

Calculation of absorbed dose to anatomical structures requires that the geometry of the applicator with its source dwell positions be defined within the patient image data set in the treatment–planning system. This process is referred to as "applicator reconstruction." The EBRT analog of applicator reconstruction is the definition of the relation between patient and the external-radiation source. Set-up uncertainties in external-beam radiation therapy (EBRT) have been widely described and discussed (ICRU, 1993b; 1999; 2010), and it is well known that these uncertainties depend on the anatomical site, the fixation of the patient, image fusion, and the level of image guidance. External-beam radiation therapy set-up uncertainties are compensated by application of planning target volume (PTV) margins (ICRU, 1993b; 1999; 2010). In brachytherapy, the reconstruction uncertainties are mainly dependent on the type of applicator, the visualization of the applicator (*i.e.*, image modality and image sequence), and image fusion procedures (Hellebust *et al.*, 2010a). As discussed in Sections 5 and 8, it is only partially possible to compensate for reconstruction uncertainties in brachytherapy with the application of a selective PTV margin in the longitudinal direction parallel to the tandem axis (Tanderup *et al.*, 2010c). Applicator-reconstruction uncertainties must be minimized, as they directly influence the assumed dose delivery (Tanderup *et al.*, 2008). The process of applicator reconstruction has been addressed in detail in textbooks and in GEC ESTRO recommendations (Hellebust *et al.*, 2010a; Kirisits *et al.*, 2011) and will only be summarized here.

The reconstruction process can be divided into two steps: (1) reconstruction of the applicator geometry including the source path, and (2) merging/fusion of applicator and anatomy (see Figure 9.1). Both steps are equally important because either incorrectly reconstructed applicator geometry or a correctly reconstructed applicator positioned incorrectly on the images would lead to incorrect calculation of the absorbed-dose distribution. The first step—reconstruction of applicator geometry and/or source path—is addressed during applicator commissioning. The source positions are identified in relation to reference points within, or in relation to the outer surface of, the applicator. The applicator geometry and source channel can be assessed from phantom scans or from technical drawings of the applicator. Reconstruction of the applicator should be verified during applicator commissioning with which the source path and the outer dimensions of the applicator are verified in order to approve the applicator for clinical use. Applicator commissioning also includes an assessment and verification of selected dwell positions by autoradiography or imaging of the source inside the applicator (Thomadsen, 2000a).

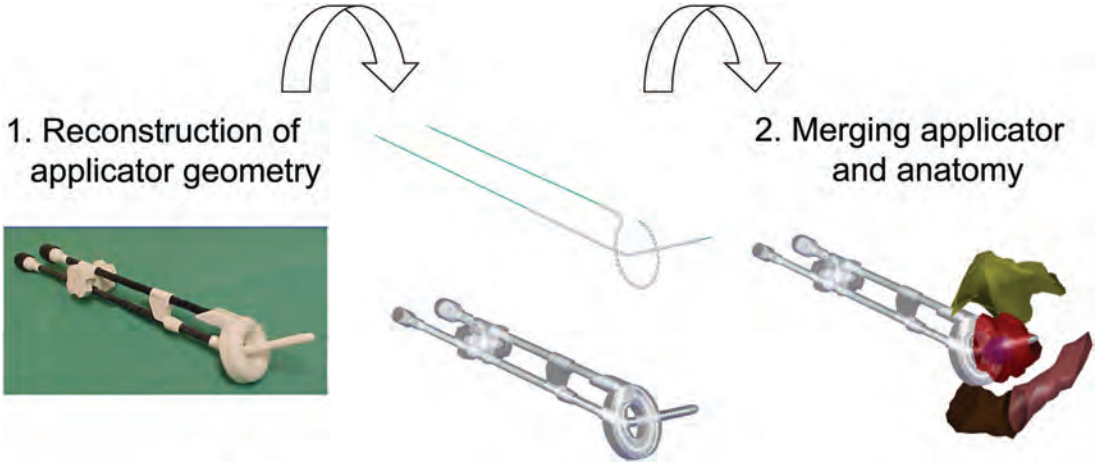

Figure 9.1. Schematic example of the two steps of applicator reconstruction: (1) reconstruction of the applicator geometry including the source paths, which may be available from applicator libraries. The applicator geometry is validated during commissioning. (2) The merging of the applicator geometry with the patient anatomy in 3D images.

The second step—merging or fusion of applicator source path and anatomical geometry—is the process in which the applicator and/or source path is defined on the individual patient images at the time of brachytherapy. This can be done by digitization directly on the acquired images with the applicator *in situ* or by importing a library file of the applicator geometry (Hellebust *et al.*, 2007). Direct digitization can be used when the source channels or marker wires are visible in the images. A library of applicators can be defined for fixed-geometry applicators such as ovoids, rings, and cylinders. Merging library applicators with the patient images can be based on fusion of reference points or by direct positioning of the applicator shape into the images according to visible structures of the applicator, such as parts of the source path or the outer surface of the applicator.

With CT images, it is possible to directly visualize the source channel either by exploiting the contrast between the applicator material and the air-filled source channel or by inserting wires with radio-opaque markers separated by fixed gaps. It has to be proven that the location of the marker strings corresponds to the source path. Marker strings have different flexibility and/or dimensions than the source wire, and the source position, especially during movement within the applicator, might not be identical to that observed with the marker strings, and discrepancies of 2 mm–3 mm have been observed (Hellebust *et al.*, 2007; 2010a).

Reconstruction of applicators with MRI presents more challenges than with CT. It is not possible to directly discriminate the source channel on MRI because there is no MR signal from either air or conventional applicator materials. Furthermore, markers used for radiographs and CT cannot be used for MRI. Special MR markers, such as catheters containing a $CuSO_4$ solution (Haack *et al.*, 2009), water (Perez-Calatayud *et al.*, 2009), glycerin (Chajon *et al.*, 2007), or ultrasound gel (Wills *et al.*, 2010), can be inserted into the source channels in plastic applicators. As with CT markers, the correspondence of the markers with the source positions has to be verified during commissioning. Fluid-filled marker catheters can change their characteristics over time, resulting in the need for constancy checks at regular intervals. Reference structures, such as needle holes or cavities filled with fluid, can be used as long as the locations relative to the dwell positions are known (Berger *et al.*, 2009; Wills *et al.*, 2010). Fluid-filled marker catheters cannot be visualized inside the source channels of titanium applicators due to magnetic-susceptibility artifacts from the metal (Haack *et al.*, 2009). The reconstruction procedure should consider uncertainties due to distortions and artifacts that can change with MRI pulse sequence. In particular, when using metallic applicators, it is essential to describe and compensate for the applicator artifacts by identifying the true position of the applicator relative to the artifacts (Haack *et al.*, 2009; Kim *et al.*, 2011). Magnetic resonance imaging slice thickness is an important parameter that has direct impact on the precision of reconstruction, and it is recommended that reconstruction be performed in an image series obtained with a slice thickness of $\leq$5 mm (Hellebust *et al.*, 2010a).

9.2 Definition of Reference Points in 3D Images

With volumetric-image-based brachytherapy, the dose prescription is often linked to target volumes and no longer to Point A (Kirisits *et al.*, 2005; Tanderup *et al.*, 2010a). However, as described in

Section 8.3.1, reporting of Point A absorbed dose is still recommended and relevant even when using volumetric imaging—see below. Bladder and rectum ICRU points as well as additional OAR points are traditionally defined according to the appearance of the bladder balloon and the vaginal wall in orthogonal x-ray images (see Section 10.3). However, equivalent points can be introduced on volumetric images (Lindegaard *et al*., 2008; Pelloski *et al*., 2005). Vaginal points (see Sections 8.4.3 and 10.3) are used for reporting in volumetric-image-based brachytherapy and can be straightforwardly positioned in CT or MRI by measuring from the surface of the applicator.

Point A location is uniquely related to the applicator geometry, and therefore the "planar imaging definition" (see Section 10.1.1) can be straightforwardly applied, step-by-step in 3D images. The sectional images are typically rotated in the treatment–planning system in order to create multiplanar images oriented according to the source channels. The surface of the vaginal applicator can be identified on the reconstructed para-coronal and para-sagittal reconstructed images. Measurements are then performed according to Figure 10.1. In several treatment–planning systems, it is possible to link reference points in a fixed relation to the applicator directly in the applicator library, which assures a reproducible definition of Point A.

The bladder balloon should contain 7 cm^3 of fluid and must be visible on the 3D images (see Section 10.3.2). With 1.5 T MRI, the balloon is visible when filled with either normal saline water or a diluted gadolinium contrast agent (Dimopoulos *et al*., 2012a). The use of x-ray contrast agents is the standard for CT imaging. The ICRU bladder point is positioned at the posterior surface of the balloon on the anterior–posterior line passing through the center of the balloon (see Section 10.3.2). When axial images are used, the ICRU bladder point will be positioned directly in the transverse-image plane, which intersects the center of the balloon. However, when para-axial images are used, the point will not be in the same para-axial image as that containing the center of the balloon because the image slices are not oriented in the anterior–posterior direction. In this case, a multiplanar reconstruction of the images can be performed, so that axial imaging planes that are orthogonal to the body axis are reconstructed, and the bladder point can then be directly positioned in these reconstructed images (see Figure 9.2).

The ICRU recto-vaginal point is related to the applicator and located 5 mm behind the posterior vaginal wall on an anterior–posterior line drawn from the middle of the vaginal sources (see Section 10.3.1). When axial images are used, the rectal point is defined in the slice that passes through the middle of the vaginal sources. As described above for the bladder point, it is advantageous to use reconstructed multiplanar images when using para-axial imaging.

9.3 Registration and Fusion of Images

9.3.1 Registration According to the Brachytherapy Applicator

In brachytherapy, the applicator, as the source of radiation, represents the reference. In an appropriate implant, even if the applicator changes its position relative to bony structures, the target volume and even parts of the OARs will move together with the applicator (Gerbaulet *et al.*, 2002b). It is therefore essential that fusion of brachytherapy images be performed with the aim of matching the

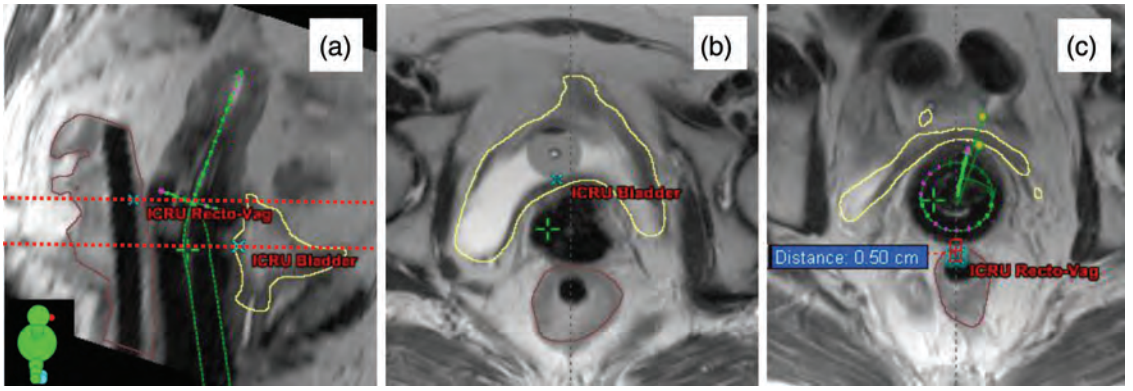

Figure 9.2. Sagittal- and axial-image planes reconstructed from a para-axial T2-weighted MR image uptake with tandem-ring applicator *in situ*. The para-axial images were oriented according to the applicator, and multiplanar reconstruction must be performed in the planning system according to the body axis in order to position the ICRU bladder and recto-vaginal points. (a) Mid-sagittal plane where the upper and lower dashed line indicates the level of the axial planes containing the ICRU recto-vaginal point and the ICRU bladder point, respectively. (b) Position of ICRU bladder point in the reconstructed axial image plane at the posterior wall of the bladder balloon. (c) Position of ICRU recto-vaginal point 5 mm posterior to the vaginal mucosa in the reconstructed axial-image plane.

brachytherapy applicator and not the bony structures (Hellebust *et al.*, 2010a).

Registration between MRI sequences with the same brachytherapy applicator is often relatively straightforward because the applicator appears as a black void on MRI in sharp contrast to the surrounding tissue. Fusion of MR and CT images can present more challenges because the applicator appears differently on these two image modalities. In CT, the source channel is readily visible, whereas the body and the surface of the applicator might not contrast with the surrounding tissue. Planning systems with automatic tools for image fusion related to the applicator have the potential to improve the fusion accuracy (Nesvacil *et al.*, 2013b). Registration between sequences from different applicator insertions can introduce some challenges if the applicator geometry is different (*e.g.*, different ring size, different tandem angulation, or different ovoid size or separation).

9.3.2 Image Fusion for Reconstruction Purposes

When contouring and reconstruction are performed in the same image series, the dose to targets and organs can be directly calculated without any image fusion. However, when necessary, several image series can be combined so that contouring is done in one image series and reconstruction in another. For example, in certain cases, the reconstruction accuracy can be increased by image fusion with supplementary imaging such as CT, sagittal or coronal MRI, 3D MRI, or other MRI sequences (Hellebust *et al.*, 2010a). This is particularly relevant in cases in which reconstruction on MRI is difficult (*e.g.*, in the case of poor visibility of needles on MRI). When different image sets are used for contouring and reconstruction, they have to be co-registered according to the applicator. Whenever possible, it is recommended that the images containing the target and OAR contours be used for dose planning. This allows for direct visualization of isodose curves on the relevant images. As MR images also contain information about the position of the applicator—although the visualization may be more difficult than on CT—fusion errors can be detected by validating the position of the applicator on MRI. It is more difficult to detect fusion errors on CT by validating contours that are transferred from MRI to CT because of the limitations with respect to visualizing the target volumes.

Fusion uncertainties will translate into absorbed-dose-calculation uncertainties. It should be noted that uncertainties can result in a miscalculation of DVH dose parameters by typically 4 % to 6 % mm^{-1} of fusion error (Tanderup *et al.*, 2008). Therefore, even small fusion uncertainties will have impact on the absorbed-dose calculation. It should always be considered whether or not fusion uncertainties are larger than reconstruction uncertainties if the reconstruction is performed directly in the image series where the contouring of target and OARs is performed. Matching to bony structures must be avoided as the applicator can move more than 5 mm in relation to bone (Datta *et al.*, 2001). This translates directly into fusion errors of more than 5 mm, which is a major deviation and unacceptable for appropriate treatment planning.

9.3.3 Fusion of Pre-EBRT and Brachytherapy Planning Images

There are considerable differences between the patient anatomy before EBRT delivery and at the time of brachytherapy with the applicator *in situ*. The tumor regression during EBRT can be substantial, amounting to from 60 % to 80 % of the pre-therapeutic tumor volume (Mayr *et al.*, 2006). Most of the shrinkage takes place during the first 2–3 weeks of EBRT. Furthermore, the pelvic organs, such as bladder, rectum, and bowel, are prone to significant movement and difference in filling. Yet another important issue is the deformation that is caused by the applicator insertion and vaginal packing. Due to these significant deformations of the anatomy, it is not possible to register tumor, bladder, rectum, sigmoid, or bowel by doing rigid bony or soft-tissue registration between pre-EBRT images (CT, MRI, PET) and the images acquired at the time of brachytherapy (Christensen *et al.*, 2001). Therefore, image fusion between diagnostic MRI and brachytherapy MRI cannot directly aid the contouring of the CTV_{IR}, due to the changes in anatomy. However, structures that are in close relation to bone, such as lymph nodes, can be more reliably fused from EBRT to brachytherapy images using registration according to bony structures.

Deformable volume registration is becoming available, in which each tissue volume element (voxel) in one 3D image is matched with the corresponding voxel in a second image (Brock, 2010). A successful deformable registration allows the voxel to be tracked during radiotherapy, and this makes it possible to track volumes and doses from fraction to fraction. However, it is important to notice that the deformations found by registration algorithms maximize some similarity measure based on image intensities and/or delineated contours. Often regularization terms are introduced that ensure smoothness of the deformations, or model tissue parameters. The resulting deformation fields are, however, not

guaranteed to correspond to the true physical deformations. This can lead to significant dose estimation errors, especially with the large deformations and high absorbed-dose gradients present in pelvic-brachytherapy absorbed-dose distributions. Furthermore, the deformable-registration method is currently hindered by the significant pelvic-organ deformation and deformations arising from changes in organ filling or tumor shrinkage between pre-EBRT and brachytherapy images. Also, the effects of the insertion of the brachytherapy applicator represent a specific challenge because this structure is not present in pre-EBRT images. Currently, deformable registration is not yet sufficiently mature for routine registration between pre-EBRT and brachytherapy images.

9.3.4 Fusion of Target Contours between Image Series at the Time of Brachytherapy

Image fusion can be used when MRI images with the applicator *in situ* are not available for every brachytherapy fraction. In this case, the target contouring from a previous MRI can be used for treatment planning in succeeding fractions of brachytherapy (Nesvacil *et al*., 2013b).

A typical scenario could be that MRI is available for the first brachytherapy session, and succeeding fractions are planned by using CT images with the applicator *in situ* (Nesvacil *et al*., 2013b). The target contours defined on the first MRI can then be transferred to succeeding CT scans by fusing images according to the applicator, as described above. This strategy assumes that the initial target contour is still applicable to succeeding brachytherapy fractions. The shortcomings of this assumption are dependent on the timing of imaging, as the GTV, the CTV_{HR}, and the CTV_{IR} defined on MRI images early in EBRT will be prone to significant shrinkage (Kirisits *et al.*, 2006b). The combination of MRI for the first brachytherapy fraction with succeeding CTs looks promising when brachytherapy is applied toward the end of therapy or after EBRT (Nesvacil *et al.*, 2013b).

Magnetic resonance images can be obtained before the first brachytherapy fraction (pre-brachytherapy MRI) in order to prepare for the first brachytherapy application (Dimopoulos *et al*., 2012a; Fokdal *et al*., 2013; Lindegaard *et al*., 2008). If it is not possible to perform MRI with the applicator *in situ*, then pre-brachytherapy imaging can be used to also aid target contouring on CT images obtained with the applicator *in situ*. Fusion between pre-brachytherapy MRI and CT is compromised because of significant organ deformation between images acquired with and without the brachytherapy applicator. Direct transfer of the MRI target to CT is not possible because of deformation problems, and the target contour needs to be adapted interactively by the physician. Fusion of images acquired before brachytherapy into images acquired during brachytherapy can be improved by inserting a "dummy applicator" or a real applicator (Fokdal *et al*., 2013; Lindegaard *et al*., 2008) in order to establish a geometry that is as similar as possible to the situation at the time of brachytherapy delivery.

9.4. Volume Reconstruction, Voxel Size, and DVH Calculation

A DVH calculation is usually based on the reconstruction of a 3D volume from 2D contours in sectional image slices. The 3D-volume reconstruction can be performed according to different principles and varies among treatment–planning systems as well as with slice thickness (Kirisits *et al.*, 2007). Certain regions of a delineated volume are more prone to volume-reconstruction uncertainties. Examples are the regions of the first and last slice of a contour, as well as regions with significant changes in the shape of a contour from one slice to the next. In cases in which the DVH parameter is particularly dependent on the absorbed dose in such a region, there will be additional uncertainties in DVH calculations. An example would be a sigmoid loop that is in parallel with the 2D slices, and the D_{2cm^3} hotspot appears in the first slice of the sigmoid delineation. The target $D_{98\ \%}$ has also shown to be particularly uncertain when compared with $D_{90\ \%}$ (ICRU, 2010). Hotspots of the bladder and rectum are often in regions with less spatial variation, and the D_{2cm^3} variation is then typically <5 % (1 SD) (Kirisits *et al.*, 2007).

The voxel size chosen for a DVH calculation must be sufficiently small to properly represent absorbed-dose gradients. However, the gain in accuracy becomes small when moving to voxel sizes of less than 1 mm^3. With a voxel size of 1 mm^3 even 0.1 cm^3 has 100 points for absorbed-dose sampling. The $D_{98\ \%}$ depends on the absorbed-dose sampling in the lowest-absorbed dose 2 % of the target volume, but 2 % will be larger than 0.1 cm^3 for target volumes larger than 5 cm^3.

When analyzing DVH parameters, some parts of the target volumes evaluated are likely to consist of applicator volume. By definition, the applicator is not part of the target volume, but it can be time-consuming to ignore applicator parts in all slices if there is no automatic routine for this in the treatment–planning system. The volume of the applicator does not greatly influence the evaluated

parameters as long as large volumes compared with the applicator volume are considered (Pötter *et al.*, 2006). Such a case is the tandem volume inside the CTV_{HR} and the CTV_{IR} when evaluating $D_{90\ \%}$, or $D_{98\ \%}$. However, volumes, such as $D_{30\ \%}$, might include too much of the applicator volume to be a meaningful parameter, and even $D_{50\ \%}$ will be influenced when subtracting the applicator volume. When calculating DVHs, it is recommended that no part of the vaginal applicator or packing be included in the GTV or the CTV_{HR}. The CTV_{IR} has a larger volume, and $D_{90\ \%}$ is therefore less prone to variations when including parts of the vaginal applicator.

9.5 Intra-Fraction, Inter-Fraction, and Inter-Application Variations

Although adaptive-treatment–planning concepts are emerging in EBRT, the practice for the majority of patients is to generate one treatment plan and to apply this for 25–30 fractions typical of radical radiotherapy. Given this scenario, there are systematic uncertainties associated with the treatment planning, absorbed dose, or treatment geometry related to the radiotherapy equipment. These systematic uncertainties will influence all treatment fractions. A second category of uncertainties is of a random nature and is related to each treatment fraction. Random uncertainties can be further categorized into inter-fraction and intra-fraction uncertainties. Due to systematic and random uncertainties, the delivered absorbed dose likely will not be equal to the prescribed absorbed dose. More accurate assessment of absorbed dose requires repeated imaging with assessment and accumulation of dose in time (Jaffray *et al.*, 2010).

An uncertainty analysis for brachytherapy is different from that for EBRT because fewer fractions are delivered (Kirisits *et al.*, 2014). Image guidance and absorbed-dose adaptation is often performed for each brachytherapy insertion, and inter-fraction uncertainties have a different significance in such scenarios than in EBRT. The following terminology is established for description of patient-related uncertainties and variations during brachytherapy (see Figure 9.3):

Intra-fraction: Variations occurring in between imaging/dose planning and absorbed-dose delivery of the succeeding brachytherapy fraction. For PDR, the intra-fraction variation includes also variations occurring during and in between pulses. For LDR, intra-fraction variation describes variations during the entire continuous irradiation time.

Inter-fraction: Variations occurring between two fractions of brachytherapy based on the same imaging, dose planning, and application.

Inter-application: Variations occurring between two different brachytherapy applications.

In order to determine the dosimetric consequences of these variations, repeated imaging is required at relevant time points. For each time point, absorbed-dose distributions can be calculated and cumulative dose can be determined across several fractions.

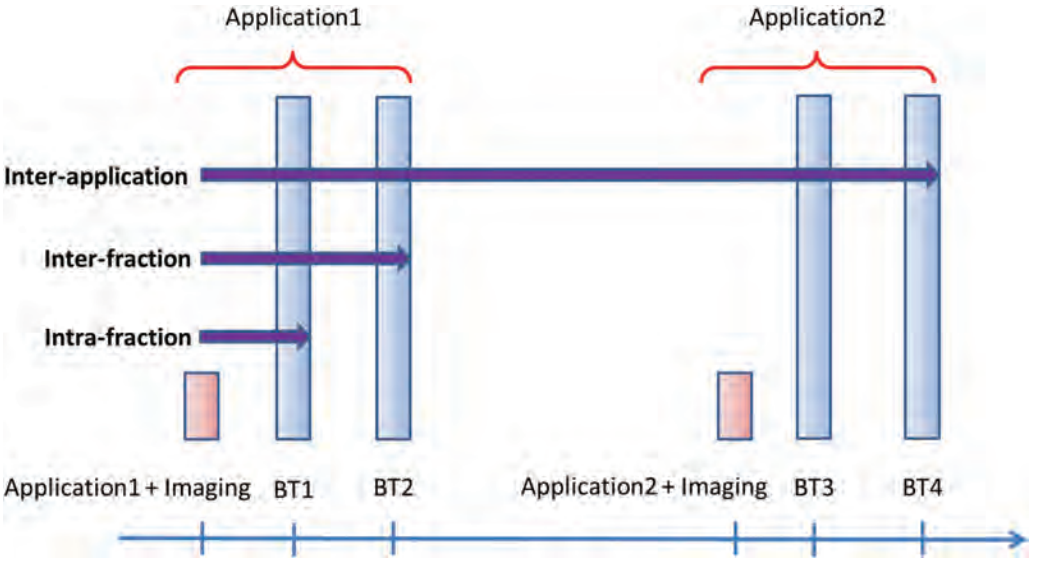

Figure 9.3. Terminology for description of patient-related variations during fractionated brachytherapy. Shown is an example of an HDR schedule with 2 applicator insertions and 4 fractions. Imaging is performed immediately after the brachytherapy application, and after contouring and treatment planning, the first HDR fraction is delivered. The applicator stays in place overnight, and fraction number 2 is delivered with the same treatment plan as for fraction 1. The same approach is repeated 1 week later for fractions 3 and 4.

9.5.1 Intra- and Inter-Fraction Variations

The static absorbed-dose distribution is the distribution of absorbed dose in a volumetric image with the brachytherapy applicator in place, and absorbed-dose determination is performed according to this snapshot of the patient anatomy. However, intra-fraction organ or applicator movement will cause certain deviations between planned and delivered absorbed dose. In image-guided brachytherapy, there is typically a 1 h to 5 h delay between imaging and absorbed-dose delivery to allow for contouring and dose planning. Applicator and/or organ movements during this period depend on the application technique and the individual patient. With PDR brachytherapy, there will be additional risk of movement during and between pulses. When delivering several HDR fractions per insertion, MR or CT imaging is not always performed for each individual fraction. In this case, inter-fraction variations are not detected and compensated for.

For an appropriate brachytherapy application, the applicator is properly fixed to the tumor, and intra-fraction organ movement will have little impact on tumor absorbed dose. Nesvacil *et al*. (2013a) evaluated inter- and intra- fraction variation data from different centers (Andersen *et al.*, 2013; De Leeuw *et al*., 2009; Hellebust *et al*., 2007; Lang *et al.*, 2013; Mohamed *et al.*, 2013). The dose deviations associated with both intra- and inter-fraction uncertainties were about 20 % to 25 % for organs at risk and about10 % for the target (CTV_{HR}) (Tanderup *et al.*, 2013). These uncertainties result in EQD2 total-dose uncertainties of typically 2 Gy–4 Gy (SD) for the CTV_{HR} and 4 Gy–8 Gy (SD) for OARs (Nesvacil *et al.*, 2013a). Contouring and reconstruction uncertainties are *per se* included in inter- and intra-fraction analyses, and therefore, the variation corresponding to actual organ and applicator motion will be smaller than the numbers indicated above (Hellebust *et al.*, 2013; Petrič *et al.*, 2013; Tanderup *et al.*, 2013).

9.5.2 Inter-Application Uncertainties

If conditions do not allow for CT or MR imaging for each applicator insertion, it might be required to utilize MRI or CT for the first brachytherapy fraction only. In this situation, succeeding fractions would be performed with the treatment plan from the first fraction. This is equivalent to the practice often used in EBRT for which a plan for all fractions is generated based on a single treatment plan developed before the first irradiation. However, EBRT is usually more robust in regard to inter-fraction uncertainties because treatment plans can be generated that take into account inter-fraction uncertainties by application of a PTV margin. In brachytherapy, the possibility of creating robust treatment plans is limited as the absorbed-dose gradients cannot be manipulated to cover a PTV with a homogeneous dose (see Section 5.5). Furthermore, the absorbed-dose gradients in brachytherapy are significant, and organ motion can cause unexpected high or low absorbed doses, although the effects of typical organ movements are smaller compared with EBRT because the organs tend to move together with the applicator.

By using only one imaging session for several brachytherapy insertions, there can be some systematic uncertainties in the delivered and reported doses. In the case of target shrinkage between subsequent brachytherapy fractions, the target dose delivered will typically be higher than estimated because the target shrinks to a region closer to the applicator where the dose is higher. Target shrinkage taking place between brachytherapy fractions can also cause OARs to move closer to the applicator and consequently receive higher absorbed doses than estimated from the first fraction. It has been demonstrated that target shrinkage could lead to a systematic underestimation of the average total dose in the target and OARs of from 4 Gy to 6 Gy when brachytherapy is initiated early during EBRT (Kirisits *et al*., 2006b). The situation becomes more stable for intracavitary applications of brachytherapy initiated toward the end of EBRT (after Week 4 to 5), after the major tumor shrinkage has taken place, in particular in small tumors treated with intracavitary brachytherapy (Mohamed *et al*., 2013). For applications with a combined intracavitary–interstitial approach, it is recommended that images for each applicator insertion be used, because the applicator geometry is not reproducible between insertions of needle applicators, and use of the same treatment plan is not desirable.

9.5.3 Summation of Dose across Treatment Applications

Dose accumulation can be performed based on serial image acquisitions and the static absorbed-dose distributions associated with each image. Several images over time are usually available with volumetric image-guided brachytherapy as the gold standard is to acquire images at least for each brachytherapy application. However, intra-fraction, inter-fraction, and inter-application variations result in deformation of organs, and it is not possible to accumulate the absorbed dose based on direct rigid registration (see Section 9.3) (Andersen *et al*., 2013; Jamema *et al*., 2013). Deformable registration is, at this time, not yet mature for routine clinical use, and

certain assumptions have to be made for dose accumulation in clinical practice. These assumptions are described in Section 8.5 as well as recommendations on dose accumulation for EBRT and brachytherapy.

9.6 Key Messages

Accurate applicator reconstruction procedures are required as the error in DVH-parameter calculation is from 5 % to 8 % mm^{-1} of reconstruction error.

Point A, ICRU bladder, and ICRU rectal points can be defined in volumetric images such as MR and CT.

Fusion of brachytherapy images is based on the brachytherapy applicator and not on bony anatomy (except for a few purposes such as assessment of lymph-node dose for which bony registration is required).

Rigid image fusion can be used for applicator reconstruction and procession of target contours.

Rigid image fusion has significant limitations for alignment of OARs and for fusion of pre-EBRT images with brachytherapy images. However, deformable registration is not yet mature for routine clinical use.

Intra- and inter-fraction dose uncertainties have a magnitude (SD) of about10 % and 20 %–25 % for target and OARs, respectively.

Using the same brachytherapy plan for several applicator insertions gives rise to inter-application uncertainties. Target shrinkage can be a source of systematic inter-application uncertainties, although this has less impact when brachytherapy is started toward the end EBRT.

Dose accumulation of EBRT and brachytherapy absorbed-dose distributions is currently performed as crude addition of DVH parameters, which relies on the assumptions of (1) homogeneous EBRT dose distribution in the region of high brachytherapy dose, and (2) similar distribution of hotspots in different brachytherapy fractions.

9.7 Summary

Volumetric (3D) absorbed-dose calculation using sectional imaging (CT, MR, US) for treatment-plan optimization and for anatomy- and contour-based absorbed-dose reporting and recording, taking into account target volumes and OAR, requires a number of steps. The process called applicator reconstruction defines the relation among the radiation source and the anatomy of the patient in the treatment–planning system, so that the absorbed-dose contribution from each source position can be calculated for each anatomical voxel. The accuracy of applicator reconstruction is of utmost importance because of the steep absorbed-dose gradients inherent to brachytherapy. Incorrect positioning of the applicator will result in absorbed-dose deviations in both target structures and OARs of up to 5 %–8 % mm^{-1} of applicator displacement. The identification of the applicator in 3D images can be achieved in multiple ways depending on imaging modality and applicator type.

Three-dimensional image registration is an integral component of image-guided brachytherapy whenever different volumetric images are combined. Contouring and applicator reconstruction can involve the acquisition of several different imaging sequences, images from different modalities, images at one single time point, and/or sequential imaging at several time points. Image registration between EBRT and brachytherapy needs specific consideration as there is significant organ deformation due to the insertion of the brachytherapy applicator and due to noticeable tumor shrinkage at the time of brachytherapy. In particular, the evaluation of accumulated doses is not trivial. It becomes especially challenging if EBRT absorbed-dose gradients are located in the high dose regions of brachytherapy; for example, when applying parametrial boost, midline block irradiation, or when performing advanced and highly conformal EBRT techniques such as IMRT or volumetric-modulated arc therapy. The utilization and application of deformable image registration for adding dose contributions of EBRT and brachytherapy is still a matter of ongoing research. To overcome the current limitations of deformable-image-registration alternative approximations are possible: by performing rigid registrations in specific regions of interest (*e.g.*, for assessment of lymph-node dose, or by performing dose estimation by matching corresponding volumes and their dose values manually).

Absorbed-dose accumulation and propagation of target contours across several brachytherapy fractions involves image registration performed with the applicator being the reference. While the nearby organs and the tumor itself are in a relatively stable configuration with respect to the applicator, they are not with the bony anatomy. Therefore, image registration using the bony anatomy as the reference is strongly discouraged for assessing the composite dose in the high-absorbed-dose region as it can lead to significant errors.

Anatomical variations in time need to be considered and include, in general, intra-fraction, inter-fraction, and inter-application variations. Intra-fraction variations can occur between imaging/dose planning and absorbed-dose delivery. Inter-fraction variations might occur between two fractions based on the same

imaging and dose planning. Inter-fraction variation in brachytherapy can occur when several fractions are delivered with the same applicator insertion. Inter-application variations might be present between two different brachytherapy applications. Intra-fraction, inter-fraction, and inter-application variations can affect the delivered absorbed dose on the order of 10 % for target and 20 % for OARs, respectively.

Static absorbed-dose distributions can be calculated in one imaging session. However, the assessment of the accumulated absorbed dose in mobile tissue requires a sequence of images with a time-dependent description of the volume variation and an absorbed-dose calculation for each time point. The development of deformable-image-registration tools can help to determine the cumulative absorbed-dose distribution in those mobile pelvic tissues. Better knowledge of the actual absorbed-dose distribution, in particular in certain OARs and their sub-structures, will ultimately result in improved understanding of dose–response and more accurate dose–response curves, which in turn can be utilized to improve absorbed-dose distributions.

Journal of the ICRU Vol 13 No 1–2 (2013) Report 89
Oxford University Press
doi:10.1093/jicru/ndw012

10. Radiographic Dose Assessment

Many facilities do not have volumetric imaging capabilities and rely on two-dimensional (2D), planar x-ray images. Although based on 2D images, the reconstructing process is not 2D; reconstructing the location of the applicator and source positions, along with any identified points, occurs in 3D space. Because soft tissues are not clearly imaged, this approach gives little accurate spatial information on the target or the normal tissue structures (unless a contrast medium is used) except for surrogates based on locations related to the applicator or skeletal anatomy or from markers, such as clips. Such imaging also does not usually provide any volumetric information. Even for facilities that perform volumetric imaging for dosimetry, radiographic imaging during the procedure can be used to assess if the placement of the applicator requires correction. Some criteria for such a judgment are discussed in Section 3.2.4.

The imaging and input methods used depend on the treatment-planning system. Localization requires the acquisition of at least two images with a known geometric relationship, allowing back-projection of the spatial location of a point shown on both images, a process known as triangulation. Details of the localization process can be found in many textbooks (Thomadsen, 2000b). The most common approach to radiographic localization for intracavitary cervical brachytherapy uses two orthogonal images, usually antero-posterior (AP) and lateral. A pair of stereo-shift images, *i.e.*, images taken with parallel beams shifted by a known distance or divergent beams separated by a known angle, is much less frequently used, and other methods are used less frequently still. The stereo-shift approach requires acquisition of only AP images or images only slightly off from AP, a significant advantage for obese patients for whom lateral images might not allow identification of structures because of poor x-ray-beam penetration. When performed with proper parameter settings, the stereo-shift approach provides accuracy comparable to orthogonal images for high-contrast, point-like objects (Adams and Meurk, 1964; Fitzgerald and Mauderli, 1975; Fletcher, 1973; Sharma *et al.*, 1982). Localizing points on a volumetric object, for example, on the surface of a Foley balloon or on a rectal wall enhanced with contrast, poses a problem when using shift imaging due to the ambiguity of the position of the point on each image. The use of orthogonal images reduces the ambiguity in localization of such points, which largely accounts for the wide acceptance of this localization method.

10.1 Target Points

10.1.1 Location of point A

Since its introduction in the 1930s by Tod and Meredith, the absorbed dose at Point A has been used as a surrogate point to specify the amount of radiation given to a patient in brachytherapy for cervical cancer (Tod and Meredith, 1938; 1953). Because of the vast experience in specifying treatments in terms of absorbed dose at Point A, this strategy is still useful. It needs to be noted that the absorbed dose at a point provides insufficient information on the application without either more information on the source distribution or reference to a protocol that describes source-distribution rules. The Manchester system accomplishes this by using a standard source-loading pattern. In such cases, the absorbed dose at a point describes the application adequately for other practitioners to understand the treatment. However, many practitioners specify the absorbed dose at Point A, but do not follow the Manchester source-loading rules. In these cases, the absorbed dose at Point A fails to define the application adequately.

The original 1938 definition of Point A was intended to indicate where the uterine artery crossed the ureter on the surface of the uterus (Tod and Meredith, 1938). This anatomic site could not be located using the imaging available at the time, so the authors developed a construction for finding that point. The construction made use of the relationships between the parts of the Manchester applicator and the patient's anatomy. For their applicator, the procedure used a line connecting the superior surfaces of the ovoids as the basis for finding Point A. This definition placed Point A sufficiently cephalad of the colpostats that it fell where the isodose surfaces run parallel to the tandem and above the high absorbed-

dose gradient that occurs near the junction of the tandem and the ovoids. In 1953, the definition was changed, so the point could be located for individual patients using radiographic localization (Tod and Meredith, 1953). Because the ovoids were not clearly imaged on radiographs, the basis for finding Point A was changed from the superior surface of the ovoids to the bottom of the tandem source train, which fell

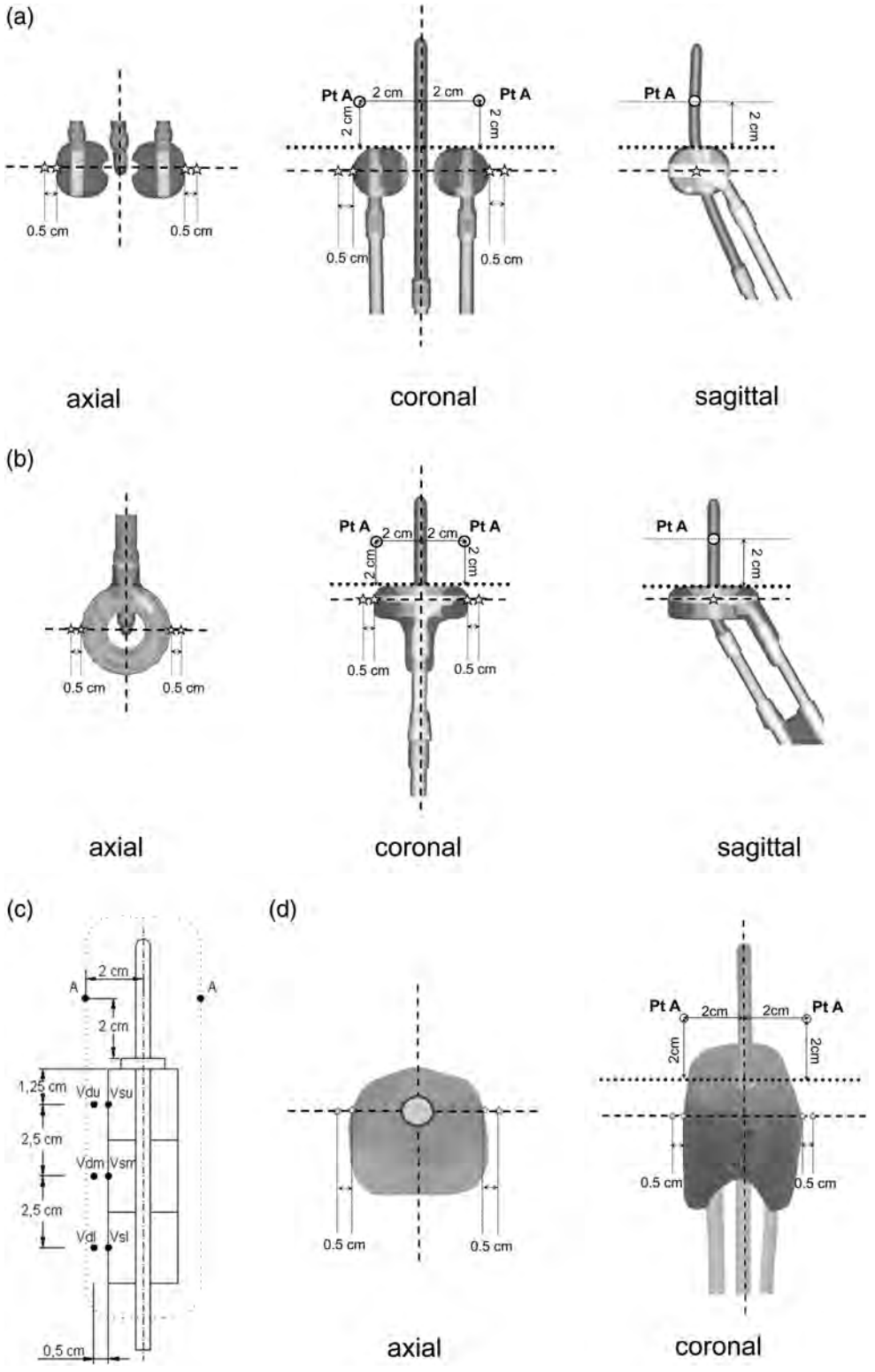

Figure 10.1. Diagrams showing the location of Point A for tandem ovoids (a), tandem ring (b), cylinder (c), and mould (d) applicators, respectively. In addition the locations of vaginal points on the surface and 5 mm from the surface are illustrated.

on the line connecting the superior surfaces of the ovoids for the Manchester applicator. This position in the Manchester applicator also coincided with the external cervical os. Some practitioners, and even some cooperative trial groups, began using the os as the basis for locating Point A for applicators with no fixed relationship between the os and the superior surface of the ovoids, such as the standard Fletcher applicator. Using the external cervical os as the base for locating Point A results in large variation of the absorbed dose at Point A for patients undergoing very similar treatments (Potish *et al.*, 1995). For this reason, the American Brachytherapy Society (ABS) and this report recommend that Point A be defined in relation to the applicator, following the original Manchester definition (Viswanathan and Thomadsen, 2012). Finding Point A follows the description below, based on the ABS recommendation:

In the treatment-planning computer,

- For tandem and ovoids, connect a line through the center of each ovoid. From the point on the tandem where this line intersects, extend superiorly along the tandem a distance equal to the radius of the ovoids (see Figure 10.1a).
- For the tandem and ring applicator, from the intersection of the plane of the center of the ring source channel and the tandem (see Figure 10.1b) move superiorly the distance from the center of the source channel to the superior surface of the ring.
- For tandem and cylinders (see Figure 10.1c) or tandem and mould (see Figure 10.1d), begin at the superior intersection of the vaginal applicator and the tandem.

From the point found above, move 2 cm further superiorly along the tandem. Define Point A on each side as 2 cm laterally on a line perpendicular with respect to the tandem from this final point on the tandem.

The transverse-point A plane is a plane perpendicular to the tandem containing point A.

10.1.2 Relationship between point A dose and the CTV_{HR} $D_{90\ \%}$

The relation between the absorbed dose at Point A and the CTV_{HR} $D_{90\ \%}$ (see Section 8.3.2) depends largely on the CTV_{HR} volume (see Figure 10.2) (Tanderup *et al.*, 2010a). For small tumors, the Point A absorbed dose is lower than the CTV_{HR} $D_{90\ \%}$, whereas for large tumors, the Point A absorbed dose is higher than the CTV_{HR} $D_{90\ \%}$. The CTV_{HR} $D_{90\ \%}$ typically varies between 60 % and 150 % of the Point-A absorbed dose. However, although the Point-A absorbed dose cannot be used to predict the target absorbed dose in individual patients, it provides a reasonable estimate of the average CTV_{HR} $D_{90\ \%}$ for a large patient population with a balanced disease-stage distribution (about one-quarter of the cases in each of Stage IB/IIA and III/IVA and half with Stage IIB) treated with radical brachytherapy. This indicates that Point A is a good representation of "an average position" of the tumor or lateral cervix wall, and that it is possible to proceed from the average dose prescription at Point A to the average dose prescribed to the CTV_{HR} without introducing any major dose escalation or reduction for such patient population as a whole.

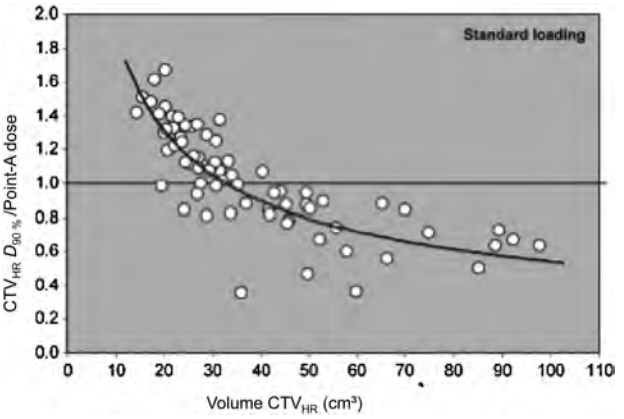

Figure 10.2. The relationship between the ratio of the CTV_{HR} $D_{90\ \%}$ to the absorbed dose at Point A as a function of the absolute volume of the CTV_{HR}, assuming the same source loading and total reference air kerma (TRAK) is used when prescribing to Point A. The data were gathered from 72 consecutive patients with locally advanced cervical cancer treated with imaged-guided intracavitary brachytherapy (Tanderup *et al.*, 2010a) (reproduced with permission).

10.1.3 Isodose-surface volumes and dimensions

A different approach to specifying the amount of radiation involves specifying the dimensions of a certain isodose-surface volume (see Section 8.7; Figure 8.13). Conventionally, this was referenced to the 60 Gy isodose line (ICRU, 1985), but it can also be the 75 Gy, 85 Gy, 125 Gy, or any other chosen line. Such references can be used within an institution to specify the dimensions of the planning-aim absorbed dose and to follow the planning procedure from an initial planning aim to the treatment prescription (see Section 8.6). It can also be used for comparison among different institutions for a given isodose-surface volume (see clinical examples in Appendix, Table 4 in each example).

In the terminology used in Section 5, prescribing the treatment to the 60 Gy isodose line would approximate prescribing the treatment to the CTV_{IR} (Gerbaulet *et al.*, 2002b; ICRU, 1985).

The dimensions of the isodose surface volumes can be also related to the dimensions of the CTV_{IR} for brachytherapy as selected through clinical examination, with or without volumetric imaging.

10.1.4 Target dose approximation

Without image-based target definition, target dose values can be only roughly estimated. Based on the clinical gynecologic examination, with or without volumetric imaging, the individual maximum width and thickness of the CTV_{HR} or the CTV_{IR} can be indicated (see examples 4, 7 and 9 in the Appendix). These dimensions can be combined with the radiographic images (see Figure 4.7) preferably on the treatment plan in relation to the applicator geometry (see Figure A7.6). When there is information from volumetric images, a full 2D contour can also be drawn in defined slice orientations related to the applicator. The dose at the outer periphery of the CTV_{HR} or the CTV_{IR} can be estimated from such approximate dimensions in width and thickness at defined levels (transverse plane at 1 cm above vaginal applicator surface, transverse-Point A plane). The uncertainties associated with this approach do not allow an accurate comparison with volumetric-image-based dose assessment. However, the method could roughly estimate a minimum dose of the order of magnitude of the $D_{98\%}$. Taking into account fractionation and EBRT, the total EQD2 for the isodose-surface volume, which roughly covers the estimated dimensions, can be estimated (see Figure 10.3 and Figure A7.6).

10.1.5 Lymph-node and Pelvic-wall points

Using external-beam treatments, a high absorbed dose can be delivered to the regional lymph nodes. Some additional absorbed dose is also frequently delivered with brachytherapy, which is higher in lymph-node areas near the applicator. Integrating the absorbed doses from the two approaches requires assessing the dose to the various lymph nodes from brachytherapy. Accounting for the absorbed dose from the external-beam treatments is discussed in Section 8.5.

With the Manchester System, the position of the most relevant lymph nodes was assumed to be at Point B, with the location of Point B determined as follows:

- For tandem and ovoids, connect a line through the center of each ovoid. From the point on the tandem where this line intersects, extend superiorly along the tandem a distance equal to the radius of the ovoids.
- From that point found immediately above, move 2 cm further superiorly along the body axis (which is not necessarily coincident with the tandem). Define Point B on each side as 5 cm lateral to this final point.

Point B fails to correlate well with relevant regional lymph nodes for cervical cancer (Lee *et al.*, 2009). Two methods recommended to locate relevant lymph nodes use the pelvic wall reference points (PWRP) or the lymphatic trapezoid as described below.

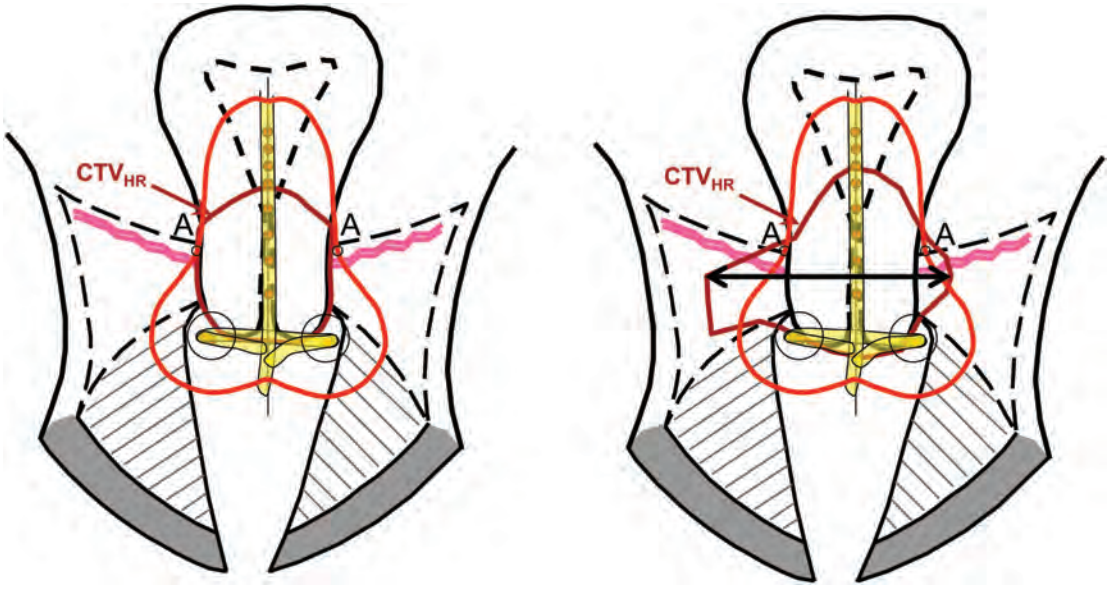

Figure 10.3. The CTV_{HR} configuration and maximum width as assessed by clinical examination in relation to the applicator. The situation on the left shows a maximum width limited to 4 cm, with 2 cm left and 2 cm right. Therefore, the Point A dose is representative of the dose covering the entire CTV_{HR}. The situation on the right shows a maximum width of 6.5 cm, with 2.5 cm left and 4 cm right. The minimum dose for such a tumor is substantially lower, approximately 80 % on the left and 43 % on the right. With 84 Gy prescribed to Point A (45 Gy EBRT + 4 × 7 Gy brachytherapy), the dose decreases to 57 Gy $EQD2_{10\ Gy}$ on the right side of the CTV_{HR} and to 78 Gy $EQD2_{10\ Gy}$ on the left side.

10.1.5.1 Pelvic wall reference points. The absorbed dose at the PWRP are intended to be representative of the absorbed dose at the distal part of the parametrium and at the obturator lymph nodes (Chassagne and Horiot, 1977). The PWRP can be visualized on AP and a lateral image and related to fixed bony structures. On an AP image, the PWRP is located at the intersection of the following (see Figure 10.4):

- A horizontal line tangential to the cephalad-most points of the acetabula (between 1 and 2 in Figure 10.4) and
- Vertical lines tangential to the inner aspect of each acetabulum.

On a lateral image, the cephalad-most points on the right and left acetabulum are first joined (a line from 1 to 2). The right PWRP (RPWRP) falls along this line, beginning at 1 and going toward the left acetabulum in proportion to the lengths 1–3 to 1–2 on the anterior radiograph. The left PWRP (LPWRP) is identified similarly.

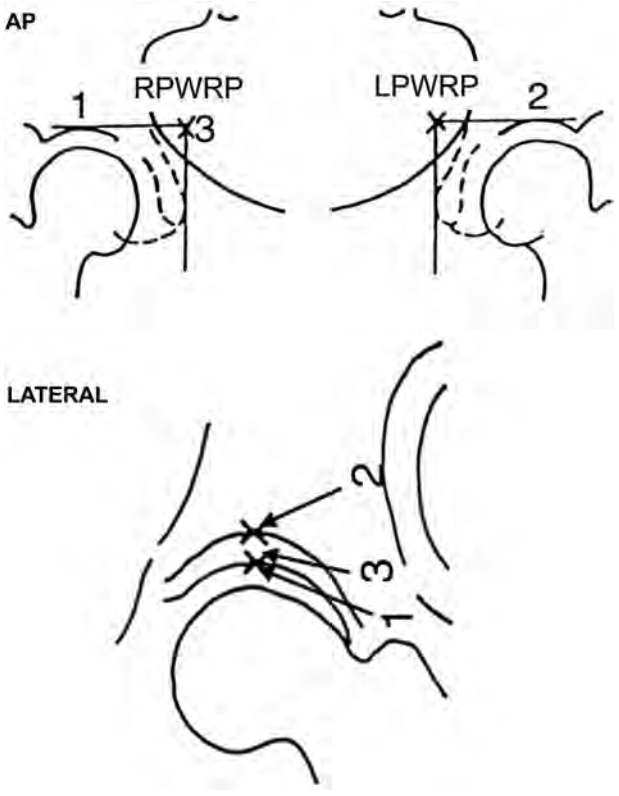

Figure 10.4. Determination of the RPWRP and LPWRP. The lateral figure shows only the placement of the RPWRP due to space limitations. The placement of the left would be similar but with the point closer to the "×" marked 2 instead of 3. Adapted from Chassagne and Horiot (Chassagne and Horiot, 1977; ICRU, 1985).

10.1.5.2 Lymphatic trapezoid. Different points identified by means of the lymphatic trapezoid are intended to be representative of the absorbed dose at the mid-external iliac, low-common iliac, and low para-aortic lymph nodes. The lymphatic trapezoid is obtained as follows (see Figure 10.5) (Fletcher, 1980):

- A line is drawn from the junction of vertebral bodies S1–S2 to the top of the symphysis.
- Then a line is drawn from the middle of that line to the middle of the anterior aspect of vertebral body L4. This line identifies the coronal plane containing the trapezoid.
- A trapezoid is constructed in the plane defined above and centered on the body axis as shown on the left in Figure 10.5, with the top 4 cm long, bottom 12 cm long, and the sides connecting the ends of those two lines.
- The absorbed doses at the inferior corners of this figure provide an estimate of the absorbed-dose rates in the mid-external iliac lymph nodes (labeled R.EXT and L.EXT for right and left external iliac nodes, respectively).
- The superior corners of the trapezoid are used to estimate the absorbed dose in the low para-aortic nodal region (labeled R.PARA and L.PARA).
- The absorbed doses at the midpoint of each side of the trapezoid are used to estimate the absorbed dose in the low common iliac lymph nodes (labeled R.COM and L.COM).

10.2 Reference Points for Upper, Mid, and Low Vagina

The vagina is simultaneously both a target tissue and an OAR as discussed in Sections 5.4.4, 6.2, and 8.4.3. In the absence of soft tissue imaging information, the superior third of the vagina is most often considered at risk of infiltration (see Figures 5.7–5.14) and treated to a therapeutic dose, while, in the absence of known disease involvement, the dose in the inferior two-thirds should be minimized.

In the treatment plan, the absorbed dose in the vagina from tandem and ovoid applicators can be specified at points located lateral to the center of, and on the surface of, the colpostats and 5 mm from that point (see Figure 10.1a) on both the right and the left of the applicator. For the ring applicator, the points are located at the lateral-most-possible dwell

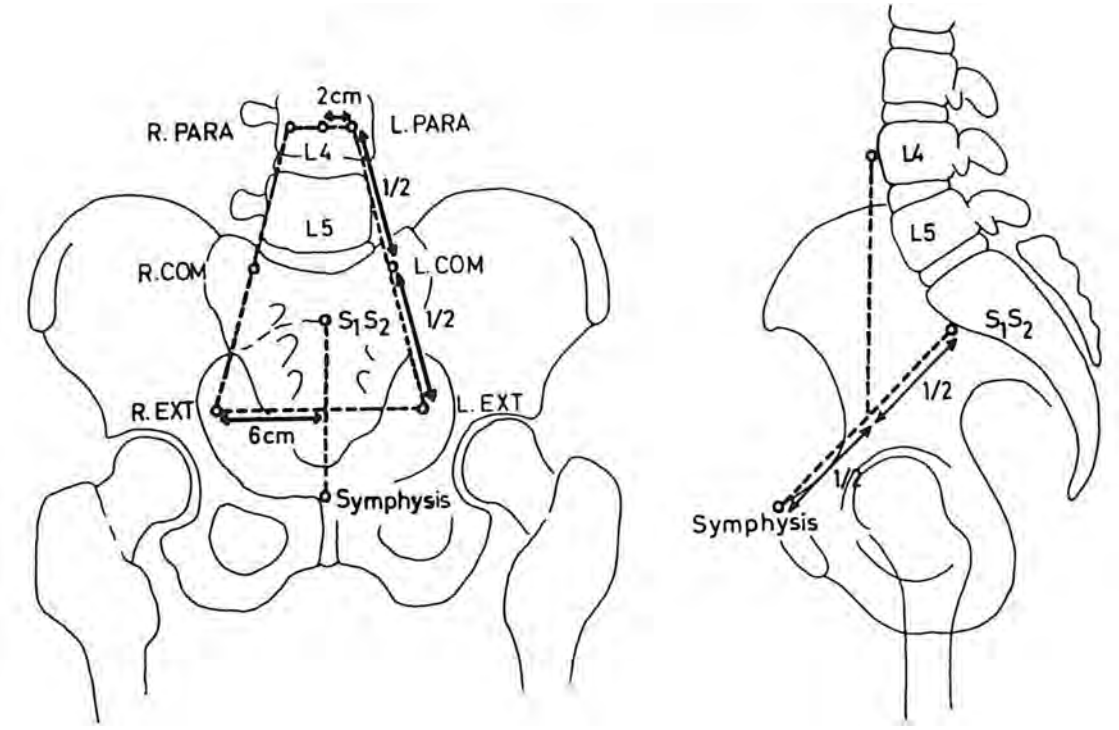

Figure 10.5. Determination of the lymphatic trapezoid. On the left is an AP view and on the right a lateral view (Fletcher, 1980; ICRU, 1985).

positions on each side of the ring, on the surface of the applicator, and 5 mm from the surface (see Figure 10.1b). If a tandem and cylinders are used, the vaginal absorbed dose is specified at the surface of the cylinders, 12.5 mm inferior to the cephalad-most extension of the cylinders, and, again, also 5 mm lateral to that point on both the left and right sides of the applicator (points VSU and VDU, respectively, in Figure 10.1d). These points should be determined in the treatment-planning system based on the known dimensions of the cylinders because applicator or patient rotations and varying magnifications make localization on the images extremely challenging.

The posterior-vaginal dose in the upper vagina is specified at the recto-vaginal point at 5 mm from the mucosal vaginal surface (ICRU reference point, see Section 10.3.1). The mid- and lower-vagina doses are defined (see Section 8.4.3 and Figure 8.12) by points at the level of the posterior-inferior border of the symphysis pubis (PIBS), 2 cm below (PIBS-2), and 2 cm above (PIBS + 2).

In vaginal brachytherapy (beyond the vagina adjacent to the portio) (*e.g.*, in Stage IIIA with major residual disease), the vaginal brachytherapy dose inside and outside the CTV has to be specified at representative sections through the upper, mid, and low vagina at 3, 6, 9, and 12 o'clock, respectively, at the surface of the applicator and at 5 mm depth (see Figures 8.12 and 10.1c).

10.3 Reference Points for the Rectum and Bladder

As noted in Sections 6.2 and 8.4, in brachytherapy of cervical carcinoma, the most important OARs are the rectum, sigmoid, bladder, and vagina. Parts of the bowel (small and large) might also receive a significant absorbed dose, but most of the bowel is usually not visible on radiographic images, so the location of points and determination of absorbed doses to reproducible bowel points is exceedingly difficult.

The discussion that follows considers techniques to locate points that indicate the dose to certain relevant locations in these critical structures. In fact, the probability of complication depends on several features of the irradiation: absorbed dose, absorbed-dose rate, fraction size, irradiated volume, and also probably complex dose–volume relationships, as discussed in Sections 6.2 and 8.4 (Barillot *et al*., 2000; Chen *et al*., 2000; Crook *et al*., 1987; Kim *et al*., 2008; Perez *et al*., 1999; Pourquier *et al*., 1996). Thus, the dose at specified points can be expected to allow only an approximate prediction of the likelihood of toxicity. However, considering the dose at these points can be useful for comparing different potential treatment techniques.

10.3.1 Recto-vaginal reference point

The point of reference for the rectal dose is located 5 mm behind the posterior vaginal wall on an AP line drawn from either the center of the vaginal sources

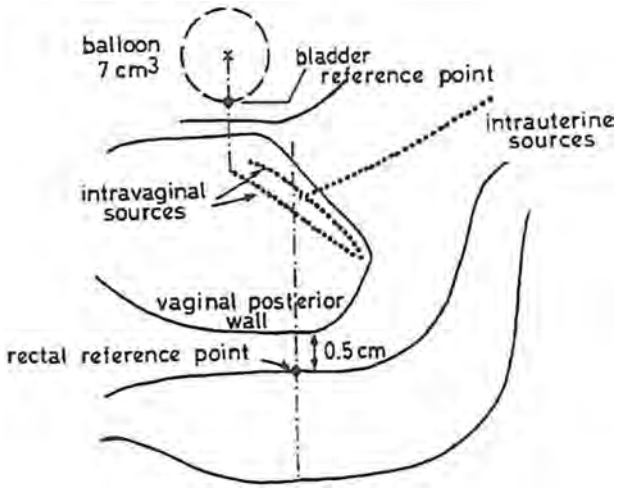

Figure 10.6. Determination of the reference points for the bladder and rectum (Chassagne and Horiot, 1977; ICRU, 1985). The ICRU-rectum reference point (ICRU, 1985) is in this report called the ICRU-recto-vaginal reference point.

or the inferior extremity of the uterine source, whichever location gives the higher absorbed dose (see Figure 10.6). This point can be determined in the treatment-planning system (see Section 9.3) or on orthogonal radiographic images. The posterior vaginal wall can be visualized with an intravaginal mold, by opacification of the vaginal cavity with radio-opaque gauze used for packing, or by a retractor. As noted in Section 10.1, localization of this point on stereo-shift images is ambiguous.

Contrast in the rectum assists in verifying the point selected. A common practice is to inject a 50 % diluted solution of barium contrast and then withdrawing as much as possible, leaving the rectal wall semiopacified.

Radio-opaque markers in the rectum are not recommended. Flaccid markers, such as chains, lie against the posterior rectal wall, which is not of interest, and rigid markers tend to distort the rectal-wall position. *In vivo* dosimetry has problems similar to radio-opaque markers in keeping the dosimeter in contact with the anterior rectal wall. Also, due to the thickness of the dosimeter, the *in vivo* absorbed dose will also not reflect the absorbed dose to the most irradiated part of the anterior rectal wall (Tanderup *et al*., 2006).

As indicated in Section 10.2, this point is also representative for the upper vaginal absorbed dose, and becomes therefore the recto-vaginal reference point.

10.3.2 Bladder reference point

The bladder reference point is related to a caudally retracted Foley balloon in the trigone of the bladder. Recommendations are that the balloon be filled with approximately 7 cm^3 of diluted radio-opaque fluid with the catheter pulled outwards and fixed to bring the balloon in reproducible contact with the bladder neck. If the balloon is nearly in the center of patient, the reference point is taken as the posterior-most point on the surface of the balloon (see Figure 10.6). This can be accomplished either in the treatment-planning system or on orthogonal radiographic images; again, localization on stereo-shift images is difficult due to the ambiguities in finding the identical point on each of the images.

The aggregate experience with this bladder point comes from patients for whom most often the balloon is situated close to the midline. If the balloon is lateral to the centers of the colpostats, the absorbed dose at the point as described is likely to be less than elsewhere on the balloon surface closer to the applicator. The bladder point does not necessarily represent the maximum absorbed dose in the trigone of the bladder in a given patient.

10.3.3 Clinical relevance of the bladder and rectal reference points

Although they are not identical, there is in general a significant correlation between the ICRU reference-point absorbed dose for the rectum and the rectal D_{2cm^3}: however, a considerable variation exists among individual patients, which means that ICRU point absorbed doses are not a good predictor of D_{2cm^3} in the individual patient (Figure 10.7). Based on data from 400 patients treated at 19 different institutions [EMBRACE study (EMBRACE, 2015)], the ICRU rectal absorbed dose is, on average, approximately 20 % larger than the rectum D_{2cm^3} with a standard deviation of 40 %. The absorbed dose at the ICRU bladder point is on average approximately 20 % smaller than the bladder D_{2cm^3} and is associated with a standard deviation of 32 %. Because of these findings, dose constraints based on the reference dose points cannot be translated directly into D_{2cm^3} constraints.

A significant number of clinical observations support a correlation between rectal complications and the absorbed dose at the ICRU rectal reference point (Barillot *et al*., 2000; Crook *et al*., 1987; Georg *et al*., 2011; Koom *et al*., 2007; Perez *et al*., 1999; Pourquier *et al*., 1996; Stryker *et al*., 1988). A correlation was also shown between the absorbed dose at Point A and the absorbed dose at the rectal reference point and rectal complications (Perez *et al*., 1999). In contrast, the ICRU bladder reference point, although simple to find and easily reproducible, does not correlate well with bladder complications (Stryker *et al*., 1988). Many, but not all, of the reports concluded that the orthogonal-film technique was adequate for assessing the maximum rectal absorbed dose but that for

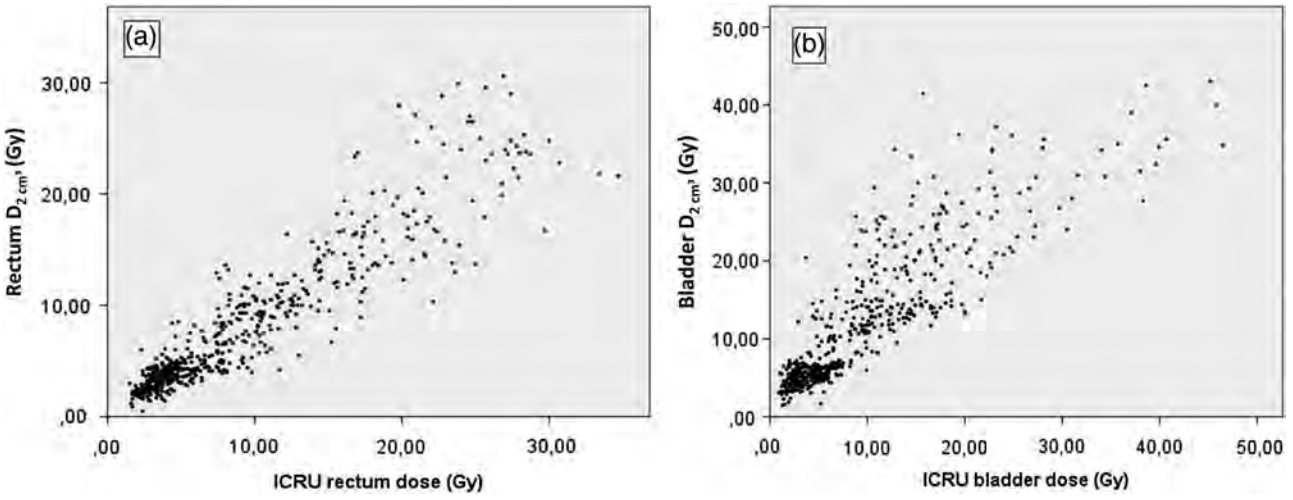

Figure 10.7. The relationship between the absorbed doses at the ICRU-defined OAR points and the D_{2cm^3} values: (a) for the rectum; and (b) for the bladder. The data exhibit a largely linear relationship but with a sizable variation for individual patients (EMBRACE, 2015) (reproduced with permission).

the bladder, a point about 2 cm cranially correlates better with bladder complications (Barillot *et al*., 2000; Hunter *et al*., 1986; Stryker *et al*., 1988). The position for this more-cranial point depends on the implantation technique, so no general recommendation for reporting a second bladder point is made.

A correlation between the ICRU recto-vaginal point as defined in this report and vaginal-morbidity (stenosis) has recently been published (Kirchheiner *et al.*, 2016).

10.3.4 Sigmoid reference point

Determining the position of the sigmoid requires infusing dilute contrast agent into the rectosigmoid and withdrawing the bulk of the contrast, leaving the wall coated as described in Section 10.3.1. Imaging with all of the contrast in place often results in obscuring the applicator information. Selecting the points of interest that represent the highest absorbed doses to that organ on the two images can be challenging. No agreement has been achieved so far on the most appropriate procedure to arrive at a reproducible location of such a sigmoid point.

10.4 Uncertainties with Radiographic Localization

Several features of radiographic localization lead to uncertainties in the localization of points used to specify absorbed doses for brachytherapy, and therefore also in the calculated absorbed doses.

- Target position. The target, and its surrogate, Point A, are inferred from the applicator. Although the applicator can be located with relatively high precision, within 2 mm (at the 2-sigma level) for most dwell positions of sources in an applicator, the applicator itself might not conform well to the patient's anatomy in the cranial–caudal direction, possibly resulting in an uncertainty of 5 mm to 7 mm (2 sigma) in the relation between the cervical os and the superior surface of the ovoids, ring, or mold, and therefore the presumed target.
- Lymph-node absorbed dose. None of the methods described in Section 10.1.5 for approximating lymph-node positions actually specify the true positions of the nodes in a particular patient, as these cannot be seen on the radiographic images without contrast opacification of the lymph chains. The absorbed doses at the lymph-node points, just as for the target points, serve as surrogates for the desired quantity. At the facility of one of the authors, the absorbed doses at the PWRP averaged 17 % of the absorbed dose at Point A, but with a relative standard deviation of 27 %. At a distance of from 5 cm to 6 cm from the applicator center, the absorbed doses at the nodal points vary by about 3 % to 4 % mm^{-1} change in the position of the point.
- OAR absorbed dose. In addition to the issues discussed above concerning how well the absorbed doses at the normal tissue points represent the absorbed doses of interest in the organs and relate to the morbidity endpoints, the absorbed doses at the normal tissue reference points also involve considerable uncertainty because they simply state the absorbed dose at standard, nominal locations, represented simply as points. As noted in Section 8.4, absorbed doses to the bladder vary greatly from those at the nominal point because the geometry of the bladder is complex and the absorbed-dose gradient through the bladder is high. As for the uncertainty of the location of the ICRU bladder reference

point, small variations in its lateral position produce little change in the determined absorbed dose, but variations in the distance from the applicator can produce variations up to 4 % mm^{-1} to 10 % mm^{-1} based on the inverse-square law.

The location of the rectal point is often based on the applicator geometry and some visible indication of the posterior vaginal wall. Usually, when the vagina is opacified with a contrast medium, the defined rectal point does fall near the anterior rectal wall. However, if the contrast material does not make good contact with the posterior vaginal wall, particularly if contrast-impregnated gauze is used, the rectal point can fall too far anteriorly and indicate an erroneously high rectal absorbed dose.

10.5 Recommendations for Reporting

Level 1: *Minimum standard for reporting*

Dose reporting:
- TRAK
- Point A dose
- Recto-vaginal reference point dose
- Bladder reference point dose

Level 2: *Advanced standard for reporting*
All that is reported in level 1 plus

Dose reporting for defined volumes:
- Estimated dose in the CTV_{HR}(according to estimated maximum width and thickness) (in the CTV_{IR} if used for prescription)
- Pelvic wall point (optional)
- Lymphatic trapezoid (optional)

Dose reporting for OARs:
- Vaginal point doses at level of sources (lateral at 5 mm)
  Lower- and mid-vagina doses (PIBS, PIBS $\pm$ 2 cm)

Level 3: *Research oriented reporting*
All that is reported in Level 1 and 2 plus

OAR volumes, points:
- Additional bladder and rectum points
- Sigmoid point
- Anal-canal point (e.g., low-vagina point)
- Vulva point (e.g., low-vagina point)
- Other points of interest

OAR-dose reporting:
- Length of treated vagina

Isodose surface volumes:
- 85 Gy EQD2 volume
- 60 Gy EQDW volume

10.6 Summary

When using radiographic imaging, soft tissue structures cannot be visualized. Therefore, doses at pre-defined, standardized reference points serve as surrogates for volumetric-dose information to targets and OARs.

The target is often represented by Point A. The recommendation by the ABS of the location of Point A is defined with fixed geometrical relations to the applicator. For small tumors, the absorbed dose at Point A is less than the CTV_{HR} $D_{90\ \%}$, while for large tumors, the absorbed dose at Point A exceeds the CTV_{HR} $D_{90\ \%}$. For specifying the absorbed dose in lymph nodes of interest, the PWRP or the points indicated by the lymphoidal trapezoid can be used as reference points. For the upper vagina, the vaginal absorbed dose is specified at points on the right and left of the vaginal applicator. The posterior-vaginal absorbed dose is specified at the recto-vaginal point at 5 mm from the mucosal vaginal surface (initial ICRU rectum point). The mid- and lower-vagina absorbed-dose values are estimated at a point at the level of the PIBS, 2 cm above (mid vagina) and 2 cm below (vaginal entrance) along the body axis. The rectal reference point is located 5 mm behind the posterior vaginal wall on an AP line drawn from either the center of the vaginal sources or the inferior extremity of the uterine source, whichever location gives the higher absorbed dose. As it is the same point used for absorbed-dose estimation for the upper vagina, this point is defined as the recto-vaginal point. The bladder reference point is usually taken on the posterior-most point on the surface of a Foley balloon filled with 7 cm^3 of diluted radio-opaque fluid, caudally retracted to the trigone of the bladder.

Journal of the ICRU Vol 13 No 1–2 (2013) Report 89
Oxford University Press
doi:10.1093/jicru/ndw014

11. Sources and Absorbed-Dose Calculation

11.1 Radionuclides

Because the sources for intracavitary applications for cervical cancer are located within the treatment volume and deposit their dose outwardly, high-energy photon emitters provide the most effective photon treatments. The most commonly used radionuclide for high-absorbed-dose-rate and pulsed brachytherapy for gynecological malignancies is ^{192}Ir, although ^{60}Co and ^{169}Yb are used in some facilities. High-dose-rate (HDR) ^{60}Co sources, with a half-life of 5.27 years, have the advantage of long usable lifetimes compared with ^{192}Ir with a half-life of 74 days. For low-dose-rate (LDR) gynecological applications, ^{137}Cs sources are the most commonly used, although some facilities still use ^{60}Co and some use ^{192}Ir, which allows the use of a smaller diameter (and thus more comfortable) tandem. A few facilities still use ^{226}Ra for LDR applications, although the use of ^{226}Ra has been discouraged (IAEA, 2006). The most common radionuclide for gynecological interstitial treatments is ^{192}Ir, although permanent implants using ^{198}Au and ^{125}I in resorbable mesh are also used. While the dose distribution depends to some extent on the particular radionuclide and encapsulation, the variations among the high-energy photon sources prove much less important than in the case of lower-energy, interstitial sources, such as ^{125}I or ^{103}Pd. For intracavitary brachytherapy, the more significant variable is the geometry of the source distribution in the uterus and vagina. Table 11.1 gives some information of interest for the more commonly used and proposed radionuclides.

11.2 Source-Strength Specification

11.2.1 Reference Air-Kerma Rate

In 1983, in line with the introduction of the *Système International d'Unités* (International System of Units, SI), the *Comité Français pour la Mesure des Rayonnements Ionisants* (CFMRI) recommended that radioactive sources be specified in terms of the reference air-kerma rate (RAKR) (CFMRI, 1983). This report also recommends that the strength of photon-emitting radioactive sources for brachytherapy be specified in terms of the quantity *RAKR*. The use of the quantity *activity* is not recommended for gynecological brachytherapy application descriptions or dosimetry.

11.2.1.1 Definition of RAKR. The RAKR (units of Gy s^{-1}), denoted by the symbol $\dot{K}_{\delta,R}$, of a source is the air-kerma rate, *in vacuo*, due to photons of energy greater than a cutoff value δ (see Section 11.2.1.4), at a reference distance of 1 m from the source center, on a transverse plane normal to and bisecting the long axis of the source (Aird *et al*., 1993; BCRU, 1984; CFMRI, 1983; ICRU, 1985; 2004b; NCS, 1991; SFPH, 1995) Air kerma is the mean sum of initial kinetic energies of all charged particles liberated in a mass dm of air by indirectly ionizing particles incident on dm. It neglects the energy that is re-radiated in the form of bremsstrahlung characteristic x rays, for example, which is small for all brachytherapy sources (Nath *et al*., 1987).

11.2.1.2 Analogs. The quantity RAKR is closely related to air-kerma strength, S_K, recommended by the American Association of Physicists in Medicine (AAPM) for specifying source strength, defined as "the product of air-kerma rate in free space and the square of the distance of the calibration point from the source center along the perpendicular bisector . . .." (Nath *et al*., 1987). The difference between the RAKR and air-kerma strength is that the air-kerma strength incorporates distance (*i.e*., the inverse relationship between air-kerma and distance for a point source) and has the unit μGy m^2 h^{-1} or allowed multiples. Numerically, the two quantities are equal when expressed in the same units of time.

11.2.1.3 Measurement. The values for $\dot{K}_{\delta,R}$ for most sources used in gynecological brachytherapy have been determined by various means depending on when they were measured. The current values for ^{137}Cs sources are derived from measurements of selected sources by various standards laboratories, traceable to measurements made several decades

Table 11.1. Physical properties of radionuclides in use and proposed for cervical brachytherapy.

Radionuclide	Half-life[a]	Conditions	Air-kerma-rate constant[b,c] (μGy m^2 h^{-1} GBq^{-1})	Effective photon energy[b,d]	Energies of emitted radiations (probabilities per disintegration >0.03) (MeV) (γ, x, β)[a]	Half-value layer (mm Pb)
^{226}Ra	1622 years	0.5 mm Pt filter	195[e]	830 keV[f]	γ: 0.047–2.448; x: 0.011–0.087	11[g] 8 (1st HVL)[g]
		1.0 mm Pt filter	182[g]	1.2 MeV[e]		
^{60}Co	3.57 years		308[h]	1.25 MeV	γ: 1.173, 1.333; β_{avg}: 0.096	11[g]
^{137}Cs	30.1 years		77.2[h]	662 keV	γ: 0.662; β_{avg}: 0.187	6[g]
^{192}Ir	73.8 days	High-dose-rate	110[i,j]	380 keV[b,e]	γ: 0.206, 0.296, 0.308, 0.317, 0.468, 0.484, 0.589, 0.604, 0.612; x: 0.0094, 0.067; Auger: 0.0068–0.00724; β_{avg}: 0.180	3[i]
		Low-dose-rate	109[i]			
		Unfiltered	114[i]			
^{169}Yb	32.0 days		42.6[i]	93 keV[e]	γ: 0.063, 0.110, 0.131, 0.177, 0.198, 0.308; x: 0.050–0.059; ce: 0.011–0.188; Auger: 0.0057, 0.0409	0.2[i,k]
^{125}I	59.4 days		33.3[i,m]	29 keV	γ: 0.035; x: 0.004, 0.027, 0.031, 0.032; ce: 0.011–0.188; Auger: 0.0037, 0.030–0.035	0.1[l] 0.03 (1st HVL)[l]
^{198}Au	2.7 days		55[n]	411 keV	γ : 0.411; β_{avg}: 0.312	3[k,l]

Note that the average photon energy pertains to an idealized point source and does not include (a) the contribution of bremsstrahlung from emitted conversion electrons and beta particles, or (b) the effects of self-absorption, encapsulation, and secondary emissions by substrates and markers.

[a]National Nuclear Data Center, information extracted from the Chart of Nuclides database, http://www.nndc.bnl.gov/chart/.

[b]Photon-energy cut-off (δ) = 10 keV (see Section 11.2.1.5).

[c]Modified from the original table by converting exposure to air kerma and mCi to GBq.

[d]Equivalent monoenergetic source energy.

[e]Depending on the filtration for radionuclides with a wide range of photon emissions.

[f]From ICRU (ICRU, 1961) citing Garrett (1958) and Wyckoff (1957), following Attix and Ritz (1957).

[g]Shalek and Stovall (1969).

[h]Attix (1967).

[i]Thomadsen (1997).

[j]Ninkovic *et al*. (2005).

[k]Nath (1995).

[l]Trott (1987).

[m]A wide variety of values are in the literature. Complicating the value for this radionuclide has been several changes in its calibration standard over the years. The value lists is a middle between several. One of the better comes from Hashemi *et al*. (1988).

[n]ICRU (1961).

ago using cavity ionization chambers with very accurately known volumes. The photon energies used for gynecological brachytherapy are too high to use a free-air chamber. For high dose-rate ^{192}Ir sources, the standards laboratories use calibrated ionization chambers and the multiple-distance technique of Goetsch *et al*. (1991). One standards lab (Physikalisch-Technische Bundesanstalt) has developed a standard for HDR ^{60}Co sources at the time of this writing. Currently, no standards exist for either ^{169}Yb or ^{241}Am. The qualification "*in vacuo*" associated with the RAKR means that the measurements must be corrected for photon attenuation and scattering in air or any other medium between source and detector, as well as for photon scattering from any nearby objects, including walls, floors, and ceilings. Before using new sources, the user is advised to check the status of the source-strength traceability.

11.2.1.4 The Energy Cutoff, δ. The energy cutoff, δ, is intended to exclude low-energy or contaminant photons (*e.g*., characteristic x rays originating in the outer layers of the metallic source cladding, that can significantly inflate $\dot{K}_{\delta,R}$ without contributing significantly to absorbed dose at clinically significant distances, greater than about 1 mm, in tissue). The chosen value for δ, typically from about 5 keV to 10 keV, is dependent upon the

application, and can result in different calculated air-kerma rates for the same source used for different applications (ICRU, 1980; 2011).

11.2.1.5 Standards Work in Progress. As explained above, the dosimetry of high-energy photon brachytherapy sources is currently based on air-kerma-rate values at 1 m, although, for clinical applications, the relevant quantity is the absorbed-dose rate in water, measured in water at short distances, of the order of from 1 cm to 8 cm. The current conversion between air kerma and absorbed dose in water, as discussed in Section 11.4, is affected by certain uncertainties, and the purpose of introducing direct calibration in water is to improve the dosimetric accuracy by avoiding this conversion step (DeWerd *et al*., 2011; Soares *et al*., 2009). Recently, within the framework of the European Metrology Research Programme, a project has been launched to establish direct measurements of absorbed dose in water (Ankerhold and Ton, 2012). A set of independent experimental devices based on calorimetry are currently under development and testing. Proof-of-principle of a brachytherapy calorimeter has shown that calorimeter-based dosimetry is possible and that a calorimeter has the potential of becoming a primary standard (Sander *et al*., 2012; Stump *et al*., 2005).

11.2.2 Survey of Previously Used Source-Strength Descriptors

11.2.2.1 Radium Mass. Historically, the strength of radium sources was specified in terms of the mass of radium (units of mg) contained in the source. The encapsulating material affects the dose rate from a radium source, with the RAKR of a source encapsulated in 1 mm of platinum being about 93 % of that of a source with a 0.5 mm thick platinum wall (Shalek and Stovall, 1969).

11.2.2.2 The Milligram-Radium Equivalent. When artificial radionuclides became available as radium substitutes for use in brachytherapy, most manufacturers specified the sources in "milligram radium equivalent" in order to simplify the use of the sources as radium substitutes. The radium mass equivalent (mg Ra equivalent) of a source is the mass of radium, *filtered by 0.5 mm* of platinum, that will produce the same exposure rate as that from the radioactive source of interest at the same distance (a distance large enough that the relation between the exposure rate and distance approximates that for point sources) (Nath *et al*., 1987). Note that 1.0 mg Ra equivalent equals 7.227 μGy h^{-1} RAKR (Nath *et al*., 1995).

Because the conventional intracavitary radium sources had 1 mm platinum encapsulation while the radium substitutes had source strengths specified in the equivalent radium mass filtered with 0.5 mm platinum, the direct substitution using nominal source strengths often results in often unintended and potentially confusing dose differences, as noted above, of about 7 % (Shalek and Stovall, 1969). Because of the ambiguities in the specification and measurement of milligram radium equivalent, specification of brachytherapy sources in terms of milligram radium equivalent is now strongly discouraged.

11.2.2.3 Contained, Apparent, and Equivalent Activity. Radioactive source strengths can be specified in terms of their activity specified in units of becquerel (Bq); the older unit was the curie (1 Ci is equivalent to 37 GBq). Due to self-absorption and filtration within the source and its encapsulation, the contained activity is of little practical interest. The "apparent activity" of a source is defined as the activity of a bare (*i.e.*, unencapsulated) point source of the same radionuclide that would deliver the same exposure rate in air, at the same distance, along the perpendicular bisector from the center of the actual source (Nath *et al*., 1987). The distance should be large enough such that the relation between the exposure rate and distance approximates that for a point source. The expression "equivalent activity" has also been used instead of apparent activity (IAEA, 1967; ICRU, 1970). Its use is no longer recommended because it could lead to some confusion, as with the expression "milligram radium equivalent." Because of energy-related differences in attenuation in tissue, sources containing different radionuclides but with the same apparent activity do not give similar dose distributions.

11.2.2.4 Exposure Rate at 1 m. The strength of a radioactive source can be specified in terms of its output. One measure of "output" was the exposure rate at a reference distance. Before introduction of the SI system, the reference exposure rate in roentgens per hour at 1 m (R h^{-1} m^2) was used (Dutreix and Wambersie, 1975; NCRP, 1974). The SI unit for exposure rate is coulombs of charge (of one sign) collected per unit mass of dry air per unit time (C kg^{-1} h^{-1} = 3.88 $\times$ 10^6 R h^{-1}). Reference air-kerma rate is determined from the exposure rate. The ions measured by the exposure rate are the result of energy absorbed in air. Most of the energy transferred is eventually absorbed in the air, but some small fraction of the energy transferred is re-radiated through bremsstrahlung, characteristic x rays, or other radiative transfers. If $g(E)$ represents the fraction of the transferred energy so re-radiated, the relationship between

exposure rate at a meter, $\dot{X}_{1m}$ and RAKR becomes,

$$\dot{K}_{\delta,R} = \frac{\bar{W}}{e} \times \frac{\dot{X}_{1m}}{[1-g(E)]}, \qquad (11.1)$$

where $\bar{W}/e$ is the mean energy required to produce an ion pair in air. The fraction g of the energy re-radiated depends on the energy, E, of the incident radiation.

11.2.3 Advantages of RAKR

The RAKR facilitates comparison of applications performed with different radionuclides. For high-energy sources, including ^{226}Ra, ^{137}Cs, ^{60}Co, and ^{192}Ir, those with the same RAKR produce absorbed-dose distributions in tissue that are very comparable. In contrast, quantities such as the air-kerma-rate constant have to be applied when comparing sources specified in terms of apparent activity. While the older exposure rate at 1 m also allows a first-order comparison between sources, RAKR currently is the recommended quantity.

11.2.4 The Air-Kerma-Rate Constant, Γ_δ

The relation between RAKR and activity, A, for a unencapsulated point source is given by (ICRU, 1980):

$$\dot{K}_{air,\delta} = A \times \Gamma_\delta, \qquad (11.2a)$$

where Γ_δ is the air-kerma-rate constant and RAKR $= \dot{K}_{air,\delta}$ at 1 m from the source. As discussed in Section 11.2.1.4, the energy cutoff, δ, is used in the definition of Γ_δ.

For radium sources, the air-kerma-rate constant is specified in terms of RAKR and the equivalent mass of radium rather than activity. The air-kerma-rate constant has been used in some clinical absorbed-dose-calculation formalisms but is now mostly used in radiation-protection calculations. Because the apparent activity a source, A_{app}, equals the activity of an unjacketed point source of the same radionuclide that produces the same air kerma rate at a distance, for a source with strength specified in apparent activity, an equation similar to 11.2a obtains,

$$\dot{K}_{air,\delta} = A_{app}\Gamma_\delta \qquad (11.2b)$$

11.3 Total Reference Air Kerma

The total reference air kerma (TRAK) is the integral of the RAKR over the treatment duration, summed for all sources, without regard to the geometry of the application. The TRAK is a purely physical quantity with the following properties:

- The TRAK is easy to calculate quickly and without ambiguity.
- The absorbed dose in any organ and the integral dose in the patient are directly proportional to the TRAK, with approximately the same relationship for most of the high-energy-photon-emitting radionuclides used in cervical brachytherapy, such as ^{226}Ra, ^{137}Cs, ^{60}Co, and ^{192}Ir.
- The inverse-square law applied to the TRAK allows an estimation of the absorbed dose during treatment at distances greater than 15 cm from the centers of the sources (*i.e.*, in the pelvis and abdomen for cervical brachytherapy). If the distance of a point from the activity-weighted center of the volume occupied by the sources is greater than twice the largest dimension of that volume, the absorbed-dose rate obtained for the point from the actual distribution of the sources differs by less than 4 % from that obtained by assuming that all of the sources are located at the activity-weighted center (Quimby, 1970),
- A simple relationship does not exist between TRAK and the absorbed dose near the sources, *i.e.*, in the gross tumor volume and the CTV or to points such as Point A. Similarly, the TRAK does not allow the shape of the treated volume to be derived. However, it has been shown that the *volume* contained within a given isodose surface can be estimated from the TRAK to within 5 % for two-thirds of implants and to within 10 % for 95 % of them (Eisbruch *et al.*, 1993; Wilkinson and Ramachandran, 1989). This is because both the volume contained within an isodose surface and TRAK reflect the integral absorbed dose, but the shape of the isodose surface depends on the geometric distributions of the sources over time,
- The conversion of the product of milligram radium equivalent and hours (mg h) to the TRAK uses a constant with a value of 7.227 μGy (mg h)$^{-1}$. This facilitates the conversion of absorbed doses from the large worldwide clinical database built up over decades using the product into TRAK. A radium source of mass 1 mg filtered with 1 mm Pt corresponds to an RAKR of 6.72 μGy h^{-1}. A set of sources with 65 mg Ra equivalent, for example, left *in situ* for 6 days (144 h) corresponds to a TRAK of 67.6 mGy.
- In intracavitary applications, there is a correlation between TRAK and isodose-surface volumes as shown in Figure 11.1a (Datta *et al.*, 2003). The relationship between the absorbed dose at Point A and TRAK is more tenuous than with the reference volume, as shown in Figure 11.1b (Tanderup *et al.*, 2010a). Although there is a general tendency toward an increasing absorbed dose to Point A with increasing TRAK, in an individual patient, the relative deviation from the linear fit could be greater than 50 %.

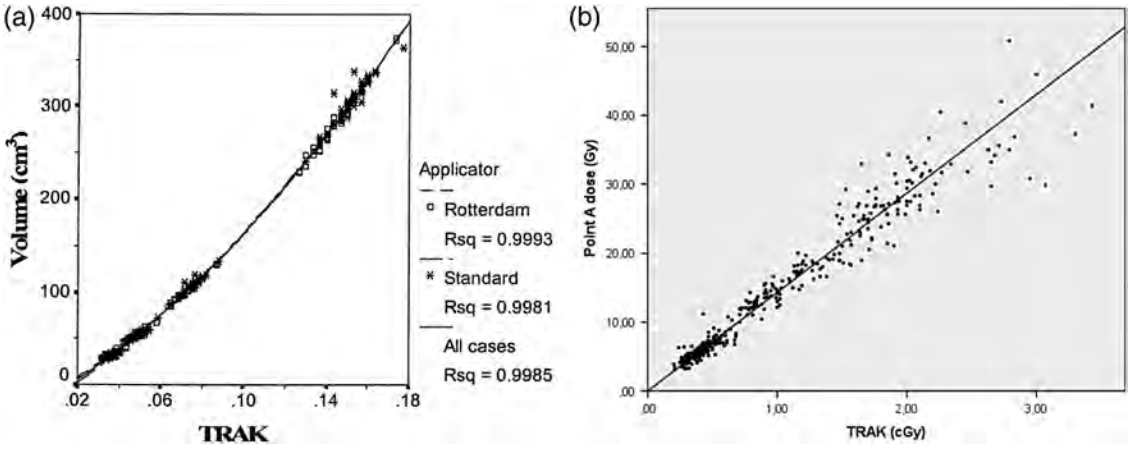

Figure 11.1. (a) The relationship between TRAK and the 60 Gy reference volume as specified in ICRU Report 38 (Datta *et al*., 2003; ICRU, 1985). (b) The relationship between TRAK and the absorbed dose at Point A (Tanderup *et al*., 2010a).

- Because biological effect varies with absorbed dose, absorbed-dose rate, and tissue type, there can be no direct relationship between TRAK and biological effect.

11.4 Absorbed-Dose Calculation

11.4.1 Absorbed-Dose-Calculation Formalism

The current model to calculate absorbed-dose distributions from a source follows the proposal by the Interstitial Collaborative Working Group (Anderson *et al*., 1990). The new formalism was adopted by Task Group No. 43 of the Radiation Therapy Committee of the AAPM (Nath *et al*., 1995; Rivard *et al*., 2004; 2007). Numerical values for the parameters for most gynecological sources currently in use can be found in the report of the joint High-Energy Photon-Emitting Brachytherapy Working Group of the AAPM and ESTRO (Perez-Calatayud *et al*., 2012). The Radiological Physics Center (RPC) maintains currently accepted, validated values for all of the absorbed-dose parameters for brachytherapy sources on their website. The model describes calculation of the absorbed-dose rate at a point (r, θ) in a medium as shown in Figure 11.2, where r is the distance from the center of the source to the point, and θ is the angle between the source axis and a line joining the center of the source to the point.

The equation for the absorbed dose to that point is

$$\dot{D}(r,\theta) = \dot{K}_{\delta,\mathrm{R}} \times 1\mathrm{m}^2 \times \Lambda \times \frac{G_\mathrm{l}(r,\theta)}{G_\mathrm{l}(r=1\,\mathrm{cm},\ \theta=\pi/2)} \times g_\mathrm{l}(r) \times F_\mathrm{l}(r,\theta), \qquad (11.3)$$

where the symbols are defined below.

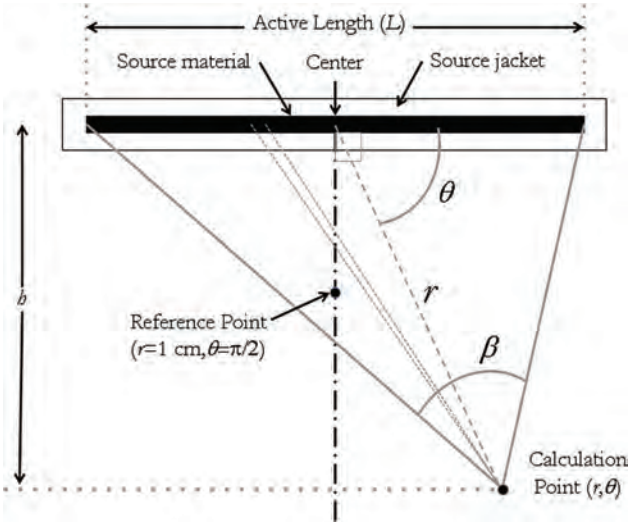

Figure 11.2. An illustration of the geometry and variables for the absorbed-dose calculation.

$\dot{K}_{\delta,\mathrm{R}}$ is the RAKR. Λ is the dose-rate constant for the radionuclide source in tissue. The dose-rate constant is defined as the ratio of absorbed-dose rate in water at a distance of 1 cm on the perpendicular bisector of the source per the product of (reference air kerma rate)$\times$(1 m^2). The dose-rate constant is characteristic of the particular source model and radionuclide. RAKR and the dose-rate constant are related in such a way that any change in the calibration standards for air-kerma strength produces a corresponding inverse change in the dose-rate constant.

$G_\mathrm{l}(r,\theta)$ is a geometric function, which accounts for the effects on the absorbed dose of the geometric relationship between the source material in the container and the point at which the absorbed dose is calculated. The geometric function is dominated by the inverse-square behavior of the contributions to

absorbed-dose rate from each volume element in the source. In the case of the ideal point source, $G_p(r,\theta)$ simply equals the inverse of the square of the distance to the source,

$$G_p(r,\theta) = \frac{1}{r^2}. \quad (11.4)$$

For a line source, $G_l(r,\theta)$ becomes

$$G_l(r,\theta) = \frac{\beta}{Lh} = \frac{\beta}{Lr\sin\theta} \quad (11.5)$$

where L is the length of the source, h the perpendicular distance from the calculation point and the source axis, and β the angle subtended by the source with respect to the point (r,θ) as shown in Figure 11.2.

The radial dose function, $g_l(r)$, accounts for absorption and scatter differences between the reference position at 1 cm and at a distance of r. The radial absorbed-dose function is calculated on the perpendicular bisector as:

$$g_l(r) = \left.\frac{\dot{D}(r)\times G_l(r=1\,\text{cm})}{\dot{D}(r=1\,\text{cm})\times G_l(r)}\right|_{\theta=\pi/2} \quad (11.6)$$

The introduction of the geometric function as defined in Equation (11.6) removes the effects of the geometry from the radial absorbed-dose function when taking the ratio of the doses at the two distances (1 cm and r).

$F_l(r,\theta)$ is the anisotropy function. This function accounts for the angular variation of absorbed-dose rate around the source due to filtration of the encapsulation and internal components and scatter in the medium, and is a function of the distance and angle. To eliminate purely geometric effects, the absorbed-dose rate is divided by the geometry function at that point. The equation for the anisotropy function is

$$F_l(r,\theta) = \left.\frac{\dot{D}(\theta)\times G_l(\theta=\pi/2)}{\dot{D}(\theta=\pi/2)\times G_l(\theta)}\right|_{\text{Evaluated at } r}. \quad (11.7)$$

When using sources for which the orientation is unknown, for example, permanent sources for which no current imaging modality can distinguish the axial direction, the point approximation would be appropriate. In that case, the absorbed-dose equation becomes

$$\dot{D}_p(r) = \dot{K}_{\delta,R}\times 1\text{m}^2\times\Lambda\times\frac{1\,\text{cm}^2}{(r)^2}\times g_p(r) \times\phi(r), \quad (11.8)$$

where the radial dose function is calculated using the point-source approximation for the geometry function,

$$g_p(r) = \frac{\dot{D}(r)\,(r)^2}{\dot{D}(r=1\,\text{cm})}, \quad (11.9)$$

and $\phi(r)$ represents the 4π average of the anisotropy function,

$$\phi(r) = \frac{\int_0^\pi \dot{D}(r,\theta)\times\sin(\theta)\times\text{d}\theta}{2\dot{D}(r,\theta=\pi/2)}. \quad (11.10)$$

With gynecological brachytherapy, the point approximation applies in very few situations, and the line model is used in most situations.

11.4.2 Inhomogeneity Correction and Applicator Influences on the Absorbed Dose

The absorbed-dose-calculation formalism presented above assumes all space is filled with water. Other approaches to dose calculation account for the true composition of the patient's anatomy and of the applicators. Although used in research for decades, they are just beginning to be incorporated into commercial treatment–planning systems. Examples of such approaches include Monte Carlo simulations and discrete-ordinance methods. Thomadsen *et al*. (2008) present a concise summary of inhomogeneity corrections in brachytherapy, and the American Association of Physicists in Medicine have issued a report on the topic (Beaulieu *et al.*, 2012). In a patient, most of the tissues differ little from water except for the bone and lung, which largely fall outside the volume of greatest interest in cervical cancer. Anatomic variations produce little change in the absorbed-dose distributions from the high-energy sources used in cervical brachytherapy. However, many applicators contain metal parts with high-atomic-number components that can distort distributions compared with calculations assuming a water medium. At the time of this writing, most treatment-planning systems have just introduced the capability to make corrections for inhomogeneities. The effect of attenuation by the applicator and/or by the sources might be more noticeable in the regions close to the axis of the applicator, for example, at rectum reference points close to the axes of vaginal ovoid sources. In practice, the attenuation by a thin applicator wall has a limited effect.

Applicators containing shielding material to reduce the absorbed dose in normal tissues [*e.g.*, tungsten disks in ovoid applicators, are used to limit the rectum or bladder absorbed dose (see Section 3.4.3) and markedly perturb the absorbed-dose distributions]. At the time of this writing, only two known commercial treatment–planning systems can make corrections for

such shielding, but it is expected that this capability will soon become widespread.

11.5 Recommendations for Reporting

Reporting of all cases should include:

(1) The radionuclide and source models used.
(2) The modality used [HDR, LDR, pulsed dose rate (PDR)].
(3) The TRAK.
(4) The geometric pattern of source-strength distribution (in RAKR or air-kerma strength) and treatment duration for LDR applications, or dwell-time pattern and source strength (in RAKR or air-kerma strength) for HDR and PDR applications.
(5) The algorithm used for the absorbed-dose determination.

11.6 Summary

The most common radionuclides used for gynecological brachytherapy vary somewhat between HDR and LDR and application techniques. For HDR intracavitary applications, ^{192}Ir is widely used, although ^{60}Co and ^{169}Yb are used to some extent, while for LDR intracavitary applications, ^{137}Cs and ^{192}Ir are used. For HDR or LDR interstitial applications, ^{192}Ir is the dominating nuclide.

The source strength should be specified in RAKR, $\dot{K}_{\delta,\mathrm{R}}$, in units of μGy h^{-1}, or equivalently, air-kerma strength, S_{K}, in units of μGy m^2 h^{-1}.

The RAKR of a source is defined as the air-kerma rate, in vacuum, due to photons of energy greater than δ, at a reference distance of 1 m from the source center, on a transverse plane normal to and bisecting the long axis of the source. In terms of older and historically used units, 1 mg Ra equivalent = 7.227 μGy h^{-1} in RAKR.

The TRAK is defined as the integral of the RAKR over the treatment duration, summed for all sources, and has units of μGy or allowed multiples, such as Gy or mGy. For a given application, absorbed doses to any point or volume are directly proportional to TRAK.

Brachytherapy absorbed-dose calculations should use the formalism found in the report of AAPM Task Group 43, described in this section.

Journal of the ICRU Vol 13 No 1–2 (2013) Report 89
Oxford University Press
doi:10.1093/jicru/ndw016

12. Treatment Planning

This section summarizes the practical aspects of clinical treatment planning for intracavitary cervical brachytherapy. Treatment planning is based on the overall planning aim for the combined dose distributions of external-beam radiotherapy (EBRT) and brachytherapy. Based on information available at diagnosis, a schedule for EBRT and brachytherapy, their relative contribution to the overall EQD2 for defined target volumes, fractionation, and timing is defined. Due to regression of the primary tumor, the target volume for brachytherapy can diminish significantly during treatment. Therefore, adaptive treatment planning is based on a reassessment of tumor and target volumes before and possibly at the time of brachytherapy. Adaptations of the brachytherapy implant itself to the anatomical situation after weeks of EBRT are also an integral part of the optimized adaptive-treatment-planning procedure. Adaptation is possible at different levels of complexity, ranging from the minimum requirement of a detailed clinical examination to image-guided approaches simulating the implantation technique and geometry (preplanning). During implantation, further optimization of the implant can be obtained by intraoperative image guidance. The final implantation geometry in relation to target volumes and organs at risks (OARs) is determined with volumetric imaging or radiographic approximation with the applicator in place. A set of dose–volume constraints for the individual brachytherapy fractions must be available prior to the optimization of dwell positions and dwell times, taking into account the pre-defined overall planning aims as well as spatial distributions of absorbed dose from previous brachytherapy and/or external-beam fractions. The method to achieve reproducible and controlled absorbed dose distributions is to start the optimization process with standardized loading patterns for the active dwell positions. In an iterative process, the dwell positions and dwell times are adjusted until an acceptable compromise between target coverage and OAR constraints is achieved. Inverse optimization and graphically assisted dose-distribution shaping should be performed with care as the spatial distribution of over-dosed and under-dosed spots within the treated volume is often changed substantially compared with the manual iterative procedure.

Clinical experience and quantitative radiobiology has shown that dose–effect curves for toxicity in the pelvis can be steep depending on the OAR and the chosen endpoint (Bentzen, 1993; Georg *et al*., 2012; Perez *et al*., 1998; Petereit *et al*., 1999; Pourquier *et al*., 1982; 1987). Figure 8.1 illustrates an example of dose–volume correlations for late rectal morbidity in cervical cancer patients treated with MRI-based brachytherapy, where a steep dose–effect is evident, especially when D_{2cm^3} is used as a descriptor of the cumulative dose of EBRT and brachytherapy EQD2 delivered to the rectum (Georg *et al*., 2009).

Considering the sharp absorbed-dose fall-offs inherent in brachytherapy, a close balance exists when attempting to deliver a curative absorbed dose to the tumor with minimal toxicity to neighboring structures (Dimopoulos *et al.*, 2009c; 2009d). The goal of treatment planning is to obtain the best possible chance for an uncomplicated cure of the individual patient (Holthusen, 1936) by careful planning of absorbed-dose delivery by a brachytherapy application (Kirisits *et al.*, 2005; 2006a; Pötter *et al.*, 2006). However, in the broadest sense, brachytherapy treatment planning should also involve an effort to implement brachytherapy into the whole treatment chain, including EBRT and concomitant chemotherapy, focusing on items such as balance of absorbed dose between EBRT and brachytherapy, overall treatment time, and brachytherapy-implant strategy (Lindegaard *et al.*, 2011). Radiographic-based gynecological brachytherapy has provided the basis for treatment planning and led to very impressive clinical results (Eifel *et al.*, 1994b; Gerbaulet *et al.*, 1995; Horiot *et al*., 1988; ICRU, 1985; Perez *et al.*, 1998; Pernot *et al*., 1995). The introduction of volumetric-image-based brachytherapy has added new information in terms of both volume for the target and OAR and how those volumes change with time, providing improved understanding (Barillot *et al.*, 1994; Haie-Meder *et al.*, 2010b; Kirisits *et al*., 2005; 2006a; Lindegaard *et al*., 2008; 2013; Pelloski *et al*., 2005; Pötter *et al*., 2007; 2011; Viswanathan *et al*., 2006b).

This section focuses on several steps of treatment planning, both at the overall strategic level and for optimization of the individual brachytherapy application. As illustrated in Figure 12.1, decisions at each step are critically linked to all previous levels of treatment planning. Pre-defined planning aims and dose constraints for the entire treatment (EBRT and brachytherapy) are essential to guide the specific treatment planning of each brachytherapy application for which (1) a set of target volumes and intended dose aims together with dose constraints for the OAR are defined, (2) the brachytherapy implant geometry is established, and (3) the absorbed-dose distribution is optimized to finally arrive at a dose prescription.

Brachytherapy offers many opportunities to achieve defined dose-planning aims. Variations of the time–dose pattern (absorbed-dose rate, fractionation) allow modification of the therapeutic window to deliver an optimal absorbed dose for the targets while sparing the OAR. Absorbed-dose delivery is performed *via* applicators, which provide the possibility for remote afterloading of the radioactive sources. Treatment planning is specific to the applicator type and location. The decision on the implant geometry and the definition of the dose-fractionation schedule are closely linked. Knowledge about the OAR close to the target volume can influence the choice of a specific fractionation schedule. After planning the time–dose pattern and the application geometry, the next step for stepping-source brachytherapy [both pulsed dose rate (PDR) and high-dose rate (HDR)] includes the determination of dwell positions inside the applicators and their respective dwell times. For low-dose-rate (LDR) brachytherapy, the choices for such optimization are often fairly limited, with the treatment time being the same for sets of sources.

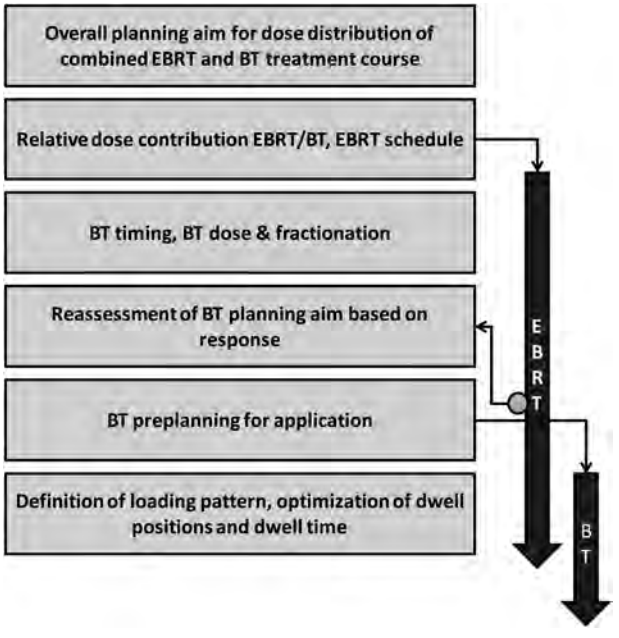

Figure 12.1. Hierarchy of action levels involved in the planning and prescription of combined EBRT and brachytherapy in locally advanced cervical cancer.

12.1 Combining EBRT and Brachytherapy: Dose and Fractionation Strategies

Clinical evidence supports the concept that definitive radiotherapy in gynecological malignancies should involve a combination of EBRT and brachytherapy to ensure optimal regional and local control and survival (Barraclough *et al.*, 2008; Beadle *et al.*, 2010; Gerbaulet *et al.*, 2002a; Han *et al.*, 2003; Lim and Sia, 2012). The whole pelvis is often treated with EBRT to 45 Gy–50 Gy at 1.7 Gy/fraction–2.0 Gy/fraction, sometimes with midline blocking after about 30 Gy of the portion of the field irradiating tissues assumed to receive high absorbed doses from the brachytherapy. Brachytherapy is added to reach total EQD2 values in the range of from 75 Gy to 95 Gy for the $D_{90\ \%}$ of the CTV_{HR} (Gerbaulet *et al.*, 2002a; Haie-Meder *et al.*, 2005; Pötter *et al.*, 2006).

Within many traditional approaches, the contribution to Point A from brachytherapy was most pronounced in early disease, whereas, in advanced disease, EBRT delivered a higher proportion of the dose. Current evidence from image-guided adaptive brachytherapy questions this approach because the relative dose contribution from EBRT and brachytherapy seems to give an optimal therapeutic ratio if approximately half the EQD2 contribution is delivered by each modality, reaching a $D_{90\ \%}$ in the CTV_{HR} of about 90 Gy EQD2 (Lindegaard *et al.*, 2013; Logsdon and Eifel, 1999; Pötter *et al.*, 2011). Attempts to replace the brachytherapy boost with advanced robotic EBRT or particle therapy have so far not produced a similarly favorable dose distribution, generally struggling to achieve the high dose in the center of the cervix without a significant increase in the pelvic volume outside the primary tumor target receiving a high dose (Assenholt *et al.*, 2008; Georg *et al.*, 2008). The relative dose contribution from EBRT and brachytherapy is also important when selecting EQD2 constraints for certain volumes of OAR, as changing the dose contribution of EBRT compared with brachytherapy will significantly influence the dose–effect curves for an OAR, mostly because of volume effects. Thus, if dose–volume histograms (DVH) constraints for total-EQD2 values are applied directly from the literature, care should be

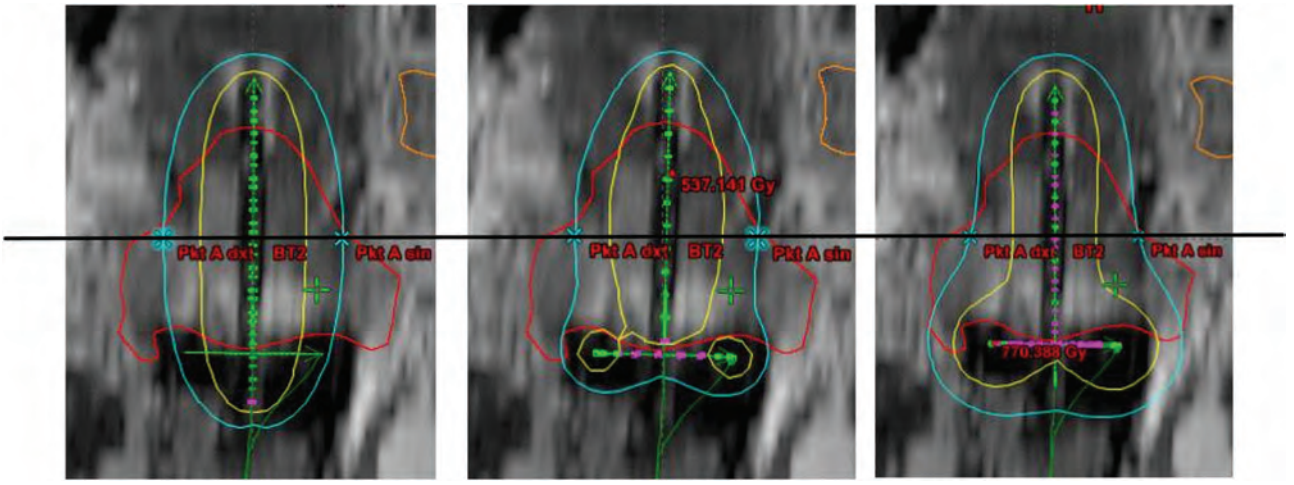

Figure 12.2. Examples of Point A-based standard loading patterns delivering the same absorbed dose to Point A, but using widely different vaginal and tandem loading. The image on the left shows an absorbed-dose distribution without vaginal loading, the middle image relates to a dose-point optimization along tandem-and-vaginal applicator, and the absorbed-dose distribution on the right is based on the same number of dwell positions with equal dwell times in the vaginal applicator and the tandem. The width of the Point A isodose volume is illustrated by the maximum width of the light blue isodose.

taken to also follow the same relative dose contribution of EBRT and brachytherapy. If the relative absorbed dose contribution of EBRT is substantially more than half of the total absorbed dose contributing to the $D_{90\ \%}$ of the CTV_{HR} or Point A, it is necessary to analyze DVH parameters that characterize the dose distribution in larger volumes of the OAR (see Section 8.4.3). On the other hand, a relatively larger dose contribution from brachytherapy accentuates the importance of the smaller OAR dose–volume metrics such as $D_{0.1cm^3}$.

Conventionally, the treatment with 3D-conformal EBRT and brachytherapy produced fixed dose distributions from the two radiation modalities and did not incorporate the effect of tumor regression during EBRT. Most often the combined dose was simply reported as a sum of physical absorbed doses of EBRT and brachytherapy to, for instance, Point A. Anatomical deformation due to the brachytherapy applicator limits the ability to calculate the true total absorbed-dose distribution from the two modalities without the assumption of homogeneity in the region of the EBRT field that covers the high-absorbed-dose portion of the brachytherapy. The traditional and widespread use of a parametrial boost is an issue that needs reconsideration in this context as this additional absorbed-dose contribution, even delivered with midline shielding, can add significant absorbed dose to those parts of the rectum, sigmoid, and bladder most exposed at brachytherapy (D_{2cm^3}) (Fenkell *et al.*, 2011; Lindegaard and Tanderup, 2012; Viswanathan *et al.*, 2012c). The use of a nodal boost should also be evaluated with regard to dose to the OARs which later will be exposed to high brachytherapy absorbed doses (Tanderup *et al.*, 2010a). With the increasing use of intensity-modulated radiotherapy (IMRT) combined with brachytherapy, examination of the homogeneity of the EBRT dose in the central part of the pelvis is also becoming very important (Tanderup *et al.*, 2010b) (see Section 8.5).

The increased complexity of treatment planning involved in image-guided adaptive brachytherapy (IGABT), including the use of composite brachytherapy applicators combining intracavitary and interstitial techniques (Dimopoulos *et al.*, 2006a) or custom-made vaginal molds (Albano *et al.*, 2008), might require a re-evaluation of the overall implant and fractionation strategy when switching from radiographic-based brachytherapy to volumetric image guidance. From the point of view of minimizing the resources involved in image-guided brachytherapy, it might be desirable to deliver more than one fraction of HDR brachytherapy using the same treatment plan and the same implant (Kirisits *et al.*, 2006b; Pötter *et al.*, 2011). However, this might reduce the advantage of outpatient treatment associated with HDR, as several hours between fractions (with the applicator in place) are needed to allow for complete recovery. For PDR, resource optimization might involve fewer, but larger, fractions delivered by an increasing number of hourly pulses to keep the average dose rate sufficiently low (Chargari *et al.*, 2009; De Brabandere *et al.*, 2008; Lindegaard *et al.*, 2008). In all circumstances, it is vital that fundamental changes in fraction size and timing of the brachytherapy boost, based on calculations, respect the limitations of the radiobiological models involved and also rests on published clinical experience.

Optimal timing of the brachytherapy in relation to EBRT involves several factors. Both MR and PET signals from the tumor are more intense before and in

the early weeks of treatment, which means that contouring of the brachytherapy target is easier in the early phase of therapy than after several weeks of EBRT (Dimopoulos *et al.*, 2012a). However, it is well known that significant tumor regression (70 %–80 %) often occurs during the first 3 weeks to 4 weeks of EBRT (Beadle *et al.*, 2009; Lim *et al*., 2008; Mayr *et al*., 2006), which can greatly improve the possibilities for target coverage and also enable a response-adapted brachytherapy prescription. As repopulation of tumor clonogens can have a detrimental effect if the overall treatment time is prolonged beyond 7 weeks (Chen *et al.*, 2003; Fyles *et al.*, 1995; Huang *et al.*, 2012; Petereit *et al*., 1995), the window of opportunity for maximal effect of IGABT for a large tumor with poor response to EBRT is likely to be the last 2 weeks to 3 weeks of a 7–8-week overall treatment time. For small and radio-responsive tumors with a CTV_{HR} volume $<30\ cm^3$, high target absorbed doses are normally achieved (Tanderup *et al.*, 2010a), and brachytherapy can therefore in these situations be delivered earlier in the course of treatment.

Applying target doses in excess of from 85 Gy to 90 Gy EQD2 within 6–8 weeks overall treatment time significantly accelerates dose delivery compared with conventional fractionation, which would take 2–3 weeks longer. Such accelerated treatment seems to be tolerable only using small-volume radiotherapy, such as IGABT (Maruyama *et al.*, 1994; Serkies *et al.*, 2001). There are no firm data on how close brachytherapy fractions can safely be combined with EBRT without risking consequential late damage (Hellebust *et al.*, 2010b; Wang *et al*., 1998). Most institutions using HDR brachytherapy deliver no more than two brachytherapy fractions for a maximal accumulated EQD2 of from 15 Gy to 20 Gy per week. For PDR brachytherapy with protracted delivery over 40–60 h with an average absorbed-dose rate of less than 0.6 Gy/h, the problem of dose intensity is less prominent.

12.2 Implant Geometry

12.2.1 Applicator type

The choice of implant geometry can be based on clinical examination and/or 3D imaging performed prior to or during the brachytherapy application. In most centers, the intracavitary applicator type, for example, tandem and ring, tandem and ovoid, or tandem with a vaginal mold, is determined by the preference of the radiation oncologist and availability of equipment. However, if several applicator types are available, the vaginal applicator type might be selected based on the vaginal geometry. With the availability of different diameters of rings or ovoids, the appropriate size is based on a clinical examination of the vagina, giving preference to the largest-size colpostats, rings, or cylinder that fit comfortably into the vaginal apex against the cervix.

Intracavitary vaginal applicators, such as colpostats and rings, allow for a laterally asymmetric absorbed-dose optimization in regions close to the vaginal sources. In contrast, the shape of the isodoses around the tandem become more and more cylindrical in the direction of the uterus, limiting the possibility of covering laterally situated target volumes at the mid and upper parts of the tandem due to absorbed doses in contra-laterally, anteriorly, and posteriorly lying OARs. In practice, the planning-aim isodose cannot be placed more than 25 mm from the tandem at the level of Point A (Kirisits *et al.*, 2006b; Kuipers *et al*., 2001). It can be pulled closer to the tandem if the OARs are receiving too high an absorbed dose, but it cannot be extended further from the tandem if targets exceed this distance. In cases of unfavorable anatomy with an asymmetric target volume, additional degrees of freedom for source-position placement are needed. Combination applicators have been developed that allow adjustments to the absorbed-dose distribution from intracavitary applicators by the addition of lateral dwell positions using interstitial needles (Dimopoulos *et al.*, 2006a; Kirisits *et al.*, 2006a; Kuipers *et al*., 2001; Nomden *et al.*, 2012; Petric *et al*., 2009; Tanderup *et al*., 2010a). This approach uses holes in the customary colpostats or rings as a guide for needle placement to keep the needles generally parallel to the intrauterine tandem. In order to minimize complications from needle insertion, blunt needles are recommended. Acceptable dose coverage 35 mm from the intrauterine tandem at the level of Point A, which usually covers at least half of the parametrium, has been reported with this combined interstitital/intracavitary approach (Kirisits *et al.*, 2006a). The additional needles for a combined intracavitary/interstitial implant can be inserted through the vagina with an accuracy of from 2 mm to 3 mm relative to their planned locations, and normally need to be inserted only 1 cm–5 cm into the tissue (Fokdal *et al*., 2013; Petric *et al.*, 2009). To increase lateral dose coverage to address distal parametrial residual disease, applications with additional obliquely directed needles have been reported (Berger *et al.*, 2010; Lindegaard and Tanderup, 2012). Free-hand oblique needle placement, in addition to intracavitary applications, has also been reported (Wakatsuki *et al.*, 2011). Despite all of these approaches, it is important to note that the absorbed-dose distributions used in published clinical series (Lindegaard *et al.*, 2013; Pötter *et al*., 2011) still largely follow from intracavitary

applications, with interstitial needles improving the dose distribution in the lateral direction. The dwell times in needles are normally limited to 10 %–20 % of that used for dwell positions in the intracavitary part of the implant (Kirisits *et al.*, 2006a).

Perineal templates consisting either of interstitial needles or catheters with or without a central vaginal obturator and uterine tandem can also be considered. Such techniques can be used for bulky cervical cancers with parametrial or vaginal spread, primary vaginal cancers, as well as recurrent cervical or endometrial cancers following previous hysterectomy. These applicators provide a higher dose at the center of the implant from the intracavitary components of the applicator while homogeneously covering the lateral parametrial disease and sparing, to some degree, the bladder and rectosigmoid (Beriwal *et al.*, 2006; 2012a; 2012b; Demanes *et al*., 1999; Dimopoulos *et al*., 2012b; Erickson *et al.*, 1996; Fokdal *et al*., 2011; Syed *et al*., 2002; Viswanathan *et al*., 2011a). The spatial distribution of absorbed dose in such implant geometries can vary substantially from intracavitary applications, especially if high-dose volumes are reduced in the central part of the implant (see Section 8.3.2).

12.2.2 Pre-planning of the implant

Pre-treatment imaging can be especially useful for difficult cases to determine the optimal applicator type, and in particular to assess the need for an interstitial approach or for an individualized vaginal applicator such as a mold (Albano *et al.*, 2008). Planning for simpler brachytherapy cases can involve a gynecological examination with a clinical drawing, whereas for more challenging cases, it might include additionally an MRI a few days before the actual implant. A pre-brachytherapy MRI with an intracavitary applicator *in situ* has been shown to be well suited for pre-planning of an individualized MRI-guided implant, including a virtual computer simulation of optimal needle positions for a combined intracavitary/interstitial implant (see Table 12.1) (Fokdal *et al*., 2013; Petric *et al.*, 2009). A pre-brachytherapy MRI without an applicator *in situ* can also be considered and is useful if only CT imaging is available with the applicator in place (Federico *et al.*, 2011).

In principle, planning for cervical brachytherapy should be performed both pre-operatively and intraoperatively—analogously to image-guided prostate brachytherapy planning (Nath *et al.*, 2009). However, presently many centers perform the detailed planning only in the post-operative phase. Table 12.1 presents a schematic overview of current possibilities for pre- and intra-operative planning of cervical cancer brachytherapy to help make the best individual choice of applicator type, implant technique, and applicator placement in relation to the anatomical situation at the time of brachytherapy. This is particularly important when large-volume disease is still present and interstitial needles have to be precisely applied to obtain the planning aim of the treatment.

12.3 Loading Pattern and 3D Absorbed-Dose Distribution without Reference to Targets

The dose distribution from brachytherapy plans is based on the time and spatial distribution of sources. With radium and its substitutes (see Section 11), the loading pattern was determined by the activity and location of the radionuclide-containing tubes combined for the treatment (see Section 3.2.3). For LDR applications, the source strength chosen for the intrauterine and vaginal applicators usually was determined according to tumor size. With the introduction of remote afterloading equipment with stepping source technology, the loading pattern became the distribution of active dwell positions in step sizes of from 1 mm to 10 mm.

The different approaches to intracavitary brachytherapy result in different absorbed-dose distributions. For example, an equal distribution of TRAK values between the tandem and ovoids produces a pear-shaped isodose with an extended width. Variations in the ratio of ovoid-to-tandem loading existed in the Paris, Stockholm, and Manchester systems. Lower ratios mean decreasing the width of the pear-shaped isodose at the level of the vaginal sources, with potentially more absorbed dose from the tandem. Without vaginal sources, the absorbed-dose distribution can be optimized to a constant width along the tandem.

In LDR tandem loadings, the most-cranial source tube usually carries a higher activity than those inferior to it. Stepping-source remote afterloading covers the length of an LDR source using several dwell positions, allowing greater flexibility in shaping the absorbed-dose distribution. The loading in the ovoids or ring can be adjusted, so that the shape of the absorbed-dose distribution becomes more conformal to the target while minimizing the absorbed dose to the rectum, bladder, and vagina.

The width, height, and thickness of the isodose volumes for the same applicator can differ substantially, based on the loading. In one study, seven different European and American institutions provided their standard loading patterns for the same tandem-ring applicator, with some examples shown in Figure 11.2 (Jürgenliemk-Schulz *et al.*, 2010) and also for the tandem-ovoid applicator (Nomden *et al.*, 2013a). The

Table 12.1. Systematic overview of pre-planning.

Pre-operative	Without volumetric imaging	Without applicator in place: Decisions on applicator type and implant geometry can be based on clinical examination assessing the vaginal and tumor topography in relation to the dimensions of the planned application, for example to estimate the lateral distance of the tumor extension into the parametrium in relation to the cervical os With applicator in place: This is used in the "mold technique," where the applicator is modeled from a vaginal impression. The outer dimensions are based on the vaginal topography, and the position of the vaginal catheters and their lengths are determined based on tumor extension and size, as identified on the vaginal impression and determined from the clinical examination The suitability of standard cylindrical vaginal applicators in relation to the vagina and tumor topography can also be considered
	With volumetric imaging	Without applicator in place: "Imaging just prior to brachytherapy" allows assessment of the configuration and the dimensions of the CTV_{HR} and the topography of OARs. "Imaging at the time of diagnosis" determines the CTV_{IR} Care has to be taken with regard to the interpretation of such imaging, because the ensuing insertion of any intracavitary applicator will substantially change the topography of the uterus and target volumes and their relation to the OARs, the vaginal axis, and also the outer body surface With applicator in place: The use of interstitial components can best be planned by imaging after inserting the intracavitary applicator including the tandem. The applicator then serves as fixed template for needle insertion during the final implantation (Fokdal *et al.*, 2013; Petric *et al.*, 2009). The image set then allows the "simulation of interstitial implant geometries and a full treatment pre-plan with regard to target coverage and OAR constraints." The most appropriate configuration for the following brachytherapy can be selected
Intraoperative	Without volumetric imaging	Before the insertion of the brachytherapy applicator, a comprehensive clinical examination under anesthesia is essential to plan implant. Information obtained from this examination in combination with any pre-operative plans will then be used to optimize the implant
	With volumetric imaging	During insertion of the applicator: The insertion of the intrauterine tandem can be guided by trans-abdominal or trans-rectal US in order to facilitate appropriate positioning in the uterine cavity. The vaginal sources can be checked in relation to the tumor extent by trans-rectal US. Needle placement into parametrial tissue can be visualized through US or with MRI With applicator in place: Post-implant imaging allows for evaluating the quality of an implant with regard to dose–volume constraints for target and OAR. If the situation is judged as inappropriate, adjustment of the application can be performed or the addition of needles in an iterative procedure supported by applicator guidance such as holes in the vaginal applicators may be used

In all situations, a comprehensive clinical examination is essential to plan the application.

width of the normalized Point A isodose volume reported in these studies ranged from 4.8 cm to 6.0 cm at the level of the ring applicators.

Standard sets of active dwell positions similar to standardized radium-tube configurations can and have been used. Without any imaging, such standard loadings are based on the clinical examination. A set of positions is activated at fixed locations inside the applicator according to the geometry of the applicator. Usually, a symmetrical loading in the vagina, with an identical number of dwell positions in the left and right ovoid or left and right portion of the ring, is used. This is based on the assumption that the vaginal applicator is oriented with the left–right axis of the applicator centered on the uterus with symmetric disease. A standard loading with the absorbed dose normalized to Point A will always result in the same absorbed-dose distribution relative to that applicator as long as the parts of the applicator are fixed with respect to each other; for applicators such as the Fletcher, in which the ovoids and the tandem are positioned independently, the absorbed-dose distribution varies from patient to patient. Ring or ovoid dwell positions usually fall approximately midway between the bladder and rectum. Non-ideal applicator placements with asymmetrical bladder or rectum positions result in unfavorable absorbed-dose distributions when using such standard applicator-based loading patterns.

Patient-specific loading patterns can be used if 3D information on the physical relationship between anatomy and applicator is available. The location of dwell positions can be adjusted relative to orientations and the position of the applicator relative to the patient's anatomy. In such cases, the dwell positions can be positioned left and right symmetrically in-between rectum and bladder, independent of the applicator orientation. More sophisticated approaches

might use fixed margins to the OAR and targets to define automatically the active positions to be used for further dwell-time optimization (auto-margins).

As an alternative to standard dwell positions and dwell weights in a standard loading, many facilities use optimization goals relative to the applicator (Nag *et al.*, 2000; Thomadsen, 1995). This approach is particularly useful for applicators without fixed relationships between the parts or when the treated length, for instance, in the tandem is adjusted for individual patients.

Because all the approaches described above create absorbed-dose distributions based on the applicator, following any of them results in highly variable absorbed dose in the CTV_{HR}. In general, when using standardized approaches, tumors with a radial width less than 2 cm tend to receive absorbed doses significantly higher than the Point A absorbed dose, whereas those with more than 2 cm receive a lower absorbed dose (Tanderup *et al.*, 2010a). Furthermore, the OARs tend to be closer to the implant in small-volume tumors, which means that OAR constraints are more often violated for small tumors when standardized approaches are applied.

12.4 Optimization of the Dose Distribution

12.4.1 General aspects of dose optimization

At present, dose planning for cervical brachytherapy is based on a limited number of dose–volume constraints and planning aims. Simple techniques have been based on the TRAK (formerly expressed in mg Ra), the absorbed dose to single points (*e.g.*, Point A), or the dimensions of reference isodose lines (*e.g.*, 60 Gy). For the OAR, radiographic planning provides additional points for dose assessment. With the use of DVHs, not only single-point absorbed doses, but dose–volume relationships can be expressed both for the target and for the OARs (rectum, sigmoid, bowel, bladder) and used as dose constraints for planning, recording, and reporting (see Section 8). However, the spatial distribution of absorbed dose is not fully described either by a set of dose points distributed throughout the treated volume or by any DVH.

An intracavitary implant produces a high-absorbed-dose region located around the applicators, in most cases enclosing the GTV and the CTV_{HR}. Combination treatments with interstitial needles should therefore maintain the high-absorbed-dose region located around the intrauterine channel because high absorbed doses in the center of the CTV seem to be more effective in terms of local control compared with homogenous absorbed-dose profiles (Viswanathan *et al.*, 2009). At the level of the lower cervix and upper vagina, the lateral width of the isodose pattern is larger than the antero-posterior thickness in order to spare the bladder and the rectum. Three-dimensional dose recommendations have been used for the rectum, sigmoid, and bladder, but not yet for the vagina (Lindegaard *et al.*, 2013; Pötter *et al.*, 2011). The situation is more complex for the vagina, which in addition to being an OAR also might be part of the brachytherapy target. Some traditional treatment approaches have used absorbed dose to vaginal points as constraints. This is also emphasized in this report, even to validate a 3D approach. In addition, there are regions around target volumes and contoured OARs (*e.g.*, the connective tissue around the uterus, the ureter, the urethra, nerves, and blood vessels where absorbed doses are not assessed). As no 3D-contouring recommendations have been defined so far, no dosimetric parameters and constraints are suggested for these structures. However, with the standard loading patterns and standardized absorbed-dose distributions, there is a large clinical experience showing that these absorbed-dose distributions are only rarely linked to major morbidity in these structures. Standard absorbed-dose distributions also deliver very high absorbed doses to the mucosa of the uterus, adjacent stroma, and whole cervix, but more moderate absorbed doses to the more distant uterine stroma, parametrium, rectum, bladder, sigmoid, nerves, vessels, urethra, and ureter. High absorbed dose occurs also in the vaginal mucosa due to the close proximity to the sources. Future research work should determine how to reduce the vaginal absorbed dose under certain clinical conditions (*e.g.*, cases with no apparent involvement of the vagina). At present, most centers maintain a conservative loading pattern along the caudal border of the CTV_{HR} leading to relative large margins between the CTV_{HR} and the treated volume.

If the cranial part of the CTV_{HR} does not reach far into the uterine corpus, loading patterns for cervical brachytherapy might not need to include the full length of the intrauterine applicator. Avoiding dwells high in the tandem without compromising the CTV_{HR} is advantageous, as the sigmoid and small bowel are often close to the applicator in that region. Reducing the superior dwells in the tandem must be done with caution if only CT is used for imaging, as this modality usually does not allow for a clear definition of the cranial extent of the cervical tumor. However, as uncertainties in applicator reconstruction unfortunately are most pronounced in the same direction, the intrauterine tip loading should not differ substantially from conventional standard loading for which there is no need for sigmoid absorbed-dose reduction (see Sections 5.4.6 and 5.5).

The use of image-defined, anatomy-based loading patterns can improve the absorbed-dose distribution

for the CTV_{HR}. The number of active dwell positions and their location inside the applicator can be adjusted based on the applicator's relationship to the target and the OARs. Margins defined to automatically perform dwell-position activation by treatment-planning software can be used to keep dwell positions at a minimum distance from an OAR. With the bladder in front and the rectum behind the vaginal applicator, this will automatically result in loading limited to the lateral parts of the ring or avoiding the most anterior and posterior positions in the ovoid.

As noted previously, asymmetric target configurations extending beyond a certain lateral distance from the tandem or the vaginal sources require placement of additional interstitial sources in order to reach appropriate dose coverage in these parts of the target. The ratio of the loading in the intrauterine, vaginal, and interstitial applicators influences the spatial distribution of absorbed dose substantially. Reported clinical experience with combined intracavitary/interstitial implants is so far based on clinical cases for which from 80 % to 90 % of the absorbed dose was delivered *via* intracavitary applicators and only from 10 % to 20 % *via* interstitial needles (Kirisits *et al.*, 2006a; Lindegaard *et al*., 2013; Pötter *et al.*, 2011).

12.4.2 Forward planning

Iterative forward planning is considered to be state-of-the-art. The absorbed-dose distribution resulting from the initial loading pattern is evaluated using the constraints for absorbed-dose points, DVH parameters, and careful anatomical inspection of the isodose distribution. If the resulting absorbed-dose distribution does not meet the planning aims, changes are made. These changes can be performed manually or with graphical tools. Great care should be taken when changing one isodose curve on only a single sectional image as this can result in unexpected absorbed-dose changes at other locations and other absorbed-dose levels (Kirisits *et al.*, 2011; Viswanathan *et al.*, 2011b). Forward planning includes, in general,

- the addition of dwell positions to increase missing coverage, either in intracavitary applicators or interstitial applicators, if available,
- scaling the absorbed-dose distribution by overall multiplication of all dwell times by a factor,
- adjusting individual dwell times for target coverage and possibly reducing individual dwell times to decrease the OAR dose.

After each iteration, the dose distribution is evaluated until either the planning aims are fulfilled or an acceptable compromise is reached. The final TRAK can be compared with a standard-plan TRAK to measure the scope of the changes relative to an initial loading pattern.

12.4.3 Inverse planning

The use of inverse planning based on volumetric parameters in brachytherapy has been reported mainly for interstitial brachytherapy (Lahanas *et al.*, 2003; Pouliot *et al.*, 2005). The objective of inverse planning is to improve the dose distribution and decrease the time to prepare a treatment plan. On the other hand, inverse optimization can take into account only clearly described objectives and constraints. Several important structures, for example, nerves, vessels, the vagina, ureter, and urethra, are not routinely contoured. Even if they were, dose constraints for these tissues are currently unknown. In addition, as most clinical experience so far has been based on forward planning, it follows that the spatial distributions of absorbed dose involved in this experience do not deviate dramatically from the conventional treatment plans from which the optimized loading patterns are derived (Kirisits *et al.*, 2006a; Tanderup *et al.*, 2010a). Major deviations from the standard pear-shaped loading pattern should be carefully studied before clinically implemented (Jamema *et al.*, 2010).

Especially for large tumors and combined intracavitary–interstitial implants, the DVH constraints on contoured organs will not restrict the algorithm from escalating absorbed doses in regions without contours. In order to control the spatial distribution of absorbed dose, many optimization approaches require additional constraints on dwell-time gradients or maximum dwell times. A special technique might be the use of different optimization rules for different parts of an implant (intracavitary *versus* interstitial applicators) while locking the dwell times and loading for the remaining already-optimized dwell positions (Trnkova *et al.*, 2009). Alternatively, "dummy" structures, similar to those commonly used in IMRT, in the region of needles, tandem, and vaginal sources can be useful (Chajon *et al.*, 2007). Such methods can be also applied to increase the conformity of the absorbed-dose distribution. However, the additional time for contouring such structures should always be balanced with the time it would take to perform a manual optimization or a manual adaptation of an inversely optimized dose plan. The potential of inverse planning also depends on the degrees of freedom in placing dwell positions and modifying dwell times. For simple target volumes that can be covered by intracavitary approaches alone, the benefit of inverse dose planning remains marginal (Jamema *et al.*, 2010; Trnková *et al.*, 2010).

However, in cases involving additional needles, resulting in a higher degree of freedom for the dose planner, the optimal solution might not be found by manual planning, but instead by a carefully developed concept of objectives with absorbed-dose and volume constraints, as well as constraints to control the dwell times in the different parts of the implant (Trnkova *et al.*, 2009).

12.4.4 Optimization by changing absorbed-dose rate in LDR and PDR treatments or fraction size in HDR brachytherapy

There is some flexibility to manipulate and optimize the absorbed-dose rate or pulse size and frequency using LDR or PDR brachytherapy. For the same total absorbed dose, an increased treatment time or higher number of pulses reduces the absorbed-dose rate, and consequently, the effective biological effect. In particular, the therapeutic window can be widened by decreasing the absorbed-dose rate, because the EQD2 for late effects in the OAR is affected more strongly by absorbed-dose rate than the EQD2 in the tumor. It is of particular interest to increase the number of pulses in cases in which the target coverage is compromised due to organs-at-risk-dose constraints. For HDR treatments, the fractions size can be adapted. Smaller-fraction doses allow for a widening of the therapeutic window.

12.5. Key Messages

- Image-guided adaptive brachytherapy is based on tumor regression obtained during 5–6 weeks of EBRT. Adaptive brachytherapy should therefore be applied toward the end, or shortly after completion, of EBRT. However, the overall treatment time including brachytherapy should not exceed 7–8 weeks.
- Adoption of certain values for the cumulative dose of EBRT and brachytherapy with regard to planning aims for the brachytherapy targets and DVH constraints for the OARs should also include adoption of the same relative dose contribution of EBRT and brachytherapy as used in the situations from which these values are taken.
- With the current dose-planning systems, an accurate calculation of the cumulative dose of EBRT and brachytherapy requires a homogenous EBRT dose distribution in the central part of the pelvis where brachytherapy is applied. When EBRT boosting of the tumor, parametria, or nodes is used, total dose summations might not be accurate, and commonly accepted dose–volume constraints might not be valid.
- Forward planning is the current standard of care, retaining a classical pear-shaped isodose distribution with a high central absorbed dose as far as possible. The optimization process should therefore preferably originate from a well-known and accepted standard loading of the given applicator.
- For combined intracavitary/interstitial implants, current clinical experience is based on a relative absorbed-dose contribution from the interstitial component of <20 %, with from 80 % to 90 % of the brachytherapy absorbed dose from the intracavitary applicator.

12.6 Summary

Treatment planning considers and encompasses the overall planning aim for the intended absorbed-dose distribution, provided by a combination of EBRT and brachytherapy. Based on the information available at diagnosis, a schedule for EBRT and brachytherapy, their relative contribution to the overall dose for defined target volumes and organs at risk, fractionation scheme, and timing is defined. Due to regression of the primary tumor, the target volume for brachytherapy can change significantly as a result of EBRT. Therefore, the adaptive-treatment-planning approach is followed, and the target volumes before and possibly during brachytherapy are reassessed. In other words, adaptation of the brachytherapy implant itself to the anatomical situation after several weeks of EBRT is an integral part of the optimized adaptive-treatment-planning procedure.

This is, however, possible at different levels of complexity, ranging from the minimum requirement of a detailed clinical examination to advanced image-guided approaches simulating the implantation technique and geometry (pre-planning). During implantation, further optimization of the implant can be obtained by intraoperative image guidance. The final implantation geometry in relation to target volumes and the OARs is determined with volumetric imaging or radiographic approximation with the applicator in place.

Taking into account the pre-defined overall planning aims and dose of previous brachytherapy and external-beam fractions, a set of treatment–planning constraints for the individual brachytherapy fractions has to be available prior to the optimization of dwell positions and dwell times. These constraints include dose and volume parameters, but should take into account also the spatial distribution of absorbed dose. The recommended method to achieve reproducible and controlled absorbed-dose distributions is to start the optimization process with standardized loading patterns for the active

dwell positions. In an iterative process, the dwell positions and dwell times can then be adjusted, until the best compromise for target and OAR constraints is achieved. Inverse and computerized treatment-plan optimization, as well as graphically assisted absorbed-dose-distribution shaping, should be performed with great care as the spatial distribution of hot and cold absorbed-dose spots within the treated volume is often changed substantially compared with the manual iterative procedure.

Journal of the ICRU Vol 13 No 1–2 (2013) Report 89
Oxford University Press
doi:10.1093/jicru/ndw015

13. Summary of the Recommendations

A short summary of the report recommendations in tabular form is provided below as an overview of the most essential conditions and parameters fundamental for reporting. More detailed tabular summaries are provided at the end of the Sections 5 through 8, 10, and 11. Recommended reporting is structured using a "level" approach:

Level 1 describes the minimum requirements that should be followed at all centers, for all patients, and represents the minimum standard of treatment;

Level 2 indicates advanced standards of dose planning and treatment that allows a more comprehensive and standardized exchange of information between centers and is based on a more complete set of parameters;

Level 3 describes new forms of planning and treatment largely related to research and development for which reporting criteria are yet to be established.

Level 1: *Minimum standard for reporting*

Volumetric-imaging approximation based on:

- Comprehensive clinical gynecologic examination
- Volumetric imaging (MR, CT, US, PET–CT) at the time of diagnosis and brachytherapy

FIGO/TNM stage

Baseline morbidity and QoL assessment

Schematic 3D documentation on a clinical diagram indicating dimensions (width, thickness, height) and volumes for:

- GTV_{init} (the GTV at diagnosis)
- GTV_{res} (the GTV at brachytherapy)
- CTV_{HR} [the GTV_{res} (if present) plus residual pathologic tissue (if present) plus whole cervix]
- (CTV_{IR}: area of GTV_{init} and/or CTV_{HR} plus safety margin if used for prescription)

Dose reporting:

- TRAK
- Point A dose
- Recto-vaginal reference-point dose
- $D_{0.1cm^3}$ and D_{2cm^3} for the bladder and rectum

Dose delivery pattern:

- Absorbed-dose rate/dose per fraction
- Number of fractions
- Time between fractions
- (Pulse number, size, time, if PDR)
- Overall treatment time
- Total EQD2 dose

Source and dose calculation:

- Radionuclide and source model
- Source strength
- Dose-calculation algorithm

Radiographic approximation based on:

- Comprehensive clinical gynecologic examination
- Radiographic imaging (plus additional volumetric 3D imaging if available)

FIGO/TNM stage

Baseline morbidity and QoL assessment

Schematic 3D documentation on a clinical diagram indicating dimensions [width, thickness, (height)] and volumes for:

- GTV_{init} (the GTV at diagnosis)
- GTV_{res} (the GTV at brachytherapy)
- CTV_{HR} [the GTV_{res} (if present) plus residual pathologic tissue (if present) plus whole cervix]
- (CTV_{IR}: area of GTV_{init} and/or CTV_{HR} plus safety margin if used for prescription)

Dose reporting:

- TRAK
- Point A dose
- Recto-vaginal reference-point dose
- Bladder reference-point dose

Dose delivery pattern:

- Absorbed-dose rate/dose per fraction
- Number of fractions
- Time between fractions
- (Pulse number, size, time, if PDR)
- Overall treatment time
- Total EQD2 dose

Source and dose calculation:

- Radionuclide and source model
- Source strength
- Dose-calculation algorithm

Level 2: *Advanced standard for reporting*
All that is reported in Level 1 plus:

Volumetric-imaging approximation based on:

3D delineation of volumes (on volumetric images with applicator):

- GTV_{res}
- CTV_{HR}
- (CTV_{IR} if used for prescription)
- With maximum width, height, thickness, and with volume

Dose reporting for defined volumes:

- $D_{98\ \%}$, $D_{90\ \%}$, $D_{50\ \%}$ for the CTV_{HR}
- ($D_{98\ \%}$, $D_{90\ \%}$ for the CTV_{IR} if used for prescription)
- $D_{98\ \%}$ for GTV_{res}
- $D_{98\ \%}$ for pathological lymph nodes

Dose reporting OARs:

- Bladder reference point dose
- $D_{0.1cm^3}$, D_{2cm^3} for sigmoid[a]
- D_{2cm^3} bowel
- Intermediate- and low-dose parameters in bladder, rectum, sigmoid, bowel
  (*e.g.*, $V_{15\ Gy}$, $V_{25\ Gy}$, $V_{35\ Gy}$, $V_{45\ Gy}$ or $D_{98\ \%}$, $D_{50\ \%}$, $D_{2\ \%}$)
- Vaginal point doses at level of sources (lateral at 5 mm)[a]
- Lower- and mid-vagina doses (PIBS, PIBS $\pm$ 2 cm)[a]

Radiographic approximation based on:

Topography for volumes (on isodose plan with applicator/on radiographs with applicator)

- GTV_{res}
- CTV_{HR}
- CTV_{IR} (if used for prescription)
- With maximum width, thickness, standard height, and with volume

Dose reporting for defined volumes:

- Estimated dose to CTV_{HR}
- (according to estimated maximum width and thickness)
- Pelvic wall point (optional)
- Lymphatic trapezoid (optional)

Dose reporting OARs:

- Vaginal point doses at level of sources (lateral at 5 mm)
- Lower- and mid-vagina doses (PIBS, PIBS $\pm$ 2 cm)

[a]Surrogate points for volumetric vaginal dose assessment.

Level 3: *Research-oriented reporting*
All that is reported in Level 1 and 2 plus:

Volumetric-imaging approximation based on:
Tumor-related volumes:
(1) GTV, CTV_{HR} sub-volumes based on functional imaging (diagnosis, during treatment, and at brachytherapy)
(2) PTV

Isodose surface volumes:
For example

- 85 Gy EQD2 volume
- 60 Gy EQD2 volume

Dose reporting for tumor:

(1) $D_{98\ \%}$ and $D_{90\ \%}$ for the CTV_{IR} even if not used for prescription
(2) $D_{90\ \%}$ for the GTV_{res}
(3) DVH parameters for the PTV
(4) $D_{50\ \%}$ for pathological lymph nodes
(5) DVH parameters for non-involved nodes (ext/int iliac, common iliac)

OAR volumes and points:

(1) Additional bladder and rectum reference points
(2) OAR sub-volumes (*e.g.*, trigonum or bladder neck, sphincter muscles)
(3) Vagina (upper, middle, lower)
(4) Anal canal (sphincter)
(5) Vulva (labia, clitoris)
(6) Other volumes/sub-volumes of interest (*e.g.*, ureter)

Dose–volume reporting for OAR:
(1) Dose–volume and dose–surface histogram parameters for additional OARs and sub-volumes
(2) Vaginal dose profiles, dose–volume, and dose–surface histograms
(3) Length of treated vagina

Radiographic approximation based on:

Isodose surface volumes: For example

- 85 Gy EQD2 volume
- 60 Gy EQD2 volume

OAR volumes, points:

(1) Additional bladder and rectum points
(2) Sigmoid point
(3) Anal-canal point (*e.g.*, low vagina point)
(4) Vulva point (*e.g.*, low vagina point)
(5) Other points of interest

OAR dose reporting:

- Length of treated vagina

The modern practice of gynecologic oncology and of brachytherapy in particular is founded in significant resources for patient work-up, imaging, preparation, treatment planning, and delivery. However, the availability of the full range of resources varies dramatically throughout the world. Hence, "recording and reporting" must reflect these variations and enhance the available information by using common agreed to communication tools. Presently, the two major routes for applying brachytherapy depend currently on the availability and utilization of imaging at the time of brachytherapy: radiographic or volumetric three-dimensional (3D) imaging (CT, MRI, US). To provide an appropriate level of reporting for both "worlds," a separation within each level is established for the clinical and volumetric approach (CT, MRI, US) on the one hand, and the clinical and radiographic approach on the other hand. This allows for appropriate attribution according to the available resources. Recommendation "boxes" are therefore organized in two columns. Exchange of information is possible within and also between the different levels and also between the different columns.

For external-beam radiotherapy reporting, the recommendations for reporting given in ICRU Reports 83, 62, and 50 (ICRU, 1993; 1999; 2010) should be followed.

In the examples provided in the Appendices, the parameters for reporting are specified for external-beam radiotherapy in a specific table, separately, as they are for brachytherapy. The contribution of EBRT and brachytherapy has to be taken into account for the various targets as well as for the OARs. For the OARs, EBRT reporting in the Appendix examples, follows a $V_{\text{absorbed dose}}$ and a $D_{\text{volume percentage}}$ approach as in ICRU Report 83 (ICRU 2010). For brachytherapy reporting, the specific recommendations given here are to be used. A total dose is provided as EQD2 by summing the contributions of EBRT and brachytherapy for specific parameters that have been proven to be feasible under certain conditions (see Section 8.5). A comprehensive reporting of both EBRT and brachytherapy contributions is particularly important if one or both varies significantly from what is regarded as "typical" in widespread practice, namely each contributing about a 50 % to the EQD2 dose to the CTV_{HR}.

Dose reporting for radiotherapy in cervical cancer relies on incorporation of both EBRT and brachytherapy doses. The variation of fractionation schemes necessitates assessment of the biological equieffective doses (EQD2), which is the prerequisite for meaningful communication and reporting. Assessment of dose follows a specific route, starting with assessment of the fractional absorbed dose, thence the fractional EQD2, and finally to the total EBRT + brachytherapy EQD2. General principles of dose assessment and reporting are summarized in Table 13.1.

Table 13.1. General principles for assessment and reporting of absorbed and equieffective EBRT and brachytherapy dose (all reporting levels).

Reporting of dose for relevant targets, OARs, and dose points:
- Planning-aim dose
- Prescribed dose
- Delivered dose

Absorbed dose and number of fractions assessed for target, OARs, dose points:
- Brachytherapy
- EBRT

Total equieffective dose (EQD2) calculated according to the linear-quadratic model through the following steps:
(1) Brachytherapy EQD2 for each fraction
(2) Total brachytherapy EQD2
(3) Total EBRT EQD2
(4) Accumulated total EBRT + brachytherapy EQD2 (based on current assumptions outlined in Sections 7.6, 8.5, 9.5.3)

Reporting of radiobiological parameters:
- α/β values for tumor and OARs; In addition, $T_{1/2}$ and recovery model for LDR and PDR treatments(At present: $\alpha/\beta = 3$ Gy for late effects in the OAR and 10 Gy for the tumor, and $T_{1/2} = 1.5$ h)

Journal of the ICRU Vol 13 No 1–2 (2013) Report 89
Oxford University Press
doi:10.1093/jicru/ndw006

Case 1: Small Cervical Cancer Stage IB1, with Positive Nodes, Treated with 3D Conformal EBRT and Concomitant Chemotherapy Plus Conformal Boost and MRI-Based PDR Brachytherapy with Mould Technique

A.1.1 General Patient Information

Age:	37 years
General condition:	good general health (WHO performance status 0)
Prior medical history:	0
Use of medication:	0
Smoking history:	0
Symptoms at presentation:	5-month history of vaginal bleeding

A.1.2 Tumor Extension at Diagnosis

A.1.2.1 Gynecological Examination (Figure A.1.1, Table A.1.1)

Tumor extension:	infiltrative tumor in the cervix, mainly in the posterior lip, no vaginal, no parametrial infiltration
Estimated size:	3 × 3 cm (width × thickness)
Biopsy result:	moderately differentiated squamous cell carcinoma

A.1.2.2 MRI of the Pelvic and Para-Aortic Area (Figure A.1.1, Table A.1.1)

Tumor extension:	tumor predominantly developed in the right part of the cervix without parametrial or vaginal involvement.
Estimated size:	3.3 × 3.0 × 2.8 cm (width × thickness × height)
Pelvic lymph nodes:	one right external iliac lymph node of 1.0 cm in small axis, no para-aortic lymph nodes

A.1.2.3 Other Findings

FDG–PET CT:	three pelvic nodes with pathological uptake (SUV max: 4.5): two along the right external iliac area (1 cm and 0.6 cm in size) and one along the left external iliac area (0.7 cm size)
Pre-therapeutic para-aortic laparoscopic lymph node dissection:	20 negative nodes

A.1.2.4 Conclusion

Thirty-seven-year-old female with a squamous cell carcinoma of the cervix, FIGO Stage IB1 with positive pelvic lymph nodes.

A.1.3 Treatment Intention

The patient was discussed in a multidisciplinary tumor board and she was offered a curative treatment using a combination of pelvic external beam radiotherapy 45 Gy, 5-weekly cycles of cisplatin 40 mg m^{-2}, and a pulsed dose-rate brachytherapy boost to the primary tumor region to a total dose of at least 60 Gy $EQD2_{10}$ to the CTV_{IR} $D_{98\ \%}$. A boost with conformal irradiation to the involved pelvic nodes was to be given after brachytherapy, to a total dose of 60 Gy, taking the contribution of brachytherapy to the nodes into account. The maximal overall treatment time including brachytherapy was to be no more than 55 days (Figure A.1.2).

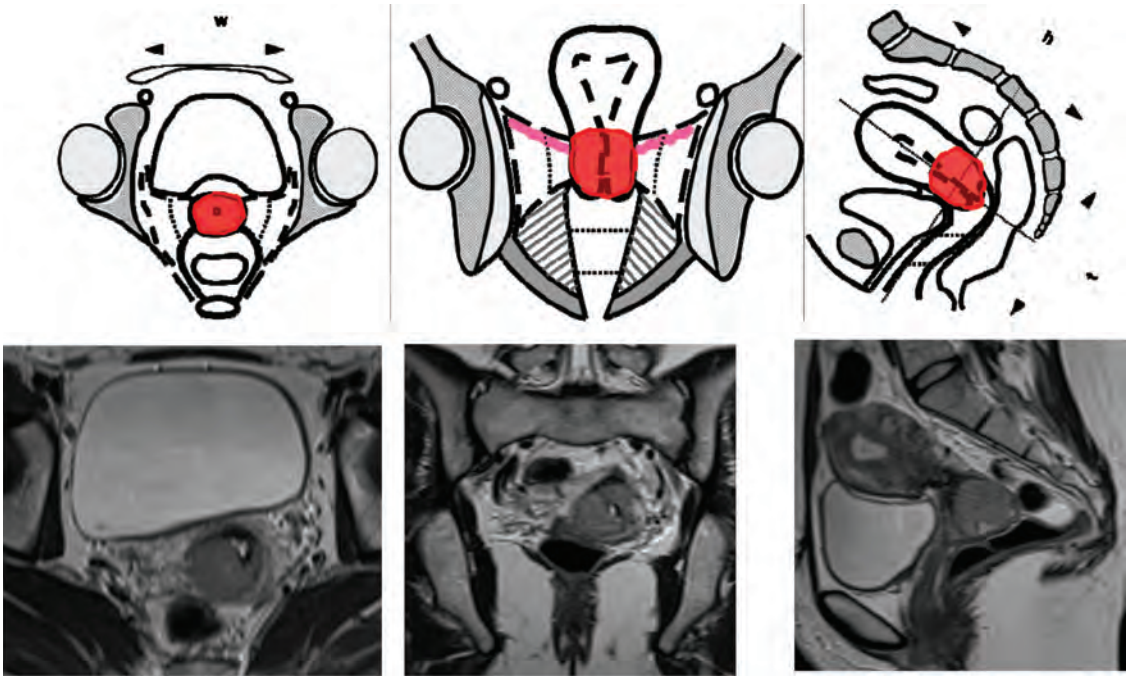

Figure A.1.1. GTV-T extension at diagnosis. Clinical drawings (up) and corresponding MRI images (below) at the time of diagnosis. Clinical drawings and corresponding MRI at diagnosis.

Table A.1.1. Dimensions and volumes of GTVs and CTVs at diagnosis and at brachytherapy.

	Diagnosis	brachytherapy
Clinical dimensions GTV, $w \times t$ (mm)	30×30	0×0
MRI dimensions GTV, $w \times t \times h$ (mm)	$33 \times 30 \times 28$	$0.5 \times 0.5 \times 0.5$
MRI volume GTV (cm^3)	14	<1
Clinical dimensions CTV_{HR}, $w \times t$ (mm)	—	25×25
MRI dimensions CTV_{HR}, $w \times t \times h$ (mm)	—	$25 \times 25 \times 40$
MRI dimensions CTV_{IR}, $w \times t \times h$ (mm)	—	$45 \times 35 \times 60$
CTV_{HR} (cm^3)	—	12
CTV_{IR} (cm^3)	—	50
Left parametrium	Not involved	Not involved
Right parametrium	Not involved	Not involved
Vagina	Not involved	Not involved
Bladder	Not involved	Not involved
Rectum	Not involved	Not involved

A.1.4 External Beam Radiotherapy

Total absorbed dose prescribed:	45 Gy to CTV-T + N1, 45 + 8 Gy to CTV-N2, 45 + 12 Gy to CTV-N3
Fractionation scheme:	25×1.8 Gy (dose distribution depicted in Figure A.1.3 and Table A.1.2), and nodal boost of 4×2 Gy and 6×2 Gy, respectively.
Target volumes:	
CTV-T	cervix, uterus, half of the vagina, both parametria
CTV-N1	pelvic lymph nodes up to aortic bifurcation all pathological nodes with pathological uptake (PET CT)
CTV-N2	two in right
CTV-N3	one in the left external iliac region

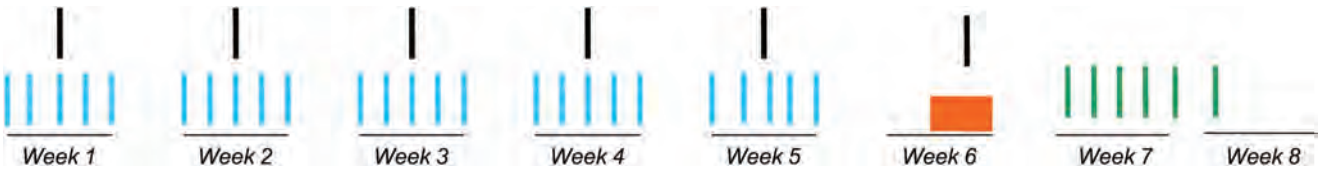

Figure A.1.2. Treatment schedule for this patient. A blue bar represents a fraction of EBRT 1.8 Gy, the orange bar represents the PDR brachytherapy fraction consisting of 60 hourly pulses, a black bar represents a course of cisplatin 40 mg m^{-2}, and green bars indicate the nodal boost delivered after brachytherapy. Overall treatment time was 50 days.

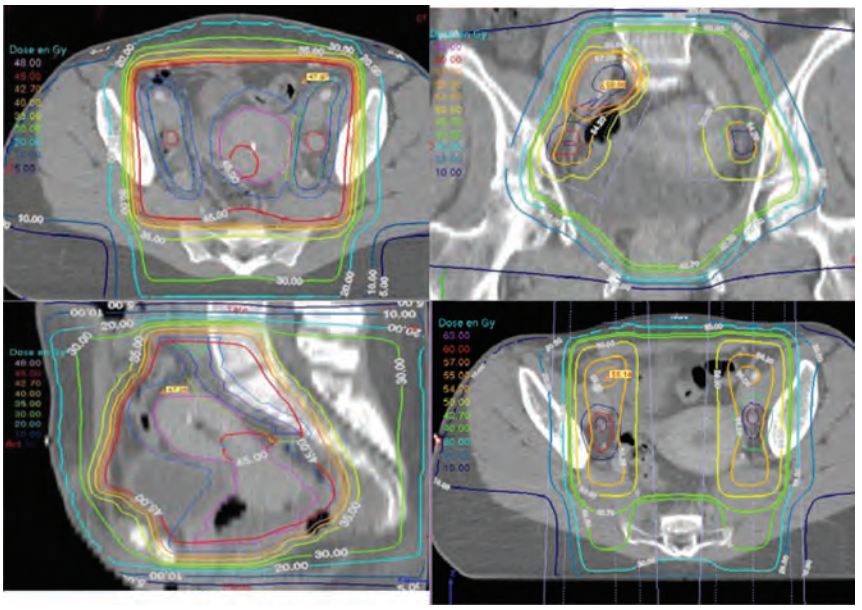

Figure A.1.3. Dose distribution of EBRT. The pelvis itself (PTV-T and PTV-N1) was treated with 45 Gy in 25 fractions. A conformal boost with two opposed fields of 8 Gy in 4 fractions were delivered to the 2 pathological nodes (PTV-N2) along the external iliac vessels bilaterally plus a complementary boost of 4 Gy in 2 fractions on the upper right iliac external node (PTV-N3), taking the brachytherapy dose contribution into account.

Table A.1.2. Absorbed dose distribution for EBRT.

Target	Volume	Planning aim		$V_{95\ \%}$[a]	$D_{98\ \%}$	$D_{50\ \%}$	$D_{2\ \%}$
PTV-T + N1	841 cm^3	45 Gy		100 %	44.7 Gy	46.6 Gy	47.6 Gy
$V_{43\ Gy}$	1089 cm^3						
$V_{57\ Gy}$	57 cm^3						
Organs at risk	$V_{35\ Gy}$	$V_{45\ Gy}$	$V_{50\ Gy}$	$V_{55\ Gy}$	$D_{98\ \%}$	$D_{50\%}$	$D_{2\%}$
Bladder	100 %	99.3 %	3.8 %	0	45.6 Gy	46.7 Gy	52.3 Gy
Rectum	78.2 %	40.5 %	0	0	33.4 Gy	43 Gy	46.4 Gy
Sigmoid	93.2 %	78.7 %	33.1 %	12.1 %	33.5 Gy	47.7 Gy	58.7 Gy
Bowel bag	385 cm^3	378 cm^3	156 cm^3	66 cm^3	19.5 Gy	47.8 Gy	58.9 Gy

[a]Volume treated to 95 % of the planning aim absorbed dose.

Applied PTV margin: 10 mm

Patient positioning: supine position (cushion supporting the knees)

Planning technique: 3DCRT, four Field box

Conformal nodal boost was planned to give:
8 Gy in 4 fractions to the left and right low external iliac macroscopic lymph nodes PTV and 12 Gy in 6 fractions to the upper right external iliac lymph node. An anterior–posterior conformal technique using 20 MV photon energy was used with two oblique fields parallel to the brachytherapy isodose shape.

Concomitant therapy: 5 weekly cycles of cisplatin 40 mg m^{-2}

Overall treatment time: CTV-T + N1 33 days

CTV-N2 46 days
CTV-N3 50 days

A.1.5 Brachytherapy

A.1.5.1 Gynecological Examination at the Time of Brachytherapy (Figure A.1.4)

Tumor extension: no residual tumor

Estimated cervical size: 2.5 × 2.5 cm (width × thickness)

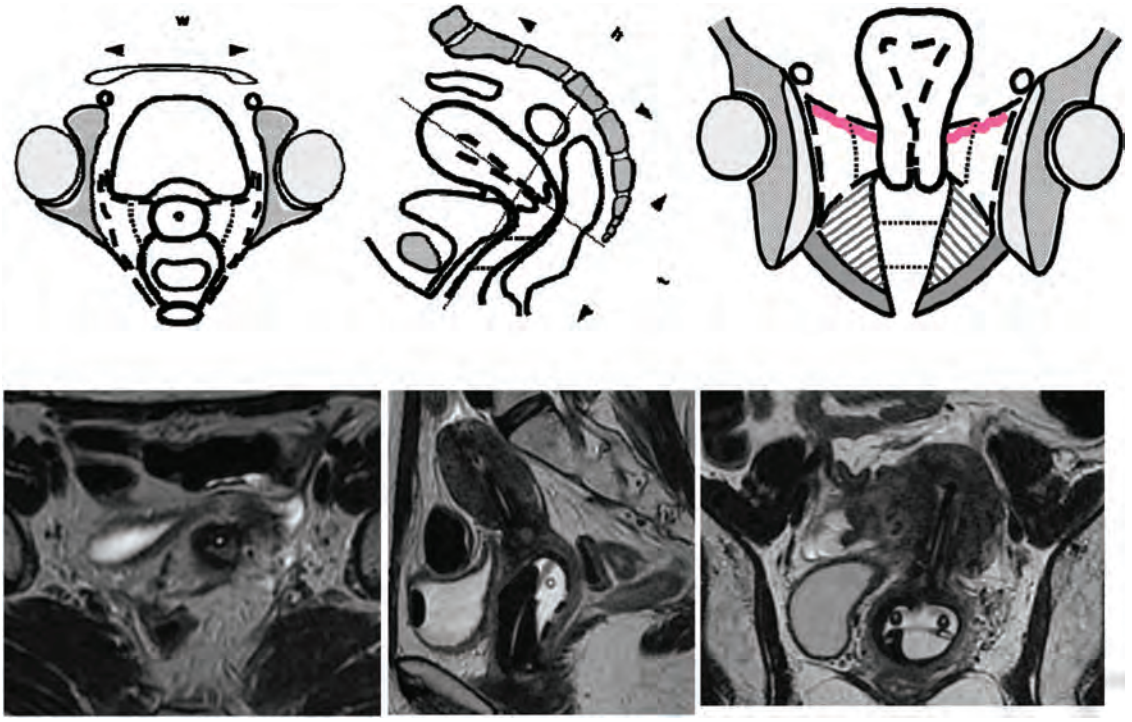

Figure A.1.4. Residual GTV and residual pathological tissue at the time of first brachytherapy. Clinical drawings (up) and corresponding MRI images (below) at the time of brachytherapy with applicator in place.

A.1.5.2 MRI of the Lower Pelvic Area at First Brachytherapy (Figure A.1.4)

Tumor extension: small persistent residual tumor 0.5 cm diameter in the peri-orificial cervical area

A.1.5.3 Treatment Planning Aim

Table A.1.3. Treatment planning aim and prescribed dose.

	Planning aim EQD2	Prescribed dose EQD2	Planning aim absorbed dose rate per pulse	Prescribed absorbed dose rate per pulse
CTV_{IR}				
$D_{98\,\%}$	$\geq$60 Gy	61.0 Gy	$\geq$0.25 Gy h^{-1}	0.30 Gy h^{-1}
Bladder				
D_{2cm^3}	$\leq$80 Gy	74.9 Gy	$\leq$0.60 Gy h^{-1}	0.51 Gy h^{-1}
Rectum				
D_{2cm^3}	$\leq$70 Gy	53.7 Gy	$\leq$0.60 Gy h^{-1}	0.22 Gy h^{-1}
Sigmoid				
D_{2cm^3}	$\leq$70 Gy	56.0 Gy	$\leq$0.60 Gy h^{-1}	0.26 Gy h^{-1}

Doses are given in EQD2 using $\alpha/\beta = 10$ Gy for target and $\alpha/\beta = 3$ Gy for organs at risk. In order to stay within institutional constraints for absorbed dose rate per pulse for D_{2cm^3} of OARs, a fractionation scheme with 60 pulses was chosen. (For the vagina, no planning aim dose constraint was applied.)

A.1.5.4 Treatment Delivery

Treatment method:	intracavitary pulsed dose-rate brachytherapy
Application:	one, after 45 Gy
Time between pulses:	1 h
Pulse number/day:	24
Total number of pulses:	60
Modality used for planning:	MRI-scan after applicator insertion
Overall treatment time:	brachytherapy alone was 3 days

A.1.5.5 Equipment Used for Brachytherapy (Figure A.1.5)

Applicator:	home-made MRI compatible mould applicator (made from a vaginal impression)
Source:	Ir-192, microselectron PDR Nucletron v2 (Nucletron), reference air kerma strength = 1914 μGy m^2 h^{-1}
Treatment planning system:	Oncentra v 4.1 (Nucletron, Veenendaal, The Netherlands) for delineation, PLATO Brachytherapy (v14.3.6) for catheter reconstruction and dosimetry
Dose calculation algorithm	AAPM TG-43

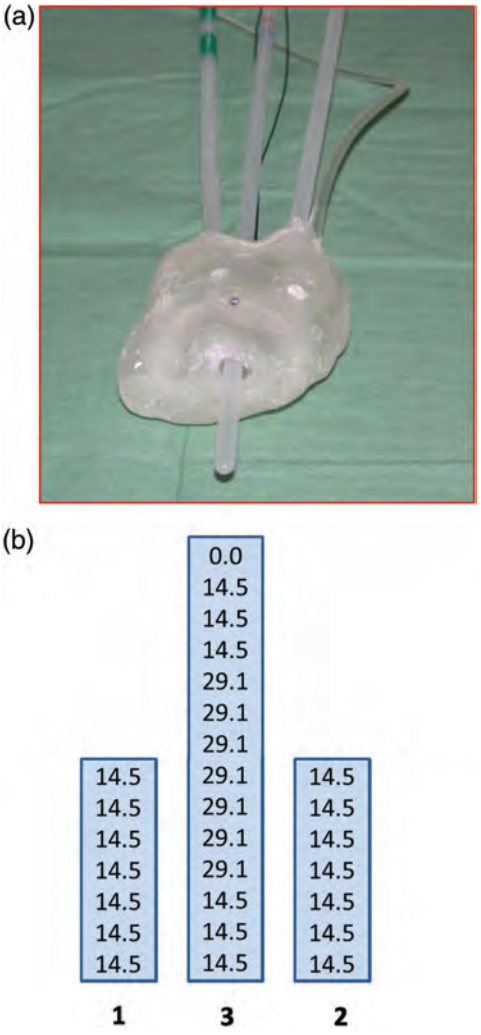

Figure A.1.5. (a) Equipment used for brachytherapy. The vaginal mould applicator was used, based on a vaginal impression. Two vaginal catheters were inserted within the mould. The length of vaginal sources was chosen, based on CTV_{IR} delineation. (b) Dwell time distribution for the vaginal part of the applicator with Catheter 1 and 2 and the intrauterine part with Catheter 3. First dwell position is on the top, all dwell times in seconds.

A.1.6 Treatment Planning and Reporting Brachytherapy and EBRT

Table A.1.4. Applicators and $EQD2_{10}$ isodose surface volumes and treatment time.

	One application
Nominal tandem length	65 mm
Nominal vaginal catheter length	30 mm
Number of pulses	60
60 Gy isodose volume EQD2	157 cm^3
75 Gy isodose volume EQD2	65 cm^3
85 Gy isodose volume EQD2	46 cm^3
TRAK	15.7 mGy

Table A.1.5a. Point-based dose reporting (Level I).

	Absorbed dose brachytherapy (Gy)	EQD2, EBRT + brachytherapy (Gy)
Point		
A		
Right	23.2	66.7
Left	20.6	63.9
Pelvic wall		
Point		
Right	3.9	47.7
Left	8.0	51.3
Bladder		
ICRU		
Point	16.8	58.3
Recto-vaginal		
ICRU		
Point	16.5	56.9
Vagina		
5 mm		
Right	19.8	60.6
Left	24.3	66.1
PIBS[a]		
+2 cm	8.6	49.9
0 cm	3.7	39.2
−2 cm	1.8	3.5

Total dose values in EQD2 were calculated using $\alpha/\beta = 10$ Gy for Point A and pelvic wall point and $\alpha/\beta = 3$ Gy for normal tissue point doses. The dose considered to be delivered at the same location by EBRT was 44.3 Gy $EQD2_{10}$ for target and 43.2 Gy $EQD2_3$ for OARs.
[a]PIBS, posterior inferior border of symphysis pubica, contribution of EBRT at PIBS + 2 cm 45.4 Gy, at PIBS 40 Gy, and at PIBS – 2 cm 3.8 Gy.

Table A.1.5b. DVH-based dose reporting (Level II).

	Absorbed dose brachytherapy (Gy)	EQD2, EBRT + brachytherapy (Gy)
GTV_{res}		
D_{98}	72.7	135.7
D_{90}	84.2	155.9
CTV_{HR}		
D_{98}	36	81.9
D_{90}	43	90.8
D_{50}	66.5	125.5
CTV_{IR}		
D_{98}	17.8	61.0
D_{90}	24.1	67.7
D_{50}	41.6	89.1
Bladder		
$D_{0.1cm^3}$	46.7	101.9
D_{2cm^3}	30.7	74.9
Rectum		
$D_{0.1cm^3}$	17.5	58.0
D_{2cm^3}	13.4	53.7
Sigmoid		
$D_{0.1cm^3}$	20.6	61.5
D_{2cm^3}	15.6	56.0

Total doses in EQD2 were calculated using $\alpha/\beta = 10$ Gy for target and $\alpha/\beta = 3$ Gy for normal tissue volumes. The dose considered to be delivered at the same location by EBRT was 44.3 Gy $EQD2_{10}$ for target and 43.2 Gy $EQD2_3$ for OARs.

A.1.6.1 Example of Dose Distribution

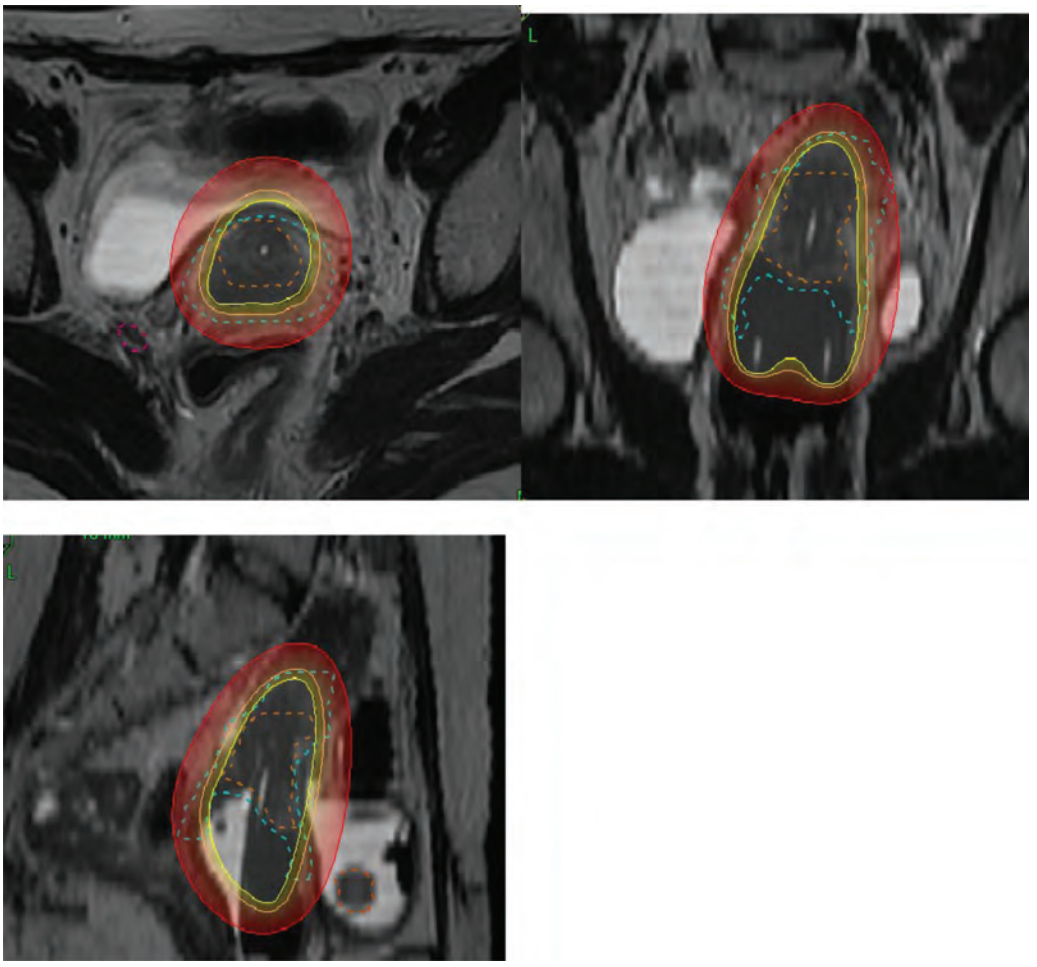

Figure A.1.6. Delineation and dose distribution at brachytherapy. Intermediate-risk CTV is in dotted blue line. High-risk CTV is in dotted orange line. Red isodose corresponds to 100 % planning aim dose, *i.e.*, 15 Gy $EQD2_{10}$ dose. Orange isodose corresponds to 200 % planning aim dose, *i.e.*, 30 Gy $EQD2_{10}$ dose. Yellow isodose corresponds to 267 % planning aim dose, *i.e.*, 40 Gy $EQD2_{10}$ dose.

A.1.7 Current Patient Status

Last treatment received:	28 June 2007
Last follow-up visit:	11 January 2013
General condition:	good
Disease-related symptoms:	none
Treatment-related symptoms:	menopausal symptoms
Treatment:	hormonal replacement therapy
Evidence of disease:	none
Assessed by:	gynecological examination, MRI-pelvis and para-aortic area

Journal of the ICRU Vol 13 No 1–2 (2013) Report 89
Oxford University Press
doi:10.1093/jicru/ndw019

Case 2: Large Cervical Cancer Stage IB2, Intracavitary, No Nodes, Treated with 3D Conformal Box EBRT and Parametrial Boost, with Concomitant Chemotherapy, and MRI-Based Intracavitary Tandem/Ring and Tandem/Ovoid HDR Brachytherapy

A.2.1 General Patient Information

Age:	47 years
General condition:	fair general health, sexually active
Prior medical history:	hypertension, diabetes mellitus
Use of medication:	antihypertensive drugs, metformin
Smoking history:	non-smoker
Symptoms at presentation:	vaginal bleeding and discharge

A.2.2 Tumor Extension at Diagnosis

A.2.2.1 Gynecological Examination (Figure A.2.1, Table A.2.1)

Tumor extension:	expanded cervix with no visible tumor or parametrial or vaginal extension. 5 cm tumor seen at hysteroscopy
Estimated size:	5×5 cm (width $\times$ thickness)
Biopsy result:	grade 3 squamous cell carcinoma

A.2.2.2 MRI of the Lower Pelvic Area (Figure A.2.1, Table A.2.1)

Tumor extension:	cervical mass measuring $5.2 \times 5.2 \times 5.7$ cm with narrowing of the cervical canal and retention of endometrial secretions. There was no uterine or parametrial spread of tumor. There was no invasion of the bladder or rectum.
Pelvic lymph nodes:	9 mm right common iliac node and a 7 mm left pelvic lymph node

A.2.2.3 Other Findings

Abdominal CT-scan:	no evidence of lymph nodes or distant metastases
FDG–PET scan:	no evidence of lymph nodes or distant metastases; intense uptake in cervix (SUV = 31.5)
CT chest:	no evidence of pulmonary metastases
Tumor marker SCC:	not obtained
Laparoscopic surgery:	none

A.2.2.4 Conclusion

Forty-nine-year-old female with a squamous cell carcinoma of the cervix, FIGO stage IB2, cT1b2, cN0, cM0.

A.2.3 Treatment Intention

The patient was discussed in a multidisciplinary tumor board and she was offered curative treatment using a combination of external beam radiotherapy 45 Gy, 5 weekly cycles of cisplatin 40 mg m^{-2}, and a brachytherapy boost to the CTV_{HR} D_{90} to a total dose of $EQD2_{10} \geq 85$ Gy (Figure A.2.2), followed by a 6th cycle of cisplatin with a 5.4 Gy pelvic nodal/parametrial boost to bring the pelvic nodes and parametria to 50.4 Gy.

A.2.4 External Beam Radiotherapy

Total dose prescribed:	45 Gy whole pelvis (WP) and 50.4 Gy pelvic nodes and bilateral parametria (blue isodose line) (Figure A.2.3).

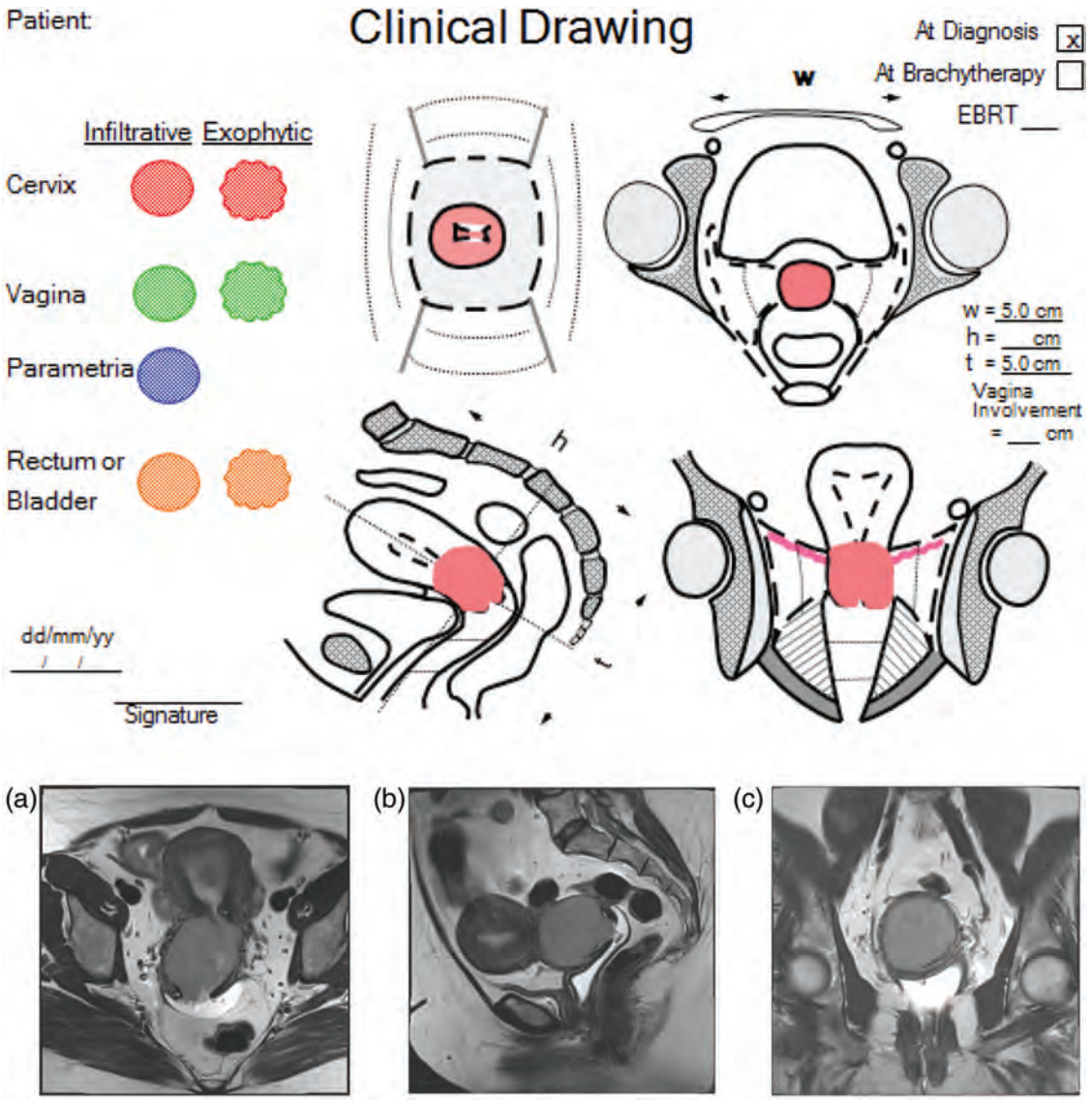

Figure A.2.1. Initial GTV extension at diagnosis. Clinical drawings (up) and corresponding MRI images (below) at the time of diagnosis.

Table A.2.1. Dimensions and volumes of GTVs and CTVs at diagnosis and at brachytherapy.

	Diagnosis	BT1	BT2	BT3	BT4	BT5
Clinical dimensions GTV, $w \times t$ (mm)	50×50	—	—	—	—	—
MRI dimensions GTV, $w \times t \times h$ (mm)	52 × 52 × 57	28 × 28 × 23	24 × 28 × 23	17 × 19 × 19	17 × 18 × 18	17 × 18 × 18
MRI volume GTV (cm^3)	69	8.1	6.8	2.8	2.5	2.3
Clinical dimensions CTV_{HR}, $w \times t$ (mm)	—	40 × 40	40 × 40	30 × 30	30 × 30	30 × 30
MRI dimensions CTV_{HR}, $w \times t \times h$ (mm)	—	40 × 38 × 39	39 × 37 × 39	32 × 30 × 38	30 × 30 × 38	30 × 28 × 37
CTV_{HR} (cm^3)	—	46.7	42.2	34.3	35.4	32.9
CTV_{IR} (cm^3)	—	99.3	86.0	84.5	86.9	87.3

Fractionation scheme:	25/28 × 1.8 Gy WP and 3/28 × 1.8 Gy AP–PA nodal/parametrial boost		
Target volumes:		CTV-T	cervix, uterus, 2/3 of the vagina, both parametria
		CTV-N	pelvic lymph nodes up to aortic bifurcation

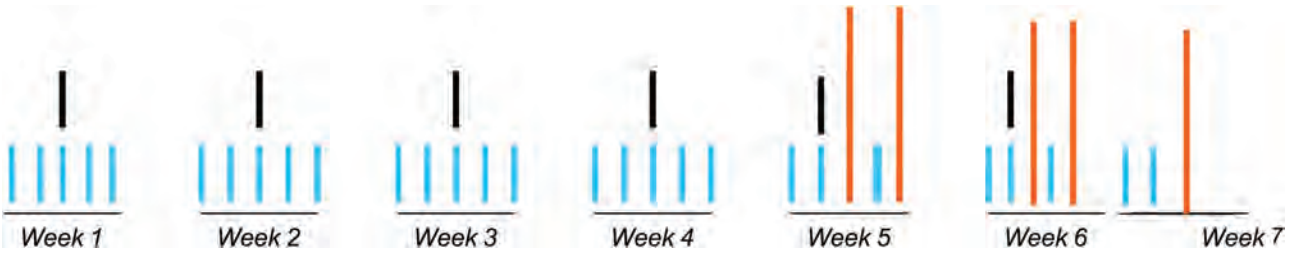

Figure A.2.2. Treatment schedule for this patient. A blue bar represents a fraction of EBRT 1.8 Gy, an orange bar represents a fraction of brachytherapy, and a black bar represents a course of cisplatin 40 mg m^{-2}, overall treatment time 45 days.

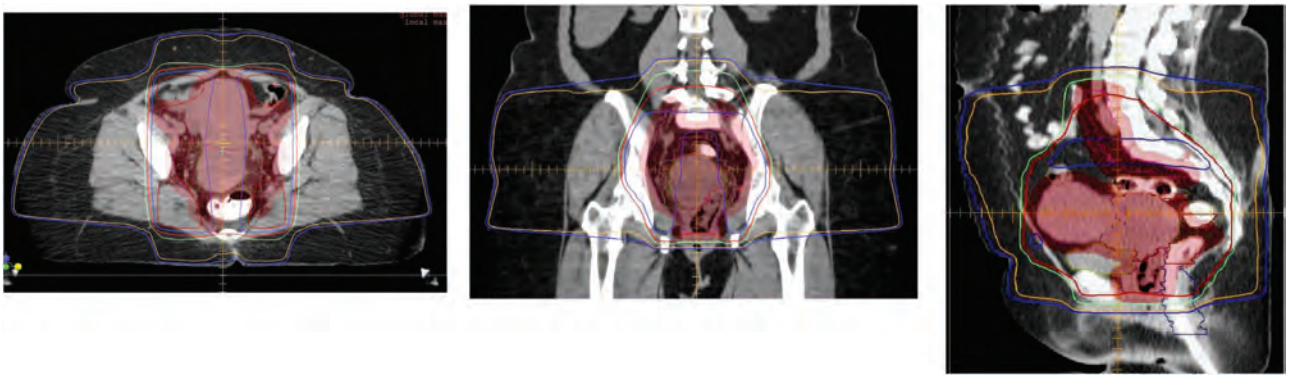

Figure A.2.3. Dose distribution of EBRT to WP (45 Gy red isodose line) and bilateral pelvic nodal and parametrial boost (50.4 Gy blue isodose line).

Table A.2.2. Absorbed dose distribution for EBRT.

Target	Volume	Planning	Aim	$V_{95\ \%}$[a]	$D_{98\ \%}$	$D_{50\ \%}$	$D_{2\ \%}$
PTV	2171 cm^3	45 Gy		95%	44.3 Gy	51.3 Gy	54.5 Gy
$V_{43\ Gy}$	2180 cm^3						
$V_{57\ Gy}$	0						
Organs at risk	$V_{35\ Gy}$	$V_{45\ Gy}$	$V_{50\ Gy}$	$V_{55\ Gy}$	$D_{98\ \%}$	$D_{50\ \%}$	$D_{2\ \%}$
Bladder	100 %	100 %	20 %	0	47.3 Gy	48.4 Gy	52 Gy
Rectum	100 %	100 %	29 %	0	48.2 Gy	48.6 Gy	54 Gy
Sigmoid	100 %	100 %	25 %	2.7 %	47.6 Gy	48.7 Gy	55 Gy
Small bowel	34 %	21 %	12 %	0.3 %	2.9 Gy	27.0 Gy	54 Gy
Large bowel	51 %	48 %	25 %	2.7 %	8.3 Gy	37.0 Gy	55 Gy

[a]Volume treated to 95 % of the planning aim absorbed dose.

Applied PTV margin:	1 cm
Patient positioning:	supine, vac-fix
Planning technique:	3DCRT, 4 Field box
Concomitant therapy:	6-weekly cycles of cisplatin 40 mg m^{-2}
Overall treatment time:	45 days (Table A.2.2)

A.2.5 Brachytherapy

A.2.5.1 Gynecological Examination at the Time of First Brachytherapy (Figure A.2.4)

Tumor extension:	regression of expanded cervix
Estimated size:	4.0 × 4.0 cm (width × thickness)

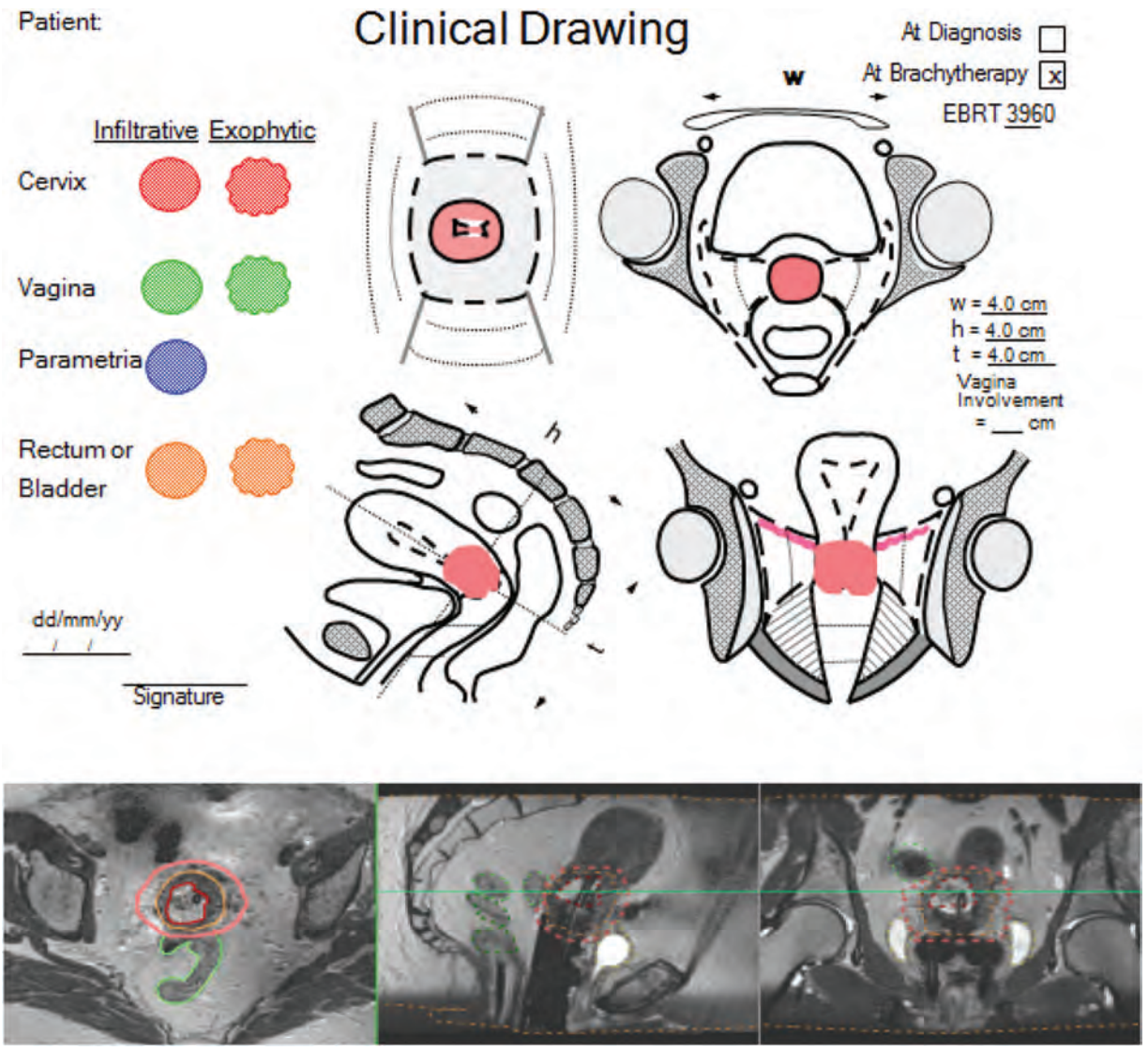

Figure A.2.4. Residual GTV at the time of first brachytherapy. Clinical drawings (up) and corresponding MRI images (below) at the time of first brachytherapy with tandem and ovoid applicator in place.

A.2.5.2 MRI of the Lower Pelvic Area at First Brachytherapy (Figure A.2.4)

Tumor extension: residual central gross tumor volume (bright zone) with surrounding residual pathological tissue (gray zones) in the cervix, width: 4.0 cm

A.2.5.3 Treatment Planning Aim

Table A.2.3. Treatment planning aim and prescribed dose

			Planning aim (Gy)	Prescribed dose (Gy)
CTV_{HR}	D_{90}	$EQD2_{10}$	≥ 85	86.3
Bladder	D_{2cm^3}	$EQD2_3$	≤ 90	79.2
Rectum	D_{2cm^3}	$EQD2_3$	≤ 70	56.4
Sigmoid	D_{2cm^3}	$EQD2_3$	≤ 75	70.1

Doses are given in EQD2 using $\alpha/\beta = 10$ Gy for target and $\alpha/\beta = 3$ Gy for organs at risk.

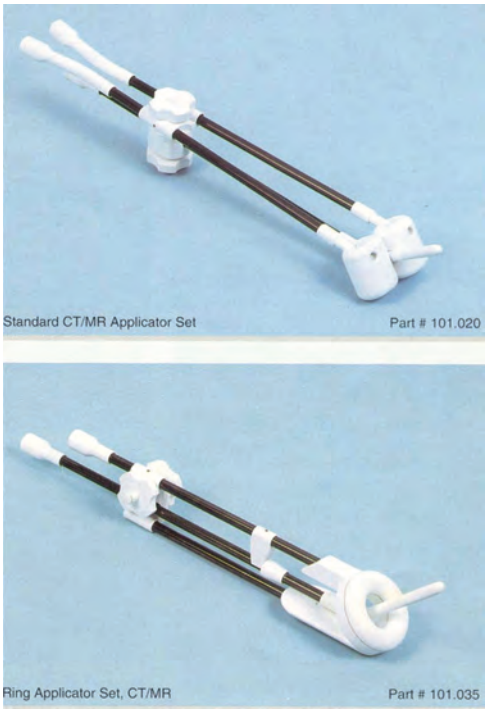

Figure A.2.5. Equipment used for brachytherapy. Tandem and ovoid Applicator (Courtesy of Nucletron an Elekta company) Tandem and ring Applicator (Courtesy of Nucletron an Elekta company).

A.2.5.4 Treatment Delivery

Treatment method:	intra-cavitary high-dose rate brachytherapy
1st application:	after 39.6 Gy
Time between fractions:	2–3D
Modality used for planning:	CT and MRI-scan after applicator insertion MRI scan for each fraction
2nd application:	after 43.2 Gy, the same procedure was followed
3rd, 4th, and 5th application:	after 45 Gy
Overall treatment time:	brachytherapy only 15 days, EBRT+brachytherapy 45 days

A.2.5.5 Equipment Used for Brachytherapy (Figure A.2.5)

Applicator	Fractions #1and #2: Tandem Ovoid applicator with a 30°, 70 mm tandem, and 30 mm outer diameter ovoids (Nucletron, Veenendaal, The Netherlands) Fractions # 3–5: Tandem Ring applicator 45° with 60 mm tandem and largest ring (34 mm nominal source channel diameter, 47 mm outer diameter) (Nucletron)
Source	Ir-192, source model mHDR-v2, air kerma strength 40 820 μGy $m^2\,h^{-1}$, with micro Selectron Afterloader (Nucletron)
Treatment planning System:	Oncentra Brachy (Nucletron an Elekta company)
Dose calculation algorithm	AAPM TG-43

A.2.6 Treatment Planning and Reporting Brachytherapy and EBRT

Table A.2.4. Applicators and $EQD2_{10}$ isodose surface volumes.

Applications	1st	2nd	3rd	4th	5th
Nominal tandem length	70 mm	70 mm	60 mm	60 mm	60 mm
Nominal ovoid/ring diameter	2 × 30 mm	2 × 30 mm	34 mm	34 mm	34 mm
60 Gy volume	327 cm^3	291 cm^3	206 cm^3	208 cm^3	208 cm^3
75 Gy volume	148 cm^3	131 cm^3	95 cm^3	97 cm^3	97 cm^3
85 Gy volume	107 cm^3	91 cm^3	68 cm^3	70 cm^3	69 cm^3
TRAK	4.6 mGy	4.2 mGy	3.3 mGy	3.4 mGy	3.4 mGy

Table A.2.5a. Point-based absorbed dose reporting (Level I).

		BT1 (Gy)	BT2 (Gy)	BT3 (Gy)	BT4 (Gy)	BT5 (Gy)	EBRT and brachytherapy (EQD2 Gy)
Point A	Right	5.6	5.1	4.9	5.1	5.1	79.3
	Left	5.7	5	5	5	5.1	79.5
Pelvic wall point	Right	1.0	0.9	0.6	0.7	0.6	51.8
	Left	1.1	1.1	0.8	0.7	0.8	52.5
Bladder	ICRU point	5.9	4.6	4.6	3.6	3.5	79.1
Recto-vaginal	ICRU point	4.2	3.7	2.3	2.4	2.3	63.8
Vagina	5 mm right	5.2	5.1	4.5	4.5	4.5	82.3
	5 mm left	5.2	5.1	4.5	4.5	4.5	82.3
PIBS	+2 cm	2.5	3.0	2.0	1.8	2.0	57.4
	0 cm	1.1	1.3	0.9	0.8	0.9	49.3
	−2 cm	0.3	0.3	0.2	0.2	0.2	4.8

Total dose values in EQD2 were calculated using $\alpha/\beta = 10$ Gy for Point A and pelvic wall point and $\alpha/\beta = 3$ Gy for normal tissue point doses. The contribution from EBRT was estimated to be within 45 Gy to 50.4 Gy depending on the location and the field arrangement.
PIBS, posterior inferior border of symphysis pubica.

Table A.2.5b. DVH-based absorbed dose reporting (Level II).

		BT1 (Gy)	BT2 (Gy)	BT3 (Gy)	BT4 (Gy)	BT5 (Gy)	EBRT and brachytherapy (Gy in EQD2)
GTV	D_{98}	5.9	4.9	7.6	8.6	7.6	96.2
	D_{90}	6.8	5.7	8.5	10.2	8.9	108
CTV_{HR}	D_{98}	4.8	4.1	5.2	5.5	5.4	78.1
	D_{90}	5.8	5.1	6.1	6.4	6.4	86.4
	D_{50}	8.9	8.5	9.1	9.9	9.9	121.1
CTV_{IR}	D_{98}	3.3	3.0	3.3	3.4	3.3	64.7
	D_{90}	4.2	3.8	4.1	4.2	4.2	70.8
	D_{50}	6.8	6.7	6.9	7.2	7.1	95.7
Bladder	$D_{0.1cm^3}$	5.7	6.3	4.5	4.8	5.1	89.4
	D_{2cm^3}	4.9	5.5	3.7	4.0	4.2	79.0
Rectum	$D_{0.1cm^3}$	2.7	3.7	2.4	2.3	2.6	61.3
	D_{2cm^3}	2.0	3.0	1.8	1.8	2.1	56.5
Sigmoid	$D_{0.1cm^3}$	4.8	4.0	4.8	5.2	5.2	82.9
	D_{2cm^3}	3.9	3.3	3.6	3.9	3.7	69.9

Total doses in EQD2 were calculated using α/β=10 Gy for target and α/β=3 Gy for normal tissue volumes.

A.2.6.1 Example of Absorbed Dose Distribution

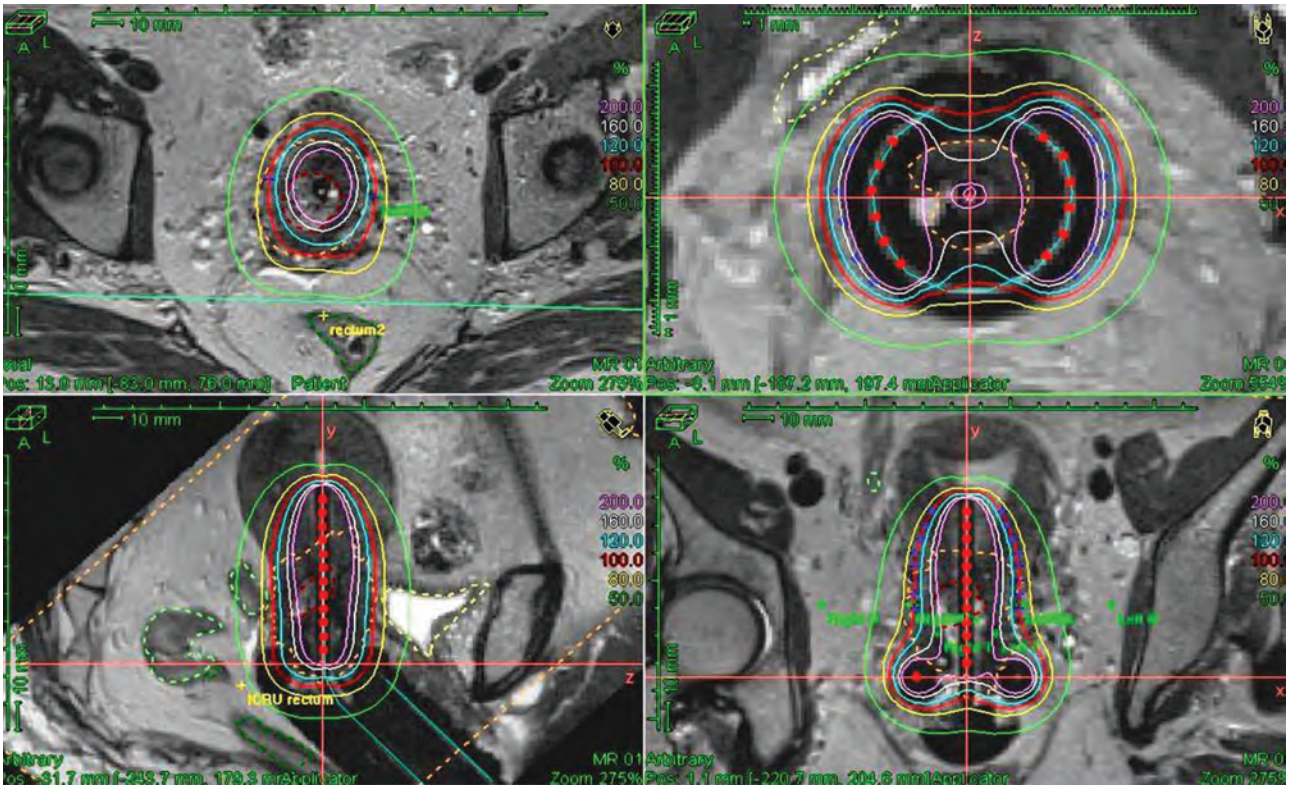

Figure A.2.6. Delineation and dose distribution at 3rd brachytherapy application on MRI with Tandem and ring applicators in place: CTV_{HR}, orange; GTV_{res}, red; bladder, thin yellow; rectum, dark green; sigmoid, light green; isodoselines normalized to 5.5 Gy: green is 50%, yellow is 80%, red is 100%, cyan is 120%, white is 160%, pink is 200%. These doses correspond to 2.75, 4.4, 5.5, 6.6, 8.8, and 11 Gy per fraction, respectively.

A.2.7 Current Patient Status

Last treatment received:	27 June 2012
Last follow-up visit:	29 October 2013
General condition:	good
Disease-related symptoms:	none
Treatment-related symptoms:	none
Evidence of disease:	none
Assessed by:	patient history, gynecological examination, MRI-pelvis, CT chest, and abdomen

Journal of the ICRU Vol 13 No 1–2 (2013) Report 89
Oxford University Press
doi:10.1093/jicru/ndw020

Case 3: Large Cervical Cancer Stage IIA2, No Nodes, Treated with 3D Conformal EBRT, with Concomitant Chemotherapy, and MRI-Based Intracavitary Tandem/Ovoid PDR Brachytherapy

A.3.1 General Patient Information

Age and gender:	female, 45 years old
General condition:	good general health, sexually active
Prior medical history:	no relevant problems
Use of medication:	no medication
Smoking history:	non-smoker
Symptoms at presentation:	postcoital vaginal bleeding

A.3.2 Tumor Extension at Diagnosis

A.3.2.1 Gynecological Examination (Figure A.3.1, Table A.3.1)

Tumor extension:	exophytic tumor in the cervix region, invasion of all fornices and the anterolateral vaginal wall over 1.5 cm
Estimated size:	6 × 6 cm (width × thickness)
Biopsy result:	grade 2 squamous cell carcinoma

A.3.2.2 MRI of the Lower Pelvic Area (Figure A.3.1, Table A.3.1)

Tumor extension:	Exophytic tumor in the cervix region 6 × 6 × 3.5 cm diameter with extension into all fornices and vaginal involvement of the anterior lateral wall over 1.5 cm and no evidence of invasion of parametria, bladder, or rectum
Pelviclymphnodes:	no involvement

A.3.2.3 Other Findings

Abdominal CT-scan:	no evidence of lymph node or distant metastases
FDG-PET scan:	no evidence of lymph node or distant metastases
Chest X-ray:	no evidence of pulmonary metastases
Tumor Marker SCC:	1.3 ng ml^{-1} (0–2.3)
Laparoscopic surgery:	no evidence of lymph node metastases at lymph node dissection (21 lymph nodes resected, 0 involved 0/21)

A.3.2.4 Conclusion

Forty-five-year old female with a squamous cell carcinoma of the cervix FIGO IIA2, cT2a2, pN0, M0.

A.3.2.5 Treatment Intention

The patient was discussed in a multidisciplinary tumor board and she was offered a curative treatment using a combination of external beam radiotherapy to the pelvis 45 Gy in 1.8 Gy fractions, with concomitant 5 weekly cycles of cisplatin 40 mg m^{-2} and a brachytherapy boost to the CTV_{HR} D_{90} to a total dose of $EQD2_{10} = 95.3$ Gy (Figure A.3.2).

A.3.3 External Beam Radiotherapy

Total dose prescribed:	45 Gy
Fractionation scheme:	25 × 1.8 Gy (dose distribution depicted in Figure A.3.3 and Table A.3.2)
Target volumes:	
CTV-T	cervix, uterus, 2/3 of the vagina, both parametria
CTV-N	pelvic lymph nodes up to iliac bifurcation
Applied PTV margin:	1 cm lateral caudal cranial, 2 cm cervix, vagina, uterus
Patient positioning:	prone position, belly board
Planning technique:	3DCRT, 4 Field box
Concomitant therapy:	5-weekly cycles of cisplatin 40 mg m^{-2}
Overalltreatmenttime:	33 days

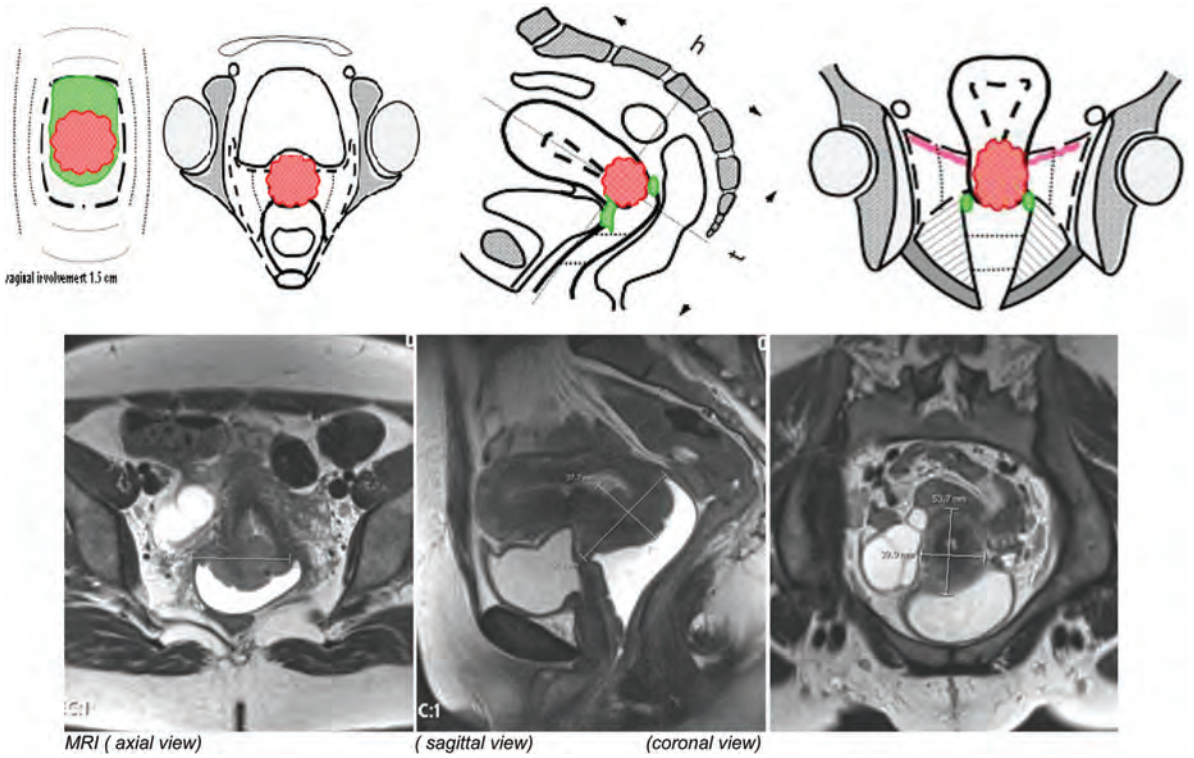

Figure A.3.1. Initial GTV extension at diagnosis. Clinical drawings (up) and corresponding MRI images (below) at the time of diagnosis.

Table A.3.1. GTV extension at diagnosis and at first brachytherapy.

	Diagnosis	Brachytherapy
Clinical GTV dimension, $w \times t$ (mm)	60 × 60	40 × 35
GTV dimension on MRI, $w \times t \times h$ (mm)	59 × 58 × 39	22 × 19 × 9
GTV on MRI (cm^3)	—	0.7
CTV_{HR} (cm^3)	—	23
CTV_{IR} (cm^3)	—	118.4
Left parametrium	Not involved	Not involved
Right parametrium	Not involved	Not involved
Vagina	Upper antero-lateral 1.5 cm	Antero-lateral fornix
Bladder	Not involved	Not involved
Rectum	Not involved	Not involved

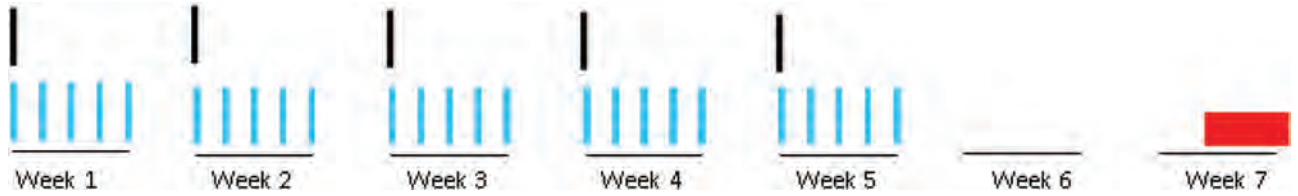

Figure A.3.2. Treatment schedule for this patient. A blue bar represents a fraction of EBRT 1.8 Gy, the red bars represent a fraction of 40 Gy PDR brachytherapy 65 pulses of 0.72 Gy to the D_{90} of the high-risk CTV and a black bar represents a course of cisplatin 40 mg m^{-2}, overall treatment time 47 days.

A.3.4 Brachytherapy

A.3.4.1 Gynecological Examination at the Time of First Brachytherapy (Figure A.3.4)

Tumor extension: residual mass with persistent infiltration of the anterolateral fornices

Estimated size: 4 × 3.5 cm (width × thickness)

A.3.4.2 MRI of the Lower Pelvic Area at Brachytherapy (Figure A.3.5)

Tumour extension: residual pathological tissue (gray zones), in the anterolateral fornices, no vaginal residual involvement

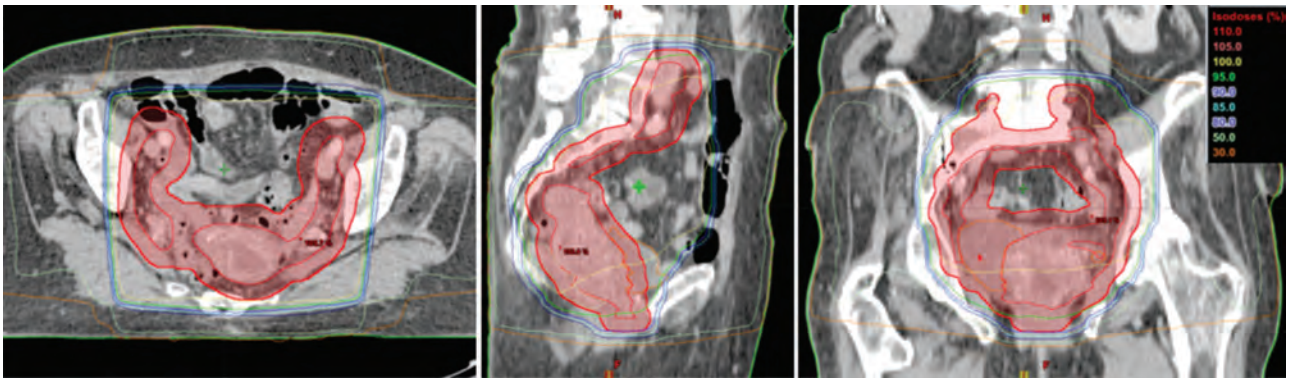

Figure A.3.3. Dose distribution of EBRT.

Table A.3.2. Absorbed dose distribution for EBRT.

Target	Volume	Planning aim dose	$V_{95\ \%}$[a]	$D_{98\ \%}$	$D_{50\ \%}$	$D_{2\ \%}$	
PTV	1784 cm^3	45 Gy	100 %	37.4 Gy	45.4 Gy	47.6 Gy	
$V_{43\ Gy}$	2465 cm^3	/	/	/	/	/	
$V_{57\ Gy}$	0	/	/	/	/	/	
OAR	$V_{35\ Gy}$	$V_{45\ Gy}$	$V_{50\ Gy}$	$V_{55\ Gy}$	$D_{98\ \%}$	$D_{50\ \%}$	$D_{2\ \%}$
Bladder	100 %	70.5 %	0 %	0 %	43.8 Gy	45.3 Gy	46.0 Gy
Rectum	99.8 %	92.1 %	0 %	0 %	40.9 Gy	46.5 Gy	47.1 Gy
Sigmoid	88.3 %	71.3 %	0 %	0 %	26.5 Gy	53 Gy	47.2 Gy
Bowelbag	125 cm^3	96 cm^3	0 %	0 %	2.9 Gy	45.3 Gy	46.7 Gy

[a]Volume treated to 95 % of the planning aim absorbed dose.

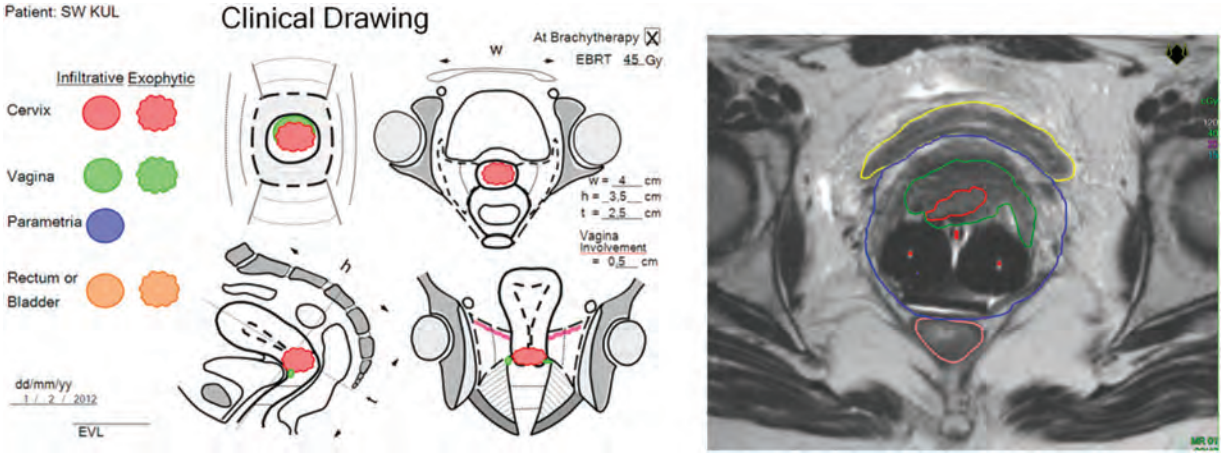

Figure A.3.4. Residual GTV and residual pathological tissue at the time of first brachytherapy. Clinical drawing of residual GTV in cervix and pathologic tissue in the anterior fornix, also visualized on MRI at the time of brachytherapy (GTV in red and cervix and pathologic gray zones in green).

A.3.4.3 Treatment Planning Aim

Table A.3.3. Treatment planning aim and prescribed dose.

			Planning aim (Gy)	Prescribed dose (Gy)
CTV_{HR}	D_{90}	$EQD2_{10}$	≥85	95.3
Bladder	D_{2cm^3}	$EQD2_3$	≤90	65.5
Rectum	D_{2cm^3}	$EQD2_3$	≤70	59.4
Sigmoid	D_{2cm^3}	$EQD2_3$	≤75	49.9

Doses are given in EQD2 using $\alpha/\beta = 10$ Gy for target and $\alpha/\beta = 3$ Gy for organs at risk.

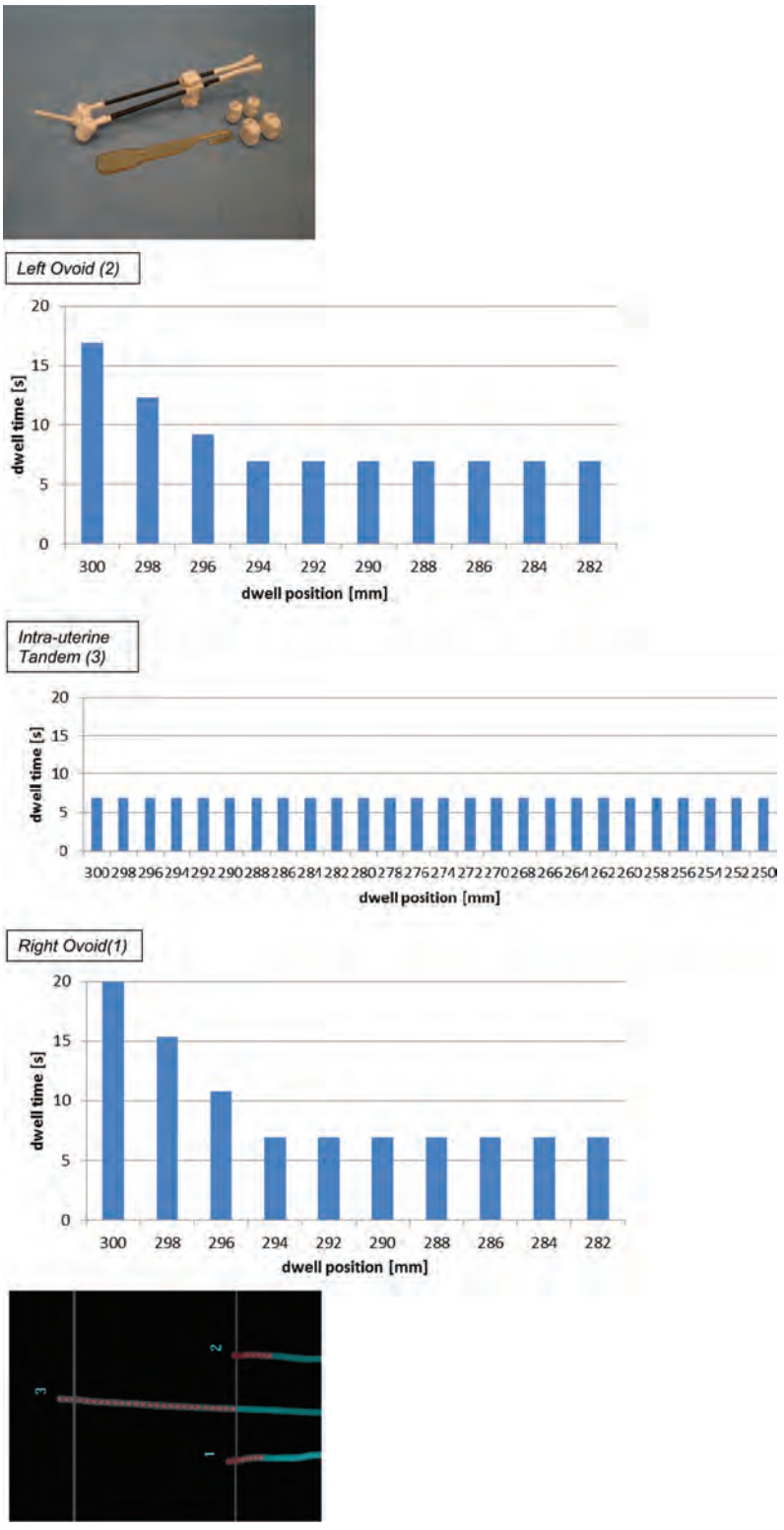

Figure A.3.5. Equipment used for brachytherapy and dwell times. MRI compatible Nucletron Standard Tandem Ovoid Applicator with 6 cm tandem and medium (2.5 cm) ovoids. Also shown is the rectal-retractor which was also inserted, as well as the small (2 cm) and large (3 cm) ovoids, which were not used in this patient. The loading was 18 mm from the tips of the ovoids and over 50 mm from the tip of the intrauterine tandem. Dwell positions were planned every 2 mm as shown in the abscises of the loading pattern graphs. Dwell times are shown in the ordinates (dwell times scaled to a different planning source strength).

A.3.4.4 Treatment Delivery

Treatment method:	PDR intracavitary brachytherapy
Application:	after 45 Gy
Pulses:	65
Time between pulses:	1 h
Modality used for planning:	MRI-scan after applicator insertion

A.3.4.5 Equipment Used for Brachytherapy (Figure A.3.5)

Applicator	standard MRI compatible tandem ovoids applicator with a 6 cm tandem and 25 mm ovoids (Nucletron, Veenendaal, The Netherlands)
Source	Ir-192, source model Flexisource, air kerma strength 4076 μGy m^2 h^{-1}, with Flexitron PDR 40 channel Afterloader (Nucletron)
Treatment planning System:	Oncentra 4.1 (Nucletron)
Dose calculation algorithm	AAPM TG-43

A.3.4.6 Treatment Reporting

Table A.3.4. Applicators and $EQD2_{10}$ isodose surface volumes.

	BT application
Nominal tandem length	60 mm
Nominal ovoid diameter	25 mm
Number of active needles	0
60 Gy volume	228.9 cm^3
75 Gy volume	138.5 cm^3
85 Gy volume	97.2 cm^3
TRAK	26.7 mGy

Table A.3.5a. Point-based absorbed dose reporting (Level I).

			Absorbed dose brachytherapy (Gy)	EQD2 EBRT + brachytherapy (Gy)
Point	A	Right	37.3	82.9
		Left	36.5	81.9
Pelvic wall	Point	Right	8.7	51.9
		Left	7.8	51.1
Bladder	ICRU	Point	18.3	58.5
Rectal	ICRU	Point	22.8	63.6
Vagina	5 mm	Right	37.3	83.7
		Left	42.4	92.0
	PIBS[a]	+2 cm	19.7	59.4
		0 cm	8.2	45.7
		−2 cm	4.4	14.1

Total dose values in EQD2 were calculated using $\alpha/\beta = 10$ Gy for point A and pelvic wall point and $\alpha/\beta = 3$ Gy for normal tissue point doses.
[a]PIBS, posterior inferior border of symphysis pubica, contribution of EBRT at PIBS + 2 cm 44.4 Gy, at PIBS 42.5 Gy, and at PIBS–2 cm 15.5 Gy.

Table A.3.5b. DVH-based absorbed dose reporting (Level II).

		Absorbed dose brachytherapy (Gy)	EQD2 EBRT + brachytherapy (Gy)
GTV_{res}	D_{98}	76.9	140.4
	D_{90}	91.5	165.9
CTV_{HR}	D_{98}	39.0	85
	D_{90}	46.9	95.3
	D_{50}	73.7	135.1
CTV_{IR}	D_{98}	22.1	65.3
	D_{90}	26.4	70
	D_{50}	43.4	90.6
Bladder	$D_{0.1cm^3}$	29.1	71.7
	D_{2cm^3}	24.3	65.5
Rectum	$D_{0.1cm^3}$	24.2	65.3
	D_{2cm^3}	19.1	59.4
Sigmoid	$D_{0.1cm^3}$	13.7	53.9
	D_{2cm^3}	9.3	49.9

Total doses in EQD2 were calculated using $\alpha/\beta = 10$ Gy for target and $\alpha/\beta = 3$ Gy for normal tissue volumes.

A.3.4.7 Example of Dose Distribution

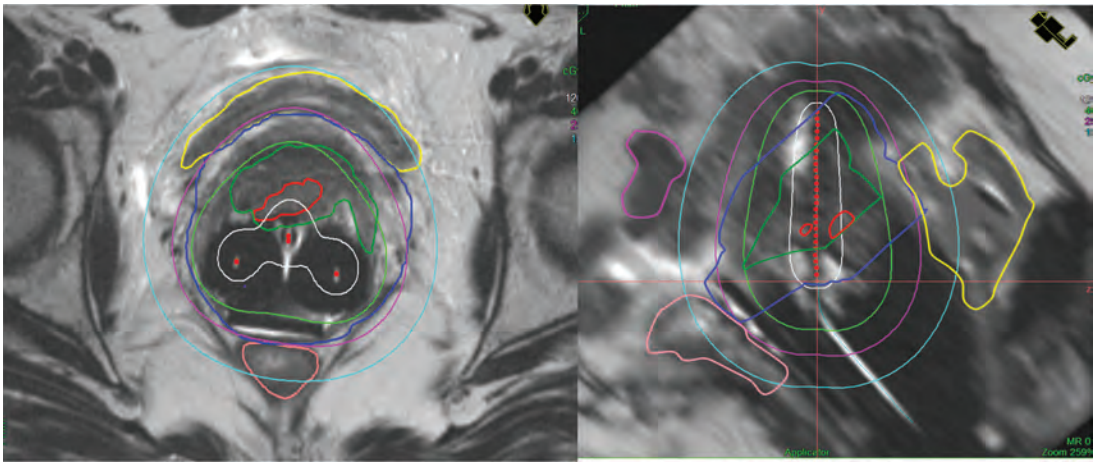

Figure A.3.6. Dose distribution for brachytherapy residual GTV (delineated in red), CTV_{HR} (in green), CTV_{IR} (in blue). The bladder is delineated in yellow, the rectum in rose. Prescribed dose was 45.2 Gy to the D_{90} of the CTV_{HR}. The isodoses are shown as: 165 Gy total EQD2 (in white), 85 Gy total EQD2 (in green covering the CTV_{HR}), 70 Gy EQD2 (in rose not entering the delineated rectum), and 60 Gy total EQD2 (covering largely the CTV_{IR}).

A.3.5 Current Patient Status

Last treatment received:	4 February 2012
Last follow-up visit:	21 May 2014
General condition:	good, works full time
Disease-related complaints:	blood loss
Treatment-related complaints:	after 27 months follow-up: normal sexual intercourse only complaints of sporadic blood loss at intercourse, no rectosigmoidal, or bladder morbidity.
Evidence of disease:	local recurrence, lymphnode recurrence, inguinal right, bilateral iliaca externa , bilateral iliaca communis, low para aortic
Assessed by:	patient history, gynecological examination, PET–CT

Journal of the ICRU Vol 13 No 1–2 (2013) Report 89
Oxford University Press
doi:10.1093/jicru/ndw021

Case 4: Cervical Cancer Stage IB1 Treated with 3D Conformal External Beam Irradiation, Concomitant Chemotherapy, and Radiograph-Based Intracavitary Tandem/Ovoid High Dose Rate Brachytherapy

A.4.1 General Patient Information

Age:	48 years
General condition:	performance status = 0 (WHO)
Prior medical history:	loop electrosurgical excision procedure (LEEP) × 2
Use of medication:	no medication
Smoking history:	former smoker (5 packyear history)
Symptoms at presentation:	1month history of postcoital vaginal bleeding

A.4.2 Tumor Extension at Diagnosis

A.4.2.1 Gynecological examination (Figure A.4.1, Table A.4.1)

Tumor extension:	firm, barrel shaped cervix measuring 4 cm in diameter with visible 2 cm exophytic lesion involving os and posterior lip, no involvement of vagina or parametrium
Estimated size:	4 × 3 cm (width × thickness)
Biopsy result:	squamous cell carcinoma, moderately differentiated, p16 strongly positive.

A.4.2.2 MRI of the Pelvis (Figure A.4.1, Table A.4.1)

Tumor extension:	4.0 × 2.8 × 3.3 cm (width × thickness × height) enhancing tumor occupying posterior cervix and extending into lower uterine segment, with minimal parametrial extension posteriorly
Pelvic lymph nodes:	no lymphadenopathy

A.4.2.3 Other Findings

Whole body FDG PET–CT:	hypermetabolic cervical mass, no lymphadenopathy, or distant metastasis.
Cr51 EDTA:	GRF = 71 ml min^{-1}

A.4.2.4 Conclusion

Forty-eight-year-old female with squamous cell carcinoma of the uterine cervix, FIGO stage IB1 TNM T1b1 N0 M0.

A.4.3 Treatment Intention

After multidisciplinary evaluation, it was decided to offer curatively intended radiochemotherapy using 3D conformal external beam radiation therapy to the pelvis (45 Gy in 1.8 Gy fractions) with 6 courses of concomitantly weekly cisplatin and a boost of high dose rate brachytherapy to the residual tumour, aiming at a total dose of $\geq$80 Gy $EQD2_{10}$ at point A. Overall treatment time 7 weeks with brachytherapy delivered in 5 fractions starting in the fourth week of treatment (Figure A.4.2).

A.4.4 External Beam Radiotherapy (Figure A.4.3 and Table A.4.2)

Total dose prescribed:	45 Gy
Fractionation scheme:	25 × 1.8 Gy 5 fractions per week
Target volumes:	cervix, uterus, upper half of the vagina, both parametria, and all pelvic nodal stations to the aortic bifurcation (L4–L5).

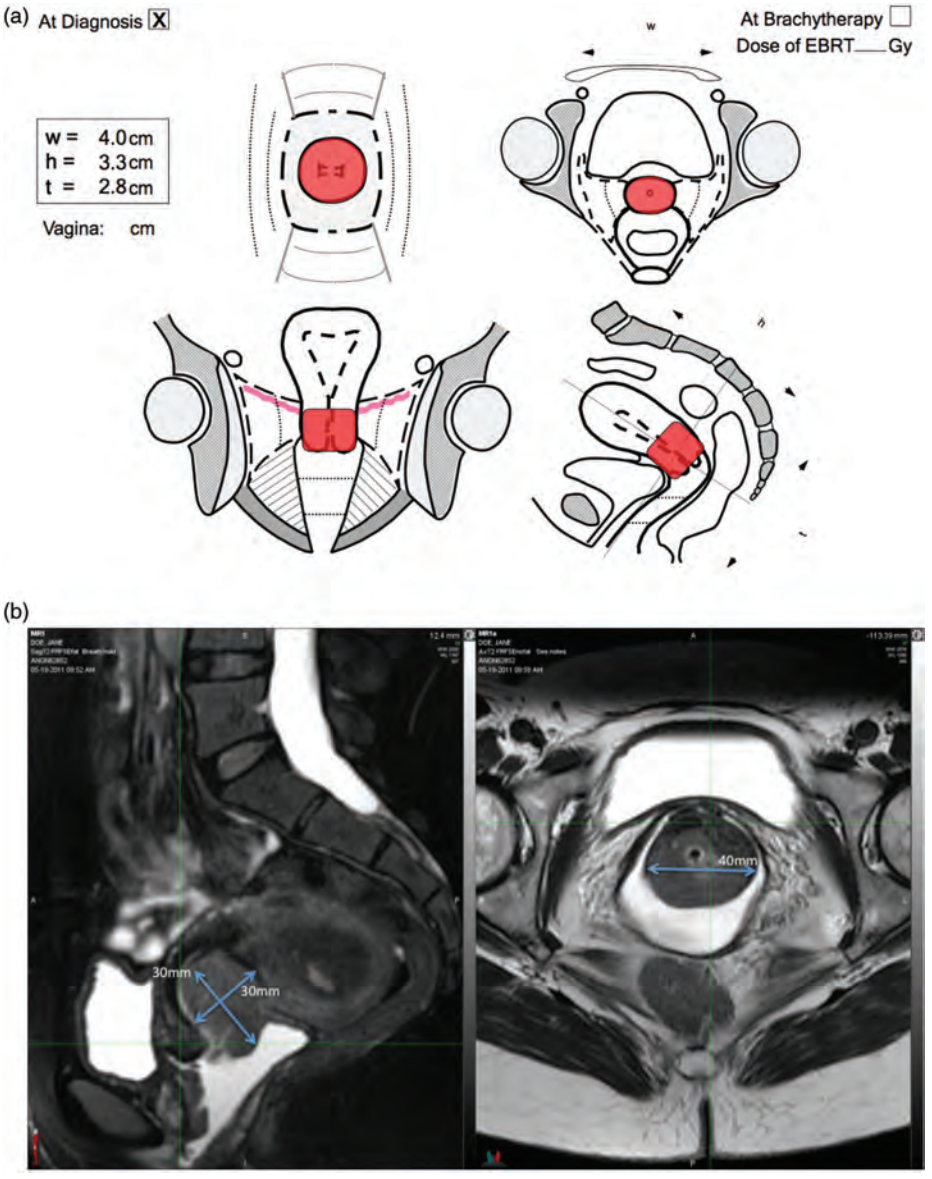

Figure A.4.1. GTV extension at diagnosis. (a) Clinical findings by gynecological examination performed at diagnosis. The initial GTV at diagnosis is indicated within the cervix and uterus (red).

Table A.4.1. Dimensions and volumes of GTVs and CTVs at diagnosis and at brachytherapy

	Diagnosis	BT1–5
Clinical dimensions GTV, $w \times t$ (mm)	40 × 30	20 × 20
MRI dimensions GTV, $w \times t \times h$ (mm)	40 × 28 × 33	—
MRI volume GTV (cm^3)	30	5[a]
Clinical dimensions CTV_{HR} $w \times t$ (mm)	—	40 × 40[a]
MRI dimensions CTV_{HR}, $w \times t \times h$ (mm)	—	—
MRI volume CTV_{HR} (cm^3)	—	—
Left parametrium	Not involved	Not involved
Right parametrium	Not involved	Not involved
Uterus	Lower part	Not involved
Vagina	Not involved	Not involved
Bladder	Not involved	Not involved
Rectum	Not involved	Not involved

[a]Estimated based on the clinical exam because no MRI was performed at the time of brachytherapy.

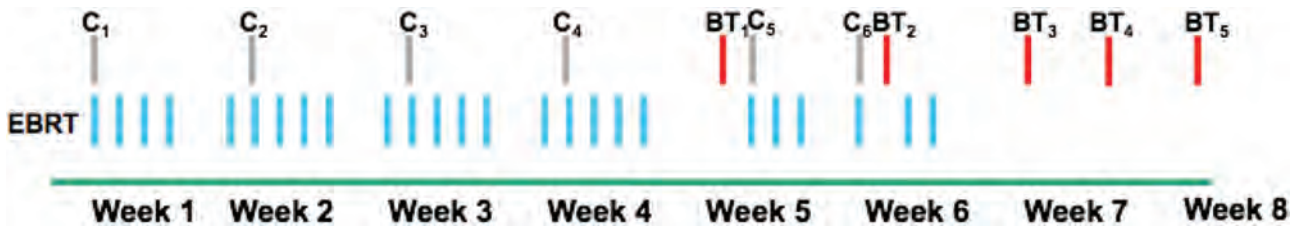

Figure A.4.2. Treatment schedule involving 49 days of treatment including weekly cisplatin (C_{1-6}), externalbeam radiotherapy (EBRT) and brachytherapy (BT_{1-5}). Treatment was initiated with EBRT (light blue bar) and weekly cisplatin (gray bar). Cisplatin was omitted on days with brachytherapy. Brachytherapy (red bars) began the day after a holiday.

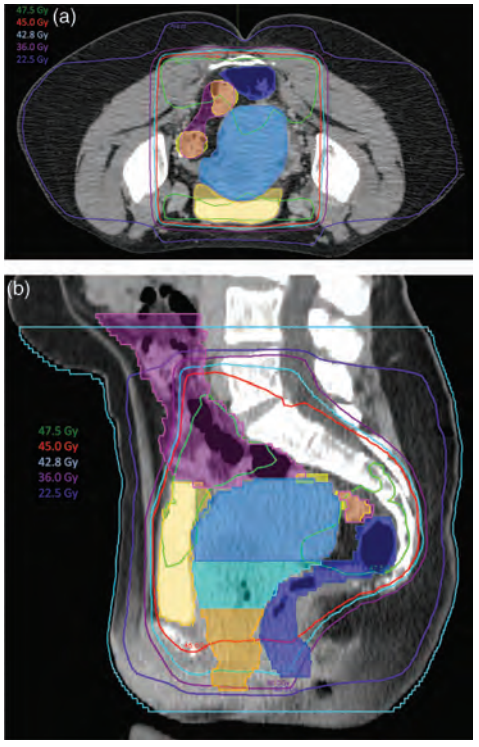

Figure A.4.3. Dose distribution of externalbeam radiotherapy: (a) transverse, and (b) sagittal. The pelvis itself (PTVE) was treated with 45 Gy in 25 fractions. The color code for the structures is: uterus, light blue; cervix, torquois; vagina, gold; rectum, dark blue; bladder, light yellow; sigmoid, dark yellow; small bowel, purple.

Applied PTV margin:	2 cm margin to block edge beyond the cervix, uterus, upper vagina/ parametrium, and targeted pelvic vasculature. Weekly orthogonal portal imaging for verification was used.
Patient positioning:	supine position with knee cushion
Planning technique:	4field 3D conformal plan
Concomitant treatment:	6 cycles of weekly cisplatin 40 mg m^{-2}
Overall treatment time:	37 days

A.4.5 Brachytherapy

A.4.5.1 Gynecological Examination at the Time of First Brachytherapy (Figure A.4.4, Table A.4.1)

Tumor extension:	involvement of posterior cervical lip
Estimated size:	2 cm × 2 cm tumor in a 4cm diameter cervix.

A.4.5.2 Treatment Planning Aim

Table A.4.2. Absorbed dose distribution for EBRT.

Target	Volume	Planning aim		$V_{95\,\%}$[a]	$D_{50\,\%}$	$D_{98\,\%}$	$D_{2\,\%}$
PTV	2219 cm^3	45 Gy		100 %	46.6	45.6	48.0
$V_{43\,Gy}$	2571 cm^3						
$V_{57\,Gy}$	0						
Organs at risk	$V_{35\,Gy}$	$V_{45\,Gy}$	$V_{50\,Gy}$	$V_{55\,Gy}$	$D_{50\,\%}$	$D_{98\,\%}$	$D_{2\,\%}$
Bladder	100 %	100 %	0 %	0 %	47.5 Gy	46.4 Gy	48.1 Gy
Rectum	99 %	89 %	0 %	0 %	48.0 Gy	39.1 Gy	48.9 Gy
Sigmoid	100 %	100 %	0 %	0 %	47.1 Gy	46.4 Gy	47.9 Gy
Bowel	365 cm^3	302 cm^3	0 cm^3	0 cm^3	28.7 Gy	1.7 Gy	48.4 Gy
Femoral head sin	5 %	0 %	0 %	0 %	27.8 Gy	26.5 Gy	40.0 Gy
Femoral head dxt	1 %	0 %	0 %	0 %	27.7 Gy	26.6 Gy	33.0 Gy

[a]Volume treated to 95 % of the planning aim absorbed dose.

A.4.5.3 Treatment Delivery

Table A.4.3. Treatment planning aim and prescribed dose for five fractions of HDR brachytherapy along with 45 Gy at 1.8 Gy per fraction from pelvic externalbeam radiation therapy.

			Planning aim	Prescribed dose
	Point A	$EQD2_{10}$	$\geq$80 Gy	78.0 Gy
Bladder	ICRU point	$EQD2_3$	$\leq$80 Gy	61.5 Gy
Rectovaginal	ICRU point	$EQD2_3$	$\leq$75 Gy	61.7 Gy

Doses are given in EQD2 using $\alpha/\beta = 10$ Gy for target and $\alpha/\beta = 3$ Gy for organs at risk. (For the vagina, no planning aim dose constraint was applied.)

Treatment method:	intracavitary HDR brachytherapy was performed with 5 fractions starting in week 4 with radiographic imaging for dosimetry
Imaging modality used for planning:	orthogonal radiographs
1st application (BT_1):	week 5, after 34.2 Gy to PTV
2nd application (BT_2):	week 6, after 41.4 Gy to PTV
3rd application (BT_3):	week 7, after 45.0 Gy to PTV
4th application (BT_4):	week 7, after 45.0 Gy to PTV
5th application (BT_5):	week 8, after 45.0 Gy to PTV
Overall treatment time:	brachytherapy alone 22 days, EBRT + brachytherapy 49 days

A.4.5.4 Equipment Used for Brachytherapy (Table A.4.4, Figure A.4.5)

Applicator:	tandem (40–55 mm) and ovoids (25 mm) applicator (Nucletron, an Elekta company, Veenendaal, The Netherlands).
Source:	^{192}Ir delivered by a microSelectron (Nucletron, an Elekta company, Veenendaal, The Netherlands)
Treatment planning system:	Oncentra (Nucletron, an Elekta company, Veenendaal, The Netherlands)
Source strength (RAKR):	20 500 μGy h^{-1} first fraction (Table A.4.4)
Dose calculation algorithm	AAPM TG43

Table A.4.4. Applicator characteristics, time/dose pattern, and isodose surface volumes for the brachytherapy fractions (BT_1 through BT_5) used this patient.

	BT1	BT2	BT3	BT4[a]	BT5
Tandem length (mm)	50	55	50	50	40
Ovoid diameters (mm)	25	25	25	25	25
Total time (s)	797.2	793.9	882.3	402.0	407.3
Volume of the prescription isodose surface (5.25 Gy) (cm^3)	143.7	135.6	147.3	148.9	142.3
Volume of the V_{85} isodose surface (6.10 Gy) (cm^3)	113.5	106.5	120.4	122.1	118.0
Volume of the V_{75} isodose surface (4.95 Gy) (cm^3)	158.6	146.9	160.0	161.1	154.0
Volume of the V_{60} isodose surface (2.92 Gy) (cm^3)	338.9	304.1	318.1	325.0	314.5
Reference air kerma rate (mGy h^{-1})	20.5	19.2	17.9	39.8	38.3
Total reference air kerma (mGy)	4.54	4.23	4.39	4.44	4.33

Brachytherapy was delivered at a high dose rate.
[a]Source exchange occurred between fractions three and four.

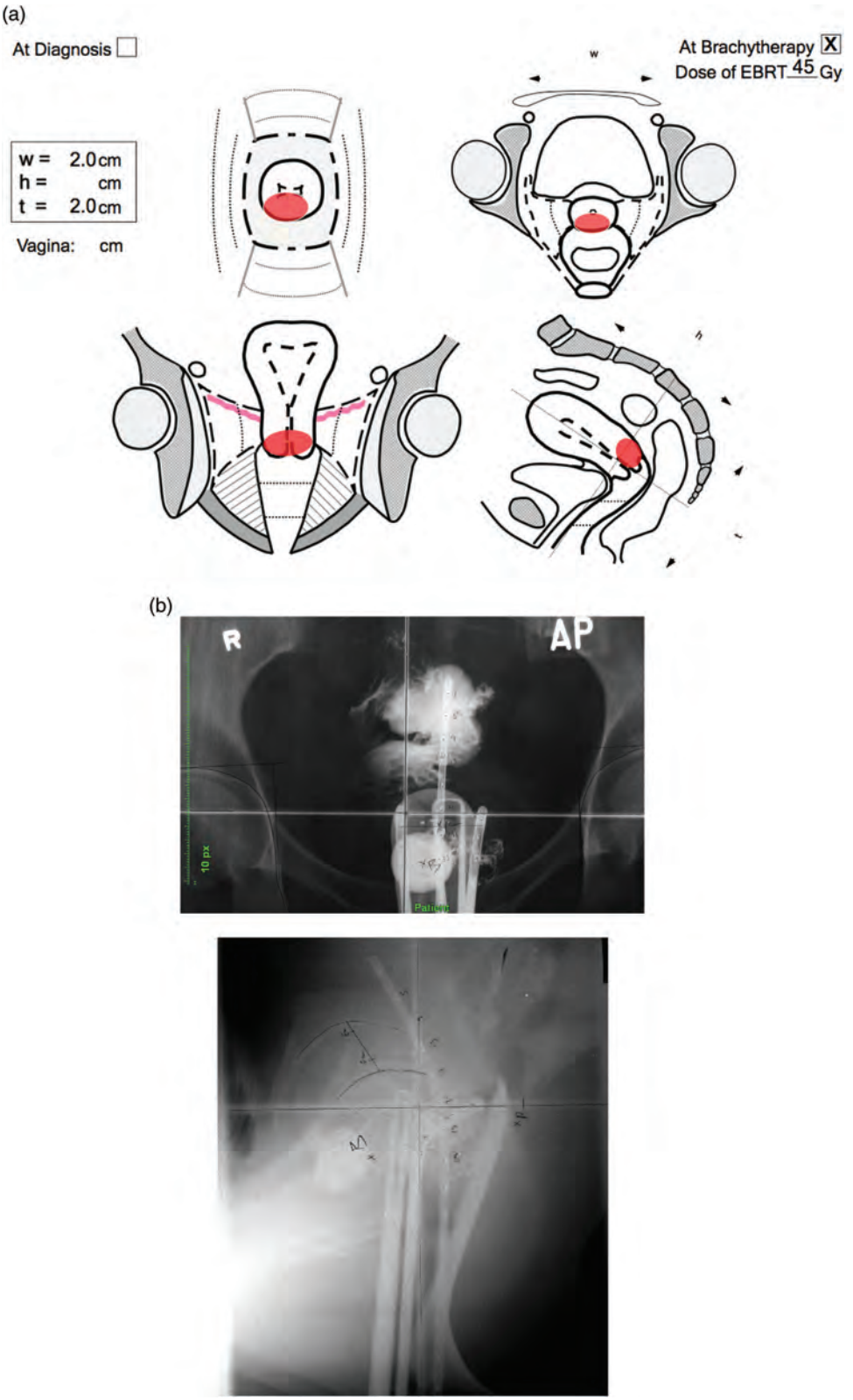

Figure A.4.4. (a) Residual GTV at first time of brachytherapy. Clinical findings by gynecological examination performed at time of the first brachytherapy fraction. The cervix was approximately 4 cm in diameter. (b) AP (upper panel) and lateral (lower panel) radiographs taken with radiographic markers in the applicators for the first brachytherapy fraction. The markers have beads at every centimeter starting with dwell position No. 1 in the tandem and the patient's right ovoid, and beads for positions Number 1 and 3, followed by beads at each centimeter from Number 3 in the patient's left ovoid. Also shown is the Foley balloon with contrast, the rectum with contrast, indications of the pelvic wall points, radioopaque threads in the gauze packing in the vagina, and the rectal retractor in the posterior vagina.

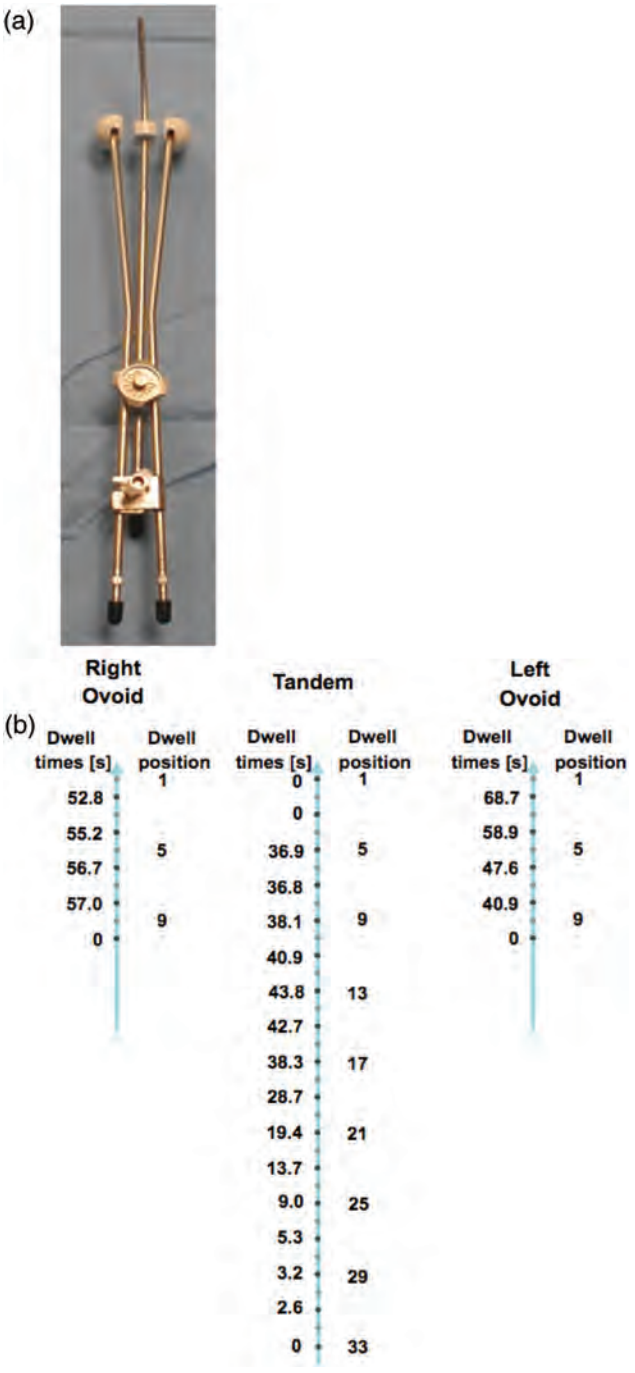

Figure A.4.5. (a) A standard HDR brachytherapy tandem and ovoid set without shielding in the ovoids (Nucletron an Elekta Company). (b) The loading pattern for the first brachytherapy application.

A.4.6 Treatment Planning and Reporting EBRT and Brachytherapy

Table A.4.5. Pointbased absorbed dose reporting (Level 1) for each brachytherapy fraction (BT_1–BT_5) and EQD2 for external beam radiotherapy (EBRT) and brachytherapy combined.

			BT1 (Gy)	BT2 (Gy)	BT3 (Gy)	BT4 (Gy)	BT5 (Gy)	EQD2 EBRT and brachytherapy (Gy)
Point	A	Right	5.4	5.3	5.2	5.3	5.3	78.0
		Left	5.1	5.2	5.3	5.2	5.2	77.2
Pelvic wall	Point	Right	0.9	1.3	0.8	1.0	1.1	48.9
		Left	1.1	0.9	1.1	1.0	0.9	48.8
Bladder	ICRU	Point	3.8	2.6	2.2	3.1	3.3	61.5
Rectovaginal	ICRU	Point	2.6	2.1	3.3	3.5	3.6	61.7
Vagina	5 mm	Right	3.9	3.9	4.0	4.0	4.0	70.8
		Left	3.9	3.9	4.0	4.0	4.0	70.8
	PIBS[a]	+2 cm	4.6	4.0	6.5	4.7	5.5	84.7
		0 cm	2.4	2.2	2.8	2.6	3.2	58.2
		−2 cm	1.4	1.2	1.7	1.5	1.8	41.5

The EQD2 was calculated assuming $\alpha/\beta = 10$ Gy for Points A, pelvic wall points, and upper vaginal points, and $\alpha/\beta = 3$ Gy for the bladder, rectal, and PIB points. The dose considered to be delivered at the same location by EBRT was 44.3 Gy $EQD2_{10}$ for target and 43.2 Gy $EQD2_3$ for OARs.
[a]PIBS, posterior inferior border of symphysis pubica, contribution of EBRT at PIBS + 2 cm 45 Gy, at PIBS 45 Gy, and at PIBS − 2 cm 43 Gy

A.4.6.1 Example of Dose Distribution (Figure A.4.6)

A.4.7 Current Patient Status

Last treatment received:	26 July 2011
Last followup visit:	7 May 2013
General condition:	excellent
Diseaserelated symptoms:	none
Treatmentrelated symptoms:	Grade 1 diarrhea, Grade 1 vaginal fibrosis
Evidence of disease:	no evidence of disease
Assesed by:	pelvic examination, pap smear, PET/CT, pelvic MRI

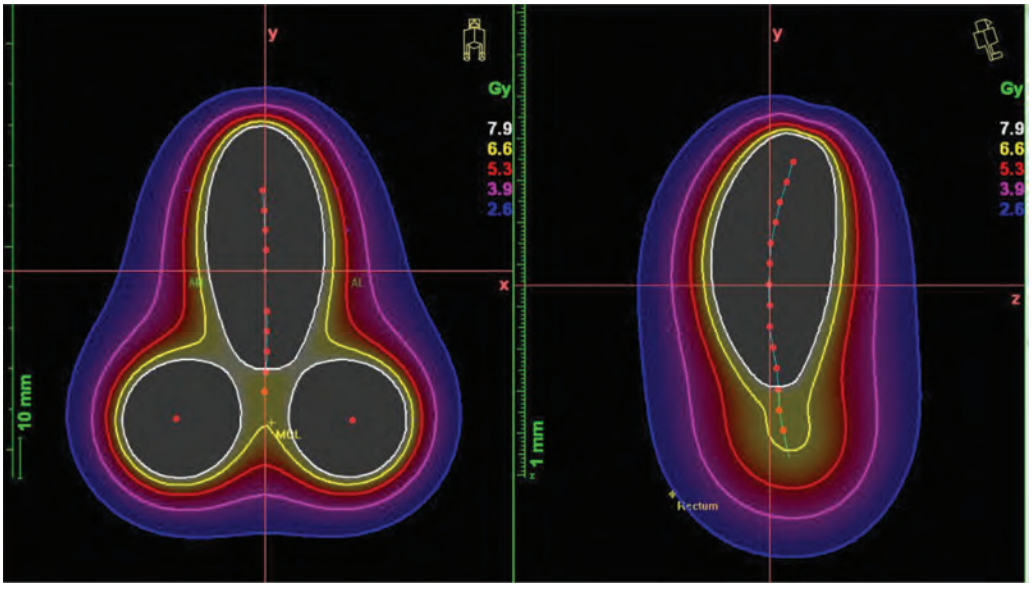

Figure A.4.6. Images in the treatment–planning system in a modified coronal plane (left) and a central sagittal plane (right) showing: optimization points as blue circles containing crosses, Points A right and left as light blue circles with crosses, active dwell positions in the plane as red dots (those out of the plane are not visualized), and selected isodose lines in the plane, corresponding to the dose prescribed to points A (5.25 Gy, rounding in the legend to 5.3 Gy), the lines corresponding to 150 %, 125 %, 100 %, 75 %, and 50 % of the prescribed dose, and the isodose line indicating the dose that would give $EQD2_{10}$ of 85 Gy (6.1 Gy) were that dose given for all five fractions following the externalbeam irradiation.

Journal of the ICRU Vol 13 No 1–2 (2013) Report 89
Oxford University Press
doi:10.1093/jicru/ndw022

Case 5: Large Cervical Cancer Stage IIB with Vaginal Involvement, No Nodes, Treated with 3D Conformal EBRT with Concomitant Chemotherapy, and MRI-Based Intracavitary and Interstitial HDR Brachytherapy Using a Tandem/Ring Applicator with Needles

A.5.1 General Patient Information

Age:	49 years
General condition:	good general health, sexually active
Prior medical history:	hypertension
Use of medication:	antihypertensive drug for number of years
Smoking history:	current smoker, approximately 25 packyears
Symptoms at presentation:	vaginal bleeding and pain in the lower abdomen

A.5.2 Tumor Extension at Diagnosis

A.5.2.1. Gynecological Examination (Figure A.5.1, Table A.5.1)

Tumor extension:	exophytic tumor in the cervix region, 1 cm extension in the posterior fornix of the vagina and both parametria infiltrated proximally
Estimated size:	6 × 4 cm (width × thickness)
Biopsy result:	Grade 3 squamous cell carcinoma with extensive invasion of the lymphovascular space

A.5.2.2 MRI of the Lower Pelvic Area (Figure A.5.1, Table A.5.1)

Tumor extension:	asymmetrical tumor in the cervix region of 5.5 cm diameter with predominantly expansive growth pattern and disruptions of the cervical ring (posterior and lateral on both sides) indicating proximal parametrial infiltration on both sides, vaginal involvement of the posterior wall approximately 1 cm, and no evidence of invasion of the bladder or rectum
Pelvic lymph nodes:	no involvement

A.5.2.3 Other Findings

FDG–PET scan:	no evidence of lymph node or distant metastases
Tumor marker SCC:	0.47 ng/ml (0–1.5)
Laparoscopic surgery:	no evidence of lymph node metastases at lymph node dissection (15 lymph nodes resected, 0 involved 0/15)

A.5.2.4 Conclusion

Forty-nine-year-old female with a squamous cell carcinoma of the cervix FIGO IIB, cT2b,pN0,M0.

A.5.3 Treatment Intention

The patient was discussed in a multidisciplinary tumor board and she was offered a curative treatment using a combination of external beam radiotherapy 45 Gy, 5 weekly cycles of cisplatin 40 mg/m^2, and a brachytherapy boost to the CTV_{HR} D_{90} to a total dose of $EQD2_{10} \geq 85$ Gy (Figure A.5.2).

A.5.4 External Beam Radiotherapy (Figure A.5.3, Table A.5.2)

Total dose prescribed:	45 Gy
Fractionation scheme:	25 × 1.8 Gy (dose distribution depicted in Figure A.5.3 and Table A.5.2)
Target volumes:	
CTV-T	cervix, uterus, half of the vagina, both parametria

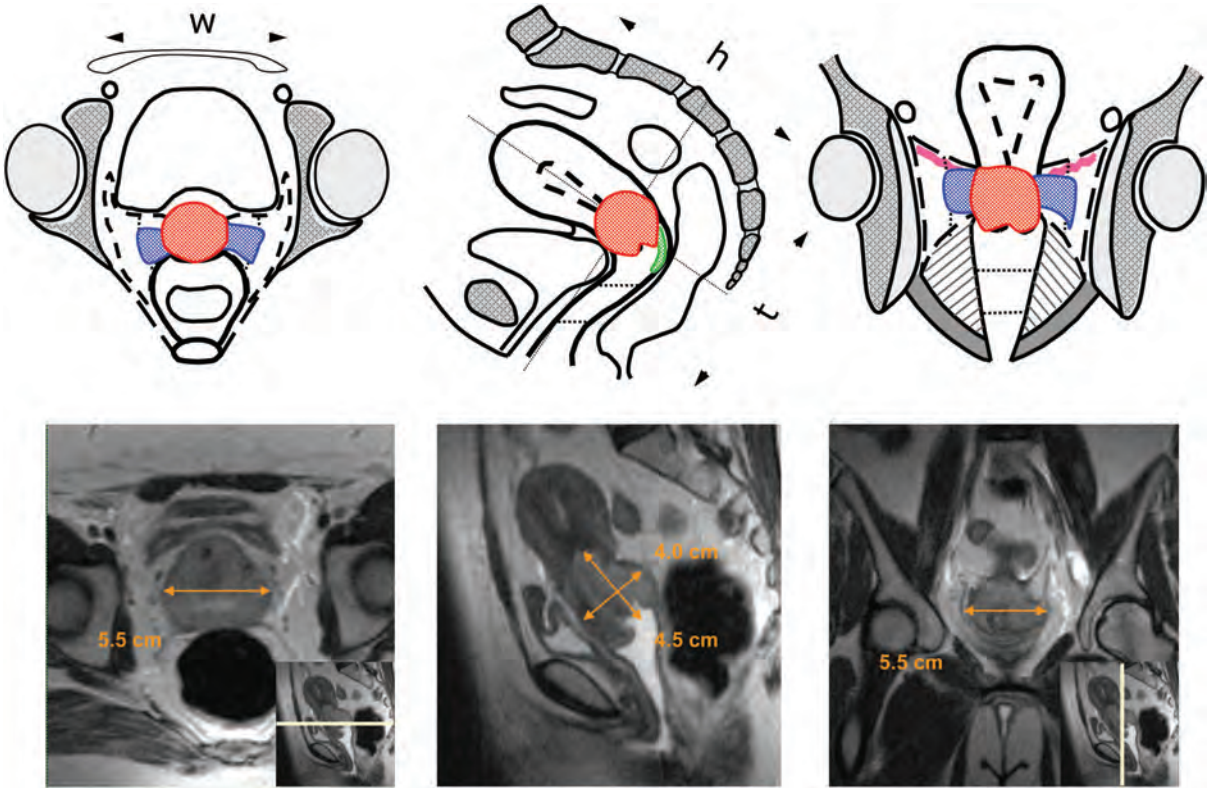

Figure A.5.1. Initial GTV extension at diagnosis. Clinical drawings (up) and corresponding MRI images (below) at the time of diagnosis.

Table A.5.1. Dimensions and volumes of GTVs and CTVs at diagnosis and at brachytherapy.

	Diagnosis	BT1 + 2	BT3 + 4
Clinical dimensions GTV, $w \times t$ (mm)	60 × 40	—	—
MRI dimensions GTV, $w \times t \times h$ (mm)	55 × 40 × 45	35 × 35 × 43	35 × 35 × 43
MRI volume GTV (cm^3)	52	33	33
Clinical dimensions CTV_{HR}, $w \times t$ (mm)	—	50 × 40	50 × 40
MRI dimensions CTV_{HR}, $w \times t \times h$ (mm)	—	48 × 35 × 43	46 × 32 × 41
CTV_{HR} (cm^3)	—	43	43
CTV_{IR} (cm^3)	—	88	88
Left parametrium	Proximal	Proximal	Proximal
Right parametrium	Proximal	Proximal	Proximal
Vagina	Upper third	Not involved	Not involved
Bladder	Not involved	Not involved	Not involved
Rectum	Not involved	Not involved	Not involved

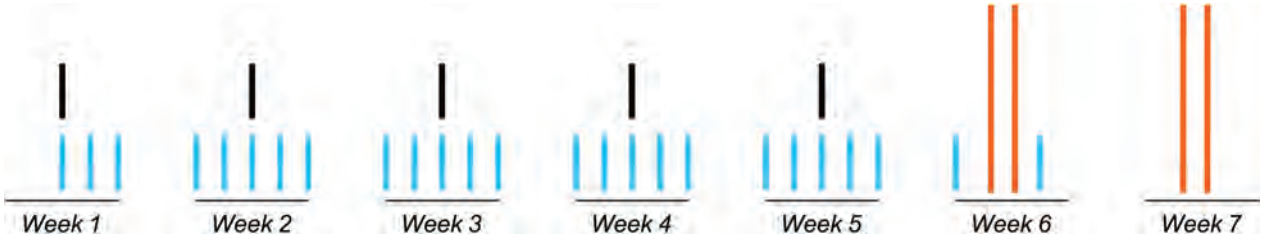

Figure A.5.2. Treatment schedule for this patient. A blue bar represents a fraction of EBRT 1.8 Gy, an orange bar represents a fraction of HDR brachytherapy, and a black bar represents a course of cisplatin 40 mg/m^2, overall treatment time 43 days.

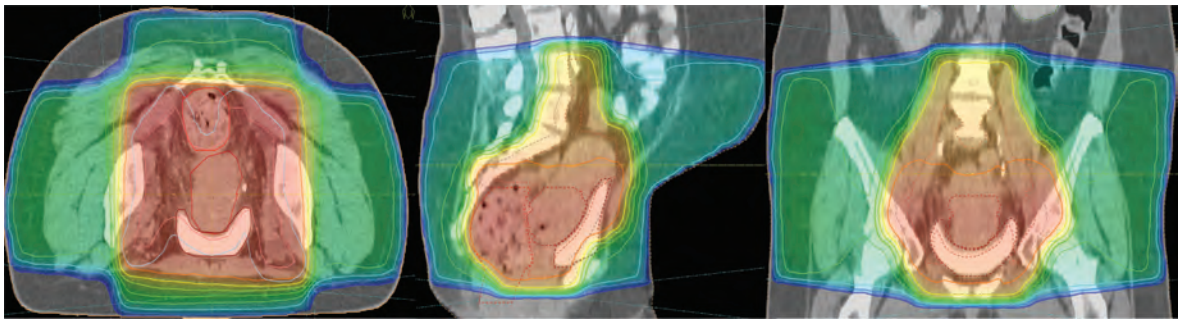

Figure A.5.3. Absorbed dose distribution of EBRT. Orange isodose corresponds to 100 % prescription dose (45 Gy). Yellow isodose corresponds to 95 % of the prescription dose. Twenty percent of the prescription dose is shown in dark blue.

Table A.5.2. Dose distribution for EBRT.

Target	Volume	Planning aim	$V_{95\ \%}$[a]	$D_{98\ \%}$	$D_{50\ \%}$	$D_{2\ \%}$	
PTV	1429 cm^3	45 Gy	94 %	41.6 Gy	45.5 Gy	47.5 Gy	
$V_{43\ Gy}$	1850 cm^3						
$V_{57\ Gy}$	0						
Organs at risk	$V_{35\ Gy}$	$V_{45\ Gy}$	$V_{50\ Gy}$	$V_{55\ Gy}$	$D_{98\ \%}$	$D_{50\ \%}$	$D_{2\ \%}$
Bladder	89.6 %	58.8 %	0	0	26.8 Gy	45.3 Gy	46.4 Gy
Rectum	73.8 %	53.7 %	0	0	13.5 Gy	45.3 Gy	47.2 Gy
Sigmoid	100.0 %	40.0 %	0	0	43.8 Gy	44.8 Gy	46.3 Gy
Bowelbag	390 cm^3	0	0	0	1.9 Gy	21.0 Gy	43.2 Gy

[a]Volume treated to 95 % of the planning aim dose.

CTV-N pelvic lymph nodes up to aortic bifurcation
Applied PTV margin: 10 mm
Patient positioning: prone position, belly board
Planning technique: 3DCRT, 4 Field box
Concomitant therapy: 5weekly cycles of cisplatin 40 mg/m^2
Overall treatment time: 37 days

A.5.5 Brachytherapy

A.5.5.1 Gynecological Examination at the Time of First Brachytherapy (Figure A.5.4, Table A.5.1)

Tumor extension: regression of tumor bulk with persistent infiltration of both parametria diminished but still present, no vaginal infiltration
Estimated size: 5 × 4 cm (width × thickness)

A.5.5.2 MRI of the Lower Pelvic Area at First Brachytherapy (Figure A.5.4, Table A.5.1)

Tumor extension: residual central gross tumor volume (bright zone) with surrounding residual pathological tissue (gray zones) in both parametria dorsolateral (left > right) and beginning recovery of the cervical stroma anterior, overall width: 3.5 cm, no vaginal residual involvement.

A.5.5.3 Treatment Planning Aim

Table A.5.3. Treatment planning aim and prescribed doses.

			Planning aim (Gy)	Prescribed dose (Gy)
CTV_{HR}	D_{90}	$EQD2_{10}$	≥85	92.3
Bladder	D_{2cm^3}	$EQD2_3$	≤90	80.6
Rectum	D_{2cm^3}	$EQD2_3$	≤70	64.3
Sigmoid	D_{2cm^3}	$EQD2_3$	≤75	51.7

Doses are given in EQD2 using $\alpha/\beta = 10$ Gy for target and $\alpha/\beta = 3$ Gy for organs at risk. (For the vagina, no planning aim dose constraint was applied.)

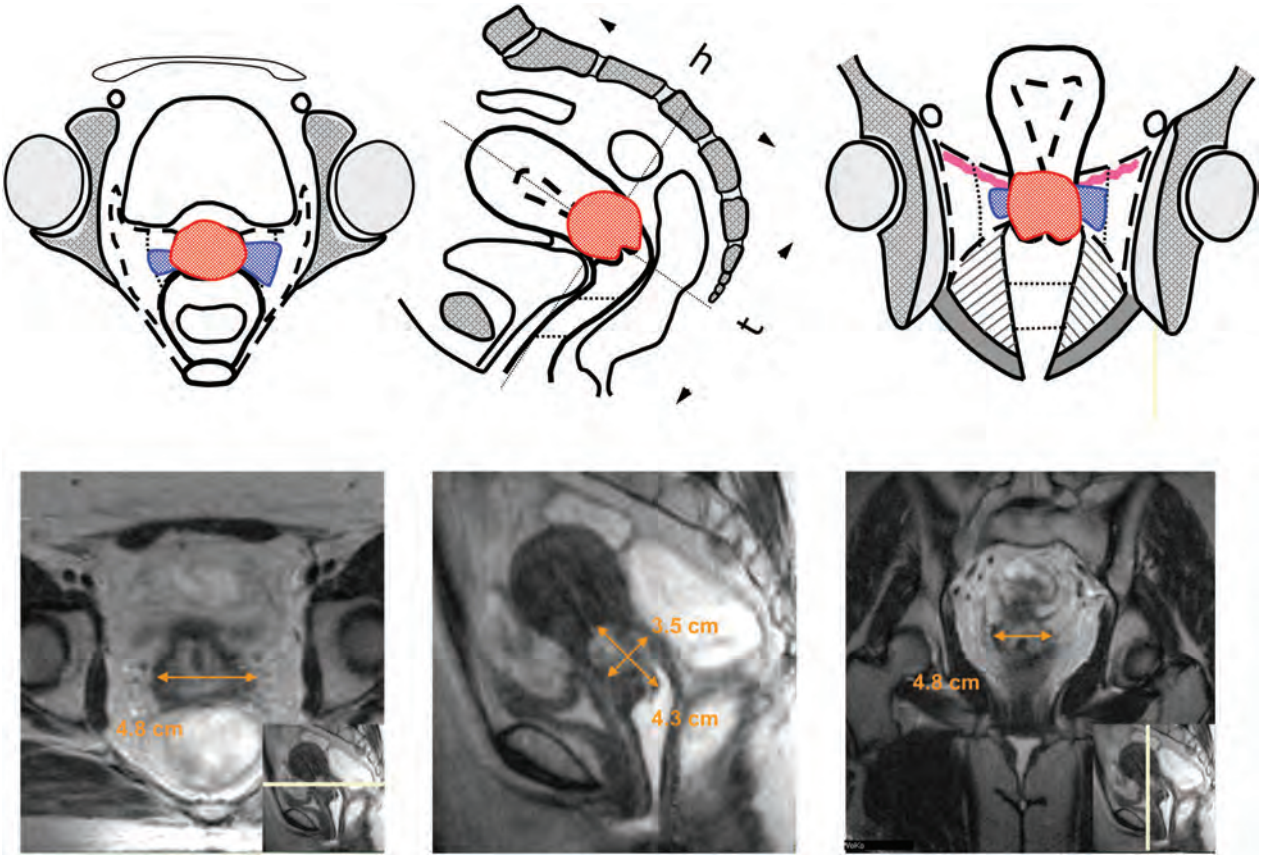

Figure A.5.4. Residual GTV and residual pathological tissue at the time of first brachytherapy: clinical drawings (upper) and corresponding MRI images (lower) at the time of first brachytherapy without applicator in place.

A.5.5.4 Treatment Delivery

Treatment method:	combined intracavitary and interstitial to ensure proper target coverage based on MRI-scan pre-brachytherapy
First application:	after 43.2 Gy
Time between fractions:	16 h
Modality used for planning:	MRI-scan after applicator insertion MRI scan before second fraction to look for changes in applicator position and organs at risk
Second application:	after 45 Gy, the same procedure was followed, 6 days after the first application
Overall treatment time:	brachytherapy alone 9 days, EBRT + brachytherapy 48 days

A.5.5.5. Equipment Used for Brachytherapy (Figure A.5.5)

Applicator	tandem ring applicator with a 6 cm tandem and a 30 mm ring, and 4 blunt titanium needles (Nucletron an Elekta Company, Veenendaal, The Netherlands) at 4, 5, 7, and 8 o'clock
Source	Ir-192, source model mHDR-v2, air kerma strength 40 820 μGy m^2 h^{-1}, with micro Selectron Afterloader (Nucletron)
Treatment planning System:	Oncentra GYN (Nucletron an Elekta Company)
Dose calculation algorithm	AAPM TG-43

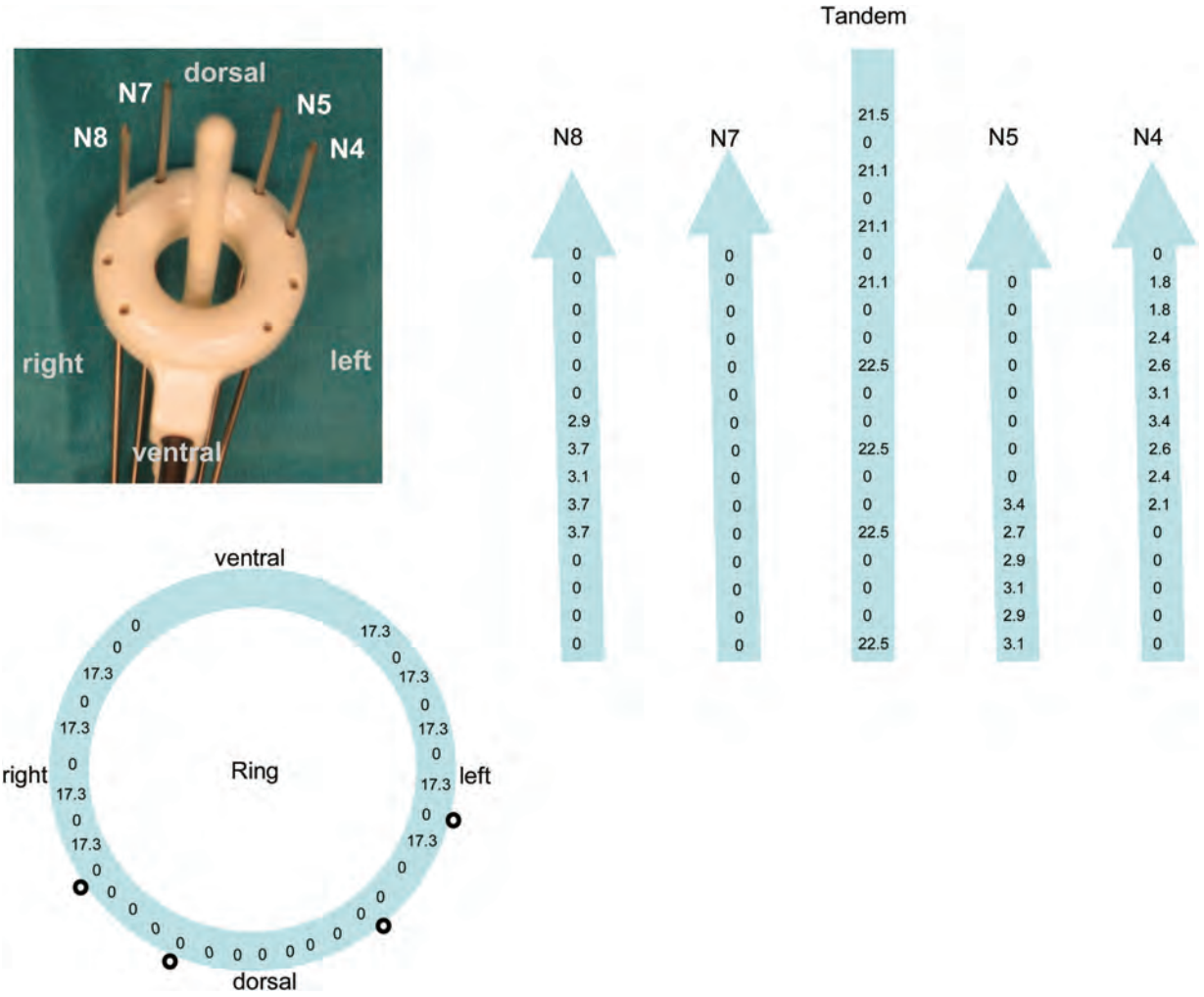

Figure A.5.5. Equipment used for brachytherapy. Tandem Ring applicator (Nucletron an Elekta Company) with needles inserted at positions N4, N5, N7, and N8 at 4, 5, 7, and 8 o'clock (ring position), respectively. The needle insertion positions were selected based on clinical examination. The ring showed a slight rotation to the right. On MRI with the applicator in place, the needle positions N4, N5 and N8 were favorable, but N7 was close to the rectum (Figure A.5.6). With delineation of CTV_{HR} and rectum, both a sufficient dose in the CTV_{HR} (D_{90} $EQD2_{10} = 92$ Gy), and dose in the rectum far below the dose constraint (D_{2cm^3} $EQD2_3 = 64$ Gy, see Table A.5.5b) could be achieved without loading of N7. Dwell times for one HDR fraction (in s) are shown for all dwell positions using a source step of 2.5 mm.

A.5.6 Treatment Planning and Reporting Brachytherapy and EBRT

Table A.5.4. Applicators and $EQD2_{10}$ isodose surface volumes

	First application	Second application
Nominal tandem length	60 mm	60 mm
Nominal ring diameter	30 mm	30 mm
Number of active needles	3	3
60 Gy volume	262 cm^3	250 cm^3
75 Gy volume	181 cm^3	168 cm^3
85 Gy volume	85 cm^3	83 cm^3
TRAK	2×4.3 mGy	2×4.2 mGy

Table A.5.5a. Point-based absorbed dose reporting (Level I)

			First application		Second application		Total dose
			BT1 (Gy)	BT2 (Gy)	BT3 (Gy)	BT4 (Gy)	EBRT + brachytherapy (EQD2 Gy)
Point	A	Right	x[a]	x[a]	x[a]	x[a]	x[a]
		Left	7.0	7.0	7.8	7.8	87.2
Pelvic Wall	Point	Right	1.1	1.1	1.0	1.0	48.2
		Left	1.0	1.0	1.1	1.1	48.2
Bladder	ICRU	Point	2.8	2.8	5.5	5.5	68.4
Recto-vaginal	ICRU	Point	2.4	2.4	3.5	3.5	57.5
Vagina	5 mm	Right	7.5	7.5	7.6	7.6	106.9
		Left	7.3	7.3	7.2	7.2	102.7
	PIBS[b]	+2 cm	5.9	5.9	6.3	6.3	88.8
		0 cm	2.6	2.6	2.4	2.4	53.4
		−2 cm	0.6	0.6	0.7	0.7	7.3

Total dose values in EQD2 were calculated using $\alpha/\beta = 10$ Gy for Point A and pelvic wall point and $\alpha/\beta = 3$ Gy for normal tissue point doses. The dose considered to be delivered at the same location by EBRT was 44.3 Gy $EQD2_{10}$ for target and 43.2 Gy $EQD2_3$ for OARs.
[a]Point A dose right not representative, as needle position is too close.
[b]PIBS, posterior inferior border of symphysis pubica, contribution of EBRT at PIBS + 2 cm 44.4 Gy, at PIBS 42.4 Gy, and at PIBS − 2 cm 5.4 Gy.

Table A.5.5b. DVH-based absorbed dose reporting (Level II)

		First application		Second application		Total dose
		BT1 (Gy)	BT2 (Gy)	BT3 (Gy)	BT4 (Gy)	EBRT + brachytherapy (EQD2 Gy)
GTV_{res}	D_{98}	10.1	10.1	10.7	10.7	115.0
	D_{90}	11.9	11.9	12.4	12.4	134.0
CTV_{HR}	D_{98}	6.5	6.5	6.7	6.7	80.8
	D_{90}	7.9	7.9	8.1	8.1	92.3
	D_{50}	11.7	11.7	11.5	11.5	127.8
CTV_{IR}	D_{98}	3.7	3.7	4.1	4.1	62.3
	D_{90}	4.6	4.6	5.3	5.3	69.0
	D_{50}	8.5	8.5	8.7	8.7	97.6
Bladder	$D_{0.1cm^3}$	7.2	7.2	7.2	7.2	102.0
	D_{2cm^3}	5.6	5.6	5.4	5.4	80.6
Rectum	$D_{0.1cm^3}$	4.8	4.8	5.0	5.0	74.2
	D_{2cm^3}	3.8	3.8	3.9	3.9	64.3
Sigmoid	$D_{0.1cm^3}$	1.9	1.9	4.4	4.4	59.9
	D_{2cm^3}	1.5	1.5	2.6	2.6	51.7

Total doses in EQD2 were calculated using $\alpha/\beta = 10$ Gy for target and $\alpha/\beta = 3$ Gy for normal tissue volumes. The dose considered to be delivered at the same location by EBRT was 44.3 Gy $EQD2_{10}$ for target and 43.2 Gy $EQD2_3$ for OARs.

A.5.6.1. Example of Dose Distribution

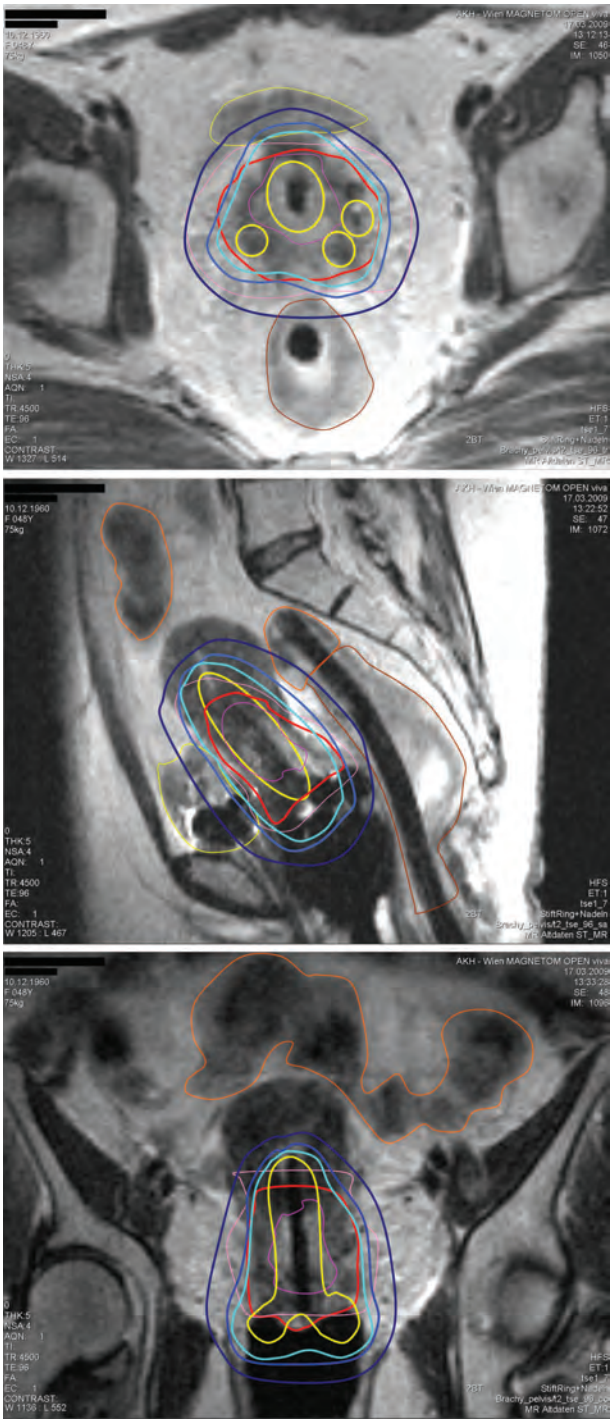

Figure A.5.6 Delineation and dose distribution at second brachytherapy application on MRI with applicators in place. CTV_{HR}, thick red; CTV_{IR}, thin pink; GTV_{res}, thin magenta; bladder, thin yellow; rectum, thin brown; bowel, thin orange; $EQD2_{10}$ isodoselines: dark blue is 60 Gy, blue is 75 Gy, cyan is 85 Gy, and yellow is 156 Gy. These doses correspond to 3.5, 5.8, 7, and 14 Gy per fraction.

A.5.7 Current patient status

Last treatment received:	18 March 2009
Last follow-up visit:	11 December 2012
General condition:	good
Disease-related symptoms:	none
Treatment-related symptoms:	after 44 months follow-up: vaginal morbidity Grade 2 (vaginal dryness and upper vaginal stenosis), rectosigmoidal morbidity Grade 1 (increased stool frequency), and bladder morbidity Grade 2 (stress incontinence).
Evidence of disease:	none
Assessed by:	patient history, gynecological examination, MRI-pelvis

Journal of the ICRU Vol 13 No 1–2 (2013) Report 89
Oxford University Press
doi:10.1093/jicru/ndw023

Case 6: Large Cervical Cancer Stage IIIB with Pathological Pelvic Nodes Treated with IMRT, Concomitant Chemotherapy, and MRI-Based Intracavitary and Interstitial Tandem/Ring Pulsed Dose Rate Brachytherapy with Needles

A.6.1 General Patient Information

Age:	57 years
General condition:	performance status = 0 (WHO)
Prior medical history:	rheumatoid arthritis
Use of medication:	no medication
Smoking history:	non-smoker
Symptoms at presentation:	6 month history of vaginal bleeding

A.6.2 Tumor Extension at Diagnosis

A.6.2.1 Gynecological Examination (Figure A.6.1, Table A.6.1)

Tumor extension:	endophytic tumor with distal parametrial invasion on the right side and proximal parametrial invasion on the left side. There was a central necrosis of 1 cm at the cervix. Vagina was not involved.
Estimated size:	8 × 5 cm (width × thickness)
Biopsy result:	squamous cell carcinoma, degree of differentiation unknown

A.6.2.2 MRI of the Pelvis (Figure A.6.1, Table A.6.1)

Tumor extension:	an expansive (52 × 48 mm, $w \times t$) tumor originating from the cervix with infiltrative growth into the distal right and proximal left parametria, but also involving the lower part of the uterus in which a large fibromyoma was present
Pelvic lymph nodes:	pathological nodes along the right and left external iliac vessels

A.6.2.3 Other Findings

Whole body FDG PET–CT:	pathological nodes along the right and left external iliac vessels. There was hydronephrosis on the right side necessitating nephrostomy
Cr-51 EDTA:	GRF = 90 ml/min

A.6.2.4 Conclusion

Fifty-seven-year-old female with squamous cell carcinoma of the uterine cervix FIGO Stage IIIB, TNM T3N1M0 (IDC-O 10: C53.9).

A.6.3 Treatment Intention and Overall Treatment Plan

At multidisciplinary team conference, it was decided to offer curatively intended radio-chemotherapy using IMRT with six courses of concomitant weekly cisplatin and a boost of pulsed dose rate brachytherapy to the CTV_{HR} D_{90} to a total dose of at least 85 Gy $EQD2_{10}$. Overall treatment time 7 weeks with brachytherapy delivered in the final 2 weeks of treatment (Figure A.6.2).

A.6.4 External Beam Radiotherapy (Figure A.6.3 and Table A.6.2)

Total dose prescribed:	50/60 Gy (PTV-T + N1/PTV-N2)
Fractionation scheme:	30 × 1.67 / 2.00 Gy (PTV-T + N1 / PTV-N2) 5 fractions per week

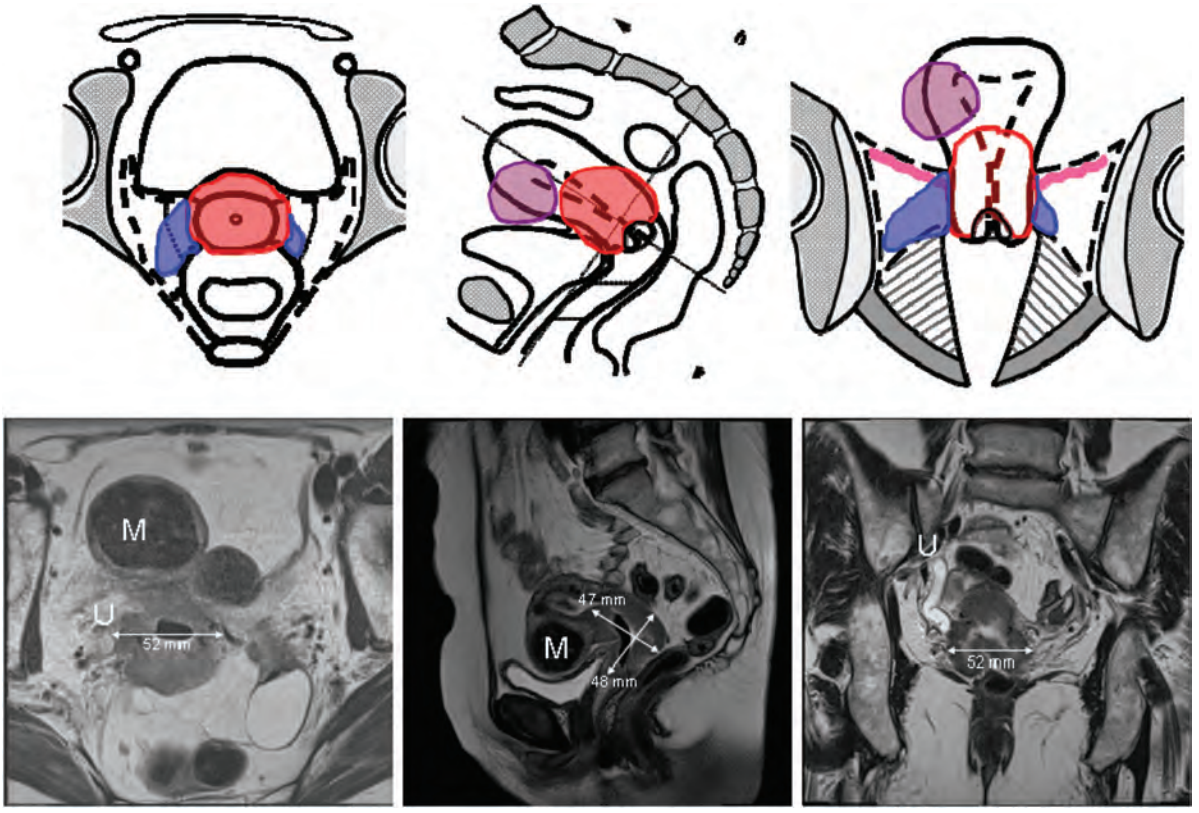

Figure A.6.1. (Upper panel) Clinical drawings performed at diagnosis. The initial GTV at diagnosis is indicated within the cervix and uterus (red), and within the parametria (blue). Necrosis at the cervix is indicated in black. (Lower panel) Transverse, sagittal, and coronal T2-weighted 1.5 T MRI of the pelvis at diagnosis. Hydroureter (U) is seen on the right side of the pelvis and a large fibromyoma (M) in the uterus. The dimensions of the GTV are indicated by arrows.

Table A.6.1. Clinical dimensions and volumes of GTVs and CTVs at diagnosis and at brachytherapy.

	Diagnosis	BT1	BT2
Clinical dimensions GTV, $w \times t$ (mm)	80×50[a]	—	—
MRI dimensions GTV, $w \times t \times h$ (mm)	$52 \times 48 \times 47$	$36 \times 29 \times 26$	$37 \times 30 \times 27$
MRI volume GTV (cm^3)	61[b]	8[c]	9[c]
Clinical dimensions CTV_{HR}, $w \times t$ (mm)	—	60×40	50×40
MRI dimensions CTV_{HR} $w \times t \times h$ (mm)	—	$51 \times 39 \times 45$	$50 \times 39 \times 43$
MRI volume CTV_{HR}[c] (cm^3)	—	41	37
MRI volume CTV_{IR}[c] (cm^3)	—	107	104
Left parametrium	Proximal	Proximal	Proximal
Right parametrium	Distal	Distal	Distal
Uterus	Lower part	Not involved	Not involved
Vagina	Not involved	Not involved	Not involved
Bladder	Not involved	Not involved	Not involved
Rectum	Not involved	Not involved	Not involved

[a]Height not evaluable by clinical examination.
[b]Calculated as $(\pi/6) \times w \times h \times t/1000$.
[c]Calculated by the treatment planning system.

Target volumes:
CTV-T cervix, uterus, upper half of the vagina, both parametria. An additional non-isotropic margin of 1–2 cm was added around the uterus in the AP–PA aspect to arrive at the ITV-T

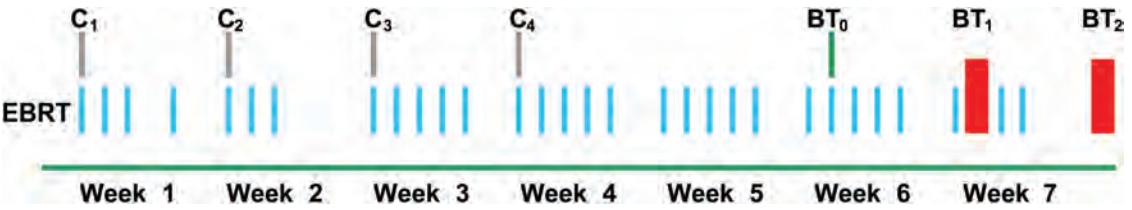

Figure A.6.2. Treatment schedule involving 50 days of treatment including weekly cisplatin (C_{1-4}) external-beam radiotherapy (EBRT) with simultaneous targeted boost (50/60 Gy in 30 fractions)) and PDR brachytherapy (BT_{1-2}). Treatment was initiated with EBRT (light blue bar) and weekly cisplatin (gray bar). Cisplatin was omitted in Weeks 5 and 6 due to leucopoenia. External-beam radiotherapy during the first 2 weeks of treatment was given over Christmas. For PDR BT (red bars), a planning intracavitary tandem-ring implant was performed in Week 6 ($BT_{0,}$ green bar). The actual implants used for treatment in Weeks 7 and 8 (Monday) were both intracavitary/interstitial implants (BT_1, BT_2). MRI with applicator *in situ* was performed for all 3 brachytherapy implants.

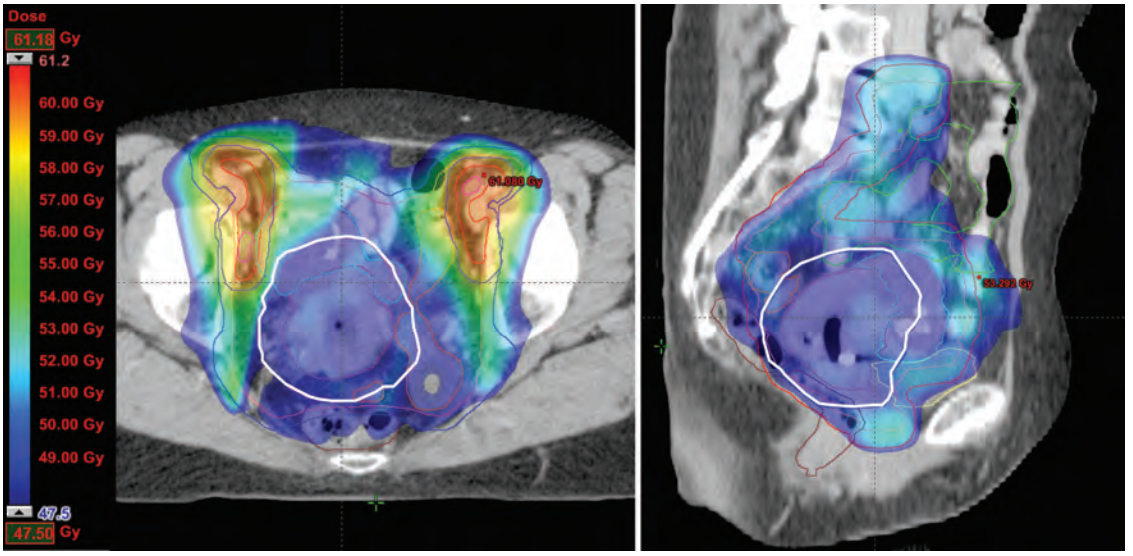

Figure A.6.3. Transversal and sagittal view of the external beam radiotherapy dose distribution for Case 6 provided by IMRT. A simultaneous integrated boost with 60 Gy in 30 fractions was delivered to pathological nodes (PTV-N2) along the external iliac vessels bilaterally. The pelvis itself (PTV-T + N1) was treated with 50 Gy in 30 fractions. A helper volume (white contour) was used to keep a homogenous dose in the organs at risk close to the primary tumor, where also brachytherapy was going to be applied. The range of the color wash is from 95 % of 50 Gy to D_{max} (47.5–61.2 Gy).

Table A.6.2. Absorbed dose and volume parameters for external-beam radiotherapy for target volumes and organs at risk.

Target	Volume	Planning aim		$V_{95\ \%}$ [a]	$D_{98\ \%}$	$D_{50\ \%}$	$D_{2\ \%}$
PTV-T + N1	1860 cm^3	50 Gy		100 %	48.3 Gy	51.5 Gy	60.6 Gy
PTV-N2	236 cm^3	60 Gy		100 %	58.5 Gy	60.1 Gy	60.9 Gy
$V_{43\ Gy}$	3149 cm^3						
$V_{57\ Gy}$	376 cm^3						
Organs at risk	$V_{35\ Gy}$	$V_{45\ Gy}$	$V_{50\ Gy}$	$V_{55\ Gy}$	$D_{98\ \%}$	$D_{50\ \%}$	$D_{2\ \%}$
Bladder	100 %	100 %	68 %	0 %	47.3 Gy	50.4 Gy	53.5 Gy
Rectum	92 %	87 %	11 %	0 %	8.4 Gy	48.9 Gy	51.4 Gy
Sigmoid	100 %	100 %	60 %	6 %	48.0 Gy	50.3 Gy	58.4 Gy
Bowel bag	1209 cm^3	1005 cm^3	680 cm^3	198 cm^3	18.5 Gy	38.9 Gy	58.8 Gy

The total GTV-N (sum of all pathological nodes) was 18 cm^3.
[a]Volume treated to 95 % of the planning aim dose, *i.e.*, 47.5 Gy for PTV-T + N1 and 57.0 Gy for PTV-N2, respectively.

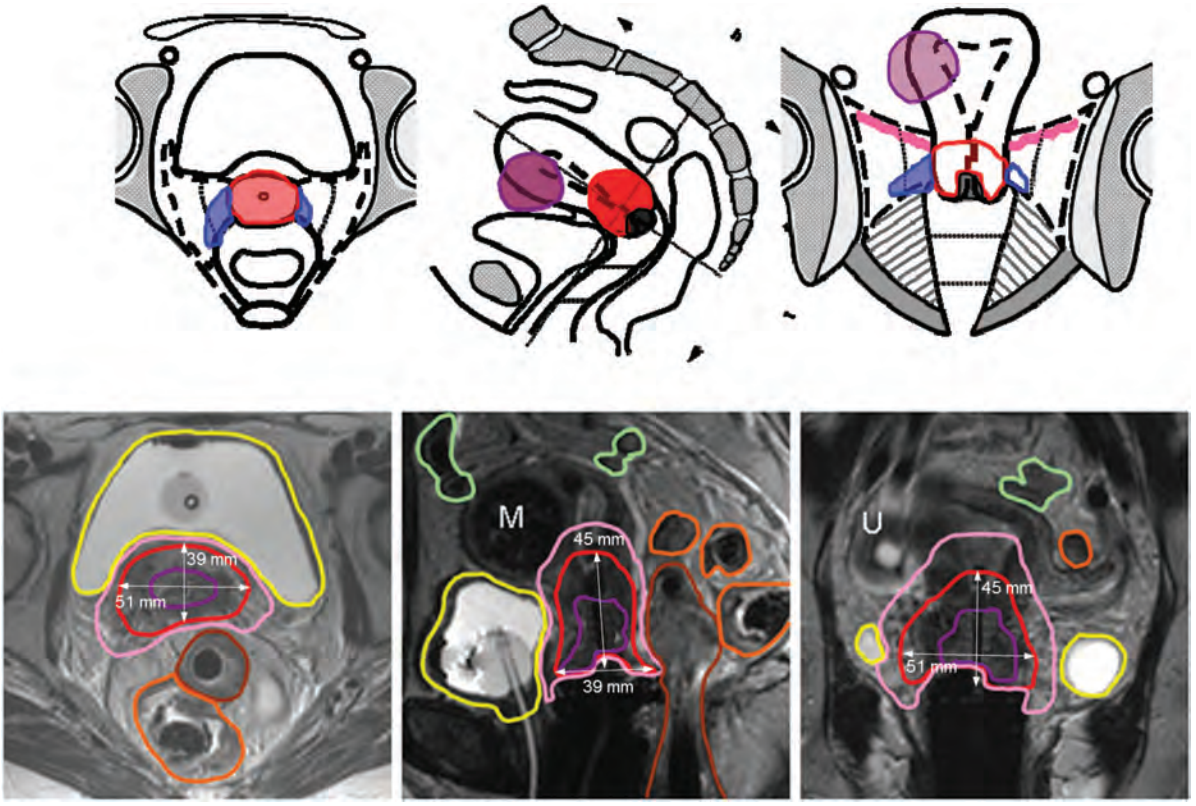

Figure A.6.4. (Upper panel) Clinical drawing performed at the time of first brachytherapy. Necrosis at the cervix is indicated in black. Residual GTV (GTV_{res}) and residual pathological tissue at the time of first brachytherapy is indicated within the cervix and uterus (red) and within parametria (blue). The fibromyoma is indicated in purple. (Lower panel) Transverse, sagittal, and coronal T2-weigthed 1.5 T MRI of the pelvis at BT_1 with the BT applicator and needles *in situ*. Hydroureter (U) is seen on the right and a large fibromyoma (M) in the uterus. The GTV_{res} (magenta), CTV_{HR} (red), and CTV_{IR} (pink) are indicated on all MRI planes together with the outer contours of the bladder (yellow), rectum (brown), sigmoid (orange), and bowel (light green). The dimensions of CTV_{HR} are indicated by arrows.

Table A.6.3. Treatment planning aims and prescribed EQD2 for total EBRT + BT.

Structure			Planning aim (Gy)	Prescribed dose (Gy)
CTV_{HR}	D_{90}	$EQD2_{10}$	≥ 85	88.9
Bladder	D_{2cm^3}	$EQD2_3$	≤ 90	71.1
Rectum	D_{2cm^3}	$EQD2_3$	≤ 70	65.6
Sigmoid	D_{2cm^3}	$EQD2_3$	≤ 70	57.4
Bowel	D_{2cm^3}	$EQD2_3$	≤ 70	53.3

The equivalent dose in 2 Gy fractions (EQD2) was calculated assuming $\alpha/\beta = 10$ Gy for tumor and $\alpha/\beta = 3$ Gy for organs at risk. The repair halftime was assumed to be 1.5 h. (No dose constraint was applied for vagina.)

CTV-N1	all pelvic nodal stations to the aortic bifurcation (L4–L5)
CTV-N2	all pathological nodes (GTV-N) found on MRI and PET–CT with a margin of up to 1 cm
Applied PTV margin:	5 mm in the axial plane and 8 mm in the cranio-caudal

Table A.6.4. Applicator characteristics, time/dose pattern, and $EQD2_{10}$ isodose surface volumes for the two brachytherapy (BT_1 and BT_2) fractions used in clinical case number 6.

	BT1	BT2
Nominal tandem length	50 mm	50 mm
Nominal ring diameter	26 mm	26 mm
Number of active needles	8	8
Number of pulses	20	20
Pulse repetition interval	60 min	60 min
Pulse irradiation time	8 min	10 min
60 Gy volume (6.1 Gy)[a]	263 cm^3	312 cm^3
75 Gy volume (12.7 Gy)[a]	95 cm^3	111 cm^3
85 Gy volume (16.5 Gy)[a]	66 cm^3	78 cm^3
TRAK	7.9 mGy	8.9 mGy

Brachytherapy was delivered by pulsed dose rate brachytherapy using a source with an air kerma strength of 4070 $\mu Gy\ m^2\ h^{-1}$.
[a]Physical dose considered to be delivered at the same location by EBRT was 50 Gy given in 30 fractions. The physical isodose level of BT used for calculating the isodose surface volume to a given $EQD2_{10}$ dose level is given in parentheses. The isodose surface volume was calculated by the treatment planning system (BrachyVision).

Table A.6.5a. Point-based absorbed dose reporting (Level 1) reporting for each brachytherapy fraction (BT_1 and BT_2) and for EQD2 for external-beam radiotherapy (EBRT) and BT combined.

			First application BT1 (Gy)	Second application BT2 (Gy)	Total dose EBRT + BT (EQD2 Gy)
Point A[a]	Right		x	x	x
	Left		x	x	x
Pelvic wall[b]	Point	Right	2.5	3.4	65.2
		Left	1.7	2.1	63.3
Bladder	ICRU	Point	10.1	12.5	70.4
Recto-vaginal	ICRU	Point	7.0	13.0	67.2
Vagina	5 mm	Right	19.4	19.0	98.6
	5 mm	Left	12.3	13.7	75.6
	PIBS	+2 cm	11.8	7.1	66.3
	PIBS	0 cm	3.9	3.0	53.5
	PIBS	−2 cm	1.8	1.6	4.6

The EQD2 was calculated assuming $\alpha/\beta = 10$ Gy for tumor and $\alpha/\beta = 3$ Gy for organs at risk. The repair halftime was assumed to be 1.5 h. Physical dose considered to be delivered at the same location by EBRT was 50 Gy given in 30 fractions.
[a]Not evaluable due to close proximity of loaded needles.
[b]Dose of EBRT at the left and right pelvic wall point was 60 Gy in 30 fractions (simultaneous integrated boost).

Table A.6.5.b. DVH-based absorbed dose reporting

		1st application BT1 (Gy)	2nd application BT2 (Gy)	Total dose EBRT + BT (EQD2 Gy)
GTV_{res}	D_{98}	20.3	21.3	94.4
CTV_{HR}	D_{98}	15.4	16.1	83.0
	D_{90}	17.3	18.5	88.9
	D_{50}	23.8	27.2	112.5
CTV_{IR}	D_{98}	7.9	7.5	63.4
	D_{90}	9.4	9.6	67.4
	D_{50}	15.5	16.5	83.7
Pathological LNs				
External iliac	D_{98}	0.8–1.3	0.7–1.2	61.3–62.3
Obturator	D_{98}	1.3–2.1	1.2–1.6	62.3–63.6
Bladder	$D_{0.1\,cm^3}$	14.2	14.2	79.5
	$D_{2\,cm^3}$	11.6	11.6	71.2
Rectum	$D_{0.1\,cm^3}$	12.7	12.2	73.8
	$D_{2\,cm^3}$	9.2	10.1	65.6
Sigmoid	$D_{0.1\,cm^3}$	8.2	11.4	66.2
	$D_{2\,cm^3}$	5.6	7.0	57.4
Bowel	$D_{0.1\,cm^3}$	3.1	8.5	56.8
	$D_{2\,cm^3}$	2.7	5.7	53.3

Dose per pulse can be found by dividing the dose from each application by 20. The total doses in EQD2 were calculated using $\alpha/\beta = 10$ Gy for target and $\alpha/\beta = 3$ Gy for normal tissue volumes. Physical dose considered to be delivered at the same location by EBRT was 50 Gy given in 30 fractions.

	plane. Daily cone-beam CT for verification was used
Patient positioning:	supine position with knee cushion
Planning technique:	6-field IMRT with simultaneous integrated boost
Concomitant treatment:	4 cycles of weekly cisplatin 40 mg/m^2. Course numbers 5–6 of cisplatin was not given due to leucopoenia.
Overall treatment time:	46 days

A.6.5 Brachytherapy

A.6.5.1 Gynecological Examination at First Time of Brachytherapy (Figure A.6.4)

Tumor extension:	tumor regression, but persistent involvement of the right distal

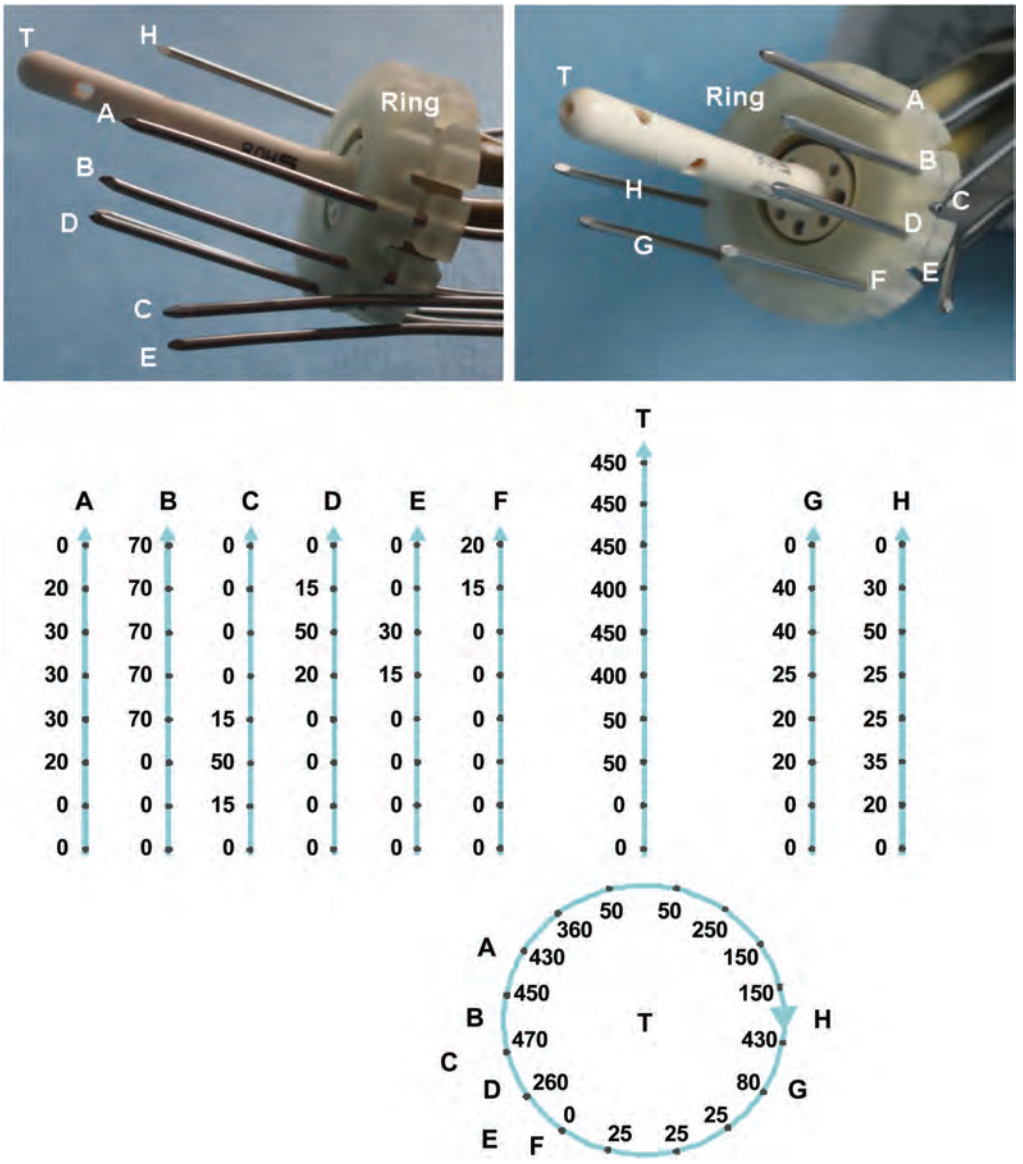

Figure A.6.5. The upper panel show the applicator configuration for BT_1 where a 50 mm tandem (T) and a 26 mm ring was combined with six interstitial titanium needles (A, B, D, F, G, H) implanted to a depth of about 3 cm through a cap attached to the ring. Two additional needles (C, E) were implanted on the outside of the needle cap in the right lower quadrant. The lower panel shows the loading pattern (nominal seconds) in each stopping position of the optimized plan for one PDR application. All stopping positions were spaced by 5 mm. A similar implant was used for BT_2.

parametrium and proximal parametrium on the left.

Estimated size: 6 × 4 cm (width × thickness)

A.6.5.2 MRI of the Pelvis at First Brachytherapy (Figure A.6.4 and Table A.6.1)

Tumor extension: both parametria involved as described above, but uterus not involved anymore.

A.6.5.3 Treatment Planning aim (Table A.6.3)

The treatment planning aim was to deliver at least 35 Gy $EQD2_{10}$ by brachytherapy to $D_{90\ \%}$ of the CTV_{HR} assuming that CTV_{HR} received 50 Gy (46.8 Gy $EQD2_{10}$) from EBRT. It was also assumed that the OAR received 50 Gy from EBRT (Figure A.6.3) close to the brachytherapy applicator.

A.6.5.4 Treatment Delivery

Treatment method: MRI with the intracavitary implant *in situ* was performed in

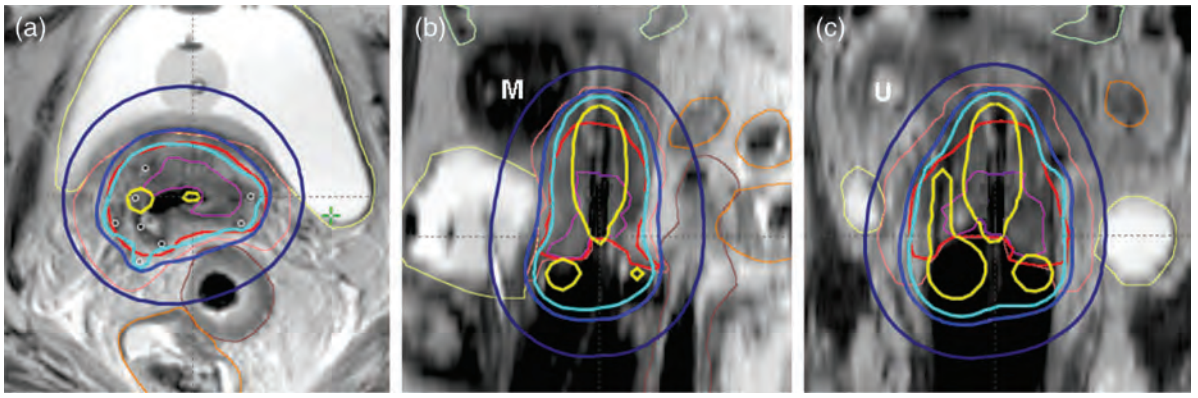

Figure A.6.6. Targets, organs at risk, and dose distribution for PDR BT_1 is shown in a para-transverse (a), para-coronal (b), and sagittal plane(c) just above the ring on a T2-weighted MRI with the brachytherapy applicator *in situ*. The fibromyoma (M) in the uterus is seen on (b) and the hydroureter (U) is seen on the right in (c). The positions of the needles are marked with white circles in (a). The brachytherapy target contours are indicated with magenta (GTV_{res}), red (CTV_{HR}), and pink (CTV_{IR}). The outer contours of organs at risk are indicated with yellow (bladder), brown (rectum), orange (sigmoid), and light green (bowel). The iso-doses shown are for 33 Gy (200 %) (yellow), 16.5 Gy (100 %) (cyan), 12.7 Gy (blue), and 6.1 Gy (dark blue), corresponding to the volumes treated to a total $EQD2_{10}$ (EBRT and brachytherapy) of 140, 85, 75, and 60 Gy, respectively.

	Week 5 for the purpose of pre-planning (BT_0) only, *i.e.,* no treatment. The actual implants (BT_1 and BT_2) used for treatment were both intracavitary/interstitial implants.
Time–dose pattern:	Pulsed dose rate brachytherapy employing 20 hourly pulses for each fraction of brachytherapy (BT_1 and BT_2).
Time between pulses:	1 h
Modality used for planning:	T1 and T2 weighted 1.5 T MRI with applicator and needles *in situ* for both BT_1 and BT_2.
First application (BT_1):	after 46.8 Gy to PTV-T + N1
Second application (BT_2):	after 50.0 Gy to PTV-T + N1, 1 week after first application
Overall treatment time:	BT alone 7 days, EBRT + brachytherapy 50 days

A.6.5.5 Equipment Used for Brachytherapy (Table A.6.4, A.6.5a and A.6.5b and Figure A.6.5)

Applicator:	tandem-ring applicator (Varian Medical Systems) with 50 mm tandem and a 25 mm ring with a custom-made cap for needle implantation. Blunt end titanium needles (Acrostac) were used for the interstitial component of the implant.
Source:	Ir-192 delivered by a GammaMed Plus afterloader (Varian Medical Systems)
Treatment planning system:	Brachy Vision (Varian Medical Systems)
Source strength (RAKR)	4.07 mGy h^{-1}
Dose calculation algorithm	AAPM TG-43

A.6.6 Treatment Planning and Reporting Brachytherapy and EBRT

A.6.6.1 Example of Dose Distribution (Figure A.6.6)

A.6.7 Current Status

Last treatment received:	2 August 2010
Last follow-up visit:	24 April 2014
General condition:	good
Disease related complaints:	none
Treatment-related complaints:	vaginal shortening G1, CX24 Quite a bit
Evidence of disease:	none
Assessed by:	gynecological examination, MRI, PET–CT, CTC V3.0, QoL EORTC C30 + CX24

Journal of the ICRU Vol 13 No 1–2 (2013) Report 89
Oxford University Press
doi:10.1093/jicru/ndw024

Case 7: Large Cervical Cancer Stage IIB, with 3D Conformal EBRT with Concomitant Chemotherapy, and Radiograph-Based Intracavitary PDR Brachytherapy with Mould Technique

A.7.1 General Patient Information

Age:	44 years
General condition:	good general condition, sexually active
Prior medical history:	ocular thrombosis treated with anti-platelets aggregates Splenectomized for thrombopenic purpura
Use of medication:	plavix
Smoking history:	non-smoker
Symptoms at presentation:	vaginal bleeding

A.7.2 Tumor Extension at Diagnosis

A.7.2.1 Gynecological Examination (Figure A.7.1 and Table A.7.1)

Tumor extension:	infiltrative tumor in the cervix involving the left vaginal and the posterior walls and extending into the left distal parametrial space. The tumor measured 5 cm in width (2 cm from the cervical os to the right and 3 cm from the os to the left). Maximum extension along the left and posterior vaginal walls measured 1 cm in height.
Estimated size:	5 × 4.5 cm (width × thickness)
Biopsy result:	well-differentiated adenocarcinoma

A.7.2.2 MRI of the Lower Pelvic Area (Figure A.7.1, Table A.7.1)

Tumor extension:	infiltrative cervical tumor extending into the left distal parametrial space. The tumor measured 5.2 cm in width, 5 cm in height, and 5 cm in thickness. No clear extension on the left vaginal wall was identified, but seen on the posterior vaginal wall with a maximal height of 1 cm.

Pelvic lymph nodes: not involved

A.7.2.3 Other Findings

Abdominal CT-scan:	not performed
FDG-PET scan:	cervix uptake with SUV_{max} 10. No nodal uptake
Chest x-ray:	not performed
Tumor Marker SCC:	not relevant (adenocarcinoma)
Laparoscopic surgery:	not performed

A.7.2.4 Conclusion

A 44-year-old female with well-differentiated adenocarcinoma of the cervix, FIGO stage IIB, cT2bN0M0.

A.7.3 Treatment Intention

The case was reviewed at tumor board and the patient was offered curative-intent treatment. This consisted of external-beam radiotherapy 45 Gy to the pelvis concurrent with weekly cisplatin 40 mg/m^2 and followed by a brachytherapy boost to the primary tumor region to a total dose of at least 60 Gy $EQD2_{10}$ to the intermediate-risk CTV D_{98} (D_{98} $CTV_{IR} \geq 15$ Gy $EQD2_{10}$ for brachytherapy alone).

A.7.4 External-Beam Radiotherapy

Total dose prescribed:	45 Gy
Fractionation scheme:	25 × 1.8 Gy
Target volumes:	

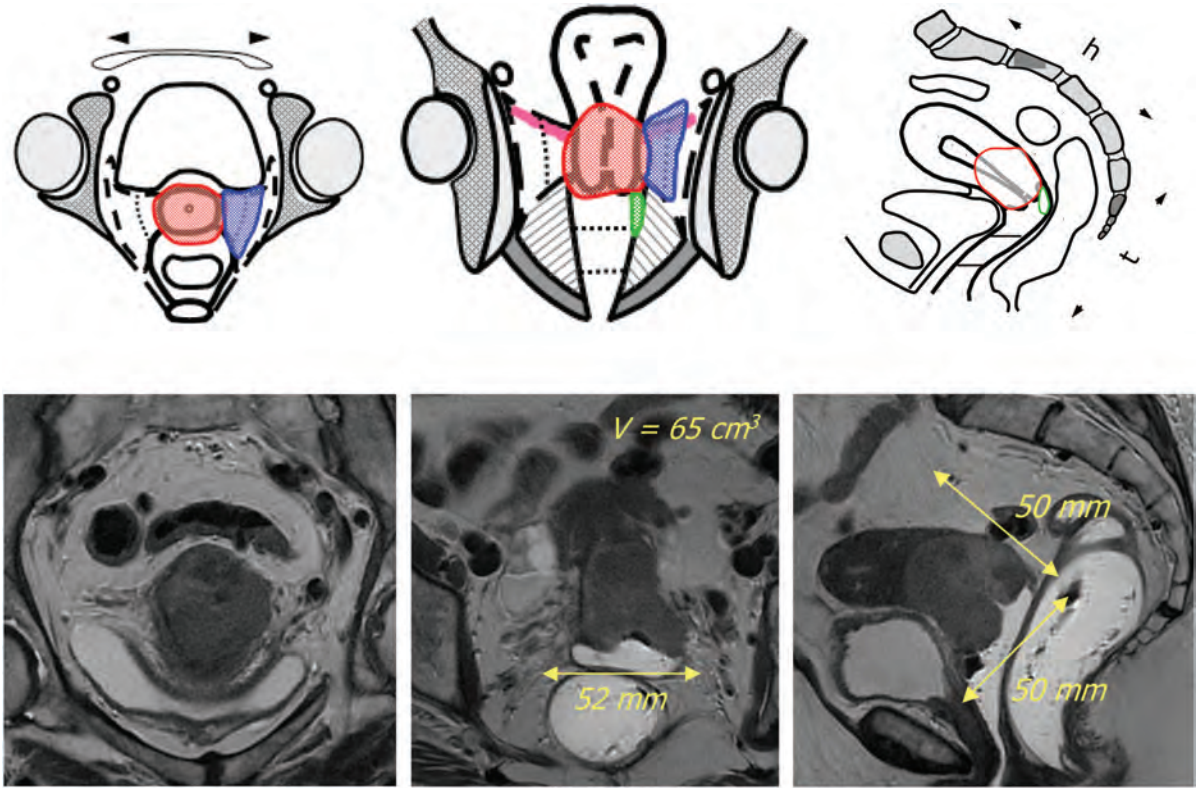

Figure A.7.1. Initial GTV extension at diagnosis. Clinical drawings (up) and corresponding MRI images (below) at the time of diagnosis.

Table A.7.1. Clinical dimensions and volumes of GTVs and CTVs at diagnosis and at the time of brachytherapy.

	Diagnosis	Brachytherapy
Clinical dimensions GTV, $w \times t$ (mm)	50 × 45	—
MRI dimensions GTV, w × t × h (mm)	52 × 50 ×50	—
MRI volume GTV (cm^3)	65	—
Clinical dimensions CTV_{HR}, $w \times t$ (mm)	—	35 × 30
Clinical dimensions CTV_{IR}, $w \times t$ (mm)	—	55 × 40
Left parametrium (MRI)	Distal	Proximal
Right parametrium (MRI)	Not involved	Not involved
Vagina	Proximal 1/3 (1 cm)	Not involved
Bladder	Not involved	Not involved
Rectum	Not involved	Not involved

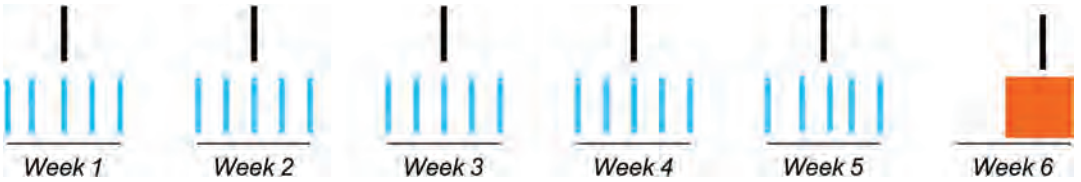

Figure A.7.2. Treatment schedule for this patient. Pelvic external-beam radiotherapy delivered a dose of 45 Gy, by fractions of 1.8 Gy/fraction, 5 times per week. Radiotherapy was intensified by chemotherapy, consisting of weekly CDDP 40 mg m^{-2}. Brachytherapy was delivered by PDR with 30 hourly pulses with simultaneous chemotherapy. A blue bar represents a fraction of EBRT 1.8 Gy, an orange bar represents a fraction of PDR brachytherapy, and a black bar represents a course of cisplatin 40 mg/m^2, overall treatment time 40 days.

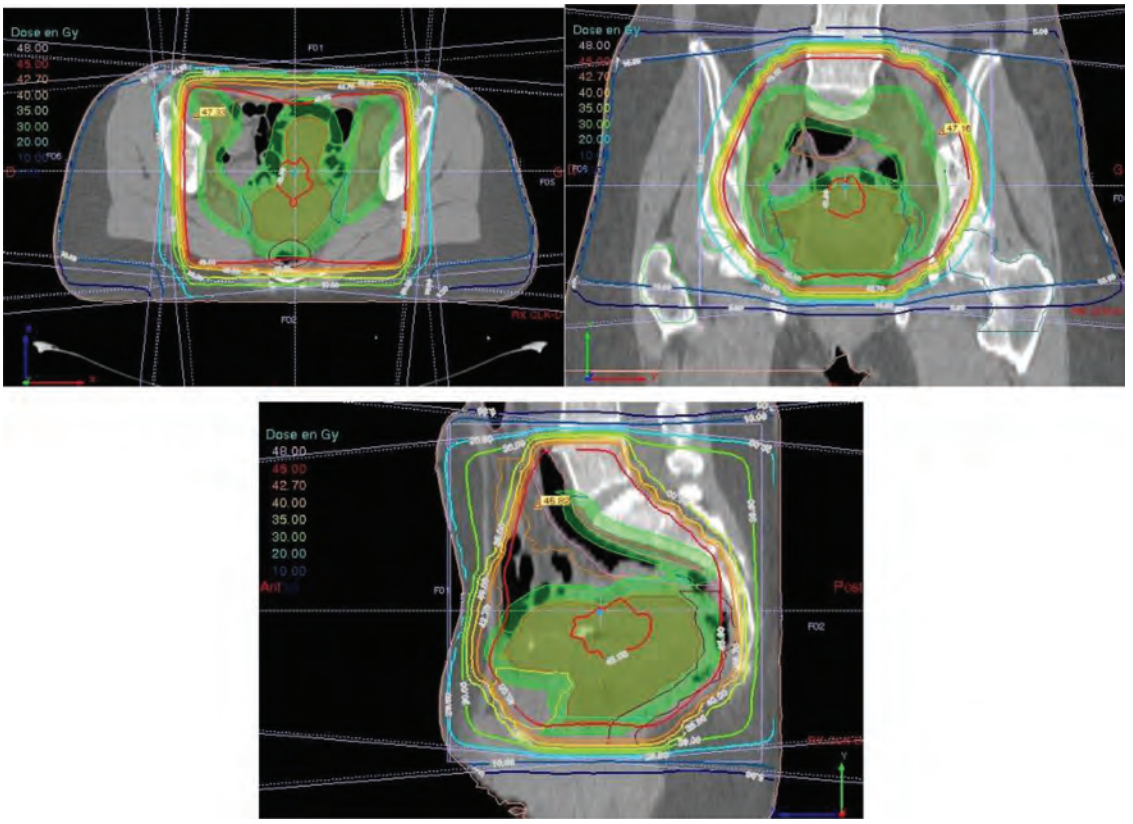

Figure A.7.3. Dose distribution of EBRT. The pelvis itself (PTV) was treated with 45 Gy in 25 fractions.

Table A.7.2. Absorbed dose distribution for EBRT.

Target	Volume	Planning aim		$V_{95\,\%}$[a]	$D_{98\,\%}$ (Gy)	$D_{50\,\%}$ (Gy)	$D_{2\,\%}$ (Gy)
PTV	1086 cm^3	45 Gy		100 %	44.9	46	47.2
$V_{43\,Gy}$	2398 cm^3						
$V_{57\,Gy}$	0						
Organs at risk	$V_{35\,Gy}$	$V_{45\,Gy}$	$V_{50\,Gy}$	$V_{55\,Gy}$	$D_{98\,\%}$	$D_{50\,\%}$	$D_{2\,\%}$
Bladder	100 %	89.1 %	0	0	41.7	45.6	46.1
Rectum	100 %	86.5 %	0	0	43.9	45.4	45.7
Sigmoid	100 %	95 %	0	0	42.8	43.8	46.6
Bowelbag	428 cm^3	355 cm^3	0	0	11.2	45.7	47.2

[a]Volume treated to 95 % of the planning aim absorbed dose.

CTV-T	cervix, uterus, half of the vagina, both parametria
CTV-N	pelvic lymph nodes up to aortic bifurcation
Applied PTV margin:	10 mm
Patient positioning:	supine position (cushion supporting the knees)
Planning technique:	3DCRT, 4 field box
Concomitant therapy:	5weekly cycles of cisplatin 40 mg/m^2
Overall treatment time:	33 days

A.7.5 Brachytherapy

A.7.5.1 Gynecological Examination at the First Time of Brachytherapy (Figure A.7.4)

Tumor extension:	at the time of brachytherapy, the tumor had shrunk in size: the tumor width at the level of the cervix was 25 mm and the remaining infiltration of the left proximal parametrium was 10 mm width, thickness was 30 mm, the vaginal infiltration had disappeared. The cervix was still infiltrated mainly on the anterior lip.

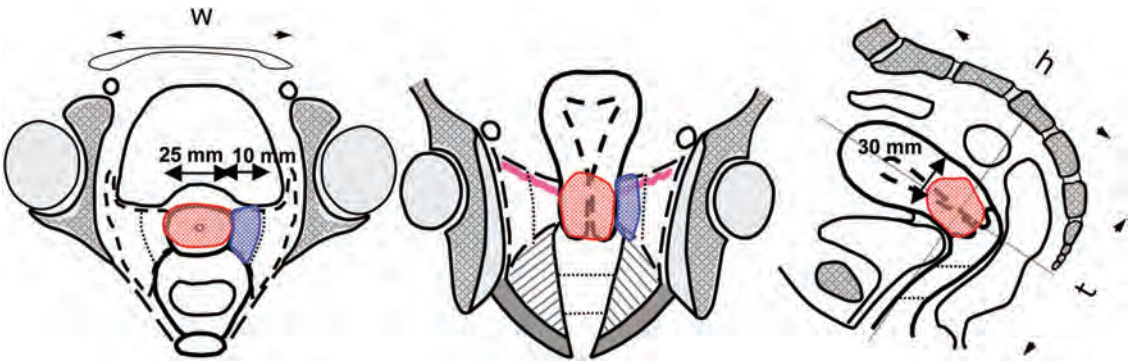

Figure A.7.4. Residual GTV and residual pathological tissue at the time of brachytherapy.

A.7.5.2 Treatment Planning Aim

Table A.7.3. Treatment planning aim.

		Planning aim EQD2 (Gy)	Prescribed EQD2 (Gy)	Planning aim absorbed dose rate (Gy h^{-1})	Prescribed absorbed dose rate (Gy h^{-1})
CTV_{IR}	D_{98}	≥60	60	≥0.25	0.52
Bladder	ICRU	≤85	48.6	≤0.60	0.23
Rectum	ICRU	≤75	60.2	≤0.60	0.55

Doses are given in EQD2 using $\alpha/\beta = 10$ Gy for target and $\alpha/\beta = 3$ Gy for organs at risk. In order to stay within institutional constraints for dose rate per pulse for point doses for OARs, a fractionation scheme with 30 pulses was chosen. (For the vagina, no planning aim dose constraint was applied.)

A.7.5.3 Treatment Delivery

Treatment method:	intracavitary pulsed dose-rate brachytherapy. Mould technique made from a vaginal impression performed after concomitant chemoradiation
Modality used for planning:	the CTV_{HR} and CTV_{IR} were clinically defined; these volumes were then integrated into two radiographs (anteroposterior and lateral) taken isocentrically, with radiographic markers indicating the source travel in the applicators
Number of applications:	one, after 45 Gy of EBRT
Total dose:	15 Gy to the D_{98} of CTV_{IR}
Time between pulses:	1 h
Pulse number/ day:	24
Total number of pulses:	30
Pulse size:	0.5 Gy to the reference isodose
Modality used for planning:	x-rays after applicator insertion
Overall treatment time:	brachytherapy alone 3 days, EBRT + brachytherapy 40 days

A.7.5.4 Equipment Used for Brachytherapy (Figure A.7.5)

Applicator	tandem with a vaginal mould, tandem length of 5.5 cm, right vaginal catheter of 3 cm, and left vaginal catheter of 4 cm
Source	PDR Gammamed (Varian)
Treatment planning system:	Brachyvision (Varian Medical Systems)
Dose calculation algorithm:	AAPM TG-43

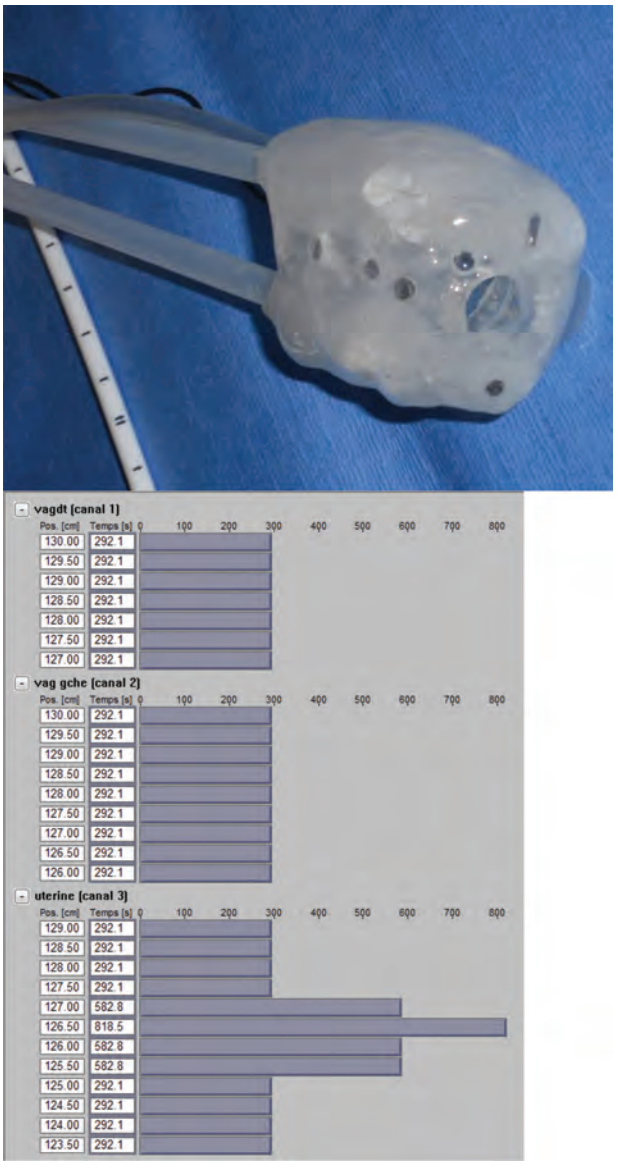

Figure A.7.5. Equipment used for brachytherapy. Brachytherapy mould applicator made from a vaginal impression performed after concomitant chemoradiation, with a central tandem and two vaginal catheters. The dwell pattern is shown for the vaginal catheters in Canal 1 and 2 and for the intrauterine in Canal 3.

A.7.6 Treatment Planning and Reporting Brachytherapy and EBRT

A.7.6.1. Example of Dose Distribution

Table A.7.4. Applicators and $EQD2_{10}$ isodose surface volumes.

	Brachytherapy
Nominal tandem length	5.5 cm
Left vaginal catheter	4 cm
Right vaginal catheter	3 cm
60 Gy volume	158 cm^3
75 Gy volume	74 cm^3
85 Gy volume	52 cm^3
TRAK	14.2 mGy

Table A.7.5. Point-based dose reporting (Level I).

			Application BT1 (Gy)	Total dose EBRT + BT (EQD2 Gy)
Point	A	Right	27.2	75.2
		Left	26	73.5
Pelvic wall	Point	Right	3.1	46.9
		Left	4.8	48.5
Bladder	ICRU	Point	6.9	48.6
Recto-vaginal	ICRU	Point	16.4	60.2
Vagina	5 mm	Right	20.9	67.5
		Left	34.4	95.7
	PIBS[a]	+2 cm	6	47.8
	PIBS	0 cm	3.5	42.4
	PIBS[a]	−2 cm	2.1	4.9

Total dose values in EQD2 were calculated using $\alpha/\beta = 10$ Gy for Point A and pelvic wall point and $\alpha/\beta = 3$ Gy for normal tissue point doses.
[a]PIBS, posterior inferior border of symphysis pubica, contribution of EBRT at PIBS + 2 cm 44.4 Gy, at PIBS 42.4 Gy, and at PIBS– 2 cm 5.4 Gy.

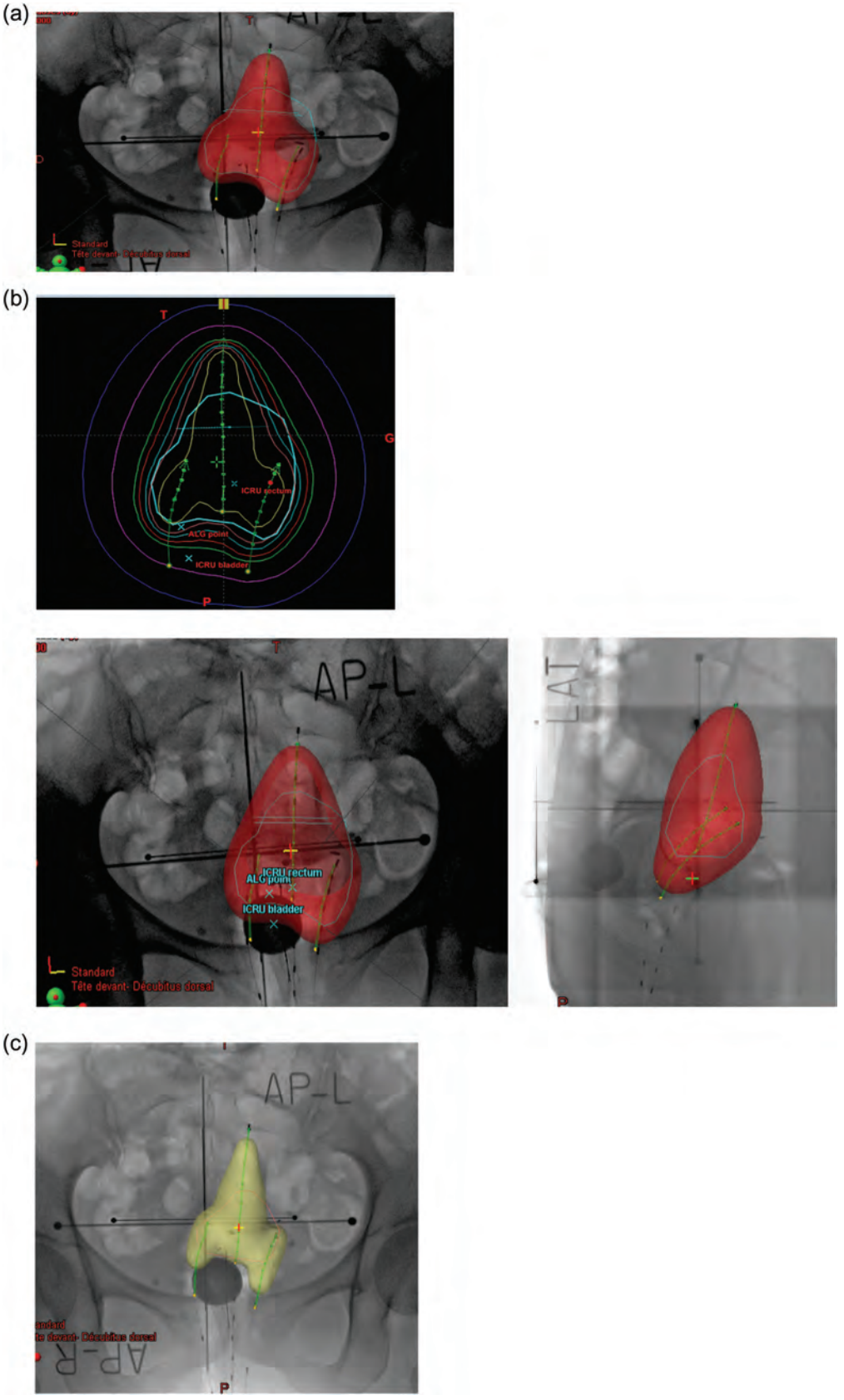

Figure A.7.6. (a) Drawing of the target (CTV_{IR}) (blue line) on the x ray with representation of the 3D isodose corresponding to 15 Gy $EQD2_{10}$. Isodose distribution and target drawing are shown on the coronal view (AA′ prescription, without optimization). (b) Optimization process to undergo the CTV_{IR} coverage with the prescription isodose (15 Gy EQD_{10}). (c) Optimization process to undergo the CTV_{HR} coverage with the prescription isodose (15 Gy) to the CTV_{IR}. Forty gray EQD_{10} isodose volume (in yellow) and CTV_{HR} line (in pink).

A.7.7 Current Patient Status

Six months after treatment, the patient presented with a clinical supraclavicular lymph node. PET–CT revealed multiple para-aortic lymph nodes and confirmed the supraclavicular lymph node, with a complete response at the level of the pelvis. The patient received concomitant chemoradiation to the para-aortic area and the supraclavicular lymph node. Three months after this treatment, PET–CT showed still a complete response within the pelvis, a partial response on the para-aortic and supraclavicular nodes, but evidenced lung metastases. Despite new chemotherapy regimen, the patient died from her metastases 12 months after the end of treatment.

Journal of the ICRU Vol 13 No 1–2 (2013) Report 89
Oxford University Press
doi:10.1093/jicru/ndw025

Case 8: Large Cervical Cancer Stage IIIB with No Nodes, Treated with 3D Conformal Box with Concomitant Chemotherapy and MRI-Based Intracavitary and Interstitial HDR Brachytherapy with Tandem/Ring Applicator and Needles

A.8.1 General Patient Information

Age:	35 years
General condition:	good general health, sexually active
Prior medical history:	no significant medical history
Use of medication:	no medication
Smoking history:	no
Symptoms at presentation:	vaginal white discharge and backache

A.8.2 Tumor Extension at Diagnosis

A.8.2.1 Gynecological Examination (Figure A.8.1, Table A.8.1)

Tumor extension:	endophytic growth at the cervix involving both lips right parametrium involved up to lateral pelvic wall; left parametrium not involved; extensive tumor necrosis vagina involved: posterior 4 cm; anterior and right lateral fornix <0.5 cm.
Estimated size:	6×5 cm (width $\times$ thickness); maximum width from the cervical canal: left: 2 cm; right: 4 cm
Biopsy result:	poorly differentiated squamous cell carcinoma

A.8.2.2 MRI of the Pelvis (Figure A.8.1, Table A.8.1)

Tumor extension:	heterogeneous mass in the cervix predominantly along its right lateral, anterior, and posterior walls, measuring $6.6 \times 6.6 \times 6.0$ cm in transverse, anterio-posterior, and cranio-caudal dimensions
Pelvic lymph nodes:	9 mm-sized right internal iliac lymph node (normal architecture): no macroscopic pelvic lymphadenopathy

A.8.2.3 Other Findings

Abdominal CT-scan:	kidneys normal; no gross para-aortic lymphadenopathy
FDG-PET scan:	not done
Chest X-ray:	no evidence of pulmonary metastases
Cystoscopy:	bladder mucosa normal
Laparoscopic surgery:	not done

A.8.2.4 Conclusion

Thirty-five-year-old female with a squamous cell carcinoma of the cervix FIGO IIIB, T3N0M0.

A.8.3 Treatment Intention

The patient was discussed in GYN Joint Clinic and she was offered a curative treatment using a combination of external beam radiotherapy 45 Gy in 25 fractions, five cycles of cisplatin (once weekly) 40 mg m^{-2} followed by a high dose rate brachytherapy boost of 7 Gy in 4 fractions (treatment schedule see Figure A.8.2) up to a total dose to the CTV_{HR} D_{90} of $\geq$85 Gy $EQD2_{10}$.

A.8.4 External Beam Radiotherapy

Total dose prescribed:	45 Gy
Fractionation scheme:	25×1.8 Gy (dose distribution depicted in Figure A.8.3 and Table A.8.2)
Target volumes:	
CTV-T	cervix, uterus, upper two thirds of the vagina, both parametria

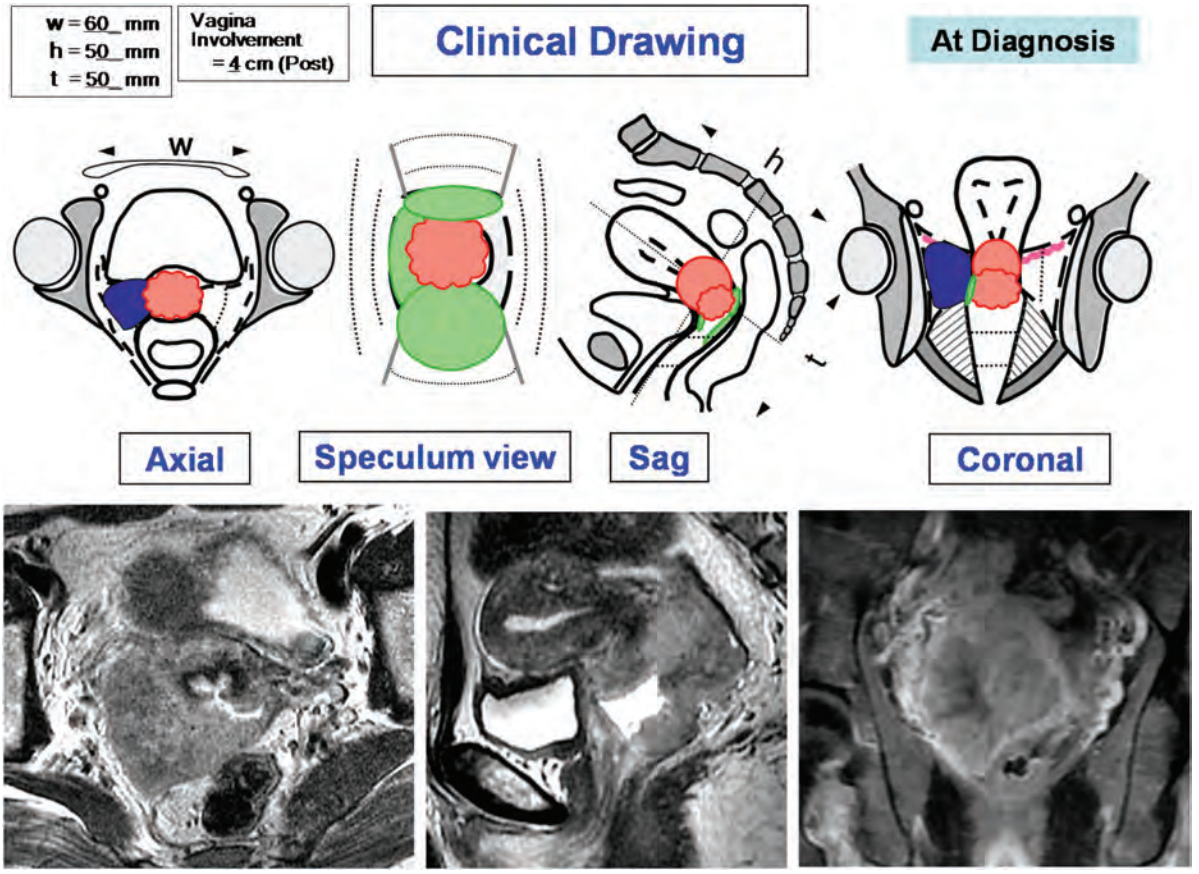

Figure A.8.1. Initial GTV extension at diagnosis. Clinical drawings (up) and corresponding MRI images (below) at the time of diagnosis.

Table A.8.1. Dimensions and volumes of GTVs and CTVs at diagnosis and at brachytherapy.

	Diagnosis	BT1 + 2	BT3 + 4
Clinical dimensions GTV, $w \times t$ (mm)	60 × 50	—	—
MRI dimensions GTV, $w \times t \times h$ (mm)	66 × 66 × 60	30 × 30 × 20	30 × 30 × 20
MRI volume GTV (cm^3)	120	19.5	15.5
Clinical dimensions CTV_{HR}, $w \times t$ (mm)	—	60 × 30	60 × 30
Width right and left		R: 40; L20	R: 40; L:20
MRI dimensions CTV_{HR}, $w \times t \times h$ (mm)	–	58 × 40 × 35	55 × 40 × 35
Width right and left		R: 45; L:15	R: 40; L:15
MRI volume CTV_{HR} (cm^3)	—	66	60
CTV_{IR} (cm^3)	—	115	106
Left parametrium (MRI)	Not involved	Not involved	Not involved
Right parametrium (MRI)	Up to pelvic wall	Up to PW	Up to PW
Vagina	Upper third	Not involved	Not involved
Bladder	Not involved	Not involved	Not involved
Rectum	Not involved	Not involved	Not involved

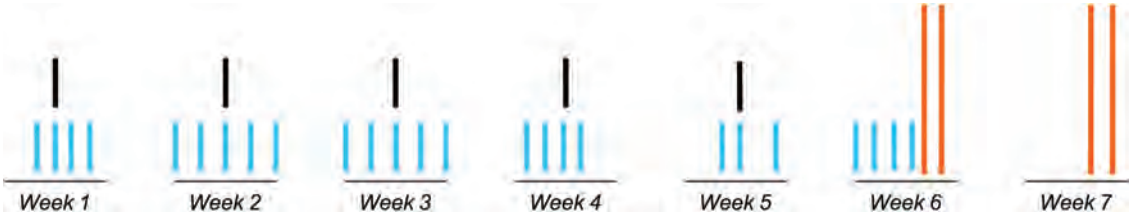

Figure A.8.2. Treatment schedule for this patient. A blue bar represents a fraction of EBRT 1.8 Gy, an orange bar represents a fraction of HDR brachytherapy 7 Gy (2 fractions within one application), and a black bar represents a course of cisplatin 40 mg m^{-2}, overall treatment time 46 days.

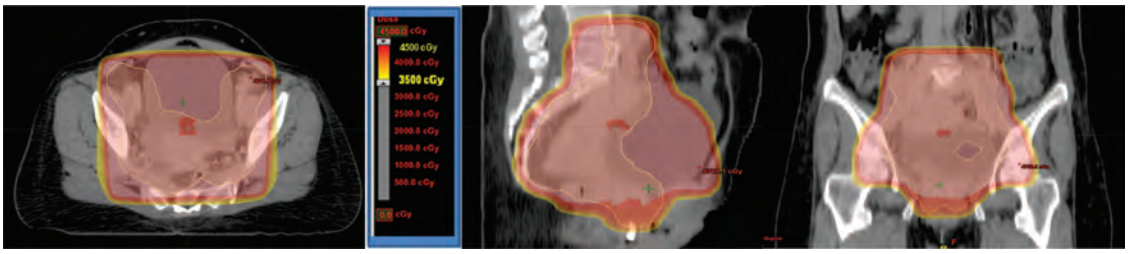

Figure A.8.3. Absorbed dose distribution of EBRT.

Table A.8.2. Absorbed dose distribution for EBRT.

Target	Volume	Planning aim		$V_{95\ \%}$ [a]	$D_{98\ \%}$	$D_{50\ \%}$	$D_{2\%}$
PTV	1584 cm^3	45 Gy		99.9%	44.5 Gy	46.4 Gy	47.8 Gy
V_{43Gy}	2886 cm^3						
V_{57Gy}	0						
Organs at risk	V_{35Gy}	$V_{45\ Gy}$	$V_{50\ Gy}$	$V_{55\ Gy}$	$D_{98\ \%}$	$D_{50\ \%}$	$D_{2\ \%}$
Bladder	95.8 %	89.9 %	0	0	28 Gy	46.0 Gy	47.3 Gy
Rectum	100 %	100 %	0	0	45.5 Gy	46.6 Gy	47.1 Gy
Sigmoid	100.0 %	100 %	0	0	46.0 Gy	46.4 Gy	46.6 Gy
Bowelbag	340 cm^3	285 cm^3	0	0	6.0 Gy	28.0 Gy	46.8 Gy

[a]Volume treated to 95% of the planning aim dose.

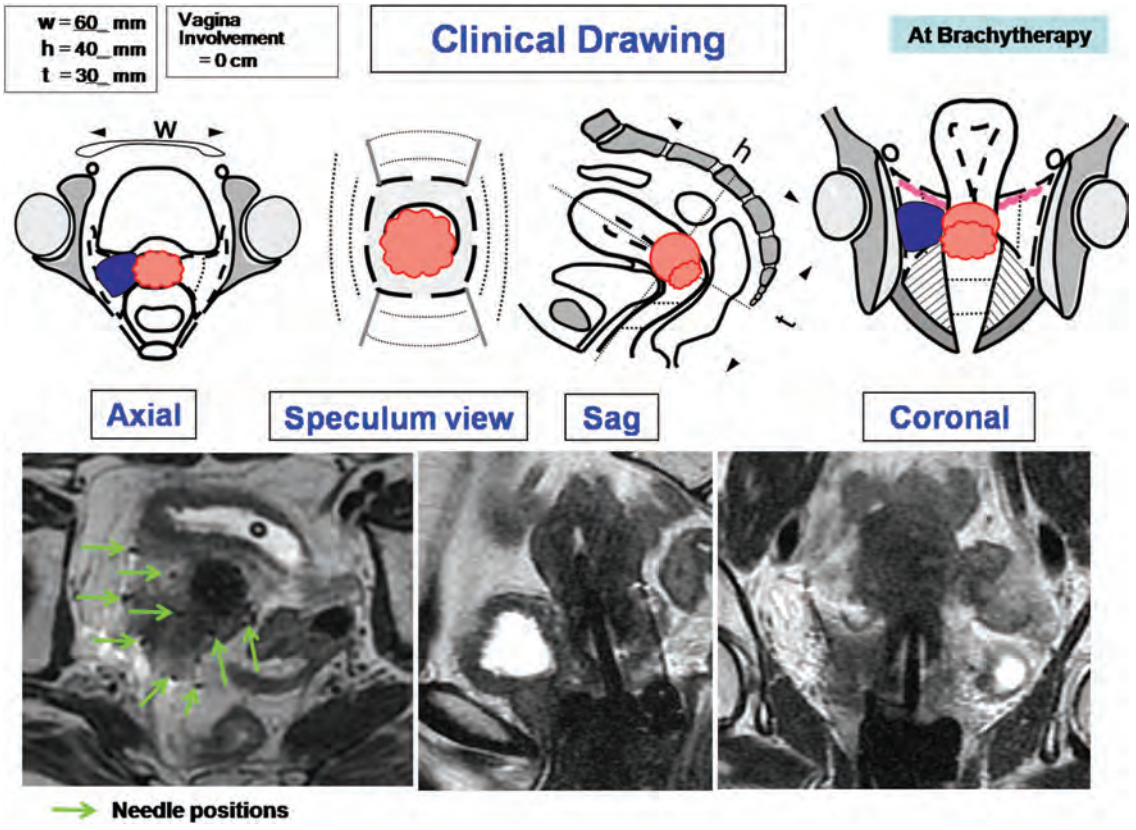

Figure A.8.4. Residual GTV and residual pathological tissue at the time of first brachytherapy: Clinical drawings (upper) and corresponding MRI images (lower) at the time of brachytherapy with applicator in place.

CTV-N pelvic lymph nodes up to aortic bifurcation

Applied PTV margins:	10 mm in superior–inferior, 7 mm in bi-lateral, and 10 mm in anterior–posterior directions
Patient positioning:	supine position with knee rest and hands over chest
Bladder filling protocol:	physiological bladder filling achieved at 45 min after emptying the bladder and drinking 750–1000 ml of water per orally.
Planning technique:	3D-CRT, 4 Field Box isocentric technique
Concomitant therapy:	5weekly cycles of cisplatin 40 mg m^{-2}
Overall treatment time:	38 days for EBRT

A.8.5 Brachytherapy

A.8.5.1 Gynecological Examination at the Time of First Brachytherapy (Figure A.8.4)

Tumor extension:	uterus ante-verted, tumor bulky, infiltrative disease over posterior lips, right fornix obliterated while rest of vagina normal; right parametrium involved up to lateral pelvic wall, left normal;
Estimated size:	6×3 (width $\times$ thickness) maximum width from the cervical canal: left: 2 cm; right: 4cm

A.8.5.2 MRI of the Lower Pelvic Area at First Brachytherapy (Figure A.8.4)

Tumor extension:	residual central gross tumor volume (bright zone, $w \times t \times h$ $30 \times 30 \times 20$) with surrounding residual pathological tissue (gray zones) in right parametrium up to lateral pelvic wall no gross vaginal residual involvement ($w \times t \times h$ $58 \times 40 \times 35$ mm), suggestive of good response at the central disease and poor at parametrium

A.8.5.3 Treatment Planning Aim

Table A.8.3. Treatment planning aim and prescribed dose.

			Planning aim (Gy)	Prescribed dose (Gy)
CTV_{HR}	D_{90}	$EQD2_{10}$	≥ 85	96.2
Bladder	D_{2cm^3}	$EQD2_3$	≤ 90	82.9
Rectum	D_{2cm^3}	$EQD2_3$	≤ 70	68.3
Sigmoid	D_{2cm^3}	$EQD2_3$	≤ 75	67.4

Doses are given in EQD2 using $\alpha/\beta = 10$ Gy for target and $\alpha/\beta = 3$ Gy for organs at risk. (No dose constraints were applied for the vagina.)

A.8.5.4 Treatment Delivery

Treatment method:	Combined intracavitary and interstitial application with Vienna II style applicator and needles on right half of the ring; additional needles with add-on ring to cover right distal parametrium; implant based on pelvic examination findings at brachytherapy
First application:	after 45 Gy
Time between fractions:	16 h
Modality used for planning:	MRI-scan after first applicator insertion CT scan before second fraction for assessment of changes in applicator position and organs at risk
Second application:	1 week after first brachytherapy application, the same procedure as for first application
Overall treatment time:	brachytherapy alone 9 days, EBRT + BT 46 days

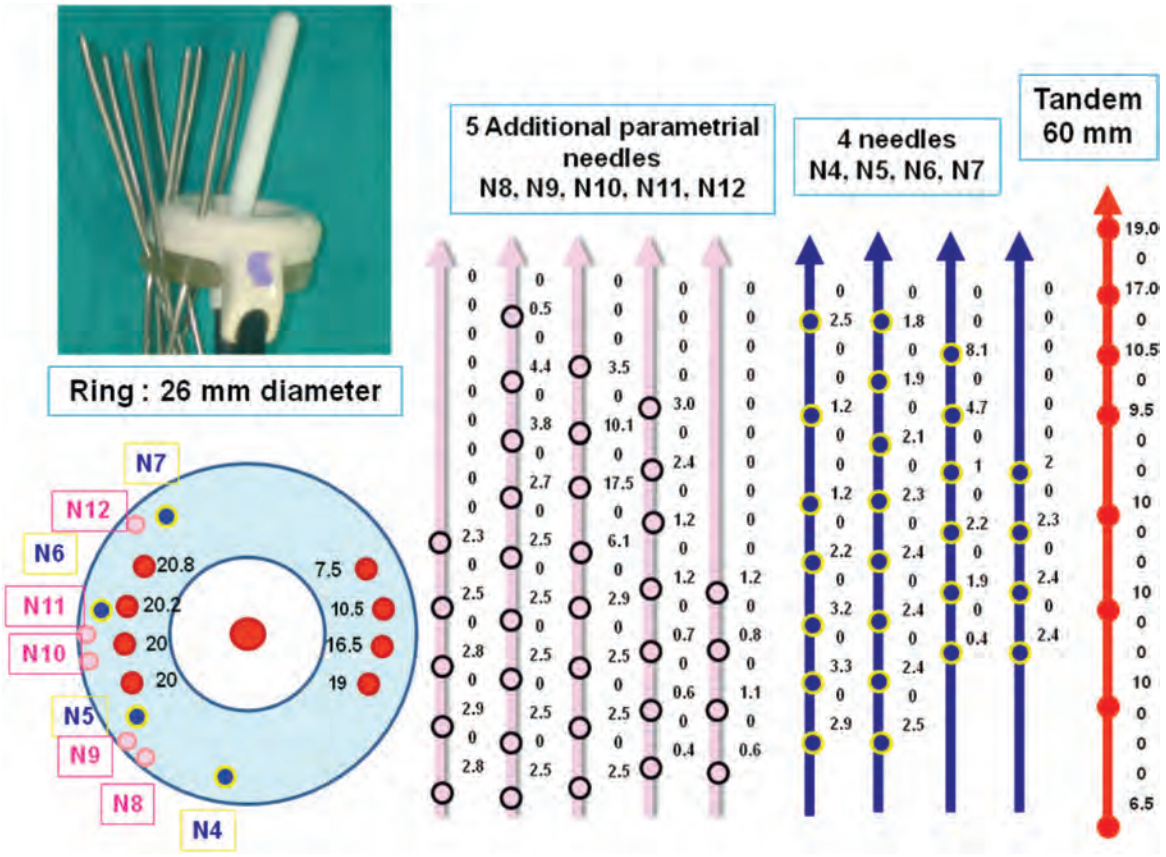

Figure A.8.5. Equipment used for brachytherapy.

A.8.5.5 Equipment Used for Brachytherapy (Figure A.8.5)

Applicator	tandem ring applicator ("Vienna II style") with a 6 cm tandem and a 26 mm ring with 7 holes (Nucletron, Veenendaal, The Netherlands) along with additional add-on-cap to insert needles into lateral parametrium
Source	Ir-192, source model mHDR—V 2, air kerma strength 46470 μGy m^2 h^{-1}, with micro Selectron Afterloader (Nucletron)
Treatment planning system:	Oncentra 4.1 (Nucletron)
Dose calculation algorithm	AAPM TG-43

Tandem ring applicator with needles inserted at positions N4, N5, N6, N7 through standard holes of Vienna applicator (26 mm ring). Additional needles in the right parametrium inserted under the guidance of add-on cap to the ring at N8, N9, N10, N11, N12. The needle insertion positions were selected based on clinical examination. The ring showed a slight rotation in the clock-wise direction. On MRI with the applicator in place, the needle positions N4, N5, and N6 were favorable, while N7 was close to the bladder (Figure A.8.6). With delineation of CTV_{HR} and rectum, both a sufficient dose in the CTV_{HR} (D_{90} $EQD2_{10} = 96.2$ Gy), and dose in the rectum and sigmoid below the dose constraint (D_{2cm^3} $EQD2_3 = 68.3$ and 67.4 Gy, see Table A.8.5b) could be achieved with the use of needles in two planes. Dwell times (in s) are shown for all dwell positions using a source step of 2.5 mm.

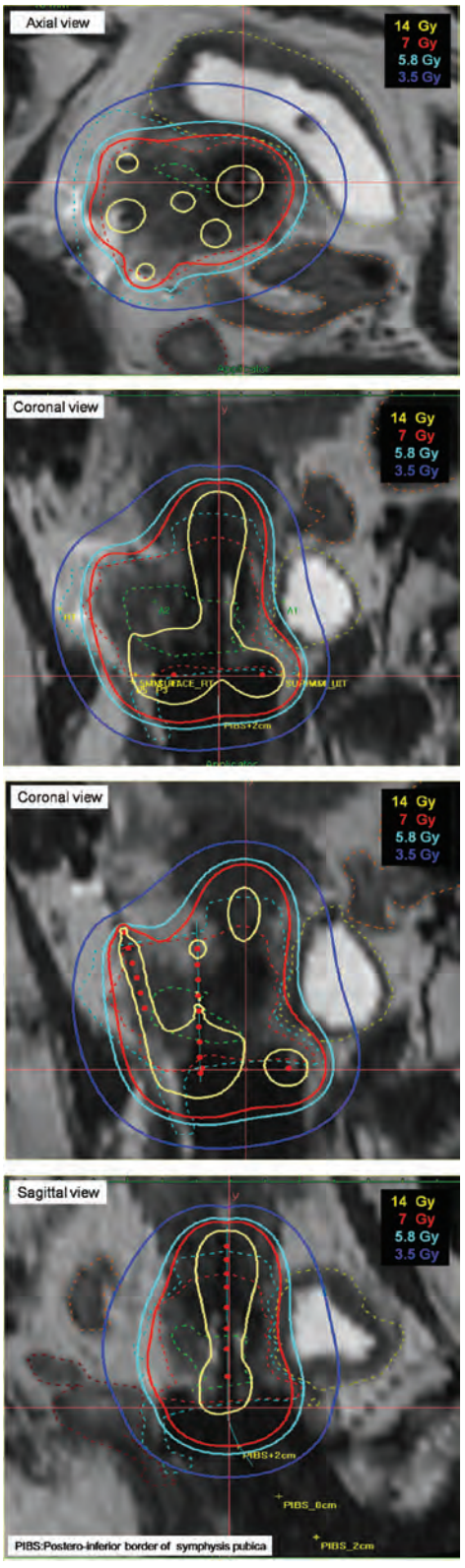

Figure A.8.6. Delineation and dose distribution at second brachytherapy application on MRI with applicators in place. CTV_{HR}, dotted red; CTV_{IR}, dotted light blue; GTV_{res}, dotted light green; bladder, dotted yellow; rectum, dotted brown; sigmoid, dotted orange; $EQD2_{10}$ isodose lines: dark blue is 60 Gy, light blue is 75 Gy, red is 85 Gy, and yellow is 156 Gy. These doses correspond to 3.5, 5.8, 7, and 14 Gy per fraction.

A.8.6 Treatment Planning and Reporting Brachytherapy and EBRT

Table A.8.4. Applicators and $EQD2_{10}$ isodose surface volumes.

	First application	Second application
Nominal tandem length	60 mm	60 mm
Nominal ring diameter	26 mm	26 mm
Number of active needles	12	12
60 Gy volume	290 cm^3	280 cm^3
75 Gy volume	175 cm^3	165 cm^3
85 Gy volume	70 cm^3	60 cm^3
TRAK	2 × 5 mGy	2 × 4.8 mGy

Table A.8.5a. Point-based absorbed dose reporting.

	First application		Second application		Total dose
	BT1 (Gy)	BT2 (Gy)	BT3 (Gy)	BT4 (Gy)	EBRT + BT (EQD2 Gy)
Point					
A					
Right	x[a] (Needle)	x[a]	x[a]	x[a]	x[a]
Left	5.0	5.0	6.0	6.0	72.8
Pelvic wall					
Point					
Right	4.0	4.0	4.2	4.2	63.5
Left	1.5	1.5	1.6	1.6	50.2
Bladder					
ICRU					
Point	5.5	5.5	5.7	5.7	81.7
Recto-vaginal					
ICRU					
Point	4.7	4.7	4.9	4.9	73.2
Vagina					
5 mm					
Right	13.0	13.0	7.6	7.6	158.6
Left	6.2	6.2	7.2	7.2	95.4
PIBS[b]					
+2 cm	6.5	6.5	6.3	6.3	91.3
0 cm	2.1	2.1	2.4	2.4	50.4
−2 cm	1.1	1.1	0.7	0.7	4.6

Total dose values in EQD2 were calculated using $\alpha/\beta = 10$ Gy for Point A and pelvic wall point and $\alpha/\beta = 3$ Gy for normal tissue point doses. The dose considered to be delivered at the same location by EBRT was 44.3 Gy $EQD2_{10}$ for target and 43.2 Gy $EQD2_3$ for OARs.

[a]Point A dose right not representative, as needle position is too close.

[b]PIBS, posterior inferior border of symphysis pubica, contribution of EBRT at PIBS + 2 cm 45 Gy, at PIBS 43.3 Gy, and at PIBS – 2 cm 2.8 Gy.

Table A.8.5b. DVH-based absorbed dose reporting (Level II).

	First application		Second application		Total dose
	BT1 (Gy)	BT2 (Gy)	BT3 (Gy)	BT4 (Gy)	EBRT + BT (EQD2 Gy)
GTV_{res}					
$D_{98\,\%}$	10.4	10.4	10.5	10.5	115.5
$D_{90\,\%}$	11.6	11.6	11.2	11.2	125.6
CTV_{HR}					
$D_{98\,\%}$	7.3	7.3	7.0	7.0	85.1
$D_{90\,\%}$	8.6	8.6	8.3	8.3	96.2
$D_{50\,\%}$	12.3	12.3	12.6	12.6	137.4
CTV_{IR}					
$D_{98\,\%}$	4.1	4.1	3.8	3.8	62.6
$D_{90\,\%}$	5.7	5.7	5.5	5.5	73.4
$D_{50\,\%}$	10.1	10.1	9.5	9.5	109.0
Bladder					
$D_{0.1\,cm^3}$	7.1	7.1	6.5	6.5	96.6
$D_{2\,cm^3}$	5.9	5.9	5.5	5.5	82.9
Rectum					
$D_{0.1\,cm^3}$	6.2	6.2	5.6	5.6	85.3
$D_{2\,cm^3}$	4.4	4.4	4.2	4.2	68.3
Sigmoid					
$D_{0.1\,cm^3}$	5.6	5.6	5.2	5.2	79.5
$D_{2\,cm^3}$	4.3	4.3	4.1	4.1	67.4

Total doses in EQD2 were calculated using $\alpha/\beta = 10$ Gy for target and $\alpha/\beta = 3$ Gy for normal tissue volumes. The dose considered to be delivered at the same location by EBRT was 44.3 Gy $EQD2_{10}$ for target and 43.2 Gy $EQD2_3$ for OARs.

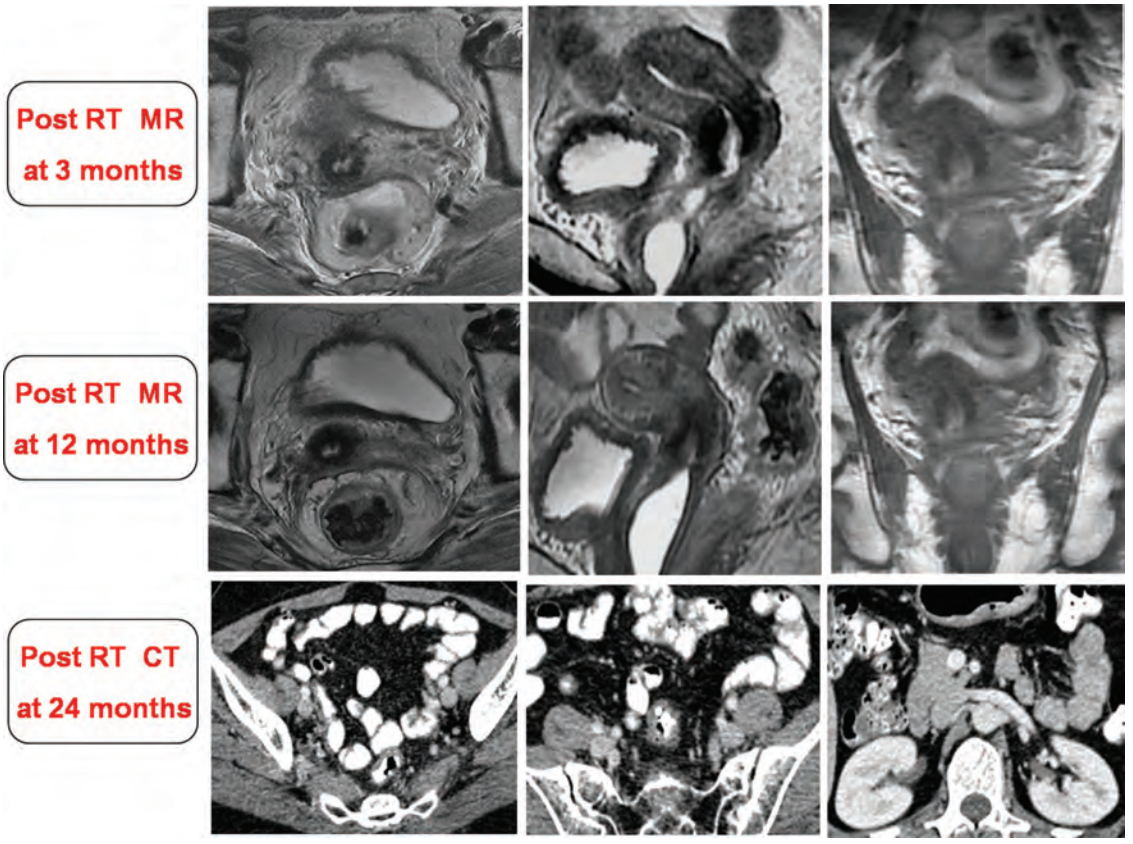

Figure A.8.7. Representative MR at 3 months, 12 months, and CT at 24 months. Representative axial, sagittal, and coronal images of MR at 3 months showing complete response; MR at 12 months showing right parametrial fibrosis and CT (axial slices only) at 24 months showing no evidence of pelvic or para-aortic lymphadenopathy.

A.8.6.1 Example of Dose Distribution

A.8.7 Current Patient Status (Figure 8.7)

Last treatment received:	11 February 2012
Last follow-up visit:	25 August 2014
General condition:	good
Disease-related complaints:	none clinically so far
Treatment-related complaints:	after 24 months follow-up: menopausal symptoms. No co-morbidity identified clinically so far
Evidence of disease:	MR at 3 months: complete response with cervix pulled to right MR at 1 year: no evidence of disease at the cervix or parametrium, right parametrium fibrosed, and no pelvic nodes CT abdomen and pelvis at 2 years: no evidence of pelvic or para-aortic lymph nodes. Kidneys normal
Assessed by:	none patient history, gynecological examination, MRI-pelvis, and CT abdomen and pelvis

Journal of the ICRU Vol 13 No 1–2 (2013) Report 89
Oxford University Press
doi:10.1093/jicru/ndw026

Case 9: Cervical Cancer Stage IIA2 Treated with 3D Conformal External-Beam Irradiation, Concomitant Chemotherapy, and Radiograph-Based Intracavitary Low Dose-Rate Brachytherapy with Tandem and Ovoids

A.9.1 General Patient Information

Age:	47 years
General condition:	performance status = 0 (WHO)
Prior medical history:	prior medical history unremarkable
Use of medication:	no medication
Smoking history:	cigar smoker
Symptoms at presentation:	post-coital bleeding, some right pelvic pain, some nausea

A.9.2 Tumor Extension at Diagnosis

A.9.2.1 Gynecological Examination (Figure A.9.1, Table A.9.1)

Tumor extension:	5 cm exophytic cervix tumor, also a 1 cm lesion in right fornix not contiguous with the cervical tumor. No parametrial extension
Estimated size:	5 cm × 2.3 cm × 5 cm (width × thickness × height)
Biopsy result:	squamous cell carcinoma, moderately/poorly differentiated with abundant necrosis, p16 strongly positive.

A.9.2.2 CT of the Pelvis (Figure A.9.1, Table A.9.1)

Pelvic lymph nodes:	no indication of nodal involvement

A.9.2.3 Other Findings

Whole body FDG PET–CT:	hypermetabolic cervical mass (50 mm width × 23 mm thickness × 50 mm height), no lymphadenopathy, or distant metastasis. This was confirmded by MRI.

A.9.2.4 Conclusion

A 47-year-old female with squamous cell carcinoma of the uterine cervix, FIGO stage IIA2 (T2a2N0M0).

A.9.3 Treatment Intention

After multidisciplinary evaluation, it was decided to offer curatively intended radio-chemotherapy using 3D conformal external beam radiation therapy to the pelvis (45 Gy in 1.8 Gy fractions) with five courses of concomitantly weekly cisplatin and a boost of low-dose-rate brachytherapy, aiming at a total dose of $\geq$90 Gy $EQD2_{10}$ at Point A. Overall treatment time 7 weeks with brachytherapy delivered in two fractions starting in the sixth week of treatment (Figure A.9.2).

A.9.4. External Beam Radiotherapy (Figure A.9.3 and Table A.9.2)

Total dose prescribed:	45 Gy
Fractionation scheme:	25 × 1.8 Gy 5 fractions per week
Target volumes:	GTV-cervix, uterus, upper vagina, internal, external, and common iliac lymph nodes, presacral lymph nodes
Critical structures:	bladder, rectum, parametria, small bowel, right femoral head, left femoral head
Applied PTV margin:	treatment fields based on anatomic landmarks, 1 cm margin to block edge beyond the cervix, uterine corpus, upper vagina/parametrium, and targeted pelvic vasculature. Weekly orthogonal portal imaging for verification was used.
Patient positioning:	prone with belly board
Planning technique:	3-field 3D conformal plan

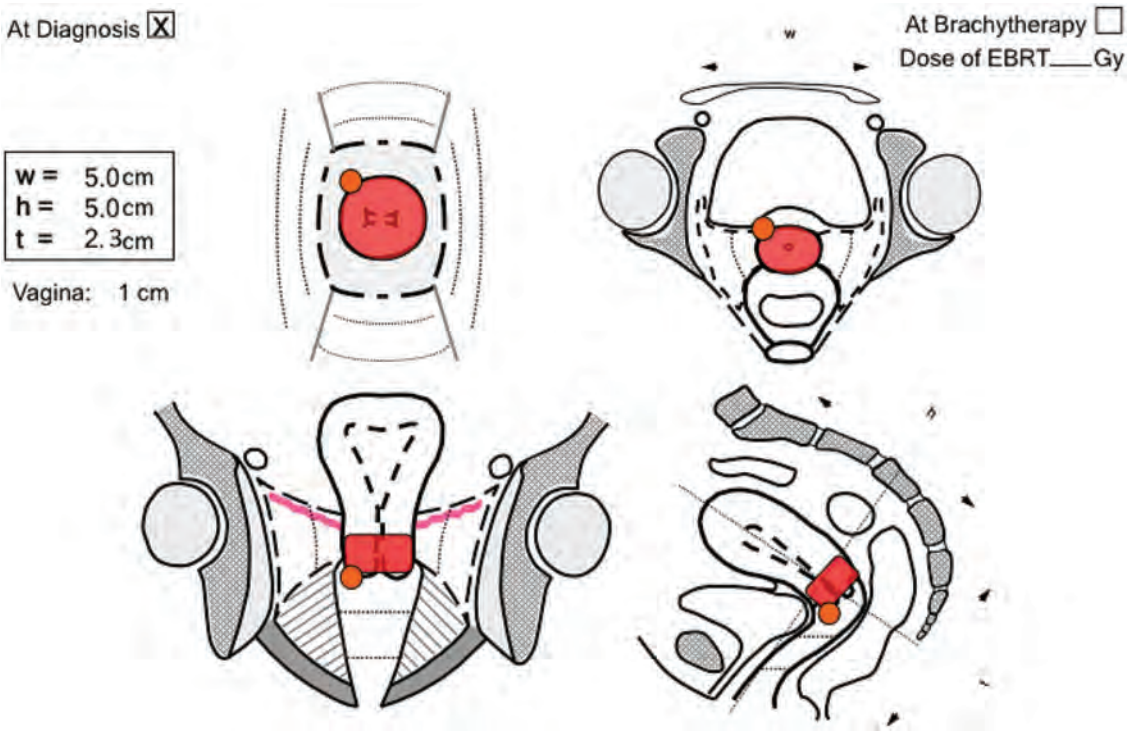

Figure A.9.1. GTV extension at diagnosis. Clinical findings by gynecological examination performed at diagnosis. The initial GTV at diagnosis is indicated within the cervix (red, with the 1 cm lesion in the right fornix indicated in orange) (height, as assessed with PET/CT and MRI not shown).

Table A.9.1. Dimensions and volumes of GTVs and CTVs at diagnosis and at brachytherapy

	Diagnosis	BT1-2
Clinical dimensions GTV, $w \times t$ (mm)	50 × 25	20 × 20
MRI/PET–CT dimensions GTV, $w \times t \times h$ (mm)	50 × 23 × 50	—
MRI/PET–CT volume GTV (cm^3)	25 cm^3	—
Clinical dimensions CTV^a_{HR}, $w \times t$ (mm)	—	40 × 30
MRI dimensions CTV_{HR}, $w \times t \times h$ (mm)	—	—
MRI volume CTV_{HR} (cm^3)	—	—
Left parametrium	Not involved	Not involved
Right parametrium	Not involved	Not involved
Uterus	Lower part	Not involved
Vagina	1 cm lesion in right fornix	Not involved
Bladder	Not involved	Not involved
Rectum	Not involved	Not involved

[a]Estimated based on the clinical exam because no MRI was performed at the time of brachytherapy.

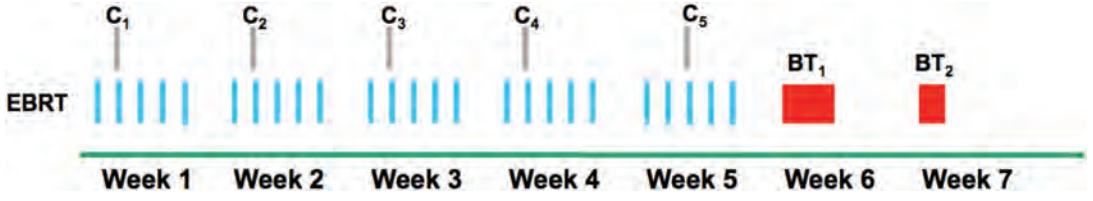

Figure A.9.2. Treatment schedule involving 45 days of treatment including weekly cisplatin (C_{1-6}), external beam radiotherapy (EBRT), and brachytherapy (BT_{1-2}). Treatment was initiated with EBRT (light blue bar) and weekly cisplatin (gray bar). Brachytherapy (red bars) began after the EBRT.

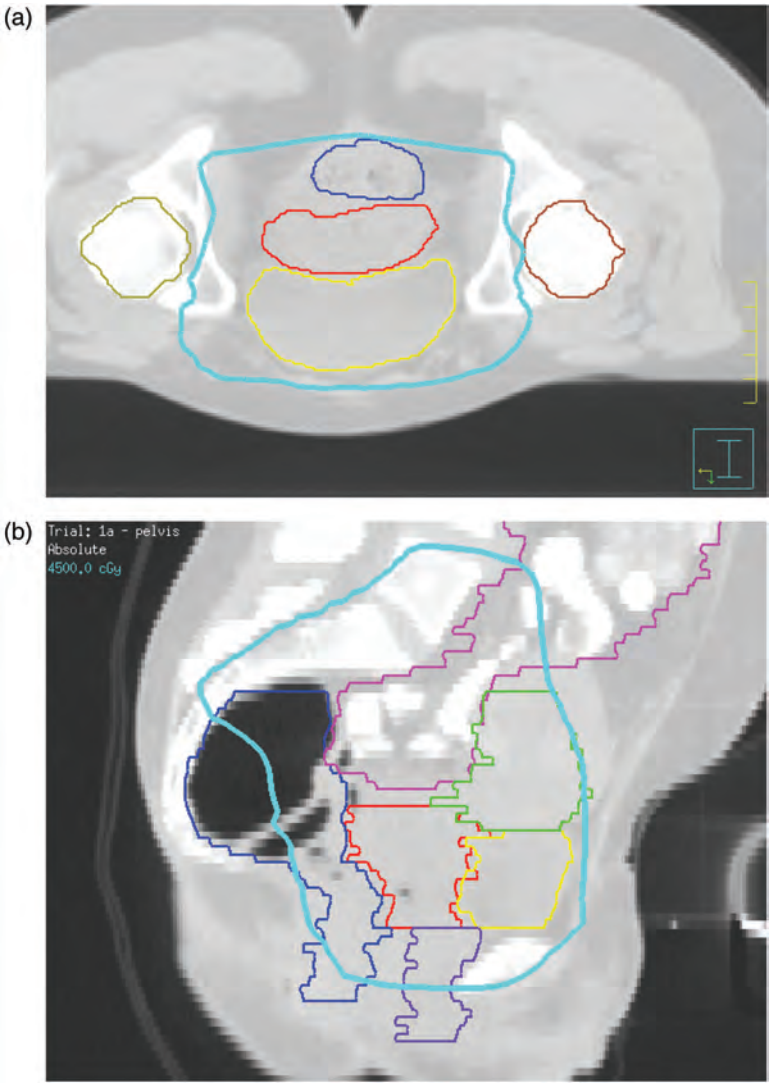

Figure A.9.3. Dose distribution of external-beam pelvic radiotherapy: (a) transverse and (b) sagittal. The GTV and cervix is shown in red based on the PET–CT findings (confirmed by MRI), the bladder in yellow, the rectum in blue, the right femoral head in brown, the left femoral head in gold, the uterus in green, the small bowel in magenta, and the vagina in purple. The PTV encompassing the 45 Gy volume is shown in cyan.

Table A.9.2. Absorbed dose distribution for pelvic EBRT

Target	Volume	Planning aim		$V_{95\ \%}$[a]	$D_{50\ \%}$	$D_{98\ \%}$	$D_{2\ \%}$
PTV	1834 cm^3	45 Gy		100 %	46.75	45.25	48.3
$V_{43\ Gy}$	2431 cm^3						
$V_{57\ Gy}$	0						
Organs at risk	$V_{35\ Gy}$	$V_{45\ Gy}$	$V_{50\ Gy}$	$V_{55\ Gy}$	$D_{50\ \%}$	$D_{98\ \%}$	$D_{2\ \%}$
Bladder	100 %	99 %	0 %	0 %	47.2 Gy	45.3 Gy	48.5 Gy
Rectum	100 %	55 %	0 %	0 %	48.0 Gy	39.1 Gy	48.9 Gy
Psoas	39 %	27.4 %	0	0	18.25 Gy	1.75 Gy	48.25 Gy
Rt. femoral head	25 %	0 %	0 %	0 %	25.5 Gy	20.5 Gy	43.5 Gy
Lt femoral head	18 %	0 %	0 %	0 %	24.25 Gy	19 Gy	43.25 Gy
Small Bowel	39 %	28 %	0 %	0 %	22.5 Gy	1.25 Gy	47.5 Gy

[a]Volume treated to 95 % of the planning aim absorbed dose.

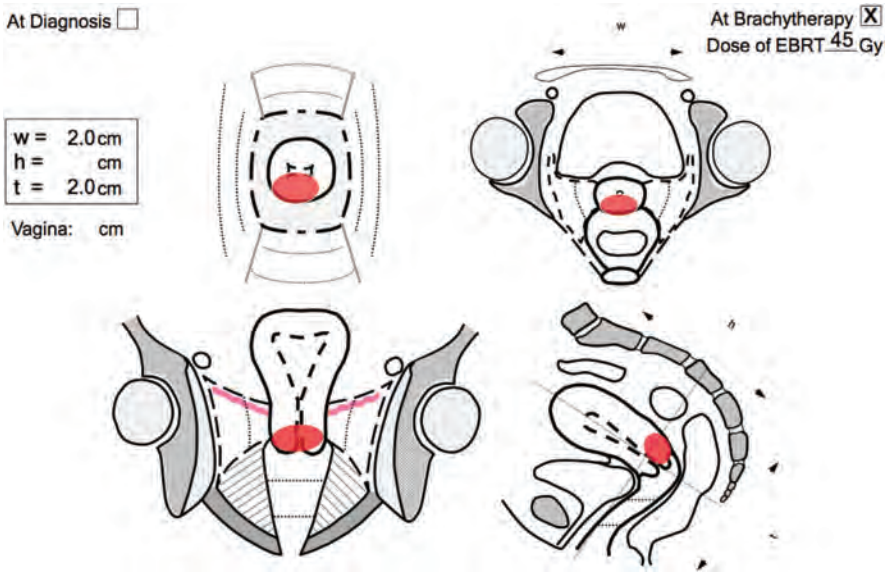

Figure A.9.4. Residual GTV at first time of brachytherapy. Clinical findings by gynecological examination performed at the time of the first brachytherapy fraction.

Concomitant treatment: 5 cycles of weekly cisplatin 40 mg/m^2
Overall treatment time: 35 days

A.9.5 Brachytherapy

A.9.5.1 Gynecological Examination at the Time of First Brachytherapy (Figure A.9.4, Table A.9.1)

Tumor extension: involvement of posterior cervical lip
Estimated size: 2 cm × 2 cm

MRI at the time of first brachytherapy was not performed.

A.9.5.2 Treatment Planning Aim

A.9.5.3 Treatment Delivery

Treatment method: intracavitary LDR BT was performed with 2 fractions starting in Week 6 with orthogonal radiographic imaging for dosimetry.
Imaging modality used for planning: orthogonal film (CT used to determine if the tandem had perforated the uterus)
1st application (BT_1): week 6, after 45 Gy to PTV-E
2nd application (BT_2): week 7, after 45 Gy to PTV-E
Overall treatment time: brachytherapy alone 10 days, EBRT + BT 45 days

Table A.9.3. Treatment planning aim and prescribed dose for two fractions of LDR BT along with 45 Gy at 1.8 Gy per fraction from pelvic external beam radiation therapy

		Planning aim EQD2 (Gy)	Prescribed EQD2 (Gy)	Planning aim absorbed dose rate (Gy h^{-1})	Prescribed absorbed dose rate (Gy h^{-1})
	Point A	≥80	91.0	>0.5	0.6
Bladder	ICRU	≤80	63.0	<0.37	0.31
Recto-vaginal	ICRU	≤75	52.6	<0.37	0.17

Doses are given in EQD2 using $\alpha/\beta = 10$ Gy for target and $\alpha/\beta = 3$ Gy for organs at risk. (For the vagina, no planning aim dose constraint was applied.)

Table A.9.4. Applicator characteristics, time/dose pattern, and isodose surface volumes for the brachytherapy fractions (BT_1 and BT_2) used for this patient

	BT1	BT2
Tandem length (mm)	60	60
Ovoid diameters (mm)	25	25
Total time (h)	48.3	26.8
Volume of the prescription isodose surface (30 Gy and 15 Gy) (cm^3)	121.1	143.1
Volume of the V_{85} isodose surface (cm^3)	157.4	183.8
Volume of the V_{75} isodose surface (cm^3)	190.8	221.8
Volume of the V_{60} isodose surface (cm^3)	266.4	308.2
Reference air kerma rate ($\mu Gy\ h^{-1}$)	442	442
Total reference air kerma (mGy)	21.35	11.85

Brachytherapy was delivered at a low dose rate.

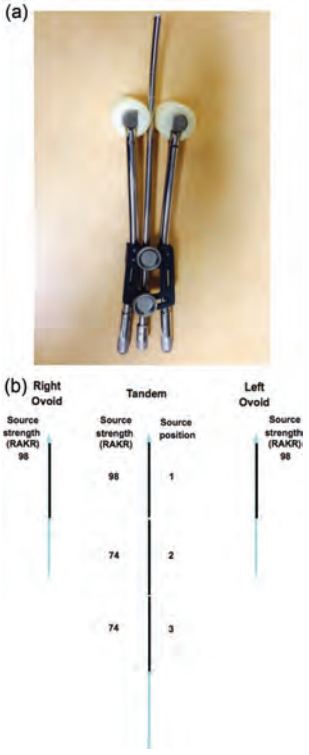

Figure A.9.5. (a) A standard LDR Fletch-Suit-Delcos brachytherapy tandem and ovoid set with shielding in the ovoids. (b) The loading pattern for the first brachytherapy application. The arrows point cephalad. The units are in cGy-cm^2/h.

A.9.5.4 Equipment Used for Brachytherapy (Table A.9.4, Figure A.9.5)

Applicator:	Tandem (60 mm) and ovoids (25 mm) applicator (Fletcher-Suit-Delcos, Best Medical, USA).
Source:	^{137}Cs (Amersham Searle, USA)
Treatment planning system:	BrachyVision V.9.0 (Varian Inc., USA)
Dose calculation algorithm	AAPM TG-43

A.9.6 Treatment Planning and Reporting EBRT and Brachytherapy

A.9.7 Current Patient Status

Last treatment received:	18 November 2011
Last follow-up visit:	2 September 2014
General condition:	excellent
Disease-related symptoms:	none
Treatment-related symptoms:	none
Evidence of disease:	no evidence of disease
Assessed by:	pelvic examination, pap smear, PET/CT, pelvic MRI

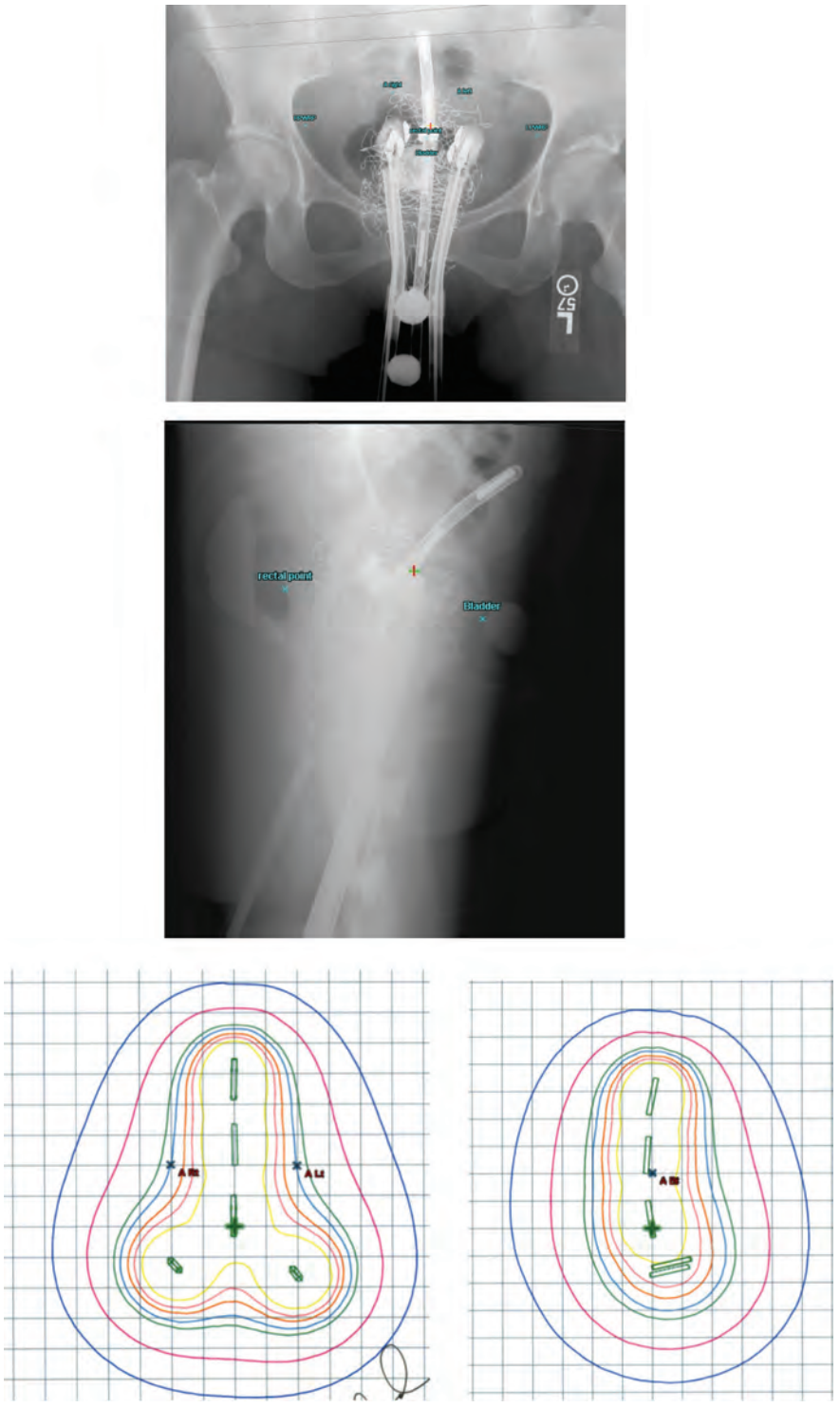

Figure A.9.6. AP (upper panel) and lateral (middle panel) radiographs taken with radiographic markers in the applicators for the first brachytherapy fraction. The markers have length of 2 cm with 2 cm between markers. Also shown is the Foley balloon with contrast, the rectum with contrast, indications of the pelvic wall points and radio-opaque threads in the gauze packing in the vagina. Images in the treatment planning system in a modified coronal plane (lower left) and a sagittal plane (lower right) showing the A points as light blue crosses and the active length of the Cs-137 seeds and green rectangles. The isodose lines shown in the figure are 60 Gy in yellow (200% of the prescription dose), 45 Gy in salmon, 37.5 Gy in orange, 30 Gy (prescribed dose) in blue, 25.5 Gy in green, 15 Gy in magenta and 9 Gy in blue.

Table A.9.5. Point-based absorbed dose reporting (Level 1) for each brachytherapy fraction (BT_1 and BT_2) and for external-beam radiotherapy (EBRT) and brachytherapy combined

		BT1 (Gy)	BT2 (Gy)	EBRT and BT (EQD2)
Point A	Right	31.9	15.1	93.5
	Left	28.1	14.9	88.5
Pelvic wall point	Right	5.8	3.5	52.4
	Left	7.8	3.4	54.2
Bladder	Reference point	15.3	7.9	63.0
Recto-vaginal	Reference point	7.9	4.8	52.6
Vagina 5 mm	Right	55.4	27.8	168.6
	left	55.4	27.1	167
	+2 cm	6.8	4.9	54.6
PIBS[a]	0 cm	3.8	2.5	47.4
	−2 cm	2.4	1.5	6.0

The equivalent dose in 2 Gy fractions (EQD2) was calculated assuming $\alpha/\beta = 10$ Gy for Points A, pelvic wall points, and upper vaginal points, and $\alpha/\beta = 3$ Gy for the bladder, rectal, and PIBS points. The dose considered to be delivered at the same location by EBRT was 44.3 Gy $EQD2_{10}$ for target and 43.2 Gy $EQD2_3$ for OARs.

[a]PIBS, posterior inferior border of symphysis pubica, *c*ontribution of EBRT at PIBS + 2 cm 47.1 Gy, at PIBS 45 Gy, and at PIBS− 2 cm 5.5 Gy.

Journal of the ICRU Vol 13 No 1–2 (2013) Report 89
Oxford University Press
doi:10.1093/jicru/ndw013

References

Aaltonen, P., Brahme, A., Lax, I., Levernes, S., Naslund, I., Reitan, J.B. and Turesson, I. (1997). "Specification of dose delivery in radiation therapy. Recommendation by the Nordic Association of Clinical Physics (NACP)," *Acta Oncol.* **36**(Suppl. 10), 1–32.

Adams, G.D. and Meurk, M.L. (1964). "The use of a computer to calculate isodose information surrounding distributed gynaecological radium sources," *Phys. Med. Biol.* **18**, 533–540.

Adler, L. (1919). "Die Radiumbehandlung maligner Tumoren in der Gynäkologie. Grundlagen, Technik, und Erfolge nebst Bericht über 250 behandelte Fälle," Strahlentherapie Sonderband 4.

Ahmed, R.S., Kim, R.Y., Duan, J., Meleth, S., De Los Santos, J.F. and Fiveash, J.B. (2004). "IMRT dose escalation for positive para-aortic lymph nodes in patients with locally advanced cervical cancer while reducing dose to bone marrow and other organs at risk," *Int. J. Radiat. Oncol. Biol. Phys.* **60**, 505–512.

Ahmad, R., Hoogeman, M.S., Quint, S., Mens, J.W., Osorio, E.M. and Heijmen, B.J. (2012). "Residual setup errors caused by rotation and non-rigid motion in prone-treated cervical cancer patients after online CBCT image-guidance," *Radiother. Oncol.* **103**, 322–326.

Aird, E.G.A., Jones, C.H., Joslin, C.A.F., Klevenhagen, S.K., Rossiter, M.J., Welsh, A.D., Wilkinson, J.M., Woods, J.M. and Wright, S.J. (1993). Recommendations for Brachytherapy Dosimetry: Report of a Joint BIR/IPSM Working Party (British Institute of Radiology, London).

Albano, M., Dumas, I. and Haie-Meder, C. (2008). "Brachytherapy at the Institut Gustave-Roussy: personalized vaginal mould applicator: technical modification and improvement," *Cancer Radiother.* **12**, 822–826.

Amit, A., Schink, J., Reiss, A. and Lowenstein, L. (2011). "PET/CT in gynecologic cancer: present applications and future prospects—a clinician's perspective," *Obstet. Gynecol. Clin. North Am.* **38**, 1–21, vii.

Andersen, E.K., Kristensen, G.B., Lyng, H. and Malinen, E. (2011). "Pharmacokinetic analysis and k-means clustering of DCEMR images for radiotherapy outcome prediction of advanced cervical cancers," *Acta Oncol.* **50**, 859–865.

Andersen, E.S., Noe, K.O., Sorensen, T.S., Nielsen, S.K., Fokdal, L., Paludan, M., Lindegaard, J.C. and Tanderup, K. (2013). "Simple DVH parameter addition as compared to deformable registration for bladder dose accumulation in cervix cancer brachytherapy," *Radiother. Oncol.* **107**, 52–57.

Anderson, L.L., Nath, R., Weaver, K.A., Nori, D., Phillips, T.L., Son, Y.H., Chiu-Tsao, S.T., Meigooni, A.S., Meli, J.A. and Smith, V. (1990). *Interstitial Brachytherapy: Physical, Biological, and Clinical Considerations* (Raven Press, New York).

Anderson, C., Lowe, G., Wills, R., Inchley, D., Beenstock, V., Bryant, L., Chapman, C. and Hoskin, P.J. (2013). "Critical structure movement in cervix brachytherapy," *Radiother. Oncol.* **107**, 39–45.

Ankerhold, U. and Ton, M.P. (2012). "European research projects for metrology in brachytherapy and external beam cancer therapy," *Metrologia* **49**, S161–S167.

Assenholt, M.S., Petersen, J.B., Nielsen, S.K., Lindegaard, J.C. and Tanderup, K. (2008). "A dose planning study on applicator guided stereotactic IMRT boost in combination with 3D MRI based brachytherapy in locally advanced cervical cancer," *Acta Oncol.* **47**, 1337–1343.

Attix, F.H. and Ritz, V.H. (1957). "A determination of the gamma-ray emission of radium," *J. Res. Natl. Bur. Std.* **59**, 293–306.

Baalbergen, A., Ewing-Graham, P.C., Hop, W.C., Struijk, P. and Helmerhorst, T.J. (2004). "Prognostic factors in adenocarcinoma of the uterine cervix," *Gynecol. Oncol.* **92**, 262–267.

Barbera, L. and Thomas, G. (2009). "Management of early and locally advanced cervical cancer," *Semin. Oncol.* **36**, 155–169.

Barillot, I., Horiot, J.C., Maingon, P., Bone-Lepinoy, M.C., Vaillant, D. and Feutray, S. (1994). "Maximum and mean bladder dose defined from ultrasonography. Comparison with the ICRU reference in gynaecological brachytherapy," *Radiother. Oncol.* **30**, 231–238.

Barillot, I., Horiot, J.C., Maingon, P., Truc, G., Chaplain, G., Comte, J. and Brenier, J.P. (2000). "Impact on treatment outcome and late effects of customized treatment planning in cervix carcinomas: baseline results to compare new strategies," *Int. J. Radiat. Oncol. Biol. Phys.* **48**, 189–200.

Barraclough, L.H., Swindell, R., Livsey, J.E., Hunter, R.D. and Davidson, S.E. (2008). "External beam boost for cancer of the cervix uteri when intracavitary therapy cannot be performed," *Int. J. Radiat. Oncol. Biol. Phys.* **71**, 772–778.

Batley, F. and Constable, W.C. (1967). "The use of the 'Manchester System' for treatment of cancer of the uterine cervix with modern after-loading radium applicators," *J. Can. Assoc. Radiol.* **18**, 396–400.

Batten, G.W., Jr. (1968). "The M.D. Anderson method for the computation of isodose curves around interstitial

and intracavitary radiation sources. II. Mathematical and computational aspects," *Am. J. Roentgenol. Radium Ther. Nucl. Med.* **102**, 673–676.

BCRU (1984). "British Committee on Radiation Units and Measurements. Specification of brachytherapy sources," *Br. J. Radiol.* **57**, 941–942.

Beadle, B.M., Jhingran, A., Salehpour, M., Sam, M., Iyer, R.B. and Eifel, P.J. (2009). "Cervix regression and motion during the course of external beam chemoradiation for cervical cancer," *Int. J. Radiat. Oncol. Biol. Phys.* **73**, 235–241.

Beadle, B.M., Jhingran, A., Yom, S.S., Ramirez, P.T. and Eifel, P.J. (2010). "Patterns of regional recurrence after definitive radiotherapy for cervical cancer," *Int. J. Radiat. Oncol. Biol. Phys.* **76**, 1396–1403.

Beaulieu, L., Carlsson Tedgren, A., Carrier, J-F., Davis, S.D., Mourtada, F., Rivard, M.J., Thomson, R.M., Verhaegen, F., Wareing, F.T. and Williamson, J.F. (2012). "Report of the Task Group 186 on Model-Based Dose Calculation Methods in Brachytherapy Beyond The TG-43 Formalism: Current Status and Recommendations for Clinical Implementation." *Med. Phys*. **39**, 6208–6236.

Bedford, J.S. and Hall, E.J. (1966). "Threshold hypoxia: its effect on the survival of mammalian cells irradiated at high and low dose-rates," *Br. J. Radiol.* **39**, 896–900.

Beiner, M.E. and Covens, A. (2007). "Surgery insight: radical vaginal trachelectomy as a method of fertility preservation for cervical cancer," *Nat. Clin. Pract. Oncol.* **4**, 353–361.

Benedetti-Panici, P., Maneschi, F., Scambia, G., Greggi, S., Cutillo, G., D'Andrea, G., Rabitti, C., Coronetta, F., Capelli, A. and Mancuso, S. (1996). "Lymphatic spread of cervical cancer: an anatomical and pathological study based on 225 radical hysterectomies with systematic pelvic and aortic lymphadenectomy," *Gynecol. Oncol.* **62**, 19–24.

Bentivegna, E., Uzan, C., Gouy, S., Leboulleux, S., Duvillard, P., Lumbroso, J., Haie-Meder, C., Schlumberger, M. and Morice, P. (2010). "Correlation between [18f]fluorodeoxyglucose positron-emission tomography scan and histology of pelvic nodes in early-stage cervical cancer," *Anticancer Res.* **30**, 1029–1032.

Bentzen, S.M. (1993). "Quantitative clinical radiobiology," *Acta Oncol.* **32**, 259–275.

Bentzen, S.M. and Baumann, M. (2002). "The linear-quadratic model in clinical practice," pp. 134–146 in *Basic Clinical Radiobiology*, 3rd ed., Steel, G.G., Ed. (Oxford University Press, London).

Bentzen, S.M. and Joiner, M.C. (2009). "The linear quadratic approach in clinical practice," pp. 120–134 in *Basic Clinical Radiobiology*, 4th ed., Joiner, M.C. and van der Kogel, A., Eds. (CRC Press, Boca Raton, Florida).

Bentzen, S.M. and Thames, H.D. (1991). "Clinical evidence for tumor clonogen regeneration: interpretations of the data," *Radiother. Oncol.* **22**, 161–166.

Bentzen, S.M., Overgaard, J., Thames, H.D., Overgaard, M., Vejby Hansen, P., von der Maase, H. and Meder, J. (1989a). "Clinical radiobiology of malignant melanoma," *Radiother. Oncol.* **16**, 169–182.

Bentzen, S.M., Overgaard, M., Thames, H.D., Christensen, J.J. and Overgaard, J. (1989b). "Early and late normal-tissue injury after postmastectomy radiotherapy alone or combined with chemotherapy," *Int. J. Radiat. Biol.* **56**, 711–715.

Bentzen, S.M., Saunders, M.I. and Dische, S. (1999). "Repair halftimes estimated from observations of treatment-related morbidity after CHART or conventional radiotherapy in head and neck cancer," *Radiother. Oncol.* **53**, 219–226.

Bentzen, S.M., Agrawal, R.K., Aird, E.G., Barrett, J.M., Barrett-Lee, P.J., Bliss, J.M., Brown, J., Dewar, J.A., Dobbs, H.J., Haviland, J.S., Hoskin, P.J., Hopwood, P., Lawton, P.A., Magee, B.J., Mills, J., Morgan, D.A., Owen, J.R., Simmons, S., Sumo, G., Sydenham, M.A., Venables, K. and Yarnold, J.R. (2008). "The UK Standardisation of Breast Radiotherapy (START) Trial A of radiotherapy hypofractionation for treatment of early breast cancer: a randomised trial," *Lancet Oncol.* **9**, 331–341.

Bentzen, S.M., Constine, L.S., Deasy, J.O., Eisbruch, A., Jackson, A., Marks, L.B., Ten Haken, R.K. and Yorke, E.D. (2010). "Quantitative analyses of normal tissue effects in the clinic (QUANTEC): an introduction to the scientific issues," *Int. J. Radiat. Oncol. Biol. Phys.* **76**, S3–S9.

Bentzen, S.M., Dorr, W., Gahbauer, R., Howell, R.W., Joiner, M.C., Jones, B., Jones, D.T., van der Kogel, A.J., Wambersie, A. and Whitmore, G. (2012). "Bioeffect modeling and equieffective dose concepts in radiation oncology—terminology, quantities and units," *Radiother. Oncol.* **105**, 266–268.

Berger, D., Dimopoulos, J., Georg, P., Georg, D., Pötter, R. and Kirisits, C. (2007). "Uncertainties in assessment of the vaginal dose for intracavitary brachytherapy of cervical cancer using a tandem-ring applicator," *Int. J. Radiat. Oncol. Biol. Phys.* **67**, 1451–1459.

Berger, D., Dimopoulos, J., Pötter, R. and Kirisits, C. (2009). "Direct reconstruction of the Vienna applicator on MR images," *Radiother. Oncol.* **93**, 347–351.

Berger, D., Pötter, R., Dimopoulos, J.A. and Kirisits, C. (2010). "New Vienna applicator design for distal parametrial disease in cervical cancer," *Brachytherapy* **9**, S51–S52.

Beriwal, S., Bhatnagar, A., Heron, D.E., Selvaraj, R., Mogus, R., Kim, H., Gerszten, K., Kelley, J. and Edwards, R.P. (2006). "High-dose-rate interstitial brachytherapy for gynecologic malignancies," *Brachytherapy* **5**, 218–222.

Beriwal, S., Demanes, D.J., Erickson, B., Jones, E., De Los Santos, J.F., Cormack, R.A., Yashar, C., Rownd, J.J. and Viswanathan, A.N. (2012a). "American Brachytherapy Society consensus guidelines for interstitial brachytherapy for vaginal cancer," *Brachytherapy* **11**, 68–75.

Beriwal, S., Rwigema, J.C., Higgins, E., Kim, H., Houser, C., Sukumvanich, P., Olawaiye, A., Richard, S., Kelley, J.L., Edwards, R.P. and Krivak, T.C. (2012b). "Three-dimensional image-based high-dose-rate interstitial brachytherapy for vaginal cancer," *Brachytherapy* **11**, 176–180.

Bipat, S., Glas, A.S., van der Velden, J., Zwinderman, A.H., Bossuyt, P.M. and Stoker, J. (2003). "Computed

tomography and magnetic resonance imaging in staging of uterine cervical carcinoma: a systematic review," *Gynecol. Oncol.* **91**, 59–66.

Bipat, S., van den Berg, R.A., van der Velden, J., Stoker, J. and Spijkerboer, A.M. (2011). "The role of magnetic resonance imaging in determining the proximal extension of early stage cervical cancer to the internal os," *Eur. J. Radiol.* **78**, 60–64.

Björkholm, E. (1997). "The development of brachytherapy and complementary external irradiation in the treatment of cervical carcinoma Radiumhemmet, Stockholm 1910–1996," pp. 71–76 in *Integration of External Beam Therapy and Brachytherapy in the Treatment of Cervix Cancer: Clinical, Physical and Biological Aspects* (European Society for Radiotherapy and Oncology, Brussels, Belgium).

Blasko, J.C., Grimm, P.D. and Ragde, H. (1993). "Brachytherapy and organ preservation in the management of carcinoma of the prostate," *Semin. Radiat. Oncol.* **3**, 240–249.

Bosch, F.X., Lorincz, A., Munoz, N., Meijer, C.J. and Shah, K.V. (2002). "The causal relation between human papillomavirus and cervical cancer," *J. Clin. Pathol.* **55**, 244–265.

Boyle, P., Golia, S., Daly, P., Johnston, P.G. and Robertson, C. (2003). "Cancer mortality in Ireland, 1926–1995," *Ann. Oncol.* **14**, 323–332.

Brenner, D.J. (2008). "The linear-quadratic model is an appropriate methodology for determining isoeffective doses at large doses per fraction," *Semin. Radiat. Oncol.* **18**, 234–239.

Brixey, C.J., Roeske, J.C., Lujan, A.E., Yamada, S.D., Rotmensch, J. and Mundt, A.J. (2002). "Impact of intensity-modulated radiotherapy on acute hematologic toxicity in women with gynecologic malignancies," *Int. J. Radiat. Oncol. Biol. Phys.* **54**, 1388–1396.

Brock, K.K. (2010). "Results of a multi-institution deformable registration accuracy study (MIDRAS)," *Int. J. Radiat. Oncol. Biol. Phys.* **76**, 583–596.

Brooks, S., Bownes, P., Lowe, G., Bryant, L. and Hoskin, P.J. (2005). "Cervical brachytherapy utilizing ring applicator: comparison of standard and conformal loading," *Int. J. Radiat. Oncol. Biol. Phys.* **63**, 934–939.

Brooks, R.A., Rader, J.S., Dehdashti, F., Mutch, D.G., Powell, M.A., Thaker, P.H., Siegel, B.A. and Grigsby, P.W. (2009). "Surveillance FDG-PET detection of asymptomatic recurrences in patients with cervical cancer," *Gynecol. Oncol.* **112**, 104–109.

Buchali, A., Koswig, S., Dinges, S., Rosenthal, P., Salk, J., Lackner, G., Bohmer, D., Schlenger, L. and Budach, V. (1999). "Impact of the filling status of the bladder and rectum on their integral dose distribution and the movement of the uterus in the treatment planning of gynaecological cancer," *Radiother. Oncol.* **52**, 29–34.

Buijsen, J., van den Bogaard, J., van der Weide, H., Engelsman, S., van Stiphout, R., Janssen, M., Beets, G., Beets-Tan, R., Lambin, P. and Lammering, G. (2012). "FDG-PET-CT reduces the interobserver variability in rectal tumor delineation," *Radiother. Oncol.* **102**, 371–376.

Burghardt, E., Hofmann, H.M., Ebner, F., Haas, J., Tamussino, K. and Justich, E. (1989). "Magnetic resonance imaging in cervical cancer: a basis for objective classification," *Gynecol. Oncol.* **33**, 61–67.

Burke, T.W. (2008). "The origins of multidisciplinary cancer care," *Gynecol. Oncol.* **110**, S2–S3.

Castadot, P., Lee, J.A., Geets, X. and Gregoire, V. (2010). "Adaptive radiotherapy of head and neck cancer," *Semin. Radiat. Oncol.* **20**, 84–93.

Castadot, P., Geets, X., Lee, J.A. and Gregoire, V. (2011). "Adaptive functional image-guided IMRT in pharyngolaryngeal squamous cell carcinoma: is the gain in dose distribution worth the effort?," *Radiother. Oncol.* **101**, 343–350.

Castelnau-Marchand, P., Chargari, C., Maroun, P., Dumas, I., Del Campo, E.R., Cao, K., Petit, C., Martinetti, F., Tafo-Guemnie, A., Lefkopoulos, D., Morice, P., Haie-Meder, C. and Mazeron, R. (2015). "Clinical outcomes of definitive chemoradiation followed by intracavitary pulsed-dose rate image-guided adaptive brachytherapy in locally advanced cervical cancer," *Gynecol. Oncol*. **139**, 288–294.

Cavalli, F. (2006). "Cancer in the developing world: can we avoid the disaster?," *Nat. Clin. Pract. Oncol.* **3**, 582–583.

CFMRI (1983). Center for Functional Magnetic Resonance Imaging. Recommendations pour la Determination des Doses Absorbees en Curietherapie (San Diego, California).

Chajon, E., Dumas, I., Touleimat, M., Magne, N., Coulot, J., Verstraet, R., Lefkopoulos, D. and Haie-Meder, C. (2007). "Inverse planning approach for 3-D MRI-based pulse-dose rate intracavitary brachytherapy in cervix cancer," *Int. J. Radiat. Oncol. Biol. Phys.* **69**, 955–961.

Chargari, C., Magne, N., Dumas, I., Messai, T., Vicenzi, L., Gillion, N., Morice, P. and Haie-Meder, C. (2009). "Physics contributions and clinical outcome with 3D-MRI-based pulsed-dose-rate intracavitary brachytherapy in cervical cancer patients," *Int. J. Radiat. Oncol. Biol. Phys.* **74**, 133–139.

Charra-Brunaud, C., Harter, V., Delannes, M., Haie-Meder, C., Quetin, P., Kerr, C., Castelain, B., Thomas, L. and Peiffert, D. (2012). "Impact of 3D image-based PDR brachytherapy on outcome of patients treated for cervix carcinoma in France: results of the French STIC prospective study," *Radiother. Oncol.* **103**, 305–313.

Chassagne, D. and Horiot, J.C. (1977). "[Proposals for common definitions of reference points in gynecological brachytherapy (author's transl)]," *J. Radiol. Electrol. Med. Nucl.* **58**, 371–373.

Chassagne, D. and Pierquin, B. (1966). "[Plesiocurietherapy of vaginal cancers by plastic mold with iridium 192 (non-radioactive preparation). (Preliminary note)]," *J. Radiol. Electrol. Med. Nucl.* **47**, 89–93.

Chen, S.W., Liang, J.A., Yang, S.N., Liu, R.T. and Lin, F.J. (2000). "The prediction of late rectal complications following the treatment of uterine cervical cancer by high-dose-rate brachytherapy," *Int. J. Radiat. Oncol. Biol. Phys.* **47**, 955–961.

Chen, S.W., Liang, J.A., Yang, S.N., Ko, H.L. and Lin, F.J. (2003). "The adverse effect of treatment prolongation in cervical cancer by high-dose-rate intracavitary brachytherapy," *Radiother. Oncol.* **67**, 69–76.

Chen, C.C., Lin, J.C., Jan, J.S., Ho, S.C. and Wang, L. (2011). "Definitive intensity-modulated radiation therapy with concurrent chemotherapy for patients with locally advanced cervical cancer," *Gynecol. Oncol.* **122**, 9–13.

Chou, H.H., Chang, T.C., Yen, T.C., Ng, K.K., Hsueh, S., Ma, S.Y., Chang, C.J., Huang, H.J., Chao, A., Wu, T.I., Jung, S.M., Wu, Y.C., Lin, C.T., Huang, K.G. and Lai, C.H. (2006). "Low value of [18F]-fluoro-2-deoxy-D-glucose positron emission tomography in primary staging of early-stage cervical cancer before radical hysterectomy," *J. Clin. Oncol.* **24**, 123–128.

Christensen, G.E., Carlson, B., Chao, K.S., Yin, P., Grigsby, P.W., Nguyen, K., Dempsey, J.F., Lerma, F.A., Bae, K.T., Vannier, M.W. and Williamson, J.F. (2001). "Image-based dose planning of intracavitary brachytherapy: registration of serial-imaging studies using deformable anatomic templates," *Int. J. Radiat. Oncol. Biol. Phys.* **51**, 227–243.

Coia, L., Won, M., Lanciano, R., Marcial, V.A., Martz, K. and Hanks, G. (1990). "The Patterns of Care Outcome Study for cancer of the uterine cervix. Results of the Second National Practice Survey," *Cancer* **66**, 2451–2456.

Compton, C.C., Byrd, D.R., Garcia-Aguilar, J., Kurtzman, S.H., Olawaiye, A. and Washington, M.K., Eds. (2012). *AJCC Cancer Staging Atlas. A Companion to the Seventh Editions of the AJCC Cancer Staging Manual and Handbook* (Springer: New York).

Corn, B.W., Hanlon, A.L., Pajak, T.F., Owen, J. and Hanks, G.E. (1994). "Technically accurate intracavitary insertions improve pelvic control and survival among patients with locally advanced carcinoma of the uterine cervix," *Gynecol. Oncol.* **53**, 294–300.

Croke, J.M. and El-Sayed, S. (2012). "Multidisciplinary management of cancer patients: chasing a shadow or real value? An overview of the literature," *Curr. Oncol.* **19**, e232–e238.

Crook, J.M., Esche, B.A., Chaplain, G., Isturiz, J., Sentenac, I. and Horiot, J.C. (1987). "Dose–volume analysis and the prevention of radiation sequelae in cervical cancer," *Radiother. Oncol.* **8**, 321–332.

Cunningham, D.E., Stryker, J.A., Velkley, D.E. and Chung, C.K. (1981). "Routine clinical estimation of rectal, rectosigmoidal, and bladder doses from intracavitary brachytherapy in the treatment of carcinoma of the cervix," *Int. J. Radiat. Oncol. Biol. Phys.* **7**, 653–660.

Cuzick, J. (2010). "Long-term cervical cancer prevention strategies across the globe," *Gynecol. Oncol.* **117**(2 Suppl.), S11–S14.

Cuzick, J., Arbyn, M., Sankaranarayanan, R., Tsu, V., Ronco, G., Mayrand, M.H., Dillner, J. and Meijer, C.J. (2008). "Overview of human papillomavirus-based and other novel options for cervical cancer screening in developed and developing countries," *Vaccine* **26**(Suppl. 10), K29–K41.

Daisne, J.F., Duprez, T., Weynand, B., Lonneux, M., Hamoir, M., Reychler, H. and Gregoire, V. (2004). "Tumor volume in pharyngolaryngeal squamous cell carcinoma: comparison at CT, MR imaging, and FDG PET and validation with surgical specimen," *Radiology* **233**, 93–100.

Dale, R.G., Coles, I.P., Deehan, C. and O'Donoghue, J.A. (1997). "Calculation of integrated biological response in brachytherapy," *Int. J. Radiat. Oncol. Biol. Phys.* **38**, 633–642.

Datta, N.R., Kumar, S., Das, K.J., Pandey, C.M., Halder, S. and Ayyagari, S. (2001). "Variations of intracavitary applicator geometry during multiple HDR brachytherapy insertions in carcinoma cervix and its influence on reporting as per ICRU Report 38," *Radiother. Oncol.* **60**, 15–24.

Datta, N.R., Das, K.J., Basu, R. and Singh, U. (2003). "Total reference air kerma: to what extent can it predict intracavitary volume enclosed by isodose surfaces during multiple high-dose rate brachytherapy?," *Brachytherapy* **2**, 91–97.

Davidson, M.T., Yuen, J., D'Souza, D.P., Radwan, J.S., Hammond, J.A. and Batchelar, D.L. (2008). "Optimization of high-dose-rate cervix brachytherapy applicator placement: the benefits of intraoperative ultrasound guidance," *Brachytherapy* **7**, 248–253.

De Brabandere, M., Mousa, A.G., Nulens, A., Swinnen, A. and Van Limbergen, E. (2008). "Potential of dose optimisation in MRI-based PDR brachytherapy of cervix carcinoma," *Radiother. Oncol.* **88**, 217–226.

Delclos, L., Fletcher, G.H., Sampiere, V. and Grant, W.H., III. (1978). "Can the Fletcher gamma ray colpostat system be extrapolated to other systems?," *Cancer.* **41**, 970–979.

Delclos, L., Fletcher, G.H., Moore, E.B. and Sampiere, V.A. (1980). "Minicolpostats, dome cylinders, other additions and improvements of the Fletcher-suit afterloadable system: indications and limitations of their use," *Int. J. Radiat. Oncol. Biol. Phys.* **6**, 1195–1206.

De Leeuw, A.A., Moerland, M.A., Nomden, C., Tersteeg, R.H., Roesink, J.M. and Jurgenliemk-Schulz, I.M. (2009). "Applicator reconstruction and applicator shifts in 3D MR-based PDR brachytherapy of cervical cancer," *Radiother. Oncol.* **93**, 341–346.

Delgado, G., Bundy, B., Zaino, R., Sevin, B.U., Creasman, W.T. and Major, F. (1990). "Prospective surgical-pathological study of disease-free interval in patients with stage IB squamous cell carcinoma of the cervix: a Gynecologic Oncology Group study," *Gynecol. Oncol.* **38**, 352–357.

Demanes, D.J., Rodriguez, R.R., Bendre, D.D. and Ewing, T.L. (1999). "High dose rate transperineal interstitial brachytherapy for cervical cancer: high pelvic control and low complication rates," *Int. J. Radiat. Oncol. Biol. Phys.* **45**, 105–112.

Denny, L. (2012). "Cervical cancer prevention: new opportunities for primary and secondary prevention in the 21st century," *Int. J. Gynaecol. Obstet.* **119**(Suppl. 1), S80–S84.

DeWerd, L.A., Ibbott, G.S., Meigooni, A.S., Mitch, M.G., Rivard, M.J., Stump, K.E., Thomadsen, B.R. and Venselaar, J.L. (2011). "A dosimetric uncertainty analysis for photon-emitting brachytherapy sources: report of AAPM Task Group No. 138 and GEC-ESTRO," *Med. Phys.* **38**, 782–801.

Diaz, J.P., Gemignani, M.L., Pandit-Taskar, N., Park, K.J., Murray, M.P., Chi, D.S., Sonoda, Y., Barakat, R.R. and Abu-Rustum, N.R. (2011). "Sentinel lymph node biopsy in the management of early-stage cervical carcinoma," *Gynecol. Oncol.* **120**, 347–352.

Dimopoulos, J., Kirisits, C., Petric, P., Georg, P., Lang, S., Berger, D. and Pötter, R. (2006a). "The Vienna applicator for combined intracavitary and interstitial brachytherapy of cervical cancer: clinical feasibility and preliminary results," *Int. J. Radiat. Oncol. Biol. Phys.* **66**, 83–90.

Dimopoulos, J., Schard, G., Berger, D., Lang, S., Goldner, G., Helbich, T. and Pötter, R. (2006b). "Systematic evaluation of MRI findings in different stages of treatment of cervical cancer: potential of MRI on delineation of target, pathoanatomic structures, and organs at risk," *Int. J. Radiat. Oncol. Biol. Phys.* **64**, 1380–1388.

Dimopoulos, J., De Vos, V., Berger, D., Petric, P., Dumas, I., Kirisits, C., Shenfield, C.B., Haie-Meder, C. and Pötter, R. (2009a). "Inter-observer comparison of target delineation for MRI-assisted cervical cancer brachytherapy: application of the GYN GEC-ESTRO recommendations," *Radiother. Oncol.* **91**, 166–172.

Dimopoulos, J., Schirl, G., Baldinger, A., Helbich, T.H. and Pötter, R. (2009b). "MRI assessment of cervical cancer for adaptive radiotherapy," *Strahlenther. Onkol.* **185**, 282–287.

Dimopoulos, J., Pötter, R., Lang, S., Fidarova, E., Georg, P., Dorr, W. and Kirisits, C. (2009c). "Dose-effect relationship for local control of cervical cancer by magnetic resonance image-guided brachytherapy," *Radiother. Oncol.* **93**, 311–315.

Dimopoulos, J., Lang, S., Kirisits, C., Fidarova, E.F., Berger, D., Georg, P., Dorr, W. and Pötter, R. (2009d). "Dose–volume histogram parameters and local tumor control in magnetic resonance image-guided cervical cancer brachytherapy," *Int. J. Radiat. Oncol. Biol. Phys.* **75**, 56–63.

Dimopoulos, J.C., Petrow, P., Tanderup, K., Petric, P., Berger, D., Kirisits, C., Pedersen, E.M., van Limbergen, E., Haie-Meder, C. and Pötter, R. (2012a). "Recommendations from Gynaecological (GYN) GEC-ESTRO Working Group (IV): basic principles and parameters for MR imaging within the frame of image based adaptive cervix cancer brachytherapy," *Radiother. Oncol.* **103**, 113–122.

Dimopoulos, J.C., Schmid, M.P., Fidarova, E., Berger, D., Kirisits, C. and Pötter, R. (2012b). "Treatment of locally advanced vaginal cancer with radiochemotherapy and magnetic resonance image-guided adaptive brachytherapy: dose–volume parameters and first clinical results," *Int. J. Radiat. Oncol. Biol. Phys.* **82**, 1880–1888.

Dische, S. and Saunders, M.I. (1989). "Continuous, hyperfractionated, accelerated radiotherapy (CHART): an interim report upon late morbidity," *Radiother. Oncol.* **16**, 65–72.

Dörr, W. (2009). "Pathogenesis of normal tissue side effects," pp. 169–190 in *Basic Clinical Radiobiology*, 4th ed., Joiner, M.C. and van der Kogel, A., Eds. (CRC Press, Boca Raton, Florida).

Dörr, W. (2011). "Late effects of chemotherapy and radiation," pp. 429–437 in *Supportive Oncology*, Davis, M.P., Feyer, P., Ortner, P. and Zimmermann, C., Eds. (Elsevier Saunders, Philadelphia, Pennsylvania).

Dörr, W. and Hendry, J.H. (2001). "Consequential late effects in normal tissues," *Radiother. Oncol.* **61**, 223–231.

Dörr, W. and van der Kogel, A.J. (2009). "The volume effect in radiotherapy," pp. 191–206 in *Basic Clinical Radiobiology*, 4th ed., Joiner, M.C. and van der Kogel, A., Eds. (CRC Press, Boca Raton, Florida).

Dresen, R.C., Beets, G.L., Rutten, H.J., Engelen, S.M., Lahaye, M.J., Vliegen, R.F., de Bruine, A.P., Kessels, A.G., Lammering, G. and Beets-Tan, R.G. (2009). "Locally advanced rectal cancer: MR imaging for restaging after neoadjuvant radiation therapy with concomitant chemotherapy. Part I. Are we able to predict tumor confined to the rectal wall?," *Radiology* **252**, 71–80.

Duenas-Gonzalez, A., Cetina, L., Mariscal, I. and de la Garza, J. (2003). "Modern management of locally advanced cervical carcinoma," *Cancer Treat. Rev.* **29**, 389–399.

Duenas-Gonzalez, A., Zarba, J.J., Patel, F., Alcedo, J.C., Beslija, S., Casanova, L., Pattaranutaporn, P., Hameed, S., Blair, J.M., Barraclough, H. and Orlando, M. (2011). "Phase III, open-label, randomized study comparing concurrent gemcitabine plus cisplatin and radiation followed by adjuvant gemcitabine and cisplatin versus concurrent cisplatin and radiation in patients with Stage IIB to IVA carcinoma of the cervix," *J. Clin. Oncol.* **29**, 1678–1685.

Dutreix, A. and Marinello, G. (1987). "The Paris system," pp. 25–42 in *Modern Brachytherapy*, Pierquin, B., Wilson, J.F. and Chassagne, D., Eds. (Year Book Medical Publishers, New York).

Dutreix, A. and Wambersie, A. (1975). "Letter: specification of gamma-ray brachytherapy sources," *Br. J. Radiol.* **48**, 1034–1035.

Eddy, G.L., Bundy, B.N., Creasman, W.T., Spirtos, N.M., Mannel, R.S., Hannigan, E. and O'Connor, D. (2007). "Treatment of ('bulky') stage IB cervical cancer with or without neoadjuvant vincristine and cisplatin prior to radical hysterectomy and pelvic/para-aortic lymphadenectomy: a phase III trial of the gynecologic oncology group," *Gynecol. Oncol.* **106**, 362–369.

Eich, H.T., Muller, R.P., Engenhart-Cabillic, R., Lukas, P., Schmidberger, H., Staar, S. and Willich, N. (2008). "Involved-node radiotherapy in early-stage Hodgkin's lymphoma. Definition and guidelines of the German Hodgkin Study Group (GHSG)," *Strahlenther. Onkol.* **184**, 406–410.

Eifel, P.J. (2006). "Chemoradiotherapy in the treatment of cervical cancer," *Semin. Radiat. Oncol.* **16**, 177–185.

Eifel, P.J. and Levenback, C., Eds. (2001). *Cancer of the Female Lower Genital Tract* (B.C. Decker, Inc.: London).

Eifel, P.J., Morris, M., Wharton, J.T. and Oswald, M.J. (1994a). "The influence of tumor size and morphology on the outcome of patients with FIGO stage IB squamous cell carcinoma of the uterine cervix," *Int. J. Radiat. Oncol. Biol. Phys.* **29**, 9–16.

Eifel, P.J., Thoms, W.W., Jr., Smith, T.L., Morris, M. and Oswald, M.J. (1994b). "The relationship between brachytherapy dose and outcome in patients with bulky

endocervical tumors treated with radiation alone," *Int. J. Radiat. Oncol. Biol. Phys.* **28**, 113–118.

Eifel, P.J., Levenback, C., Wharton, J.T. and Oswald, M.J. (1995). "Time course and incidence of late complications in patients treated with radiation therapy for FIGO stage IB carcinoma of the uterine cervix," *Int. J. Radiat. Oncol. Biol. Phys.* **32**, 1289–1300.

Eisbruch, A., Williamson, J.F., Dickson, D.R., Grigsby, P.W. and Perez, C.A. (1993). "Estimation of tissue volume irradiated by intracavitary implants," *Int. J. Radiat. Oncol. Biol. Phys.* **25**, 733–744.

Ekberg, L., Holmberg, O., Wittgren, L., Bjelkengren, G. and Landberg, T. (1998). "What margins should be added to the clinical target volume in radiotherapy treatment planning for lung cancer?," *Radiother. Oncol.* **48**, 71–77.

EMBRACE (2015). International Study on MRI-Guided Brachytherapy in Locally Advance Cervical Cancer. About Embrace, https://www.embracestudy.dk (accessed 18 September 2015) (Medical University of Vienna, Vienna, Austria).

Epstein, E., Testa, A., Gaurilcikas, A., Di Legge, A., Ameye, L., Atstupenaite, V., Valentini, A.L., Gui, B., Wallengren, N.O., Pudaric, S., Cizauskas, A., Masback, A., Zannoni, G.F., Kannisto, P., Zikan, M., Pinkavova, I., Burgetova, A., Dundr, P., Nemejcova, K., Cibula, D. and Fischerova, D. (2013). "Early-stage cervical cancer: tumor delineation by magnetic resonance imaging and ultrasound—a European multicenter trial," *Gynecol. Oncol.* **128**, 449–453.

Erickson, B.A. (2003). "The sculpted pear: an unfinished brachytherapy tale," *Brachytherapy* **2**, 189–199.

Erickson, B. and Gillin, M.T. (1997). "Interstitial implantation of gynecologic malignancies," *J. Surg. Oncol.* **66**, 285–295.

Erickson, B., Albano, K. and Gillin, M. (1996). "CT-guided interstitial implantation of gynecologic malignancies," *Int. J. Radiat. Oncol. Biol. Phys.* **36**, 699–709.

Erickson, B., Jones, R., Rownd, J., Albano, K. and Gillen, M. (2000). "Is the tandem and ring applicator a suitable alternative to the high dose rate selectron tandem and ovoid applicator?," *J. Brachyther. Int.* **16**, 131–144.

Erickson, B., Lim, K., Stewart, J., Donnelly, E., Small, W., Fyles, A. and Milosevic, M. (2011). "Adaptive radiation therapy for gynecologic cancer," pp. 351–368 in *Adaptive Radiation Therapy*, Li, X.A., Ed. (CRC Press, Boca Raton, Florida).

Esche, B.A., Crook, J.M. and Horiot, J.C. (1987a). "Dosimetric methods in the optimization of radiotherapy for carcinoma of the uterine cervix," *Int. J. Radiat. Oncol. Biol. Phys.* **13**, 1183–1192.

Esche, B.A., Crook, J.M., Isturiz, J. and Horiot, J.C. (1987b). "Reference volume, milligram-hours and external irradiation for the Fletcher applicator," *Radiother. Oncol.* **9**, 255–261.

Federico, M., Fotina, I., Hegazy, N., Kirisits, C., Sturdza, A., Georg, D. and Pötter, R. (2011). "Analysis of spatial agreement between CT (+PREBT MRI) and MRI based HRCTV delineation in cervix cancer brachytherapy," *Radiother. Oncol.* **99**(Suppl. 1), S57.

Fellner, C., Pötter, R., Knocke, T.H. and Wambersie, A. (2001). "Comparison of radiography- and computed tomography-based treatment planning in cervix cancer in brachytherapy with specific attention to some quality assurance aspects," *Radiother. Oncol.* **58**, 53–62.

Fenkell, L., Assenholt, M., Nielsen, S.K., Haie-Meder, C., Pötter, R., Lindegaard, J. and Tanderup, K. (2011). "Parametrial boost using midline shielding results in an unpredictable dose to tumor and organs at risk in combined external beam radiotherapy and brachytherapy for locally advanced cervical cancer," *Int. J. Radiat. Oncol. Biol. Phys.* **79**, 1572–1579.

Ferlay, J., Parkin, D.M. and Pisani, P. (2001). GLOBOCAN 2000: Cancer Incidence, Mortality, and Prevalence Worldwide, Version 1.0, IARC Cancer Base No. 5 (IARC Press, Lyon).

Ferlay, J., Autier, P., Boniol, M., Heanue, M., Colombet, M. and Boyle, P. (2007). "Estimates of the cancer incidence and mortality in Europe in 2006," *Ann. Oncol.* **18**, 581–592.

Fidarova, E.F., Berger, D., Schussler, S., Dimopoulos, J., Kirisits, C., Georg, P., Bachtiary, B. and Pötter, R. (2010). "Dose volume parameter D2cc does not correlate with vaginal side effects in individual patients with cervical cancer treated within a defined treatment protocol with very high brachytherapy doses," *Radiother. Oncol.* **97**, 76–79.

Finlay, M.H., Ackerman, I., Tirona, R.G., Hamilton, P., Barbera, L. and Thomas, G. (2006). "Use of CT simulation for treatment of cervical cancer to assess the adequacy of lymph node coverage of conventional pelvic fields based on bony landmarks," *Int. J. Radiat. Oncol. Biol. Phys.* **64**, 205–209.

Fiorino, C., Reni, M., Bolognesi, A., Cattaneo, G.M. and Calandrino, R. (1998). "Intra- and inter-observer variability in contouring prostate and seminal vesicles: implications for conformal treatment planning," *Radiother. Oncol.* **47**, 285–292.

Fiorino, C., Cozzarini, C., Vavassori, V., Sanguineti, G., Bianchi, C., Cattaneo, G.M., Foppiano, F., Magli, A. and Piazzolla, A. (2002). "Relationships between DVHs and late rectal bleeding after radiotherapy for prostate cancer: analysis of a large group of patients pooled from three institutions," *Radiother. Oncol.* **64**, 1–12.

Fischerova, D. (2011). "Ultrasound scanning of the pelvis and abdomen for staging of gynecological tumors: a review," *Ultrasound Obstet. Gynecol.* **38**, 246–266.

Fischerova, D., Cibula, D., Stenhova, H., Vondrichova, H., Calda, P., Zikan, M., Freitag, P., Slama, J., Dundr, P. and Belacek, J. (2008). "Transrectal ultrasound and magnetic resonance imaging in staging of early cervical cancer," *Int. J. Gynecol. Cancer* **18**, 766–772.

Fitzgerald, L.T. and Mauderli, W. (1975). "Analysis of errors in three-dimensional reconstruction of radium implants from stereo radiographs," *Radiology* **115**, 455–458.

Fleming, P., Nisar Syed, A.M., Neblett, D., Puthawala, A., George, F.W., III. and Townsend, D. (1980). "Description of an afterloading ^{192}Ir interstitial–intracavitary technique in the treatment of carcinoma of the vagina," *Obstet. Gynecol.* **55**, 525–530.

Fletcher, G.H. (1971). "Cancer of the uterine cervix. Janeway lecture, 1970," *Am. J. Roentgenol. Radium Ther. Nucl. Med.* **111**, 225–242.

Fletcher, G.H., Ed. (1973). *Textbook of Radiotherapy*, 2nd ed. (Lea and Febiger: Philadelphia, Pennsylvania).

Fletcher, G.H. (1980). "Uterine cervix," in *Textbook of Radiotherapy*, 3rd ed., Fletcher, G.H., Ed. (Lea and Febiger, Philadelphia, Pennsylvania).

Fletcher, G.H., Shalek, R.J., Wall, J.A. and Bloedorn, F.G. (1952). "A physical approach to the design of applicators in radium therapy of cancer of the cervix uteri," *Am. J. Roentgenol. Radium Ther. Nucl. Med.* **68**, 935–949.

Fletcher, G.H., Wall, J.A., Bloedorn, F.G., Shalek, R.J. and Wootton, P. (1953). "Direct measurements and isodose calculations in radium therapy of carcinoma of the cervix," *Radiology* **61**, 885–901; discussion, 901–902.

Fokdal, L., Tanderup, K., Nielsen, S.K., Christensen, H.K., Rohl, L., Pedersen, E.M., Schonemann, N.K. and Lindegaard, J.C. (2011). "Image and laparoscopic guided interstitial brachytherapy for locally advanced primary or recurrent gynaecological cancer using the adaptive GEC ESTRO target concept," *Radiother. Oncol.* **100**, 473–479.

Fokdal, L., Tanderup, K., Hokland, S.B., Røhl, L., Pedersen, E.M., Nielsen, S.K., Paludan, M. and Lindegaard, J.C. (2013). "Clinical feasibility of combined intracavitary/interstitial brachytherapy in locally advanced cervical cancer employing MRI with a tandem/ring applicator in situ and virtual preplanning of the interstitial component," *Radiother. Oncol.* **107**, 63–68.

Forouzanfar, M.H., Foreman, K.J., Delossantos, A.M., Lozano, R., Lopez, A.D., Murray, C.J. and Naghavi, M. (2011). "Breast and cervical cancer in 187 countries between 1980 and 2010: a systematic analysis," *Lancet* **378**, 1461–1484.

Fowler, J.F. (1997). "Dose reduction factors when increasing dose rate in LDR or MDR brachytherapy of carcinoma of the cervix," *Radiother. Oncol.* **45**, 49–54.

Fowler, J.F. and Van Limbergen, E.F. (1997). "Biological effect of pulsed dose rate brachytherapy with stepping sources if short half-times of repair are present in tissues," *Int. J. Radiat. Oncol. Biol. Phys.* **37**, 877–883.

Franco, E.L., Duarte-Franco, E. and Ferenczy, A. (2001). "Cervical cancer: epidemiology, prevention and the role of human papillomavirus infection," *Can. Med. Assoc. J.* **164**, 1017–1025.

Frank, S.J., Jhingran, A., Levenback, C. and Eifel, P.J. (2005). "Definitive radiation therapy for squamous cell carcinoma of the vagina," *Int. J. Radiat. Oncol. Biol. Phys.* **62**, 138–147.

Fyles, A.W., Pintilie, M., Kirkbride, P., Levin, W., Manchul, L.A. and Rawlings, G.A. (1995). "Prognostic factors in patients with cervix cancer treated by radiation therapy: results of a multiple regression analysis," *Radiother. Oncol.* **35**, 107–117.

Gadducci, A., Sartori, E., Maggino, T., Landoni, F., Zola, P., Cosio, S., Pasinetti, B., Alessi, C., Maneo, A. and Ferrero, A. (2003). "The clinical outcome of patients with stage Ia1 and Ia2 squamous cell carcinoma of the uterine cervix: a Cooperation Task Force (CTF) study," *Eur. J. Gynaecol. Oncol.* **24**, 513–516.

Garrett, C. (1958). "Modification of the basis for roentgen calibrations between 0.5 and 3 MeV," *Can. J. Phys.* **36**, 149–150.

Gebara, W.J., Weeks, K.J., Jones, E.L., Montana, G.S. and Anscher, M.S. (2000). "Carcinoma of the uterine cervix: a 3D-CT analysis of dose to the internal, external and common iliac nodes in tandem and ovoid applications," *Radiother. Oncol.* **56**, 43–48.

Geets, X., Daisne, J.F., Tomsej, M., Duprez, T., Lonneux, M. and Gregoire, V. (2006). "Impact of the type of imaging modality on target volumes delineation and dose distribution in pharyngo-laryngeal squamous cell carcinoma: comparison between pre- and per-treatment studies," *Radiother. Oncol.* **78**, 291–297.

Geets, X., Tomsej, M., Lee, J.A., Duprez, T., Coche, E., Cosnard, G., Lonneux, M. and Gregoire, V. (2007). "Adaptive biological image-guided IMRT with anatomic and functional imaging in pharyngo-laryngeal tumors: impact on target volume delineation and dose distribution using helical tomotherapy," *Radiother. Oncol.* **85**, 105–115.

Georg, D., Kirisits, C., Hillbrand, M., Dimopoulos, J. and Pötter, R. (2008). "Image-guided radiotherapy for cervix cancer: high-tech external beam therapy versus high-tech brachytherapy," *Int. J. Radiat. Oncol. Biol. Phys.* **71**, 1272–1278.

Georg, P., Kirisits, C., Goldner, G., Dorr, W., Hammer, J., Potzi, R., Berger, D., Dimopoulos, J., Georg, D. and Pötter, R. (2009). "Correlation of dose–volume parameters, endoscopic and clinical rectal side effects in cervix cancer patients treated with definitive radiotherapy including MRI-based brachytherapy," *Radiother. Oncol.* **91**, 173–180.

Georg, P., Lang, S., Dimopoulos, J., Dorr, W., Sturdza, A.E., Berger, D., Georg, D., Kirisits, C. and Pötter, R. (2011). "Dose–volume histogram parameters and late side effects in magnetic resonance image-guided adaptive cervical cancer brachytherapy," *Int. J. Radiat. Oncol. Biol. Phys.* **79**, 356–362.

Georg, P., Pötter, R., Georg, D., Lang, S., Dimopoulos, J.C., Sturdza, A.E., Berger, D., Kirisits, C. and Dorr, W. (2012). "Dose effect relationship for late side effects of the rectum and urinary bladder in magnetic resonance image-guided adaptive cervix cancer brachytherapy," *Int. J. Radiat. Oncol. Biol. Phys.* **82**, 653–657.

Gerbaulet, A.L., Kunkler, I.H., Kerr, G.R., Haie, C., Michel, G., Prade, M., Lhomme, C., Masselot, M., Albano, M., Dutreix, A. and Chassagne, D. (1992). "Combined radiotherapy and surgery: local control and complications in early carcinoma of the uterine cervix—the Villejuif experience, 1975–1984," *Radiother. Oncol.* **23**, 66–73.

Gerbaulet, A., Michel, G., Haie-Meder, C., Castaigne, D., Lartigau, E., L'Homme, C., Duvillard, P., Lusinchi, A., Marsiglia, H. and Masselot, J. (1995). "The role of low dose rate brachytherapy in the treatment of cervix carcinoma. Experience of the Gustave-Roussy Institute on 1245 patients," *Eur. J. Gynaecol. Oncol.* **16**, 461–475.

Gerbaulet, A., Pötter, R., Mazeron, J.J., Meertens, H. and Van Limbergen, E. (2002a). *The GEC ESTRO*

Handbook of Brachytherapy (European Society for Radiotherapy and Oncology, Brussels, Belgium).

Gerbaulet, A., Pötter, R. and Haie-Meder, C. (2002b). "Cervix cancer," pp. 301–363 in *The GEC ESTRO Handbook of Brachytherapy*, Gerbaulet, A., Pötter, R., Mazeron, J.J., Meertens, H. and Van Limbergen, E., Eds. (European Society for Radiotherapy and Oncology, Brussels, Belgium).

Gien, L.T., Beauchemin, M.C. and Thomas, G. (2010). "Adenocarcinoma: a unique cervical cancer," *Gynecol. Oncol.* **116**, 140–146.

Gill, B.S., Kim, H., Houser, C.J., Kelley, J.L., Sukumvanich, P., Edwards, R.P., Comerci, J.T., Olawaiye, A.B., Huang, M., Courtney-Brooks, M. and Beriwal, S. (2015). "MRI-guided high-dose-rate intracavitary brachytherapy for treatment of cervical cancer: the University of Pittsburgh experience," Int. *J. Radiat. Oncol. Biol. Phys*. **91**, 540–547.

Giraud, P., Elles, S., Helfre, S., De Rycke, Y., Servois, V., Carette, M.F., Alzieu, C., Bondiau, P.Y., Dubray, B., Touboul, E., Housset, M., Rosenwald, J.C. and Cosset, J.M. (2002). "Conformal radiotherapy for lung cancer: different delineation of the gross tumor volume (GTV) by radiologists and radiation oncologists," *Radiother. Oncol.* **62**, 27–36.

Girinski, T., Pejovic-Lenfant, M.H., Bourhis, J., Campana, F., Cosset, J.M., Petit, C., Malaise, E.P., Haie, C., Gerbaulet, A. and Chassagne, D. (1989). "Prognostic value of hemoglobin concentrations and blood transfusions in advanced carcinoma of the cervix treated by radiation therapy: results of a retrospective study of 386 patients," *Int. J. Radiat. Oncol. Biol. Phys.* **16**, 37–42.

Girinsky, T., Rey, A., Roche, B., Haie, C., Gerbaulet, A., Randrianarivello, H. and Chassagne, D. (1993). "Overall treatment time in advanced cervical carcinomas: a critical parameter in treatment outcome," *Int. J. Radiat. Oncol. Biol. Phys.* **27**, 1051–1056.

Goetsch, S.J., Attix, F.H., Pearson, D.W. and Thomadsen, B.R. (1991). "Calibration of ^{192}Ir high-dose-rate afterloading systems," *Med. Phys.* **18**, 462–467.

Goldhirsch, A., Ingle, J.N., Gelber, R.D., Coates, A.S., Thurlimann, B. and Senn, H.J. (2009). "Thresholds for therapies: highlights of the St Gallen International Expert Consensus on the primary therapy of early breast cancer 2009," *Ann. Oncol.* **20**, 1319–1329.

Gondi, V., Bentzen, S.M., Sklenar, K.L., Dunn, E.F., Petereit, D.G., Tannehill, S.P., Straub, M. and Bradley, K.A. (2012). "Severe late toxicities following concomitant chemoradiotherapy compared to radiotherapy alone in cervical cancer: an inter-era analysis," *Int. J. Radiat. Oncol. Biol. Phys.* **84**, 973–982.

Gortzak-Uzan, L., Jimenez, W., Nofech-Mozes, S., Ismiil, N., Khalifa, M.A., Dube, V., Rosen, B., Murphy, J., Laframboise, S. and Covens, A. (2010). "Sentinel lymph node biopsy vs. pelvic lymphadenectomy in early stage cervical cancer: is it time to change the gold standard?," *Gynecol. Oncol.* **116**, 28–32.

Gray, H.J. (2008). "Primary management of early stage cervical cancer (IA1-IB) and appropriate selection of adjuvant therapy," *J. Natl. Compr. Canc. Netw.* **6**, 47–52.

Green, J.A., Kirwan, J.M., Tierney, J.F., Symonds, P., Fresco, L., Collingwood, M. and Williams, C.J. (2001). "Survival and recurrence after concomitant chemotherapy and radiotherapy for cancer of the uterine cervix: a systematic review and meta-analysis," *Lancet* **358**, 781–786.

Green, J., Kirwan, J., Tierney, J., Vale, C., Symonds, P., Fresco, L., Williams, C. and Collingwood, M. (2005). "Concomitant chemotherapy and radiation therapy for cancer of the uterine cervix," *Cochrane Database Syst. Rev.* CD002225.pub2. doi:10.1002/14651858.

Gregoire, V., Levendag, P., Ang, K.K., Bernier, J., Braaksma, M., Budach, V., Chao, C., Coche, E., Cooper, J.S., Cosnard, G., Eisbruch, A., El-Sayed, S., Emami, B., Grau, C., Hamoir, M., Lee, N., Maingon, P., Muller, K. and Reychler, H. (2003). "CT-based delineation of lymph node levels and related CTVs in the node-negative neck: DAHANCA, EORTC, GORTEC, NCIC,RTOG consensus guidelines," *Radiother. Oncol.* **69**, 227–236.

Grigsby, P.W. (2007). "The role of FDG-PET/CT imaging after radiation therapy," *Gynecol. Oncol.* **107**, S27–S29.

Grigsby, P.W. (2009). "Role of PET in gynecologic malignancy," *Curr. Opin. Oncol.* **21**, 420–424.

Guerrero, M. and Li, X.A. (2006). "Halftime for repair of sublethal damage in normal bladder and rectum: an analysis of clinical data from cervix brachytherapy," *Phys. Med. Biol.* **51**, 4063–4071.

Gulliford, S.L., Foo, K., Morgan, R.C., Aird, E.G., Bidmead, A.M., Critchley, H., Evans, P.M., Gianolini, S., Mayles, W.P., Moore, A.R., Sanchez-Nieto, B., Partridge, M., Sydes, M.R., Webb, S. and Dearnaley, D.P. (2010). "Dose–volume constraints to reduce rectal side effects from prostate radiotherapy: evidence from MRC RT01 Trial ISRCTN 47772397," *Int. J. Radiat. Oncol. Biol. Phys.* **76**, 747–754.

Haack, S., Nielsen, S.K., Lindegaard, J.C., Gelineck, J. and Tanderup, K. (2009). "Applicator reconstruction in MRI 3D image-based dose planning of brachytherapy for cervical cancer," *Radiother. Oncol.* **91**, 187–193.

Haack, S., Pedersen, E.M., Jespersen, S.N., Kallehauge, J.F., Lindegaard, J.C. and Tanderup, K. (2010). "Apparent diffusion coefficients in GEC ESTRO target volumes for image guided adaptive brachytherapy of locally advanced cervical cancer," *Acta Oncol.* **49**, 978–983.

Haas, J.S., Dean, R.D. and Mansfield, C.M. (1983). "Fletcher-Suit-Delclos gynecologic applicator: evaluation of a new instrument," *Int. J. Radiat. Oncol. Biol. Phys.* **9**, 763–768.

Haas, J.S., Dean, R.D. and Mansfield, C.M. (1985). "Dosimetric comparison of the Fletcher family of gynecologic colpostats 1950–1980," *Int. J. Radiat. Oncol. Biol. Phys.* **11**, 1317–1321.

Haie, C., Pejovic, M.H., Gerbaulet, A., Horiot, J.C., Pourquier, H., Delouche, J., Heinz, J.F., Brune, D., Fenton, J., Pizzi, G., Bey, P., Brussel, R., Pillement, P., Volterrani, F. and Chassagne, D. (1988). "Is prophylactic para-aortic irradiation worthwhile in the treatment of advanced cervical carcinoma? Results of a controlled

clinical trial of the EORTC radiotherapy group," *Radiother. Oncol.* **11**, 101–112.

Haie-Meder, C., Kramar, A., Lambin, P., Lancar, R., Scalliet, P., Bouzy, J. and Gerbaulet, A. (1994). "Analysis of complications in a prospective randomized trial comparing two brachytherapy low dose rates in cervical carcinoma," *Int. J. Radiat. Oncol. Biol. Phys.* **29**, 953–960.

Haie-Meder, C., Gerbaulet, A. and Pötter, R. (2002). "Interstitial brachytherapy in gynaecological cancer," pp. 417–434 in *The GEC ESTRO Handbook of Brachytherapy*, Gerbaulet, A., Pötter, R., Mazeron, J.J., Meertens, H. and Van Limbergen, E., Eds. (European Society for Radiotherapy and Oncology, Brussels, Belgium).

Haie-Meder, C., Pötter, R., Van Limbergen, E., Briot, E., De Brabandere, M., Dimopoulos, J., Dumas, I., Hellebust, T.P., Kirisits, C., Lang, S., Muschitz, S., Nevinson, J., Nulens, A., Petrow, P. and Wachter-Gerstner, N. (2005). "Recommendations from Gynaecological (GYN) GEC-ESTRO Working Group (I): concepts and terms in 3D image based 3D treatment planning in cervix cancer brachytherapy with emphasis on MRI assessment of GTV and CTV," *Radiother. Oncol.* **74**, 235–245.

Haie-Meder, C., Chargari, C., Rey, A., Dumas, I., Morice, P. and Magne, N. (2009). "DVH parameters and outcome for patients with early-stage cervical cancer treated with preoperative MRI-based low dose rate brachytherapy followed by surgery," *Radiother. Oncol.* **93**, 316–321.

Haie-Meder, C., Morice, P. and Castiglione, M. (2010a). "Cervical cancer: ESMO Clinical Practice Guidelines for diagnosis, treatment and follow-up," *Ann. Oncol.* **21**(Suppl. 5), v37–v40.

Haie-Meder, C., Chargari, C., Rey, A., Dumas, I., Morice, P. and Magne, N. (2010b). "MRI-based low dose-rate brachytherapy experience in locally advanced cervical cancer patients initially treated by concomitant chemoradiotherapy," *Radiother. Oncol.* **96**, 161–165.

Haie-Meder, C., Siebert, F.A. and Pötter, R. (2011). "Image guided, adaptive, accelerated, high dose brachytherapy as model for advanced small volume radiotherapy," *Radiother. Oncol.* **100**, 333–343.

Hall, E.J. (1972). "Radiation dose-rate: a factor of importance in radiobiology and radiotherapy," *Br. J. Radiol.* **45**, 81–97.

Han, B.H., Wallner, K., Merrick, G., Butler, W., Sutlief, S. and Sylvester, J. (2003). "Prostate brachytherapy seed identification on post-implant TRUS images," *Med. Phys.* **30**, 898–900.

Han, K., Milosevic, M., Fyles, A., Pintilie, M. and Viswanathan, A.N. (2013). "Trends in the utilization of brachytherapy in cervical cancer in the United States," *Int. J. Radiat. Oncol. Biol. Phys.* **87**, 111–119.

Hashemi, A.M., Mills, M.D., Hogstrom, K.R. and Almond, P.R. (1988). "The exposure rate constant for a silver wire 125I seed," *Med. Phys.* **15**, 228–234.

Hatano, K., Sekiya, Y., Araki, H., Sakai, M., Togawa, T., Narita, Y., Akiyama, Y., Kimura, S. and Ito, H. (1999). "Evaluation of the therapeutic effect of radiotherapy on cervical cancer using magnetic resonance imaging," *Int. J. Radiat. Oncol. Biol. Phys.* **45**, 639–644.

Hawnaur, J.M., Johnson, R.J., Carrington, B.M. and Hunter, R.D. (1998). "Predictive value of clinical examination, transrectal ultrasound and magnetic resonance imaging prior to radiotherapy in carcinoma of the cervix," *Br. J. Radiol.* **71**, 819–827.

Hegazy, N., Pötter, R., Kirisits, C., Berger, D., Federico, M., Sturdza, A. and Nesvacil, N. (2013). "High-risk clinical target volume delineation in CT-guided cervical cancer brachytherapy: impact of information from FIGO stage with or without systematic inclusion of 3D documentation of clinical gynecological examination," *Acta Oncol.* **52**, 1345–1352.

Heirs, M., Suekarran, S., Slack, R., Light, K., Gibson, F., Glaser, A., Hawkins, M. and Phillips, R. (2012). "A systematic review of models of care for the follow-up of childhood cancer survivors," *Pediatr. Blood Cancer* **60**, 351–356.

Hellebust, T.P., Dale, E., Skjonsberg, A. and Olsen, D.R. (2001). "Inter fraction variations in rectum and bladder volumes and dose distributions during high dose rate brachytherapy treatment of the uterine cervix investigated by repetitive CT-examinations," *Radiother. Oncol.* **60**, 273–280.

Hellebust, T.P., Tanderup, K., Bergstrand, E.S., Knutsen, B.H., Roislien, J. and Olsen, D.R. (2007). "Reconstruction of a ring applicator using CT imaging: impact of the reconstruction method and applicator orientation," *Phys. Med. Biol.* **52**, 4893–4904.

Hellebust, T.P., Kirisits, C., Berger, D., Perez-Calatayud, J., De Brabandere, M., De Leeuw, A., Dumas, I., Hudej, R., Lowe, G., Wills, R. and Tanderup, K. (2010a). "Recommendations from Gynaecological (GYN) GEC-ESTRO Working Group (III): considerations and pitfalls in commissioning and applicator reconstruction in 3D image-based treatment planning of cervix cancer brachytherapy," *Radiother. Oncol.* **96**, 153–160.

Hellebust, T.P., Kristensen, G.B. and Olsen, D.R. (2010b). "Late effects after radiotherapy for locally advanced cervical cancer: comparison of two brachytherapy schedules and effect of dose delivered weekly," *Int. J. Radiat. Oncol. Biol. Phys.* **76**, 713–718.

Hellebust, T.P., Tanderup, K., Lervåg, C., Fidarova, E., Berger, D., Malinen, E., Pötter, R. and Petrič, P. (2013). "Dosimetric impact of inter-observer variability in MRI-based delineation for cervical cancer brachytherapy," *Radiother. Oncol.* **107**, 13–19.

Henriksen, E. (1949). "The lymphatic spread of carcinoma of the cervix and of the body of the uterus; a study of 420 necropsies," *Am. J. Obstet. Gynecol.* **58**, 924–942.

Henschke, U.K. (1960). "'Afterloading' applicator for radiation therapy of carcinoma of the uterus," *Radiology* **74**, 834.

Henschke, U.K., Hilaris, B.S. and Mahan, G.D. (1963). "Afterloading in interstitial and intracavitary radiation therapy," *Am. J. Roentgenol. Radium Ther. Nucl. Med.* **90**, 386–395.

Heron, D.E., Gerszten, K., Selvaraj, R.N., King, G.C., Sonnik, D., Gallion, H., Comerci, J., Edwards, R.P., Wu, A., Andrade, R.S. and Kalnicki, S. (2003). "Conventional 3D conformal versus intensity-modulated radiotherapy for the adjuvant treatment of gynecologic malignancies:

a comparative dosimetric study of dose–volume histograms small star, filled," *Gynecol. Oncol.* **91**, 39–45.

Hertel, H., Kohler, C., Grund, D., Hillemanns, P., Possover, M., Michels, W. and Schneider, A. (2006). "Radical vaginal trachelectomy (RVT) combined with laparoscopic pelvic lymphadenectomy: prospective multicenter study of 100 patients with early cervical cancer," *Gynecol. Oncol.* **103**, 506–511.

Heyman, J. (1935). "The so-called Stockholm method and the results of treatment of uterine cancer at the Radiumhemmet," *Acta Radiol.* **16**, 129–147.

Heyman, J. (1947). "Improvement of results in the treatment of uterine cancer," *J. Am. Med. Assoc.* **135**, 412–416.

Hilaris, B.S., Nori, D. and Anderson, L.L. (1988). "Brachytherapy in cancer of the cervix," pp. 244–256 in *An Atlas of Brachytherapy* (Macmillan, New York).

Hintz, B.L., Kagan, A.R., Chan, P., Gilbert, H.A., Nussbaum, H., Rao, A.R. and Wollin, M. (1980). "Radiation tolerance of the vaginal mucosa," *Int. J. Radiat. Oncol. Biol. Phys.* **6**, 711–716.

Ho, G.Y., Bierman, R., Beardsley, L., Chang, C.J. and Burk, R.D. (1998). "Natural history of cervicovaginal papillomavirus infection in young women," *N. Engl. J. Med.* **338**, 423–428.

Holthusen, H. (1936). "Erfahrungen über die Verträglichkeitsgrenze für Röntgenstrahlung und deren Nutzanwendung zur Verhütung von Schäden," *Strahlenther. Onkol.* **57**, 254–269.

Horiot, J.C., Pigneux, J., Pourquier, H., Schraub, S., Achille, E., Keiling, R., Combes, P., Rozan, R., Vrousos, C. and Daly, N. (1988). "Radiotherapy alone in carcinoma of the intact uterine cervix according to G.H. Fletcher guidelines: a French cooperative study of 1383 cases," *Int. J. Radiat. Oncol. Biol. Phys.* **14**, 605–611.

Horsman, M.R., Wouters, B.G., Joiner, M.C. and Overgaard, J. (2009). "The oxygen effect and fractionated radiotherapy," pp. 207–216 in *Basic Clinical Radiobiology*, 4th ed., Joiner, M.C. and van der Kogel, A., Eds. (CRC Press, Boca Raton, Florida).

Hoskin, P.J., Colombo, A., Henry, A., Niehoff, P., Paulsen Hellebust, T., Siebert, F.A. and Kovacs, G. (2013). "GEC/ESTRO recommendations on high dose rate afterloading brachytherapy for localised prostate cancer: an update," *Radiother. Oncol.* **107**, 325–332.

Hricak, H. and Yu, K.K. (1996). "Radiology in invasive cervical cancer,"*Am. J. Roentgenol.* **167**, 1101–1108.

Hricak, H., Lacey, C.G., Sandles, L.G., Chang, Y.C., Winkler, M.L. and Stern, J.L. (1988). "Invasive cervical carcinoma: comparison of MR imaging and surgical findings," *Radiology* **166**, 623–631.

Hricak, H., Swift, P.S., Campos, Z., Quivey, J.M., Gildengorin, V. and Goranson, H. (1993). "Irradiation of the cervix uteri: value of unenhanced and contrast-enhanced MR imaging," *Radiology* **189**, 381–388.

Hricak, H., Gatsonis, C., Coakley, F.V., Snyder, B., Reinhold, C., Schwartz, L.H., Woodward, P.J., Pannu, H.K., Amendola, M. and Mitchell, D.G. (2007). "Early invasive cervical cancer: CT and MR imaging in preoperative evaluation—ACRIN/GOG comparative study of diagnostic performance and interobserver variability," *Radiology* **245**, 491–498.

Huang, Z., Mayr, N.A., Gao, M., Lo, S.S., Wang, J.Z., Jia, G. and Yuh, W.T. (2012). "Onset time of tumor repopulation for cervical cancer: first evidence from clinical data," *Int. J. Radiat. Oncol. Biol. Phys.* **84**, 478–484.

Hunter, R.D. (1994). "Dose rate correction in LDR intracavitary therapy," pp. 55–59 in *Brachytherapy from Radium to Optimisation*, Mould, R.F., Ed. (Nucletron International BV, Veenendal, The Netherlands).

Hunter, R.D. and Davidson, S.E. (2002). "Low dose-rate brachytherapy for treating cervix carcinoma: changing dose-rate," pp. 343–353 in *Principles and Practice for Brachytherapy* (CRC Press, Boca Raton, Florida).

Hunter, R.D., Wong, F., Moore, C., Notley, H.M. and Wilkinson, J. (1986). "Bladder base dosage in patients undergoing intracavitary therapy," *Radiother. Oncol.* **7**, 189–197.

IAEA (1967). International Atomic Energy Agency. Physical Aspects of Radioisotope Brachytherapy, Technical Reports Series No. 75 (International Atomic Energy Agency, Vienna, Austria).

IAEA (2006). International Atomic Energy Agency. Applying Radiation Safety Standards in Radiotherapy, Safety Reports Series 38, STI/PUB/1205 (International Atomic Energy Agency, Vienna, Austria).

IAEA (2013). International Atomic Energy Agency. Management of Cervical Cancer: Strategies for Limited-resource Centres—A Guide for Radiation Oncologists, IAEA Human Health Reports No. 6, STI/PUB/1556 (International Atomic Energy Agency, Vienna, Austria).

IAEA/ICRU (2007). International Atomic Energy Agency/International Commission on Radiation Units and Measurements. Dose Reporting in Ion-Beam Therapy, IAEA-TECDOC-1560 (International Atomic Energy Agency, Vienna, Austria).

IAEA/ICRU (2008). International Atomic Energy Agency/International Commission on Radiation Units and Measurements. Relative Biological Effectiveness in Ion-Beam Therapy, Technical Report Series No. 461, STI/DOC/010/461 (International Atomic Energy Agency, Vienna, Austria).

ICRU (1961). International Commission on Radiation Units and Measurements. Report of the International Commission on Radiological Units and Measurements (ICRU) 1959, ICRU Report 9 (International Commission on Radiation Units and Meausrements, Bethesda, Maryland).

ICRU (1970). International Commission on Radiation Units and Measurements. Specification of High Activity Gamma-Ray Sources, ICRU Report 18 (Oxford University Press, Oxford, United Kingdom).

ICRU (1978). International Commission on Radiation Units and Measurements. An International Neutron Dosimetry Intercomparison, ICRU Report 27 (Oxford University Press, Oxford, United Kingdom).

ICRU (1980). International Commission on Radiation Units and Measurements. Radiation Quantities and Units, ICRU Report 33 (Oxford University Press, Oxford, United Kingdom).

ICRU (1985). International Commission on Radiation Units and Measurements. Dose and Volume

Specification for Reporting Intracavitary Therapy in Gynaecology, ICRU Report 38 (Oxford University Press, Oxford, United Kingdom).

ICRU (1993a). International Commission on Radiation Units and Measurements. Quantities and Units in Radiation Protection Dosimetry, ICRU Report 51 (Oxford University Press, Oxford, United Kingdom).

ICRU (1993b). International Commission on Radiation Units and Measurements. Prescribing, Recording and Reporting Photon Beam Therapy, ICRU Report 50 (Oxford University Press, Oxford, United Kingdom).

ICRU (1997). International Commission on Radiation Units and Measurements. Dose and Volume Specification for Reporting Interstitial Therapy, ICRU Report 58 (Oxford University Press, Oxford, United Kingdom).

ICRU (1998). International Commission on Radiation Units and Measurements. Fundamental Quantities and Units for Ionizing Radiation, ICRU Report 60 (Oxford University Press, Oxford, United Kingdom).

ICRU (1999). International Commission on Radiation Units and Measurements. Prescribing, Recording and Reporting Photon Beam Therapy (Supplement to Report 50), ICRU Report 62 (Oxford University Press, Oxford, United Kingdom).

ICRU (2000). International Commission on Radiation Units and Measurements. Nuclear Data for Neutron and Proton Radiotherapy and for Radiation Protection, ICRU Report 63 (Oxford University Press, Oxford, United Kingdom).

ICRU (2004a). International Commission on Radiation Units and Measurements. "Prescribing, recording and reporting electron beam therapy," ICRU Report 71, *J. ICRU* **4(1)**.

ICRU (2004b). International Commission on Radiation Units and Measurements. "Dosimetry of beta rays and low-energy photons for brachytherapy with sealed sources," ICRU Report 72, *J. ICRU* **4(2)**.

ICRU (2007). International Commission on Radiation Units and Measurements. "Prescribing, recording, and reporting proton-beam therapy," ICRU Report 78, *J. ICRU* **7(2)**.

ICRU (2010). International Commission on Radiation Units and Measurements. "Prescribing, recording, and reporting photon- beam intensity-modulated radiation therapy (IMRT)," ICRU Report 83, *J. ICRU* **10(1)**.

ICRU (2011). International Commission on Radiation Units and Measurements. "Fundamental quantities and units for ionizing radiation ICRU Report 85a (Revised)," *J. ICRU* **11(1)**.

Innocenti, P., Pulli, F., Savino, L., Nicolucci, A., Pandimiglio, A., Menchi, I. and Massi, G. (1992). "Staging of cervical cancer: reliability of transrectal US," *Radiology* **185**, 201–205.

Inoue, T. and Okumura, M. (1984). "Prognostic significance of parametrial extension in patients with cervical carcinoma Stages IB, IIA, and IIB. A study of 628 cases treated by radical hysterectomy and lymphadenectomy with or without postoperative irradiation," *Cancer* **54**, 1714–1719.

Jaffray, D.A., Lindsay, P.E., Brock, K.K., Deasy, J.O. and Tome, W.A. (2010). "Accurate accumulation of dose for improved understanding of radiation effects in normal tissue," *Int. J. Radiat. Oncol. Biol. Phys.* **76**, S135–S139.

Jamema, S.V., Kirisits, C., Mahantshetty, U., Trnkova, P., Deshpande, D.D., Shrivastava, S.K. and Pötter, R. (2010). "Comparison of DVH parameters and loading patterns of standard loading, manual and inverse optimization for intracavitary brachytherapy on a subset of tandem/ovoid cases," *Radiother. Oncol.* **97**, 501–506.

Jamema, S.V., Mahantshetty, U., Tanderup, K., Malvankar, D., Sharma, S., Engineer, R., Chopra, S., Shrivastava, S.K. and Deshpande, D.D. (2013). "Inter-application variation of dose and spatial location of D(2cm(3)) volumes of OARs during MR image based cervix brachytherapy," *Radiother. Oncol.* **107**, 58–62.

Jemal, A., Bray, F., Center, M.M., Ferlay, J., Ward, E. and Forman, D. (2011). "Global cancer statistics," *CA Cancer J. Clin.* **61**, 69–90.

Jemal, A., Center, M.M., DeSantis, C. and Ward, E.M. (2012). "Global patterns of cancer incidence and mortality rates and trends," *Cancer Epidemiol. Biomarkers Prev.* **19**, 1893–1907.

Joelsson, I. and Backstrom, A. (1970). "Applicators for remote afterloading technique for optimum pelvic dose distribution in carcinoma of the uterine cervix," *Acta Radiol. Ther. Phys. Biol.* **9**, 233–246.

Joiner, M.C. (2009). "Quantifying cell kill and cell survival," pp. 41–55 in *Basic Clinical Radiobiology*, 4th ed., Joiner, M.C. and van der Kogel, A., Eds. (CRC Press, Boca Raton, Florida).

Joiner, M.C. and Bentzen, S.M. (2002). "Time–dose relationships: the linear-quadratic approach," pp. 120–133 in *Basic Clinical Radiobiology*, 3rd ed., Steel, G.G., Ed. (Oxford University Press, London).

Joiner, M.C. and Bentzen, S.M. (2009). "Fractionation: the linear-quadratic approach," pp. 102–119 in *Basic Clinical Radiobiology*, 4th ed., Joiner, M.C. and van der Kogel, A., Eds. (CRC Press, Boca Raton, Florida).

Jones, B. and Dale, R.G. (2005). "The potential for mathematical modelling in the assessment of the radiation dose equivalent of cytotoxic chemotherapy given concomitantly with radiotherapy," *Br. J. Radiol.* **78**, 939–944.

Jürgenliemk-Schulz, I.M., Tersteeg, R.J., Roesink, J.M., Bijmolt, S., Nomden, C.N., Moerland, M.A. and de Leeuw, A.A. (2009). "MRI-guided treatment-planning optimisation in intracavitary or combined intracavitary/interstitial PDR brachytherapy using tandem ovoid applicators in locally advanced cervical cancer," *Radiother. Oncol.* **93**, 322–330.

Jürgenliemk-Schulz, I.M., Lang, S., Tanderup, K., de Leeuw, A., Kirisits, C., Lindegaard, J., Petric, P., Hudej, R. and Pötter, R. (2010). "Variation of treatment planning parameters (D90 HR-CTV, D 2cc for OAR) for cervical cancer tandem ring brachytherapy in a multicentre setting: comparison of standard planning and 3D image guided optimisation based on a joint protocol for dose–volume constraints," *Radiother. Oncol.* **94**, 339–345.

Kang, H.C., Shin, K.H., Park, S.Y. and Kim, J.Y. (2010). "3D CT-based high-dose-rate brachytherapy for cervical

cancer: clinical impact on late rectal bleeding and local control," *Radiother. Oncol.* **97**, 507–513.

Katz, A. and Eifel, P.J. (2000). "Quantification of intracavitary brachytherapy parameters and correlation with outcome in patients with carcinoma of the cervix," *Int. J. Radiat. Oncol. Biol. Phys.* **48**, 1417–1425.

Kavanagh, B.D., Pan, C.C., Dawson, L.A., Das, S.K., Li, X.A., Ten Haken, R.K. and Miften, M. (2010). "Radiation dose–volume effects in the stomach and small bowel," *Int. J. Radiat. Oncol. Biol. Phys.* **76**, S101–S107.

Kesson, E.M., Allardice, G.M., George, W.D., Burns, H.J. and Morrison, D.S. (2012). "Effects of multidisciplinary team working on breast cancer survival: retrospective, comparative, interventional cohort study of 13 722 women," *Br. Med. J.* **344**, doi: http://dx.doi.org/10.1136/bmj.e2718.

Keys, H.M., Bundy, B.N., Stehman, F.B., Okagaki, T., Gallup, D.G., Burnett, A.F., Rotman, M.Z. and Fowler, W.C., Jr. (2003). "Radiation therapy with and without extrafascial hysterectomy for bulky stage IB cervical carcinoma: a randomized trial of the Gynecologic Oncology Group," *Gynecol. Oncol.* **89**, 343–353.

Kidd, E. and Grigsby, P. (2011). "The use of positron emission tomographic imaging for image-guided therapy," pp. 41–48 in *Gynecologic Radiation Therapy: Novel Approaches to Image-Guidance and Management*, Viswanathan, A.N., Kiristis, C., Erickson, B.E. and Pötter, R., Eds. (Springer, Heidelberg).

Kidd, E.A., El Naqa, I., Siegel, B.A., Dehdashti, F. and Grigsby, P.W. (2012). "FDG-PET-based prognostic nomograms for locally advanced cervical cancer," *Gynecol. Oncol.* **127**, 136–140.

Kidd, E.A., Thomas, M., Siegel, B.A., Dehdashti, F. and Grigsby, P.W. (2013). "Changes in cervical cancer FDG uptake during chemoradiation and association with response," *Int. J. Radiat. Oncol. Biol. Phys.* **85**, 116–122.

Kim, H.K., Silver, B., Berkowitz, R. and Howes, A. (1999). "Bulky, barrel-shaped cervical carcinoma (stages IB, IIA, IIB): the prognostic factors for pelvic control and treatment outcome," *Am. J. Clin. Oncol.* **22**, 232–236.

Kim, H.J., Kim, S., Ha, S.W. and Wu, H.G. (2008). "Are doses to ICRU reference points valuable for predicting late rectal and bladder morbidity after definitive radiotherapy in uterine cervix cancer?," *Tumori* **94**, 327–332.

Kim, Y., Muruganandham, M., Modrick, J.M. and Bayouth, J.E. (2011). "Evaluation of artifacts and distortions of titanium applicators on 3.0-Tesla MRI: feasibility of titanium applicators in MRI-guided brachytherapy for gynecological cancer," *Int. J. Radiat. Oncol. Biol. Phys.* **80**, 947–955.

Kirchheiner, K., Fidarova, E., Nout, R.A., Schmid, M.P., Sturdza, A., Wiebe, E., Kranz, A., Polterauer, S., Pötter, R. and Dorr, W. (2012b). "Radiation-induced morphological changes in the vagina," *Strahlenther. Onkol.* **188**, 1010–1017.

Kirchheiner, K., Nout, R., Lindegaard, J., Petric, P., Limbergen, E.V., Jurgenliemk-Schulz, I.M., Haie-Meder, C., Pötter, R. and Dorr, W. (2012a). "Do clinicians and patients agree regarding symptoms? A comparison after definitive radiochemotherapy in 223 uterine cervical cancer patients," *Strahlenther. Onkol.* **188**, 933–939.

Kirchheiner, K., Nout, R.A., Lindegaard, J.C., Haie-Meder, C., Mahantshetty, U., Segedin, B., Jürgenliemk-Schulz, I.M., Hoskin, P.J., Rai, B., Dörr, W., Kirisits, C., Bentzen, S.M., Pötter, R. and Tanderup, K; EMBRACE Collaborative Group. (2016). Dose-effect relationship and risk factors for vaginal stenosis after definitive radio(chemo)therapy with image-guided brachytherapy for locally advanced cervical cancer in the EMBRACE study. *Radiother. Oncol.* **118**, 160–166.

Kirchheiner, K., Nout, R.A., Tanderup, K., Lindegaard, J.C., Westerveld, H., Haie-Meder, C., Petrič, P., Mahantshetty, U., Dörr, W. and Pötter, R. (2014). "Manifestation pattern of early-late vaginal morbidity after definitive radiation (chemo)therapy and image-guided adaptive brachytherapy for locally advanced cervical cancer: an analysis from the EMBRACE study," *Int. J. Radiat. Oncol. Biol. Phys.* **89**, 88–95.

Kirisits, C., Pötter, R., Lang, S., Dimopoulos, J., Wachter-Gerstner, N. and Georg, D. (2005). "Dose and volume parameters for MRI-based treatment planning in intracavitary brachytherapy for cervical cancer," *Int. J. Radiat. Oncol. Biol. Phys.* **62**, 901–911.

Kirisits, C., Lang, S., Dimopoulos, J., Berger, D., Georg, D. and Pötter, R. (2006a). "The Vienna applicator for combined intracavitary and interstitial brachytherapy of cervical cancer: design, application, treatment planning, and dosimetric results," *Int. J. Radiat. Oncol. Biol. Phys.* **65**, 624–630.

Kirisits, C., Lang, S., Dimopoulos, J., Oechs, K., Georg, D. and Pötter, R. (2006b). "Uncertainties when using only one MRI-based treatment plan for subsequent high-dose-rate tandem and ring applications in brachytherapy of cervix cancer," *Radiother. Oncol.* **81**, 269–275.

Kirisits, C., Siebert, F.A., Baltas, D., De Brabandere, M., Hellebust, T.P., Berger, D. and Venselaar, J. (2007). "Accuracy of volume and DVH parameters determined with different brachytherapy treatment planning systems," *Radiother. Oncol.* **84**, 290–297.

Kirisits, C., Tanderup, K., Hellebust, T.P. and Cormack, C. (2011). "Physics for image-guided brachytherapy," pp. 143–164 in *Gynecologic Radiation Therapy: Novel Approaches to Image-Guidance and Management*, Viswanathan, A.N., Kiristis, C., Erickson, B.E. and Pötter, R., Eds. (Springer, Heidelberg).

Kirisits, K., Rivard, M.J., Baltas, D., Ballester, F., Brabandere, M., Van der Laarse, R., Niatsetski, Y., Papagiannis, P., Hellebust, T.P., Perez-Calatayud, J., Tanderup, K., Venselaar, J.L.M. and Siebert, F.A. (2014). "Review of clinical brachytherapy uncertainties: analysis guidelines of GEC-ESTRO and the AAPM," *Radiother. Oncol.* **110**, 199–212.

Kirkpatrick, J.P., Meyer, J.J. and Marks, L.B. (2008). "The linear-quadratic model is inappropriate to model high dose per fraction effects in radiosurgery," *Semin. Radiat. Oncol.* **18**, 240–243.

Kleine, W., Rau, K., Schwoeorer, D. and Pfleiderer, A. (1989). "Prognosis of the adenocarcinoma of the cervix uteri: a comparative study," *Gynecol. Oncol.* **35**, 145–149.

Komaki, R., Brickner, T.J., Hanlon, A.L., Owen, J.B. and Hanks, G.E. (1995). "Long-term results of treatment of cervical carcinoma in the United States in 1973, 1978, and 1983: patterns of Care Study (PCS)," *Int. J. Radiat. Oncol. Biol. Phys.* **31**, 973–982.

Koom, W.S., Sohn, D.K., Kim, J.Y., Kim, J.W., Shin, K.H., Yoon, S.M., Kim, D.Y., Yoon, M., Shin, D., Park, S.Y. and Cho, K.H. (2007). "Computed tomography-based high-dose-rate intracavitary brachytherapy for uterine cervical cancer: ireliminary demonstration of correlation between dose-volume parameters and rectal mucosal changes observed by flexible sigmoidoscopy," *Int. J. Radiat. Oncol. Biol. Phys.* **68**, 1446–1454.

Kottmeier, H.L. (1954). "Modern trends in the treatment of cancer of the cervix," *Acta Radiol. Suppl.* **116**, 405–414.

Kottmeier, H.L. (1964). "Surgical and radiation treatment of carcinoma of the uterine cervix. Experience by the current individualized Stockholm technique," *Acta Obstet. Gynecol. Scand.* **43**(Suppl. 2), 1–48.

Kottmeier, H.L. and Gray, M.J. (1961). "Rectal and bladder injuries in relation to radiation dosage in carcinoma of the cervix. A 5 year follow-up," *Am. J. Obstet. Gynecol.* **82**, 74–82.

Kucera, H., Wagner, G. and Weghaupt, K. (1984). "Komplikationen der präoperativen high-dose-rate-iridium-192-vorbestrahlung beim gebärmutterhalskarzinom," *Onkologie* **7**, 244–248.

Kuipers, T., Hoekstra, C.J., van 't Riet, A., Mak, A.C., Vonk, E.J., Elders, L.H., Koster, K. and Pop, L.A. (2001). "HDR brachytherapy applied to cervical carcinoma with moderate lateral expansion: modified principles of treatment," *Radiother. Oncol.* **58**, 25–30.

Kupets, R., Thomas, G.M. and Covens, A. (2002). "Is there a role for pelvic lymph node debulking in advanced cervical cancer?," *Gynecol. Oncol.* **87**, 163–170.

Lahanas, M., Baltas, D. and Giannouli, S. (2003). "Global convergence analysis of fast multiobjective gradient-based dose optimization algorithms for high-dose-rate brachytherapy," *Phys. Med. Biol.* **48**, 599–617.

Lamarque, P. and Coliez, R. (1951). "Les cancers des organs genitaux de la femme," pp. 2549 in *Electro-Radiotherapie* (Masson, Paris).

Lambrecht, M., Deroose, C., Roels, S., Vandecaveye, V., Penninckx, F., Sagaert, X., van Cutsem, E., de Keyzer, F. and Haustermans, K. (2010). "The use of FDG-PET/CT and diffusion-weighted magnetic resonance imaging for response prediction before, during and after preoperative chemoradiotherapy for rectal cancer," *Acta Oncol.* **49**, 956–963.

Lanciano, R.M., Martz, K., Coia, L.R. and Hanks, G.E. (1991). "Tumor and treatment factors improving outcome in stage III-B cervix cancer," *Int. J. Radiat. Oncol. Biol. Phys.* **20**, 95–100.

Landoni, F., Maneo, A., Colombo, A., Placa, F., Milani, R., Perego, P., Favini, G., Ferri, L. and Mangioni, C. (1997). "Randomised study of radical surgery versus radiotherapy for stage Ib–IIa cervical cancer," *Lancet* **350**, 535–540.

Lang, S., Nulens, A., Briot, E., Kirisits, C., De Brabandere, M., Dumas, I., Dimopoulos, J., Petrow, P., Georg, D., Van Limbergen, E., Haie-Meder, C. and Pötter, R. (2006). "Intercomparison of treatment concepts for MR image assisted brachytherapy of cervical carcinoma based on GYN GEC-ESTRO recommendations," *Radiother. Oncol.* **78**, 185–193.

Lang, S., Kirisits, C., Dimopoulos, J., Georg, D. and Pötter, R. (2007). "Treatment planning for MRI assisted brachytherapy of gynecologic malignancies based on total dose constraints," *Int. J. Radiat. Oncol. Biol. Phys.* **69**, 619–627.

Lang, S., Trnkova, P., Kirisits, C., Dimopoulos, J., Georg, D. and Pötter, R. (2008). "Dose reporting for rectum and sigmoid colon in 3D image based brachytherapy for cervical cancer: the importance of the location of the recto-sigmoid junction," *Radiother. Oncol.* **88**, S91.

Lang, S., Nesvacil, N., Kirisits, C., Georg, P., Dimopoulos, J., Federico, M. and Pötter, R. (2013). "Uncertainty analysis for 3D image-based cervix cancer brachytherapy by repetitive MR imaging: assessment of DVH-variations between two HDR fractions within one applicator insertion and their clinical relevance," *Radiother. Oncol.* **107**, 26–31.

La Vecchia, C., Bosetti, C., Lucchini, F., Bertuccio, P., Negri, E., Boyle, P. and Levi, F. (2010). "Cancer mortality in Europe, 2000–2004, and an overview of trends since 1975," *Ann. Oncol.* **21**, 1323–1360.

Leblanc, E., Narducci, F., Frumovitz, M., Lesoin, A., Castelain, B., Baranzelli, M.C., Taieb, S., Fournier, C. and Querleu, D. (2007). "Therapeutic value of pretherapeutic extraperitoneal laparoscopic staging of locally advanced cervical carcinoma," *Gynecol. Oncol.* **105**, 304–311.

Leblanc, E., Gauthier, H., Querleu, D., Ferron, G., Zerdoud, S., Morice, P., Uzan, C., Lumbroso, S., Lecuru, F., Bats, A.S., Ghazzar, N., Bannier, M., Houvenaeghel, G., Brenot-Rossi, I. and Narducci, F. (2011). "Accuracy of 18-fluoro-2-deoxy-D-glucose positron emission tomography in the pretherapeutic detection of occult paraaortic node involvement in patients with a locally advanced cervical carcinoma," *Ann. Surg. Oncol.* **18**, 2302–2309.

Leborgne, F., Fowler, J.F., Leborgne, J.H., Zubizarreta, E. and Chappell, R. (1996). "Fractionation in medium dose rate brachytherapy of cancer of the cervix," *Int. J. Radiat. Oncol. Biol. Phys.* **35**, 907–914.

Leborgne, F., Fowler, J.F., Leborgne, J.H., Zubizarreta, E. and Curochquin, R. (1999). "Medium-dose-rate brachytherapy of cancer of the cervix: preliminary results of a prospectively designed schedule based on the linear-quadratic model," *Int. J. Radiat. Oncol. Biol. Phys.* **43**, 1061–1064.

Lecuru, F., Mathevet, P., Querleu, D., Leblanc, E., Morice, P., Darai, E., Marret, H., Magaud, L., Gillaizeau, F., Chatellier, G. and Dargent, D. (2011). "Bilateral negative sentinel nodes accurately predict absence of lymph node metastasis in early cervical cancer: results of the SENTICOL study," *J. Clin. Oncol.* **29**, 1686–1691.

Lederman, M. and Lamerton, L.F. (1948). "Dosage estimation and distribution in the radium treatment of carcinoma of the cervix uteri; a new method and its clinical applications," *Br. J. Radiol.* **21**, 11–26.

Lee, A.W., Sze, W.M., Fowler, J.F., Chappell, R., Leung, S.F. and Teo, P. (1999). "Caution on the use of altered fractionation for nasopharyngeal carcinoma," *Radiother. Oncol.* **52**, 207–211.

Lee, L.J., Sadow, C.A., Russell, A. and Viswanathan, A.N. (2009). "Correlation of point B and lymph node dose in 3D-planned high-dose-rate cervical cancer brachytherapy," *Int. J. Radiat. Oncol. Biol. Phys.* **75**, 803–809.

Lee, L.J., Das, I.J., Higgins, S.A., Jhingran, A., Small, W., Jr., Thomadsen, B., Viswanathan, A.N., Wolfson, A. and Eifel, P. (2012). "American Brachytherapy Society consensus guidelines for locally advanced carcinoma of the cervix. Part III: low-dose-rate and pulsed-dose-rate brachytherapy," *Brachytherapy* **11**, 53–57.

Leer, J.W. (2011). "The future development of radiation oncology in Europe: a personal view," *Radiother. Oncol.* **100**, 7–9.

Lenz, M. (1927). "Radiotherapy of cancer of the cervix at the Radium Institute, Paris, France," *Am. J. Roentgenol. Radium Ther.* **17**, 335–342.

Letschert, J.G., Lebesque, J.V., de Boer, R.W., Hart, A.A. and Bartelink, H. (1990). "Dose–volume correlation in radiation-related late small-bowel complications: a clinical study," *Radiother. Oncol.* **18**, 307–320.

Letschert, J.G., Lebesque, J.V., Aleman, B.M., Bosset, J.F., Horiot, J.C., Bartelink, H., Cionini, L., Hamers, J.P., Leer, J.W. and van Glabbeke, M. (1994). "The volume effect in radiation-related late small bowel complications: results of a clinical study of the EORTC Radiotherapy Cooperative Group in patients treated for rectal carcinoma," *Radiother. Oncol.* **32**, 116–123.

Levitchi, M., Charra-Brunaud, C., Quetin, P., Haie-Meder, C., Kerr, C., Castelain, B., Delannes, M., Thomas, L., Desandes, E. and Peiffert, D. (2012). "Impact of dosimetric and clinical parameters on clinical side effects in cervix cancer patients treated with 3D pulse-dose-rate intracavitary brachytherapy," *Radiother. Oncol.* **103**, 314–321.

Lim, A. and Sia, S. (2012). "Outcomes of chemoradiotherapy in cervical cancer—the Western Australian experience," *Int. J. Radiat. Oncol. Biol. Phys.* **82**, 1431–1438.

Lim, K., Chan, P., Dinniwell, R., Fyles, A., Haider, M., Cho, Y.B., Jaffray, D., Manchul, L., Levin, W., Hill, R.P. and Milosevic, M. (2008). "Cervical cancer regression measured using weekly magnetic resonance imaging during fractionated radiotherapy: radiobiologic modeling and correlation with tumor hypoxia," *Int. J. Radiat. Oncol. Biol. Phys.* **70**, 126–133.

Lim, K., Kelly, V., Stewart, J., Xie, J., Cho, Y.B., Moseley, J., Brock, K., Fyles, A., Lundin, A., Rehbinder, H. and Milosevic, M. (2009). "Pelvic radiotherapy for cancer of the cervix: is what you plan actually what you deliver?," *Int. J. Radiat. Oncol. Biol. Phys.* **74**, 304–312.

Lim, K., Small, W., Jr., Portelance, L., Creutzberg, C., Jurgenliemk-Schulz, I.M., Mundt, A., Mell, L.K., Mayr, N., Viswanathan, A., Jhingran, A., Erickson, B., De los Santos, J., Gaffney, D., Yashar, C., Beriwal, S., Wolfson, A., Taylor, A., Bosch, W., El Naqa, I. and Fyles, A. (2011). "Consensus guidelines for delineation of clinical target volume for intensity-modulated pelvic radiotherapy for the definitive treatment of cervix cancer," *Int. J. Radiat. Oncol. Biol. Phys.* **79**, 348–355.

Lindegaard, J.C. and Tanderup, K. (2012). "Counterpoint: time to retire the parametrial boost," *Brachytherapy* **11**, 80–83.

Lindegaard, J.C., Tanderup, K., Nielsen, S.K., Haack, S. and Gelineck, J. (2008). "MRI-guided 3D optimization significantly improves DVH parameters of pulsed-dose-rate brachytherapy in locally advanced cervical cancer," *Int. J. Radiat. Oncol. Biol. Phys.* **71**, 756–764.

Lindegaard, J., Pötter, R., van Limbergen, E. and Haie-Meder, C. (2011). "Clinical aspects of treatment planning," pp. 119–130 in *Gynecologic Radiation Therapy: Novel Approaches to Image-Guidance and Management*, Viswanathan, A.N., Kiristis, C., Erickson, B.E. and Pötter, R., Eds. (Springer, Heidelberg).

Lindegaard, J.C., Fokdal, L.U., Nielsen, S.K., Juul-Christensen, J. and Tanderup, K. (2013). "MRI-guided adaptive radiotherapy in locally advanced cervical cancer from a Nordic perspective," *Acta Oncol.* **52**, 1510–1519.

Ling, C.C., Spiro, I.J., Mitchell, J. and Stickler, R. (1985). "The variation of OER with dose rate," *Int. J. Radiat. Oncol. Biol. Phys.* **11**, 1367–1373.

Ling, C.C., Humm, J., Larson, S., Amols, H., Fuks, Z., Leibel, S. and Koutcher, J.A. (2000). "Towards multidimensional radiotherapy (MD-CRT): biological imaging and biological conformality," *Int. J. Radiat. Oncol. Biol. Phys.* **47**, 551–560.

Liversage, W.E. (1969). "A general formula for equating protracted and acute regimes of radiation," *Br. J. Radiol.* **42**, 432–440.

Logsdon, M.D. and Eifel, P.J. (1999). "Figo IIIB squamous cell carcinoma of the cervix: an analysis of prognostic factors emphasizing the balance between external beam and intracavitary radiation therapy," *Int. J. Radiat. Oncol. Biol. Phys.* **43**, 763–775.

Louie, K.S., de Sanjose, S., Diaz, M., Castellsague, X., Herrero, R., Meijer, C.J., Shah, K., Franceschi, S., Munoz, N. and Bosch, F.X. (2009). "Early age at first sexual intercourse and early pregnancy are risk factors for cervical cancer in developing countries," *Br. J. Cancer* **100**, 1191–1197.

Lukka, H., Hirte, H., Fyles, A., Thomas, G., Elit, L., Johnston, M., Fung, M.F. and Browman, G. (2002). "Concurrent cisplatin-based chemotherapy plus radiotherapy for cervical cancer—a meta-analysis," *Clin. Oncol. (R. Coll. Radiol.)* **14**, 203–212.

Lutgendorf-Caucig, C., Fotina, I., Gallop-Evans, E., Claude, L., Lindh, J., Pelz, T., Knausl, B., Georg, D., Pötter, R. and Dieckmann, K. (2012). "Multicenter evaluation of different target volume delineation concepts in pediatric Hodgkin's lymphoma. A case study," *Strahlenther. Onkol.* **188**, 1025–1030.

Maffione, A.M., Piva, M., Tsamita, C.S., Nanni, C., Castellucci, P., Ambrosini, V., Lopci, E., Musto, A., Rampin, L., Grassetto, G., Marzola, M.C., Massaro, A., Cracco, E., Al-Nahhas, A., Fanti, S. and Rubello, D. (2009). "Positron-emission tomography in gynaecologic malignancies," *Arch. Gynecol. Obstet.* **280**, 521–528.

Magee, B.J., Logue, J.P., Swindell, R. and McHugh, D. (1991). "Tumour size as a prognostic factor in carcinoma of the cervix: assessment by transrectal ultrasound," *Br. J. Radiol.* **64**, 812–815.

Magne, N., Chargari, C., Vicenzi, L., Gillion, N., Messai, T., Magne, J., Bonardel, G. and Haie-Meder, C. (2008). "New trends in the evaluation and treatment of cervix cancer: the role of FDG-PET," *Cancer Treat. Rev.* **34**, 671–681.

Magne, N., Chargari, C., SanFilippo, N., Messai, T., Gerbaulet, A. and Haie-Meder, C. (2010). "Technical aspects and perspectives of the vaginal mold applicator for brachytherapy of gynecologic malignancies," *Brachytherapy* **9**, 274–277.

Mahantshetty, U., Tiwana, M.S., Jamema, S., Mishra, S., Engineer, R., Deshpande, D. and Shrivastava, S. (2011a). "Additional rectal and sigmoid mucosal points and doses in high dose rate intracavitary brachytherapy for carcinoma cervix: a dosimetric study," *J. Cancer Res. Ther.* **7**, 298–303.

Mahantshetty, U., Swamidas, J., Khanna, N., Engineer, R., Merchant, N.H., Deshpande, D.D. and Shrivastava, S. (2011b). "Reporting and validation of gynaecological Groupe Euopeen de Curietherapie European Society for Therapeutic Radiology and Oncology (ESTRO) brachytherapy recommendations for MR image-based dose volume parameters and clinical outcome with high dose-rate brachytherapy in cervical cancers: a single-institution initial experience," *Int. J. Gynecol. Cancer* **21**, 1110–1116.

Mahantshetty, U., Khanna, N., Swamidas, J., Engineer, R., Thakur, M.H., Merchant, N.H., Deshpande, D.D. and Shrivastava, S. (2012). "Trans-abdominal ultrasound (US) and magnetic resonance imaging (MRI) correlation for conformal intracavitary brachytherapy in carcinoma of the uterine cervix," *Radiother. Oncol.* **102**, 130–134.

Martinez, A., Cox, R.S. and Edmundson, G.K. (1984). "A multiple-site perineal applicator (MUPIT) for treatment of prostatic, anorectal, and gynecologic malignancies," *Int. J. Radiat. Oncol. Biol. Phys.* **10**, 297–305.

Martinez, A., Edmundson, G.K., Cox, R.S., Gunderson, L.L. and Howes, A.E. (1985). "Combination of external beam irradiation and multiple-site perineal applicator (MUPIT) for treatment of locally advanced or recurrent prostatic, anorectal, and gynecologic malignancies," *Int. J. Radiat. Oncol. Biol. Phys.* **11**, 391–398.

Marnitz, S., Kohler, C., Roth, C., Fuller, J., Hinkelbein, W. and Schneider, A. (2005). "Is there a benefit of pretreatment laparoscopic transperitoneal surgical staging in patients with advanced cervical cancer?," *Gynecol. Oncol.* **99**, 536–544.

Maruyama, Y., Bowen, M.G., Van Nagell, J.R., Gallion, H.H., DePriest, P. and Wierzbicki, J. (1994). "A feasibility study of 252Cf neutron brachytherapy, cisplatin + 5-FU chemo-adjuvant and accelerated hyperfractionated radiotherapy for advanced cervical cancer," *Int. J. Radiat. Oncol. Biol. Phys.* **29**, 529–534.

Mayr, N.A., Yuh, W.T., Taoka, T., Wang, J.Z., Wu, D.H., Montebello, J.F., Meeks, S.L., Paulino, A.C., Magnotta, V.A., Adli, M., Sorosky, J.I., Knopp, M.V. and Buatti, J.M. (2006). "Serial therapy-induced changes in tumor shape in cervical cancer and their impact on assessing tumor volume and treatment response," *Am. J. Roentgenol.* **187**, 65–72.

Mayr, N.A., Wang, J.Z., Zhang, D., Grecula, J.C., Lo, S.S., Jaroura, D., Montebello, J., Zhang, H., Li, K., Lu, L., Huang, Z., Fowler, J.M., Wu, D.H., Knopp, M.V. and Yuh, W.T. (2010a). "Longitudinal changes in tumor perfusion pattern during the radiation therapy course and its clinical impact in cervical cancer," *Int. J. Radiat. Oncol. Biol. Phys.* **77**, 502–508.

Mayr, N.A., Yuh, W.T., Jajoura, D., Wang, J.Z., Lo, S.S., Montebello, J.F., Porter, K., Zhang, D., McMeekin, D.S. and Buatti, J.M. (2010b). "Ultra-early predictive assay for treatment failure using functional magnetic resonance imaging and clinical prognostic parameters in cervical cancer," *Cancer* **116**, 903–912.

Mazeron, J.J., Simon, J.M., Le Pechoux, C., Crook, J.M., Grimard, L., Piedbois, P., Le Bourgeois, J.P. and Pierquin, B. (1991). "Effect of dose rate on local control and complications in definitive irradiation of T1-2 squamous cell carcinomas of mobile tongue and floor of mouth with interstitial iridium-192," *Radiother. Oncol.* **21**, 39–47.

Mazeron, J.J., Van Limbergen, E., Scalliet, P. and Lartigau, E. (2002). "Radiobiology of brachytherapy," in *The GEC-ESTRO Handbook of Brachytherapy* (European Society for Radiotherapy and Oncology, Brussels, Belgium).

Mazeron, R., Gilmore, J., Champoudry, J., Dumas, I., Helou, J., Maroun, P., Martinetti, F., Gerbaulet, A. and Haie-Meder, C. (2014). "Volumetric evaluation of an alternative bladder point in brachytherapy for locally advanced cervical cancer," *Strahlenther. Onkol.* **190**, 41–47.

Mazeron, R., Dumas, I., Rivin, E., Martin, V., Benhabib-Boukhelif, W., Tailleur, A., Guemnie-Tafo, A., Martinetti, F., Chargari, C., Lefkopoulos, D. and Haie-Meder, C. (2015a). "D2 cm(3)/DICRU ratio as a surrogate of bladder hotspots localizations during image-guided adaptive brachytherapy for cervical cancer: assessment and implications in late urinary morbidity analysis," *Brachytherapy* **14**, 300–307.

Mazeron, R., Castelnau-Marchand, P., Dumas, I., del Campo, E.R., Kom, L.K., Martinetti, F., Farha, G., Tailleur, A., Morice, P., Chargari, C., Lefkopoulos, D. and Haie-Meder, C. (2015b). "Impact of treatment time and dose escalation on local control in locally advanced cervical cancer treated by chemoradiation and image-guided pulsed-dose rate adaptive brachytherapy," *Radiother. Oncol.* **114**, 257–263.

McAlpine, J., Schlaerth, J.B., Lim, P., Chen, D., Eisenkop, S.M. and Spirtos, N.M. (2004). "Radiation fields in gynecologic oncology: correlation of soft tissue (surgical) to radiologic landmarks," *Gynecol. Oncol.* **92**, 25–30.

McCabe, M.S. and Jacobs, L.A. (2012). "Clinical update: survivorship care—models and programs," *Semin. Oncol. Nurs.* **28**, e1–e8.

McKenzie, A.L., van Herk, M. and Mijnheer, B. (2000). "The width of margins in radiotherapy treatment plans," *Phys. Med. Biol.* **45**, 3331–3342.

Meredith, W.J. (1950). "Dosage distribution and dosage in carcinoma of the uterine cervix," *Radiology* **54**, 386–391.

Meredith, W.J. (1967). *Radium Dosage: The Manchester System* (Livingstone, Edinburgh).

Michalski, J.M., Gay, H., Jackson, A., Tucker, S.L. and Deasy, J.O. (2010). "Radiation dose–volume effects in radiation-induced rectal injury," *Int. J. Radiat. Oncol. Biol. Phys.* **76**, S123–S129.

Milam, M.R., Frumovitz, M., dos Reis, R., Broaddus, R.R., Bassett, R.L., Jr. and Ramirez, P.T. (2007). "Preoperative lymph-vascular space invasion is associated with nodal metastases in women with early-stage cervical cancer," *Gynecol. Oncol.* **106**, 12–15.

Mitchell, D.G., Snyder, B., Coakley, F., Reinhold, C., Thomas, G., Amendola, M., Schwartz, L.H., Woodward, P., Pannu, H. and Hricak, H. (2006). "Early invasive cervical cancer: tumor delineation by magnetic resonance imaging, computed tomography, and clinical examination, verified by pathologic results, in the ACRIN 6651/GOG 183 Intergroup Study," *J. Clin. Oncol.* **24**, 5687–5694.

Mohamed, S., Nielsen, S.K., Fokdal, L.U., Lindegaard, J.C. and Tanderup, K. (2013). "Feasibility of applying one treatment plan for succeeding fractions in image guided brachytherapy in cervix cancer," *Radiother. Oncol.* **107**, 32–38.

Mohamed, S., Lindegaard, J.C., de Leeuw, A., Jürgenliemk-Schulz, I.M., Pötter, R., Kirisits, C. and Tanderup, K. (2014). "Brachytherapy vaginal dose de-escalation in locally advanced cervical cancer," *Radiother. Oncol.* **111**, S101.

Mohan, R., Ding, I.Y., Toraskar, J., Chui, C., Anderson, L.L. and Nori, D. (1985). "Computation of radiation dose distributions for shielded cervical applicators," *Int. J. Radiat. Oncol. Biol. Phys.* **11**, 823–830.

Mongioj, V., Orlandi, E., Palazzi, M., Deponti, E., Marzia, F., Stucchi, C., Sangalli, C., Fallai, C., Zonca, G., Olmi, P. and Pignoli, E. (2011). "Set-up errors analyses in IMRT treatments for nasopharyngeal carcinoma to evaluate time trends, PTV and PRV margins," *Acta Oncol.* **50**, 61–71.

Montana, G.S., Fowler, W.C., Varia, M.A., Walton, L.A., Mack, Y. and Shemanski, L. (1986). "Carcinoma of the cervix, stage III. Results of radiation therapy," *Cancer* **57**, 148–154.

Morgia, M., Cuartero, J., Walsh, L., Jezioranski, J., Keeler, K., Xie, J., Massey, C., Williamson, D., Cho, Y.B., Oh, S., Fyles, A. and Milosevic, M. (2013). "Tumor and normal tissue dosimetry changes during MR-guided pulsed-dose-rate (PDR) brachytherapy for cervical cancer," *Radiother. Oncol.* **107**, 46–51.

Morice, P., Piovesan, P., Rey, A., Atallah, D., Haie-Meder, C., Pautier, P., Sideris, L., Pomel, C., Duvillard, P. and Castaigne, D. (2003). "Prognostic value of lymphovascular space invasion determined with hematoxylin-eosin staining in early stage cervical carcinoma: results of a multivariate analysis," *Ann. Oncol.* **14**, 1511–1517.

Mottet, N., Bellmunt, J., Bolla, M., Joniau, S., Mason, M., Matveev, V., Schmid, H.P., Van der Kwast, T., Wiegel, T., Zattoni, F. and Heidenreich, A. (2011). "EAU guidelines on prostate cancer. Part II: treatment of advanced, relapsing, and castration-resistant prostate cancer," *Eur. Urol.* **59**, 572–583.

Muschitz, S., Petrow, P., Briot, E., Petit, C., De Crevoisier, R., Duvillard, P., Morice, P. and Haie-Meder, C. (2004). "Correlation between the treated volume, the GTV and the CTV at the time of brachytherapy and the histopathologic findings in 33 patients with operable cervix carcinoma," *Radiother. Oncol.* **73**, 187–194.

Nag, S. (2006). "Controversies and new developments in gynecologic brachytherapy: image-based intracavitary brachytherapy for cervical carcinoma," *Semin. Radiat. Oncol.* **16**, 164–167.

Nag, S., Erickson, B., Thomadsen, B., Orton, C., Demanes, J.D. and Petereit, D. (2000). "The American Brachytherapy Society recommendations for high-dose-rate brachytherapy for carcinoma of the cervix," *Int. J. Radiat. Oncol. Biol. Phys.* **48**, 201–211.

Nag, S., Chao, C., Erickson, B., Fowler, J., Gupta, N., Martinez, A. and Thomadsen, B. (2002). "The American Brachytherapy Society recommendations for low-dose-rate brachytherapy for carcinoma of the cervix," *Int. J. Radiat. Oncol. Biol. Phys.* **52**, 33–48.

Narayan, K., van Dyk, S. and Bernshaw, D. (2011). "Australia: Peter Maccullum Cancer Center, Melbourne," pp. 167–172 in *Gynecologic Radiation Therapy: Novel Approaches to Image-Guidance and Management*, Viswanathan, A.N., Kiristis, C., Erickson, B.E. and Pötter, R., Eds. (Springer, Heidelberg).

Nath, R. (1995). "Physical Properties and Clinical Uses of Brachytherapy Radionuclides," in *Brachytherapy Physics* (Medical Physics Publishing Corporation, Madison, WI).

Nath, R., Anderson, L.L., Jones, D., Ling, C., Loevinger, R., Williamson, J. and Hanson, W.F. (1987). Specification of Brachytherapy Source Strength, AAPM Report No. 21 (American Association of Physicists in Medicine, New York).

Nath, R., Anderson, L.L., Luxton, G., Weaver, K.A., Williamson, J.F. and Meigooni, A.S. (1995). "Dosimetry of interstitial brachytherapy sources: recommendations of the AAPM Radiation Therapy Committee Task Group No. 43. American Association of Physicists in Medicine," *Med. Phys.* **22**, 209–234.

Nath, R., Bice, W.S., Butler, W.M., Chen, Z., Meigooni, A.S., Narayana, V., Rivard, M.J. and Yu, Y. (2009). "AAPM recommendations on dose prescription and reporting methods for permanent interstitial brachytherapy for prostate cancer: report of Task Group 137," *Med. Phys.* **36**, 5310–5322.

NCI (2015). National Cancer Institute. Cisplatin and Radiation Therapy With or Without Carboplatin and Paclitaxel in Patients with Locally Advanced Cervical Cancer (OUTBACK), http://clinicaltrials.gov/show/NCT01414608 (accessed 6 January 2016) (National Cancer Institute, Bethesda, Maryland).

NCLACCMAC (2003). "Neoadjuvant Chemotherapy for Locally Advanced Cervical Cancer Meta-analysis Collaboration. Neoadjuvant Chemotherapy for Locally Advanced Cervical Cancer: a systematic review and meta-analysis of individual patient data from 21 randomised trials," *Eur. J. Cancer* **39**, 2470–2486.

NCRP (1974). National Council on Radiation Protection and Measurements. Specification of Gamma-Ray Brachytherapy Sources, NCRP Report No. 41 (National

Council on Radiation Protection and Measurement, Bethesda, Maryland).

NCS (1991). Netherlands Commission on Radiation Dosimetry. Recommendations for Dosimetry and Quality Control of Radioactive Sources Used in Brachytherapy, NCS Report (Netherlands Commission on Radiation Dosimetry, Delft, The Netherlands).

Nesvacil, N., Tanderup, K., Hellebust, T.P., De Leeuw, A., Lang, S., Mohamed, S., Jamema, S.V., Anderson, C., Pötter, R. and Kirisits, C. (2013a). "A multicentre comparison of the dosimetric impact of inter- and intrafractional anatomical variations in fractionated cervix cancer brachytherapy," *Radiother. Oncol.* **107**, 20–25.

Nesvacil, N., Pötter, R., Sturdza, A., Hegazy, N., Federico, M. and Kirisits, C. (2013b). "Adaptive image guided brachytherapy for cervical cancer: a combined MRI-/CT-planning technique with MRI only at first fraction," *Radiother. Oncol.* **107**, 75–81.

Newman, G. (1996). "Increased morbidity following the introduction of remote afterloading, with increased dose rate, for cancer of the cervix," *Radiother. Oncol.* **39**, 97–103.

Newton, M. (1975). "Radical hysterectomy or radiotherapy for stage I cervical cancer. A prospective comparison with 5 and 10 years follow-up," *Am. J. Obstet. Gynecol.* **123**, 535–542.

Nguyen, P.L., Chen, R.C., Hoffman, K.E., Trofimov, A., Efstathiou, J.A., Coen, J.J., Shipley, W.U., Zietman, A.L. and Talcott, J.A. (2010). "Rectal dose–volume histogram parameters are associated with long-term patient-reported gastrointestinal quality of life after conventional and high-dose radiation for prostate cancer: a subgroup analysis of a randomized trial," *Int. J. Radiat. Oncol. Biol. Phys.* **78**, 1081–1085.

Niemierko, A. (1997). "Reporting and analyzing dose distributions: a concept of equivalent uniform dose," *Med. Phys.* **24**, 103–110.

Nijkamp, J., de Haas-Kock, D.F., Beukema, J.C., Neelis, K.J., Woutersen, D., Ceha, H., Rozema, T., Slot, A., Vos-Westerman, H., Intven, M., Spruit, P.H., van der Linden, Y., Geijsen, D., Verschueren, K., van Herk, M.B. and Marijnen, C.A. (2012). "Target volume delineation variation in radiotherapy for early stage rectal cancer in the Netherlands," *Radiother. Oncol.* **102**, 14–21.

Ninkovic, M.M., Raicevic, J.J. and Adrovic, F. (2005). "Air kerma rate constants for gamma emitters used most often in practice," *Radiat Prot Dosimetry* **115**, 247–250.

Njeh, C.F. (2008). "Tumor delineation: the weakest link in the search for accuracy in radiotherapy," *J. Med. Phys.* **33**, 136–140.

Nkiwane, K.S., Pötter, R., Tanderup, K., Federico, M., Lindegaard, J.C. and Kirisits, C. (2013). "Single line source with and without vaginal loading and the impact on target coverage and organ at risk doses for cervix cancer Stages IB, II, and IIIB: treatment planning simulation in patients treated with MRI-guided adaptive brachytherapy in a multicentre study (EMBRACE)," *Brachytherapy* **12**, 317–323.

Nkiwane, K.S., Pötter, R., Fokdal, L.U., Hoskin, P., Pearcey, R., Segedin, B., Mahantshetty, U. and Kirisits, C. (2015). "Use of bladder dose points for assessment of the spatial dose distribution in the posterior bladder wall in cervical cancer brachytherapy and the impact of applicator position," *Brachytherapy* **14**, 252–259.

NNDC (2015). National Nuclear Data Center. Chart of Nuclides, http://www.nndc.bnl.gov/chart/ (accessed 18 September 2015) (Brookhaven National Laboratory, Upton, New York).

Nomden, C.N., de Leeuw, A.A., Moerland, M.A., Roesink, J.M., Tersteeg, R.J. and Jurgenliemk-Schulz, I.M. (2012). "Clinical use of the Utrecht applicator for combined intracavitary/interstitial brachytherapy treatment in locally advanced cervical cancer," *Int. J. Radiat. Oncol. Biol. Phys.* **82**, 1424–1430.

Nomden, C.N., de Leeuw, A.A., Roesink, J.M., Tersteeg, R.J., Moerland, M.A., Witteveen, P.O., Schreuder, H.W., van Dorst, E.B. and Jürgenliemk-Schulz, I.M. (2013b). "Clinical outcome and dosimetric parameters of chemoradiation including MRI guided adaptive brachytherapy with tandem-ovoid applicators for cervical cancer patients: a single institution experience," *Radiother. Oncol*. **107**, 69–74.

Nomden, C.N., de Leeuw, A.A., Van Limbergen, E., de Brabandere, M., Nulens, A., Nout, R.A., Laman, M., Ketelaars, M., Lutgens, L., Reniers, B. and Jurgenliemk-Schulz, I.M. (2013a). "Multicentre treatment planning study of MRI-guided brachytherapy for cervical cancer: comparison between tandem-ovoid applicator users," *Radiother. Oncol.* **107**, 82–87.

Noordhuis, M.G., Eijsink, J.J., Roossink, F., de Graeff, P., Pras, E., Schuuring, E., Wisman, G.B., de Bock, G.H. and van der Zee, A.G. (2011). "Prognostic cell biological markers in cervical cancer patients primarily treated with (chemo) radiation: a systematic review," *Int. J. Radiat. Oncol. Biol. Phys.* **79**, 325–334.

Noyes, W.R., Peters, N.E., Thomadsen, B.R., Fowler, J.F., Buchler, D.A., Stitt, J.A. and Kinsella, T.J. (1995). "Impact of 'optimized' treatment planning for tandem and ring, and tandem and ovoids, using high dose rate brachytherapy for cervical cancer," *Int. J. Radiat. Oncol. Biol. Phys.* **31**, 79–86.

O'Leary, M., Krailo, M., Anderson, J.R. and Reaman, G.H. (2008). "Progress in childhood cancer: 50 years of research collaboration, a report from the Children's Oncology Group," *Semin. Oncol.* **35**, 484–493.

Oliver, R. (1964). "A comparison of the effects of acute and protracted gamma-radiation on the growth of seedlings of *Vicia Faba*. Part II. Theoretical calculations," *Int. J. Radiat. Biol. Relat. Stud. Phys. Chem. Med.* **8**, 475–488.

Olpin, J. and Tempany, C.M. (2011). "Imaging in gynecologic malignancies," pp. 3–18 in *Gynecologic Radiation Therapy: Novel Approaches to Image-Guidance and Management*, Viswanathan, A.N., Kiristis, C., Erickson, B.E. and Pötter, R., Eds. (Springer, Heidelberg).

Olszewska, A.M., Saarnak, A.E., de Boer, R.W., van Bunningen, B.N. and Steggerda, M.J. (2001). "Comparison of dose–volume histograms and dose-wall histograms of the rectum of patients treated with intracavitary brachytherapy," *Radiother. Oncol.* **61**, 83–85.

Overgaard, J. (2011). "Advancing radiation oncology through scientific publication—100 volumes of Radiotherapy and Oncology," *Radiother. Oncol.* **100**, 1–6.

Paley, P.J., Goff, B.A., Minudri, R., Greer, B.E., Tamimi, H.K. and Koh, W.J. (2000). "The prognostic significance of radiation dose and residual tumor in the treatment of barrel-shaped endophytic cervical carcinoma," *Gynecol. Oncol.* **76**, 373–379.

Parkin, D.M., Bray, F., Ferlay, J. and Pisani, P. (2005). "Global cancer statistics, 2002," *CA Cancer J. Clin.* **55**, 74–108.

Patel, F.D., Negi, P.S., Sharma, S.C., Kapoor, R., Singh, D.P. and Ghoshal, S. (1998). "Dose rate correction in medium dose rate brachytherapy for carcinoma cervix," *Radiother. Oncol.* **49**, 317–323.

Paterson, R. (1948). *The Treatment of Malignant Disease by Radium and X-Rays, Being a Practice of Radiotherapy* (Edward Arnold, London).

Paterson, R. (1954). "Radiotherapy in cancer of the cervix; rising cure rates follow improvement in technique," *Acta Radiol. Suppl.* **116**, 395–404.

Pecorelli, S. (2009). "Revised FIGO staging for carcinoma of the vulva, cervix, and endometrium," *Int. J. Gynaecol. Obstet.* **105**, 103–104.

Pelloski, C.E., Palmer, M., Chronowski, G.M., Jhingran, A., Horton, J. and Eifel, P.J. (2005). "Comparison between CT-based volumetric calculations and ICRU reference-point estimates of radiation doses delivered to bladder and rectum during intracavitary radiotherapy for cervical cancer," *Int. J. Radiat. Oncol. Biol. Phys.* **62**, 131–137.

Perez, C.A., Breaux, S., Madoc-Jones, H., Bedwinek, J.M., Camel, H.M., Purdy, J.A. and Walz, B.J. (1983). "Radiation therapy alone in the treatment of carcinoma of uterine cervix. I. Analysis of tumor recurrence," *Cancer* **51**, 1393–1402.

Perez, C.A., Breaux, S., Bedwinek, J.M., Madoc-Jones, H., Camel, H.M., Purdy, J.A. and Walz, B.J. (1984). "Radiation therapy alone in the treatment of carcinoma of the uterine cervix. II. Analysis of complications," *Cancer* **54**, 235–246.

Perez, C.A., Kuske, R. and Glasgow, G.P. (1985). "Review of brachytherapy techniques for gynecologic tumors.," *Encocuriether. Hypertherm. Oncol.* **1**, 153–175.

Perez, C.A., Fox, S., Lockett, M.A., Grigsy, P.W., Camel, H.M., Galakatos, A., Kao, M.-S. and Williamson, J. (1991). "Impact of dose in outcome of irradiation alone in carcinoma of the uterine cervix: analysis of two different methods," *Int. J. Radiat. Oncol. Biol. Phys.* **21**, 885–898.

Perez, C.A., Grigsby, P.W., Castro-Vita, H. and Lockett, M.A. (1995). "Carcinoma of the uterine cervix. I. Impact of prolongation of overall treatment time and timing of brachytherapy on outcome of radiation therapy," *Int. J. Radiat. Oncol. Biol. Phys.* **32**, 1275–1288.

Perez, C.A., Grigsby, P.W., Chao, K.S., Mutch, D.G. and Lockett, M.A. (1998). "Tumor size, irradiation dose, and long-term outcome of carcinoma of uterine cervix," *Int. J. Radiat. Oncol. Biol. Phys.* **41**, 307–317.

Perez, C.A., Grigsby, P.W., Lockett, M.A., Chao, K.S. and Williamson, J. (1999). "Radiation therapy morbidity in carcinoma of the uterine cervix: dosimetric and clinical correlation," *Int. J. Radiat. Oncol. Biol. Phys.* **44**, 855–866.

Perez-Calatayud, J., Kuipers, F., Ballester, F., Granero, D., Richart, J., Rodriguez, S., Tormo, A. and Santos, M. (2009). "Exclusive MRI-based tandem and colpostats reconstruction in gynaecological brachytherapy treatment planning," *Radiother. Oncol.* **91**, 181–186.

Perez-Calatayud, J., Ballester, F., Das, R.K., DeWerd, L.A., Ibbott, G.S., Meigooni, A.S., Ouhib, Z., Rivard, M.J., Sloboda, R.S. and Williamson, J.F. (2012). Dose Calculation for Photon-Emitting Brachytherapy Sources with Average Energy Higher than 50 keV: Full Report of the AAPM and ESTRO, Report 229 (American Association of Physicists in Medicine, College Park, Maryland).

Pernot, M., Malissard, L., Hoffstetter, S., Luporsi, E., Peiffert, D., Aletti, P., Kozminski, P. and Bey, P. (1994). "The study of tumoral, radiobiological, and general health factors that influence results and complications in a series of 448 oral tongue carcinomas treated exclusively by irradiation," *Int. J. Radiat. Oncol. Biol. Phys.* **29**, 673–679.

Pernot, M., Hoffstetter, S., Peiffert, D., Carolus, J.M., Guillemin, F., Verhaeghe, J.L., Marchal, C., Luporsi, E., Beckendorf, V., Stines, J., Marchal, C., Luporsi, E., Beckendorf, V. and Stines, J. (1995). "[Statistical study of a series of 672 cases of carcinoma of the uterine cervix. Results and complications according to age and modalities of treatment]," *Bull. Cancer* **82**, 568–581.

Pernot, M., Luporsi, E., Hoffstetter, S., Peiffert, D., Aletti, P., Marchal, C., Kozminski, P., Noel, A. and Bey, P. (1997). "Complications following definitive irradiation for cancers of the oral cavity and the oropharynx (in a series of 1134 patients)," *Int. J. Radiat. Oncol. Biol. Phys.* **37**, 577–585.

Petereit, D.G., Sarkaria, J.N., Chappell, R., Fowler, J.F., Hartmann, T.J., Kinsella, T.J., Stitt, J.A., Thomadsen, B.R. and Buchler, D.A. (1995). "The adverse effect of treatment prolongation in cervical carcinoma," *Int. J. Radiat. Oncol. Biol. Phys.* **32**, 1301–1307.

Petereit, D.G., Sarkaria, J.N., Pötter, D.M. and Schink, J.C. (1999). "High-dose-rate versus low-dose-rate brachytherapy in the treatment of cervical cancer: analysis of tumor recurrence—the University of Wisconsin experience," *Int. J. Radiat. Oncol. Biol. Phys.* **45**, 1267–1274.

Peters, W.A., III,, Liu, P.Y., Barrett, R.J., II, Stock, R.J., Monk, B.J., Berek, J.S., Souhami, L., Grigsby, P., Gordon, W., Jr. and Alberts, D.S. (2000). "Concurrent chemotherapy and pelvic radiation therapy compared with pelvic radiation therapy alone as adjuvant therapy after radical surgery in high-risk early-stage cancer of the cervix," *J. Clin. Oncol.* **18**, 1606–1613.

Petric, P., Dimopoulos, J., Kirisits, C., Berger, D., Hudej, R. and Pötter, R. (2008). "Inter- and intraobserver variation in HR-CTV contouring: intercomparison of transverse and paratransverse image orientation in 3D-MRI assisted cervix cancer brachytherapy," *Radiother. Oncol.* **89**, 164–171.

Petrič, P., Hudej, R. and Music, M. (2009). "MRI assisted cervix cancer brachytherapy pre-planning, based on insertion of the applicator in para-cervical anaesthesia: preliminary results of a prospective study," *J. Contemp. Brachyther.* **1**, 163–169.

Petrič, P., Pötter, R. and Van Limbergen, E. (2011). "Adaptive contouring of the target volume and organs at risk," pp. 99–118 in *Gynecologic Radiation Therapy: Novel Approaches to Image-Guidance and Management*, Viswanathan, A.N., Kirisits, C., Erickson, B.E. and Pötter, R., Eds. (Springer, Heidelberg).

Petrič, P., Hudej, R., Rogelj, P., Blas, M., Tanderup, K., Fidarova, E., Kirisits, C., Berger, D., Dimopoulos, J., Pötter, R. and Hellebust, T.P. (2013). "Uncertainties of target volume delineation in MRI guided adaptive brachytherapy of cervix cancer: a multi-institutional study," *Radiother. Oncol.* **107**, 6–12.

Pettersson, F. and Benedet, J.L. (1998). "History of the annual report," *J. Epidemiol. Biostat.* **3**, 1–2.

Pierquin, B. (1964). *Précis de Curiethérapie, Endocuriethérapie et Plésiocuriethérapie* (Masson, Paris).

Pierquin, B. and Marinello, G. (1997). *A Practical Manual of Brachytherapy* (Medical Physics Publishing, Madison, Wisconsin).

Pohle, E.A. (1950). "Carcinoma of the cervix," pp. 371–458 in *Clinical Radiation Therapy* (Lea and Febiger, Philadelphia, PA).

Polo, A., Salembier, C., Venselaar, J. and Hoskin, P. (2010). "Review of intraoperative imaging and planning techniques in permanent seed prostate brachytherapy," *Radiother. Oncol.* **94**, 12–23.

Portelance, L., Chao, K.S., Grigsby, P.W., Bennet, H. and Low, D. (2001). "Intensity-modulated radiation therapy (IMRT) reduces small bowel, rectum, and bladder doses in patients with cervical cancer receiving pelvic and para-aortic irradiation," *Int. J. Radiat. Oncol. Biol. Phys.* **51**, 261–266.

Potish, R.A. and Gerbi, B.J. (1986). "Role of point A in the era of computerized dosimetry," *Radiology* **158**, 827–831.

Potish, R.A. and Gerbi, B.J. (1987). "Cervical cancer: intracavitary dose specification and prescription," *Radiology* **165**, 555–560.

Potish, R., Gerbi, B. and Engler, G.P. (1995). "Dose prescription, dose specification, and applicator geometry in intracavitary therapy," pp. 379–410 in *Brachytherapy Physics* (Medical Physics Publishing, Madison, Wisconsin).

Pötter, R. (2009). "Image-guided brachytherapy sets benchmarks in advanced radiotherapy," *Radiother. Oncol.* **91**, 141–146.

Pötter, R. and Van Limbergen, E. (2002). "Oesophageal cancer," pp. 515–538 in *The GEC ESTRO Handbook of Brachytherapy*, Gerbaulet, A., Pötter, R., Mazeron, J.J., Meertens, H. and Van Limbergen, E., Eds. (European Society for Radiotherapy and Oncology, Brussels, Belgium).

Pötter, R., Knocke, T.H., Fellner, C., Baldass, M., Reinthaller, A. and Kucera, H. (2000). "Definitive radiotherapy based on HDR brachytherapy with iridium 192 in uterine cervix carcinoma: report on the Vienna University Hospital findings (1993–1997) compared to the preceding period in the context of ICRU 38 recommendations," *Cancer Radiother.* **4**, 159–172.

Pötter, R., Van Limbergen, E., Gerstner, N. and Wambersie, A. (2001a). "Survey of the use of the ICRU 38 in recording and reporting cervical cancer brachytherapy," *Radiother. Oncol.* **58**, 11–18.

Pötter, R., Van Limbergen, E., Dries, W., Popowski, Y., Coen, V., Fellner, C., Georg, D., Kirisits, C., Levendag, P., Marijnissen, H., Marsiglia, H., Mazeron, J.J., Pokrajac, B., Scalliet, P. and Tamburini, V. (2001b). "Prescribing, recording, and reporting in endovascular brachytherapy. Quality assurance, equipment, personnel and education," *Radiother. Oncol.* **59**, 339–360.

Pötter, R., Gerbaulet, A. and Haie-Meder, C. (2002a). "Endometrium cancer," pp. 365–402 in *The GEC ESTRO Handbook of Brachytherapy*, Gerbaulet, A., Pötter, R., Mazeron, J.J., Meertens, H. and Van Limbergen, E., Eds. (European Society for Radiotherapy and Oncology, Brussels, Belgium).

Pötter, R., Van Limbergen, E. and Wambersie, A. (2002b). "Reporting in brachytherapy. Dose and volume specification," pp. 154–215 in *The GEC ESTRO Handbook of Brachytherapy*, Gerbaulet, A., Pötter, R., Mazeron, J.J., Meertens, H. and Van Limbergen, E., Eds. (European Society for Radiotherapy and Oncology, Brussels, Belgium).

Pötter, R., Haie-Meder, C., Van Limbergen, E., Barillot, I., De Brabandere, M., Dimopoulos, J., Dumas, I., Erickson, B., Lang, S., Nulens, A., Petrow, P., Rownd, J. and Kirisits, C. (2006). "Recommendations from gynaecological (GYN) GEC ESTRO working group (II): concepts and terms in 3D image-based treatment planning in cervix cancer brachytherapy-3D dose volume parameters and aspects of 3D image-based anatomy, radiation physics, radiobiology," *Radiother. Oncol.* **78**, 67–77.

Pötter, R., Dimopoulos, J., Georg, P., Lang, S., Waldhausl, C., Wachter-Gerstner, N., Weitmann, H., Reinthaller, A., Knocke, T.H., Wachter, S. and Kirisits, C. (2007). "Clinical impact of MRI assisted dose volume adaptation and dose escalation in brachytherapy of locally advanced cervix cancer," *Radiother. Oncol.* **83**, 148–155.

Pötter, R., Kirisits, C., Fidarova, E.F., Dimopoulos, J.C., Berger, D., Tanderup, K. and Lindegaard, J.C. (2008a). "Present status and future of high-precision image guided adaptive brachytherapy for cervix carcinoma," *Acta Oncol.* **47**, 1325–1336.

Pötter, R., Fidarova, E., Kirisits, C., Lang, S., Reinthaller, A. and Dimopoulos, J. (2008b). "3D MRI-based brachytherapy for cervical cancer," *Expert Rev. Obstet. Gynecol.* **3**, 351.

Pötter, R., Georg, P., Dimopoulos, J.C., Grimm, M., Berger, D., Nesvacil, N., Georg, D., Schmid, M.P., Reinthaller, A., Sturdza, A. and Kirisits, C. (2011). "Clinical outcome of protocol based image (MRI) guided adaptive brachytherapy combined with 3D conformal radiotherapy with or without chemotherapy in patients with locally advanced cervical cancer," *Radiother. Oncol.* **100**, 116–123.

Pötter, R., Eriksen, J.G., Beavis, A.W., Coffey, M., Verfaillie, C., Leer, J.W. and Valentini, V. (2012). "Competencies in radiation oncology: a new approach for education and training of professionals for radiotherapy and oncology in Europe," *Radiother. Oncol.* **103**, 1–4.

Pötter, R., Federico, M., Sturdza, A., Fotina, I., Hegazy, N., Schmid, M., Kirisits, C. and Nesvacil, N. (2016). "Value of Magnetic Resonance Imaging without or with applicator in place for target definition in cervix cancer brachytherapy," *Int. J. Radiat. Oncol. Biol. Phys.* **94**, 588–597.

Pouliot, J., Lessard, E. and Hsu, I.C. (2005). "Chapter 21: Advanced 3D planning," pp. 393–413 in *Brachytherapy Physics*, 2nd ed. (Medical Physics Publishing, Madison, Wisconsin).

Pourquier, H., Dubois, J.B. and Delard, R. (1982). "Cancer of the uterine cervix: dosimetric guidelines for prevention of late rectal and rectosigmoid complications as a result of radiotherapeutic treatment," *Int. J. Radiat. Oncol. Biol. Phys.* **8**, 1887–1895.

Pourquier, H., Delard, R., Achille, E., Daly, N.J., Horiot, J.C., Keiling, R., Pigneux, J., Rozan, R., Schraub, S. and Vrousos, C. (1987). "A quantified approach to the analysis and prevention of urinary complications in radiotherapeutic treatment of cancer of the cervix," *Int. J. Radiat. Oncol. Biol. Phys.* **13**, 1025–1033.

Pourquier, H., Dubois, J.B. and Delard, R. (1996). "Radiation therapy of cervical cancer with dosimetric prevention of late pelvic complications," *Bull. Cancer Radiother.* **83**, 135–143.

Pritchard-Jones, K., Kaatsch, P., Steliarova-Foucher, E., Stiller, C.A. and Coebergh, J.W. (2006). "Cancer in children and adolescents in Europe: developments over 20 years and future challenges," *Eur. J. Cancer* **42**, 2183–2190.

Querleu, D., Leblanc, E., Cartron, G., Narducci, F., Ferron, G. and Martel, P. (2006). "Audit of preoperative and early complications of laparoscopic lymph node dissection in 1000 gynecologic cancer patients," *Am. J. Obstet. Gynecol.* **195**, 1287–1292.

Quimby, E.H. (1970). "Dosage with radioactive materials," pp. 241–284 in *Physical Foundations of Radiology* (Harper and Row, New York).

Quinn, M.A., Benedet, J.L., Odicino, F., Maisonneuve, P., Beller, U., Creasman, W.T., Heintz, A.P., Ngan, H.Y. and Pecorelli, S. (2006). "Carcinoma of the cervix uteri. FIGO 26th Annual Report on the Results of Treatment in Gynecological Cancer," *Int. J. Gynaecol. Obstet.* **95**(Suppl. 1), S43–S103.

Raaymakers, B.W., Lagendijk, J.J., Overweg, J., Kok, J.G., Raaijmakers, A.J., Kerkhof, E.M., van der Put, R.W., Meijsing, I., Crijns, S.P., Benedosso, F., van Vulpen, M., de Graaff, C.H., Allen, J. and Brown, K.J. (2009). "Integrating a 1.5 T MRI scanner with a 6 MV accelerator: proof of concept," *Phys. Med. Biol.* **54**, N229–N237.

Reade, C. and Elit, L. (2012). "Trends in gynecologic cancer care in North America," *Obstet. Gynecol. Clin. North Am.* **39**, 107–129.

Reinhardt, M.J., Ehritt-Braun, C., Vogelgesang, D., Ihling, C., Hogerle, S., Mix, M., Moser, E. and Krause, T.M. (2001). "Metastatic lymph nodes in patients with cervical cancer: detection with MR imaging and FDG PET," *Radiology* **218**, 776–782.

Rijkmans, E.C., Nout, R.A., Rutten, I.H., Ketelaars, M., Neelis, K.J., Laman, M.S., Coen, V.L., Gaarenstroom, K.N., Kroep, J.R. and Creutzberg, C.L. (2014). "Improved survival of patients with cervical cancer treated with image-guided brachytherapy compared with conventional brachytherapy" *Gynecol. Oncol.* **135**, 231–238.

Rivard, M.J., Coursey, B.M., DeWerd, L.A., Hanson, W.F., Huq, M.S., Ibbott, G.S., Mitch, M.G., Nath, R. and Williamson, J.F. (2004). "Update of AAPM Task Group No. 43 Report: a revised AAPM protocol for brachytherapy dose calculations," *Med. Phys.* **31**, 633–674.

Rivard, M.J., Butler, W.M., DeWerd, L.A., Huq, M.S., Ibbott, G.S., Meigooni, A.S., Melhus, C.S., Mitch, M.G., Nath, R. and Williamson, J.F. (2007). "Supplement to the 2004 update of the AAPM Task Group No. 43 Report," *Med. Phys.* **34**, 2187–2205.

Roberts, S.A., Hendry, J.H., Swindell, R., Wilkinson, J.M. and Hunter, R.D. (2004). "Compensation for changes in dose-rate in radical low-dose-rate brachytherapy: a radiobiological analysis of a randomised clinical trial," *Radiother. Oncol.* **70**, 63–74.

Rodemann, H.P. and Wouters, B.G. (2011). "Frontiers in molecular radiation biology/oncology," *Radiother. Oncol.* **101**, 1–6.

Rodrigus, P., De Winter, K., Venselaar, J.L. and Leers, W.H. (1997). "Evaluation of late morbidity in patients with carcinoma of the uterine cervix following a dose rate change," *Radiother. Oncol.* **42**, 137–141.

Roh, J.W., Seo, S.S., Lee, S., Kang, K.W., Kim, S.K., Sim, J.S., Kim, J.Y., Hong, E.K., Cho, D.S., Lee, J.S. and Park, S.Y. (2005). "Role of positron emission tomography in pretreatment lymph node staging of uterine cervical cancer: a prospective surgicopathologic correlation study," *Eur. J. Cancer* **41**, 2086–2092.

Rose, P.G., Adler, L.P., Rodriguez, M., Faulhaber, P.F., Abdul-Karim, F.W. and Miraldi, F. (1999). "Positron emission tomography for evaluating para-aortic nodal metastasis in locally advanced cervical cancer before surgical staging: a surgicopathologic study," *J. Clin. Oncol.* **17**, 41–45.

Rose, P.G., Ali, S., Whitney, C.W., Lanciano, R. and Stehman, F.B. (2011). "Outcome of stage IVA cervical cancer patients with disease limited to the pelvis in the era of chemoradiation: a Gynecologic Oncology Group study," *Gynecol. Oncol.* **121**, 542–545.

Roy, M., Bouchard-Fortier, G., Popa, I., Gregoire, J., Renaud, M.C., Tetu, B. and Plante, M. (2011). "Value of sentinel node mapping in cancer of the cervix," *Gynecol. Oncol.* **122**, 269–274.

Saibishkumar, E.P., Patel, F.D., Sharma, S.C., Karunanidhi, G., Sankar, A.S. and Mallick, I. (2006). "Results of external-beam radiotherapy alone in invasive cancer of the uterine cervix: a retrospective analysis," *Clin. Oncol. (R. Coll. Radiol.)* **18**, 46–51.

Sala, E., Wakely, S., Senior, E. and Lomas, D. (2007). "MRI of malignant neoplasms of the uterine corpus and cervix," *Am. J. Roentgenol.* **188**, 1577–1587.

Sander, T., Duane, S., Lee, N.D., Thomas, C.G., Owen, P.J., Bailey, M. and Palmans, H. (2012). "NPL's new absorbed dose standard for the calibration of HDR 192Ir brachytherapy sources," *Metrologia* **49**, S184–S188.

Sandler, B. (1942). "Radium therapy of carcinoma cervix," *J. Obstet. Gynecol. Br. Emp.* **49**, 101–148.

Sapru, S., Mohamed, S., Fokdal, L., Nkiwane, K., Swamidas, J., Mahantshetty, U., Kirisits, C., Pötter, R., Christian Lindegaard, J. and Tanderup, K. (2013). "Dose to the non-involved uterine corpus with MRI guided brachytherapy in locally advanced cervical cancer," *Radiother. Oncol.* **107**, 93–98.

Scalliet, P., Landuyt, W. and van der Schueren, E. (1989). "Repair kinetics as a determining factor for late tolerance of central nervous system to low dose rate irradiation," *Radiother. Oncol.* **14**, 345–353.

Scheidler, J., Hricak, H., Yu, K.K., Subak, L. and Segal, M.R. (1997). "Radiological evaluation of lymph node metastases in patients with cervical cancer. A meta-analysis," *J. Am. Med. Assoc.* **278**, 1096–1101.

Schmid, R., Kirisits, C., Syeda, B., Wexberg, P., Siostrzonek, P., Pokrajac, B., Georg, D., Glogar, D. and Poetter, R. (2004). "Quality assurance in intracoronary brachytherapy. Recommendations for determining the planning target length to avoid geographic miss," *Radiother. Oncol.* **71**, 311–318.

Schmid, M.P., Kirisits, C., Nesvacil, N., Dimopoulos, J.C., Berger, D. and Pötter, R. (2012). "Local recurrences in cervical cancer patients in the setting of image-guided brachytherapy: a comparison of spatial dose distribution within a matched-pair analysis," *Radiother. Oncol.* **100**, 468–472.

Schmid, M.P., Pötter, R., Brader, P., Kratochwil, A., Goldner, G., Kirchheiner, K., Sturdza, A. and Kirisits, C. (2013a). "Feasibility of transrectal ultrasonography for assessment of cervical cancer," *Strahlenther. Onkol.* **189**, 123–128.

Schmid, M.P., Mansmann, B., Federico, M., Dimopoulous, J.C., Georg, P., Fidarova, E., Dorr, W. and Pötter, R. (2013b). "Residual tumour volumes and grey zones after external beam radiotherapy (with or without chemotherapy) in cervical cancer patients. A low-field MRI study," *Strahlenther. Onkol.* **189**, 238–245.

Schuetz, M., Schmid, M.P., Pötter, R., Kommata, S., Georg, D., Lukic, D., Dudczak, R., Kletter, K., Dimopoulos, J., Karanikas, G. and Bachtiary, B. (2010). "Evaluating repetitive 18F-fluoroazomycin-arabinoside (18FAZA) PET in the setting of MRI guided adaptive radiotherapy in cervical cancer," *Acta Oncol.* **49**, 941–947.

Schwarz, G. (1969). "An evaluation of the Manchester system of treatment of carcinoma of the cervix," *Am. J. Roentgenol. Radium Ther. Nucl. Med.* **105**, 579–585.

Serkies, K., Kobierska, A., Konopa, K., Sawicki, T. and Jassem, J. (2001). "The feasibility study on continuous 7-day-a-week external beam irradiation in locally advanced cervical cancer: a report on acute toxicity," *Radiother. Oncol.* **61**, 197–202.

SFPH (1995). Société Française des Physiciens d'Hôpital. Contrôle de Qualité en Curiethérapie par Iridium-192 à Haut Débit de Dose (Commission de Curiethérapie, Société Française des Physiciens d'Hôpital, Paris).

Shalek, R.J. and Stovall, M. (1968). "The M.D. Anderson method for the computation of isodose curves around interstitial and intracavitary radiation sources. I. Dose from linear sources," *Am. J. Roentgenol. Radium Ther. Nucl. Med.* **102**, 662–672.

Shalek, R.J. and Stovall, M.A. (1969). "Dosimetry in implant therapy," pp. 743–807 in *Radiation Dosimetry* (Academic Press, New York).

Sharma, S.C., Williamson, J.F. and Cytacki, E. (1982). "Dosimetric analysis of stereo and orthogonal reconstruction of interstitial implants," *Int. J. Radiat. Oncol. Biol. Phys.* **8**, 1803–1805.

Sherris, J., Herdman, C. and Elias, C. (2001). "Cervical cancer in the developing world," *West. J. Med.* **175**, 231–233.

Shin, K.H., Kim, T.H., Cho, J.K., Kim, J.Y., Park, S.Y., Park, S.Y., Kim, D.Y., Chie, E.K., Pyo, H.R. and Cho, K.H. (2006). "CT-guided intracavitary radiotherapy for cervical cancer: comparison of conventional point A plan with clinical target volume-based three-dimensional plan using dose-volume parameters," *Int. J. Radiat. Oncol. Biol. Phys.* **64**, 197–204.

Sievert, R.M. (1921). "Die intensitätsverteilung der primären γ-strahlung in der nähe medizinischer radiumpräparate," *Acta Radiol.* **1**, 89.

Sironi, S., Buda, A., Picchio, M., Perego, P., Moreni, R., Pellegrino, A., Colombo, M., Mangioni, C., Messa, C. and Fazio, F. (2006). "Lymph node metastasis in patients with clinical early-stage cervical cancer: detection with integrated FDG PET/CT," *Radiology* **238**, 272–279.

Small, W., Jr., Mell, L.K., Anderson, P., Creutzberg, C., De Los, S.J., Gaffney, D., Jhingran, A., Portelance, L., Schefter, T., Iyer, R., Varia, M., Winter, K. and Mundt, A.J. (2008). "Consensus guidelines for delineation of clinical target volume for intensity-modulated pelvic radiotherapy in postoperative treatment of endometrial and cervical cancer," *Int. J. Radiat. Oncol. Biol. Phys.* **71**, 428–434.

Smeenk, R.J., Hopman, W.P., Hoffmann, A.L., van Lin, E.N. and Kaanders, J.H. (2012). "Differences in radiation dosimetry and anorectal function testing imply that anorectal symptoms may arise from different anatomic substrates," *Int. J. Radiat. Oncol. Biol. Phys.* **82**, 145–152.

Soares, C.G., Douysset, G. and Mitch, M.G. (2009). "Primary standards and dosimetry protocols for brachytherapy sources," *Metrologia* **46**, S80–S98.

Sobin, L.H., Gospodarowicz, M.K. and Wittekind, C., Eds. (2009). *TNM Classification of Malignant Tumours*, 7th edn (Wiley-Blackwell, Oxford).

Specenier, P. and Vermorken, J.B. (2013). "Cetuximab: its unique place in head and neck cancer treatment," *Biologics* **7**, 77–90.

Specht, L., Yahalom, J., Illidge, T., Berthelsen, A.K., Constine, L.S., Eich, H.T., Girinsky, T., Hoppe, R.T., Mauch, P., Mikhaeel, N.G. and Ng, A. (2014). "Modern radiation therapy for Hodgkin lymphoma: field and dose guidelines from the International Lymphoma Radiation Oncology Group (ILROG)," *Int. J. Radiat. Oncol. Biol. Phys.* **89**, 854–862.

Steel, G.G. (1991). "The ESTRO Breur lecture. Cellular sensitivity to low dose-rate irradiation focuses the problem of tumour radioresistance," *Radiother. Oncol.* **20**, 71–83.

Steel, G.G., Ed. (2002). *Basic Clinical Radiobiology*, 3rd ed. (Oxford University Press, London).

Steenbakkers, R.J., Duppen, J.C., Fitton, I., Deurloo, K.E., Zijp, L.J., Comans, E.F., Uitterhoeve, A.L., Rodrigus, P.T., Kramer, G.W., Bussink, J., De Jaeger, K., Belderbos, J.S., Nowak, P.J., van Herk, M. and Rasch, C.R. (2006). "Reduction of observer variation using matched CT-PET for lung cancer delineation: a three-dimensional analysis," *Int. J. Radiat. Oncol. Biol. Phys.* **64**, 435–448.

Stehman, F.B., Bundy, B.N., DiSaia, P.J., Keys, H.M., Larson, J.E. and Fowler, W.C. (1991). "Carcinoma of the cervix treated with radiation therapy. I. A multi-variate analysis of prognostic variables in the Gynecologic Oncology Group," *Cancer* **67**, 2776–2785.

Stitt, J.A., Fowler, J.F., Thomadsen, B.R., Buchler, D.A., Paliwal, B.P. and Kinsella, T.J. (1992). "High dose rate intracavitary brachytherapy for carcinoma of the cervix: the Madison system: I. Clinical and radiobiological considerations," *Int. J. Radiat. Oncol. Biol. Phys.* **24**, 335–348.

Stout, R. and Hunter, R.D. (1989). "Clinical trials of changing dose rate in intracavitary low dose rate therapy," pp. 219–222 in *Brachytherapy*, Mould, R.F., Ed. (Nucletron International BV, Veenendal, The Netherlands).

Stryker, J.A., Bartholomew, M., Velkley, D.E., Cunningham, D.E., Mortel, R., Craycraft, G. and Shafer, J. (1988). "Bladder and rectal complications following radiotherapy for cervix cancer," *Gynecol. Oncol.* **29**, 1–11.

Stump, K.E., DeWerd, L.A., Rudman, D.A. and Schima, S.A. (2005). "Active radiometric calorimeter for absolute calibration of radioactive sources," *Rev. Sci. Instrum.* **76**, 033504–033509.

Sturdza, A., Pötter, R., Ulrik Fokdal, L., Haie-Meder, C., Tan, L.T., Mazeron, R., Petric, P., Segedin, B., Jurgenliemk-Schulz, I.M., Nomaden, C., Gillham, C., McArdle, O., Van Limbergen, E., Janssen, H., Hoskin, P., Lowe, G., Tharavichitkul, E., Villafranca, E., Mahantshetty, U., Georg, P., Kirchheiner, K., Kirisits, C., Tanderup, K. and Lindegaard, J.C. (2016). "Image Guided Brachytherapy in Locally Advanced Cervical Cancer: improved pelvic control and survival in RetroEMBRACE, a Multicenter chohort study," *Radiother. Oncol.*, in press.

Sugawara, Y., Eisbruch, A., Kosuda, S., Recker, B.E., Kison, P.V. and Wahl, R.L. (1999). "Evaluation of FDG PET in patients with cervical cancer," *J. Nucl. Med.* **40**, 1125–1131.

Suit, H.D., Moore, E.B., Fletcher, G.H. and Worsnop, R. (1963). "Modification of Fletcher ovoid system for afterloading, using standard-sized radium tubes (milligram and microgram)," *Radiology* **81**, 126–131.

Swift, P.S., Purser, P., Roberts, L.W., Pickett, B., Powell, C.B. and Phillips, T.L. (1997). "Pulsed low dose rate brachytherapy for pelvic malignancies," *Int. J. Radiat. Oncol. Biol. Phys.* **37**, 811–817.

Syed, A.M.N., Puthawala, A.A. and Neblett, D. (1986). "Transperineal interstitial-intracavitary 'Syed-Neblett' applicator in the treatment of carcinoma of the uterine cervix," *Endocurie Hypertherm. Oncol.* **2**, 1–13.

Syed, A.M., Puthawala, A.A., Abdelaziz, N.N., el-Naggar, M., Disaia, P., Berman, M., Tewari, K.S., Sharma, A., Londrc, A., Juwadi, S., Cherlow, J.M., Damore, S. and Chen, Y.J. (2002). "Long-term results of low-dose-rate interstitial-intracavitary brachytherapy in the treatment of carcinoma of the cervix," *Int. J. Radiat. Oncol. Biol. Phys.* **54**, 67–78.

Tamaki, T., Ohno, T., Noda, S.E., Kato, S. and Nakano, T. (2015). "Filling the gap in central shielding: three-dimensional analysis of the EQD2 dose in radiotherapy for cervical cancer with the central shielding technique," *J. Radiat. Res*. **56**, 804–810.

Takehara, K., Shigemasa, K., Sawasaki, T., Naito, H. and Fujii, T. (2001). "Recurrence of invasive cervical carcinoma more than 5 years after initial therapy," *Obstet. Gynecol.* **98**, 680–684.

Tammela, J., Bundy, B. and Odunsi, K. (2004). "Reassessment of pelvic lymph node debulking in advanced cervical cancer," *Gynecol. Oncol.* **92**, 1014–1015.

Tan, L., Blake, P., Hoskin, P., Davidson, S., Rathmell, A., Bidmead, M., Lee, C. and Wilkins, M. (2009). *Implementing Image-Guided Brachytherapy for Cervix Cancer in the UK* (The Royal College of Radiologists, London).

Tan, L.T., Jones, B., Gee, A. and Kingston, R.E. (1997a). "An audit of the treatment of carcinoma of the uterine cervix using external beam radiotherapy and a single line source brachytherapy technique," *Br. J. Radiol.* **70**, 1259–1269.

Tan, L.T., Jones, B. and Shaw, J.E. (1997b). "Radical radiotherapy for carcinoma of the uterine cervix using external beam radiotherapy and a single line source brachytherapy technique: the Clatterbridge technique," *Br. J. Radiol.* **70**, 1252–1258.

Tanderup, K., Christensen, J.J., Granfeldt, J. and Lindegaard, J.C. (2006). "Geometric stability of intracavitary pulsed dose rate brachytherapy monitored by in vivo rectal dosimetry," *Radiother. Oncol.* **79**, 87–93.

Tanderup, K., Fokdal, L., Sturdza, A., Haie-Meder, C., Mazeron, R., Van Limbergen, E., Jürgenliemek-Schulz, I., Petric, P., Hoskin, P., Dörr, W., Bentzen, S., Kirisits, C., Lindegaard, J. and Pötter, R. (2016). "Effect of tumor dose, volume and overall treatment time on local control after radiochemotherapy including MRI guided brachythernapy of locally advanced cervical cancer," *Radiother. Oncol.*, in press.

Tanderup, K., Hellebust, T.P., Lang, S., Granfeldt, J., Pötter, R., Lindegaard, J.C. and Kirisits, C. (2008). "Consequences of random and systematic reconstruction uncertainties in 3D image based brachytherapy in cervical cancer," *Radiother. Oncol.* **89**, 156–163.

Tanderup, K., Nielsen, S.K., Nyvang, G.B., Pedersen, E.M., Rohl, L., Aagaard, T., Fokdal, L. and Lindegaard, J.C. (2010a). "From point A to the sculpted pear: MR image guidance significantly improves tumour dose and sparing of organs at risk in brachytherapy of cervical cancer," *Radiother. Oncol.* **94**, 173–180.

Tanderup, K., Georg, D., Pötter, R., Kirisits, C., Grau, C. and Lindegaard, J. (2010b). "Adaptive management of cervical cancer radiotherapy," *Semin. Radiat. Oncol.* **20**, 121–129.

Tanderup, K., Pötter, R., Lindegaard, J.C., Berger, D., Wambersie, A. and Kirisits, C. (2010c). "PTV margins should not be used to compensate for uncertainties in 3D image guided intracavitary brachytherapy," *Radiother. Oncol.* **97**, 495–500.

Tanderup, K., Nesvacil, N., Pötter, R. and Kirisits, C. (2013). "Uncertainties in image guided adaptive cervix cancer brachytherapy: impact on planning and prescription," *Radiother. Oncol.* **107**, 1–5.

Tanderup, K., Eifel, P.J., Yashar, C.M., Pötter, R. and Grigsby, P.W. (2014). "Curative radiation therapy for locally advanced cervical cancer: brachytherapy is not optional," *Int. J. Radiat. Oncol. Biol. Phys.* **88**, 537–539.

Taylor, A. and Powell, M.E.B. (2008). "An assessment of interfractional uterine and cervical motion: implications for radiotherapy target volume definition in gynaecological cancer," *Radiother. Oncol.* **88**, 250–257.

Taylor, A., Rockall, A.G., Reznek, R.H. and Powell, M.E. (2005). "Mapping pelvic lymph nodes: guidelines for delineation in intensity-modulated radiotherapy," *Int. J. Radiat. Oncol. Biol. Phys.* **63**, 1604–1612.

Thames, H.D. (1985). "An 'incomplete-repair' model for survival after fractionated and continuous irradiations," *Int. J. Radiat. Biol. Relat. Stud. Phys. Chem. Med.* **47**, 319–339.

Thames, H.D. and Suit, H.D. (1986). "Tumor radioresponsiveness versus fractionation sensitivity," *Int. J. Radiat. Oncol. Biol. Phys.* **12**, 687–691.

Thames, H.D., Bentzen, S.M., Turesson, I., Overgaard, M. and Van den Bogaert, W. (1990). "Time–dose factors in radiotherapy: a review of the human data," *Radiother. Oncol.* **19**, 219–235.

Thomadsen, B. (1995). "Clinical implementation of HDR intracavitary and translunimal brachytherapy," pp. 641–677 in *Brachytherapy Physics* (Medical Physics Publishing, Madison, Wisconsin).

Thomadsen, B. (1997). "Brachytherapy Source Material," in *Categorical Course in Brachytherapy Physics* (RSNA Publications, Oak Brook, IL).

Thomadsen, B. (2000a). "Quality management for dosimetric treatment planning," pp. 210–239 in *Achieving Quality in Brachytherapy* (Institute of Physics Publishing, London).

Thomadsen, B. (2000b). *Achieving Quality in Brachytherapy* (Institute of Physics Publishing, London).

Thomadsen, B.R., Williamson, J.F., Rivard, M.J. and Meigooni, A.S. (2008). "Anniversary paper: past and current issues, and trends in brachytherapy physics," *Med. Phys.* **35**, 4708–4723.

Thomas, G. (1999). "Improved treatment for cervical cancer—concurrent chemotherapy and radiotherapy," *N. Engl. J. Med.* **340**, 1198–2000.

Thwaites, D.I. and Malicki, J. (2011). "Physics and technology in ESTRO and in radiotherapy and oncology: past, present and into the 4th dimension," *Radiother. Oncol.* **100**, 327–332.

Tod, M.C. (1941). "The optimum dosage in the treatment of carcinoma of the uterine cervix by radiation," *Br. J. Radiol.* **14**, 23–29.

Tod, M.C. (1947). "Optimum dosage in the treatment of cancer of the cervix by radiation," *Acta Radiol.* **28**, 564–575.

Tod, M. and Meredith, W.J. (1938). "A dosage system for use in the treatment of cancer of the uterine cervix," *Br. J. Radiol.* **11**, 809–824.

Tod, M. and Meredith, W.J. (1953). "Treatment of cancer of the cervix uteri, a revised Manchester method," *Br. J. Radiol.* **26**, 252–257.

Touboul, C., Uzan, C., Mauguen, A., Gouy, S., Rey, A., Pautier, P., Lhomme, C., Duvillard, P., Haie-Meder, C. and Morice, P. (2010). "Prognostic factors and morbidities after completion surgery in patients undergoing initial chemoradiation therapy for locally advanced cervical cancer," *Oncologist* **15**, 405–415.

Touboul, C., Uzan, C., Mauguen, A., Gouy, S., Rey, A., Pautier, P., Haie-Meder, C. and Morice, P. (2011). "Survival and prognostic factors after completion surgery in patients undergoing initial chemoradiation therapy for locally advanced cervical cancer," *Gynecol. Obstet. Fertil.* **39**, 274–280.

Tozzi, R., Lavra, F., Cassese, T., Campanile, R.G., Pedicini, V., Bignardi, M., Scorsetti, M. and Bertuzzi, A. (2009). "Laparoscopic debulking of bulky lymph nodes in women with cervical cancer: indication and surgical outcomes," *Br. J. Obstet. Gynaecol.* **116**, 688–692.

Trimble, E.L. (2009). "Cervical cancer state-of-the-clinical-science meeting on pretreatment evaluation and prognostic factors, September 27–28, 2007: proceedings and recommendations," *Gynecol. Oncol.* **114**, 145–150.

Trnkova, P., Pötter, R., Baltas, D., Karabis, A., Fidarova, E., Dimopoulos, J., Georg, D. and Kirisits, C. (2009). "New inverse planning technology for image-guided cervical cancer brachytherapy: description and evaluation within a clinical frame," *Radiother. Oncol.* **93**, 331–340.

Trnková, P., Baltas, D., Karabis, A., Stock, M., Dimopoulos, J., Georg, D., Pötter, R. and Kirisits, C. (2010). "A detailed dosimetric comparison between manual and inverse plans in HDR intracavitary/interstitial cervical cancer brachytherapy," *J. Contep. Brachyther.* **2**, 163–170.

Trnková, P., Fidarova, E., Berger, D., Georg, D., Pötter, R. and Kirisits, C. (2016). "Vagina wall: dosimetric parameters—comparison for several treatment planning approaches with respect to vagina," *J. Contep. Brachyther.*, submitted for publication.

Trott, N.G. (1987). "Radionuclides in brachytherapy: radium and after," *Br. J. Radiol.* (Suppl. 21), 1–54.

Trott, K.R., Doerr, W., Facoetti, A., Hopewell, J., Langendijk, J., van Luijk, P., Ottolenghi, A. and Smyth, V. (2012). "Biological mechanisms of normal tissue damage: importance for the design of NTCP models," *Radiother. Oncol.* **105**, 79–85.

Turesson, I. (1990). "Radiobiological aspects of continuous low dose-rate irradiation and fractionated high dose-rate irradiation," *Radiother. Oncol.* **19**, 1–15.

Turesson, I. and Thames, H.D. (1989). "Repair capacity and kinetics of human skin during fractionated radiotherapy: erythema, desquamation, and telangiectasia

after 3 and 5 year's follow-up," *Radiother. Oncol.* **15**, 169–188.

Uzan, C., Souadka, A., Gouy, S., Debaere, T., Duclos, J., Lumbroso, J., Haie-Meder, C. and Morice, P. (2011). "Analysis of morbidity and clinical implications of laparoscopic para-aortic lymphadenectomy in a continuous series of 98 patients with advanced-stage cervical cancer and negative PET-CT imaging in the para-aortic area," *Oncologist* **16**, 1021–1027.

Vale, C., Thierny, J.F. and Stewart, L.A. (2008). "Reducing uncertainties about the effects of chemoradiotherapy for cervical cancer: a systematic review and meta-analysis of individual patient data from 18 randomized trials," *J. Clin. Oncol.* **26**, 5802–5812.

Valentini, V., Aristei, C., Glimelius, B., Minsky, B.D., Beets-Tan, R., Borras, J.M., Haustermans, K., Maingon, P., Overgaard, J., Pahlman, L., Quirke, P., Schmoll, H.J., Sebag-Montefiore, D., Taylor, I., Van Cutsem, E., Van de Velde, C., Cellini, N. and Latini, P. (2009). "Multidisciplinary rectal cancer management: 2nd European rectal cancer consensus conference (EURECA-CC2)," *Radiother. Oncol.* **92**, 148–163.

van de Bunt, L., van der Heide, U.A., Ketelaars, M., de Kort, G.A. and Jurgenliemk-Schulz, I.M. (2006). "Conventional, conformal, and intensity-modulated radiation therapy treatment planning of external beam radiotherapy for cervical cancer: the impact of tumor regression," *Int. J. Radiat. Oncol. Biol. Phys.* **64**, 189–196.

van de Bunt, L., Jürgenliemk-Schulz, I.M., de Kort, G.A.P., Roesink, J.M., Tersteeg, R.J.H.A. and van der Heide, U.A. (2008). "Motion and deformation of the target volumes during IMRT for cervical cancer: what margins do we need?," *Radiother. Oncol.* **88**, 233–240.

Van de Kamer, J.B., De Leeuw, A.A., Moerland, M.A. and Jurgenliemk-Schulz, I.M. (2010). "Determining DVH parameters for combined external beam and brachytherapy treatment: 3D biological dose adding for patients with cervical cancer," *Radiother. Oncol.* **94**, 248–253.

Van de Putte, G., Lie, A.K., Vach, W., Baekelandt, M. and Kristensen, G.B. (2005). "Risk grouping in stage IB squamous cell cervical carcinoma," *Gynecol. Oncol.* **99**, 106–112.

van der Kogel, A.J. (2009). "The dose rate effect," pp. 162–168 in *Basic Clinical Radiobiology*, 4th ed., Joiner, M.C. and van der Kogel, A., Eds. (CRC Press, Boca Raton, Florida).

Van de Steene, J., Linthout, N., de Mey, J., Vinh-Hung, V., Claassens, C., Noppen, M., Bel, A. and Storme, G. (2002). "Definition of gross tumor volume in lung cancer: inter-observer variability," *Radiother. Oncol.* **62**, 37–49.

Van Dyk, S., Narayan, K., Fisher, R. and Bernshaw, D. (2009). "Conformal brachytherapy planning for cervical cancer using transabdominal ultrasound," *Int. J. Radiat. Oncol. Biol. Phys.* **75**, 64–70.

van Elmpt, W., De Ruysscher, D., van der Salm, A., Lakeman, A., van der Stoep, J., Emans, D., Damen, E., Ollers, M., Sonke, J.J. and Belderbos, J. (2012). "The PET-boost randomised phase II dose-escalation trial in non-small cell lung cancer," *Radiother. Oncol.* **104**, 67–71.

van Herk, M., Remeijer, P., Rasch, C. and Lebesque, J.V. (2000). "The probability of correct target dosage: dose-population histograms for deriving treatment margins in radiotherapy," *Int. J. Radiat. Oncol. Biol. Phys.* **47**, 1121–1135.

Van Hoe, L., Vanbeckevoort, D., Oyen, R., Itzlinger, U. and Vergote, I. (1999). "Cervical carcinoma: optimized local staging with intravaginal contrast-enhanced MR imaging—preliminary results," *Radiology* **213**, 608–611.

Vargas, C., Yan, D., Kestin, L.L., Krauss, D., Lockman, D.M., Brabbins, D.S. and Martinez, A.A. (2005). "Phase II dose escalation study of image-guided adaptive radiotherapy for prostate cancer: use of dose–volume constraints to achieve rectal isotoxicity," *Int. J. Radiat. Oncol. Biol. Phys.* **63**, 141–149.

Vincens, E., Balleyguier, C., Rey, A., Uzan, C., Zareski, E., Gouy, S., Pautier, P., Duvillard, P., Haie-Meder, C. and Morice, P. (2008). "Accuracy of magnetic resonance imaging in predicting residual disease in patients treated for stage IB2/II cervical carcinoma with chemoradiation therapy: correlation of radiologic findings with surgicopathologic results," *Cancer* **113**, 2158–2165.

Viswanathan, A.N. and Thomadsen, B. (2012). "American Brachytherapy Society consensus guidelines for locally advanced carcinoma of the cervix. Part I: general principles," *Brachytherapy* **11**, 33–46.

Viswanathan, A.N., Lee, H., Hanson, E., Berkowitz, R.S. and Crum, C.P. (2006a). "Influence of margin status and radiation on recurrence after radical hysterectomy in Stage IB cervical cancer," *Int. J. Radiat. Oncol. Biol. Phys.* **65**, 1501–1507.

Viswanathan, A.N., Cormack, R., Holloway, C.L., Tanaka, C., O'Farrell, D., Devlin, P.M. and Tempany, C. (2006b). "Magnetic resonance-guided interstitial therapy for vaginal recurrence of endometrial cancer," *Int. J. Radiat. Oncol. Biol. Phys.* **66**, 91–99.

Viswanathan, A.N., Dimopoulos, J., Kirisits, C., Berger, D. and Pötter, R. (2007). "Computed tomography versus magnetic resonance imaging-based contouring in cervical cancer brachytherapy: results of a prospective trial and preliminary guidelines for standardized contours," *Int. J. Radiat. Oncol. Biol. Phys.* **68**, 491–498.

Viswanathan, A.N., Cormack, R., Rawal, B. and Lee, H. (2009). "Increasing brachytherapy dose predicts survival for interstitial and tandem-based radiation for stage IIIB cervical cancer," *Int. J. Gynecol. Cancer* **19**, 1402–1406.

Viswanathan, A.N., Yorke, E.D., Marks, L.B., Eifel, P.J. and Shipley, W.U. (2010). "Radiation dose–volume effects of the urinary bladder," *Int. J. Radiat. Oncol. Biol. Phys.* **76**, S116–S122.

Viswanathan, A.N., Erickson, B.E. and Rownd, J. (2011a). "Image-based approaches to interstitial brachytherapy," pp. 247–259 in *Gynecologic Radiation Therapy: Novel Approaches to Image-Guidance and Management*, Viswanathan, A.N, Kiristis, C., Erickson, B.E. and Pötter, R., Eds. (Springer, Heidelberg).

Viswanathan, A.N., Kirisits, C., Erickson, B. and Pötter, R., Eds. (2011b). *Gynecologic Radiation Therapy: Novel Approaches to Image-Guidance and Management* (Springer, Heidelberg).

Viswanathan, A.N., Moughan, J., Small, W., Jr., Levenback, C., Iyer, R., Hymes, S., Dicker, A.P., Miller, B., Erickson, B. and Gaffney, D.K. (2012a). "The quality of cervical cancer brachytherapy implantation and the impact on local recurrence and disease-free survival in radiation therapy oncology group prospective trials 0116 and 0128," *Int. J. Gynecol. Cancer* **22**, 123–131.

Viswanathan, A.N., Beriwal, S., De Los Santos, J.F., Demanes, D.J., Gaffney, D., Hansen, J., Jones, E., Kirisits, C., Thomadsen, B. and Erickson, B. (2012b). "American Brachytherapy Society consensus guidelines for locally advanced carcinoma of the cervix. Part II: high-dose-rate brachytherapy," *Brachytherapy* **11**, 47–52.

Viswanathan, A.N., Creutzberg, C.L., Craighead, P., McCormack, M., Toita, T., Narayan, K., Reed, N., Long, H., Kim, H.J., Marth, C., Lindegaard, J.C., Cerrotta, A., Small, W., Jr. and Trimble, E. (2012c). "International brachytherapy practice patterns: a survey of the Gynecologic Cancer Intergroup (GCIG)," *Int. J. Radiat. Oncol. Biol. Phys.* **82**, 250–255.

Vliegen, R.F., Beets, G.L., Lammering, G., Dresen, R.C., Rutten, H.J., Kessels, A.G., Oei, T.K., de Bruine, A.P., van Engelshoven, J.M. and Beets-Tan, R.G. (2008). "Mesorectal fascia invasion after neoadjuvant chemotherapy and radiation therapy for locally advanced rectal cancer: accuracy of MR imaging for prediction," *Radiology* **246**, 454–462.

Vogelius, I.R. and Bentzen, S.M. (2013). "Meta-analysis of the alpha/beta ratio for prostate cancer in the presence of an overall time factor: bad news, good news, or no news?," *Int. J. Radiat. Oncol. Biol. Phys.* **85**, 89–94.

Wachter-Gerstner, N., Wachter, S., Reinstadler, E., Fellner, C., Knocke, T.H. and Pötter, R. (2003a). "The impact of sectional imaging on dose escalation in endocavitary HDR-brachytherapy of cervical cancer: results of a prospective comparative trial," *Radiother. Oncol.* **68**, 51–59.

Wachter-Gerstner, N., Wachter, S., Reinstadler, E., Fellner, C., Knocke, T.H., Wambersie, A. and Pötter, R. (2003b). "Bladder and rectum dose defined from MRI based treatment planning for cervix cancer brachytherapy: comparison of dose–volume histograms for organ contours and organ wall, comparison with ICRU rectum and bladder reference point," *Radiother. Oncol.* **68**, 269–276.

Wakatsuki, M., Ohno, T., Yoshida, D., Noda, S.E., Saitoh, J., Shibuya, K., Katoh, H., Suzuki, Y., Takahashi, T. and Nakano, T. (2011). "Intracavitary combined with CT-guided interstitial brachytherapy for locally advanced uterine cervical cancer: introduction of the technique and a case presentation," *J. Radiat. Res.* **52**, 54–58.

Walstam, R. (1954). "The dosage distribution in the pelvis in radium treatment of carcinoma of the cervix," *Acta Radiol.* **42**, 237–250.

Walstam, R. (1965). "A remotely controlled afterloading apparatus," *Acta Radiol.* **326**, 84–100.

Wang, C.J., Leung, S.W., Chen, H.C., Sun, L.M., Fang, F.M., Huang, E.Y., Hsiung, C.Y. and Changchien, C.C. (1998). "The correlation of acute toxicity and late rectal injury in radiotherapy for cervical carcinoma: evidence suggestive of consequential late effect (CQLE)," *Int. J. Radiat. Oncol. Biol. Phys.* **40**, 85–91.

Wang, J.Z., Mayr, N.A., Zhang, D., Li, K., Grecula, J.C., Montebello, J.F., Lo, S.S. and Yuh, W.T. (2010). "Sequential magnetic resonance imaging of cervical cancer: the predictive value of absolute tumor volume and regression ratio measured before, during, and after radiation therapy," *Cancer* **116**, 5093–5101.

Wang, D., Bosch, W., Kirsch, D.G., Al Lozi, R., El Naqa, I., Roberge, D., Finkelstein, S.E., Petersen, I., Haddock, M., Chen, Y.L., Saito, N.G., Hitchcock, Y.J., Wolfson, A.H. and DeLaney, T.F. (2011). "Variation in the gross tumor volume and clinical target volume for preoperative radiotherapy of primary large high-grade soft tissue sarcoma of the extremity among RTOG sarcoma radiation oncologists," *Int. J. Radiat. Oncol. Biol. Phys.* **81**, e775–e780.

Weiss, E., Richter, S., Krauss, T., Metzelthin, S.I., Hille, A., Pradier, O., Siekmeyer, B., Vorwerk, H. and Hess, C.F. (2003). "Conformal radiotherapy planning of cervix carcinoma: differences in the delineation of the clinical target volume. A comparison between gynaecologic and radiation oncologists," *Radiother. Oncol.* **67**, 87–95.

Weiss, E., Wu, J., Sleeman, W., Bryant, J., Mitra, P., Myers, M., Ivanova, T., Mukhopadhyay, N., Ramakrishnan, V., Murphy, M. and Williamson, J. (2010). "Clinical evaluation of soft tissue organ boundary visualization on cone-beam computed tomographic imaging," *Int. J. Radiat. Oncol. Biol. Phys.* **78**, 929–936.

Westerveld, H., Pötter, R., Dankulchai, P., Dörr, W., Sora, M.C., Pötter-Lang, S., Berger, D. and Kirisits, C. (2013). "Vaginal dose point reporting in cervical cancer patients treated with combined 2D/3D external beam radiotherapy and 2D/3D brachytherapy," *Radiother. Oncol.* **107**, 99–105.

WHO (World Health Organization) (2000) *International Classification of Diseases for Oncology (ICD-O)*, 3rd ed. (World Health Organization, Geneva).

Wilkinson, J.M. and Ramachandran, T.P. (1989). "The ICRU recommendations for reporting intracavitary therapy in gynaecology and the Manchester method of treating cancer of the cervix uteri," *Br. J. Radiol.* **62**, 362–365.

Wilkinson, J.M., Hendry, J.H. and Hunter, R.D. (1980). "Dose-rate considerations in the introduction of low-dose-rate afterloading intracavitary techniques for radiotherapy," *Br. J. Radiol.* **53**, 890–893.

Wilkinson, J.M., Moore, C.J., Notley, H.M. and Hunter, R.D. (1983). "The use of Selectron afterloading equipment to simulate and extend the Manchester System for intracavitary therapy of the cervix uteri," *Br. J. Radiol.* **56**, 409–414.

Wills, R., Lowe, G., Inchley, D., Anderson, C., Beenstock, V. and Hoskin, P. (2010). "Applicator reconstruction for HDR cervix treatment planning using images from 0.35 T open MR scanner," *Radiother. Oncol.* **94**, 346–352.

Withers, H.R., Taylor, J.M. and Maciejewski, B. (1988). "Treatment volume and tissue tolerance," *Int. J. Radiat. Oncol. Biol. Phys.* **14**, 751–759.

Wong, E.K., Truong, P.T., Kader, H.A., Nichol, A.M., Salter, L., Petersen, R., Wai, E.S., Weir, L. and Olivotto, I.A. (2006). "Consistency in seroma contouring for partial breast radiotherapy: impact of guidelines," *Int. J. Radiat. Oncol. Biol. Phys.* **66**, 372–376.

Wright, J.D., Dehdashti, F., Herzog, T.J., Mutch, D.G., Huettner, P.C., Rader, J.S., Gibb, R.K., Powell, M.A., Gao, F., Siegel, B.A. and Grigsby, P.W. (2005). "Preoperative lymph node staging of early-stage cervical carcinoma by [18F]-fluoro-2-deoxy-D-glucose-positron emission tomography," *Cancer* **104**, 2484–2491.

Wu, D.H., Mayr, N.A., Karatas, Y., Karatas, R., Adli, M., Edwards, S.M., Wolff, J.D., Movahed, A., Montebello, J.F. and Yuh, W.T. (2005). "Interobserver variation in cervical cancer tumor delineation for image-based radiotherapy planning among and within different specialties," *J. Appl. Clin. Med. Phys.* **6**, 106–110.

Wyckoff, H. (1957). "Modification of the basis for roentgen calibrations between 0.5 and 3 MeV," *NBS Tech. News Bull*. 41.

Yan, D. (2010). "Adaptive radiotherapy: merging principle into clinical practice," *Radiat. Oncol.* **20**, 79–83.

Young, R.H. and Clement, P.B. (2002). "Endocervical adenocarcinoma and its variants: their morphology and differential diagnosis," *Histopathology* **41**, 185–207.